Further characterisation of the envelope stress responses of *Salmonella* Typhimurium

Hannah Charlotte Wells

4006879

A Thesis submitted to the University of East Anglia in accordance with the requirements of the degree of Doctor of Philosophy

School of Biological Sciences

September 2015

Abstract

Salmonella serovars are enteric pathogens of economic and clinical importance. The ability of *Salmonella spp.* to sense and adapt to exogenous stresses contributes towards infection severity and prevalence. The envelope stress responses promote survival within and between hosts by maintaining envelope homeostasis and promoting the rapid response to environmental insults. In this study, we present the first comprehensive analysis of the Cpx regulated transcriptome in *S*. Typhimurium, identifying 116 genes as novel members of the *S.* Typhimurium Cpx regulon. Transcriptomic analyses, EMSAs and mutant screens further establish CpxAR as a major contributor to *S*. Typhimurium virulence through regulation of SPI-1, and as a regulator of post-transcriptional modification through the positive and negative regulation of small regulatory RNAs (*invR*, *omrA* and *omrB*). Our data confirm Cpx contribution to copper tolerance, a positive regulator of the heat shock sigma factor *rpoH* and adds polyamine homeostasis and regulation of host cell apoptosis to the growing list of Cpx regulated processes.

Furthermore, we present the first transcriptomic investigation into the ZraSR two-component signal transduction system and characterisation of its accessory protein, ZraP. We suggest ZraR mediated positive regulation of the virulence factors MntH and GroEL, GroSL, DnaK and ClpB (the heat shock chaperones). In addition, we show critical requirement of ZraSR for maximal carbon-starvation induced cross-resistance to heat and polymyxin B. The ZraR regulon described here includes functional groups required to promote survival within the *Salmonella* containing vacuole and genes contributing towards anaerobic metabolism. This work provides the foundations for investigating the contribution of ZraSR to *Salmonella* host-pathogen interactions and the potential this newly characterised ESR has as a target for investigating *Salmonella* survival within host cells. Together these investigations highlight the potential ESRs could hold as critical contributors to *Salmonella* pathogenicity and as therapeutic targets for the treatment of *Salmonella* infections.

Table of contents

List of tables..... 9
List of figures..... 11
List of abbreviations..... 14
Acknowledgements..... 17
1. Introduction..... 18
1.1 The origins of *Salmonella*..... 19
1.2 *Salmonella* pathogenicity..... 20
1.2.1 Source of infection..... 20
1.2.2 Salmonellosis..... 21
1.2.3 Enteric fever..... 22
1.2.4 *Salmonella* infection methods..... 24
1.2.5 Genetic and physiological differences between typhoidal and non-typhoidal *Salmonella enterica* subspecies..... 29
1.2.6 Emergence of invasive non-typhoidal *Salmonella* strains (iNTS)..... 30
1.3 Current treatments and disease prevention..... 31
1.3.1 Current *Salmonella* vaccines..... 32
1.4 Bacterial stress responses..... 33
1.5 Envelope stress responses..... 35
1.6 The extracytoplasmic-function sigma factor: Sigma E (σ^E)... 36
1.6.1 Extracytoplasmic sigma factors..... 36
1.6.2 Sigma E – RpoE..... 38
1.6.3 The σ^E regulon of *Salmonella*..... 39
1.6.3.1 The σ^E regulon and virulence..... *42*
1.6.4 Effect of σ^E on post-transcriptional regulation..... 44
1.6.5 The β-barrel assembly machinery (BAM) complex and σ^E.. 44
1.6.6 HtrA (DegP)..... 46
1.6.7 CpxAR and σ^E..... 47
1.7 The Cpx pathway..... 47
1.7.1 Two-component signal transduction (2CST) systems..... 48
1.7.2 Cpx-envelope response..... 48
1.7.3 Cpx and pathogenesis..... 50
1.7.4 Cpx and antibiotics..... 51
1.7.5 Cpx and antimicrobial compounds..... 55
1.7.6 *Salmonella* biofilms and Cpx..... 55
1.7.7 The CpxP-like superfamily..... 56
1.7.7.1 Structural similarities..... *57*
1.7.7.2 Spy..... *58*
1.7.7.3 ZraP..... *59*
1.8 The phage shock protein (PSP) System..... 60
1.9 Rcs phosphorelay response..... 62
1.10 Outer membrane vesicles as a stress response..... 65
1.11 BaeSR..... 66
1.12 ZraPSR..... 68

1.13 Thesis overview..... 69
1.13.1 Research gap..... 69
1.13.2 Aims..... 69
2. Materials and methods..... 70
2.1 Materials..... 71
2.2 Bacterial strains and plasmids..... 71
2.3 Bacterial culture conditions..... 71
2.3.1 Media..... 71
2.3.2 Overnight cultures..... 71
2.3.3 Long-term strain stocks..... 74
2.3.4 Aerobic batch culture..... 74
2.3.5 Anaerobic growth analysis in Hungate tubes..... 75
2.4 General laboratory techniques..... 75
2.4.1 Polymerase chain reaction (PCR)..... 75
2.4.2 Colony PCR..... 76
2.4.3 PCR product purification..... 78
2.4.4 Plasmid DNA extraction and purification..... 78
2.4.5 Bacterial transformation..... 78
2.4.5.1 Production of electrocompetent cells..... 78
2.4.5.2 Electroporation..... 79
2.4.5.3 Production of chemically competent cells..... 79
2.4.5.4 Heat shock transformation..... 80
2.4.6 *De novo* mutagenesis via the lambda (λ) red method..... 80
2.4.6.1 Production of competent cells for mutagenesis..... 80
2.4.6.2 Generation of FRT-flanked resistance gene construction..... 81
2.4.6.3 Mutant verification..... 81
2.4.6.4 P22 transduction..... 85
2.4.6.4.1 Lysate production of donor strain..... 85
2.4.6.4.2 Transduction of recipient strain with lysate..... 85
2.4.6.4.3 Detection of lysogens using UCB indicator (green) plates..... 85
2.4.6.5 Antibiotic resistance cassette removal..... 86
2.4.7 DNA electrophoresis..... 86
2.4.8 Extraction of DNA from agarose gels..... 87
2.4.9 Site-directed mutagenesis (SDM)..... 87
2.4.10 Complementation studies..... 88
2.4.10.1 Ligations..... 88
2.4.11 Spot plates..... 88
2.4.12 Disc diffusion assays..... 92
2.4.13 β-Galactosidase assays..... 92
2.4.14 Long-term carbon-starvation survival (LT-CSS) assays... 93
2.4.15 Carbon-starvation induced cross-resistance (CSIXR) assays..... 93
2.4.16 Protein purification..... 94
2.4.16.1 Test expression assay..... 94
2.4.16.1.1 Expression sample analysis by SDS-PAGE..... 94

2.4.16.2 Large-scale cell harvest..... *95*
2.4.16.3 Cell lysate collection and Fast Protein Liquid Chromatography (FPLC)..... *96*
2.4.16.4 Protein concentration and buffer exchange..... *96*
2.4.17 SDS polyacrylamide gel electrophoresis (SDS-PAGE)..... 97
2.4.18 Native PAGE and formaldehyde chemical cross-linking of protein oligomers..... 97
2.4.19 Western blot..... 99
2.4.19.1 Membrane transfer, ponceau red staining and membrane blocking..... *99*
2.4.19.2 Antibody staining and blot imaging..... *99*
2.4.20 Bradford assay..... 99
2.4.21 Electrophoretic motility shift assays (EMSAs)..... 100
2.4.21.1 CpxR phosphorylation..... *100*
2.4.21.2 EMSA 6-FAM™-fluorescein labelled probe production..... *100*
2.4.21.3 EMSA reaction and gel imaging..... *101*
2.4.22 RNA Extraction and analysis..... 102
2.4.22.1 Cell harvesting..... 102
2.4.22.2 Chromosomal DNA and total RNA extraction, purification, quality and quantity assessment..... *102*
2.4.23 Quantitative real-time polymerase chain reaction (qRT-PCR)..... 104
2.4.23.1 cDNA synthesis..... *104*
2.4.23.2 qRT-PCR primer design..... *104*
2.4.24 Microarray..... 106
2.4.24.1 Direct labelling of SL1344 reference genomic DNA. *106*
2.4.24.2 Array hybridisation and washing..... *107*
2.4.24.3 Scanning, normalisation and data analysis..... *108*
2.4.25 Analytical ultracentrifugation (AUC)..... 108
2.4.26 Protein aggregation assays..... 109
2.4.27 Malate dehydrogenase (MDH) activity assays..... 109
2.4.28 Biofilm assays..... 110
3 The CpxR regulated transcriptome of *Salmonella* Typhimurium.. 112
3.1 Introduction..... 113
3.1.1 Induction of the Cpx pathway by NlpE..... 113
3.1.2 Previous transcriptomic analysis of the Cpx regulon..... 114
3.2 Aim..... 118
3.3 Experimental design..... 118
3.3.1 Bacterial strains and plasmids..... 118
3.3.2 Growth curves during batch culture..... 119
3.3.3 NlpE overexpression..... 119
3.3.4 Microarray..... 119
3.4 Results..... 120
3.4.1 Overexpression of NlpE has no negative impact on the growth of *Salmonella* Typhimurium SL1344 or a Δ*cpxR* mutant of this strain..... 120

3.4.2 Analysis of genes differentially expressed in SL1344 WT and Δ*cpxR* strains post Cpx induction..... 121
3.4.2.1 Comparison of transcriptomic data in SL1344 to current literature..... *122*
3.4.2.2 Previously unidentified members of the Cpx regulon. *136*
3.4.2.2.1 Cpx and Salmonella virulence..... *136*
3.4.2.2.2 Regulation including sRNAs..... *138*
3.4.2.2.3 Metal stress and homeostasis..... *140*
3.4.2.2.4 Metabolic functions and respiration..... *141*
3.4.2.2.5 Genes of unknown or hypothetical function..... *142*
3.4.2.2.6 Transport and efflux systems..... *143*
3.5 Discussion and future work..... 151
3.5.1 Cpx regulon members, identified previously in *E. coli*, with unchanging transcription following induction of the Cpx response in SL1344 strains..... 151
3.5.1.1 Sigma factors and genes products involved in regulation..... *152*
3.5.1.2 Confirmation of Cpx mediated regulation of well-characterised periplasmic chaperones and proteases..... *153*
3.5.1.3 Cell division..... *157*
3.5.1.4 Chemotaxis and cell components..... *158*
3.5.1.5 Genes of unknown function..... *159*
3.5.2 Novel Cpx regulated genes..... 159
3.5.2.1 Cpx and pathogenicity..... *160*
3.5.3 sRNAs..... 162
4 Phenotypic analysis of newly discovered and uncharacterised members of the Cpx regulon..... 164
4.1 Introduction..... 165
4.1.1 Analysis of new Cpx regulon members – An introduction. 165
4.1.2 *Salmonella* response to copper stress and the contribution of CpxAR to copper tolerance..... 166
4.1.2.1 An introduction to metal stress..... *166*
4.1.2.2 Impact of copper on virulence of Salmonella..... *167*
4.1.2.3 Salmonella response to copper..... *168*
4.1.3 Role of polyamines in Enteric bacteria..... 169
4.1.3.1 Polyamine synthesis and homeostasis..... *170*
4.1.3.2 Polyamines and virulence..... *172*
4.2 Aim..... 174
4.3 Experimental design..... 174
4.3.1 Purification of His_{10}-CpxR protein..... 174
4.3.2 Electrophoretic motility shift assays (EMSAs)..... 175
4.3.2.1 CpxR phosphorylation..... *175*
4.3.2.2 EMSA probe production..... *175*
4.3.2.3 EMSA reaction and gel imaging..... *175*
4.3.3 β-Galactosidase assays..... 176
4.3.4 Sensitivity spot plates 176

4.3.5 Disc diffusion assays..... 176
4.3.6 Spermidine survival assays..... 176
4.3.7 Real-time quantitative PCR..... 177
4.4 Results 177
4.4.1 Shortlist of new Cpx regulon members for further analysis. 177
4.4.2. Regulation of proposed Cpx regulon members was confirmed by qRT-PCR..... 179
4.4.3 *in silico* analysis of CpxR binding motifs within the promoter regions of identified Cpx regulon members in SL1344..... 180
4.4.4 Confirmation of CpxR-mediated regulation of new Cpx regulon members and CpxR-P:DNA complex formation..... 184
4.4.4.1 Purification of S. Typhimurium CpxR (SL4009) for use in DNA binding assays..... 184
4.4.4.2 Visualisation of DNA:CpxR-P Interactions – Direct regulation of cstA, yqaE, SL3646, yccA, ydgF, eco, slrP and ybiJ by CpxR-P confirmed through the formation of promoter-CpxR-P complexes..... 188
4.4.5 Phenotypic analysis of uncharacterised, newly identified *S*. Typhimurium Cpx-regulon members..... 188
4.4.5.1 Antibiotic and antimicrobial compound screens suggest yqaE involvement in response to ampicillin and oxidative stress..... 191
4.4.5.2 YdgFE contributes to S. Typhimurium survival during spermidine stress..... 193
4.4.5.3 ScsA, as well as ScsBCD, contributes towards copper sulphate tolerance in S. Typhimurium..... 195
4.4.5.4 Characterisation of the SL3010/3009 operon: Expression levels across growth phases and regulation by other ESRs..... 201
4.4.5.4.1 SL3010 and SL3009 are up-regulated upon entry into stationary phase and increasing cell density..... 201
4.4.5.4.2 Involvement of SL3010/09 in adhesion of S. Typhimurium to abiotic surfaces..... 204
4.5 Discussion and future work..... 206
4.5.1 The multidrug efflux system YdgFE assists *S*. Typhimurium in overcoming spermidine toxicity..... 208
4.5.2 *yqaE* involvement in *S*. Typhimurium response to ampicillin and oxidative stress..... 211
4.5.3 Cross-regulation of SL3010/SL3009 by Cpx, Bae and Zra ESRs and the influence of Cpx regulated genes on biofilm formation..... 213
4.5.4 Confirmation of Scs operon involvement in copper tolerance of *S*. Typhimurium..... 215
4.5.5 Summary..... 217
5 Characterisation of the *S*. Typhimurium ZraPSR ESR..... 219
5.1 Introduction……..……..... 220
5.1.1 The Zra 2CST system..... 220

5.1.2 ZraR is a σ^{54} bacterial enhancer binding protein (bEBP).... 221
5.1.3 Zinc – How bacteria respond to fluctuations in zinc availability and maintenance of zinc homeostasis..... 223
5.1.4 Importance of zinc in host pathogen interactions and *Salmonella* virulence..... 226
5.1.5 Contribution of the Bae ESR system to zinc tolerance..... 230
5.2 Aims……..……..……..... **232**
5.3 Experimental design……..……..……..... **232**
5.3.1 Growth assays……..... 232
5.3.2 ZraR overexpression and microarray analysis....……..... 232
5.3.3 Real time quantitative PCR.....……..……..... 233
5.3.4 LT-CSS and CSIXR assays.....……..... 233
5.4 Results……..... **233**
5.4.1 Zinc sensitivity of SL1344 WT following deletion of ZraSR and the CpxP-like family of molecular chaperones..... 233
5.4.2 Transcription of *zraR* increases in response to elevated environmental zinc..... 238
5.4.3 ZraR is negatively regulated by its cognate, periplasmic protein ZraP and expression of both genes correlates with this feedback inhibition across growth phases in SL1344... 239
5.4.4 Contribution of ZraSR to carbon starvation induced cross resistance (CSIXR) of *S*. Typhimurium..... 241
5.4.5 Overexpression of ZraR and analysis of the ZraR regulated transcriptome in SL1344..... 242
5.4.5.1 Comparison of transcriptomic data from ZraR overexpression in SL1344 to current literature..... 244
5.4.5.1.1 ESR genes: Comparisons to Bae, Cpx, and σ^E regulons and genes involved in envelope homeostasis..... 246
5.4.5.1.2 Functional groups with members differentially regulated by ZraR over expression..... 254
5.4.6 Analysis of *zraR* and *zraP* during anaerobic growth..... 255
5.4.7 The contribution of the Bae ESR to zinc tolerance in *S.* Typhimurium, *S*. Enteritidis and *E. coli* is not universal..... 256
5.5 Discussion and future work..... **261**
6 Analysis of ZraP function and structure – How zinc influences ZraP chaperone activity and quaternary structure..... **271**
6.1 Introduction..... **272**
6.1.1 Biochemical analysis of ZraP..... 272
6.1.2 ZraP higher-order structure analysis..... 275
6.2 Aims..... **276**
6.3 Experimental design..... **276**
6.3.1 Site-directed mutagenesis (SDM) 276
6.3.2 Purification of WT and recombinant ZraP protein..... 276
6.3.3 Protein aggregation assays..... 277
6.3.4 Malate dehydrogenase (MDH) activity assays..... 277
6.3.5 Analytical ultracentrifugation (AUC)..... 277

6.3.6 Native PAGE and formaldehyde chemical cross-linking of protein oligomers..... 278
6.4 Results..... 278
6.4.1 ZraP protects MDH from denaturation by guanidine hydrochloride (GdnHCl)..... 278
6.4.2 Production and purification of ZraP site directed mutants. 279
6.4.3 Chaperone activity of ZraP is zinc dependent, requires residues G120-Y125 and occurs independently of an LTXXQ motif conserved within the CpxP-like superfamily of molecular chaperones..... 281
6.4.4 ZraP-SDMB is unable to form higher order multimers..... 285
6.4.4.1 ZraP-SDMB predominantly forms monomers as seen by chemical cross-linking..... 285
6.4.4.2 Mutations within the ZraP-SDMB motif impacts on the formation of multimeric structures of ZraP..... 289
6.5 Discussion and future work..... 295
6.5.1 ZraP chaperone activity and higher order oligomerisation is hindered by alanine substitution mutations at residues G120-Y125..... 295
7 General discussion..... 303
7.1 Context..... 304
7.1.1 Why study the ESRs of *Salmonella*?..... 305
7.2 ZraSR – More than a zinc sensing system?..... 306
7.3 The CpxP-like family of periplasmic chaperones..... 313
7.4 The Cpx ESR and *Salmonella* virulence..... 316
7.5 Concluding remarks..... 319
8 References..... 321
9 Appendices..... 376

List of tables

Table 1 Virulence phenotypes associated with Cpx mutants..... 52

Table 2 The Rcs phosphorelay system and virulence..... 64

Table 3 Strains used during this study..... 72

Table 4 Plasmids used during this study..... 73

Table 5 PCR reaction components..... 76

Table 6 Primers used for the generation of cloning products and pBAD/*Myc* His A sequencing primers..... 77

Table 7 Thermocycling steps for PCR..... 77

Table 8 Primers used for the production of knockout mutants..... 83

Table 9 Primers used to verify the production of knockout gene mutant strains..... 84

Table 10 PCR reagents and reaction composition for site-directed mutagenesis..... 89

Table 11 Site-directed mutagenesis primers for mutation of specific amino acid residues within *zraP*..... 90

Table 12 Double restriction enzyme digestion of PCR amplified insert DNA and plasmid DNA..... 91

Table 13 Reaction composition and conditions for ligations..... 91

Table 14 *L*-arabinose and IPTG titration used during test expression assays..... 95

Table 15 Components and composition of SDS polyacrylamide protein gels..... 98

Table 16 Components and composition of native polyacrylamide protein gels..... 98

Table 17 Composition of Bradford assay reaction..... 100

Table 18 Oligonucleotides used to produce 6-FAM™-fluorescein labelled probes..... 102

Table 19 Composition of EMSA reactions..... 103

Table 20 Primers used during qRT-PCR..... 105

Table 21 Microarray hybridisation buffer..... 108

Table 22 77 genes repressed by CpxR in *Salmonella* Typhimurium SL1344..... 128

Table 23 63 genes induced by CpxR in *Salmonella* Typhimurium SL1344..... 132

Table 24 New members of the Cpx regulon of *S*. Typhimurium..... 145

Table 25 Shortlist of 27 genes differentially regulated >2-fold (FDR <0.05) during our transcriptomic analyses selected for further investigation..... 178

Table 26 Summary of qRT-PCR results confirming expression levels observed during microarray analysis..... 183

Table 27 Presence and location of CpxR-P binding motifs..... 186

Table 28 Sensitivity screens of *S*. Typhimurium SL1344 WT and six deletion mutants..... 192

Table 29 97 genes up-regulated by ZraR overexpression in *S.* Typhimurium SL1344 that do not belong to the σ^{54} regulon..... 249

Table 30 Summary of AUC data for ZraP WT and ZraP variants..... 292

Table 31 Zinc requirements and toxic levels..... 309

List of figures

Figure 1 Model of *Salmonella* evolution..... 20

Figure 2 Total populations at 'high-risk' from typhoid fever in endemic regions..... 25

Figure 3 A cartoon depiction of the diverse chemical and physical stresses inflicted upon *Salmonella* in host and non-host environments.. 34

Figure 4 Diagrammatic representation of the five main ESRs, their inducing cues, pathway components and examples of the genes they regulate..... 37

Figure 5 Genetic organisation of the *S.* Typhimurium *rpoE* operon (A) and comparison of the *E. coli* and *S.* Typhimurium *rpoE* promoter regions (B) 41

Figure 6 Representation of a simple gene disruption strategy..... 82

Figure 7 The reversible oxidation of malate to oxaloacetate by MDH..... 110

Figure 8 Overview of the Cpx two-component signal transduction system, components and inducing cues..... 115

Figure 9 Growth of SL1344p*nlpE* and Δ*cpxR*p*nlpE* in LB broth batch culture is unaffected by overexpression of NlpE from the P_{BAD} plasmid.. 121

Figure 10 Comparison of known CpxR regulon members to those identified in *S*. Typhimurium..... 123

Figure 11 Relative percentage of genes up-/down-regulated in SL1344Δ*cpxR* compared to SL1344 WT following NlpE overexpression 135

Figure 12 Regulation of *Salmonella* Pathogenicity Island-1 by CpxR..... 139

Figure 13 Polyamine synthesis and transport..... 173

Figure 14 Quantitative real-time PCR showing mRNA levels of selected target genes (A-R) 182

Figure 15 Sequence logo for the CpxR-P recognition weight matrix in *E. coli* (A) and *Salmonella* (B)..... 185

Figure 16 Purification of N-terminal 10xHis tagged CpxR purification at >95% purity as judged by SDS-PAGE..... 187

Figure 17 Formation of CpxR-P-promoter complexes for *cstA*, *yqaE*, *SL3646*, *yccA, ydgF*, *eco*, *slrP* and *ybiJ* 6-FAM fluorescein labelled promoter regions..... 189

Figure 18 Formation of CpxR-P-promoter complexes for *yihE*, *tsr*, *deoA* and *rpoH* 6-FAM fluorescein labelled promoter regions in the absence of poly(dI•dC) 190

Figure 19 Deletion of *yqaE* renders *S*. Typhimurium more sensitive to ampicillin [10 µg] and hydrogen peroxide [30% and 15% v/v]..... 193

Figure 20 *S*. Typhimurium SL1344 WT and Δ*ydgFE* double mutants do not differ in sensitivity to spermidine (2 mM) when grown in liquid culture..... 196

Figure 21 *S*. Typhimurium SL1344 and *ydgFE* double mutants do not differ in sensitivity to spermidine (2 mM) when grown on solid media..... 198

Figure 22 S. Typhimurium *ydgFE* double mutant exhibits sensitivity to spermidine at concentrations greater than 4 mM when grown on solid media..... 198

Figure 23 Growth of SL1344 WT, Δ*cpxR*, Δ*scsA* and *cpxA** strains on LB agar containing 4 mM $CuSO_4$, under aerobic conditions, at 37°C for ~48 hours..... 199

Figure 24 Sensitivity of Δ*scsA* and Δ*cpxR*Δ*scsA* to 3mM $CusO_4$ (A) cannot be fully complemented when Δ*scsA* is expressed *in trans* (B)..... 200

Figure 25 Sensitivity of Δ*scsA* and Cpx mutants to 4 mM $CusO_4$ when grown overnight in batch culture (LB)..... 200

Figure 26 β-galactosidase assays of SL3010/3009 *lacZ*-promoter fusions show increased SL3010/3009 expression upon entry into stationary phase and with increased cell density..... 202

Figure 27 β-galactosidase assays of SL3010/3009 *lacZ*-promoter fusions show cross-regulation of this uncharacterised operon by Cpx, Bae and Zra ESRs..... 203

Figure 28 Increased biofilm formation of Δ*SL3009* and Δ*SL3010*Δ*SL3009* mutants compared to SL1344 WT..... 205

Figure 29 Biofilm formation of Δ*ybiJ* and Δ*ydgFE* mutants does not significantly differ to SL1344 WT (100%)..... 205

Figure 30 Diagram of *zraPSR* operon..... 222

Figure 31 Zinc transporters in Enterobacteria..... 227

Figure 32 Representation of Bae regulon and members involvement in zinc tolerance..... 231

Figure 33 Impacts of high $ZnCl_2$ (A) and $ZnSO_4$ (B) concentrations on the growth rate (μ) of SL1344..... 236

Figure 34 Growth of SL1344 WT and strains lacking *zraSR*, *zraP* and the Cpx family of molecular chaperones are unaffected by exposure to $ZnSO_4$..... 237

Figure 35 Expression of *zraR* in a SL1344 WT background when cultured in MOPS with increasing $ZnCl_2$ concentrations (0-1 mM)..... 239

Figure 36 Expression of *zraR* and *zraP* peak upon entry into exponential growth phase..... 240

Figure 37 ZraSR contributes towards *S*. Typhimurium CSIXR to cAMP and heat..... 243

Figure 38 Diagrammatic summary of transcription changes to 186 genes differentially regulated >2-fold following ZraR overexpression in *S*. Typhimurium SL1344..... 245

Figure 39 Fold change of the CpxP family of molecular chaperones in S. Typhimurium SL1344 following ZraR overexpression..... 248

Figure 40 Anaerobic growth of *S*. Typhimurium SL1344 is unaffected by deletion of *zraSR* or *baeR*..... 256

Figure 41 Deletion of *baeR* does not impact on zinc tolerance..... 259

Figure 42 Growth rate constants (μ) and mean generation times (*Td*) of *baeR* deletion mutants are unchanged compare to WT equivalents when exposed to $ZnSO_4$ in rich (A and B) and minimal (C and D) media 260

Figure 43 Diagrammatic representations of the known crystal structures of the Cpx family of molecular chaperones..... 275

Figure 44 ZraP protects MDH function during chemical denaturation with GdnHCl..... 279

Figure 45 Elution profiles and SDS-PAGE analysis of ZraP recombinant proteins..... 283

Figure 46 ZraP protects MDH from thermal aggregation, independently of amino acid substitutions within LTTEQ and HRGGGH motifs..... 286

Figure 47 ZraP-SDMB protects MDH from thermal aggregation, activity that is lost upon the addition of zinc chloride..... 287

Figure 48 Native PAGE of formaldehyde cross-linked ZraP WT and ZraP variants..... 289

Figure 49 Preliminary sedimentation equilibrium analysis of recombinant ZraP oligomers at 7,000 rpm and 10,000 rpm..... 291

Figure 50 Sedimentation equilibrium analysis of recombinant ZraP oligomers at 23,000 rpm and 30,000 rpm..... 293

Figure 51 Sedimentation equilibrium analysis of recombinant ZraP-SDMB oligomers at 23,000 rpm and 30,000 rpm..... 294

List of abbreviations

(v/v)	Volume per volume
(w/v)	Weight per volume
2CST	Two-component signal transduction
AIEC	Adherent invasive *E. coli*
Amp	Ampicillin
AMP	Antimicrobial peptides
APS	Ammonium persulfate
ATR	Acid tolerance reponse
AUC	Analytical ultracentrifugation
BAM	β-barrel assembly machinery
bEBP	Bacterial enhancer binding protein
BSA	Bovine serum albumin
$CaCl_2$	Calcium chloride
cDNA	Complementary DNA
CFU	Colony forming unit
Cm	Chloramphenicol
CSIXR	Carbon starvation induced cross-resistance
Ct	Calculated threshold
DMSO	Dimethyl sulfoxide
DNA	Deoxyribonucleic acid
Dnase I	Deoxyribnuclease I
DTT	Dithiothreitol
ECF	Extracytoplasmic function
EDTA	Ethylenediaminetetraacetic acid
EHEC	Enterohaemorrhagic *Escherichia coli*
EPEC	Enteropathogenic *Escherichia coli*
ESR	Envelope stress response
ETEC	Enterotoxigenic *Escherichia coli*
FDR	False discovery rate
FPLC	Fast protein liquid chromatography
FRT	Flippase recognition target
GdnHCl	Guanidine hydrochloride
HIC	Higher-income countries
HiC	High carbon
His	Histidine
HK	Histidine kinase
HRP	Horseradish peroxidase
HU	Hydroxy urea
IEC	Intestinal epithelial cells
IM	Inner membrane
iNTS	Invasive non-typhoidal *Salmonella*
IPTG	Isopropyl β-D-1-thiogalactopyranoside
Kan	Kanamycin

kDa	Kilodalton
KEGG	Kyoto Encyclopaedia of Genes and Genomes
Km	Kanamycin
L	Litre
LMIC	Low and middle income countries
LoC	Low carbon
LPS	Lipopolysaccharide
LTCSS	Long-term carbon starvation survival
MDH	Malate dehydrogenase
MDR	Multidrug resistant
Min	Minute
mL	Millilitre
mM	Millimolar
mm	Millimetre
MOPS	3-(N-morpholino)propanesulfonic acid
mRNA	Messenger RNA
N-PAGE	Native polyacrylamide gel electrophoresis
NE	Neutrophil elastase
NF-kB	Nuclear factor kappa-light-chain-enhancer of activated B cells
NoC	No carbon/carbon-free
NTS	Non-typhoidal *Salmonella*
OM	Outer membrane
OMP	Outer membrane protein
ORF	Open reading frame
PBP	Penicillin binding protein
PBS	Phosphate buffered saline
PCR	Polymerase chain reaction
PMN	Polymorphonuclear leukocytes
Poly(dIdC)	Poly(deoxyinosinic-deoxycytidylic)
PP	Periplasmic protein
PPIase	Peptidyl-prolyl cis-trans isomerase
PSP	Phage shock protein
qRT-PCR	Quantitative real-time polymerase chain reaction
^{R}	Resistance
RNA	Ribonucleic acid
RNAP	RNA polymerase
RNS	Reactive nitrogen species
ROS	Reactive oxygen species
rpm	Revolutions per minute
RR	Response regulator
RT	Room temperature (18-24°C)
SCV	*Salmonella* containing vacuole
SD	Standard deviation
SDS	Sodium dodecyl sulphate
SDS-PAGE	Sodium dodecyl sulphate polyacrylamide gel electrophoresis

sec	Second(s)
SO	Sulfite oxidase
STEC	Shiga-toxin producing *Escherichia coli*
STM	*Salmonella* Typhimurium
str.	Strain
substr.	Substrain
TAT	Twin-arginine translocation
TBE	Tris/Borate/EDTA
TBS	Tris buffer saline
TBST	Tris buffer saline Tween20
TEMED	*N,N,N′,N′*-Tetramethylethylenediamine
Tet	Tetracycline
TLR	Toll-like receptor
Tm	Melting temperature
TTSS	Type three secretion system
UPEC	Uropathogenic *Escherichia coli*
V	Volts
Van	Vancomycin
WHO	World Heath Organisation
WT	Wild type
µL	Microlitre

Acknowledgements

Firstly, thank you to UEA for funding and the John and Pamela Salter Charitable Trust for additional financial contributions. My supervisory team Dr Gary Rowley, Dr Tom Clarke and Dr Jonathan Todd have provided invaluable expertise, help and advice during my time at UEA and I am incredibly grateful to them. I would like to thank Gary specifically for his guidance, encouragement and patience. Your continued support has been invaluable and I owe a lot to the time you've given me over the last four years. Thank you also for the many beverages and pep talks when science (and life) weren't going as planned. Thank you to Dr Tom Clarke for his much appreciated technical support, especially throughout my ZraP project.

I am particularly grateful to Dr Corinne Appia-Ayme and Dr Matt Sullivan for their guidance and training when I started; to Elaine Patrick for being the best technician a PhD student could ask for and to all other members of the Rowley lab for your support and friendships. In particular, a big thank you to Tom Williams for assistance with carbon starvation assays and Rhiannah Zalm and Isabel Johnston for all of your technical support during my final months of research.

I am truly grateful to members of Lab 1.29 for their friendship and generosity during my 7 years at UEA and to the Hutchings research group, past and present, for your technical and emotional support. My PhD would not have been the same without your 'Food Days' and Spotify sessions. To Chris Beckwith and John Munnoch, thanks for the BBQs, laughter and write-up counselling sessions. I'm lucky to call you my friends and proud that we made it through together.

To my Mum, Dad, Lorna and Ash, thank you for putting up with me during the stressful times and for always being a phone call away when I needed you. And finally I'd like to thank Tom Howson for being my best friend, late-night lab taxi, guidance councillor and motivator over these last 4 years. Without your unwavering support and love I wouldn't have made it this far and I thank you from the bottom of my heart.

1 Introduction

1.1 The origins of *Salmonella*

The *Salmonella* genus consists of two species, *Salmonella bongori* and *Salmonella enterica*, that diverged from a common ancestor with *Escherichia coli* ~100-150 million years ago (Fookes et al., 2011, Doolittle et al., 1996). *S. bongori*, a commensal of cold-blooded animals, is subcategorised into eight serovars whereas the *Salmonella enterica* species is vastly more substantial, comprising of six subspecies: *enterica* (I), s*alamae* (II), *arizonae* (IIIa), *diarizonae* (IIIb), *houtenae* (IV) and *indica* (VI) (Figure 1). This nomenclature reflects current understanding of *Salmonella* taxonomy, as published by the Judicial Commission of the International Committee on the Systematics of Prokaryotes (2005) (Tindall et al., 2005, Issenhuth-Jeanjean et al., 2014).

S. enterica subspecies I-VI are further divided into >2500 serovars based on the presence of distinct surface antigens (somatic 'O', flagella 'H' and capsular Vi) (Fookes et al., 2011, McClelland et al., 2001, Porwollik et al., 2002, Baumler et al., 1998, Sabbagh et al., 2010). This subtyping of *S. enterica* predominately occurs through serotyping, identification of these surface antigens through agglutination reactions with specific antibodies. However, the use of molecular biology techniques in serovar identification has become more prominent during the last two decades (Wattiau et al., 2011, Baumler et al., 1998, Porwollik et al., 2002). As of September 2014 there were 2659 *Salmonella* serovars, 1586 within subspecies *enterica* (Issenhuth-Jeanjean et al., 2014). The WHO Collaborating Centre for Reference and Research on *Salmonella* (WHO-Salm) are set to publish their most recent Kauffman-White-Le Major scheme report (comprising the antigenic formulae of *Salmonella* serovars) in December 2015.

S. enterica subspecies I (*S. enterica* subsp. *enterica*) is adapted to warm-blooded animals and contains pathotypes that are both promiscuous and host-adapted. This subspecies is responsible for virtually all cases of *S. enterica* infections in humans and is the focus of the majority of *Salmonella* research. Only 1,342 cases of infection from *S. enterica* subspecies II-IV occurred in the US between 1985-2010, and subspecies VI is rarely isolated

from humans (Abbott et al., 2012). The subspecies I serovar at the focus of this study is *S*. Typhimurium.

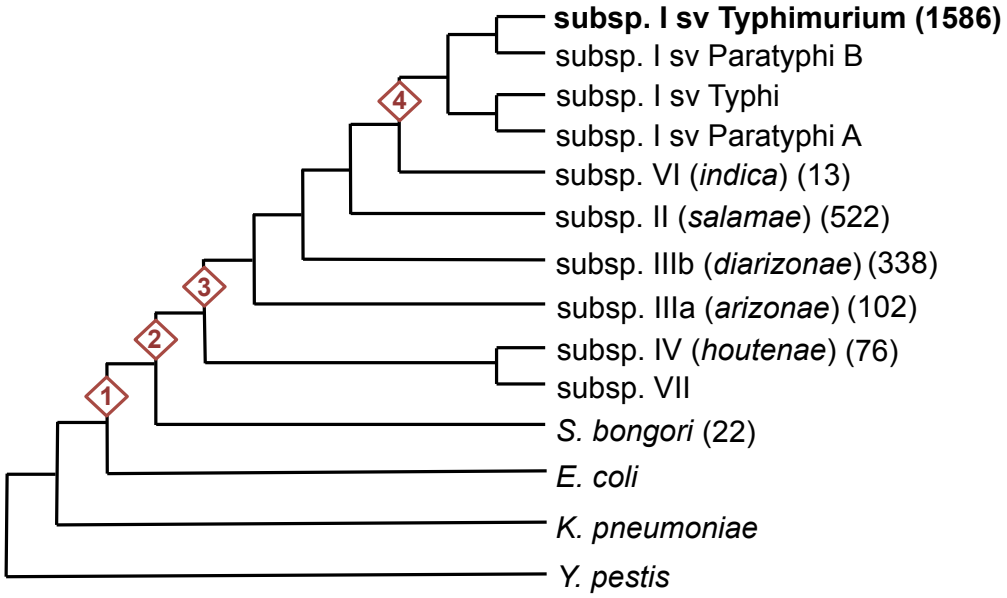

Figure 1: **Model of *Salmonella* evolution.** 1) Acquisition of SPI-1 TTSS by *Salmonella*'s common ancestor. 2) Acquisition of SPI-2 TTSS by the *Salmonella enterica* ancestor; divergence of the two *Salmonella* species. 3) *Salmonella enterica* subspecies acquire the ability to phase shift multiple flagellin subunits, allowing host immune response avoidance. 4) Further subspecies differentiation: subspecies I acquires the ability to colonise warm-blooded hosts. The number of serovars present in each species and subspecies is shown in parenthesis. Adapted from Ellermeier (2006).

1.2 *Salmonella* pathogenicity

S. enterica are pathogenic Enterobacteriaceae, responsible for four disease outcomes: enteric fever (typhoid fever and paratyphoid fever), salmonellosis/enterocolitis, bacteraemia and chronic asymptomatic carriage. Of these four states, human enteric fever and salmonellosis are the two most common and both will be discussed here. Although *S. enterica* serovars are some of the most studied pathogens (Boyle et al., 2007) they are still responsible for significant morbidity and mortality across low- and middle-income countries (LMICs) (Mogasale et al., 2014). This results from their ability to infect a broad host range and establish persistent infections, coupled with increasing antibiotic resistance.

1.2.1 Sources of infection

Salmonella infections in humans vary in symptoms and severity from asymptomatic colonisation (no disease manifestation) to systemic typhoid

fever, which can be fatal if untreated. An estimated 95% of *Salmonella* infections originate from foodborne sources, with contaminated eggs and poultry the typical transmission vehicle (Strelkauskas, 2010). However, outbreaks attributed to the contamination of fresh produce are increasing (Fatica and Schneider, 2011). As fresh produce is often consumed raw, the lack of cooking makes pathogen elimination difficult. Sealing cut produce in packaging, modifying packaging atmospheres to high CO_2/N_2 and washing vegetables in a chlorine dioxide solution can reduce bacterial growth rates and viable colony counts (Hanning et al., 2009, Jin and Lee, 2007, Pasha et al., 2014). Globalisation of the modern food market makes these treatments and the prevention of contamination ever more important. Infected food and drink can travel vast distances in short time frames, making the source of contamination difficult to find and disease containment challenging.

Chronic carriers of *S*. Typhi are another reservoir for disease spread. With treatment, 95-97% of typhoid fever patients recover from the acute phase of the disease, however 3-5% develop chronic infections of the gall bladder (Merselis et al., 1964, Levine et al., 1982). These patients shed large *S*. Typhi numbers in their faeces and urine contaminating water sources and food. With 25% of carriers experiencing no clinical manifestations of disease (asymptomatic carriers) identification of infected individuals is difficult (Parry et al., 2002, Sinnott and Teall, 1987). These carriers are highly contagious and can continue to shed bacteria for decades (Shpargel et al., 1985). As typhoid is spread by close contact with an infected individual (horizontal transmission) in addition to ingestion of contaminated material, asymptomatic carriers, as well as diseased patients, are important contributors to disease spread (Gonzalez-Escobedo et al., 2011).

1.2.2 Salmonellosis

S. enterica serovars are one of the leading causes of gastrointestinal infections worldwide (~10-30% of cases annually) (Pang et al., 1995, Strelkauskas, 2010). Salmonellosis (also called *Salmonella* enterocolitis) is a specific form of bacterial gastroenteritis in humans. *S. enterica* subspecies I (*enterica*) is the leading cause of salmonellosis, with disease outcomes differing substantially between serovars (Jones et al., 2008). The most

recently published figures for the United States of America confirmed three of the ~2600 *S. enterica* serovars (Typhimurium, Enteritidis and Newport) were responsible for ~40% of *Salmonella* infections, with 20 serovars in total causing ~70% of cases (Centers for Disease Control and Prevention (CDC), 2014). These non-typhoidal *Salmonella* (NTS) strains are broadly adapted host-generalists and predominantly cause self-limiting infections, characterised by localised inflammation of the intestinal epithelium, vomiting, abdominal cramps and diarrhoea or constipation (Haraga et al., 2008). Symptoms usually occur 8-72 hours post ingestion of contaminated material and although unpleasant, the vast majority of cases require no treatment. The host immune system usually removes the infection within 2-5 days. Only immunocompromised patients: those burdened with chronic medical conditions (i.e. HIV/AIDS, cancer patients) and/or the very young and old require treatment with antibiotics or hospitalisation to replace fluid loss. Regarding risk groups, Laupland et al. (2010) observed an increase in NTS occurrence with male gender and increasing age, however no such correlations were observed for typhoidal *Salmonella* bacteraemia, where a decrease in incidents with advancing age was observed.

In addition to salmonellosis, *S. enterica* serovars can cause severe and progressive life threatening systemic infections, such as bacteraemia and enteric fever, in humans. One *S. enterica* serovar, *S*. Typhimurium, is of particular interest because it causes enterocolitis and bacteraemia in humans, but a systemic, typhoid-like illness in mice. This makes *S.* Typhimurium a useful typhoid model in the laboratory and the greatest contributor to typhoid research (Baumler et al., 1998).

1.2.3 Enteric fever

Enteric fever is the common name referring to two illnesses: typhoid fever and paratyphoid fever (Crump and Mintz, 2010). Both are systemic, socially and economically significant infections caused by human-restricted serovars of *S. enterica* subspecies I: *S*. Typhi, *S*. Paratyphi A, *S*. Paratyphi B, *S*. Paratyphi C and *S*. Sendai (*S*. Typhi alone causes typhoid fever).

The symptoms of typhoid fever develop over four weeks, starting with high fever, abdominal cramps, vomiting and diarrhoea or constipation. The disease progresses to enlargement of the liver and spleen, severe weight loss and deterioration of mental state (World Health Organisation (WHO), 2015). If left untreated, haemorrhagic necrosis can occur resulting in tissue perforation and a systemic spread of the infection. Despite continued efforts to improve treatment and disease prevention techniques, a recent investigation into typhoid fever burden in LMICs (where vaccines are most likely to be deployed) estimated 223,000 fatalities from ~21 million cases per annum (estimated risk-unadjusted burden) (Mogasale et al., 2014). Although improved sanitation has reduced the incidence of *S.* Typhi infection in higher-income countries (HICs) (sporadic outbreaks remaining relatively constant), typhoid fever is still highly endemic in the vast majority of LMICs with the majority of cases on the Indian subcontinent (Buckle et al., 2012, Crump et al., 2004, Bhutta et al., 1996). The endemic population in LMICs for 2010 was estimated at 5.6 billion, with 29% (1.6 billion people) at 'high-risk' of typhoid infection (Mogasale et al., 2014) (Figure 2).

Incidence records of typhoid fever are limited by the geographical occurrence of the disease. Southern China is one region of particular interest as *S*. Paratyphi A has overtaken *S*. Typhi as the dominant cause of infection (Jin, 2008). There is significant overlap in symptoms between typhoid and paratyphoid with differential fever presentation, abdominal distension and general malaise the clearest indications of typhoid (Bhutta, 2006, World Health Organisation (WHO), 2015). Many countries across Africa and Asia lack the appropriate technology for correct diagnosis and differentiation between *S*. Typhi and *S*. Paratyphi serovars (Parry et al., 2002). If available, a combination of serology (40-60% positive) and organism cultures from patient stool and blood samples (up to 80% positive) are the most effective diagnostic techniques (Tam et al., 2008, World Health Organisation (WHO), 2015, Johnston et al., 2009). In Africa, high HIV rates, wide-spread poverty, insufficient infrastructure, political upheaval and mass migration all negatively impact diagnosis, treatment and hinder long-term clinical and epidemiological studies (Wain et al., 2014). With poor diagnostics, this further disrupts the effective collection of data and appropriate treatment. Paediatric cases

specifically are believed to be under-reported and difficult to diagnose, due to milder or asymptomatic presentation of the disease in some children and problems of collecting sufficient volumes of blood from young patients (Sinha et al., 1999).

The continued prevalence of *S. enterica* infections worldwide, the substantial impact on human health and the economic burden associated with this, highlight the importance of understanding the mechanisms by which *Salmonella* are able to sense their environment, adapt accordingly and cause infection. As *Salmonella* infections are spread through direct contact with contaminated material, both in the wider environment and during food product processing, the continued prevalence of this pathogen and the indiscriminate nature of infection make it an important research focus. Our understanding of how bacterial pathogens (e.g. *S.* Typhi and *S.* Typhimurium) perceive changes in their internal and external environments are crucial for our understanding of how these important pathogens survive and cause disease.

1.2.4 *Salmonella* infection methods

The pathogenicity of *Salmonella* is, in part, due to the presence of sophisticated molecular machinery encoded by *Salmonella* pathogenicity islands (SPIs). These clusters of virulence-associated genes are large unstable elements of the chromosome characterised by their differing GC content (37-47% lower than the rest of the genome), their atypical codon usage and the location of many SPIs next to a tRNA gene (Kelly et al., 2009, Feng et al., 2011). These charcteristics imply acquisition of these genomic islands through horizontal transfer events. At the present time, 21 SPIs have been characterised: 11 are present in *S*. Typhimurium and *S*. Typhi (SPIs-1 to 6, 9, 11, 12, 13 and 16), one is *S*. Typhimurium specific (SPI-14) and four SPIs (SPI-7, 15, 17 and 18) are only found in *S*. Typhi (Shah et al., 2005, Sabbagh et al., 2010) (Appendix A, Table A1). Tight regulation of all SPIs by environmental, spatial and genetic factors is essential to ensure expression of virulence genes only occurs when needed. Before an infection can be

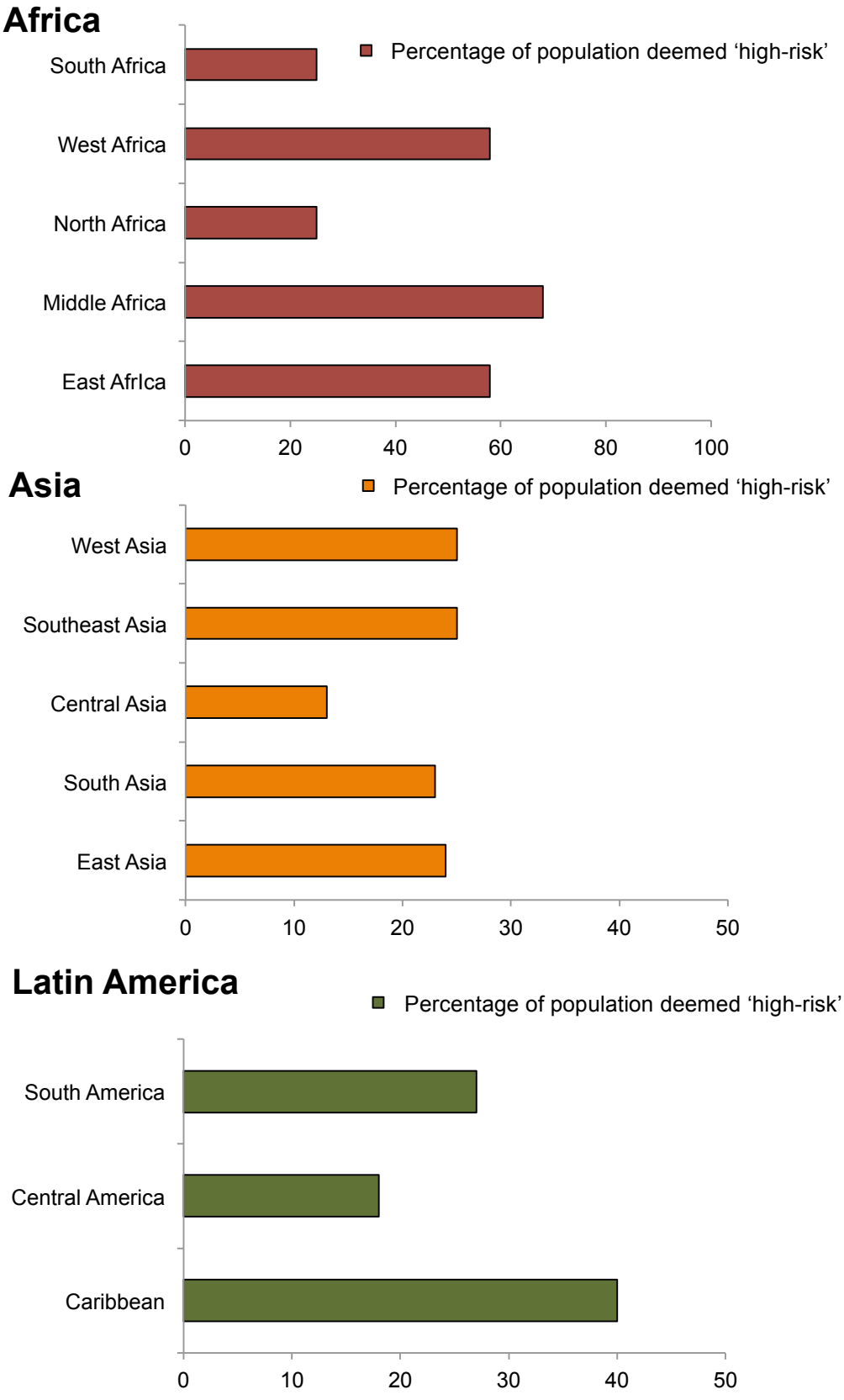

Figure 2: Total populations at 'high-risk' from typhoid fever in endemic regions, categorised by continent. 'High-risk' defined as "rural population lacking access to improved water and urban population living in slums". Adapted from Mogasale et al. (2014).

established, *Salmonella* must first survive the low pH gastric juices of the stomach upon entering the host, which provides the body with a protective barrier against many pathogens. *Salmonella* has an effective acid tolerance response (ATR) involving several ATR regulators (i.e. RpoS, Ada, Fur, OmpR, PhoPQ) (Bang et al., 2002, Bearson et al., 1998) that control the expression of novel sRNAs (i.e. DsrA, ArcZ) and 105 acid shock proteins, expressed across log and stationary growth phases (Suar and Ryan, 2015, Foster, 1991). Together these allow *Salmonella* survival when passing through the stomach and into the intestinal lumen (Garcia-del Portillo et al., 1993a).

SPI-1 and SPI-2 contain genes encoding type-three secretion systems (TTSS). These secretion systems are macromolecular structures that evolved from the flagella basal body, consisting of a motor, needle complex and a translocon through which effector proteins are delivered into host cells (Srikanth et al., 2011, Stebbins and Galan, 2003, Schmidt and Hensel, 2004, Thomson et al., 2008). SPI-1 is required for *Salmonella* invasion of host cells, which preferentially occurs at the microfold (M) and epithelial cells of the distal small intestines (Jones et al., 1994, Clark et al., 1994, Kohbata et al., 1986). Expression of SPI-1 is induced by high osmolarity, near neutral pH and O_2 tension at this location, initiating SPI-1 TTSS formation and priming *Salmonella* for invasion (Valdez et al., 2009, Altier, 2005, Wisner et al., 2012, Garmendia et al., 2003). Equally, repression of SPI-1 occurs upon exposure to bile and short-chain fatty acids, as these environmental cues indicate entry into the small and large intestines respectively (Altier, 2005).

The basal body of the SPI-1 TTSS comprises an IM ring of PrgH and PrgK, multiple IM proteins (SpaP, SpaQ, SpaR, SpaS and InvA), an ATPase (InvC) and the OM secretin, InvG (Kubori et al., 1998, Kubori et al., 2000). From this secretin the needle complex formed by PrgI extends, with SipB and SipC forming a translocon at the needle end. When this translocon comes into contact with the wall of the small intestine, *Salmonella* effector proteins are translocated into the host cell cytosol or secreted directly into the intestinal milieu. Excreted effector proteins, including the Sip proteins, SopE and

SopB, induce changes to the cytoskeletal structure of the infected cell through manipulation of host cell machinery and activation of Rho GTPases, nuclear factor NF-$_K$B and AP-1 transcription factor (Hardt et al., 1998, Stender et al., 2000). SipA and SipC induce membrane ruffling through the bundling of actin fibres (McGhie et al., 2001, Zhou et al., 1999), a key process during *Salmonella* invasion of non-phagocytic epithelial cells (Srikanth et al., 2011). Once cellular invasion has occurred, the endocytosed bacteria survive within the *Salmonella* containing vacuole (SCV) where effectors, i.e. SptP and SspH1, function to maintain homeostasis. This is achieved through the reversal of the host cell membrane changes that occurred during invasion, preventing inflammatory mechanisms of the host cell (Fu and Galan, 1999, Galan and Zhou, 2000).

A second TTSS encoded by SPI-2 is important for survival and growth within the SCV and during the systemic phase of infection (Fields et al., 1986, Shea et al., 1996, Ochman et al., 1996, Cirillo et al., 1998, Karasova et al., 2010). Forest et al. (2010) report that SPI-2 is not required for the survival of *S*. Typhi inside macrophages, contradicting another studies where deletion of genes involved in SPI-2 and aromatic biosynthesis pathway (*ssaV* and *aroC*) in *S*. Typhi causes severe attenuation (Khan et al., 2003). The majority of research in other *S. enterica* serovars provides evidence of intracellular growth defects associated with mutations within SPI-2.

SPI-2 is absent from *S*. bongori, suggesting *S*. *enterica* acquired SPI-2 after these two species diverged (Ochman and Groisman, 1996). SPI-2 genes are only expressed upon entry into the host cell where they are induced by this low pH (4-5), low Mg^{2+} and low Ca^{2+} environment (Cirillo et al., 1998, Pfeifer et al., 1999). The global 2CST systems PhoPQ and EnvZ/OmpR, and SsrAB encoded within SPI-2, are positive regulators of SPI-2 genes under these conditions (Fass and Groisman, 2009, Cirillo et al., 1998). In the absence of these inducing signals, H-NS binds to SPI-2 preventing transcription (SPI-2 function and expression are reviewed by Figueira and Holden (2012) and Fass and Groisman (2009).

Some SPI-1 effectors remain after SCV formation and work in combination with SPI-2 effectors to manipulate the host's cytoskeletal components. For instance, in a murine model SopB persists for up to 12 hours post infection, aiding maintenance of the SCV and long-term systemic infection in mice (Lawley et al., 2006).

S. Typhimurium exhibits similar levels of attenuation when SPI-2 genes are deleted individually or in combination, suggesting cooperation of these effector proteins within the SCV and an equal contribution to intracellular survival and virulence (Jiang et al., 2004, Beuzon et al., 2000, Ruiz-Albert et al., 2002, Freeman et al., 2003, Knodler et al., 2003). There are currently 28 SPI-2 effector proteins known to be translocated across the phagosomal membrane into the host cell cytoplasm (Figueira and Holden, 2012). Within hours of internalisation within the SCV, SPI-2 TTSS secretes effectors SifA, SseF, SseG, SopD2 and PipB2 to promote *Salmonella*-induced filament (Sif) formation (Knodler and Steele-Mortimer, 2005, Stein et al., 1996, Jiang et al., 2004). Sif are long filamentous membrane structures that extend into the host cell, stabilising SCV formation and increasing its size to allow *Salmonella* replication within (Knodler et al., 2003, Garcia-del Portillo et al., 1993b, Haraga et al., 2008). A *sifA* deletion mutant is unable to form Sif, the vacuolar membrane surrounding these mutants is quickly lost and the Δ*sifA* mutant is released into the macrophage cytosol where it is killed (Beuzon et al., 2002, Beuzon et al., 2000). These results suggested SifA as an essential component of SCV integrity and may explain the severe attenuation of *sifA* deletion strains in mice (Brumell et al., 2001). However, Ruiz-Albert et al., (2002) showed strains unable to excrete SifA did not lose SCV integrity implying SifA is an important but not essential contributor to SCV maintenance (Beuzon et al., 2000). This was later confirmed through investigations into SseJ and SopD2 (Ruiz-Albert et al., 2002, Schroeder et al., 2010).

In addition to Sif formation, SPI-2 effector proteins also interfere with the host cell's immune signalling. SpvC conducts irreversible phosphate removal within the macrophage, inhibiting MAP kinase signal cascades and reducing

cytokine release from infected macrophages (Mazurkiewicz et al., 2008). Although a large number of other SPI-2 effectors have an uncharacterised function (e.g. SifB, PipB, SseK1, GtgE, SteABDE and CigR) the importance of SPI-2 as a whole in *Salmonella* virulence cannot be understated and investigations are continuing to fully elucidate the SPI-2s contribution to *Salmonella* intracellular survival (Figueira and Holden, 2012).

Typhoidal and NTS strains utilise SPI-1 and SPI-2 during invasion of the intestinal epithelium of the small intestine. However, these serovars differ in their subsequent course of infection (Liu et al., 1988). NTS strains remain at the epithelial layer causing: localised inflammation, the infiltration of polymorphonuclear leukocytes (PMNs) into the intestinal lumen and diarrhoea (Haraga et al., 2008). Typhoidal strains have the ability to spread to, and infect, multiple organ systems through the invasion and manipulation of macrophages. The ability of *S. enterica* strains to cause intestinal disease is directly correlated to their ability to recruit PMNs across cell monolayers without the need to invade epithelial cell layers, with *S.* Typhimurium recruiting the vast majority of neutrophils over the first 1-3 hours of infection (Coburn et al., 2007, McCormick et al., 1995). The established genetic and physiological differences between NTS strains and *S*. Typhi, which promote differential disease progression, are outlined below.

1.2.5 Genetic and physiological differences between typhoidal and non-typhoidal *Salmonella enterica* subspecies

S. Typhimurium and *S*. Typhi share approximately 90% of their genome, but the genetic differences preventing *S*. Typhimurium from causing typhoid fever in humans are still poorly understood (Sabbagh et al., 2010). These disparities could be due to differential regulation of shared genes; regulatory pathways may vary between these serovars and gene products may function differently (Barquist et al., 2013). Other differences may also reside within the 10% of genetic material not shared. Wain et al. (2014) highlight the importance of recent developments in large-scale transposon knockout libraries, a technology that can be used for assessing function at the genome level. This methodology could have huge potential for finding new drug and

vaccine targets via uncovering the genetic factors that differ between *S*. Typhi and other NTS strains (Langridge et al., 2009, Barquist et al., 2013, Wain et al., 2014, Sabbagh et al., 2010).

Host physiology may also influence *S*. Typhi and *S*. Typhimurium disease manifestation. Toll-like receptor 11 (TLR11) is present in the mouse intestine but is not expressed in humans (Roach et al., 2005) and recognises flagellin on the surface of *S*. Typhimurium (Mathur et al., 2012). *S*. Typhi is human-restricted and unable to establish infections in mice (Tsolis et al., 1999b). However, once orally dosed with *S*. Typhi, *tlr11*$^{-/-}$ mice become infected and *S*. Typhi disseminates to the gallbladder, liver, spleen and kidneys (Mathur et al., 2012). Mathur et al. (2012) also show successful vaccination of *tlr11*$^{-/-}$ against *S*. Typhi. Because of its host specificity, *S*. Typhi research has been hindered by the lack of a suitable animal model able to successfully reproduce the immunological features of human infection. *tlr11*$^{-/-}$ mice therefore represent a useful animal model not only for investigating the microbiology and immunology of *S*. Typhi infections, but an appropriate model for the development of future vaccines.

1.2.6 Emergence of invasive non-typhoidal *Salmonella* strains (iNTS)

Non-typhoidal serovars predominantly cause self-limiting gastroenteritis and salmonellosis; only rarely will cases present with bacteraemia (Laupland et al., 2010). However, with a fatality rate of 20-25% in children and up to 50% in HIV infected adults, invasive NTS (iNTS) strains are an emerging threat in sub-Saharan Africa (Kingsley et al., 2009, Vugia et al., 1993). Although this phenomenon has not yet been reported in Asia (Deen et al., 2012), typhoid fever presenting in patients with HIV was observed in HICs almost two decades ago (Manfredi et al., 1998).

iNTS strains predominately belong to *S*. Typhimurium and *S*. Enteritidis serovars. High incidence of malaria, malnutrition and HIV in sub-Saharan Africa has provided an 'ecological and immunological niche' for the evolution of a multidrug resistant (MDR) iNTS genotype of *S*. Typhimurium, ST313 (Feasey et al., 2012). Following genomic degradation, the acquisition of

pseudogenes and genetic deletions, ST313 is now genetically distinct from ST19, the most commonly found *S*. Typhimurium genotype worldwide (to which SL1344, used throughout this thesis, belongs) (Kingsley et al., 2009, Achtman et al., 2012). The newly emerging ST313 genotype is phagocytosed more efficiently and is highly resistant to killing in macrophages, allowing survival and replication within these immune cells (Ramachandran et al., 2015). ST313 therefore behaves in a more similar manner to *S*. Typhi and *S*. Paratyphi A/B/C. Once within intestinal macrophages, the infected host cells enter the bloodstream resulting in systemic spread of the bacteria: bacteraemia, septicaemia and meningitis (Ramachandran et al., 2015, de Jong et al., 2012).

1.3 Current treatments and disease prevention

Typhoid fever requires early treatment with antibiotics otherwise serious complications or death can result. The 'first line' antibiotics for treatment are chloramphenicol, ampicillin and trimethoprim/sulfamethoxazole. However, strains of *S*. Typhi and *S*. Paratyphi resistant to all three drugs have been present since the late 1980's (Parry et al., 2002, Brusch et al., 2015, Bhan et al., 2005). In addition to continued high numbers of enteric fever cases across LMICs, the presence of MDR strains poses a major problem for the future. Infections from MDR serovars are increasing rapidly in endemic regions, such as Asia and Africa, and in the UK due to infected returning travellers (Mirza et al., 1996, Mermin et al., 1999, Threlfall and Rowe, 1991). As a cost effective drug with minimal side effects, ciprofloxacin became a suitable alternative (Brusch et al., 2015). However, sporadic resistance to first-generation fluoroquinolones and cephalosporins is also on the rise (Capoor and Nair, 2010). Worryingly, patients who have been infected with fully or partially resistant strains experience more relapse incidents than non-resistant strains; even once the bacterial load has been cleared (Chau et al., 2007). This resistance prevalence increases mortality rates and treatment costs, posing a huge indirect economic burden as well as cost to life (Paterson and Maskell, 2010). The development of *S*. Typhi and *S*. Paratyphi vaccines is becoming ever more important if the health, social and economic impacts of enteric fever are to be reduced.

1.3.1 Current *Salmonella* vaccines

In addition to the emergence of MDR strains, the critical importance of developing new *Salmonella* vaccines and treatments is further emphasised by the fact that two typhoid vaccines currently available have an efficacy of ~60-70% (Fraser et al., 2007). There are also no licenced vaccines against paratyphoid or NTS serotypes available, although there is evidence to suggest typhoid fever vaccines do offer some cross-resistance to paratyphoid strains and common NTS strains (Nisini et al., 1993, D'Amelio et al., 1988, Wahid et al., 2014, Wahid et al., 2012, Pakkanen et al., 2012, Pakkanen et al., 2014, Tagliabue et al., 1986).

The first *S*. Typhi vaccine was developed in the 19th century and consisted of heat-inactivated, phenol preserved cells (Wright and Leishman, 1900, Ivanoff et al., 1994). Whole cell paratyphoid A and B vaccines, utilised by the military in the early 20th century, quickly followed (Ivanoff et al., 1994). Although effective in reducing disease, whole cell vaccines were highly reactogenic, producing high fever, headaches and malaise in vaccinated individuals and were discounted as a viable long-term method of immunisation against enteric fever (Ivanoff et al., 1994, Tennant and Levine, 2015). Orally administered, live attenuated vaccines are now widely regarded as the way forward. This approach offers long lasted efficiency, the ability to carry heterologous antigens and to induce mucosal, cellular and humeral immune responses while being well tolerated (Gamazo and Irache, 2007, Paterson and Maskell, 2010). They are also practical to administer to large populations, relatively cheap to produce and do not generate hazardous wastes (i.e. needles, syringes) that are difficult to handle and dispose of in the field (Pasetti et al., 2011, Mestecky et al., 2008).

Three typhoid fever vaccines are currently licenced for use: Ty21a (Vivotif®), an orally administered, live-attenuated vaccine (PaxVaxCorporation); the parenteral capsular Vi polysaccharide preparations (Vi) Typherix® (GSK) or Typhim Vi® (Sanofi Pasteur); and Typbar TCV®, Vi polysaccharide conjugated to tetanus toxoid (Bharat Biotech and Peda Typh™) (Pakkanen et al., 2015, Tennant and Levine, 2015). Ty21a also provides moderate

protection against *S*. Paratyphoid B (MacLennan et al., 2014), and Pakkanen et al. (2015) show that the former two vaccines can be administered simultaneously, resulting in an enhanced immune response to *S*. Typhi, *S*. Paratyphoid and NTS serotypes. This could offer additional protection to those in high-risk areas (Figure 2), but there are yet to be any licenced vaccines available for *Salmonella* serovars other than *S*. Typhi.

One vaccine candidate, the *S*. Typhi Ty2 Δ*aroC* Δ*ssaV* mutant strain ZH9, also called M01ZH09 and Typhella®, has passed phase I and phase II clinical trials where it was shown to be a safe, single dose vaccine that is well tolerated by adults and children in the UK, USA and Vietnam, a typhoid endemic country (Hindle et al., 2002, Kirkpatrick et al., 2005, Kirkpatrick et al., 2006, Lyon et al., 2010, Tran et al., 2010). Typhella® was acquired by the biopharmaceutical company Prokarium in 2012 and is yet to undertake stage III clinical trials. Instead, the company is using ZH9 as the typhoid component of its duel typhoid-ETEC diarrhoea vaccine Typhetec® alongside investigations for ZH9 use a vaccine delivery vector (Prokarium, 2015, Tennant and Levine, 2015).

Determining essential *Salmonella* virulence factors provides potential genetic targets for *S. enterica* vaccine development. Deletions of genes involved in the envelope stress responses (ESRs) of *S. enterica* serovars (*htrA*, *cpxR*, *clpXP*, described later in this work) have produced attenuated strains, which can be used in the design and development of new live vaccines for humans and animal reservoirs (Nandre et al., 2014, Tennant et al., 2011, Baumler et al., 1994, Johnson et al., 1991, Chatfield et al., 1992). Our understanding of how *S.* Typhi and *S.* Typhimurium perceive changes in host and external environments is not only crucial for our understanding of how these important pathogens survive and cause disease, but critical if we are going to reduce the significant impact of these pathogens on human health.

1.4 Bacterial stress responses

Organisms must possess the ability to sense and respond to their environment in order to survive. Universal mechanisms are utilised to recruit

a multifaceted response to environment fluctuations and the stresses they provoke. Studying microbial responses to these rapidly changing conditions could provide an insight into the stress response systems utilised across other forms of life, as well as pathogenic bacteria associated with foodborne infections, such as *E. coli* and *S. enterica* subspecies. Enteric pathogens are of particular interest due to the diverse range of conditions they encounter, both *in vivo* and in environmental reservoirs (Boor, 2006, McBroom and Kuehn, 2007) (Figure 3).

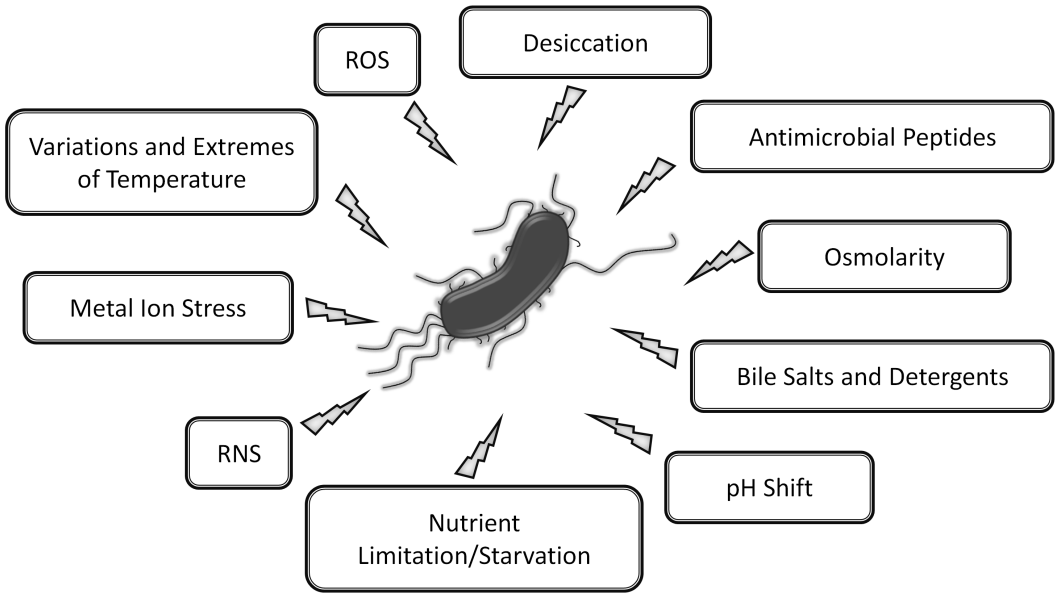

Figure 3: A cartoon depiction of the diverse chemical and physical stresses inflicted upon *Salmonella* in host and non-host environments. Taken from Runkel et al. (2013).

For the pathogen to survive, proliferate and infect host tissues, such stresses (Figure 3) need to be recognised and responded to. This huge range of insults have adverse impacts on bacterial physiology, including virulence, growth and antimicrobial resistance, often resulting in the inhibition and/or death of bacteria at an individual cell, and population level, if an appropriate stress response is not successfully launched (McMahon et al., 2007). Each consequence of stress requires a controlled regulatory response through

coordinated programs of gene expression and protein activity, involving alternative sigma factors and two-component signal transduction (2CST) systems. These responses provide resistance to a range of general stresses or in a stress-specific manner, affording the bacteria an adaptive advantage in each new host environment. Organisms that maintain this advantage are subsequently able to evade, endure or manipulate innate immune effectors and cause persistent infections. This results in a continued recognition of microbial signal molecules and leads to the signs and symptoms of disease (Ohl and Miller, 2001).

1.5 Envelope stress response

In contrast to Gram-positive bacteria, the envelope of Gram-negatives contains two lipid bilayers: an inner (or cytoplasmic) membrane (IM) and an outer membrane (OM), separated by a periplasmic space. The periplasm contains a thin peptidoglycan layer that maintains structural integrity and rigidity. The periplasm of *E. coli* has a diffusion coefficient significantly lower (100-fold) than that of the cytoplasm, due to a rise in protein density and subsequent increase in viscosity (Brass et al., 1986). The oxidising nature of the periplasm provides conditions where proteins can be stabilised by disulphide bonds (S-S) (Merdanovic et al., 2011), an environment that differs greatly to aqueous solutions used *in vitro*, including the lack of ATP.

Proteins of the OM and periplasm must be translocated across the IM by two pathways: the classical secretion system, Sec, and the Twin arginine translocation system (TAT) (Merdanovic et al., 2011). If these translocated proteins become damaged by environmental stresses at any point during their production or translocation, they are either: repaired, degraded by periplasmic proteases or, as a last resort, aggregated. Protein aggregation can hinder cell membrane integrity and cause a physical obstruction within the periplasmic space; it is therefore avoided wherever possible. Disruption to envelope homeostasis induces tightly regulated, coordinated transduction mechanisms, known collectively as the envelope stress responses (ESRs). Consisting of at least five complementary extracytoplasmic pathways each ESR has a role in maintaining envelope integrity; the alternative sigma factor

RpoE (σ^E) responds to misfolded OM proteins, the Cpx pathway monitors cell surface assembly, the phage shock proteins (PspABCDEF) detect disruption to the proton motive force, the Bae pathway protects against antimicrobial agents, while the RcsCDB phosphorelay system is activated in response to peptidoglycan stress and contributes to intrinsic antibiotic resistance. Although each has a defined role (only briefly highlighted above) cross talk between these pathways forms an important network in the response to stress. These pathways overlap at numerous phases; including the inducing signals which stimulate activity of regulon members. A summary of these ESRs is shown in Figure 4 and each ESR is described in detail below.

1.6 The extracytoplasmic function sigma factor: sigma E (σ^E)

1.6.1 Extracytoplasmic sigma factors

Alterations in gene expression at a transcriptional level are fundamentally controlled by interactions of sigma factors with the catalytic core of RNA polymerase (RNAP) (Borukhov and Nudler, 2003). Extracytoplasmic function (ECF) sigma factors, a family of alternative sigma factors, were originally recognised in *Streptomyces coelicolor* and are so called as they regulate function outside of the cytoplasm (Lonetto et al., 1994, Missiakas and Raina, 1998). The ECF class of sigma factors share common features. They are often co-transcribed with a transmembrane anti-sigma factor, recognise promoter elements containing an 'AAC' codon at the -35 region, and control cell envelope functions, such as secretion, transport and extracytoplasmic stress (Helmann, 2002). ECF sigma factors are much smaller than other sigma factors (20 to 25 kDa), they differ in structure to core sigma factors at region 2 (responsible for binding to RNAP and -10 recognition) and in the recognition helix of their helix-turn-helix motif (required for -35 recognition) (Lonetto et al., 1994, Raivio and Silhavy, 2001). Because of these differences, it is region 2 that is believed to dictate promoter specificity between ECF sigma factors (Lonetto et al., 1994).

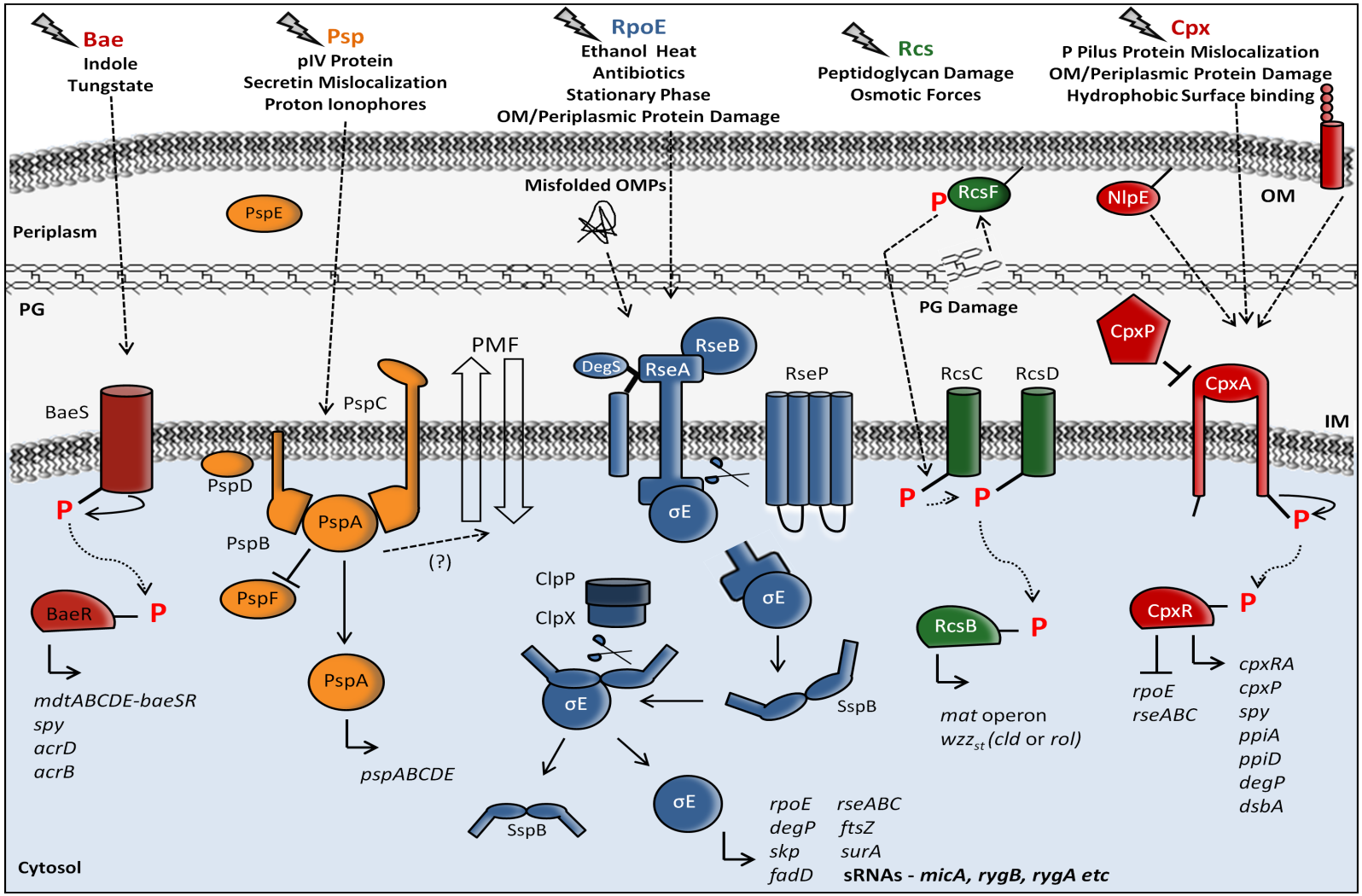

Figure 4: Diagrammatic representation of the five main ESRs, their inducing cues, pathway components and examples of the genes they regulate. Stress signals are shown as dashed arrows. The movement of phosphate (P) is represented as dotted arrows. The movement/release of proteins are shown by solid arrows. Cleavage events are represented by scissors. Taken from Runkel et al. (2013).

The use of a cognate membrane-bound anti-sigma factor enables ECF sigma factors to detect extracytoplasmic inducing cues (Raivio and Silhavy, 2001). In the absence of an inducing cue the ECF sigma factor is bound to an anti-sigma factor at the IM, preventing association with RNAP core enzyme. This association will only occur in the presence of an inducer. The inducing cue disrupts the sigma binding activity of the anti-sigma factor and the ECF sigma factor is released. Association with RNAP can now occur allowing DNA binding and transcription initiation.

1.6.2 Sigma E - RpoE

RpoE (sigma E, σ^E) is one of the most studied ECF sigma factors. Since its discovery in *E. coli* (Erickson and Gross, 1989), σ^E has become the best characterised of the ESRs and is responsible for the regulation of a number of genes in *E. coli* and *Salmonella* spp. (Rowley et al., 2006, Skovierova et al., 2006) (Appendix B, Table B1). There are, however, significant differences between the function of this sigma factor in these organisms. In *E. coli* σ^E is an essential sigma factor (De Las Penas et al., 1997). However, this is not the case in *Salmonella*. Deletion of *rpoE* negatively impacts *Salmonella* virulence, with RpoE essential for survival during invasion of macrophages *in vitro* and in host tissue *in vivo* (Humphreys et al., 1999). *S*. Typhimurium Δ*rpoE* strains also present increased sensitivity to antimicrobial peptides (AMPs), acid and oxidative stress (Humphreys et al., 1999, Crouch et al., 2005, Testerman et al., 2002, Muller et al., 2009, Bang et al., 2005). Because of the differences in *E. coli* and *Salmonella* Δ*rpoE* phenotypes, it is unsurprising that *rpoE* regulation differs in these organisms (Figure 5). Although the *rpoE* operons of *E. coli* and *Salmonella* are similar in their organisation, three promoters are located upstream of *rpoE* in *S*. Typhimurium (*rpoEp1*, *rpoEp2* and *rpoEp3*) with two promoters present in *E. coli* (P1 and P2) (Miticka et al., 2003). Miticka et al. (2003) highlighted the inducing conditions of σ^E in *S*. Typhimurium and confirmed σ^E involvement in carbon starvation, cold shock, and repression of *rpoE* by another ESR system, CpxAR (discussed later). Cold shock was the greatest inducer of

rpoEp3 expression and produced the greatest contrast to results obtained in *E. coli* (Dartigalongue et al., 2001).

The signalling pathway for σ^E has been well characterised in *E. coli*. Under non-inducing conditions, σ^E is bound to the IM spanning anti-sigma factor, RseA, covering its RNAP binding domain and preventing σ^E/RNAP interactions. The presence of misfolded OM proteins (OMPs) activates cleavage of RseA by DegS, an IM anchored serine protease, and YaeL, a zinc metalloprotease (Alba and Gross, 2004). Under non-stress conditions, DegS is inactive due to auto-inhibition. During stress, DegS recognises the exposed C-termini of mis-localised and misfolded OMPs and cleaves RseA to a truncated form at the periplasmic C-terminus. YaeL then releases the RseA/σ^E complex from the membrane and cleaves RseA at its transmembrane segment. σ^E is finally released into the cytoplasm by proteases, such as ClpX, which subsequently degrade this anti-sigma factor (Figure 4). This release allows binding of σ^E to RNAP and σ^E mediated gene transcription can now occur (De Las Penas et al., 1997, Dartigalongue et al., 2001, Skovierova et al., 2006). Such defined regulation is a commonly adopted mechanism by ECF sigma factors, allowing the organism to activate specific regulatory systems only in response to defined signals.

1.6.3 The σ^E regulon of *Salmonella*

The σ^E regulon of *E. coli* has been extensively studied and is still growing. Regulon members include genes and sRNAs involved in primary metabolism, sensory function, OMP assembly, phospholipid and LPS biogenesis and modification, protein folding, biofilm formation and genes of unknown function (Li et al., 2015a, Rowley et al., 2006, Kabir et al., 2005, Dartigalongue et al., 2001, Rhodius et al., 2006, Rezuchova et al., 2003, Chassaing and Darfeuille-Michaud, 2013). Characterisation of the *Salmonella* σ^E regulon is essential for understanding the differences in *E. coli* and *S.* Typhimurium Δ*rpoE* phenotypes, and the critical contribution σ^E makes to *Salmonella* virulence. When compared with other regulators important for *Salmonella* virulence (i.e. *rpoS*, *slyA*, *ssrAB* etc.) an *rpoE*

mutant exhibits the greatest sensitivity to the intracellular environment (Li et al., 2015b). Because *S*. Typhimurium Δ*rpoE* strains are attenuated, the σ^E regulon of *Salmonella* could contain important targets for the potential development and design of new *S*. Typhi, *S*. Paratyphi and NTS vaccines.

Skovierova et al. (2006) were the first to decribe the σ^E regulon in *Salmonella*, utilising a two-plasmid system developed by Rezuchova et al. (2003) in *E. coli* to locate promoters that recognised RNAP bound to σ^E. This group discovered 62 genes directly regulated by σ^E in *S*. Typhimurium, with 39 orthologues previously identified as members of the σ^E regulon in *E. coli* (Appendix B, Table B1). The remaining 23 genes were newly identified σ^E regulon members specific to *S*. Typhimurium (*ptr*, *recD*, *tolR*, *oppA*BCDF, *stm1741*, *eno*, *yggT*, *yggU*, *yggW*, *yjfO*, *yjfN*, *yiaD*, *dedD*, *ydcG*, *yfeK*, *yfeL*, *stm1250*, *stm1251*). Of the σ^E-regulated genes identified by Skovierova et al. (2006), several were important for *Salmonella* cell envelope integrity (*tol-pal* gene cluster, *ptr* periplasmic protease III), DNA repair and recombination (*ptr* is co-transcribed with *recC* and *recBD genes*) and assembly of proteins at the OM (*bamA* and *bamD*) The latter two were new cellular functions that had not been connected with the σ^E regulon in any organism prior to this study. All genes identified by Skovierova et al. (2006), and all other σ^E regulon members (genes with a σ^E binding site identified or regulation by σ^E experimentally shown) are listed in Table B1.

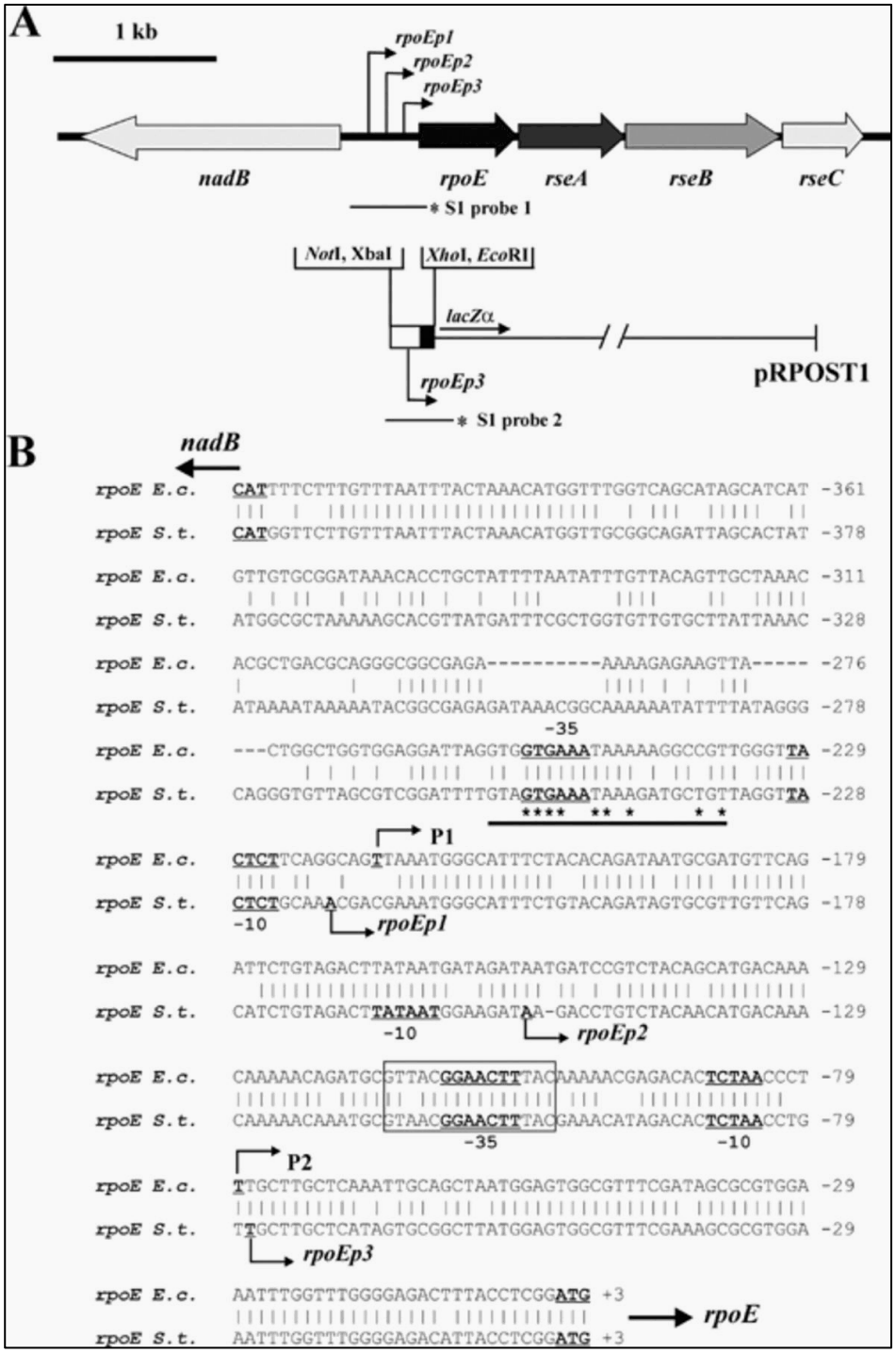

Figure 5: Genetic organisation of the *S.* Typhimurium *rpoE* operon (A) and comparison of the *E. coli* and *S.* Typhimurium *rpoE* promoter regions (B). A) Bent arrows denote the positions of *rpoE* promoters. Lines below the maps and open box indicates DNA fragments (5′-labelled at the end marked with an asterisk) used as probes in S1-nuclease mapping experiments and the position of a 240-bp fragment (comprising the *rpoE*-dependent *rpoEp3* promoter) in plasmid pRPOST1 in Miticka et al. (2003). Relevant restriction sites are indicated. B) Bent arrows indicate transcription start point (TSP) of *rpoE* promoters. The −10 and −35 boxes and initiation codons of *nadB* and *rpoE* are bold and underlined. CpxR recognition sequence (De Wulf et al., 2002) is indicated by a box around the sequence. Thick line below the sequence denotes the putative cAMP-CRP binding site (Kolb et al., 1993). Asterisks denote positions identical with the consensus sequence. Numbers refer to nucleotide position upstream of *rpoE* ATG codon with A as +1. Nucleotide sequences are parts of the overlapping sections deposited in GenBank/EMBL/DDJB databases under accession numbers AE000343 and AE000344 for *E. coli* K12 MG1655, AE008819 and AE008820 for *S.* Typhimurium LT2. Taken from Miticka et al. (2003).

1.6.3.1 The σ^E regulon and virulence

σ^E is associated with the virulence of a variety of human pathogens, *Vibrio* sp., *Proteus* sp., *Staphylococcus* sp., *Yersinia* sp, and *Streptococcus* sp., as well as *Salmonella* (Brown and Gulig, 2009, Liu et al., 2015, Weiss et al., 2014, Heusipp et al., 2003, Jones et al., 2003, Kovacikova and Skorupski, 2002). One study in adherent-invasive *E. coli* (AIEC) (strain LF82) showed crucial σ^E involvement in regulating adhesion, invasion and biofilm formation in this strain, but not in the non-pathogenic model organism *E. coli* K12, MG1655 (Chassaing and Darfeuille-Michaud, 2013). AIEC colonise ileal lesions in Crohn's disease patients, where the bacteria invade intestinal epithelial cells (IEC) and macrophages, resulting in disease. The σ^E regulon was defined in AIEC following this discovery and was shown to control AIEC-IEC interactions and biofilm formation through the regulation of 12 genes, specifically *waaWVL* (Chassaing et al., 2015) (Table B1).

Deletion of *rpoE* significantly reduces the ability of *S*. Typhimurium to cause disease in mice, regardless of the method of infection (oral, intravenous or intraperitoneal) (Humphreys et al., 1999, Crouch et al., 2005, Testerman et al., 2002). Δ*rpoE* mutants are more sensitive to oxidative stress and AMPs than their isogenic parent strain and are unable to survive AMP and reactive oxygen species (ROS) attack from the host immune system (Crouch et al., 2005). Li et al. (2015b) conducted a broad scale microarray analysis of σ^E-regulated genes in *S*. Typhimurium when cultured in rich and acid minimal media (LBM) at different stages of growth (log, 4 hours, 20 hours). These conditions replicate those of intracellular growth and a summary of σ^E-regulated genes in *S*. Typhimurium from this study are shown in Table B2.

One set of *Salmonella* virulence genes included within the *S*. Typhimurium σ^E regulon is SPI-2 (Osborne and Coombes, 2009, Yoon et al., 2009, Li et al., 2015b). σ^E up-regulates SPI-2 expression in *S*. Typhimurium ATCC 14028s by increasing transcription of the SPI-2 regulator *ssrB*, under conditions that mimic the early stages of infection (LPM, 4 hours) (Li et al., 2015b). Li et al. (2015b) observed σ^E-mediated up-regulation of SPI-2 during conditions that simulate late stages of infection (LPM 20 hours). This was a

result of down-regulation of the SPI-2 repressor H-NS, counteracting the silencing of H-NS on SPI-2 genes. In support of these data, Osborne and Coombes (2009) showed fine-tuning by σ^E of a subset of SsrB-regulated virulence genes (*sseB*, *sseG*, *sseL*, *sifA*, *srfN*) (Table B1). Both studies therefore provide additional evidence to explain the reduced viability of *rpoE* deletion mutants within macrophages (Humphreys et al., 1999, Yoon et al., 2009). When *rpoE* is absent, bacteria are unable to regulate the environment within the SCV, reducing intracellular replication and leaving an already AMP and ROS sensitive mutant further exposed to these threats within the host cell.

In *S*. Typhi, σ^S (RpoS/σ^{38}) and σ^E are important for a coordinated response to hyperosmotic shock (Du et al., 2011b). σ^S is another alternative sigma factor, which like σ^E is induced during times of stress and is also required for *S*. Typhimurium virulence (Coynault et al., 1996, Nickerson and Curtiss, 1997). Osmotic shock is an important stress response for understanding *Salmonella* pathogenicity because enteric pathogens are exposed to high osmolarity in the lumen of the host intestine (~300 nM NaCl) compared to contaminated food or water (~50 nM) (Huang et al., 2007a, Du et al., 2011b). Although genes responding to osmotic shock are independently regulated by σ^S and σ^E (Miticka et al., 2003, Hengge-Aronis, 1996, Balaji et al., 2005), co-regulation by σ^S and σ^E had not previously been investigated. A total of 38 σ^S and σ^E co-regulated genes were highlighted by Du et al. (2011b), approximately half of which were hypothetical proteins. Of the genes of known or putative function, genes involved in the successful invasion of the host epithelium (*osmB*, *osmC*, *osmY* and *otsBC*) and cellular metabolism (*nar*-, *gln*- and *ugp*- operons) were present. This group also provide evidence to suggest the possible regulation of flagella by σ^E in *S*. Typhi during hyperosmotic stress (Du et al., 2011a). Many of these genes have previously been assigned to the σ^S or σ^E regulon (Table B1), confirming the significant overlap of σ^S and σ^E regulation in *S*. Typhi during hyperosmotic stress (Du et al., 2011b).

1.6.4 Effect of σ^E on post-transcriptional regulation

Li et al. (2015a) estimated that approximately 58% of the *S*. Typhimurium genome could be σ^E regulated (under three growth conditions tested), with an even distribution of σ^E up-regulated and σ^E down-regulated genes. This study states that as association of RNAP/σ^E with the promoter region of genes generally results in the 'switching on' of expression (direct regulation), no direct interaction of σ^E and the promoter regions of down-regulated genes would occur. Regulation of σ^E down-regulated genes would therefore result from post-translational events, either through the interaction of σ^E with sRNAs and/or indirect regulation of these genes by an array of other regulators within the σ^E regulon (Li et al., 2015a).

Genome wide analysis in *E. coli* and *Salmonella* has identified approximately 80-100 sRNAs in these species (Gottesman, 2004). Although the role of a large number remains unknown, sRNAs that have been characterised are involved in a huge array of functions (Runkel et al., 2013). Within the σ^E regulon are sRNAs involved in reducing protein aggregation through the degradation of mRNAs. RygB and MicA (SraD) are strictly controlled by σ^E (Johansen et al., 2006). These RNAs bind to the RNA chaperone Hfq to form a complex that subsequently interacts with unstable porin mRNAs (OmpA, OmpC and OmpF) to facilitate their remodelling (Runkel et al., 2013, Sugawara and Nikaido, 1992, Sugawara and Nikaido, 1994, Prehna et al., 2012). In 2014 a third σ^E regulated sRNA was identified called MicL (Guo et al., 2014). This sRNA is also involved in combating membrane stress by repressing the synthesis of OMPs to restore envelope homeostasis (Guo et al., 2014). The overexpression of porins is a well-established inducer of the σ^E ESR because of their accumulation within the periplasm. Removing excess porins through the use of sRNAs allows fine-tuning of porin levels within the envelope and alleviates said inducing signal and stress (Douchin et al., 2006, Kroger et al., 2012).

1.6.5 The β-barrel assembly machinery (BAM) complex and σ^E

The β-barrel assembly machinery (BAM) complex (BamABCDE) is responsible for the folding and insertion of OMP into the OM (Werner and

Misra, 2005, Wu et al., 2005, Doerrler and Raetz, 2005, Malinverni et al., 2006). BamA (YaeT) is an OM protein, which forms the core component of the BAM complex. The lipoproteins BamB (YfgL), BamC (NlpB), BamD (YfiO) and BamE (SmpA) are coupled to BamA and anchored at the periplasmic face of the OM (Wu et al., 2005). Homologues of the BAM complex are present across α-, β- and γ-proteobacteria (Wu et al., 2005) and all *bam* genes are regulated by σ^E in S*almonella* and *E. coli* (Rhodius et al., 2006, Skovierova et al., 2006).

Following synthesis in the cytoplasm, proteins destined for the OM must pass across the IM and through the periplasm before folding and insertion can occur (Merdanovic et al., 2011). This is a highly regulated and controlled process and upon entry into the periplasm, the nascent OMP associates with a number of periplasmic chaperones; including Skp, HtrA (DegP) and SurA, all of which belong to the *Salmonella* σ^E regulon (Knowles et al., 2009, Lewis et al., 2009, Dartigalongue et al., 2001). HtrA, a protease involved in the activation of the σ^E pathway, has chaperone activity at low temperatures and all three Skp, HtrA and SurA chaperones are required for maintenance of envelope homeostasis (Strauch and Beckwith, 1988, Dartigalongue et al., 2001). In the presence of negatively charged phospholipids, Skp binds specifically to numerous OMPs (e.g. OmpA, OmpC, OmpF and LamB) and SurA binds multiple OMPs through high affinity binding to aromatic amino acids present in these proteins (Chen and Henning, 1996, Bitto and McKay, 2003, Qu et al., 2009, Patel et al., 2009, Hennecke et al., 2005, Merdanovic et al., 2011). Single and double knockout mutants of the genes encoding Skp, HtrA and SurA highlight their importance. Inactivation of Skp significantly attenuates *S.* Typhimurium during infection of mice (Rowley et al., 2011), but no affect of *skp* deletion was observed during growth under stress *in vitro*, suggesting a role for this chaperone in the mammalian host environment. Although null mutations of *skp*, *htrA* and *surA* in *E. coli* are viable, double mutations of *htrA* and *skp* are lethal due to aggregated proteins accumulating in the periplasm (Chen and Henning, 1996, Schafer et al., 1999), and *surA* and *skp* double mutants result in reduced OMP levels (Rizzitello et al., 2001).

The *smpA* gene in *S.* Typhimurium, encoding BamE, has two promoters: the distal promoter (*smpAp1*) is regulated by σ^E whereas the proximal promoter (*smpAp2*) is not (Lewis et al., 2008). *smpAp2* is, however, only conserved across the Enterobacteriales order. Lewis et al., (2009) observed significant attenuation of *smpA* deletion strains in a murine model following oral and parenteral infection. Unlike *rpoE* mutants, this deletion strain does not have reduced replication within macrophages *in vitro*. Mutations in genes encoding BAM complex proteins may therefore produce good live vaccine candidates due to this attenuation. Deletion of the HtrA chaperone also results in reduced *Salmonella* virulence and is discussed below.

1.6.6 HtrA (DegP)

HtrA (DegP) belongs to the HtrA family of PDZ-domain containing proteases, containing two PDZ domains and a trypsin-like protease domain. *htrA* was the first σ^E-regulated gene identified as important for *S.* Typhimurium virulence (Johnson et al., 1991, Baumler et al., 1994). HtrA is the only protease identified as a heat shock protein that is also involved in the degradation of misfolded proteins (Miot and Betton, 2004, Strozen et al., 2005), shown by the requirement of HtrA in *E. coli* for surviving temperatures higher than 42°C (Lipinska et al., 1989, Erickson and Gross, 1989). Although not an essential protein in *S.* Typhimurium, *htrA* deletion mutants do show reduced replication and survival within macrophages (Baumler et al., 1994), increased sensitivity to killing by ROS (Johnson et al., 1991) and are highly attenuated in a murine model of *Salmonella* infection (Humphreys et al., 1999, Chatfield et al., 1992). These different roles for HtrA in *E. coli* and *S.* Typhimurium are unsurprising given the fact they are under the control of different promoters. In *E. coli* a single, σ^E dependent promoter governs *htrA*, whereas three promoters: *htrAp1, htrAp2* and *htrAp3*, have been identified in *S*. Typhimurium (Lewis et al., 2009). Both *htrAp1* and *htrAp2* are believed to be under the control of the principle sigma factor σ^{70}, but only *htrAp3* is σ^E dependent. Expression of this protein is also up regulated upon the induction of the Cpx-response systems (Kim et al., 2011, Raffa and Raivio, 2002) and overexpression of the lipoproteins NlpE and YafY (Miyadai et al., 2004).

Muller et al. (2009) demonstrated σ^E activation in *S.* Typhimurium in response to acid stress. This occurs independently of HtrA or the unfolded OMP signal, although it requires processing of RseA by YaeL. qRT-PCR analysis monitored the relative expression levels of four, σ^E mediated genes, *fkpA*, *rpoH*, *surA* and *rpoE* (Muller et al., 2009). FkpA, like SurA, is a peptidyl-prolyl isomerase that functions in the periplasm as a protein folding catalyst and *rpoH* encodes a heat shock sigma factor. All of these σ^E-regulated genes were induced significantly in WT *Salmonella* at pH 4.5 (Muller et al., 2009). These results concur with the findings of Rowley and colleagues (2005) who had previously showed that an *rpoE* mutant strain is less virulent than a *degS* mutant, suggesting σ^E activation through a different mechanism during *Salmonella*-host interactions (Rowley et al., 2005). Although *Salmonella* encounter low pH during passage through the stomach, pH 4-5 is also encountered inside the SCV, triggering the expression of virulence genes required for intracellular survival (Rathman et al., 1996, Alpuche Aranda et al., 1992).

1.6.7 CpxAR and σ^E

The *rpoEp3* promoter is essential for *rpoE* expression under σ^E inducing conditions and in the *S.* Typhimurium *cpxA** strain where induction of this promoter occurred at similar levels to that in the *rpoE* mutant (Humphreys et al., 2004). It was suggested by Humphreys et al. (2004) that reduced *cpxA** virulence may result from *rpoE* repression. Mutations in both CpxAR and σ^E pathways affect *Salmonella* virulence and infection differently: CpxA* strains are able to survive within macrophages, while *rpoE* deletion strains cannot, and CpxA* strains have reduced adherence to eukaryotic cells, whereas *rpoE* mutant strains do not.

1.7 The Cpx pathway

One of the best-studied examples of a two-component signal transduction (2CST) system is the Cpx pathway. As the most prevalent signalling pathways in nature, and the most common method used by bacteria to assess their environments, 2CST systems are fundamental to understanding bacterial adaptation and how pathogenic bacteria respond and adapt to

environmental stresses (Stock et al., 2000). Two other 2CST systems are also ESRs, the BaeSR and ZraSR pathways, discussed later.

1.7.1 Two-component signal transduction (2CST) systems

As well an IM, periplasm and OM, the cell envelopes of Gram-negative bacteria also contain a vast number of exposed surface structures, such as porins, flagella, adhesins and secretion systems. These are composed of numerous protein subunits, all of which need to be tightly regulated during synthesis, folding and export to ensure final protein assembly occurs correctly (Ruiz et al., 2009, Thanassi et al., 2012). Such appendages are so important that they are recognised as potential targets for live vaccine development and multiple biotechnological applications (Steadman et al., 2014, Nicolay et al., 2015). It is essential that any damage occurring to the cell envelope is recognised and dealt with efficiently to ensure bacterial survival; aided by the contribution of 2CST systems. These signalling pathways consist of a histidine sensor kinase (HK), typically located in the IM, and a partner cytoplasmic response regulator (RR) (Capra and Laub, 2012, Gao and Stock, 2009, MacRitchie et al., 2008a). However, it is also recognised that auxiliary sensing proteins assist the various domains of HK and RRs in integrating a number of inducing signals (Buelow and Raivio, 2010).

1.7.2 Cpx-envelope response

The CpxAR 2CST system comprises of the HK CpxA, the RR CpxR and a periplasmic accessory protein, CpxP (Rainwater and Silverman, 1990, Danese et al., 1995, Weber and Silverman, 1988, Raivio and Silhavy, 2001, Otto and Silhavy, 2002, MacRitchie et al., 2008a). CpxA was originally identified as a sensor protein during sequence analysis in *E. coli* (Nixon et al., 1986). The product of *cpxR*, situated immediately upstream of *cpxA*, was subsequently confirmed as its cognate RR (Dong et al., 1993, Raivio and Silhavy, 1997), establishing CpxAR as a 2CST pathway.

A three-stage cascade of phosphorylation events controls the functional state of the Cpx system. Firstly, envelope stress generates a signal perceived at,

and transduced across, the OM. This activates autophosphorylation of CpxA at a conserved histidine residue and the phosphate group is subsequently transferred to a conserved aspartate residue of CpxR, in a process called transphosphorylation. This active form of CpxR (CpxR-P) can now bind to targeted regions of DNA, initiating Cpx mediated transcription. The Cpx regulon members consequently ameliorate the envelope stress by degrading and refolding damaged and misfolded proteins, maintaining envelope homeostasis. Finally, dephosphorylation of the RR occurs to return the system to its pre-induced state (Gao and Stock, 2009, Rowley et al., 2006, Hunke et al., 2012).

CpxP belongs to the Cpx regulon, acting as a negative regulator of the Cpx pathway. This was demonstrated through the overproduction of periplasmic localised CpxP, resulting in down-regulation of the Cpx signalling cascade (Raivio and Silhavy, 1999). Although a repressor of the Cpx pathway, induction of *cpxAR* can occur in the presence and absence of CpxP and another accessory protein, new lipoprotein E (NlpE) (DiGiuseppe and Silhavy, 2003, Hunke et al., 2012). New lipoprotein E (NlpE) is an OM lipoprotein involved in the activation of Cpx ESR in response to adhesion to hydrophobic surfaces (Otto and Silhavy, 2002). NlpE is discussed in more detail during the introduction to Chapter 3.

CpxP and CpxA form a structural dimer due to polar bond interactions, blocking the sensor domain of CpxA and preventing signal induction, referred to as CpxP-mediated Cpx inhibition (Tschauner et al., 2014). Environmental stresses (e.g. alkaline pH and high salt concentrations) disrupt these bonds, causing a conformational change in CpxP and dissociation from CpxA. Competition with CpxP from misfolded P-pili subunits and other misfolded PPs also leads to dissociation and breakdown of the CpxP-CpxA complex (Isaac et al., 2005, Zhou et al., 2011, Hunke et al., 2012). Once dissociated, the SK domain of CpxA is exposed and a phosphorylation cascade initiated. CpxP-mediated repression of the Cpx pathway is also alleviated by the degradation of CpxP by another periplasmic protein, HtrA. Degradation by HtrA is an important component of the Cpx response as an *htrA* mutant

renders the Cpx response partially inactive (Buelow and Raivio, 2005). As previously described this protease has chaperone activity, is involved in activation of the σ^E ESR and is essential for the heat shock response in *E. coli*. However, the Cpx response can be initiated in the absence of *htrA*, and this protease is not essential for Cpx activation.

The contribution of the Cpx pathway to pathogenicity, antibiotic resistance, biofilm formation and the CpxP family of molecular chaperones is detailed below. The contribution of the Cpx ESR to copper stress in *Salmonella* spp. and our current understanding of the Cpx regulon are discussed within the introduction to Chapter 3 (3.1.2 and 3.1.4) and will therefore not be discussed here.

1.7.3 Cpx and pathogenesis

The Cpx signal transduction system has been linked to pathogenesis of several Gram-negative pathogens (Table 1). Humphreys et al. (2004) provided evidence supporting direct involvement of this ESR in *Salmonella* virulence. Although null mutations in *S.* Typhimurium *cpxR* and *cpxA* did not reduce attachment or internalisation of eukaryotic cells, constitutive expression of the Cpx pathway (*cpxA** mutation) does (Humphreys et al., 2004). These results concur with numerous studies in *E. coli*, highlighting the importance of a functional Cpx pathway for adhesion to inanimate surfaces (Otto and Silhavy, 2002). However, the specific adhesion factor affected was not determined in this instance (Humphreys et al., 2004).

The Cpx response promotes virulence in uropathogenic *E. coli* (UPEC), with the loss of CpxAR significantly hindering localised and systemic infection in zebra fish, and the ability of UPEC to colonise the murine bladder (Debnath et al., 2013). CpxAR is also essential for virulence of the murine intestinal pathogen *Citrobacter rodentium*, used as a model for enteropathogenic *E. coli* (EPEC) and enterohaemorrhagic (EHEC) *E. coli* (Thomassin et al., 2015). CpxAR is the first 2CST system associated with pathogenicity in this species, with expression levels increasing during the early stages of infection.

However, there is evidence that the Cpx response both promotes and inhibits virulence in EPEC (Vogt and Raivio, 2012) (Table 1). A *cpxR* deletion mutant of the human isolate EPEC O127:H6 has diminished levels of bundle-forming pili and severely reduced adherence to epithelial cells *in vitro* (Nevesinjac and Raivio, 2005). However, inhibition of bundle-forming pili expression also occurred following activation of the Cpx response, along with inhibition of motility and type III secretion (Vogt et al., 2010, MacRitchie et al., 2008b, Vogt and Raivio, 2012). These latter results are surprising given the need for a functional Cpx response during attachment to host cells in EPEC and other pathogens (Nevesinjac and Raivio, 2005, Debnath et al., 2013) and investigations into the attachment of Cpx mutants to host cells *in vivo* is required to specify the influence of Cpx on EPEC virulence. EPEC is not the only organism where Cpx acts positively and negatively on virulence. The regulation of several *Legionella pneumophila* secreted substrates is ambiguous following CpxR expression (Table 1). Combined these results from EPEC and *L. pneumophila* do suggest Cpx involvement in regulation of virulence in these organisms, possibly through multiple pathways under a variety of growth conditions and further investigations are needed to establish the exact level of Cpx regulation on Pili formation in EPEC and Icm/Dot type IV secretion system components in *L. pneumophila*.

1.7.4 Cpx and antibiotics

There is paradoxical evidence for the role of Cpx in response to antibiotics, especially aminoglycoside antibiotics and small toxic molecules, such as hydroxyl urea (HU). Aminoglycosides, for example gentamicin, amikacin and kanamycin, directly target the 30S subunit of the ribosome and cause mistranslation through tRNA mismatching and the production of misfolded and misfunctioning proteins (Davis, 1987, Weisblum and Davies, 1968). The exact means of aminoglycoside mediated cell death has long been enigmatic.

Table 1: **Virulence phenotypes associated with Cpx mutants**. *Organisms where Cpx has both a positive and negative effect on virulence. Adapted from Vogt and Raivio (2012).

Organism	Virulence Phenotype	Reference
Cpx response promotes virulence		
EPEC*	*cpxR* null mutant has decreased elaboration of bundle-forming pilus and decreased adherence to cultured cells	(Nevesinjac and Raivio, 2005)
UPEC	*cpxAR* deletion reduces localised and systemic infection in zebra fish and colonisation of the murine bladder	(Debnath et al., 2013)
Citrobacter rodentium	CpxAR essential for *in vivo* virulence; severely reduced morbidity of mice when infected with Δ*cpxAR*	(Thomassin et al., 2015)
Shigella spp.	*cpxR* null mutation abolishes expression of TTSS transcriptional regulator VirF; *cpxA* deletion post-transcriptionally reduces expression of InvE regulator	(Nakayama and Watanabe, 1995, Mitobe et al., 2005)
*Legionella pneumophila**	CpxR directly activates expression of several Icm/Dot type IV secretion system components, as well as some secreted substrates	(Gal-Mor and Segal, 2003, Vincent et al., 2006, Altman and Segal, 2008)
Xenorhabdus nematophila	*cpxR* mutant has reduced virulence in the insect host *Manduca sexta*, likely related to its decreased growth rate in insecta, increased stimulation of antimicrobial peptide production and reduced expression of the pathogenesis regulator LrhA	(Herbert et al., 2007, Herbert Tran and Goodrich-Blair, 2009)
Cpx response inhibits virulence		
EPEC*	Activation of Cpx response inhibits bundle-forming pilus expression, type III secretion and motility	(MacRitchie et al., 2008b, Vogt et al., 2010, Vogt and Raivio, 2012)
Salmonella enterica serovar Typhimurium	*cpxA** constitutively active mutation inhibits adherence to cultured cells and reduces virulence in mice	(Humphreys et al., 2004)

Table 1 continued

Organism	Virulence Phenotype	Reference
Vibrio cholerae	CpxA activation reduces expression of two major virulence factors cholerae toxin (CT) and toxin-coregulated pilus (TCP); affects cAMP receptor protein (CRP) function to hinder expression of the regulators ToxT and TcpP.	(Acosta et al., 2015)
Yersinia pseudotuberculosis	*cpxA* mutation inhibits type III secretion and adherence to host cells, via down-regulation of the adhesin invasin	(Carlsson et al., 2007a, Carlsson et al., 2007b)
*Legionella pneumophila**	CpxR inhibits expression of several Icm/Dot type IV-secreted substrates	(Altman and Segal, 2008)
Haemophilus ducreyi	Cpx inhibits expression of several virulence determinants, including LspB-LspA2 and DsrA; Δ*cpxA* pathway-activating mutation renders *H. ducreyi* avirulent in human volunteers	(Labandeira-Rey et al., 2010, Spinola et al., 2010, Labandeira-Rey et al., 2009)

One controversial (and since disputed) model was presented by Collins and colleagues (2007, 2008). These published works suggested aminoglycosides trigger hydroxyl radical formation, leading through multiple processes to aminoglycoside-induced oxidative stress and cell death. Said processes included the perturbation of metabolism and respiration, increased superoxide formation, iron-catalysed Fenton chemistry and subsequent reactions with endogenous hydrogen peroxide (Kohanski et al., 2008, Kohanski et al., 2007, Dwyer et al., 2007). The formation of hydroxyl radicals post gentamycin treatment was only possible (in that study) if both Cpx and Arc 2CST systems were intact and active, making them 'essential' for antibiotic-mediated oxidative stress and cell death (Kohanski et al., 2008). The initial significance of Collins and colleagues' proposal for the development of novel antibiotics was huge. However, two recent studies published in *Science* provided additional evidence to contradict the ROS model of Collins and colleagues (Liu and Imlay, 2013, Keren et al., 2013).

Studies conducted prior to the ROS hypothesis showed that overexpression of CpxR increased the mRNA levels of several drug exporter genes, including *acrD* and *macA* (Hirakawa et al., 2003). This increase resulted in *E. coli* resistance to the bile salt deoxycholate, the aminocoumarin antibiotic novobiocin and the aminoglycosides amikacin and kanamycin (Hirakawa et al., 2003). When the Cpx system is rendered constitutive (*cpxA** mutation), strains are also highly resistant to amikacin and kanamycin, and HU in a CpxR dependant manner (Rainwater and Silverman, 1990, Humphreys et al., 2004, Mahoney and Silhavy, 2013). The resistance associated with *cpxA** strains is not due to the many pleiotropic effects associated with constitutive expression of Cpx because overexpression of NlpE, inducing the Cpx pathway, also results in HU resistance, although this occurs to a lesser extent than that observed for *cpxA**. As *cpxA** is a stronger Cpx inducer than NlpE, this suggests HU resistance correlates with Cpx activity levels (Mahoney and Silhavy, 2013, Vogt and Raivio, 2012).

Although *cpxA* deletion also results in resistance to HU, amikacin and gentamycin (Davies et al., 2009, Kohanski et al., 2008, Mahoney and

Silhavy, 2013), this is not due to Cpx induction by HU and aminoglycoside antibiotics, as suggested by (Kohanski et al., 2010, Kohanski et al., 2007, Kohanski et al., 2008). Instead, Mahoney and Silhavy (2013) state such resistance occurs because of disruption to all three key CpxA activities: 1) the ability of CpxA to act as a phosphatase (in the absence of inducing stimuli), 2) to maintain unphosphorylated CpxR levels and 2) CpxA autokinase and kinase activation of CpxR (Raivio and Silhavy, 1997). These conclusions, coupled with evidence presented by Lui and Imlay (2013) and Keren et al. (2013) suggests Cpx involvement in antibiotic-mediated ROS stress and cell death.

1.7.5 Cpx and antimicrobial compounds

Antimicrobial peptides are ubiquitously produced by the mammalian innate immune system and have emerged as a potential treatment for microbial infections (Zasloff, 2002). Due to the presence of negatively charged lipopolysaccharides (LPS) on the surface of Gram-negative bacteria, most of these effective AMPs are cationic. However, resistance to AMPs is also becoming a problem; the strategies imparted by *Salmonella* spp. to resist AMPs are reviewed by (Matamouros and Miller, 2015). The AMP ApoEdpL-W is derived from human apolipoprotein E, and functions through perturbation of the lipid bilayer. Activation of the Cpx pathway directly contributes towards tolerance of this AMP, polymyxin B and melittin in *E. coli*, with exposure to sub-lethal concentrations of ApoEdpL-W inducing the Cpx response and two other ESRs: σ^E and RcsCDB (Audrain et al., 2013). The involvement of Cpx and other ESRs in response to AMP stress are not surprising given their modes of action, and more investigations are needed if bacterial resistance to AMPs is to be understood in sufficient depth and overcome.

1.7.6 *Salmonella* biofilms and Cpx

The ability of *Salmonella* to adhere to living and abiotic structures is an important part of their life cycle and virulence strategy (Steenackers et al., 2012). Biofilms are defined as complex, structured communities of bacterial cells that are adherent to living and abiotic surface (Costerton et al., 1999,

Steenackers et al., 2012, Donlan and Costerton, 2002, Hall-Stoodley and Stoodley, 2009). Within the host, *Salmonella* adhesion to epithelial cells and gallstones play an essential role in *Salmonella* invasion and asymptomatic carriage (Crawford et al., 2010). They are clinically relevant environments allowing *Salmonella* and other pathogens to persist within the host and non-host environments and affording protection to treatment from antibiotics (Otto and Silhavy, 2002).

The regulation of genes within a biofilm is complex and multi-layered, including multiple ESRs with genes belonging to the σ^E, Cpx and PSP regulons of *E. coli* up-regulated in response to biofilm formation (Beloin et al., 2004). Adaptation to environmental stresses, adhesion and motility (through alterations to chemo- and energy- taxis) are all involved in the transition of bacteria from planktonic to biofilm growth and all are moderated, to some extent, by Cpx (Dorel et al., 2006). Components of four types of surface organelles are negatively regulated by activation of the Cpx pathway: F pili, required for strong adherence to abiotic surfaces (*tra* gene) (Gubbins et al., 2002); P pili, needed for adherence of uropathogenic *E. coli* to host cells within the urinary tract (*pap* genes) (Hernday et al., 2004); curli, important for initial adhesion and cell-cell interactions, as well as adhesion to abiotic surfaces (*csgB*, *csgB*) (Prigent-Combaret et al., 2001) and the type IV bundle forming pili (*bfp* genes), required for virulence of EPEC (Nevesinjac and Raivio, 2005). Together these appendages are important for all stages of biofilm formation, from initial adhesion to host tissues to the stabilisation of larger multicellular matrices. Due to their essential role in adhesion, regulation of pili by the Cpx pathway it critical for the host cell invasion and virulence of both *E. coli* and *Salmonella* (Leclerc et al., 1998, Dorel et al., 1999) and understanding the regulatory mechanisms of biofilm formation is an important step in understanding how persistent biofilms can be broken down and prevented.

1.7.7 The CpxP-like superfamily

Enteric bacteria such as *E. coli* and *Salmonella* possess the CpxP superfamily of molecular chaperones: *cpxP*, *spy* and *zraP* (Appia-Ayme et

al., 2012). As briefly mentioned, the Cpx ESR is involved in AMP protection in *E. coli*. In *Salmonella*, both *cpxP* and *spy* are up-regulated in the presence of polymyxin B (Bader et al., 2003). As polymyxin B disrupts the OM through binding to the negative charges on LPS, it is not surprising to see ESR involvement in the bacterial response to such cationic AMPs. Single deletions of *cpxP*, *spy* and *zraP* all show sensitivity to polymyxin B (Appia-Ayme et al., 2012). Removal of all three genes presented the most severe response, with no viable cells remaining post polymyxin B exposure. This sensitivity, in collaboration with an array of increasingly sensitive phenotypes displayed by the CpxP superfamily double mutants, shows the importance of this group of chaperones in response to this AMP (Appia-Ayme et al., 2012).

1.7.7.1 Structural similarities

The protein sequence identity between ZraP and Spy, and ZraP and CpxP, is 13% and 12% respectively, with Spy and CpxP sharing 29% identity (Appia-Ayme et al., 2012, Raivio and Silhavy, 1999). The crystal structure of the ZraP monomer (PDB code 3LAY) shows two α-helices with residues 123-151 disordered, coming together to form a decameric structure. Sedimentation equilibrium experiments indicate that ZraP requires zinc to stabilise this oligomeric structure and function effectively, although there are no zinc ions present in the structure of ZraP (Appia-Ayme et al., 2012, Zhou et al., 2011). Upon comparing the crystal structure of ZraP to those of Spy (PDB code 3O39) and CpxP (PDB code 3QZC), a third α-helix is present in these two proteins, absent from ZraP. If present, the position of this third helix would interfere with the decameric structure of ZraP (Appia-Ayme et al., 2012).

Various phenotypic analysis of *cpxP*, *zraP* and *spy* single, double and triple mutants have shown an overlapping requirement of *S.* Typhimurium for these three proteins. This, along with similarities in: structural, regulatory and chaperone activity, point to a functional overlap of this CpxP superfamily of proteins in maintaining envelope homeostasis (Appia-Ayme et al., 2012).

1.7.7.2 Spy

Spy is an abundant periplasmic protein, first identified in spheroplasts (Hagenmaier et al., 1997). It is up-regulated in large quantities by stimuli that induce the Rcs phosphorelay response and the Cpx and Bae ESR pathways (Rcs and Bae are discussed later) (Merdanovic et al., 2011, Raffa and Raivio, 2002). Despite sequence homologies of Spy being present in a wide variety of enterobacteria, proteobacteria and cyanobacteria (Raffa and Raivio 2002), the physiological role of this highly abundant protein has only recently come to light. Work by Quan et al. (2011) confirmed that Spy acts as an ATP independent molecular chaperone *in vivo*. Previous hypotheses suggested Spy might be involved in OM protein biogenesis, due to deletion of Spy causing an induction of genes under the control of σ^E (Raivio et al., 2000). However, this has not been observed. Instead, Quan et al. (2011) hypothesised that due to overexpression of Spy resulting in accumulation of a previously highly unstable protein, Spy functions as a chaperone to facilitate protein folding in the periplasm. Aggregation of malate dehydrogenase (MDH) denatured by heat treatment, ethanol and urea is significantly reduced in the presence of Spy, even at sub stoichiometric concentrations. This effective inhibition suggests the highly efficient nature of Spy as a molecular chaperone (Quan et al., 2011). The ATP independent nature of Spy's chaperone activity is not unusual for a protein which functions outside of the periplasm (Quan et al., 2011). However, the results were unexpected, as ATP is usually required by chaperones at the sub stoichiometric concentrations at which Spy functions (Powers and Balch, 2011, Saibil, 2008).

Evans et al. (2011) showed that Spy modulates aggregation of the major curli subunit CsgA by inhibiting polymerisation *in vitro*, and overexpression of Spy reduces curli biogenesis *in vivo*. As CsgA must pass through the periplasm prior to curli formation at the OM, these results suggest Spy contributes towards protecting the cell from amyloid formation in the periplasm, adding more weight to support Spy as a crucial regulator of envelope homeostasis (Evans et al., 2011).

Despite the structural similarities of Spy and CpxP, Spy does not share the ability of CpxP to inhibit activation of the Cpx pathway (Raivio et al., 2000) and it does not influence the expression of Bae-, Cpx-, σ^E-, Rcs- and Psp-regulated genes (Quan et al., 2011). Spy therefore does not have an identified regulatory function and appears to solely act as a molecular chaperone.

1.7.7.3 ZraP

ZraP contains two proposed zinc-binding domains and preferentially binds zinc over other metals, suggesting a role for this protein in zinc homeostasis and/or as a modulator of zinc transporters (Noll et al., 1998, Appia-Ayme et al., 2012). Regulation of *zraP* in *E. coli* is dependent on ZraSR (also known in the literature as HydHG), a zinc responsive two-component regulator, and RpoN (σ^N or σ^{54}) (Leonhartsberger et al., 2001) with investigations in *S.* Typhimurium supporting this (Appia-Ayme et al., 2012).

Appia-Ayme et al. (2012) conducted the first functional characterisation of ZraP, casting new light over this member of the CpxP family of regulatory proteins and highlighting its contribution to envelope homeostasis. *In vitro* analysis of ZraP, similar to assays conducted to investigate Spy (Quan et al., 2011), showed that ZraP was able to suppress aggregation of malate dehydrogenase (MDH) as effectively, if not better than, Spy (Appia-Ayme et al., 2012).

In *E. coli*, transcription of all three CpxP superfamily members is up-regulated in the presence of zinc sulphate (Graham et al., 2009). Due to the ability of ZraP to preferentially bind zinc over other metals, it was hypothesised that chaperone activity of ZraP would increase in the presence of Zn^{2+}, and this was observed upon the addition of known concentrations of $ZnCl_2$ (Appia-Ayme et al., 2012). An increase in MDH aggregation when ZraP and EDTA, a chelator of Zn^{2+}, were present confirmed the zinc dependent nature of ZraP chaperone activity (Appia-Ayme et al., 2012).

A comparison of *zraR* expression in *zraP* deletion strains of *S.* Typhimurium compared to the isogenic parent revealed that the absence of ZraP results in a 12-fold up-regulation of the response regulator ZraR, whilst overexpression of ZraP in a WT *S*. Typhimurium background results in the down-regulation of ZraR. As *zraP* is regulated by ZraR, this results in a negative feedback loop, similar to that observed for CpxP and CpxR. Quan et al (2011) showed that, unlike CpxP, Spy does not have a regulatory mechanism and functions solely as a highly efficient chaperone. The evidence presented by Appia-Ayme et al. (2012) does indicate a regulatory function for ZraP, and in that respect this protein shares a closer mechanism to CpxP than Spy.

1.8 The phage shock protein (PSP) system

The phage shock (Psp) response was first reported in *E. coli* following the discovery of phage shock protein A (PspA). This 25kDa protein was induced in high concentrations following the prolonged synthesis of phage gene IV protein (pIV) during filamentous phage infection (Brissette et al., 1990). pIV belongs to the secretin family of OM proteins and is an essential component of the phage particle exit channel required for phage extrusion from the cell (Joly et al., 2010, Russel, 1994).

The Psp operon is encoded by two loci in *E. coli* and *Salmonella*: the *pspABCDE* operon; *PspF*, a positive regulator of *pspA* is divergently transcribed to it*;* and the separate *pspG* gene (Huvet et al., 2011). In the absence of an inducing condition, PspA is bound to PspF, preventing induction of transcription (Elderkin et al., 2002, Elderkin et al., 2005, Joly et al., 2009). However, when an inducing signal is present (i.e. filamentous phage infection, loss of IM integrity) the concentration of PspB and/or PspC increases in the cytoplasm, sequestering PspA and releasing PspF (Darwin, 2005). This subsequently activates transcription of *pspA* and *pspG*.

This ESR system is involved in repairing damage to the IM (Kobayashi et al., 2007) and maintenance of the proton motive force (PMF) in *E. coli* and *Salmonella* (Kleerebezem et al., 1996, Becker et al., 2005, Model et al., 1997). Because disruption to the PMF negatively impacts metabolite

production, motility and translocation of flagellin, anaerobic respiration and TTSS secreted effector molecule (Wallrodt et al., 2014, Galan, 2008, Minamino and Namba, 2008), Psp is considered important for a broad range of cellular functions.

The Psp system is present in all *Enterobacteriacae* and is regulated by σ^{54} in conjunction with PspF as a bacterial enhancer binding protein (bEBP) (Joly et al., 2010). One study by Huvet et al. (2011) in *E. coli* showed transcription of *pspE* could occur independently to *pspABCD*, from a *pspE*-specific σ^{70} dependant promoter. A similar result has recently been observed in *S*. Typhimurium (Kroger et al., 2013), suggesting that PspE may function independently of the main Psp operon in an as yet undetermined role. PspE is a thiosulfate sulfurtransferase (TST) and Wallrodt et al. (2013) provided evidence of PspE contribution to *S*. Typhimurium virulence, but only in combination with another TST, GlpE. This supports the hypothesis of PspE functioning independently from the Psp operon, but the mechanisms of PspE (and GlpE) contribution to *S*. Typhimurium remained elusive.

Three additional studies have linked the *psp* operon to *Salmonella* virulence through a possible role in host-pathogen interactions. During *S*. Typhimurium infection of macrophages and epithelial cells, all *psp* genes are highly expressed (Eriksson et al., 2003, Hautefort et al., 2008), with *psp* induction also observed during a genome expression analysis of non-proliferating *S*. Typhimurium in fibroblast cells (Nunez-Hernandez et al., 2013). Homologues of PspA in *Pseudomonas aeruginosa* are also important for biofilm formation and virulence in this organism (Mace et al., 2008) suggesting Psp involvement in virulence of a range of pathogens.

Several links between the Psp system and σ^{E} response have been observed, which may contribute one explanation to Psp involvement in *Salmonella* virulence. PspA was recently described as σ^{E} regulated in *S. Typhimurium* (Li et al., 2015a). σ^{E} is expressed in high levels upon entry into stationary phase (Miticka et al., 2003) and PspA is able to compensate for loss of σ^{E} during stationary phase survival, with mutations in *rpoE* strongly

inducing expression of the Psp regulon (Becker et al., 2005). Becker and colleagues (2005) also showed in *S.* Typhimurium that increased expression of *pspA* resulted from disruption of the PMF and deletion of *rpoE* (in alkaline conditions). Although *rpoE* deletion reduces the PMF, double deletions of *rpoE* and *PspA* also have a stationary phase survival defect, which is more pronounced than single mutations in each locus (Becker et al., 2005). This indicates complementarity between these two ESRs and the necessity of the σ^E regulon for PMF maintenance. The affect of σ^E on the PMF requires more attention to elucidate whether this outcome is a consequence of the σ^E regulon directly or due to indirect disruption of the cell envelope (Becker et al., 2005).

1.9 Rcs phosphorelay response

The RcsCDB phosphorelay system, once again discovered in *E. coli*, was originally described as a capsular synthesis regulatory system (regulator of capsular synthesis genes). In *S.* Typhimurium genes encoding core Rcs components, *rcsDB and rcsC*, are co-transcribed from a single locus as two converging transcriptional units (Clarke, 2012, Pescaretti Mde et al., 2010).

Initiation of the phosphorelay response begins with activation of the pathway via RcsF, an OM protein, or RcsC, which is anchored to the cytoplasmic face of the IM (Majdalani et al., 2005). Several phosphotransfer events then take place from RcsC to RcsD at the IM, and RcsB, situated in the cytoplasm. How RcsF transduces this initiation signal to RcsC remains unknown. However, inducers of the Rcs phosphorelay that act through RcsF have been shown to perturb the OM where RcsF is localised (Holtje, 1998, Majdalani et al., 2005). Activation of the Rcs phosphorelay is further complicated by an array of accessory proteins (RcsA, TviF, IgaA/YrfF) which, although not playing an active part in the phosphoreplay, contribute to modulating signalling activity of the core components mentioned above (for a review of all Rcs accessory and core components see Clarke (2012)).

Phylogenetic analysis showed that the Rcs ESR is limited to the Enterobacteriacae order and in *S*. Typhimurium, Rcs is induced in response

to osmotic shock, elevated temperature (Erickson and Detweiler, 2006), copper stress (Pontel et al., 2010) and cationic AMPs (Farris et al., 2010). The Rcs phosphorelay response is linked to pathogenicity of other enteric and plant pathogens. Evidence of Rcs involvement in virulence of *E. coli*, *Yersinia* spp., and *S*. Typhimurium is summarised in Table 2. Additional inducing conditions identified in *E. coli*, although this list is not exhaustive, include LPS biosynthesis, metabolic stress, acidic phospholipids and the overproduction of DjlA, HupAB, LolA/OmpG (Clarke, 2012).

The Rcs system also contributes to intrinsic antibiotic resistance and is activated by damage to peptidoglycan (Laubacher and Ades, 2008). The peptidoglycan layer of the cell envelope maintains cell structure and integrity and new peptidoglycan subunits are incorporated into this layer during cell growth by penicillin binding proteins (PBPs). Laubacher and Ades (2008) demonstrated that the inhibition of penicillin binding protein 2 by amdinocillin resulted in the activation of Rcs and other existing stress responses, including the Cpx and σ^E pathways.

Table 2: The Rcs phosphorelay system and virulence. Adapted from Clarke (2012).

Species	Potential role in pathogenicity	Reference
EHEC	Regulation of genes in LEE pathogenicity island	(Tobe et al., 2005, Morgan et al., 2013)
S. Typhimurium	Resistance to cationic AMPs, regulation of yecI	(Farris et al., 2010, Erickson and Detweiler, 2006)
Y. enterocolitica	Regulation of Ysa type 3 secretion system Attachment to mammalian cells	(Venecia and Young, 2005, Hinchliffe et al., 2008)
Y. pseudotuberculosis	Attachment to mammalian cells	(Hinchliffe et al., 2008)

1.10 Outer membrane vesicles as a stress response

This newly established ESR is described as a complementary mechanism for managing envelope stress, entirely independent to the other ESR pathways previously described (McBroom and Kuehn, 2007).

Vesicular release occurs throughout the growth of Gram-negative bacteria and involving the blebbing out and subsequent fission of the OM (reviewed by (McBroom and Kuehn, 2005, Mayrand and Grenier, 1989). This allows controlled regulation of envelope components through the removal of unwanted material, as well as providing intercellular messaging and transport vehicles. A role for vesicles in host-pathogen interactions has been indicated as they provide an alternative means for the release of toxins to host cells and surrounding environments (McBroom and Kuehn, 2005, Kuehn and Kesty, 2005). McBroom and Kuehn (2007) have suggested that during envelope stress, such releases allow removal of toxic protein species and other damaged material. Vesiculation would maintain envelope homeostasis and promote cellular survival in an advantageous manner through this “selective disposal” of misfolded polypeptides. This was supported by the observation of a positive correlation between increases in vesiculation and bacterial survival, with this ‘bulk-flow mechanism’ sufficiently relieving envelope stresses in the absence of previously described ESRs (McBroom and Kuehn, 2007).

Due to the independent nature of OM vesicle production, there appears not to be a regulatory link between this stress response and those previously described. How this novel ESR is induced and the means by which cells transmit such signals to the OM vesicle machinery is still unknown and requires further investigation. The regulatory mechanisms controlling vesicle contents also requires more attention as this selective process is essential for the correct application of vesiculation as an ESR.

1.11 BaeSR

The BaeSR stress response was first discovered during a search for new 2CST systems, and was later characterised as the third ESR (Raffa and Raivio, 2002). However, compared to the σ^E and Cpx ESRs, little work has been conducted into BaeSR. This ESR is yet to be characterised in depth, most likely due to the fact that deletion of *baeS* or *baeR* produce few noticeably phenotypes (Appia-Ayme et al., 2011).

Overexpression of the RR, BaeR, increases bacterial resistance to beta-lactam antibiotics, novobiocin (an aminocoumarin antibiotic) and bile salts in *E. coli* (Raffa and Raivio, 2002). Functional overlap with the Cpx-pathway has been observed as double deletion mutants of the RR in both two-component systems (*baeR* and *cpxR*) present an increased sensitivity to envelope stress than the single mutants alone. An overlap is also observed in the genes regulated by the Cpx and BaeSR pathways, of which *spy* is a prominent example. However, the core BaeSR regulon in *E. coli* contains three genes, amongst others, encoding members of the resistance nodulation-cell division (RND) family of multidrug transporters; *mdtA*, *acrB* and *acrD* (Bury-Mone et al., 2009). Sodium tungstate (Na_2WO_4) is a natural substrate of MdtABC influx pumps (Leblanc et al., 2011). In *S*. Typhimurium *baeR* is up-regulated in the presence of tungstate and *baeR* deletion mutants have an increased sensitivity to tungstate compared to the isogenic parent strain (Appia-Ayme et al., 2011). Strains carrying mutations in *mdtABCD* and/or *acrAB* or *acrD* lose their ability to grow on tungstate, whereas single mutations of the RND efflux pump systems do not show sensitivity. CpxR also regulates transcription of *mdtA and acrD*, but a *cpxR* deletion does not result in tungstate sensitivity. BaeR is therefore the primary regulatory of these genes in response to tungstate waste removal and is critically required for *S.* Typhimurium resistance to Na_2WO_4 (Appia-Ayme et al., 2011). Functional overlap between these RND transporters exists for waste disposal of tungstate from the cell, suggesting a role for BaeSR in *Salmonella* survival from the stresses inflicted from water and soil where tungstate concentrations can fluctuate.

Expression of BaeSR is also growth phase linked, like σ^E, as induction of *baeSR* increases during stationary phase growth when grown in LB (alkaline conditions) (Appia-Ayme et al., 2011, Miticka et al., 2003). Other inducers of BaeR activity include: iron, copper, zinc and high concentrations of indole, a compound found in the intestines and faeces due to bacterial decomposition of tryptophan.

Indole at μM concentrations is utilised by bacteria as a signalling molecule in the intestines of humans and other mammals (Botsford and Demoss, 1972), a process encouraged by the induction of *tnaA* (an indole producing tryptophanase) by the alkaline pH and low nutrient concentrations present within the intestines (Han et al., 2011). The survival rate of a *S*. Typhimurium *baeR* mutant is no different to the isogenic parent strain in the presence of mM indole concentrations (Appia-Ayme et al., 2011). However, in a *baeR* deletion strain of *E. coli*, 1 mM indole significantly reduces cell viability (Raffa and Raivio, 2002). *E. coli* is an indole producer whereas *Salmonella* is not and it has been hypothesised that differences in survival of these mutant strains is a result of dissimilarities in the indole producing and sensing pathways of these two bacterial species (Appia-Ayme et al., 2011).

BaeSR is required for *Salmonella enterica* serovar Dublin (*S.* Dublin) colonisation and subsequent systemic salmonellosis in orally infected cattle (Pullinger et al., 2010). Appia-Ayme and colleagues (2011) ascertained that in a murine typhoid model, BaeSR is not required for *S.* Typhimurium infection, with no significant attenuation of a *baeR* mutant observed, compared to the isogenic parent strain SL1344, after oral infection.

The BaeSR system is also associated with zinc stress tolerance in *E. coli* and *S*. Typhimurium (Nishino et al., 2007, Wang and Fierke, 2013). This function of the Bae ESR with be discussed in Chapter 5 and will therefore not be mentioned here.

1.12 ZraPSR

The ZraPSR system is discussed in detail in Chapter 5. Below is a brief introduction to this newly characterised ESR.

The majority of investigations conducted on the ZraSR 2CST system are associated with zinc homeostasis in *E. coli*. Zinc plays an essential role in cell metabolism. However, at high concentrations, accumulation of this metal is cytotoxic and strict homeostatic mechanisms are needed to prevent this. Numerous *E. coli* genes involved in such processes, including *zraR*, have been identified; regulated by zinc inducible promoters (Outten et al., 1999). In response to elevated Zn^{2+} concentrations, both the RR, ZraR, and the HK, ZraS activate *zraP*, which is divergently transcribed from *zraSR* (Franke et al., 2001). Within the *zraP-zraSR* intergenic region, a σ^{54} dependent promoter is located where it is believed ZraR, as a bEBP, binds. Noll et al. (1998) showed that in the absence of transcriptional activators, this promoter is completely switched off, whereas the weak constitutive promoter of *zraSR* allows for basal levels of expression of both the RR and SK (Ravikumar et al., 2011, Noll et al., 1998, Leonhartsberger et al., 2001).

Although originally described as a zinc responsive 2CST system, Appia-Ayme et al. (2011) provided the first evidence of the involvement of ZraPSR in envelope stress. A regulatory link, directly or indirectly, between ZraPSR and the BaeSR system was observed; overexpression of BaeR results in significant transcriptional repression of *zraP*. Other links between ZraP and BaeR have been indicated in the presence of tungstate (Appia-Ayme et al., 2011) and this compound was shown to induce all ESR pathways, but in a *baeR* mutant background, *zraP* and *zraSR* were both highly up-regulated at the transcriptional level. These results concur with previous observations in *E. coli* that showed repression of *baeR* upon zinc addition, proposed to be a result of ZraPSR up-regulation (Graham et al., 2012).

1.13 Thesis overview

1.13.1 Research gap

Our understanding of the response of Gram-negative bacteria to exogenous stresses and envelope damage is fundamental to our understanding of how pathogens adapt to and survive the threats inflicted upon them from the host and wider environment. The ESRs provide a potential pool of untapped resources for novel treatment and vaccine development because of their critical involvement in aiding adaption to host environments, surviving within the diverse microenvironments encountered within the host and the direct association of many ESR proteins with pathogenicity.

1.13.2 Aims

The intention of this thesis is to expand our understanding of the ESRs in the broad-host range generalist *S*. Typhimurium, knowledge that could be transferable to non-typhoidal and typhoidal *Salmonella* strains, as well as related pathogens i.e. *E. coli* spp., *Shigella* spp., *Yersina* spp. and *Vibrio* spp. This thesis specifically aims to:

- Characterise the Cpx regulon of *Salmonella* through a combined transcriptomic approach (Chapter 3).
- Identify the processes through which new Cpx regulon members contribute towards envelope homeostasis, pathogenicity and other Cpx associated processes (Chapter 4).
- Characterise the regulon of a newly identified stress response, ZraSR, and confirm the contribution of this 2CST system to *Salmonella* physiology (Chapter 5).
- Confirm the role of the ZraSR auxiliary protein ZraP as a zinc-responsive molecular chaperone and the contribution of zinc to the structure and function of this chaperone (Chapter 6).

2 Materials and methods

2.1 Materials

Chemicals and reagents used are laboratory standard grade or above, purchased from Sigma Aldrich (UK) or Thermo Fisher Scientific (UK) unless otherwise stated. All media and solutions were made using dH_2O, except those involving RNA where 0.1 µm filtered, molecular biology grade water (not treated with DEPC, nuclease and protease free) was used (Sigma W 4502; referred to as Sigma H_2O).

2.2 Bacterial strains and plasmids

Bacterial strains used in this work are *Salmonella enterica* subspecies and *Escherichia coli* K-12 derivatives. The isogenic parent strain, from which the majority of deletion mutants were derived from, is *Salmonella enterica* subspecies *enterica* serovar Typhimurium strain SL1344 (referred to as SL1344). For ease of description, SL1344 will be refered to as our 'wild-type' (WT) strain throughout this work. A comprehensive list of strains and plasmids used in this study are described in Table 3 and Table 4 respectively.

2.3 Bacterial culture conditions

2.3.1 Media

Media compositions are shown in Appendix C. As SL1344 is a histidine (His) auxotroph, His (40 mg/mL) was added to defined media where applicable. When required, media were supplemented with the appropriate antibiotic (Appendix C) at concentrations: 100 µg/mL ampicillin (Amp), 10 µg/mL chloramphenicol (Cm), 50 µg/mL kanamycin (Km) and 5 µg/mL tetracycline (Tet) unless otherwise stated.

2.3.2 Overnight cultures

Bacterial strains were aseptically streaked onto LB agar (1.5% w/v) plates (supplemented with antibiotics [2.3.1] where applicable) from DMSO stocks or Microbank™ bead stocks (2.3.3). Streak plates were incubated overnight at 37°C for 14-18 hours and stored at 4°C for a maximum of two weeks.

Table 3: **Strains used during this study**.

Strain	Description	Reference
Salmonella Strains		
SL1344	*Salmonella enterica* serovar Typhimurium 4/74, *hisG*, *rpsL*	(Hoiseth and Stocker, 1981), (McClelland et al., 2001)
P125109 (PT4)	*Salmonella enterica* serovar Enteritidis, phage type 4 (PT4)	(Barrow, 1991, Thomson et al., 2008)
Escherichia coli Strains		
MG1655	Prototroph; K-12 derivative*; F-, lambda-, rph-1*	(Guyer et al., 1981) (Lacey et al., 2010)
803	*met-*	(Wood, 1966)
Top10	*mcrA, Δ(mrr-hsdRMS-mcrBC), Phi80lacZ(del)M15, ΔlacX74, deoR, recA1, araD139, Δ(ara-leu)7697, galU, galK, rpsL(SmR), endA1, nupG*	Invitrogen™
XL10-Gold	*endA1, glnV44, recA1, thi-1, gyrA96, relA1, lac, Hte, Δ(mcrA)183, Δ(mcrCB-hsdSMR-mrr)173, F'[proAB lacI^{q}ZΔM15 Tn10(Tet^{R} Amy Cm^{R})]*	Stratagene™
Salmonella Mutant Strains		
Δ*baeR*	SL1344 Δ*baeR*::pCP20	(Appia-Ayme et al., 2011)
Δ*baeR* (PT4)	P125109 Δ*baeR*::pCP20	This study
Δ*baeR ΔcpxAR*	SL1344 Δ*baeR*::*kan* Δ*cpxAR*::*cat*	(Appia-Ayme et al., 2011)
Δ*baeR* Δ*cpxR* Δ*zraSR*	SL1344 Δ*baeR*::pCP20 Δ*cpxR*::*cat* Δ*zraSR*::*kan*	(Appia-Ayme et al., 2011)
Δ*cpxA-cpxA**	SL1344 Δ*cpxA*::pCP20-cpxA*	(Humphreys et al., 2004)
Δ*cpxAR*	SL1344 Δ*cpxAR*::*kan*	(Humphreys et al., 2004)
Δ*cpxP*	SL1344 Δ*cpxP*::*cat*	(Appia-Ayme et al., 2011)
Δ*cpxP Δspy*	SL1344 Δ*cpxP*::*cat* Δ*spy*::*kan*	(Appia-Ayme et al., 2011)
Δ*cpxP* Δ*spy* Δ*zraP*	SL1344 Δ*cpxP*::pCP20 Δ*spy*::*kan* Δ*zraP*::*cat*	(Appia-Ayme et al., 2011)
Δ*cpxP* Δ*zraP*	SL1344 Δ*cpxP*::*cat* Δ*zraP*::*kan*	(Appia-Ayme et al., 2012)
Δ*cpxR*	SL1344 Δ*cpxR*::*kan*	(Humphreys et al., 2004)
Δ*rpoE*	SL1344 Δ*rpoE*::*kan*	(Humphreys et al., 1999)
Δ*scsA*	SL1344 Δ*scsA*::*cat*	This study
Δ*SL3009*	SL1344 Δ*SL3010*::*cat*	This study
Δ*SL3009 ΔSL3010*	SL1344 Δ*SL3009*/*10*::*cat*	This study
Δ*spy*	SL1344 Δ*spy*::*kan*	(Appia-Ayme et al., 2011)
Δ*stm3388*	SL1344 Δ*stm3388*::*kan*	This study
Δ*ydgEF*	SL1344 Δ*ydgEF*::*cat*	This study
Δ*ydiP*	SL1344 Δ*ydiP*::*cat*	This study
Δ*yncJ*	SL1344 Δ*yncJ*::*kan*	This study
Δ*yqaE*	SL1344 Δ*yqaE*::*kan*	This study
Δ*zraP*	SL1344 Δ*zraP*::*cat*	(Appia-Ayme et al., 2012)
Δ*zraSR*	SL1344 Δ*zraSR*::*cat*	(Appia-Ayme et al., 2011)

Table 4: **Plasmids used during this study**.

Plasmids	Description	Reference
pBAD/*Myc*-His A	pBR322 origin, *ara*BAD promoter(P_{BAD}) C-terminal *Myc* epitope tag, C-terminal 6xHis tag, *rrnB* transcription termination region, *araC;* Amp^R	Invitrogen™
pCP20	Temperature sensitive replication and thermal induction of FLP synthesis; Amp^R; Cm^R	(Cherepanov and Wackernagel, 1995)
pET16*b*	pBR322 origin, N-terminal Xa cleavage site, cloning and expression vector for expressing N-terminal 10xHis tagged proteins; Amp^R	Novagen™
pKD3	pANT-Sγ derivative; Amp^R; Cm^R	(Datsenko and Wanner, 2000)
pKD4	pANT-Sγ derivative containing a FRT-flanked Km^R; Amp^R	(Datsenko and Wanner, 2000)
pKD46	pINT-ts derivative containing *araC*-ParaB and γ, β, exo genes; Amp^R	(Datsenko and Wanner, 2000)
pMP220	Wide host range, promoterless-*lacZ* probe vector; Tet^R	(Zaat et al., 1987) (Spaink et al., 1987)
pUC57	Derivative of pUC19, cloning vector, production of nested deletions with ExoIII; Amp^R	Thermo Scientific™
Overexpression Constructs		
p*scsA*	*scsA* gene in pBAD *Myc*/His A expression plasmid without 6xHis epitope; Amp^R	This study
p*nlpE*	*nlpE* gene in pBAD *Myc*/His A expression plasmid without 6xHis epitope; Amp^R	(Humphreys et al., 2004)
His Tagged Protein Constructs		
p*zraP*6xHIS	*zraP* gene in pBAD *Myc*/His A expression plasmid in phase with C-terminal 6xHis epitope; Amp^R	This study
p*zraR*6xHIS	*zraR* gene in pBAD *Myc*/His A expression plasmid in phase with C-terminal 6xHis epitope; Amp^R	This study
pET16b*cpxR*	*cpxR* gene in pET16*b* expression plasmid in phase with N-terminal 10xHis epitope; Amp^R	This study
pUC57*cpxR*	*cpxR* gene in pUC57 cloning vector for sub-cloning, synthesised by GenScript™; Amp^R	This study
LacZ Fusion Constructs		
pR3009/10	Promoter region of S*L3009/10* in pBAD *Myc*/His A expression plasmid without the 6xHis epitope; Tet^R	This study
pRscsA	Promoter region of *scsA* in pBAD *Myc*/His A expression plasmid without the 6xHis epitope; Tet^R	This study
Site Direct Mutagenesis Constructs		
p*zraP*LTTEA	*zraP* gene, with Q48A mutation, in pBAD *Myc*/His A expression plasmid in phase with C-terminal 6xHis epitope; Amp^R	This study

Table 4 continued

Plasmids	Description	Reference
p*zraP*AAAAA	*zraP* gene, with L44A; T45A; T46A; E47A; Q48A mutations, in pBAD *Myc*/His A expression plasmid in phase with C-terminal 6xHis epitope; Amp^R	This study
p*zraP*HRGGAH	*zraP* gene, with G134A mutation, in pBAD *Myc*/His A expression plasmid in phase with C-terminal 6xHis epitope, Amp^R	This study
p*zraP*GGC-AAA	*zraP* gene, with G120A; G121A; C122A; G123A; G124A; Y125 mutations, in pBAD *Myc*/His A expression plasmid in phase with C-terminal 6xHis epitope, Amp^R	This study
pUC57*zraP*GGC-AAA	*zraP* gene, with G120A; G121A; C122A; G123A; G124A; Y125 mutations, in pUC57 cloning vector; Amp^R	This study

Stationary phase, overnight cultures were produced by inoculating 10 mL LB broth with a single colony, picked from streak plates using a heat sterilised inoculation loop or autoclaved wooden toothpicks. Cultures were incubated at 37°C, plus 200-250 rpm agitation, for a minimum of 12 hours.

2.3.3 Long-term strain stocks

Strains were stored at -80°C in the form of Microbank™ (Prolab Diagnostics), produced following manufacturer's instructions, or DMSO stocks, made by adding 1.8 mL of fresh overnight culture (2.3.2) to 50 µL DMSO (>99%), inverting to mix and snap freezing at -80°C.

2.3.4 Aerobic batch culture

Batch culture growth curves were conducted using 50 mL of relevant media in sterile 250 mL volume conical flasks, supplemented with the appropriate antibiotic, and inoculated 1:100 (v/v) from overnight cultures (2.3.2). For strains harbouring overexpression vectors, 0.02% (w/v) *L*-arabinose was added to the media to switch on the pBAD/*Myc* His A promoter. Cultures were grown at 37˚C, 200 rpm for 24-hours unless otherwise stated.

To measure cell density, 1 mL of culture was collected at regular intervals and the OD at 600nm measured. If OD_{600} > 1, 0.1 mL of culture was diluted 1:10 (v/v) in the appropriate media prior to measuring OD. The OD_{600} value of undiluted culture was calculated by correcting for the dilution factor. Growth rate was calculated by plotting the log value of OD_{600} against time. From the straight line produced (during exponential [log] phase) the specific growth rate (μ) of cultures were calculated from the line gradient using Equation 1: *t* is time, ln represents the natural log (loge), N2 is the OD_{600} value at *t*2 and N1 is the OD_{600} value at *t*1. The dimension of μ is reciprocal time and is therefore expressed as reciprocal hours (hr^{-1}).

Equation 1:

$$\ln(N2/N1)=\mu(t2-t1)$$

All growth curves were conducted in triplicate, as a minimum, to allow for statistical analysis.

2.3.5 Anaerobic growth analysis in Hungate tubes

Overnight cultures (2.3.2) (1 mL aliquots) were washed twice in MGN media (Appendix C) before 100 μL was added to pre-autoclaved Hungate tubes containing 10 mL MGN media, plus additions. Cultures were incubated statically at 37˚C and the OD_{600} measured every two hours, over a 12-hour period. All growth curves were conducted in triplicate, as a minimum.

2.4 General laboratory techniques

2.4.1 Polymerase chain reaction (PCR)

Polymerase chain reaction (PCR) was conducted using ultra-stable *Taq* DNA Polymerase and *Phusion*™ high-fidelity DNA polymerase and their reagents (Table 5). Template DNA was purified chromosomal DNA, PCR product, plasmid DNA and synthesised constructs; stated where appropriate. Calculating specific primer melting temperatures (T_m) and adjusting values accordingly for each enzyme used, determined the annealing temperature

(T_a). Elongation time was calculated as one minute per one kilobase-pair (Kbp) of product. PCR programmes (Table 7) were conducted using a DNA engine PTC 300 (BIORAD) PCR machine. Primers used for the generation of cloning products are shown in Table 6. All primers used throughout this work were synthesised by Integrated DNA Technologies (IDT).

2.4.2 Colony PCR

Purified template DNA was substituted with a single bacterial colony of interest, re-suspended in PCR reaction mix (Table 5). The initial denaturing stage of the PCR programme chosen was extended to 5 min at 98°C to allow cell lysis and DNA release. The remaining stages of the chosen programme were completed as standard (Table 7).

Table 5: **PCR reaction components**.

Reagent	**Volume (µL)**	
Ultra-stable *Taq* DNA Polymerase		
2X BioMix (Bioline)	12.5	25
Forward primer (5'-3') [20 µM]	0.5	1
Reverse primer (3'-5') [20 µM]	0.5	1
Template DNA	Variable	Variable
Nuclease-free dH_2O	Σ 25	Σ 50
Phusion® High Fidelity (HF) DNA Polymerase		
5X Phusion HF Buffer	5	10
10 mM dNTPs	1	1
Forward primer (5'-3') [20 µM]	1	2
Reverse primer (3'-5') [20 µM]	1	2
Template DNA	Variable	Variable
Phusion DNA polymerase	0.5	0.5
Nuclease-free dH_2O	Σ 25	Σ 50

Table 6: **Primers for the generation of cloning products and pBAD/*Myc* His A sequencing primers**

Gene	Primers	Sequence (5'-3')
cpxR	cpxR_GeneFWD	AAAACCATGGGTAATAAAATCCTGTTAG
	cpxR_GeneREV	AAAAAAGCTTTGAAGCGGAAACCATCAG
scsA	scsA_GeneFWD	AAAACCATGGGTGCGAAACAACAACGGA
	scsA_GeneREV	AAAAGAATTCTCATTCACGGAAGACACAA
zraP	zraP_GeneFWD	TAACCATGGTGAAACGGAACAATAAATCAG
	zraP_GeneHISREV	AAAAGAATTCTTTACCAGTTTCCCATACCC
zraR	zraR_GeneFWD	AAAACCATGGGTGTGATACGCGGAAAAA
	zraR_GeneHISREV	AAAAGAATTCACGGCTGAGTTTAGCCAG
Sequencing primers		
	pBAD_FWD*	TTATCGCAACTCTCTACTG
	pBAD_REV[¥]	TGATTTAATCTGTATCAGGC

*FWD, forward primer. [¥]REV, reverse compliment primer. Restriction enzyme sites are underlined. All restriction enzymes used throughout this work are listed in Appendix F.

Table 7: **Thermocycling steps for PCR**

PCR Stages	Routine PCR		Mutagenesis		Site-Directed Mutagenesis		RNA Quality Control		qRT-PCR		EMSA	
	Temp (˚C)	Time (min)	Temp (˚C)	Time (min)	Temp (˚C)	Time (min)	Temp (˚C)	Time (min)	Temp (˚C)	Time	Temp (˚C)	Time (min)
1) Initial Denaturation	96	2	96	3	95	2	94	3	95	10 min	98	2
2) Denaturation	92	0.5	95	0.5	95	0.33	94	0.25	95	15 sec	98	0.5
3) Annealing	52-65*	0.5	52-58*	0.5	60	0.17	58	0.33	58	15 sec	55	0.5
4) Elongation	72	0.5-3[¥]	72	0.5-2.5[¥]	68	2.5	72	0.17	72	10 sec	72	0.5
5) Repeat stages 2-4	(29x)		(29x)		(18x)		(28x)			(x39)	(25x)	
6) Final elongation	72	5	72	10	68	5	72	3	65-95[†]	5 sec	72	5

* Annealing temperature (T_a) was ascertained by calculating the primer melting temperatures (T_m) and adjusting values accordingly; 5˚C below the minimum T_a for each primer pair.
[¥]Elongation time was set as 1 min per 1 Kbp. [†]Increase temperatures from 65˚C to 95˚C in 5 sec steps, recording fluorescence at each step to measure speed of dsDNA denaturing.

2.4.3 PCR product purification

PCR products were purified using a QIAquick™ PCR Purification Kit (QIAGEN) as per the manufacturer's instructions. Products were eluted from purification columns in 50 µL of nuclease-free dH_2O and stored at -20°C.

2.4.4 Plasmid DNA extraction and purification

QIAprep™ Spin Miniprep Kit (QIAGEN) and QIAprep™ Spin Midiprep Kit (QIAGEN) were used for plasmid extraction and purification. For low copy number plasmids, the maximum volume of culture advised by the manufacture was adopted (10 mL and 100 mL respectively). The volume of buffers utilised in the subsequent steps were adjusted accordingly: QIAprep™ Spin Miniprep Kit buffers P1, P2 and N3 volumes were doubled, QIAprep™ Spin Midiprep Kit buffer volumes remained unchanged from manufacturer's guidelines. Plasmid DNA was eluted from QIAprep™ spin columns (Miniprep Kit) in 50 µL of nuclease-free dH_2O. The same volume of nuclease-free dH_2O was used for resuspension of air-dried DNA pellets (Midiprep Kit). Plasmid DNA was analysed for concentration and purify on a NanoDrop 2000c UV-Vis spectrophotometer (Thermo Scientific) with NanoDrop 2000 software (Thermo Scientific) and stored at -20°C.

2.4.5 Bacterial transformation

Two methods of bacterial transformation were adopted during this work, 1) electroporation, using electrocompetent cells, and 2) heat shock transformation, requiring $CaCl_2$ treated, chemically competent cells. Heat shock transformation was the preferred methodology. During transformation of low yield exogenous DNA or during mutagenesis (2.4.6.2) electroporation was the more effective and reliable technique.

2.4.5.1 Production of electrocompetent cells

Overnight cultures (2.3.2) of desired strains were used to inoculate (1% v/v) 50 mL Lennox broth (Appendix C) and incubated at 37°C, 200-250 rpm until an OD_{600} 0.4-0.6 was achieved, as measured on a SpectraMax™ M5 spectrophotometer (Molecular Devices), referenced to media only control. Cells were harvested by centrifugation at 4000 x *g*, 4°C, the supernatant

removed and pelleted cells gently resuspended, on ice, in 15 mL ice-cold 30% (v/v) glycerol. Cell harvesting and resuspension was repeated three times. During final re-suspension, a reduced volume of 2 mL was used, aliquoted as 100 µL or 50 µL volumes in 1.5 mL microcentrifuge tubes, on ice. Electrocompetent cells are best used on day of production and this was adhered to where possible. Otherwise, aliquots were snap frozen in liquid nitrogen before storing at -80°C.

2.4.5.2 Electroporation

MicroPulser™ Electroporation Cuvettes (BIO-RAD): 0.2 cm cuvette gap width (green cap); were chilled for ~15 min at -20°C before use. Aliquots of electrocompetent cells, 50 µL or 100 µL, were defrosted on ice (~10 min) before the addition of exogenous DNA (2-5 µL); adjusted for desired concentration (>5 µL exogenous DNA was used for mutagenesis transformations; 2.4.6.2). Following transfer of this transformation reaction mix to a pre-chilled electroporation cuvette, cells were subjected to a single electrical pulse in MicroPulser™ Electroporation Apparatus (BIO-RAD) at a voltage of 2.5 kV (programme EC2), ensuring electroporation cuvettes were dry and condensation free prior to use. A maximum of 1 mL LB broth was added to the transformation reaction, mixed by gentle pipetting and transferred to a 1.5 mL microcentrifuge tube. This was incubated at 37°C, 200 rpm, for ~1.5 hours to allow for cell recovery.

Recovered cultures were subsequently spread aseptically, in 100 µL and 900 µL volumes (the latter was concentrated by centrifugation and resuspended in ~100 µL before spreading), onto agar plates of appropriate selective media. Once dried, plates were incubated at 37˚C (unless otherwise stated) for 12-16 hours to allow selection of successful transformants and single colony formation.

2.4.5.3 Production of chemically competent cells

Overnight cultures (2.3.2) of desired strains were used to inoculate (1% v/v) 50 mL LB broth (Appendix C) and incubated at 37°C, 200-250 rpm until an OD_{600} 0.4-0.6 was achieved, as measured on a SpectraMax™ M5

spectrophotometer (Molecular Devices), referenced to media only control. Cells were harvested by centrifugation at 4000 x *g*, 4°C, supernatant removed and pelleted cells gently resuspended, on ice, in 30 mL of ice-cold 1M $CaCl_2$. Cell harvesting and resuspension was repeated three times. Final resuspension, aliquoting and storage were as described for 2.4.5.2.

2.4.5.4 Heat shock transformation

Aliquots of chemically competent cells (2.4.5.3) (50 µL or 100 µL) were defrosted on ice (~10 min) before exogenous DNA (2-10 µL) was added, adjusted for desired concentration. This transformation reaction mix was incubated on ice for one hour, heat shocked at 42°C in a water bath (1 min) and returned to ice (1 min) before the addition of 1 mL, pre-warmed (37°C), LB broth. Cells were incubated at 37˚C, 200 rpm, for a minimum of one hour before being spread on to the appropriate selective media.

2.4.6 *De novo* mutagenesis via the lambda (λ) red method

Deletion mutants were produced by replacing genes of interest with an antibiotic cassette (Figure 6) (Datsenko and Wanner, 2000). A linear PCR product (FRT-flanked resistance gene construct) was produced (2.4.6.2) and purified (2.4.3) before transformation (2.4.5.2) into an appropriate host strain (2.4.6.1). Following knockout mutant verification (2.4.6.3), P22 transfection into a clean genetic background (2.4.6.4) and selection for non-lysogens (2.4.6.5), long-term strain stocks were produced for each mutant strain (2.3.3).

2.4.6.1 Production of competent cells for mutagenesis

The helper plasmid pKD46 encodes the λ-red bacteriophage recombinase genes (*exo*, *bet*, *gam*) under the control of an *L*-arabinose inducible promoter ($_p$BAD). Via homologous recombination, this system allows replacement of a gene of interest with an antibiotic cassette of choice. An overnight culture (2.3.2) of SL1344 (or an alternative strain of interest) harboring pKD46 was produced (incubated at 30°C to maintain pKD46; this plasmid carries a temperature sensitive origin of replication) and used to inoculate (1% v/v) 50 mL LB broth containing Amp (100 µg/mL) and *L*-arabinose (1 mM). Cells

were incubated at 30˚C, 200 rpm, until an OD_{600} of 0.48-0.6 was reached, and harvested by centrifugation (4000 x *g*, 4°C, for 10 min). Cell pellets were gently resuspended in ice-cold 10% (v/v) glycerol (15 mL) and subjected to centrifugation as before. This process was repeated twice before a final resuspension in 1 mL ice-cold 10% (v/v) glycerol, allowing 10 x 100 µL aliquots in 1.5 mL microcentrifuge tubes. If not used immediately, competent cells were snap frozen in liquid nitrogen and stored at -80˚C.

2.4.6.2 Generation of FRT-flanked resistance gene construction

All mutagenesis primers are shown in Table 8. Primer pairs specific to the gene of interest, containing 40 bp homologous extensions flanking the gene of interest and 20 bp complementary to the 5' and 3' ends of the antibiotic cassette (Figure 6), were used to PCR amplify the FRT-flanked, antibiotic resistance cassette of plasmids pKD3 and/or pKD4 (2.4.1). Following purification (2.4.3) this product was used to transform the strain of choice harboring plasmid pKD46 (Figure 6; 2.4.5.1). Successful transformants were selected for by spread plating onto the appropriate media and incubating at 37˚C overnight.

2.4.6.3 Mutant verification

Knockout mutants were confirmed by colony PCR (2.4.2) and comparing the PCR product produced to that obtained for the isogenic parent strain. The antibiotic cassettes of pKD3 and pKD4 are of known sizes (Cm; 1300 bp and Km; 1700 bp respectively) allowing size comparison between the WT SL1344 gene and the cassette now replacing the gene in the mutant strain. Mutant verification primers are shown in Table 9. External verification primers of 20 bp lengths were designed 50-200 bp up-/downstream of the gene of interest, allowing amplification of the gene or antibiotic cassette, in WT and mutant strains respectively. Reverse complementary internal verification primers of 20 bp lengths amplify a 95-105 bp fragment within the gene of interest in the WT strain (Table 9), but do not produce a PCR product in the mutant strain due to gene absence. External and internal primer pairs were used in conjunction with internal, reverse complimentary

cassette primers (Table 9), to confirm presence and location of the antibiotic cassette.

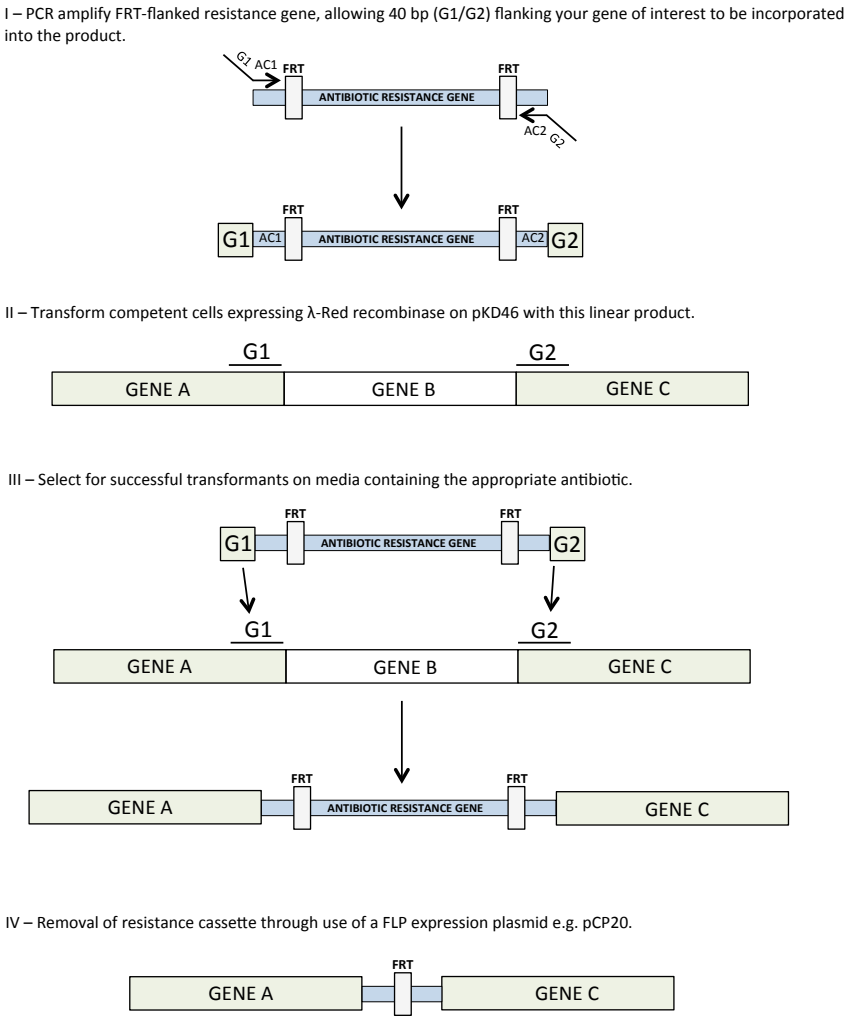

Figure 6: Representation of a simple gene disruption strategy. I – Primer composition for antibiotic cassette amplification; G1 and G2 corresponding to 40 bp homology extensions flanking your gene of interest, priming sites AC1 and AC2 are 20 bp homologous to 5' and 3' ends of the antibiotic resistance cassette of pKD3 (Cm^R) and pKD4 (Km^R) plasmids. II- Transformation of competent cells expressing λ-Red recombinase (encoded on pKD46) with PCR product allows (III) homologous recombination of this product and selection of successful transformants on appropriate selective media. IV) If required, the antibiotic cassette removed using a FLP expression plasmid. Adapted from Datsenko and Wanner (2000).

Table 8: Primers used for the production of knockout mutants

Gene	Forward Primer (5'-3')	Reverse Primer (5'-3')
baeR (PT4)	ATGACTGAATTACCCATTGATGAAAACACGCCGCGCATTTGTGTAGGCTGGAGCTGCTTC	CTTCCCAGCGATATCCCACCCCGTAGACCGCGCGTATAAACATATGAATATCCTCCTTAG
scsA	ATGGCGAAACAACAACGGATGGGCTGGTGGTTTCTTTGCCGTGTAGGCTGGAGCTGCTTC	TCATTCACGGAAGACACAAAATCGTAGATGTACCCGTAATCATATGAATATCCTCCTTAG
SL3009/SL3010	TAGCCGGAAGTACCGGTATTGTTCTGCTGTCTGCTGCAGCGTGTAGGCTGGAGCTGCTTC	TAACCCACGCCAAGATTAAAACCATTGCTATTAAGGCTTCCATATGAATATCCTCCTTAG
SL3646	ATGCAGCAATATATCGGTATTGATGTGGGAGGAACTCACGGTGTAGGCTGGAGCTGCTTC	TTAGCCTCGGTCGAGCTTTTGCTGCGCCAGCCAGACGGCGCATATGAATATCCTCCTTAG
STM3388	ATGCCGGTTAGTGAGTACAACCACATCCTTGTGGCGGTTTGTGTAGGCTGGAGCTGCTTC	TTATTTTGAGTTGATATTATATATTGACCTTGTGAATATACATATGAATATCCTCCTTAG
ydgEF	ATGTTTTACTGGATTTTATTAGCTCTGGCTATCGCGACTGGTGTAGGCTGGAGCTGCTTC	TCAGGCAAATTTGATCATGACCATTCCGGCGAGCAGCAATCATATGAATATCCTCCTTAG
yncJ	ATGCTTACAAAAACGTTATCAGTAGTTTTACTGACCTGTGGTGTAGGCTGGAGCTGCTTC	ATAGCTTTCTGGTTTGCGCGATTTCTGCCAGTTGTGGTGCCATATGAATATCCTCCTTAG
Δ*yqaE*	ATGGGTTTCTGGAGAATTGTATTTACGATTATTTTGCCTCGTGTAGGCTGGAGCTGCTTC	TTAATGACGCATCTGAACCCAAAATGCGTGGATAAGCCCCCATATGAATATCCTCCTTAG
Δ*zraSR*	GGGGCTATTTTCCATTATGGTCATTCGCGACTATGGCCGTGTGTAGGCTGGAGCTGCTTC	GCAGCGTTTTGCGCGTAATGCCCAATTGACGGGCGGCTTCCATATGAATATCCTCCTTAG

Table 9: Primers used to verify the production of knockout gene mutant strains

Gene	Forward Primer (5'-3')	Reverse Primer (5'-3')
baeR (PT4)	CATTACAGTAGAGTTACCGC	TACCAGGCGACACGCATCCG
scsA	GCGCCAGTGGCTAAGATAAC	CTCACCGTTAGCGGACGTAT
SL3009	CTTTGTGGAGATGATGGATT	ATACAGCAGGCTGGGGGATA
SL3009/SL3010	CTTAATACATGCCAGTAAGG	AATCCATCATCTCCACAAAG
SL3646	AAAGAATTCCGATTTACCGCCTAACTCCA	TTATCGCACGGCGATGTAAC
stm3388	AAAGAATTCCAAAAGCCGTATCGTCTGGT	CCCACAAGTTATGATCTTTATAAGC
ydgEF	AAATCTAGAAATTCGGCATCGGGTCATCC	GCTATATCCGTCACCGGCTTTCGCG
yncJ	ATTGGCATCATAGCCTCACG	TTCAGTGAGCCCTGAAGCGC
yqaE	AAAGAATTCAGCCCATAATAACCCCAAGC	GCGGTTACCGCGTCCCAGAGTTT
zraSR	ATACGATTACATAAAGATGC	AAACTAACGGCTGAGTTTAG
Internal Antibiotic Cassette Primers		
pKD3_REV*		TTATACGCAAGGCGACAAGG
pKD4_REV*		CAGTCATAGCCGAATAGCCT

*REV, reverse compliment primer

2.4.6.4 P22 transduction

Transduction using bacteriophage P22 is required to prevent additional undesirable recombination events, once gene deletion in a SL1344 pKD46 strain is accomplished. This process involves three stages: production of donor strain (verified knockout mutant) lysate, transduction of a recipient strain (WT SL1344 in this case) with the lysate and selection for stable, non-lysogens following transduction.

2.4.6.4.1 Lysate production of donor strain

An overnight culture (2.3.2) of the verified knockout mutant (2.4.6.3), containing the appropriate selective antibiotic, was sub-cultured (1% v/v inoculum) in 10 mL LB broth and incubated at 37°C, 200 rpm, for one hour. To this, 20 µL of bacteriophage P22 lysate was added and incubation continued for six additional hours. Cultures were transferred to a chloroform resistant tube (Falcon™ 15 mL conical centrifugation tube) and 1 mL of chloroform added, was gently mixed by inversion and incubated at 4°C for a minimum of two hours. Cell debris was pelleted by centrifugation (4000 x *g*, 4°C, 15 min) and the supernatant (lysate) transferred to a new Falcon™ tube without disturbing the chloroform phase and stored at 4°C.

2.4.6.4.2 Transduction of recipient strain with lysate

From overnight cultures of our recipient strain (e.g. SL1344) (2.3.2), 100 µL was taken for use in transduction. To this aliquot, 10 µL of lysate (2.4.6.4.1) was added and the reaction incubated at 37°C for 45 min. Cells were spread on to LB agar (1.5% w/v) plates, containing the appropriate antibiotic, and incubated overnight at 37°C. Streak plates of non-transduced recipient strain cells and pure lysate were used as negative controls.

2.4.6.4.3 Detection of lysogens using UCB indicator (green) plates

A selected number of colonies produced from transduction (2.4.6.4.2) were streaked on to UCB indicator plates (Bochner, 1984), commonly referred to as green plates, and incubated overnight at 37°C. Green plates allow for selection of non-lysogens due to the high concentration of glucose present in the media. *Salmonella* ferment the glucose during growth producing an

acidic environment. In the presence of lysing cells, pH indicator within the media turns dark green, allowing light green/white, non-lysing, stable mutants to be selected for and streaked onto their respective antibiotic containing LB agar (1.5% w/v). Mutants were verified as described in 2.4.6.3.

2.4.6.5 Antibiotic resistance cassette removal

Removing an antibiotic cassette is required to produce multiple gene knockouts, or to ensure removal of the gene of interest did not result in transient effects on the transcription of downstream genes. The FLP-recombinase encoded on the pCP20 plasmid allowed for removal of the antibiotic cassette between the flippase recognition target (FRT) sites (Figure 6) by site-directed recombination.

The temperature sensitive plasmid pCP20 was introduced into the strain of interest by electroporation (2.4.5.1) and recovered at 30˚C, 200 rpm, in LB containing Amp. Cultures were spread onto LB agar (1.5% w/v), containing Amp, and incubated overnight at 30˚C. From this plate, single colonies were picked to 10 mL LB and incubated at 43˚C overnight. This overnight culture was diluted to 10^{-6}, spread onto LB agar (1.5% w/v) and incubated at 37˚C for 12 hours minimum. Single colonies were patched consecutively onto three types of LB agar (1.5% w/v): LB plus the antibiotic of the cassette being removed, LB plus Amp and LB only, in that order. Only strains which had lost their antibiotic resistance; those which only grow on LB, were taken forward.

2.4.7 DNA electrophoresis

Separation, visualisation and analysis of the size and quality of PCR products and other DNA fragments was conducted using 1% (w/v) agarose gel electrophoresis, prepared using 1 x TBE electrophoresis buffer, unless otherwise stated (Appendix D for buffer compositions). Agarose gels contained 2 µg/mL ethidium bromide. DNA loading buffer (5x) (BIOLINE) was adding to samples prior to loading (1:5) where required and 1 kb Hyperladder (BIOLINE) or 100 bp ladder (NEB) were used as size markers. Electrophoresis occurred at 110 V (Sub-Cell GT electrophoresis system,

BIOLINE) for 30-45 min, unless otherwise stated and visualisation of DNA was by UV-light, using a Molecular Imager® Gel Doc™ System (BIO-RAD).

2.4.8 Extraction of DNA from agarose gels

Following agarose gel electrophoresis of restriction enzyme digested vector or PCR product; extraction of said DNA fragments from agarose gel was sometimes required. Allowing for removal of impurities, unwanted DNA of an incorrect size or undigested vector from the sample, gel extraction was conducted using a QIAquick™ Gel Extraction Kit (QIAGEN) as per manufacturer's instruction. Final elution of extracted and washed DNA from QIAquick™ Spin Columns was in 50 µL nuclease-free dH_2O and analysed for concentration and purify on a NanoDrop 2000c UV-Vis spectrophotometer (Thermo Scientific; software NanoDrop 2000, Thermo Scientific). Samples were stored at -20°C.

2.4.9 Site-directed mutagenesis (SDM)

Specific amino acids of ZraP were mutated at the codon level using a QuikChange® Lightning Site-Directed Mutagenesis Kit (Agilent Technologies), as per manufacturer's instruction. In brief, mutant strand synthesis occurred using SDM primers (Table 11; Appendix E) incorporated into the PCR product. PCR reagents and programme used are outlined in Table 10 and Table 7 respectively. Template DNA, parental methylated and hemi-methylated DNA, not containing the desired mutation were removed through *Dpn I* enzyme digestion; 1 µL of *Dpn I* enzyme and 4 µL of buffer were added to the SDM reaction, mixed by flicking and incubated (37˚C, up to one hour). The remaining undigested mutated plasmid was transduced into electrocompetent XL10-Gold® Ultracompetent Cells provided with the SDM kit. The control plasmid pUC18 was used to assess transformation efficiency. Successful SDM constructs were confirmed by plasmid purification (2.4.4) and sequenced (Eurofins MWG Operon Value Read) using specifically designed sequencing primers (Table 5).

2.4.10 Complementation studies

In order to verify phenotypes of deletion mutants, the genes of interest were cloned into the low-copy number protein expression vector pBAD/*Myc* His A (Invitrogen) (without a C-Terminal 6xHis Tag; native STOP codon of the gene remained intact) under the control of the plasmid's *L*-arabinose inducible promoter.

Genes were amplified by PCR (2.4.1) using primers in Table 4, incorporating desired restriction enzyme sites at the 5' and 3' ends (see Appendix F for all restriction enzymes used). PCR product and vector were subjected to double restriction enzyme digests (Table 12), with the appropriate enzymes, for a minimum of one hour, at 37°C, producing overlapping sticky ends. Digested products were purified by PCR purification (2.4.3) or gel electrophoresis (2.4.7) and gel extraction (2.4.8), and ligated into pBAD/*Myc* His A using T4 DNA ligase 1U/µl (Invitrogen) (2.4.10.1; Table 13). Electrocompetent recipient cells, i.e. *E. coli* TOP10 (Invitrogen), were prepared and transformed by heat shock (2.4.5.3) with 10 µL of ligation reaction. Cells were also transformed with undigested vector as a positive control to assess transformation efficiency. Successful transformants were selected for on LB agar (1.5% w/v) plates containing Amp, confirmed by plasmid extraction (2.4.4) and sequencing (Eurofins MWG Operon Value Read) using specifically designed sequencing primers (Table 7). The confirmed construct was transduced into the desired mutant strain (2.4.5.2).

2.4.10.1 Ligations

Ligation ratios were calculated using an online calculation tool (http://www.insilico.uni-duesseldorf.de/Lig_Input.html) (Table 13). Ligation reactions were as per manufacturers' instruction (Table 13) and ligation products were stored at 4°C. Vector only (religation control), insert only and minus T4 DNA ligase reactions were included as negative controls.

2.4.11 Spot plates

Overnight cultures (2.3.2) of the investigative strains, including SL1344 WT as a comparative control, were serial diluted 10-fold in 1 x PBS to 10^{-8} using

aseptic technique. LB agar (1.5% w/v) plates (control) and the same media containing the compound of interest, stated within the relevant results chapter(s), were prepared and 10 µL of appropriate overnight dilutions (typically 10^{-3} to 10^{-8}) spotted consecutively onto control and test media. After drying at RT, spot plates were incubated (37˚C, 12 hours minimum) until single colonies were visible. CFU mL^{-1} was calculated by multiplying colony numbers by the dilution rate. Survival percentages were calculated from CFU mL^{-1} to allow comparisons to SL1344 WT controls. All spot plates were conducted in biological triplicate, as a minimum, to allow for statistical analysis.

Table 10: PCR reagents and reaction composition for site-directed mutagenesis

Reagent	Volume (µL)
QuikChange® Lightning Mutagenesis Reaction	
10X QuikChange Lightning Buffer	5
dNTP Mix	1
QuikSolution Reagent	1.5
Forward SDM Primer [125 ng]	1
Reverse SDM Primer [125 ng]	1
dsDNA Template - p*zraP*6xHIS [100 ng/uL]	2
Nuclease-free dH_2O	37.5
QuikChange Lightning Enzyme	1
QuikChange® Lightning Control Reaction	
10X QuikChange Lightning Buffer	5
dNTP Mix	1
QuikSolution Reagent	1.5
Control Primer #1 [125 ng]	1.25
Control Primer #2 [125 ng]	1.25
pWhitescript 4.5 kb plasmid [5 ng/uL]	5
Nuclease-free dH_2O	34
QuikChange Lightning Enzyme	1

Table 11: Site-directed mutagenesis primers for mutation of specific amino acid residues within *zraP*

Primers	Residues Mutated	Sequence (5'-3')
ATTEQ_FWD	L44A	GGAGGTAGCCCGGCAACTACGGAACAGCAGGCGACGGCG
ATTEQ_REV		CGCCGTCGCCTGCTGTTCCGTAGTTGCCGGGCTACCTCC
LATEQ_FWD	T45A	GGAGGTAGCCCGTTAGCTACGGAACAGCAGGCGACGGCG
LATEQ_REV		CGCCGTCGCCTGCTGTTCCGTAGCTAACGGGCTACCTCC
LTTEQ-A_FWD	L44A, T45A, T46A, E47A, Q48A	GGAGGTAGCCCGTTAACTACGGAAGCGCAGGCGACGGCG
LTTEQ-A_REV		CGCCGTCGCCTGCGCTTCCGTAGTTAACGGGCTACCTCC
HRGGGH-A_FWD	H130A, R131A, G132A, G133A, G134A, H135A	GCTATGGCGGCGGTTATGCTCGCGGCGGCGGTCACATGGGTATGG
HRGGGH-A_REV		CCATACCCATGTGACCGCCGCCGCGAGCATAACCGCCGCCATAGC
HRGGAH_FWD	G134A	GCTATGGCGGCGGTTATCATCGCGGCGGCGCTCACATGGGTATGG
HRGGAH_REV		CCATACCCATGTGAGCGCCGCCGCGATGATAACCGCCGCCATAGC
HRGGGA_FWD	H135A	GCTATGGCGGCGGTTATCATCGCGGCGGCGGTGCCATGGGTATGG
HRGGGA_REV		CCATACCCATGGCACCGCCGCCGCGATGATAACCGCCGCCATAGC

Table 12: Double restriction enzyme digestion of PCR amplified insert DNA and plasmid DNA.

Component	Volume (µL)	
	Insert DNA/PCR Product	*Vector/Plasmid DNA*
DNA	1 µg	1 µg
[¥]Enzyme I	1	1
[¥]Enzyme II	1	1
10 x Restriction Enzyme Buffer H	2	5
dH_2O	Σ20	Σ50
Temperature	*37°C*	*37°C*
Time	*3-12* hours*	*3-12* hours*

* A maximum of 12 hours digestion time was adopted only if both enzymes used did not exhibit star activity.
[¥]All restriction enzymes used during this work and their cut site sequences are listed in Appendix F.

Table 13: Reaction composition and conditions for ligations.

Component	Volume to Add (µL)					
Insert: Vector (Molar Ratios)	*1:1*	*1:3*	*1:5*	[§]*Vector Only* (1uL)	[§]*Insert Only* (1uL)	[§]*Ligase Only* 0
5 x T4 DNA Ligase Reaction Buffer	4	4	4	4	4	4
dH_2O	Σ20	Σ20	Σ20	Σ20	Σ20	Σ20
T4 DNA Ligase	0.5	0.5	0.5	0.5	0.5	0.5
Temperature	*16°C*	*16°C*	*16°C*	*16°C*	*16°C*	*16°C*
Time	*Overnight*	*Overnight*	*Overnight*	*Overnight*	*Overnight*	*Overnight*

[§]Control ligations; religation control, insert DNA control and ligase enzyme only.

2.4.12 Disc diffusion assays

Top agar plates were produced for all strains of interest, including SL1344 as a comparative control. From overnight cultures (2.3.2), 10 mL fresh LB were inoculated (10% v/v) and incubated for one hour at 37˚C, 200 rpm. LB agar (0.75% w/v), pre-warmed to ~60˚C, was aliquoted into sterile 5 mL Bijou tubes in 4 mL volumes, and kept molten in a 50˚C water bath. To ensure the LB agar temperature was not too high, Bijou tubes were removed from the water bath and left to cool at RT for 2-3 min before the addition of 100 µL of the 10% subculture. This molten agar culture was immediately poured over pre-set 1.5% (w/v) LB agar plates and left to set at RT.

Sterile Whatman® antibiotic assay discs (6 mm) were aseptically placed onto pre-poured and set top agar plates and impregnated with 10 µL of the compound of interest, stated where appropriate in the corresponding results chapter(s). Plates were incubated at 37˚C for a minimum of 12 hours and the zone of inhibition (mm^2) recorded. All assays were conducted in biological and technical triplicate, as a minimum, to allow for statistical analysis.

2.4.13 β-Galactosidase assays

Overnight cultures (2.3.2), supplemented with Tet, of SL1344 WT and deletion mutants harbouring *lacZ* fusion constructs (Table 4) or empty pMP220 vector (background control) were inoculated (1% v/v) into fresh 50 mL LB broth and incubated at 37°C, 200 rpm, for the duration of the experiment. Samples were taken at times corresponding to lag, early-log, mid-log, late-log and stationary phases of growth. The OD_{600} of these samples were measured and a sample of culture permeabilised with Z-buffer (Appendix D) to a final volume of 1 mL. Permeabilised cultures were supplemented with 1 drop of 0.1% SDS in 1 x PBS and 2 drops of chloroform from a Pasteur pipette. Following incubation (30°C, 5 min), 200 µL of ONPG (4 mg/mL) solution (Appendix D) was added and the reaction proceeded at 30˚C. At the initiation of *o*-nitrophenol production (yellowing of the solution), 400 µL of 1M Na_2CO_3 was added to increase pH and cease the reaction. The suspension was centrifuged (2 min, 14,800 x *g*) to remove cell debris and the OD_{420} measured immediately on a SpectraMax M5

spectrophotometer (Molecular Devices), referenced with Z-buffer. β-galactosidase activity was determined in Miller units, using the equation of Zhang and Bremer (1995). Background readings from the empty pMP220 containing cultures were subtracted to determine an accurate level of expression. All assays were conducted in triplicate, as a minimum, to allow for statistical analysis.

2.4.14 Long-term carbon starvation survival (LT-CSS) assays

LT-CSS assays were conducted as described in Kenyon et al. (2002). Overnight cultures (2.3.2) of SL1344 and deletion mutants were diluted 1:100 into 4 mL high carbon (HiC) MOPS media, grown for approximately five hours (37°C, 200 rpm) and normalised to 0.35 OD_{600}. Normalised culture was used to inoculate (10% v/v) carbon-free (NoC) MOPS, and incubated as previosuly. Samples were collected at regular periods over 21 days and plated, in triplicate, onto LB agar (1.5% w/v) to determine CFU mL^{-1}, with the maximum viability typically around 5 x 10^8 CFU mL^{-1}.

2.4.15 Carbon starvation induced cross-resistance (CSIXR) assays

The method of Kenyon et al. (2002) was used to assay CSIXR to heat and polymyxin B (PmB). Overnight cultures (2.3.2) of SL1344 WT and selected deletion mutants were used to inoculate low-carbon (LoC) MOPS defined media (1% v/v), and incubated (37°C, 200 rpm), for ~29 hours to generate 24 hour carbon-starved cells: the additional five hours incubation was required to allow all remaining, available carbon to be exhausted. These cultures were diluted 1:100 into HiC MOPS and grown for approximately five hours to allow cells to enter exponential phase of growth. These exponential and carbon-starved cells were normalised to an OD_{600} of 0.35 and diluted 1:100 into M9 minimal salts buffer (Appendix C). An initial sample was taken to determine the viable cell count (usually ~3-5 x 10^6 CFU mL^{-1}) before cells were exposed to high temperature stress (55˚C, 16 min) or PmB (0.1 mg/mL, one hour). Upon completion, samples were collected and spread at appropriate dilutions (~ 10^{-3} to 10^{-5}) onto LB agar (1.5% w/v), in triplicate, to determine CFU mL^{-1}. Initial and final CFU mL^{-1} were calculated by counting the number of colonies following overnight incubation (37°C) of spread plates.

2.4.16 Protein purification

Proteins were tagged with a 6xHis C-terminal or 10xHis N-terminal epitope and purified from whole cell lysate, post overexpression, using a 1 mL capacity HisTrap™ HP column (GE Healthcare Life Sciences) on an ÄKTAFPLC (GE Healthcare Life Sciences). Genes were cloned into overexpression vectors under the control of *L*-arabinose or IPTG inducible promoters or sub-cloned from GenScript synthesised constructs (Table 4).

2.4.16.1 Test expression assay

Small-scale test expression assays were conducted to ascertain stable and high yielding conditions for recombinant protein overexpression. Overnight cultures (2.3.2), supplemented with Amp (100 µg/mL), of host strains harbouring the overexpression construct (Table 4) and empty vector controls were used to inoculate 10 mL LB broth (1% v/v) containing Amp (50 µg/mL), in quintuplicate, and labelled sequentially 1-5. Cultures were incubated (37°C, 200 rpm) for three hours or until 0.5-1 OD_{600}. 'Zero time point' samples were taken by collecting 1 mL samples from each culture; cells were harvested by centrifugation (2 min, 14,800 x *g*) and the supernatant removed prior to storing pellets at -20°C. Four 10-fold serial dilutions of the inducer, 20% *L*-arabinose (20% - $2x10^{-3}$%) or IPTG (1 M-0.1 mM) in sterile dH_2O, were aseptically produced and added to the quintuplicate cultures (Table 14). Cultures were incubated for four hours (37°C, 200 rpm) and 1 mL samples collected and harvested as per 'zero time point' samples. Cell pellets were snap frozen and stored at -20°C.

2.4.16.1.1 Expression sample analysis by SDS-PAGE

To confirm overexpression and stability of recombinant proteins prior to large-scale purification, samples (both *L*-arabinose and IPTG induced) were analysed by SDS-PAGE (2.4.16). Sample cell pellets were defrosted on ice (or analysed immediately post collection) and resuspended in 50 µL SDS loading buffer (Appendix D) containing β-mercaptoethanol (1:19) before boiling (100°C, 5 min). Cell debris was pelleted by centrifugation (30 sec, 14,800 x *g*) and 5-10 µL of sample loaded onto SDS-PAGE gels (15% v/v acrylamide) with 3 µL PageRuler™ Prestained Protein Ladder (Thermo

Table 14: ***L*-arabinose and IPTG titration used during test expression assays**, to ascertain appropriate inducing conditions for recombinant protein overexpression

Culture	Volume to Add (µL)	Stock Solution	Final Concentration
L-arabinose		*(%)*	*(%)*
1	100	20	0.2
2	100	2	2×10^{-2}
3	100	0.2	2×10^{-3}
4	100	2×10^{-2}	2×10^{-4}
5	100	2×10^{-3}	2×10^{-4}
IPTG		*(mM)*	*(mM)*
1	100	1000	10
2	100	100	1
3	100	10	0.1
4	100	1	10^{-2}
5	100	0.1	10^{-3}

Scientific) as a marker. Samples were electrophoresed (180 V, one hour) in 1 x TGS running buffer (Appendix D) using Mini-PROTEAN® Tetra Cell systems (BIO-RAD), and stained with SimplyBlue™ SafeStain Coomassie® G-250 (Life Technologies) (RT, one hour minimum) with gentle agitation. Gels were imaged using white light on a Molecular Imager® Gel Doc™ System (BIO-RAD).

2.4.16.2 Large-scale cell harvest

Once protein overexpression conditions had been established through test expression assays (2.4.15.1), the appropriate conditions were repeated with a larger volume of culture to maximise protein yield. Overnight cultures (2.3.2), supplemented with Amp, were produced in 20 mL volumes and used to inoculate (2% v/v) 1 L LB broth containing Amp in 2 L conical flasks. Cultures were incubated (37˚C, 200 rpm), and 1 mL samples harvested after three hours growth, as described in 2.4.15.1. Overexpression was induced upon the addition of 10 mL *L*-arabinose or 10 mL IPTG at an appropriate concentration determined in 2.4.15.1. Cultures were incubated for a further four hours (37°C, 200 rpm) before 1 mL samples were collected and analysed by SDS-PAGE, as described previously (2.4.15.1 and 2.4.15.1.1 respectively), to confirm overexpression and stability of recombinant proteins

at these larger volumes. Remaining culture was transferred to 95 x 191 mm, 1 L volume polycarbonate centrifugation bottles (Beckman Coulter) and cells harvested by centrifugation (12 min, 6100 x *g*, 4°C) in a Beckman Coulter Avanti® J-20 high performance centrifuge using a JLA-8.1000 rotor (Beckman Coulter). Cell pellets were transferred to 50 mL Falcon™ conical centrifugation tubes, snap frozen and stored at -20°C.

2.4.16.3 Cell lysate collection and fast protein liquid chromatography (FPLC)

Cell pellets (2.4.15.2) were defrosted on ice and resuspended in 20 mL 1 x PBS with two cOmplete, mini, EDTA-free® protease inhibitor cocktail tablets (Roche), 40 µg DNase I and 50 mg lysozyme. Samples were subjected to three passes through French® Press and lysate centrifuged in an Eppendorf® 5804R, (10,600 x g, 30 min, 4°C) to remove cell debris. After centrifugation, His-tagged protein was purified from the supernatant through binding to a HisTrap™ HP column (GE Healthcare Life Sciences) on a ÄKTAFPLC (GE Healthcare Life Sciences), and eluted in 1 mL fractions across a 1 x PBS/imidazole (0-300 mM) gradient. Protein quality and purity was ascertained by SDS-PAGE (2.4.16); 10 µL of fractions were diluted in 50 µL SDS loading buffer, and treated as described in 2.4.15.1.1 prior to imaging.

2.4.16.4 Protein concentration and buffer exchange

Protein fractions (2.4.15.3) of sufficient purity (2.4.16), were combined and concentrated using Amicon® Ultra-15 Centrifugal Filter Units (10,000 NMWL) (4000 x *g*, RT), to approximately 500 µL. Protein samples were diluted in 10 mL of their desired storage buffer; HEPES 50 mM (ZraP and recombinant versions) and CpxR storage buffer (Appendix D) (CpxR) and again concentrated to ~500 µL as previously. This process was repeated three times before a final concentration to 500 µL – 1 mL, aliquoted into appropriate volumes, snap frozen and stored at -20˚C or -80˚C. Protein concentration was determined through A_{280} analysis using a NanoDrop 2000c UV-Vis spectrophotometer (Thermo Scientific), Bradford assay (2.4.19) and/or by Qubit™ Protein Assay Kits with a Qubit® 2.0 Fluorometer (Invitrogen), as per manufacturer's instruction. Western Blotting (2.4.18)

confirmed protein presence and the lack of contaminants (≥ 95% purity) confirmed by SDS-PAGE (2.4.16)

2.4.17 SDS polyacrylamide gel electrophoresis (SDS-PAGE)

SDS-PAGE allows denatured proteins to be separated according to size along an acrylamide gel matrix. A standard resolving gel of 15% (w/v) ProtoGel™, Acrylamide/methylene Bis-Acrylamide solution (37.5:1 ratio) (National Diagnostics) and a stacking gel (5% w/v), was used throughout this research (Table 15), cast using Mini-PROTEAN® Tetra handcast systems (BIO-RAD) (0.75 mm and 1 mm combs and integrated spacer plates) and left to polymerise at RT, 30 min minimum. Gels were electrophoresed at 180 V in 1 x TGS running buffer (Appendix D) using Mini-PROTEAN® Tetra Cell systems (BIO-RAD) (~1 hour) and stained with SimplyBlue™ SafeStain Coomassie® G-250 stain (Life Technologies) as per manufacturer's instruction. Gels were imaged using white light on a Molecular Imager® Gel Doc™ System (BIO-RAD).

2.4.18 Native PAGE and formaldehyde chemical cross-linking of protein oligomers

Native polyacrylamide gels (6% acrylamide w/v) (Table 16) as SDS-PAGE gels (2.4.16) (1 mm combs and integrated spacer plates) and left to polymerise at RT for one hour minimum. Protein samples (1 mg/mL) in 20 µL volumes were treated with 1% (v/v) formaldehyde (pH 8) for 1 min. The reaction was terminated upon 2 M glycine addition, before 10 µL SDS loading buffer was added. Of this sample, 10 µL was loaded on to native polyacrylamide gels (pre-run at 120 V, 15 min) and electrophoresed at 120 V in 1 x TBE running buffer (Appendix D) using Mini-PROTEAN® Tetra Cell systems (BIO-RAD) (~1 hour). Gels were stained and imaged as described 2.4.16.

Table 15: Components and composition of SDS polyacrylamide protein gels

Component	Stock Solution	Volume	Final Concentration
Resolving Gel			
Acrylamide/Bis-Acrylamide	30% (w/v)	10 mL	15%
[*]Tris-HCl, pH 8.8	1.5 M	5 mL	375 mM
[*]SDS	10% (w/v)	100 µL	0.05%
dH_2O		4.795 mL	
[§]TEMED	>99%	5 µL	0.5%
[§*]APS	20% (w/v)	100 µL	0.1%
Stacking Gel			
Acrylamide/Bis-Acrylamide	30% (w/v)	1.66 mL	5%
[*]Tris-HCl, pH 6.8	0.5 M	1.26 mL	63 mM
[*]SDS	10% (w/v)	50 µL	0.05%
dH_2O		6.975 mL	
[§]TEMED	>99%	5 µL	1%
[§*]APS	20% (w/v)	50 µL	0.1%

* Solubilised in dH_2O. [§] Reagents added directly before gel casting; catalyse polymerisation of acrylamide.

Table 16: **Components and composition of native polyacrylamide protein gels**.

Component	Stock	Volume	Final Concentration
Acrylamide/ Bis-Acrylamide	30% (w/v)	3.96 mL	6%
TBE Buffer	10 x	2 mL	1 x
dH_2O		13.93 mL	
[§]TEMED	>99%	10 µL	0.5%
[§*]APS	20% (w/v)	100 µL	0.1%

2.4.19 Western blot

2.4.19.1 Membrane transfer, Ponceau red staining and membrane blocking

Protein samples were subjected to SDS-PAGE (2.4.16; 2.4.15.1.1) prior to nitrocellulose Biodyne A membrane (Pall Corporation) transfer in a Trans-Blot® SD Semi-Dry Transfer Cell (BIO-RAD). Three layers of blotting paper, equal size to the gel, were soaked in 1 x transfer buffer (Appendix D) and placed on the transfer cell anode plate. Nitrocellulose membrane was soaked in 100% methanol (1 min), followed by washing in transfer buffer (5 min), and placed on top of the blotting paper. The SDS polyacrylamide gel of proteins to be transferred was placed on top of the membrane, followed by three more layers of soaked blotting paper before transfer took place (10 V, one hour). The membrane was briefly washed in 1 x TBS and stained with Ponceau Red (1:10 of 2% w/v) Ponceau S in 30% trichloracetic acid and 30% sulfosalicylic acid) to confirm transfer. To de-stain, the membrane was washed in dH_2O until clear. A blocking solution of 5% (w/v) fat-free skimmed milk powder in 1 x TBST (Appendix D) was poured over the membrane and incubated (RT, ~1 hour with gentle agitation).

2.4.19.2 Antibody staining and blot imaging

Anti-His antibody, conjugated to horseradish peroxidase (HRP), (QIAGEN) was diluted 1:20,000 in blocking solution (5% w/v fat-free skimmed milk powder in 1 x TBST.) The membrane was incubated in 20 mL of this antibody suspension (RT, one hour with gentle agitation) and washed three times in 1 x TBST (10 min) with gentle agitation. His-tagged proteins were detected using a luminol-based chemiluminescent detection system (QIAGEN).

2.4.20 Bradford assay

The Bradford dye-binding method (Bradford, 1976), provides a simple technique for the quantification of protein at low concentrations by comparing protein samples of unknown concentration to a standard curve produced from BSA samples of known concentration. Bovine serum albumin (BSA)

standards (from 1 mg/ml stock in dH_2O) and unknown samples were diluted in Bradford Dye Reagent solution (BIO-RAD) and dH_2O (Table 17) in 1.6 mL cuvettes (semi-micro disposable polystyrene 10 mm path length; Fisherbrand) and mixed by inverting. Absorbance was measured at A_{595} and a standard curve produced by plotting BSA standards A_{595} values against their known protein concentration (mg/mL). Using this, the protein concentration of unknown samples was deduced from their A_{595} values.

Table 17: **Composition of Bradford assay reaction** mix, BSA standards for production of a standard curve and unknown samples to be tested

Sample	BSA (µL)	dH_2O (mL)	Bradford Reagent (mL)
†*Standards*			
1	0	0.8	0.2
2	1	0.8	0.2
3	5	0.795	0.2
4	10	0.790	0.2
5	20	0.780	0.2
6	40	0.760	0.2
	*Unknown Sample**		
As many as required	*2*	0.78	0.2

*Unknown sample volume can be increased as required to produce a sufficient colorimetric change if low protein concentration is present. †Increase concentration of standards as required.

2.4.21 Electrophoretic motility shift assays (EMSAs)

2.4.21.1 CpxR phosphorylation

Phosphorylation of His_{10}-CpxR was conducted as described by Hung et al. (2001) with minor alterations. CpxR (100 pmol) was incubated in phosphorylation buffer (100 mM Tris [pH 7.5], 10 mM $MgCl_2$, 125 mM KCl, 50 mM acetyl phosphate [lithium potassium salt; Sigma]) (30˚C, one hour) in a final volume of 50 µL.

2.4.21.2 EMSA 6-FAM™-fluorescein Labelled Probe Production

Fluorescently labelled DNA probes were generated by PCR amplification of target gene promoters (~200-400 bp in length, upstream of the initiation codon) using sequence specific oligonucleotides (Table 18). Positive and negative control probes were produced by amplifying the promoter region of

cpxP, known to contain a CpxR binding site with CpxR binding previously confirmed (positive control), and *wraB*, a gene whose expression levels are not influenced by CpxR and promoter region does not contain a proposed or known CpxR binding motif (negative control). Following purification (2.4.3), PCR products were diluted 1:50 to minimise carry-over of unlabelled DNA. Universal 6-FAM™-fluorescein labelled primers (Table 18) were used to amplify 1:50 template DNA during a second round of PCR, producing 6-FAM™ labelled probes. Labelled probes were purified as previously described (2.4.3) before use in EMSA reactions.

2.4.21.3 EMSA reaction and gel imaging

EMSAs were as described by Shimada et al. (2013), with minor alterations, because this protocol had successfully determined factors that affect the strength and specificity of CpxR-P:DNA binding e.g. buffer ionic strength, pH, appropriate glycerol and Mg^{2+} concentrations. Phosphorylated CpxR (CpxR-P) at various concentrations (2.4.20.1) were incubated (30˚C, one hour) with 6-FAM™ tagged probes (0.5 pmol) in EMSA buffer (10 mM Tris-HCl [pH 7.5], 10 mM NaCl, 1 mM $MgCl_2$, 1 mM EDTA [pH 8.0], 5 mM DTT, 5% glycerol and 30 mM acetyl phosphate) (Table 19). Poly(dIdC) was used as a non-specific binding competitor. DNA loading dye solution (40% glycerol, 0.025% bromophenol blue, 0.025% xylene cyanol) (1:5) was added and the reaction immediately subjected to native PAGE (2.4.17) in 1 x TBE buffer (30 mA, 4°C). Gels were visualised using a Typhoon FLA 9500 laser scanner (GE Healthcare) with LBP/BPB1 emission filter, Ex_{max} 495 nm Em_{max} 576 nm, at 50 µM resolution. A Typhoon FLA 9500 laser system and filters provided results comparable in resolution and sensitivity to those obtained for radiolabelled probes. Bromophenol blue can bind to proteins and inhibit some binding reactions, however no such issues were observed under the conditions tested here. Poly(dI•dC) was added to all reactions unless otherwise stated, ensuring CpxR-P binding to labelled probes was specific. This commonly used polymer provided an excess of non-specific binding sites to out-compete any low-affinity binding.

Table 18: **Composition of EMSA reactions** in the presence and absence of poly(dIdC)

CpxR-P (pmol)	EMSA Buffer (µL)	Fluorescein labelled probe (pmol)	Poly(dIdC) [1 µg/µL] (µL) Minus	Plus	dH_2O
0	9.8	0.5	0	1	Σ20
25	9.8	0.5	0	1	Σ20
50	9.8	0.5	0	1	Σ20

2.4.22 RNA extraction and analysis

2.4.22.1 Cell harvesting

To stabilise mRNA, four OD units of cells were incubated on ice (30 min), in a 5:1 ratio of phenol ethanol solution (5% v/v phenol [pH 4.3], 95% v/v ethanol). Samples were centrifuged (4000 x *g*, 10 min, at 4°C), the supernatant removed and the cell pellet resuspended in the residual liquid before being transferred to pre-chilled, RNAse-free 1.5 mL microcentrifuge tubes. Remaining residual liquid was removed following a 1 min centrifugation (14,800 x *g*) and pellets frozen at -80°C.

2.4.22.2 Chromosomal DNA and total RNA extraction, purification, quality and quantity assessment

Chromosomal DNA was isolated from 10 mL SL1344 overnight culture (2.3.2), using a Genomic DNA isolation kit (QIAGEN). Total RNAs were isolated using a SV Total RNA Isolation kit (Promega) and treated with Turbo DNA-*free*™ (Ambion Life Technologies) as per manufacturer's instruction. Sigma H_2O (50 µL) was used during final elution for both extraction methods. Chromosomal DNA was stored at -20°C. RNA samples were snap frozen and stored at -80°C. An RNA aliquot (5 µL) was removed prior to storage for quality and quantity assessments, preventing repeated freeze-thaw of RNA samples, which increases the risk of RNA damage and subsequent degradation.

Table 19: Oligonucleotides used to produce 6-FAM™-fluorescein labelled probes for use in EMSA reactions with CpxR-P

Gene	Forward Primer (5'-3')	Reverse Primer (5'-3')
Controls		
cpxP	CTAAAACGACGGCCAGTAGGGAAGTCAGCTCTCGGTC	CAGGAAACAGCTATGACTGCTCCCAAAATCTTTTCTG
wraB	CTAAAACGACGGCCAGTTGCGCCATGGTTTCAATGTG	CAGGAAACAGCTATGACACGTCGTAGTAGGCCGCTTAC
Unknown Targets		
cstA	CTAAAACGACGGCCAGTCAACAAGGATCGTCCCATTT	CAGGAAACAGCTATGACAGCTGGGTGGACATTGAGTT
cueP (SL3616)	CTAAAACGACGGCCAGTTTTCCTTCACCATCGAAAGC	CAGGAAACAGCTATGACCAGAAAAGCGGATTCTGAGG
deoA	CTAAAACGACGGCCAGTAAGAGGCGCTGATTCGTAAA	CAGGAAACAGCTATGACGCAATCTGCCCTTCAGAGAT
eco	CTAAAACGACGGCCAGTGCTTCGACGGGATAAATCAA	CAGGAAACAGCTATGACCACTGACAACAGATTAACACATTCA
rpoH	CTAAAACGACGGCCAGTATCGTTCGATGAGTGCCTGT	CAGGAAACAGCTATGACGCAACGAGAATATCACCCACT
scsA	CTAAAACGACGGCCAGTGTTATACGGCTGGCCTTCGT	CAGGAAACAGCTATGACGCGGTACAAACCATTACCA
SL3009	CTAAAACGACGGCCAGTCGGTATGGGCAGACGATAAT	CAGGAAACAGCTATGACGCGGCCATAATATTTCCTGA
SL3010	CTAAAACGACGGCCAGTCTCTCCATAGCCGTTTCCTG	CAGGAAACAGCTATGACATTATCGTCTGCCCATACCG
SL3646 (STM3681)	CTAAAACGACGGCCAGTTTCACCTGGCTGAATACGTG	CAGGAAACAGCTATGACACGTGAGTTCCTCCCACATC
slrP	CTAAAACGACGGCCAGTCGTCATTTTAATCTTATATG	CAGGAAACAGCTATGACATATCTCTTCTTTTAAAGGC
STM3388	CTAAAACGACGGCCAGTGCATTGTAAGTCCGCTTTTCA	CAGGAAACAGCTATGACTAGCGACAGCAAATGAAACC
tsr	CTAAAACGACGGCCAGTAGTAGCGGTAAGCCACCAGA	CAGGAAACAGCTATGACATAGCGCCAATACCAGCAGT
ybiJ	CTAAAACGACGGCCAGTCGAACTTCCCCACGGCGAAA	CAGGAAACAGCTATGACCTGGCTTTACAGAGTCGAGG
yccA	CTAAAACGACGGCCAGTACGTATTGATCGCCTCCACT	CAGGAAACAGCTATGACACGATCACGCGATGATGTAA
ydgF	CTAAAACGACGGCCAGTGGAACAATGATATCTGCGGC	CAGGAAACAGCTATGACACAATTATCCGCAGTGTTGC
yedY	CTAAAACGACGGCCAGTAGCCTGGGAGCTAACCGTAT	CAGGAAACAGCTATGACCGCTGATGCCTAATGCTTTT
yihE	CTAAAACGACGGCCAGTCCATTCCAGGGATTCAAAAA	CAGGAAACAGCTATGACGTTCAAACAGCGCATCCAT
yqaE	CTAAAACGACGGCCAGTCGAACCGCAAAGCATACATA	CAGGAAACAGCTATGACCCAGAAACCCATATACACTCCA
Universal M13-flurosceine Labelled Primers	GTAAAACGACGGCCAGT	CAGGAAACAGCTATGAC

Chromosomal DNA and total RNA samples were quantified at A_{260} and A_{280} using a NanoDrop 2000c. RNA quality was assessed by size chromatography on an Experion™ RNA StdSens Chip (BIO-RAD) using the Experion™ Automated Electrophoresis Station (BIO-RAD). Absence of DNA contamination was verified by PCR and visualised by agarose (2% w/v) gel electrophoresis (180 V, 20-30 min). Gels were visualised as described previously (2.4.7), also allowing RNA quality to be assessed.

2.4.23 Quantitative real-time polymerase chain reaction (qRT-PCR)

qRT-PCR was performed as according to Appia-Ayme et al. (2012). Gene specific primers (~60°C Tm) were designed (2.4.21.2) to amplify an internal gene fragment of 95-100 bp (Table 20). Experiments were performed in biological triplicate with three technical replicates. Three 10-fold serial dilutions of chromosomal DNA (2.4.20.2) was used for standardisation. The calculated threshold cycle (C_t) for each gene was normalised to that of reference genes *rpoD* and *ampD*; chosen as housekeeping genes whose expression levels remained constant across conditions tested. CFX manager software (BIO-RAD) was used for data analysis.

Cells were subjected to mRNA stabilisation and total RNA extraction (2.4.20). Following TurboDNAse (2U/ µL) treatment total RNA was subjected to quantity and quality analysis (2.4.20.2) and used as template for cDNA synthesis (2.4.21.1). Real-time PCR quantifications were realised on a 5-fold dilution of the total cDNA obtained, using the BIO-RAD CFX96™ instrument and SensiMix™ SYBR No-ROX kit (BIOLINE) (Table 7).

2.4.23.1 DNA synthesis

Total RNAs (2 µg) were reverse-transcribed from random hexamers (Invitrogen) with Superscript™ II Reverse Transcriptase (Invitrogen) according to manufacturer's instruction. cDNA was diluted 5-times and stored long-term at -20˚C.

2.4.23.2 qRT-PCR primer design

qRT-PCR primers were designed using *Primer3* (v. 0.4.0) primer design software (http://bioinfo.ut.ee/primer3-0.4.0/primer3/) with a product size

range of 95-105 bp and 'General Primer Picking Conditions' of; primer size 18-22 bp, GC content 50-60% and melting temperatures (T_m) of 58°C-62°C. Primers were diluted 1:4 with nuclease-free dH_2O to the 250 nM.

Table 20: **Primers used during qRT-PCR** to amplify 95-105 bp internal fragments of target genes. *rpoD* and *ampD* were used as housekeeping reference genes.

Gene	Forward Primer (5'-3')	Reverse Primer (5'-3')
cueP (SL3616)	CAGGGAGAAATGCCGAATAA	CCGTTTCGATAGCTTTGCAT
baeR	CGAAAGCCCGTTAATGATTG	TACCCGGTTCAAGCGATAAG
cpxP	TAACCGAACATCAGCGTCAG	CCGATGCATTGTCTCCATTT
deoA	ATTCATGCCAAAGACGAAGC	ACGATAGACCGAAGGTGTGC
eco	AAAGGAATGAAGCGGCAAGT	CAATCCACATTCAGCGTTTG
rpoH	ACGCTGATCCTGTCTCACCT	TTGCCTTCCTGGATCAAATC
rpoN	CAATGACGCCTCAGCTACAA	TCAAGCAGCGGGTTATTTTC
scsA	GCTCCTCCTCGACAGATGAC	AAGGATAGCGCCTTCAAAGA
SL3009	CCTCTTCAGCAAACCCGTAA	ATGCCATCCTGAGCTGATTT
SL3010	ATGAAATGTCACCGGACTGG	ACGGGTTGTTACACGACCAT
SL3646	CATAAAATCGCGTCAACCAG	CCATTCGTTCGAAGATCACA
SL4465	TCGATCGCCTGATTTTTACC	AGCGCTTCTCCAGACGATAA
slrP	ATATGCAGCGGCTAATGTCC	ATGCAGTGGTCGAGTTACCC
spy	GCCAATGATGCAGCATAAAG	TAATGTCGCGAATTTGTTGC
stm3388	TCGATAGATGCGCCCTTTAC	CATCAGTTCCCGTTCGTTTT
tsr	CGGTGAAGTCCGTAATCTGG	CAGCGTCGAACCTACATCAA
ybiJ	ATGGCCTGGAAGCTAAACTG	TGCCGCTCATTTTGTCATTA
yccA	CGCGGTGTTTATCCTGATTT	TGACGGTCGCACGAATATAG
ydgF	AGCGTGCTGCTATTTGATGA	TTACGCGTCCCTGATTTGAT
yedY	TAACGCCGGAAGATAAGGTG	CACGGTTCGGTTTTCAGACT
yihE	GTTATCTTGGCCGATTGCAT	GAATACCTGGCGAGGTTCAA
yjiY	CCAACGCTGGCAGTAGGTAT	AACAGCGCTTCGAACAGAAT
yncJ	TACTGACCTGTGCGCTGTTT	GGCTTCGTGTCTAAGCTGGT
yqaE	GCTCGGCGTACTTTTAGGAA	ACCCAAAATGCGTGGATAAG
zraP	GCAACAATGACGGTATGTGG	GCGCTGGTCTGCGTATAGTA
zraR	GTTCGGTTAATTGCCGCTAC	ATTTCAATCGCCACCACATT
Reference Genes		
rpoD	CGTACCCAGGAACGTCTGAT	CAGGTTTCGCTGGTTTCATT
ampD	ATGACGAAAAACCGTCCTTG	GGATCTATCGTTCCGGTGAA

2.4.24 Microarray

Total RNA samples were labelled with fluorescent dye Cy5-dCTP (Amersham) (2.4.23.1) and combined with SL1344 genomic DNA (reference), labelled with Cy3-dCTP dye using Gibco Bioprime DNA labelling system (2.4.23.2). Following hybridisation and incubation (2.4.23.3), array slides were scanned using a GenePix 4000A scanner (Axon Instruments, Inc.) and quantified using GenePix Pro 7.0 software (Axon Instruments, Inc.). Data was normalised using the Batch Anti Banana Algorithm in R (BABAR) (Alston et al., 2010) and further analysed using GeneSpring 7.3 Software (Agilent). As Cy dyes are light sensitive: reactions were kept in dark conditions during incubation steps and labelling.

2.4.24.1 Direct labelling of SL1344 reference genomic DNA

Samples were held on ice between incubation steps and labelled using the Gibco Bioprime DNA labelling system. The following protocol produces sufficient labelled gDNA for five hybridisations and was repeated twice to ensure sufficient labelled DNA for 8 x 15K array hybridisation.

Chromosomal DNA was isolated (2.4.20.2) and 2 µg brought to a volume of 21 µL in Sigma dH_2O. Reaction buffer mix/2.5 x random primers from Gibco Bioprime DNA labelling system was added (20 µL), samples incubated (100˚C, 5 min), followed by chilling on ice for 5 min. A dNTP mix (10x) (produced separately to the DNA labelling system [1.2 mM each dATP, dGTP, dTTP; 0.6 mM dCTP; 10 mM Tris, pH8.0; 1 mM EDTA]) was added (5 µL) on ice, followed by Cy3-dCTP (3 µL) and 1 unit of Klenow enzyme (1 µL) (Gibco Bioprime DNA labelling system). Samples were collected by brief centrifugation and incubated at 37˚C overnight.

Following labelling, unincorporated/quenched Cy dyes and residual reagents were removed (2.4.3), eluted twice in 50 µL Sigma H_2O to maximize recovery. Samples were stored in the dark, at 4˚C, for hybridisation later the same day. Samples should not be stored for prolonged periods and should be labelled as close to hybridisation as possible.

2.4.24.2 Array hybridisation and washing

To prevent impurities, 8 x 15K array slides should be handled in low dust environments while wearing clean, powder-free gloves. Hybridisations were carried out in 50 µL reactions (Table 21). Following labelling, all sample volumes were reduced from 100 µL to ~16 µL in a concentrator 5301 (Eppendorf®) at 30˚C. Labelled gDNA sample volumes were measured and divided equally (1/5) between the labelled cDNA samples. Total volumes of combined samples were brought to 21.5 µL with Sigma H_2O, and denatured at 94˚C, 2 min. Following sample collection by brief centrifugation and cooling (RT, 1 min), labelled cDNA/gDNA samples were mixed with 37.5 µL of hybridisation buffer (Table 21). An Agilent SureHyb backing (gasket) slide was placed onto a SureHyb Microarray Hybridisation Chamber (Agilent) base and 40 µL of hybridisation mix pipetted onto the center of each segment on the gasket slide, one per array, ensuring the liquid did not touch the gasket silicone edges. An OGT array slide was lowered on top of the gasket slide (Agilent label face down) allowing the array surface to come into contact with the hybridisation mix. The chamber was sealed and secured with clamps, ensuring that the hybridisation mix was moving freely across the whole array surface. The array can be gently tapped upon a hard surface to loosen any bubbles that may have become attached to the gasket silicone edges. The array slide, in its assembly, was incubated at 55˚C for 60 hours, rotating horizontally, within a blacked-out hybridisation oven.

The array slide, post hybridisation, required washing before scanning could take place. Once released from the hybridisation chamber, the array slide was submerged in wash solution 1 (Appendix D) and the gasket slide removed. The microarray was washed in wash solution 1, with gentle mixing, at RT for 5 min. This washing was repeated in wash solution 2 (Appendix D) and the array was dried by centrifugation in an array microcentrifuge for 30 sec. This removed residual liquid without splashing or exposing the array to dust and impurity contaminants.

2.4.24.3 Scanning, normalisation and data analysis

The dried microarray slide was inserted, array side (Agilent label) down, into a Genepix 4000A scanner (Axon Instruments, Inc.) and scanned according to the manufacturer's instruction. Scanned images were filtered and quantified using Genepix Pro 7.0 (Axon Instruments, Inc.) software, allowing each spot to be aligned, normalised for signal intensity by removing any background fluorescence and the green/red (Cy3/Cy5) ratio calculated. Data were normalised using the Batch Anti Banana Algorithm in R (BABAR) (Alston et al., 2010) and analysed with GeneSpring 7.3 (Agilent) software, with a false discovery rate (FDR) of 0.05.

Table 21: **Microarray hybridisation buffer**, composition per hybridisation reaction and volumes required per 8x array slide

Component	Per 50 µL hybridisation (µL)	Volume for 8 x Array Slide*
¥12xMES 7.04% *MES free acid monohydrate* *19.03% MES Sodium salt*	5	45
5 M Sodium chloride	12	108
Formamide (>99%)	12	108
0.5 M EDTA, pH 8.0	2.5	22.5
10% Triton x 100	6	54

*Volumes adjusted to 9x hybridisation to allow for any pipetting error present. ¥1.22 M MES in dH_2O, pH should be 6.5-6.7; without adjustment, 0.2 µm filter sterilised and stored at 4˚C.

2.4.25 Analytical ultracentrifugation (AUC)

Samples of 60 µM ZraP or recombinant site-directed mutants (ZraP-LTXXA, ZraP-AAAAA, ZraP-HRGGAH and ZraP-SDMB) in 50 mM Tris/HCl pH 7.5, 50 mM NaCl, with 60 µM $ZnCl_2$ or 10 mM EDTA were centrifuged, at 3950, 8050, 42,600 or 72,450 x *g*, at 20°C, in an An50-Ti rotor. Absorbance was monitored at A_{280} and scans were recorded every 5 hours to ensure equilibrium was achieved. Once reached, a total of five scans per sample were recorded, and a single species model was used to fit the sample scans using the program Ultrascan II (Demelar, 2005), to calculate the apparent weight average molecular mass, taken to be the concentration at the middle point using Equation 2, where *c* is the concentration (as OD) at radius *r*, and ω is the angular velocity (in radians/sec), $\overline{\nu}$ is the partial specific volume and

ρ is the solvent density. Individual scans were fitted separately to determine the standard deviation (SD) of the fit. ZraP has a partial specific volume (protein volume divided by molecular mass) of 0.712 mL g^{-1}, calculated from the amino acid sequence using SEDNTERP (version 1.05).

Equation 2

$$\overline{M}_{w,app} = \frac{d\ln(c)}{dr^2}\frac{2RT}{\omega^2(1-\bar{\nu}\rho)}$$

The monomeric molecular weight was calculated for ZraP and recombinant site-directed mutants from residues 27-151, predicted to remain after the removal of the signal peptide at amino acid position 26/27.

2.4.26 Protein aggregation assays

This work was conducted as described by Quan et al. (2011) with minor alterations. *L*-MDH, purified from pig heart mitochondria, was added to a fluorescence cuvette containing 50 mM HEPES/NaOH, pH 7.5, pre-warmed to 43˚C, at a final concentration of 213 nM. Assays were run in the presence and absence of WT ZraP or recombinant site-directed mutants with a range of zinc chloride concentrations (0-10 μM). Rate of *L*-MDH aggregation under each condition was monitored by light scattering at a $\lambda_{excitation}/\lambda_{emission}$ of 360 nm, with a CARY Eclipse fluorimeter, equipped with a temperature controller set to 43˚C. WT ZraP and buffer only controls were conducted to validate *L*-MDH aggregation levels. Assays were run in a minimum of triplicate for each condition tested, the average taken and normalised to background to produce final results.

2.4.27 Malate dehydrogenase (MDH) activity assays

MDH reduces oxaloacetate to malate while oxidising NADH to NAD^+ (Figure 7) Residual activity of MDH after guanidine hydrochloride (GdnHCl) treatment, in the absence and presence of ZraP was measured through the oxidation of NADH, using oxaloacetate as a substrate. Samples of 70 μM MDH in 50 mM HEPES pH 7.4 alone or with addition of 70 μM ZraP, 1 mM $ZnCl_2$ and 0-2 M of GdnHCl (in 2 mM increments) were incubated for 20 min

at RT. Cuvettes containing 50 mM HEPES, pH 7.4, 0.1 mM NADH and 4 µL of GdnHCl treated MDH sample were incubated at 25°C and the absorbance measured at 340 nm using a Hitachi U-3310 UV-visible spectrophotometer. The reaction was initiated by the addition of 2 µL oxaloacetate and the rate of decrease in absorbance used to calculate the rate of NADH oxidation, using an NADH absorbance coefficient of 6.22 mM^{-1} cm^{-1}. Control samples of untreated MDH were used to calculate and compare NADH oxidation rates.

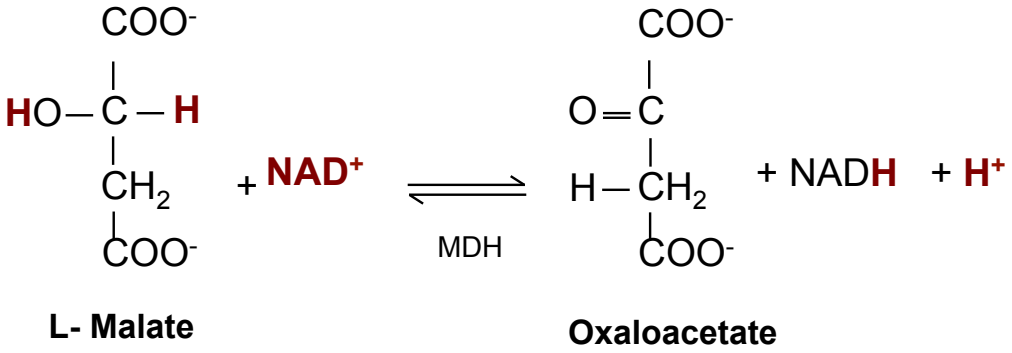

Figure 7: The reversible oxidation of malate to oxaloacetate by MDH using the reduction of NAD+ to NADH.

2.4.28 Biofilm assays

All biofilm assays were conducted as described by (Hamilton et al., 2009) with minor alterations. An overnight culture (2.4.2) for each strain was used to inoculate 10 mL of sterile CFA medium (1% v/v) (Appendix C) and incubated overnight at 37˚C, 200 rpm. Growth was determined by measuring OD_{600nm} and cells were standardised to 10^6 by dilution in fresh CFA medium. Each strain was inoculated in octuplicate into sterile, flat bottomed polystyrene 96-well plates (Nunc), sealed with a sterile lid (Nunc) to avoid contamination and incubated statically, at 25°C, for 24-72 hours. After the desired time period, planktonic cells, and media, were removed by inverting and gently shaking the 96-well plate. Wells were washed twice with 1 x PBS, dried at 60°C for one hour and stained with 125 µL 1% of Crystal Violet (CV) solution (Appendix D) for 10 min. Surplus CV solution was removed from wells and plates were repeatedly washed in dH_2O until all excess CV was removed (no further colour change in dH_2O was seen). A 200 µL solution of 20% acetone in ethanol (>99.8%) was used to de-stain wells for 10 min,

mixing well by pipetting. An 80 µL aliquot of solubilised CV was transferred to a new polystyrene 96-well plate, and the absorbance at OD_{590}. Media only controls were conducted to allow background staining to be deducted from final OD_{590} values.

3 The CpxR regulated transcriptome of *Salmonella* Typhimurium

3.1 Introduction

3.1.1 Induction of the Cpx pathway by NlpE

The importance of the Cpx ESR system in sensing and responding to numerous stresses, including alkaline pH, hydrophobic surface binding, P pilus protein mislocalisation and OM/periplasmic protein damage has been widely documented (1.7) and numerous virulence phenotypes are associated with Cpx response mutations (Table 1). Studies investigating the Cpx regulon, predominately conducted in *E. coli*, have highlighted genes positively and negatively regulated by Cpx. These function to alleviate stresses sensed by the Cpx system and contribute towards the maintenance of envelope integrity, prevent toxic build up of misfolded and denatured proteins within the periplasm, or as virulence and adhesion factors.

The OM lipoprotein NlpE (New lipoprotein E) is one of four proteins that participate in signal sensing for the Cpx system. Although originally identified as a multicopy suppressor of LamB-LacZ-PhoA toxicity (Snyder et al., 1995), Otto and Silhavy (2002) demonstrated the requirement of NlpE for induction of the Cpx response upon adhesion to hydrophobic surfaces. This involvement of CpxAR in adhesion was further supported by a reduction in the number of cells adhering and disruption of the dynamic cell-surface interaction of CpxAR deletion mutants (Otto and Silhavy, 2002). A brief summary of the importance of *Salmonella* adhesion and biofilm formation was included during the main introduction (1.7.5).

Association to the OM is critical for NlpE to function correctly in a signalling capacity and acyl chains anchor NlpE to the periplasmic side of the OM (Matsuyama et al., 1995, Matsuyama et al., 1997, Yakushi et al., 2000, Miyadai et al., 2004). The molecular mechanism(s) by which NlpE detects envelope stresses at the OM and transmits these signals to CpxA at the IM are still unclear. There are two hypotheses for how this interaction may occur. Firstly, overloading and disruption of the periplasmic folding machinery may result in NlpE misfolding, preventing recognition by the Lol transport system (required to insert NlpE into the OM) and mislocalisation to

the IM. Secondly, it is possible that during hydrophobic surface adhesion the inherently unstable N-terminal domain of NlpE becomes unfolded, allowing direct interaction between the C-terminus of NlpE and the IM (Hirano et al., 2007, Vogt and Raivio, 2012). Both means of interaction could occur independently or in addition to each other in response to stress and both are yet to be confirmed.

NlpE is not involved in signal sensing for all Cpx inducing conditions because NlpE null strains retain their ability to activate Cpx at a high pH and during PapG subunit overexpression (DiGiuseppe and Silhavy, 2003). NlpE does not activate the Bae signal transduction pathway, indicating no overlap between Cpx and other ESRs in this instance (Raffa and Raivio, 2002). Investigations into activation kinetics of Cpx pathway induction by NlpE acknowledge NlpE as a strong and specific activator of the Cpx pathway (Pogliano et al., 1997). Therefore, this OM protein is not involved in sensing multiple envelope stresses and overexpression of NlpE is an established, specific Cpx stimulus.

3.1.2 Previous transcriptomic analysis of the Cpx regulon

Seminal ESR research was conducted in non-pathogenic, laboratory strains of *E. coli* and transcriptomic analysis into the Cpx regulon of pathogenic strains and other species are relatively new. Five studies have been published to date utilising NlpE overexpression as a Cpx inducing cue in two species. Three of these studies identified Cpx regulon members in the model *E. coli* strain MC4100 and EPEC strain E2348/69 (Price and Raivio, 2009, Vogt et al., 2010, Raivio et al., 2013) and the two additional studies focused on the role of Cpx in the coccobacilli bacterium *Haemophilus ducreyi* (Gangaiah et al., 2013, Labandeira-Rey et al., 2010), the causative agent of the sexually transmitted disease chancroid. In addition to these broad-scale transcriptomic studies, De Wulf et al. (2002) used promoter recognition sites to identify CpxR-P target operons, Yamamoto and Ishihama (2005) identified the copper-inducible promoters for Cpx and Bury-Mone et al. (2009) compared the global transcriptional responses of the five main ESRs in

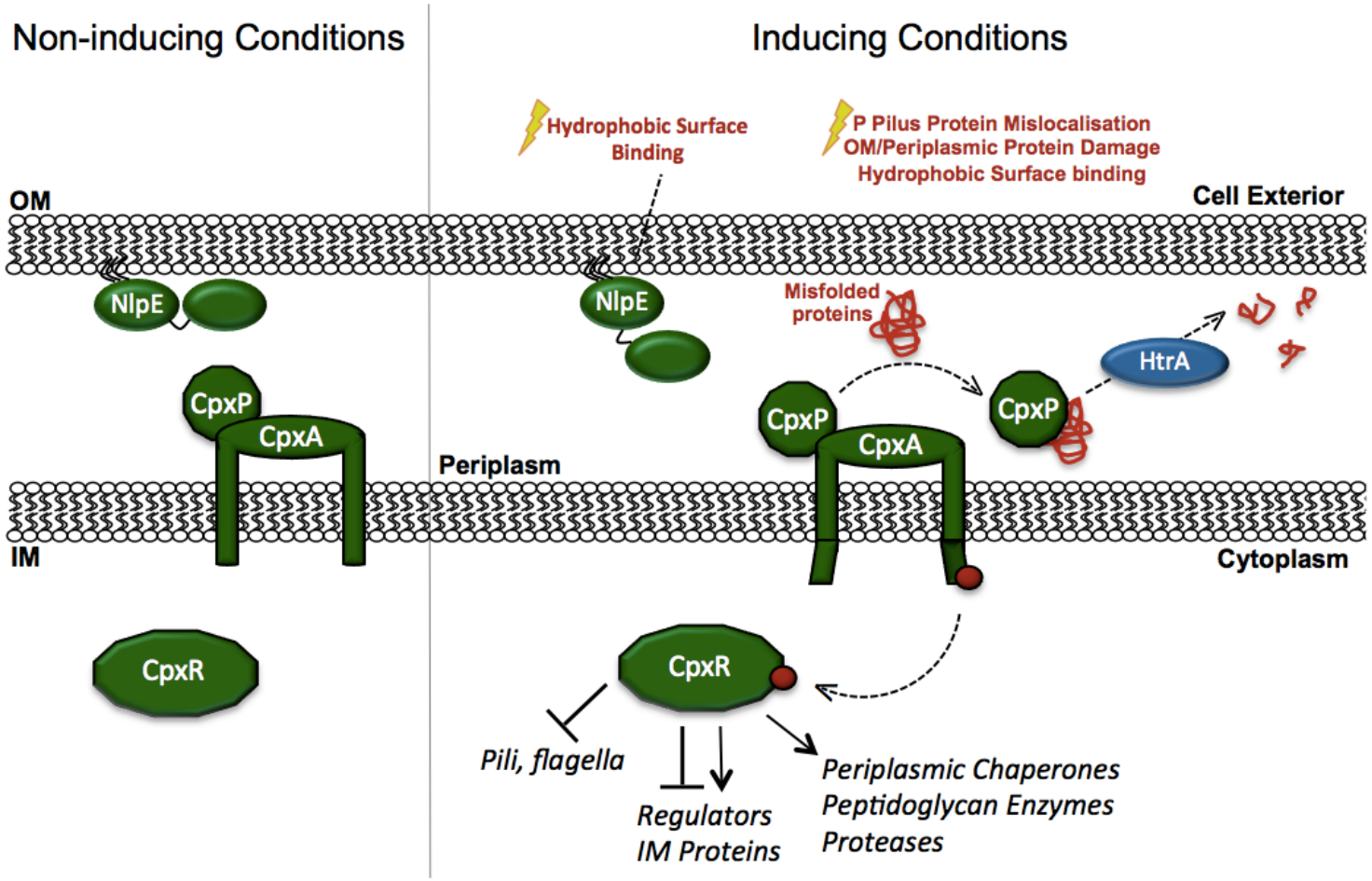

Figure 8: Overview of the Cpx two-component signal transduction system, components and inducing cues (adapted from Vogt et al., 2013). Under non-inducing conditions (left) the RR, CpxR, is unphosphorylated and "switched off" due to phosphatase activity of the HK, CpxA. The CpxA inhibitory protein CpxP, in the presence of inducing cues (indicated in red), is titrated away from CpxA and degraded by HtrA. Autophosphorylation of CpxA occurs, transfer of the phosphate group (red circle) to CpxR 'activates' the RR (CpxR-P) allowing DNA binding and regulation of transcription.

parallel, providing additional insights into the Cpx response. All three of these latter studies used *E. coli* K-12 derivatives as genetic backgrounds, likely chosen as the Cpx response, and its first regulon members, were originally characterised in MC4100 (Cosma et al., 1995, Danese and Silhavy, 1997).

No large-scale or transcriptomic analyses of the Cpx regulon in any *Salmonella* serovar has been published to date. All known Cpx regulon members identified from the current literature are summarised in Appendix G, Table G1 (see in table citations for references). In addition to descriptions of these Cpx regulated genes and their functions, information regarding the presence of a CpxR-P binding site, the *in vivo* effect of CpxR-P binding and if *in vitro* binding of CpxR-P to these sites has been experimentally proven, have been included where possible (Table G1).

Induction of Cpx by NlpE overexpression was utilised in the work presented here to allow the first transcriptomic analysis and comparison of *S.* Typhimurium SL1344 WT and *cpxR* deletion strains, through the use of microarrays. Price and Raivio (2009) showed that deletion of *cpxR* alone does not offer a strong (i.e. greater than 2-fold) change in gene expression for the majority of proposed Cpx-regulated genes. Other Cpx inducing cues, such as alkaline pH (Danese and Silhavy, 1997) or overproduction of P-pilus components: PapE, PapG and BfpA, (Jones et al., 1997, Nevesinjac and Raivio, 2005), are vastly more general and would result in activation of other stress responses, for example the σ^E pathway. Although NlpE overexpression produces a reduced phenotype (relatively) when compared to constitutive expression of *cpxA* (*cpxA**) there are many pleiotropic effects as a result of the *cpxA** mutation. Phenotypes associated with *cpxA** in *E. coli* and *Salmonella* strains include an increase in tolerance to aminoglycoside antibiotics (amikacin and kanamycin), hydroxyurea (Rainwater and Silverman, 1990, Thorbjarnardottir et al., 1978, Mahoney and Silhavy, 2013, Humphreys et al., 2004), alkaline pH (Danese and Silhavy, 1998), copper (De Wulf et al., 1999) and the bactericidal toxins colicins A and K (Plate, 1976). Despite these increased tolerances, CpxA* strains are also more sensitive to high temperatures (McEwen and Silverman, 1980)

and SDS (Cosma et al., 1995), and present abnormal FtsZ formation, cell cleavage (McEwen and Silverman, 1982, McEwen et al., 1983, Pogliano et al., 1998) and swarming in *E. coli* (De Wulf et al., 1999). Specific changes to the bacterial envelope when *cpxA* is constitutively expressed include deficiency of OmpF and Braun lipoprotein in the OM (McEwen and Silverman, 1982, McEwen et al., 1983). When grown on succinate, *L*-lactose and *L*-proline, *cpxA** strains present reduced growth (Rainwater and Silverman, 1990, Plate and Suit, 1981), but they are able to utilise *L*-serine as a sole carbon source (Morris and Newman, 1980, Newman et al., 1982, Su et al., 1989).

Due to the specific nature of the NlpE inducing cue, it can be proposed that any effects resulting from NlpE overexpression are due to activation of the Cpx 2CST system and subsequent downstream effects resulting from this, rather than interference of NlpE with other ESR systems. In combination, these findings make NlpE overexpression the most desirable Cpx induction method available.

Despite the use of NlpE overexpression in investigating Cpx-regulated genes in both model and clinically relevant strains of *E. coli* (EPEC, UPEC) and *H. ducreyi*), the importance of elucidating *Salmonella* specific Cpx regulated genes and further enhancing our understanding of the Cpx 2CST system in this organism cannot be understated. Significant differences within the ESRs of *Salmonella* and other organisms have been identified during the *Salmonella* ESR studies already completed. The most noteworthy of these differences is σ^E (RpoE), the extracytoplasmic function (ECF) sigma factor that is essential in *E. coli* (De Las Penas et al., 1997) (1.1.7). A viable *rpoE* deletion strain is producible in *Salmonella* spp. but Δ*rpoE* strains exhibit severe attenuation in murine models (Humphreys et al., 1999, Crouch et al., 2005, Testerman et al., 2002). A *Salmonella rpoE* deletion mutant is defective for survival and proliferation within epithelial and macrophage cell lines and is therefore of significant importance during *Salmonella* infection and as a potential target for the development of typhoid fever vaccines

(Humphreys et al., 1999, Kenyon et al., 2002, Testerman et al., 2002). Several periplasmic chaperones belonging to the σ^E and Cpx regulons, originally identified in model *E. coli* strains, also have key contributions to *Salmonella* pathogenicity (e.g. HtrA [DegP], Skp, SurA) (see 1.2 for *Salmonella* pathogenicity review).

Through the identification of novel Cpx regulated genes in *S.* Typhimurium one can add to the broader knowledge collected in distinct and related species, in addition to identifying *Salmonella* specific Cpx regulated genes. These specific genes could provide greater insights into how *Salmonella* spp. responds to environmental and envelope stresses, how this organism responds to stresses inflicted upon it from the host, and how it establishes infection. This work ultimately aims to reveal new genes important for *Salmonella* survival and pathogenesis, and consequently potential targets for the treatment and prevention of *Salmonella* spp. infections.

3.2 Aim

The aim of this chapter was to 1) define the CpxR regulon in *Salmonella* Typhimurium to broaden our understanding of the physiological importance of Cpx and 2) to identify *Salmonella* specific, CpxR regulated genes.

3.3 Experimental design

All assays were conducted in biological and technical triplicate, as a minimum, to allow for statistical analysis unless otherwise stated.

3.3.1 Bacterial strains and plasmids

Our SL1344 WT, and SL1344 Δ*cpxR*::*Kan* (hereafter referred to as Δ*cpxR*) strains were transformed with p*nlpE*† (2.4.5.3). Control strains, SL1344 WT and Δ*cpxR* expressing empty pBAD/Myc His A, were generated in the same manner.

3.3.2 Growth curves during batch culture

For measurement of aerobic growth, LB broth or MOPS minimal media were used for batch cultures (2.3.4).

3.3.3 NlpE overexpression

SL1344p*nlpE* and Δ*cpxR*p*nlpE* overnight cultures were diluted 1:100 (v/v) into 50 mL LB broth supplemented with 100 µg/mL ampicillin, in biological quadruplicate. Cultures were grown at 37˚C, 200 rpm to an OD_{600} of 1. *L*-arabinose at 0.02% (w/v) was added and cultures incubated, as previously, for four hours to allow accumulation of NlpE within the bacterial periplasm.

Non-inducing controls were produced for SL1344p*nlpE* and Δ*cpxR*p*nlpE*. Growth conditions were identical to that described above, except for the omission of *L*-arabinose; dH_2O was added instead. In the absence of *L*-arabinose, P_{BAD} produces very low levels of expression. Therefore, additional negative controls were also produced, consisting of SL1344 WT and Δ*cpxR* harbouring empty pBAD Myc His A vectors, grown in the presence of 0.02% (w/v) *L*-arabinose as described for our experimental strains. Comparison of these controls to our experimental strains ensured all significant changes in gene expression during microarray analysis resulted from NlpE overexpression and subsequent induction of the Cpx system, not from the overexpression vector, the presence of *L*-arabinose or methodology used.

3.3.4 Microarray

Cells were collected for all samples after NlpE overexpression (3.3.3), mRNA stabilised and total RNA extracted (2.4.20). Once RNA had been quantified and quality assessed (2.4.20.2), samples were labeled with fluorescent dye Cy5-dCTP (Amersham) (2.4.22.1) and combined (1:5) with SL1344 genomic DNA (reference), labeled with Cy3-dCTP dye using Gibco Bioprime DNA labeling system (2.4.22.2). gDNA/cDNA experimental samples and standards were hybridised to an OGT array slide (8 x 15K arrays) and incubated for 60 hours (2.4.22.3). Slides were scanned on a GenePix 4000A scanner (Axon Instruments, Inc.) and quantified using GenePix Pro 7.0 software (Axon Instruments, Inc.). Normalisation of data was performed

using the Batch Anti Banana Algorithm in R (BABAR) (Alston et al., 2010) and further analyses using GeneSpring 7.3 Software (Agilent). A 2-fold cut off threshold was employed with a false discovery rate (FDR) of <0.05. As Cy dyes are light sensitive: reactions were kept in dark conditions during incubation and exposed to minimal light during, and post, labelling. Experiments were conducted in triplicate as a minimum.

3.4 Results

3.4.1 Overexpression of NlpE has no negative impact on the growth of *S.* Typhimurium SL1344 or a Δ*cpxR* mutant of this strain

Overexpression of NlpE is an established Cpx inducing cue (Price and Raivio, 2009, Raivio et al., 2013, Gangaiah et al., 2013, Labandeira-Rey et al., 2010). Prior to transcriptomic investigations, we wished to confirm that overexpression of NlpE from the plasmid P_{BAD} had no detrimental impact on growth.

SL1344p*nlpE* and Δ*cpxR*p*nlpE* were cultured as described in 3.3.3 to induce transcription of *nlpE*. The OD_{600} values for both strains were measured across a ten-hour period of growth, the natural log (ln) plotted against time (Figure 9) and the specific growth rate (μ) calculated using Equation 1 (3.3.4). Growth rates for SL1344p*nlpE* and Δ*cpxR*p*nlpE* were μ=0.97 hr^{-1} and μ=1.01 hr^{-1} respectively. No significant difference in μ was seen between these strains in the presence of *L*-arabinose (0.02% w/v). Negative, empty vector controls (SL1344pBAD/*Myc* His A and Δ*cpxR* pBAD/*Myc* His A) cultured under the same conditions also exhibited no negative effects on growth as a result of pBAD/*Myc* His A introduction (data not shown).

At 0.02% (w/v), our inducer (*L*-arabinose) had previously been shown to induce NlpE expression *in trans* at sufficient levels to activate the Cpx pathway of *E. coli* (Snyder et al., 1995). In SL1344 this *L*-arabinose concentration did not have a negative impact on cell growth (Figure 9). Our SL1344p*nlpE* and Δ*cpxR*p*nlpE* strains were subsequently used in microarray

studies to compare the transcriptomes of SL1344 WT and Δ*cpxR* under the same conditions of NlpE overexpression presented here.

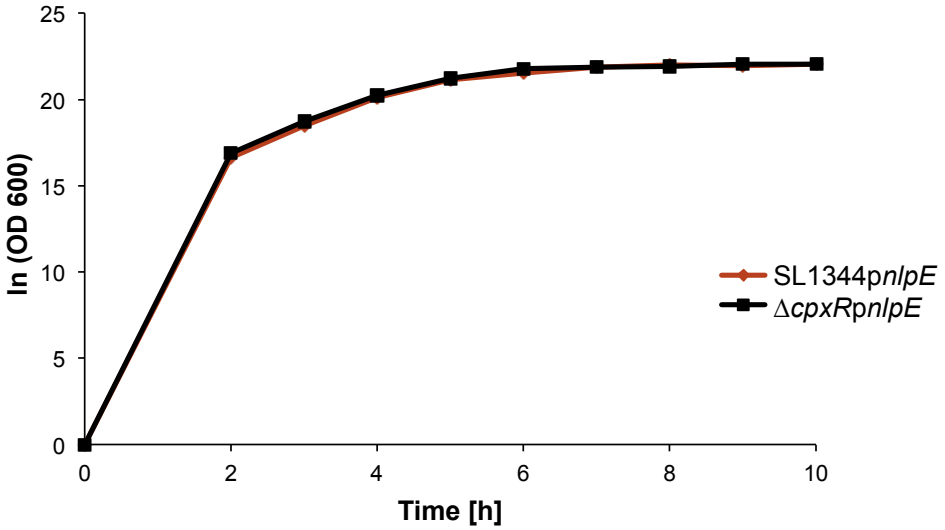

Figure 9: Growth of SL1344p*nlpE* and Δ*cpxR*p*nlpE* is unaffected by overexpression of NlpE from the P_{BAD} plasmid. Growth curves of ln(OD_{600}) values collected hourly over a 10 hour period of growth, in LB broth (3.3.2). Growth rates (μ) were 0.97 hr^{1} and 1.01 hr^{1} for SL1344p*nlpE* and Δ*cpxR*p*nlpE* respectively.

3.4.2 Analysis of genes differentially expressed in SL1344 WT and Δ*cpxR* strains post Cpx induction

The CpxR regulated transcriptome in *S.* Typhimurium was evaluated using NlpE overexpression. Our genetic background for these investigations was *S*. Typhimurium SL1344 (WT and SL1344Δ*cpxR*), chosen because no broad-scale studies of the Cpx regulon (e.g. microarray analysis) have been conducted to date in any *Salmonella* serovar and SL1344 is an established *Salmonella* strain where ESRs and virulence have been studied previously.

Following statistical filtering, 144 genes were differentially regulated between SL1344 WT and Δ*cpxR* (> 2-fold, FDR <0.05) (Appendix H; Table H1). Of these 144 genes, 77 were induced in the absence of CpxR (CpxR repressed) (Table 22), and 67 were repressed (CpxR activated) (Table 23). These 144 genes were compared to a list of all known Cpx regulon members (112 genes) generated from the current literature (Appendix G). 28 of our 144 genes had been assigned Cpx-mediated regulation prior to this study (highlighted yellow in Table H1, Table 22, Table 23) and are discussed below.

To better understand the regulatory networks controlled by CpxR, our 144 genes were categorised according to the Kyoto Encyclopaedia of Genes and Genomes (KEGG), using GeneSpring 7.3 Software in combination with current literature. A total of 38 categories were analysed, with changes in expression observed in all but nine of these categories (Figure 11). Raw values for the number of genes up-/down-regulated in each category are shown in Table H1. Categories of most relevance to our study will be discussed further, including genes belonging to SPI-1, where 29 genes were negatively regulated by CpxR, membrane stress and cell envelope components, which saw expression of six and 11 genes change respectively (Figure 12).

3.4.2.1 Comparison of transcriptomic data in SL1344 to current literature

Of genes identified as Cpx-regulated from current literature (Table G1), 28 (~20%) had expression levels change significantly (more than 2-fold; FDR <0.05) during our investigation. We first assessed expression of seven established *E. coli* Cpx regulon members (i.e. *cpxA*, *cpxP*, *htrA* (*degP*), *rdoA-dsbA*, *ppiA, skp* (*hlpA*) and *spy*) to 1) confirm regulation of these well-characterised genes in *S*. Typhimurium and 2) to confirm our methodology as an accurate means of determining Cpx-regulated gene expression (Figure 10). These genes are defined as 'established Cpx regulon members' because multiple research groups have confirmed their Cpx-mediated regulation (Cao et al., 2007, Danese et al., 1995, Danese and Silhavy, 1997, Pogliano et al., 1997).

As expected, *cpxA* and *cpxP* were induced significantly by CpxR in SL1344, ~22-fold and 90-fold respectively (Table 23). PpiA and HtrA, fundamental to maintaining periplasmic quality were both positively regulated by CpxR (9.86-fold and 9.22-fold) (Table 23). One of the largest transcriptional changes was observed for *spy*, where a 53.3-fold decrease in expression was observed in our *cpxR* null strain (Table 23, Figure 10). The periplasmic chaperone Spy is up-regulated by both Cpx and Bae ESRs and has had Cpx mediated regulation confirmed by multiple studies (Table H1). Another periplasmic

chaperone *skp*, important for *Salmonella* pathogenesis (Rowley et al., 2011), was repressed 3.22-fold by CpxR in SL1344 (Table 22). The *rdoA*(*yihE*)-*dsbA* operon, encoding a regulatory kinase and disulphide oxidase, was under positive regulation by CpxR (~3-fold). *In vitro* analysis of non-pathogenic *E. coli* confirmed CpxR-P binding to the *rodA*(*yihE*)-*dsbA* promoter (Pogliano et al., 1997). A CpxR-P binding motif (AGTAAAACCTTGTAAG) almost identical to the putative CpxR-P binding site identified in *E. coli* (GTAAAAGCTTGTAAG) (De Wulf et al., 2002), is located ~420 bp upstream of the *yihE* start codon in *S*. Typhimurium (Table 27, Appendix K). If this regulation is confirmed in *Salmonella*, the involvement of the RdoA (YihE) kinase in programmed cell death could provide a useful target for attenuating *Salmonella* strains and improving treatment through the enhancement of antimicrobial lethality (Dorsey-Oresto et al., 2013).

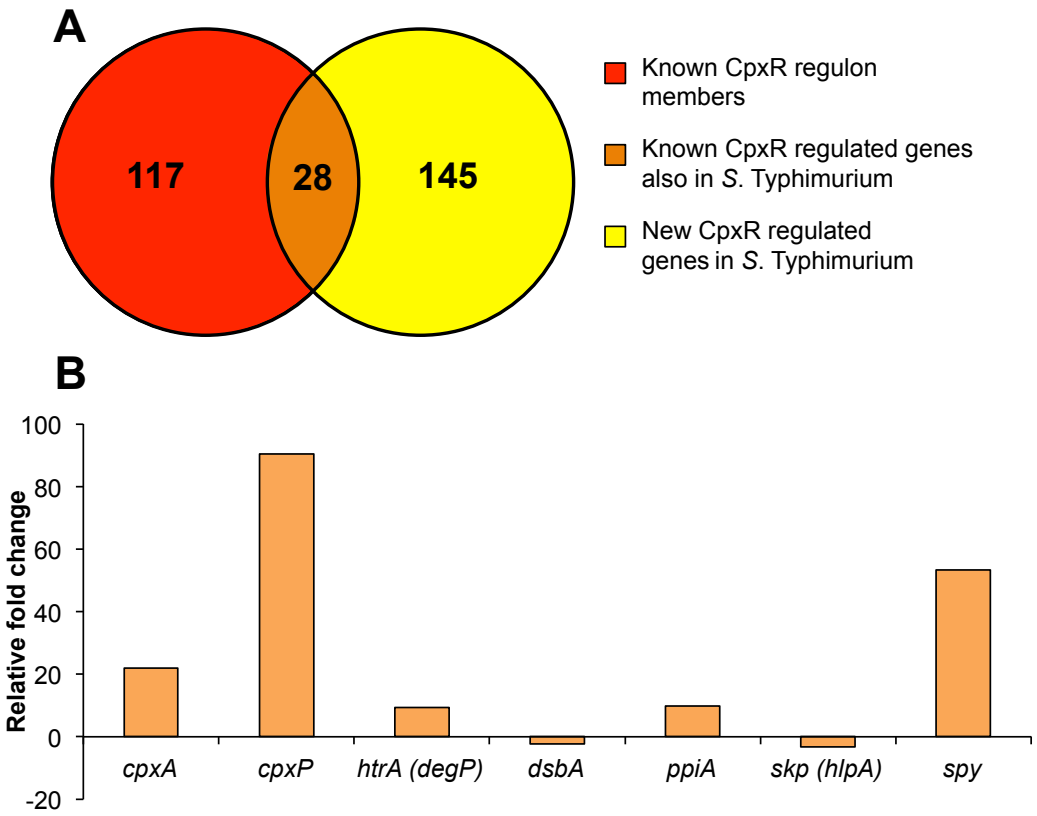

Figure 10: **Comparison of known CpxR regulon members to those identified in *S.* Typhimurium.** A) Venn diagram of Cpx regulon members identified in Enterobacteria (145) that were also CpxR regulated in S. Typhimurium (28). Change in expression level of established *E. coli* Cpx regulon members in SL1344 when CpxR was presence following overexpression of *nlpE*.

The remaining Cpx regulon members from the literature were identified in diverse genetic backgrounds, using an array of methodologies and growth conditions (Table G1). Of the known Cpx regulated genes not yet mentioned, *csrB*, *rpoE*, *rseA*, and *yjiY* exhibited negative regulation by CpxR in *S*. Typhimurium (Table 22). Those genes positively regulated by CpxR included *psd*, *ycfS*, *ygjA*, *tsr*, *htpX* and *rpoH* (Table 23). The direction of transcriptional change for all of these genes in *S*. Typhimurium concurs with those identified in other organisms (Table G1). However, *ppiD*, encoding a second PPIase that is positively regulated by Cpx in *E. coli* (Dartigalongue and Raina, 1998), did not see transcription levels alter significantly (>2-fold) in our data. This was also the case for *ung* and *ompC*, two genes with CpxR binding domains and under weak positive Cpx-regulation in *E. coli* (Table 22).

Raivio et al. (2013) presented a group of 38 'core' genes uniformly regulated by CpxR in *E. coli*, including a set of 12 '*y genes'* of unknown function. Expression of these genes changed in response to NlpE overexpression independently of the strain (MC4100 or EPEC E2548/69) or medium (LB broth and DMEM/F12) used (Table G1). 34 of these 38 genes are present within the genome of *S*. Typhimurium and of these, 10 were up-regulated in *S.* Typhimurium in a CpxR-dependent manner: *cpxP* (90-fold) and *spy* (53-fold) as already mentioned, *dsbA* (2.5-fold), *dacC* (2.1-fold), *slt* (4.7-fold), *yebE* (48-fold), *yncJ* (50-fold), *ynfD* (4.7-fold), *yqaE* (24.4-fold) and *yccA* (40-fold) (Table 22). Of these 10 genes, five were classified as 'y genes' of unknown function (Raivio et al., 2013).

The *yccA* gene, although annotated in *S*. Typhimurium SL1344 as a hypothetical protein (Chaudhuri et al., 2004), is believed to be a putative IM protein that functions to modulate FtsH proteolysis and contributes to copper stress tolerance in *E. coli* BW21553 and 2K1056 (Yamamoto and Ishihama, 2006, Price and Raivio, 2009). To the best of our knowledge, no investigations into the regulation of *yccA* or the function of its protein product (YccA) have been conducted in *Salmonella* species. Protein-protein BLAST (BLASTP) analysis show YccA of SL1344 (SL1025) and *E. coli* str. K-12 share 96% (184 of 192 residues) sequence identity, at the amino acid level

(Appendix I). The 40-fold reduction in *yccA* expression observed in our *cpxR* null strain was one of the largest decreases of any gene in our data set (Table 22). Confirmation of *yccA* regulation and phenotypic analysis of an SL1344Δ*yccA* strain was undertaken in Chapter 4.

Raivio et al. (2013) was the first study to provide evidence for Cpx regulation of *yqaE*. The 24.4-fold induction of *yqaE* in our data (Table 22) was 4-6 times greater than the levels seen by Raivio et al. (2013) in *E. coli*, in any of the strains used. Prior to the Raivio and colleagues (2013) publication, other investigations had shown direct, negative regulation of YqaE at the posttranscriptional level by the small, non-coding RNA CyaR (De Lay and Gottesman, 2009). No changes in *cyaR* transcription, or *crp* (encoding a regulator of CyaR), were observed during our analysis. *In silico* analysis in SL1344 shows the presence of a CpxR-P consensus-binding motif within the promoter of *yqaE* (Chapter 4 - Table 27, Appendix K), suggesting possible direct regulation of *yqaE* by CpxR at the transcriptional level in *S.* Typhimurium. A similar binding motif was proposed in *E. coli* (Raivio et al., 2013), but this is yet to be experimentally demonstrated in this species. Confirmation of *yqaE* regulation and phenotypic analysis of an SL1344Δ*yqaE* strain was undertaken in Chapter 4.

Two other 'y genes' of unknown function, *yqjA* and *ycfS*, were not Cpx regulated in the Raivio et al. (2013) study, but were positively regulated by Cpx in *E. coli* BW21553 (>3-fold) in response to elevated copper concentrations (Yamamoto and Ishihama, 2006, Yamamoto and Ishihama, 2005). *yqjA* and *ycfS* exhibited Cpx-mediated induction in *S.* Typhimurium, 5-fold and 7.67-fold respectively (Table 23), but further investigations are needed to determine the contribution of these genes to copper tolerance in both *Salmonella* and *E. coli* spp.

Another gene of unknown function, *yjiY*, has a potential CpxR-P binding motif within its promoter region in *E. coli* (102-116 bp 5' ATG)(De Wulf et al., 2002) (Table H1) and has been described by Bury-Mone et al. (2009) as PspF regulated. No *in vivo* binding of CpxR-P to said binding site and no

experimental evidence supporting this proposed CpxR regulation of *yjiY* has been published to date. In our data, expression of *yjiY* decreased 2.38-fold when CpxR was present (Table 22), suggesting negative regulation of *yjiY* by Cpx in SL1344. The gene product of *yjiY* is annotated in *Salmonella* LT2 as a putative starvation response protein (Chaudhuri et al., 2004) and our *in silico* analysis reveals a proposed CpxR binding motif ~370 bp upstream of the *yjiY* start codon in SL1344 (Chapter 4 - Table 27, Appendix K). This motif is located between *yjiY* and a known Cpx regulon member, *tsr*. Direct negative regulation of *tsr* by CpxR-P has been identified through EMSAs and northern blot analysis (De Wulf et al., 1999) and the *tsr* gene was adopted previously for genetic and biochemical verification of CpxR-P targets (De Wulf et al., 2002). Surprisingly, transcription of *tsr* in our study increased when CpxR was present 2.78-fold (Table 23), in direct contrast to observations in *E. coli*. Tsr therefore appears to be positively regulated by Cpx in *S*. Typhimurium, under our conditions tested (Table 23). This proposed regulation of *yjiY* and *tsr* is investigated further during Chapter 4.

Our 144 Cpx regulon members of *S*. Typhimurium did not include any previously identified Cpx-regulated genes involved in: protein secretion and envelope management (*secA*), specific envelope components (*ompC*, *ompF*, *acrD*, *mdtABCD*, *nanC*, and *efeU*); chemotaxis and cell surface appendages (*motAB-cheAW*, *aer*, *csgBAC* and *csgDEFG*), cell division (*minCDE*) and known and proposed virulence loci (*mviM*, *pap* and *bfp*). The *motAB-cheAW* genes encode flagella motor proteins and chemotaxis regulators respectively. None saw significant changes to expression in our SL1344 data, despite being highlighted as directly Cpx regulated by De Wulf et al. (1999). Several proposed CpxR regulated genes of unknown function, or those with a function unrelated to the bacterial envelope (*aroG*, *aroK*, *ftnB*, *ung*, *ybaJ* and *ydeH*) also saw no significant changes in expression in *S*. Typhimurium.

Genes involved in transcriptional regulation, including RNA polymerase sigma factors, do belong to the Cpx-regulon of *S*. Typhimurium. The extracytoplasmic function sigma factor and important ESR protein σ^E (*rpoE*),

and *rseA*, encoding the anti-sigma factor that negatively regulates σ^E, were both significantly down-regulated (2.48-fold and 2.77-fold respectively; Table 22). However, two other members of the *rpoE* operon previously described as Cpx-regulated and located directly downstream of *rseA* (*rseBC*), did not see transcription change >2-fold in our data and did not pass our statistical filtered. Raivio et al. (2013) observed induction of *rpoE* and *rseA* by NlpE overexpression, concurring with our results for *S*. Typhimurium. However, these results disagree with previous examinations by Price and Raivio (2009) where the *rpoE-rseABC* operon saw Cpx mediated inhibition. Raivio et al. (2013) hypothesised that as the Price and Raivio (2009) study utilised transcriptional reporters and microarray analyses, a combination of transcriptional and post-transcriptional inputs led to an accumulation of *rpoE-rseABC* mRNA under Cpx inducing signals. Alternatively it is possible that NlpE-dependent events, independent of the Cpx system, may induce this *rpoE-rseABC* operon. However, the specific nature of our inducing cue and confirmation of NlpE induced Cpx-regulation by qRT-PCR would suggest this latter hypothesis is unlikely, but further testing is required to confirm both possibilities.

The heat shock sigma factor RpoH (σ^H or σ^{32}) is under negative regulation from the Cpx system in *E. coli* (Danese and Silhavy, 1997). However, transcription of *rpoH* was down regulated 3.1-fold in our Δ*cpxR* strain (Table 23), suggesting a positive regulatory role for CpxR on RpoH in *S*. Typhimurium. In SL1344, a possible CpxR-P binding site is located ~730 bp upstream of *rpoH* initiation codon (Chapter 4 - Table 27, Appendix K) and the direct binding of CpxR-P to the promoter region of *rpoH* in SL1344 is investigated in Chapter 4.

Table 22: **77 genes repressed by CpxR in *Salmonella* Typhimurium SL1344**. All genes were induced greater than 2-fold (FDR <0.05) in SL1344Δ*cpxR* following NlpE overexpression, compared to SL1344 WT. Genes are listed according to fold change (highest to lowest) to three significant figures. The locus tags for both *S*. Typhimurium LT2 (STM) and *S*. Typhimurium SL1344 (SL) are shown.

Locus Tag		Gene Name	Description	Fold Change[†]
SL Number	STM Number			
SL1190	STM1254		Putative outer membrane lipoprotein	12.97
SL4251	STM4315		Putative DNA-binding protein	10.73
SL2856	STM2876	*hilA*	Invasion protein regulator	7.64
SL4248	STM4312		Hypothetical protein	7.36
SL2854	STM2874	*prgH*	Needle complex inner membrane protein	6.76
SL2043	STM2066	*sopA*	Effector protein secreted by SPI-I, type-III secretion system	6.55
SL2850	STM2870	*orgA*	Needle complex assembly protein	6.40
SL2869	STM2890	*spaP*	Surface presentation of antigens protein	6.37
SL2875	STM2896	*invA*	Needle complex export protein	6.32
SL2879	STM2900	*invH*	Needle complex outer membrane lipoprotein precursor	6.10
SL3112	STM3138		Putative methyl-accepting chemotaxis protein	5.92
SL2852	STM2872	*prgJ*	Needle complex minor subunit	5.27
SL2874	STM2895	*invB*	Secretion chaperone	5.22
SL2853	STM2873	*prgI*	Needle complex major subunit	5.06
SL2851	STM2871	*prgK*	Needle complex inner membrane lipoprotein	5.04
SL2848	STM2868	*orgC*	Putative cytoplasmic protein	4.66
SL2873	STM2894	*invC*	Needle complex assembly protein	4.64
SL2876	STM2897	*invE*	Invasion protein	4.46
SL2860	STM2881	*iacP*	Acyl carrier protein	4.46
SL2871	STM2892	*invJ*	Needle length control protein	4.41
SL2878	STM2899	*invF*	Invasion regulatory protein	4.36
SL2855	STM2875	*hilD*	Invasion protein regulatory protein	4.28
SL1263	STM1328		Putative outer membrane protein	4.27

Table 22 continued

Locus Tag		Gene Name	Description	Fold Change[†]
SL Number	**STM Number**			
SL2857	STM2877	*iagB*	Invasion protein precursor	4.26
SL4238	STM4301	*dcuB*	Anaerobic C4-dicarboxylate transporter	4.10
SL2870	STM2891	*spaO*	Surface presentation of antigens protein	3.65
SL2861	STM2882	*sipA*	Secreted effector protein	3.61
SL2865	STM2886	*sicA*	Secretion chaperone	3.58
SL4250	STM4314		Putative regulatory protein	3.55
SL2877	STM2898	*invG*	Outer membrane secretin precursor	3.50
SL2859	STM2879	*sicP*	Secretion chaperone	3.46
SL1999	STM2023	*cbiM*	Cobalt transport protein	3.37
SL2868	STM2889	*spaQ*	Needle complex export protein	3.34
SL2225	STM2255	*napC*	Cytochrome C-type protein	3.31
SL2862	STM2883	*sipD*	Translocation machinery component	3.30
SL1189	STM1253		Putative inner membrane protein	3.30
SL1186	STM1250		Putative cytoplasmic protein	3.26
SL2863	STM2884	*sipC*	Translocation machinery component	3.20
SL2864	STM2885	*sipB*	Translocation machinery component	3.20
SL4239	STM4302		Putative cytoplasmic protein	3.18
SL0536	STM0543	*fimA*	Fimbrin	3.15
		invR	Small non-coding regulatory RNA	3.14
SL0226	STM0225	*hlpA*	Periplasmic chaperone	3.14
SL2867	STM2888	*spaR*	Needle complex export protein	3.04
SL3783	STM3817	*ccmC*	Haem exporter protein	2.93
SL2674	STM2703		Hypothetical protein	2.92
SL2003	STM2027	*cbiH*	Precorrin-3B C(17)-methyltransferase	2.91
SL2796	STM2811	*proX*	Glycine betaine-binding periplasmic protein precursor	2.90

Table 22 continued

Locus Tag		Gene Name	Description	Fold Change[†]
SL Number	STM Number			
SL3782	STM3815	*ccmE;ccmD*	Cytochrome c-type biogenesis protein	2.88
SL1030	STM1091	*sopB*	SigD; Salmonella outer protein B; Effector protein secreted by SPI-I, type-III secretion system	2.86
SL2858	STM2878	*sptP*	Protein tyrosine phosphatase/GTPase activating protein	2.82
SL2603	STM2639	*rseA*	Sigma-E factor regulatory protein	2.77
SL2163	STM2186		Putative oxidoreductase	2.76
SL3784	STM3818	*ccmB*	Haem exporter protein	2.75
SL2378	STM2410	*yfeA*	Hypothetical protein	2.66
SL1872	STM1939		Putative glucose-6-phosphate dehydrogenase	2.65
SL2521	STM2559	*cadA*	Lysine decarboxylase 1	2.65
	STM2966	*csrB*	Possible regulatory RNA	2.58
SL2056	STM2079	*wzzB*	Lipopolysaccharide O-antigen chain length regulator	2.57
SL2001	STM2025	*cbiK*	Vitamin B12 biosynthetic protein	2.54
SL2604	STM2640	*rpoE*	RNA polymerase sigma-E factor (sigma-24)	2.48
SL2000	STM2024	*cbiL*	Cobalt-precorrin-2 C(20)-methyltransferase	2.46
SL1184	STM1246	*pagC*	Virulence membrane protein PAGC precursor	2.43
SL2011	STM2035	*cbiA*	Cobyrinic acid a,c-diamide synthase	2.41
SL4463	STM4532	*yjiY*	Putative carbon starvation protein	2.38
SL0407	STM0413	*tsx*	Nucleoside channel	2.35
SL0776	STM0800	*slrP*	Leucine-rich repeat-containing protein	2.31
SL1996	STM2020	*cbiO*	Cobalt transporter ATP-binding subunit	2.28
SL2020	STM2044	*pduH*	Propanediol dehydratase reactivation protein	2.25
SL1278	STM1344	*ydiV*	Hypothetical protein; possible putative diguanylate cyclase/ phosphodiesterase domain 1	2.23
	STM14_1500		Hypothetical protein; located directly upstream of PagC (outer membrane invasion protein [STM1246])	2.20

Table 22 continued

Locus Tag		Gene Name	Description	Fold Change[†]
SL Number	**STM Number**			
SL1177	STM1239		Putative cytoplasmic protein	2.14
SL1799	STM1867	*pagK*	PhoPQ-activated gene	2.14
SL2490	STM2528		Putative dimethylsulfoxide reductase	2.14
SL1181	STM1242	*envE*	Putative envelope protein; Probable EnvE precursor	2.10
SL3105	STM3131		Putative cytoplasmic protein	2.05
SL1265	STM1330		Putative DNA/RNA non-specific endonuclease	2.02

[†]Denotes change in expression level in SL1344Δ*cpxR* compared to SL1344 WT following overexpression of *nlpE*.

Table 23: **63 genes induced by CpxR in *Salmonella* Typhimurium SL1344**. All genes were repressed greater than 2-fold (FDR <0.05) in SL1344Δ*cpxR* following NlpE overexpression, compared to SL1344 WT. Genes are listed according to fold change (highest to lowest) to three significant figures. The locus tags for both *S*. Typhimurium LT2 (STM) and *S*. Typhimurium SL1344 (SL) are shown.

Locus Tag		Gene Name	Description	Fold Change[†]
SL Number	STM Number			
SL4009	STM4060	*cpxP*	Periplasmic repressor protein	0.01
SL1243	STM1308	*spy*	Periplasmic protein; Induced by Cpx and BaeSR stress response systems	0.02
SL1533	STM1603	*yncJ*	Putative periplasmic protein	0.02
SL1814	STM1880	*yebE*	Putative inner membrane protein	0.02
SL1025	STM1085	*yccA*	Hypothetical protein	0.02
SL2780	STM2796	*yqaE*	Putative transport protein	0.04
SL4007	STM4058	*cpxA*	Two-component sensor protein	0.05
SL3009	STM3030		Hypothetical protein	0.05
SL1773	STM1844	*htpX*	Heat shock protein X; possible putative metalloprotease	0.07
SL3616	STM3650	*cueP*	Hypothetical protein; proposed copper sensitivity protein	0.08
SL0799	STM0823	*ybiJ*	Hypothetical protein	0.08
SL3439	STM3472	*ppiA*	Peptidyl-prolyl cis-trans isomerase A (rotamase)	0.10
SL0210	STM0209	*htrA*	Serine endoprotease; also known as *degP*.	0.11
SL3010	STM3031		Ail/OmpX-like protein	0.11
SL4008	STM4059	*cpxR*	DNA-binding transcriptional regulator	0.12
SL0088	STM0087	*folA*	Dihydrofolate reductase	0.13
SL1152	STM1215	*ycfS*	Putative periplasmic protein	0.13
SL1699	STM1771	*chaA*	Calcium/sodium: proton antiporter	0.14
SL1052	STM1113	*scsA*	Suppression of copper sensitivity protein A	0.15
SL3350	STM3377	*yedY*	Putative sulphite oxidase subunit	0.17
SL4124	STM4189	*yjbB*	Periplasmic transport protein	0.19
SL0500	STM0507	*ybbA*	Putative ABC transporter ATP-binding protein	0.19

Table 23 continued

Locus Tag		Gene Name	Description	Fold Change[†]
SL Number	STM Number			
SL3161	STM3187	*ygiB*	Hypothetical protein	0.19
SL3199	STM3226	*yqjA*	Hypothetical protein	0.20
SL2232	STM2262	*eco*	Ecotin precursor	0.21
SL1430	STM1500	*ynfD*	Putative outer membrane protein	0.21
SL4509	STM4582	*slt*	Lytic murein transglycosylase	0.21
SL3351	STM3378	*yedZ*	Putative sulfite oxidase subunit	0.22
SL3162	STM3188	*ygiC*	Putative glutathionylspermidine synthase	0.25
SL1404	STM1473	*ompN*	Outer membrane protein N precursor	0.25
SL4294	STM4360	*miaA*	tRNA delta(2)-isopentenylpyrophosphate transferase	0.26
SL3200	STM3227	*yqjB*	Hypothetical protein	0.26
SL4285	STM4348	*psd*	Phosphatidylserine decarboxylase	0.27
SL1054	STM1115	*scsC*	Suppression of copper sensitivity protein C	0.27
SL3438	STM3471	*yhfG*	Hypothetical protein	0.29
SL1811	STM1877		Putative amidohydrolase	0.30
SL1055	STM1116	*scsD*	Suppression of copper sensitivity protein D	0.31
SL1053	STM1114	*scsB*	Suppression of copper sensitivity protein B	0.31
SL3944	STM3996	*yihE*	Serine/threonine protein kinase	0.31
SL3646	STM3681		Putative transcriptional regulator	0.31
SL1412	STM1482	*ydgF*	Multidrug efflux system protein MdtJ	0.32
SL1261	STM1326	*pfkB*	6-phosphofructokinase 2	0.32
SL3533	STM3568	*rpoH*	RNA polymerase factor sigma-32	0.32
SL0808	STM0833	*ompX*	Outer membrane protein X	0.33
SL3201	STM3228	*yqjC*	Putative periplasmic protein	0.33
		omrB	Small RNA	0.33

Table 23 continued

Locus Tag		Gene Name	Description	Fold Change[†]
SL Number	STM Number			
	STM3229	*yqjD*	Putative inner membrane protein	0.34
		omrA	Small RNA	0.34
SL3437	STM3470	*fic*	Cell filamentation protein	0.34
SL3352	STM3379	*accB*	Acetyl-CoA carboxylase biotin carboxyl carrier protein subunit	0.35
SL1260	STM1325	*ydiZ*	Putative cytoplasmic protein	0.35
SL3361	STM3388		Putative signal transduction protein	0.36
SL4464	STM4533	*tsr*	Methyl-accepting chemotaxis protein I	0.36
SL4450	STM4519		Putative NAD-dependent aldehyde dehydrogenase	0.37
SL3353	STM3380	*accC*	Acetyl-CoA carboxylase biotin carboxyl carrier protein subunit	0.37
SL1413	STM1483	*ydgE*	Multidrug efflux system protein MdtI	0.38
SL3365	STM3392	*yhdV*	Putative outer membrane lipoprotein	0.40
SL3203	STM3231	*yqjK*	Putative inner membrane protein	0.40
SL4510	STM4583	*trpR*	Probable Trp operon repressor	0.41
SL4495	STM4568	*deoA*	Thymidine phosphorylase	0.41
SL3945	STM3997	*dsbA*	Periplasmic protein disulphide isomerase I	0.42
SL3202	STM3230	*yqjE*	Putative inner membrane protein	0.43
SL0731	STM0749	*pal*	Peptidoglycan- associated outer membrane lipoprotein	0.44
SL3928	STM3974	*tatB*	Sec independent translocase protein	0.47
SL4298	STM4364	*hflC*	FtsH protease regulator	0.47
SL0839	STM0863	*dacC*	D-alanyl-D-alanine carboxypeptidase fraction C	0.47
SL3229	STM3256		Phosphotransferase system mannitol/fructose-specific IIA component	0.48

[†]Denotes change in expression level in SL1344Δ*cpxR* compared to SL1344 WT following overexpression of *nlpE*. Values <0.5 represent level of expression reduction.

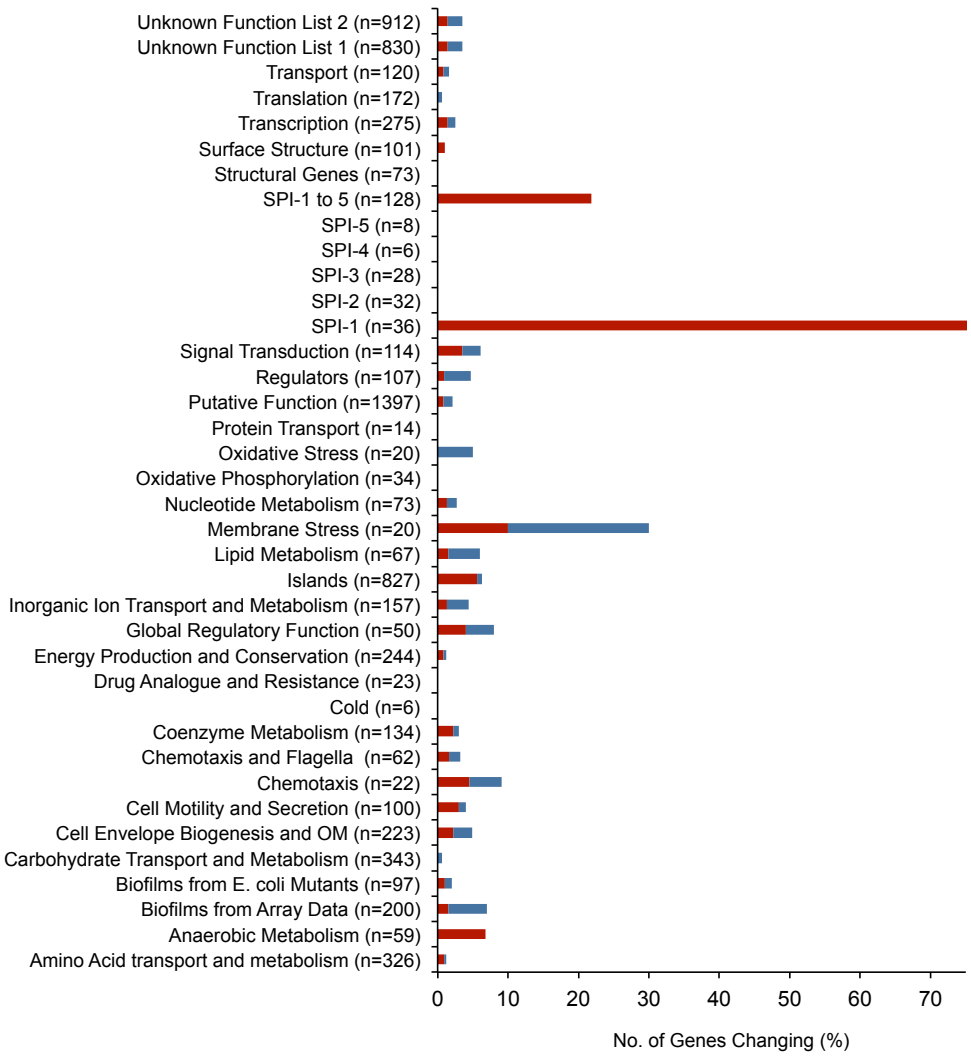

Figure 11: Relative percentage of genes up-/down-regulated in SL1344Δ*cpxR* compared to SL1344 WT following NlpE overexpression. Genes of interest were categorised according to Kyoto Encyclopaedia of Genes and Genomes (KEGG) pathways and current literature (x-axis). **Red bars** = [%] of genes up-regulated (CpxR repressed) and **blue bars** = [%] of genes down-regulated (CpxR activated) in *cpxR* null background compared to SL1344 WT post NlpE overexpression. n=total number of genes per functional category. Cut-off threshold = 2-fold; FDR < 0.05. See Appendix B, Table B2 for raw value summaries.

3.4.2.2 Previously unidentified members of the CpxR regulon

As decribed in 3.4.2.1, of the 144 genes differentially regulated in SL1344 WT and Δ*cpxR* (post NlpE overexpression), 28 had been assigned some form of Cpx-mediated regulation prior to this study (Table H1, highlighted yellow). To the best of our knowledge, the remaining 116 genes have not been highlighted as Cpx regulated in *Salmonella* or any other species (Table 24). A selection of these individual genes and operons, including *Salmonella* specific genes, will be discussed here. For ease of discussion, genes are grouped according to their function and/or the regulatory network they belong to. Of these the most interesting were virulence genes, those of unknown or hypothetical function, metal stress and homeostasis, and regulatory genes and small RNAs.

3.4.2.2.1 Cpx and Salmonella virulence

The majority of genes down regulated by CpxR in our data are critically important for *Salmonella* virulence and infection strategies (Figure 11). SPI-1 encodes a TTSS that delivers effector proteins into eukaryotic cells during invasion. Expression of *hilA*, the central positive regulator of the SPI-1 TTSS genes, was repressed 7.64-fold (Table 22). Unsurprising, 29 of the 36 SPI-1 members (80%) were also repressed by CpxR in our SL1344 WT strain (Figure 12, Table 22). Expression of the remaining seven SPI-1 genes (*avrA*, *sprB*, *hilC*, *orgB*, *stm2880*, *spaS* and *invI*) did reduce more than 2-fold in SL1344 WT, but they did not pass the statistical filtering imposed. Of the 29 significantly changing SPI-1 genes, only *invE* has had regulation by Cpx confirmed experimentally (Table H1). In *S*. Typhimurium, CpxA represses *hilA* in a pH-dependent manner, but this was observed independently of CpxR (Nakayama et al., 2003). The authors hypothesised that CpxA functioned through another RR to repress HilA, and SPI-1, activity. Transcription of *hilA* is also controlled in a feed-forward loop with the response regulator SirA, one of four known HilA regulators. The second, HilD, activates the remaining two *hilA* regulators: HilC and RtsA (Johnston et al., 1996). A significant decrease in *hilD* expression was observed (4.28-fold) when CpxR was present (Table 22). However, expression of *silA*, *hilC* or *rtsA* did not change during our analysis. No changes were also observed for *virF*,

encoding a second regulator of SPI-1, shown to be CpxR dependent in *Shigella flexneri*. In *Shigella*, InvE (VirB) and VirF tightly regulate TTSSs and CpxR is responsible for positive regulation of both (Tobe et al., 1993, Mitobe et al., 2005, Nakayama and Watanabe, 1995, Nakayama and Watanabe, 1998). In our Δ*cpxR* mutant, *invE* transcription increased 4.46-fold (Table 23). In a Δ*cpxA* mutant of *S. sonnei*, little effects on *invE* and *virF* transcription were observed at a neutral pH (Mitobe et al., 2005). However, InvE was reduced at the protein level, suggesting post-transcriptional regulation of InvE by Cpx in this species (Mitobe et al., 2005, Vogt and Raivio, 2012).

SlrP is an E3 ubiquitin ligase and is secreted by SPI-1 and SPI-2 TTSS secretion into eukaryotic host cells during infection, where it mediates ubiquitination of ubiquitin and thioredoxin (Bernal-Bayard and Ramos-Morales, 2009). Transcription of *slrP* was repressed 2.21-fold by CpxR during our microarray analyses (Table 22). A recent publication highlighted three genetic factors as novel regulators of *slrP* in *S.* Typhimurium; LeuO, Lon and the 2CST system PhoQ/PhoP (Cordero-Alba and Ramos-Morales, 2014). None of these newly discovered regulators of SlrP saw significant changes to their transcription levels in our data set, suggesting these regulators were not indirectly responsible for the reduction in *slrP* transcription observed. We have identified a 17 bp CpxR-P binding motif ~460 bp upstream of the *slrP* transcriptional start site in SL1344 (Table 27, Appendix K) and possible direct regulation of *slrP* by CpxR is discussed in more detail in 3.5.2 and Chapter 4.

The periplasmic serine protease, ecotin, provides *E. coli* with protection from neutrophil elastase (NE) (Eggers et al., 2004), a protease secreted during inflammation by immune cells to aid bacterial killing (Belaaouaj et al., 2000). Despite the importance of ecotin for *E. coli* intracellular survival, no investigations into the molecular mechanisms of ecotin or its regulation of have taken place to date. Our study shows a 5-fold increase in transcription of the ecotin precursor (*eco*) in a CpxR dependent manner (Table 22), highlighting possible involvement of the Cpx response in activating

transcription of this important protease. In addition to this, a potential CpxR binding motif is situated ~250 bp upstream of the *eco* initiation site (Table 27, Appendix K) adding wright to the theory that CpxR directly regulates this protease in *S*. Typhimurium. Investigations into Cpx-mediated regulation of *eco* are continued in Chapter 4.

3.4.2.2.2 Regulation including sRNAs

Two putative transcriptional regulators were highlighted as CpxR activated during our study, SL3361 (STM3388) and SL3646 (STM3681) (Table 23). The protein product of *stm3388* contains a GGDEF-EAL domain. This classification of proteins is associated with biofilm formation through the regulation of cell surface assembly components (Kader et al., 2006). Kader et al. (2006) implicated *stm3388* in the regulation of CsgD, a positive regulator of thin aggressive fimbriae (*agf* - more recently referred to as exopolysaccharide cellulose and proteinaceous curli fimbriae) and multicellular rdar (red dry and rough) morphotype. Transcription of *stm3388* increased 2.78-fold in our SL1344 WT strain, highlighting a positive regulatory affect of CpxR on this gene (Table 23). However, the absence of a CpxR-P binding motif within the promoter region of *stm3388* (Table 27) suggests this regulation may occur in an indirect manner.

The second transcriptional regulator, *SL3646* (*stm3681*), is located between *aldB* and *selB* in *S.* Typhimurium SL1344. Post Cpx induction, *SL3646* expression was ~3-fold higher in the presence of CpxR (Table 23). We located a potential CpxR-P consensus binding motif ~426 bp upstream of the *SL3646* start codon (Table 27). Bioinformatic analysis demonstrated sequence similarity, at the amino acid level, between SL3646 and the NagC-like transcriptional regulators in *E. coli* (AAC73497.1). Protein homologues are present in *E. hermannii* and *E. vulneris*, 72% and 71% identity at the amino acid level, and other Enterobacteriacae: *Citrobacter rodentium* (69% identify), *Enterobacter* and *Cronobacter* species (identities of <68%) (data not shown) (Altschul et al., 1990, Boratyn et al., 2013). Very little information for *SL3646* is available in the literature and to the best of our knowledge no

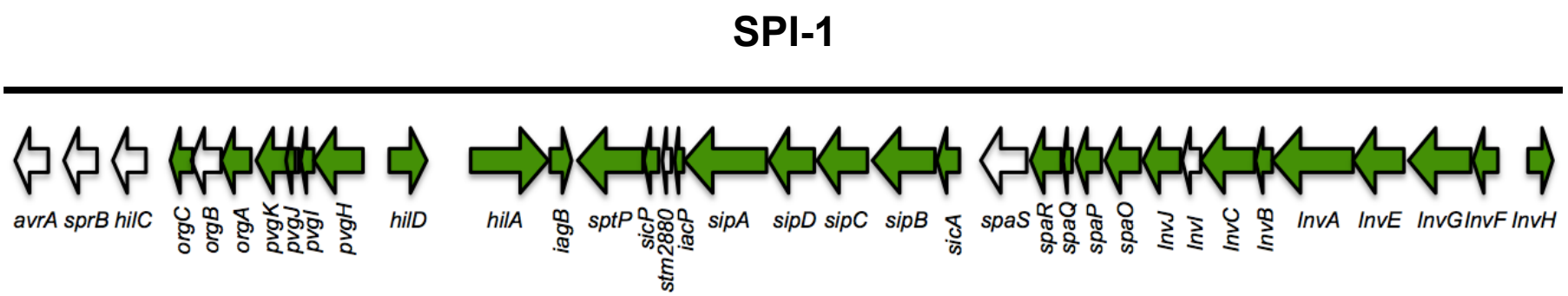

Figure 12: Regulation of *Salmonella* Pathogenicity Island-1 by CpxR. Genes of SPI-1 which levels of transcription changed > 2-fold following NlpE overexpression in a *cpxR* null strain compared to WT SL1344. Genes highlighted GREEN saw a significant increase in expression levels; genes that saw no significant change in expression are **WHITE**. Threshold = 2-fold cut off; FDR<0.05. Adapted from (Dieye et al., 2009).

investigations concerning SL3646 regulation or function have been carried out.

The importance of small RNAs in a regulatory and signalling capacity is becoming increasingly apparent, and a possible role of the Cpx system is regulating these important small molecules has recently come to light (Vogt et al., 2014). Within the 144 genes differentially regulated between our SL1344 WT and Δ*cpxR* strains, four encode small RNAs: *csrB* (up regulated 2.58-fold), *invR* (up regulated 3.14-fold), *omrA* and *omrB* (both down regulated ~3-fold) (Table 22, Table 23). As shown in Table G1, CsrB was previously identified as a CpxR regulated sRNA in *E. coli* (Bury-Mone et al., 2009) but to the best of our knowledge no regulation by CpxR, either direct or indirect, has been shown in the literature for any of the other sRNAs, *invR*, *omrA* and *omrB* identified here.

3.4.2.2.3 Metal stress and homeostasis

CueP (SL3616), regulated by CueR, is an abundant copper binding PP which confers copper resistance in *Salmonella* (Pontel and Soncini, 2009, Yoon et al., 2014a, Abriata et al., 2014, Yoon et al., 2014b, Osman et al., 2010). As the macrophage phagosome contains elevated copper concentrations, CueP is believed to have an important role in *S*. Typhimurium survival within host immune cells (Yoon et al., 2014b). Cpx has been linked to copper tolerance and the regulation of copper-inducible promoters in *E. coli* (Yamamoto and Ishihama, 2005, Yamamoto and Ishihama, 2006), so it was unsurprising to see several copper tolerance genes (*cueP*, *scsABCD*) down regulated in the absence of *cpxR*. *cueP* transcription reduced 12.85-fold, *scsA*, 6.74-fold; *scsB*, 3.2-fold; *scsC*, 3.67-fold and *scsD*, 3.25-fold (Table 22). No data has been published on the regulation of *cueP* by CpxR, despite the presence of a probable CpxR-P binding motif ~400 bp upstream of the *cueP* start codon (Table 27). Genes encoding all four members of the suppression of copper sensitivity (Scs) operon (*scsABCD* – *SL1052-SL1054*) were significantly down regulated during our microarray analysis (CpxR activated). This operon is absent from

E. coli however homologues are found in other Enterobacteria. Although studies have focused on the role of the Scs operon in copper tolerance, redox stress and pathogenicity (Gupta et al., 1997, Anwar et al., 2013), no studies have provided evidence as to the genetic regulation of this operon in *S*. Typhimurium or any species where this operon is present. Following bioinformatic analyses, no obvious CpxR binding motif was located within the promoter of *scsA* (Table 27), suggesting CpxR independent regulation of this operon. Investigations into the role of CueP and the Scs operon in the copper tolerance response of *S*. Typhimurium and regulation by Cpx are continued in Chapter 4.

3.4.2.2.4 Metabolic functions and respiration

Among the 18 genes encoding proteins involved in respiration and metabolism that presented differential expression in SL1344 WT and Δ*cpxR* (Table H1), the *SL3350-SL3351* operon, encoding YedYZ, was induced ~5-fold by CpxR. Biochemical and biophysical characterisation of YedYZ in *E. coli* confirmed that YedZ, a membrane intrinsic cytochrome *b* with six putative transmembrane helices, anchors YedY, a molybdoenzyme, to the cytoplasmic membrane (Brokx et al., 2005). Together these proteins function as a sulfite oxidase (SO), conserved across a range of Gram-negative bacteria (Brokx et al., 2005, Loschi et al., 2004). Very few bacterial SO family enzymes have been characterised in detail. Those that have exhibit a huge variation in structural conformation and are involved in a range of metabolic processes: host colonisation, sulfite detoxification, organosulfonate degradation and energy production from sulphur compounds (Kappler, 2011). YedYZ is yet to be assigned a metabolic function and there is no information available in the current literature on the regulation of this system in *Salmonella*. However, as was the case for *SL3009-SL3010*, no CpxR-P consensus-binding motif is located within the *yedYZ* operon promoter (Table 27), but possible regulation by the ESR Bae, in addition to Cpx, has been observed at times of envelope stress (Appia-Ayme et al., unpublished observations).

Transcription of the *deoA* gene, annotated in *S.* Typhimurium as a thymidine phosphorylase, was induced 2.42-fold in SL1344 WT by CpxR (Table 23). Bioinformatic analysis shows 98 orthologues of *S*. Typhimurium LT2 *deoA* within the Enterobacteriaceae family (data not shown) and investigations into the structure and function of the *deo* operon date back three decades (Valentin-Hansen et al., 1984). Our data highlights possible *deoA* activation by CpxR, either directly or indirectly, under our test conditions. DeoA is up regulated in response to glyphosate stress, a broad-spectrum herbicide, in a new *Enterobacter* species (Fei et al., 2013). However, as stated by Fei et al. (2013) bacteria exposed to stresses of this nature are consequently exposed to oxidative, acidic and osmotic stress and the changes in global regulation observed could be due to these related effects. Two possible CpxR-P binding motifs were situation upstream of the *deoA* initiation codon at ~266 bp and ~460 bp (Table 27), the latter of which is situation within the *deoC* gene.

The remaining 15 genes in this functional category include four of the eight members of the *ccm* operon, *ccmBCDE*, involved in the maturation of *c*-type cytochromes (Thony-Meyer et al., 1995). All saw significant repression (>2.75-fold) by CpxR during our transcriptomic analysis (Table 22). A possible CpxR-P binding motif is located ~890 bp upstream of *ccmA* (Table 27), however this gene and *ccmFGH* did not pass the statistical filtering (2-fold change cut-off; FDR<0.05) imposed.

3.4.2.2.5 Genes of unknown or hypothetical function

In total, 61 genes of unknown function were defined as Cpx-regulated following KEGG pathway analysis (Figure 11). These genes have no known function assigned to them, are annotated according to sequence and structural homology only or are listed as hypothetical proteins. Of these 61 (42% of the total 144 genes) 25 were CpxR repressed (up regulated in SL1344 WT) (Table 22) and 36 were CpxR activated (down regulated in SL1344 WT compared to Δ*cpxR*) (Table 23, Figure 11). Several of these genes have been previously reported as Cpx regulated and were described in 3.4.2.

One gene of unknown function, *ybiJ*, was up regulated ~12-fold in the presence of CpxR (Table 23). This fold-change makes *ybiJ* one of the most positively regulated, previously unknown, Cpx regulon members in our data. To the best of our knowledge, no information into the regulation of *ybiJ* in any bacterial species exists in current literature. A possible role for YbiJ, the small (86 amino acid), low-molecular weight protein product of this gene, has been proposed in biofilm formation of UPEC *E. coli* (strain CFT073) (Hancock et al., 2010), but this is yet to be determined and no function of YbiJ has been assigned in any species. BLASTP analysis of YbiJ from SL1344 WT indicates an 80% sequence homology (69 of 86 residues) at the amino acid level with YbiJ of UPEC *E. coli* str. CFT073 (Appendix J). Both the function of YbiJ and its mode of regulation in *S*. Typhimurium warrant further investigation.

Bioinformatic analysis of the *stm3030-3031* (*SL3009-SL3010*) operon in *S*. Typhimurium LT2 theys they encode an YfdX-like protein and an OmpX-like OMP, with a possible role in virulence (data not shown). Both genes were substantially down regulation in the absence of CpxR, 18.4-fold and 9.25-fold respectively (Table 23). A role for STM3031 in ceftriaxone resistance of *S*. Typhimurium has been alluded to and a decrease in STM3031 levels in a Δ*cpxAR* double mutant (Hu et al., 2005, Hu et al., 2009). However, no CpxR-P binding sites have been located within the promoter region of this operon during our investigations (Table 27) and possible regulation by another ESR, BaeSR, has been suggested (Hu et al., 2005, Hu et al., 2009). This suggests indirect or combined regulation of this operon by the Cpx system and/or other ESRs.

3.4.2.2.6 Transport and efflux systems

The YdgFE two-component system (also known as MdtJI in *E. coli*) is annotated in SL1344 as a multidrug efflux system (Chaudhuri et al., 2004). Both genes were significantly down regulated (*ydgF* 3.17-fold and *ydgE* 2.64-fold) in our *cpxR* null strain (Table 23), highlighting a possible positive regulation by CpxR. Investigations in *E. coli* suggest a role for YdgFE in

resistance to SDS, deoxycholate, nalidixic acid and fosfomycin, when the ORF was expressed in multicopy and overexpression vectors (Nishino and Yamaguchi, 2001). An additional function as a potential spermidine efflux system has also been alluded to (Higashi et al., 2008). Work to date on this SMR type transporter system has only been conducted in derivatives of *E. coli* K-12 (Nishino and Yamaguchi, 2001, Carper et al., 1991, Higashi et al., 2008) and W3100 (Hirakawa et al., 2005). No regulatory information has been published for YdgFE, or homologues of these genes in *S*. Typhimurium or related species. A proposed CpxR-P binding motif is situated ~160 bp upstream of the *ydgF* transcriptional start site (Table 27) and *S*. Typhimurium YdgF and YdgE are 84% and 83% homologous, at the amino acid level, with their equivalents in these *E. coli* stains (Appendix J).

According to the genome sequence database EcoGene, *chaA* (*SL1699* in SL1344) encodes a Ca^{2+}/H^{+}-K^{+}/H^{+} antiporter, which extrudes K^{+} ions, and Na^{2+} ions at an alkaline pH (Rudd, 2000). This source also states *chaA* is regulated by osmolarity and pH. Analysis of the *E. coli* IM proteome showed ChaA has 11 predicted transmembrane domains with the C-terminus localised to the periplasm (Daley et al., 2005). Levels of *chaA* transcription were 7.18-fold higher in *S*. Typhimurium when CpxR was present (Table 23). Although a potential CpxR-P binding site has been described ~100 bp upstream of the *chaA* gene of *E. coli*, *in vivo* effects of CpxR-P binding or evidence of CpxR-P binding *in vitro* are yet to be shown (De Wulf et al., 2002). Our *in silico* analysis revealed a proposed CpxR-P binding motif ~ 400bp upstream of the *chaA* start codon in SL1344 (Table 27) a site which is located between *chaA*-*chaB*.

Table 24: **New members of the Cpx regulon of *S*. Typhimurium.** All genes are differentially regulated in SL1344 WT and SL1344 Δ*cpxR* following induction of the Cpx response by NlpE overexpression and have had no Cpx regulation assigned to them, in any bacterial species, previously. Values >2 are up-regulated in Δ*cpxR*, values <0.5 are down regulated in Δ*cpxR* compared to SL1344 WT.

Locus Tag		Gene Name	Description	Fold Change[†]
SL Number	STM Number			
Unknown/Hypothetical Proteins				
SL0799	STM0823	*ybiJ*	Hypothetical protein	0.08
SL1177	STM1239		Putative cytoplasmic protein	2.14
SL1186	STM1250		Putative cytoplasmic protein	3.26
SL1260	STM1325	*ydiZ*	Putative cytoplasmic protein	0.35
SL1278	STM1344	*ydiV*	Hypothetical protein; possible putative diguanylate cyclase/phosphodiesterase domain 1	2.23
SL2163	STM2186		Putative oxidoreductase	2.76
SL2378	STM2410	*yfeA*	Hypothetical protein	2.66
SL2674	STM2703		Hypothetical protein	2.92
SL3009	STM3030		Hypothetical protein	0.05
SL3105	STM3131		Putative cytoplasmic protein	2.05
SL3112	STM3138		Putative methyl-accepting chemotaxis protein	5.92
SL3161	STM3187	*ygiB*	Hypothetical protein	0.19
SL3162	STM3188	*ygiC*	Putative glutathionylspermidine synthase	0.25
SL3200	STM3227	*yqjB*	Hypothetical protein	0.26
SL3201	STM3228	*yqjC*	Putative periplasmic protein	0.33
SL3202	STM3230	*yqjE*	Putative inner membrane protein	0.43
SL3203	STM3231	*yqjK*	Putative inner membrane protein	0.40
SL3229	STM3256		Phosphotransferase system mannitol/fructose-specific IIA component	0.48
SL3350	STM3377	*yedY*	Putative sulfite oxidase subunit	0.17
SL3351	STM3378	*yedZ*	Putative sulfite oxidase subunit	0.22

Table 24 continued

Locus Tag		Gene Name	Description	Fold Change[†]
SL Number	STM Number			
SL3438	STM3471	*yhfG*	Hypothetical protein	0.29
SL4239	STM4302		Putative cytoplasmic protein	3.18
SL4248	STM4312		Hypothetical protein	7.36
	STM14_1500		Hypothetical protein; located directly upstream of PagC (outer membrane invasion protein [STM1246])	2.20
	STM3229	*yqjD*		0.34
Virulence				
SL0776	STM0800	*slrP*	Leucine-rich repeat-containing protein	2.31
SL1030	STM1091	*sopB*	SigD; Salmonella outer protein B; Effector protein secreted by SPI-I, type-III secretion system	2.86
SL1184	STM1246	*pagC*	Virulence membrane protein PAGC precursor	2.43
SL1799	STM1867	*pagK*	PhoPQ-activated gene	2.14
SL2043	STM2066	*sopA*	Effector protein secreted by SPI-I, type-III secretion system	6.55
SL2232	STM2262	*eco*	Ecotin precursor	0.21
SL2848	STM2868	*orgC*	Putative cytoplasmic protein	4.66
SL2850	STM2870	*orgA*	Needle complex assembly protein	6.40
SL2851	STM2871	*prgK*	Needle complex inner membrane lipoprotein	5.04
SL2852	STM2872	*prgJ*	Needle complex minor subunit	5.27
SL2853	STM2873	*prgI*	Needle complex major subunit	5.06
SL2854	STM2874	*prgH*	Needle complex inner membrane protein	6.76
SL2855	STM2875	*hilD*	Invasion protein regulatory protein	4.28
SL2856	STM2876	*hilA*	Invasion protein regulator	7.64
SL2857	STM2877	*iagB*	Invasion protein precursor	4.26
SL2858	STM2878	*sptP*	Protein tyrosine phosphatase/GTPase activating protein	2.82
SL2859	STM2879	*sicP*	Secretion chaperone	3.46
SL2860	STM2881	*iacP*	Acyl carrier protein	4.46

Table 24 continued

Locus Tag		Gene Name	Description	Fold Change[†]
SL Number	STM Number			
SL2861	STM2882	*sipA*	Secreted effector protein	3.61
SL2862	STM2883	*sipD*	Translocation machinery component	3.30
SL2863	STM2884	*sipC*	Translocation machinery component	3.20
SL2864	STM2885	*sipB*	Translocation machinery component	3.20
SL2865	STM2886	*sicA*	Secretion chaperone	3.58
SL2867	STM2888	*spaR*	Needle complex export protein	3.04
SL2868	STM2889	*spaQ*	Needle complex export protein	3.34
SL2869	STM2890	*spaP*	Surface presentation of antigens protein	6.37
SL2870	STM2891	*spaO*	Surface presentation of antigens protein	3.65
SL2871	STM2892	*invJ*	Needle length control protein	4.41
SL2873	STM2894	*invC*	Needle complex assembly protein	4.64
SL2874	STM2895	*invB*	Secretion chaperone	5.22
SL2875	STM2896	*invA*	Needle complex export protein	6.32
SL2877	STM2898	*invG*	Outer membrane secretin precursor	3.50
SL2878	STM2899	*invF*	Invasion regulatory protein	4.36
SL2879	STM2900	*invH*	Needle complex outer membrane lipoprotein precursor	6.10
Regulation				
SL3361	STM3388		Putative signal transduction protein	0.36
SL3646	STM3681		Putative transcriptional regulator	0.31
SL4250	STM4314		Putative regulatory protein	3.55
SL4251	STM4315		Putative DNA-binding protein	10.73
SL4298	STM4364	*hflC*	FtsH protease regulator	0.47
SL4510	STM4583	*trpR*	Probable Trp operon repressor	0.41

Table 24 continued

Locus Tag		Gene Name	Description	Fold Change[†]
SL Number	STM Number			
Small RNAs				
		invR	Small non-coding regulatory RNA	3.14
		omrA	Small RNA	0.34
		omrB	Small RNA	0.33
Transport/Efflux Systems				
SL0407	STM0413	*tsx*	Nucleoside channel	2.35
SL0500	STM0507	*ybbA*	Putative ABC transporter ATP-binding protein	0.19
SL1412	STM1482	*ydgF*	Multidrug efflux system protein MdtJ	0.32
SL1413	STM1483	*ydgE*	Multidrug efflux system protein MdtI	0.38
SL1699	STM1771	*chaA*	Calcium/sodium: proton antiporter	0.14
SL2796	STM2811	*proX*	Glycine betaine-binding periplasmic protein precursor	2.90
SL3928	STM3974	*tatB*	Sec independent translocase protein	0.47
SL4124	STM4189	*yjbB*	Periplasmic transport protein	0.19
SL4238	STM4301	*dcuB*	Anaerobic C4-dicarboxylate transporter	4.10
Cell envelope components				
SL0808	STM0833	*ompX*	Outer membrane protein X	0.33
SL1181	STM1242	*envE*	Putative envelope protein; Probable EnvE precursor	2.10
SL1189	STM1253		Putative inner membrane protein	3.30
SL1190	STM1254		Putative outer membrane lipoprotein	12.97
SL1263	STM1328		Putative outer membrane protein	4.27
SL1404	STM1473	*ompN*	Outer membrane protein N precursor	0.25
SL3010	STM3031		Ail/OmpX-like protein	0.11
SL3365	STM3392	*yhdV*	Putative outer membrane lipoprotein	0.40

Table 24 continued

Locus Tag		Gene Name	Description	Fold Change[†]
SL Number	STM Number			
Cell surface				
SL0536	STM0543	*fimA*	Fimbrin	3.15
SL2056	STM2079	*wzzB*	Lipopolysaccharide O-antigen chain length regulator	2.57
Metal stress and homeostasis				
SL1052	STM1113	*scsA*	Suppression of copper sensitivity protein A	0.15
SL1053	STM1114	*scsB*	Suppression of copper sensitivity protein B	0.31
SL1054	STM1115	*scsC*	Suppression of copper sensitivity protein C	0.27
SL1055	STM1116	*scsD*	Suppression of copper sensitivity protein D	0.31
SL1996	STM2020	*cbiO*	Cobalt transporter ATP-binding subunit	2.28
SL1999	STM2023	*cbiM*	Cobalt transport protein	3.37
SL2000	STM2024	*cbiL*	Cobalt-precorrin-2 C(20)-methyltransferase	2.46
SL2001	STM2025	*cbiK*	Vitamin B12 biosynthetic protein	2.54
SL2003	STM2027	*cbiH*	Precorrin-3B C(17)-methyltransferase	2.91
SL2011	STM2035	*cbiA*	Cobyrinic acid a,c-diamide synthase	2.41
SL3616	STM3650	*cueP*	Hypothetical protein; proposed copper sensitivity protein	0.08
Respiration and metabolism				
SL0088	STM0087	*folA*	Dihydrofolate reductase	0.13
SL1261	STM1326	*pfkB*	6-phosphofructokinase 2	0.32
SL1811	STM1877		Putative amidohydrolase	0.30
SL1872	STM1939		Putative glucose-6-phosphate dehydrogenase	2.65
SL2020	STM2044	*pduH*	Propanediol dehydratase reactivation protein	2.25
SL2225	STM2255	*napC*	Cytochrome C-type protein	3.31

Table 24 continued

Locus Tag		Gene Name	Description	Fold Change[†]
SL Number	STM Number			
SL2490	STM2528		Putative dimethylsulfoxide reductase	2.14
SL2521	STM2559	*cadA*	Lysine decarboxylase 1	2.65
SL3352	STM3379	*accB*	Acetyl-CoA carboxylase biotin carboxyl carrier protein subunit	0.35
SL3353	STM3380	*accC*	Acetyl-CoA carboxylase biotin carboxyl carrier protein subunit	0.37
SL3437	STM3470	*fic*	Cell filamentation protein	0.34
SL3782	STM3815	*ccmE;ccmD*	Cytochrome c-type biogenesis protein	2.88
SL3783	STM3817	*ccmC*	Haem exporter protein	2.93
SL3784	STM3818	*ccmB*	Haem exporter protein	2.75
SL4294	STM4360	*miaA*	tRNA delta(2)-isopentenylpyrophosphate transferase	0.26
SL4450	STM4519		Putative NAD-dependent aldehyde dehydrogenase	0.37
SL4495	STM4568	*deoA*	Thymidine phosphorylase	0.41
SL1265	STM1330		Putative DNA/RNA non-specific endonuclease	2.02

[†]Denotes change in expression level in SL1344Δ*cpxR* compared to SL1344 WT following overexpression of *nlpE*. Values <0.5 represent level of expression reduction.

3.5 Discussion and future work

The work presented here includes the first broad-scale, transcriptomic analysis of the *Salmonella* Cpx regulon. We utilised NlpE overexpression, a Cpx specific inducing cue, to define the transcriptional response of *S.* Typhimurium SL1344 to stimulation of the Cpx ESR pathway. This work expands upon similar studies in *E. coli* (Raivio et al., 2013, Price and Raivio, 2009), the human pathogen *H. ducreyi* (Labandeira-Rey et al., 2010, Labandeira-Rey et al., 2009) and other microarray studies where the Cpx-regulon was defined through overexpression of unphosphorylated CpxR or strains lacking the Cpx response (Bury-Mone et al., 2009). Together, these investigations provide a detailed description of how the Cpx ESR responds to disruption of envelope homeostasis through the genes this pathway regulates.

3.5.1 Cpx regulon members, identified previously in *E. coli*, with unchanging transcription following induction of the Cpx response in SL1344 strains

Of the 144 genes differentially regulated in our SL1344 WT and Δ*cpxR* strains (Table H1), 53% were CpxR activated (77 genes - Table 22), and 47% were CpxR repressed (67 genes - Table 23). These results were compared to all known Cpx-regulated genes available in the current literature (Table G1) to ascertain new and previously identified Cpx regulon members within our data set. Bury-Mone et al. (2009) conducted global analysis of extracytoplasmic stress signalling in model *E. coli* strains. From their investigations, 35 proposed Cpx regulon members were identified, of which only four were present in our data set: *yebE*, *csrB*, *spy* and *cpxP*. Of the remaining 31 genes not present in our data, almost half (14 genes) exhibited a less than 2-fold change in expression levels (Bury-Mone et al., 2009). If equivalent changes were observed for these 31 genes in our *S*. Typhimurium study, they would have been discounted during statistical filtering due to the 2-fold change threshold applied. When the Cpx regulon of *E. coli* presented by Bury-Mone et al. (2009) is compared to those in Price and Raivio (2009), a second transcriptomic study of the Cpx regulon in MC4100, only *yebE*, *spy* and *cpxP* were present in both studies. Bury-Mone et al. (2009) used

MG1655 *cpxR* deletion strains, *cpxR* overexpression and *lacZ* transcriptional fusions during transcriptome analysis to identify Cpx regulon members, not a specific Cpx-inducing cue, as utilised by the Raivio group and our study. Deletion of *cpxR* alone does not induce transcriptional change for the majority of proposed Cpx-regulated genes (Price and Raivio, 2009) and overexpression of CpxR could result in large amounts of unphosphorylated RR. A *lux* reporter system utilised by Price and Raivio (2009) is also more sensitive than the *lacZ* promoter fusions published by Bury-Mone et al. (2009), which may provide explanations for the absence of several predicted regulon members in the Bury-Mone et al. (2009) study.

3.5.1.1 Sigma factors and gene products involved in regulation

Negative regulation of the RpoE (σ^E) promoter *rpoE*P3 by Cpx has been demonstrated in *S*. Typhimurium (Miticka et al., 2003). Our data concurs with Miticka et al., (2003); *rpoE* expression was 2.48-fold lower in our WT strain compared to Δ*cpxR* (Table 22), a similar reduction to that observed in *E. coli* by Price and Raivio (2009). The σ^E operon also consists of *rseA* and *rseBC*, which contribute towards σ^E activation. Expression of *rseA* reduced concurrently with *rpoE* (Table 22), but *rseBC* exhibited no significant changes in their transcriptional levels (data not shown). It is expected that any effects of Cpx induction on these two genes were not observed post differential analysis due to inconsistencies in fluorescence during array scanning, and therefore missed the 2-fold cut off threshold applied to our data. There are several hypotheses as to why *rpoE* is negatively regulated by the Cpx ESR. As σ^E is essential in *E. coli* and *Salmonella rpoE* null strains are rendered avirulent and sick (De Las Penas et al., 1997, Humphreys et al., 1999), optimised expression of this sigma factor is essential. Excessive repression by Cpx would be detrimental to cell survival. Both Cpx and σ^E ESRs are self-regulating and this coupled with negative regulation of σ^E by Cpx suggests a tightly controlled feedback loop, allowing the cell to control the number of active ESRs and the intensity of their induction in response to stress. There is significant overlap in the stress signals that induce the Cpx and σ^E stress responses with both responding to p-pilus misassembly and toxic accumulation of misfolded proteins in the periplasm. The σ^E regulon is

extensive and still growing (Table B2). If both ESRs are activated simultaneously, certain genes regulated by σ^E may be detrimental to the Cpx pathway during activation. If so, negative regulation by Cpx may be a response to activation of singular or multiple σ^E regulon members.

Cpx, σ^E and RpoH (σ^H or σ^{32}) respond in a coordinated manner to stress signals. Positive regulation of the heat shock sigma factor σ^H by σ^E has been identified in several bacterial species (Nuss et al., 2009, Bury-Mone et al., 2009). Danese and Silhavy (1997) also showed negative regulation of *rpoH* by Cpx in *E. coli* through binding of CpxR-P to the *rpoH*1 promoter. However, no evidence of *rpoH* regulation by Cpx was presented by Raivio and colleagues (2009, 2013). The current understanding in *E. coli* is that when Cpx represses expression of the *rpoE-rseABC* operon, Cpx indirectly represses *rpoH* through this reduction in σ^E. σ^H may then be further repressed through binding of CpxR-P to the *rpoH*P1 promoter (Danese and Silhavy, 1997). Our study concurs with the negative regulation of *rpoE* by Cpx, as described above. However, surprisingly, our data suggested positive regulation of *rpoH* by Cpx in *S*. Typhimurium. Transcription of *rpoH* increased 3.1-fold when CpxR was present (Table 23), the opposite of what has been proposed in *E. coli*. The repression of *rpoH* that occurs following negative regulation of σ^E by Cpx is therefore not observed in *S*. Typhimurium. One explanation is that in *Salmonella*, it appears that Cpx counteracts any detrimental effects on *rpoH* expression as a result of *rpoE* down-regulation through *rpoH* activation. The presence of a possible CpxR binding motif within the promoter region of *rpoH* (approximately 730 bp upstream of the ATG start codon) (Table 27; Chaper 4) suggests the up-regulation of *rpoH* observed occurs in a direct manner and the specific nature of this regulation is investigated and discussed in Chapter 4.

3.5.1.2 Confirmation of Cpx mediated regulation of well-characterised periplasmic chaperones and proteases

As several Cpx inducing cues result in the accumulation and misfolding of periplasmic proteins, it was unsurprising for several proteases and chaperones to be among the first Cpx regulated genes identified in *E. coli*

(Danese and Silhavy, 1997, Danese and Silhavy, 1998, Quan et al., 2011, Danese et al., 1995, Pogliano et al., 1997) (Table G1). Of these well characterised Cpx-regulated genes, several envelope folding and degrading factors: the chaperones CpxP, Spy and Skp (HlpA), the protease and chaperone HtrA, the disulphide oxidase DsbA and the peptidyl-proyl-isomerase PpiA, were all under Cpx control in *Salmonella*, further confirming their status as Cpx regulated (*dsbA*, induced 2.4-fold; *htrA*, induced 9.32-fold; *spy*, induced 53.3-fold; *ppiA*, induced 9.86-fold).

The prominence of Skp (HlpA) as a key component of protein folding in the periplasm is well documented (Missiakas et al., 1996, Thome and Muller, 1991). Studies have identified *skp* as under the regulation of σ^E (Dartigalongue et al., 2001, Skovierova et al., 2006) and Cpx (De Wulf et al., 2002) due to a proposed CpxR-P binding site located approximately 120 bp upstream of the *skp* start codon. Our data provide experimental evidence in *S*. Typhimurium to support the suggested Cpx regulation of *skp* by De Wulf et al. (2002) in *E. coli*. Studies of Skp in *S*. Typhimurium have shown the importance of this periplasmic protein in virulence (Rowley et al., 2011). With Skp now an established member of the Cpx-regulon in *Salmonella*, our data including the repression of SPI-1 and its regulators by the Cpx response (3.5.2.1), add further weight to the contribution of the Cpx response towards regulating *Salmonella* virulence factors.

Cpx regulation of the *ppiA* gene was first described by Pogliano et al. (1997) in MC4100 derivatives, where, following RNA transcript analysis, expression from the *ppiA* P1 promoter increased 2.5-fold when NlpE was overexpressed. This induction was only observed in the presence of CpxAR and did not occur in strains absent of this operon (Pogliano et al., 1998). This concurs with the data presented here, although our observed induction of *ppiA* was almost four times greater than that witnessed by Pogliano et al. (1997). During that study, expression of both *dsbA* and *degP* (*htrA*) was higher than *ppiA*. In *Salmonella*, *ppiA* and *htrA* were up-regulated ~9-fold, and *dsbA* 2.5-fold. This 4-fold increase in *ppiA* levels may result from the differential regulation of sigma factors σ^E and σ^H also seen in our data. There

is substantial evidence to support overlap of genes regulated by the envelope stress responses. For example, Cpx modulates BaeR-mediated transcriptional regulation and can also nullify some effects of σ^E deletion (Hirakawa et al., 2005, Connolly et al., 1997). To assess the impact of such overlap, a Cpx-regulon *lux* reporter library could be constructed and induction measured (through luminescence assays) in our Δ*cpxR* and NlpE overexpression backgrounds, an SL1344 *cpxA** strain, SL1344 with constitutive Bae expression, SL1344 Δ*rpoE* or SL1344 harbouring an *rpoE* overexpression plasmid. This would allow basal levels of transcription and the relative strength of Cpx regulation for all Cpx-regulon members discussed here to be determined. This large-scale screening may also identify not previously observed associations between the ESRs and improve our understanding of those less characterised ESRs, such as BaeSR.

Although several established members of the Cpx regulon were further confirmed as Cpx regulated during our analysis, some examples were absent from our 144 differentially regulated genes. Three genes, *ppiD*, *ung* and *ompC*, identified as weakly or moderately regulated by the *E. coli* Cpx response system (Dartigalongue and Raina, 1998, De Wulf et al., 2002), were not present in our data set post differential analysis. Like *ppiA*, *ppiD* encodes a PPIase and acts as a multicopy suppressor of *surA* (Dartigalongue and Raina, 1998). Dartigalongue and Raina (1998) overexpressed the phosphatase PrpA in MC4100 to show *ppiD* regulation by Cpx at the transcriptional level (overexpression of *prpA* constitutively expresses the Cpx pathway) (Missiakas and Raina, 1997). Transcription of *ppiD* was uneffected by *cpxR* and *cpxA* deletions in *H. ducreyi* (Labandeira-Rey et al., 2010) and *ppiD* has not been identified as Cpx regulated in other similar transcriptomic studies (Raivio et al., 2013, Bury-Mone et al., 2009). The *cpxA24* allele is a strong inducer of the Cpx response and this also had no affect on *ppiD* expression (Price and Raivio, 2009). Despite the presence of a CpxR-P consensus-binding motif upstream of the *ppiD* σ^{70} promoter, CpxR-P binding has never been demonstrated (De Wulf et al., 2002, Dartigalongue and Raina, 1998). What effect, if any, Cpx has on *ppiD* expression therefore remains questionable. To the best of our knowledge the

only Cpx inducing cue to impact *ppiD* regulation is PrpA overexpression (Missiakas and Raina, 1997). Whether this phosphatase has a transient effect on *ppiD* expression or if *ppiD* induction by Cpx is specific to this inducing cue remains unclear. However evidence is building to question PpiD as an established Cpx regulon member, in *E. coli* and *Salmonella*.

Transcription of *ompC* is only slightly (~1.4-fold increase) affected by constitutive expression of *cpxA* (Price and Raivio, 2009), with no differences seen during NlpE overexpression. De Wulf et al. (2002) highlighted a CpxR-P binding motif 425-439 bp upstream of the *ompC* start codon, with expression data showing positive (<2-fold) regulation by Cpx in a combination of Cpx deletion backgrounds. However, fluorescence assays utilising chromosomal *ompC* cyan fluorescent protein (CFP) fusions showed a 3-fold increase in *ompC* expression, during NlpE overexpression and in CpxA* strains of MG1655 (Batchelor et al., 2005). Batchelor et al. (2005), De Wulf et al. (2002) and Raivio et al. (2013) suggest minimal regulation of OmpC by Cpx in *E. coli*. This was not observed in our data set for *Salmonella*. Despite the presence of a CpxR-P binding motif within the promoter of *ompC* in *E. coli*, no potential binding site was found during our bioinformatic analysis of the 1000bp upstream of *ompC* in *S*. Typhimurium LT2 (data not shown). It is yet to be determined if OmpC transcription changes slightly in CpxA* *Salmonella* strains, as was the case in *E. coli* (Price and Raivio, 2009), but the lack of a CpxR binding motif and any substantial changes in transcription in our data, as observed for well-characterised Cpx regulon members, suggests this regulation results from pleiotropic effects as a result of constitutive *cpxA* expression and not direct Cpx regulation. Our *in silico* analysis coupled with the lack of significant changes to *ompC* transcription in our microarray concludes that OmpC is not Cpx regulated in *S*. Typhimurium.

Raivio et al. (2013), like us, observed no significant changes to *ompC*, *ppiD* or *ung* expression following transient NlpE overexpression. Given the similarity in genetic backgrounds used by Raivio et al. (2013) and other studies where Cpx regulation of these three genes was witnessed (Raffa and

Raivio, 2002, Raivio and Silhavy, 1997, De Wulf et al., 2002, Ogasawara et al., 2007, Price and Raivio, 2009, Dartigalongue and Raina, 1998), there are limited explanations for the differences seen. Either the inducing methodology employed by us and Raivio et al. (2013) were not sufficient to witness the small effects of Cpx on regulation of *ompC*, *ppiD* or *ung*, or regulation by Cpx is dependent on other factors not present during these investigations. The theory that our methods of Cpx induction were not adequately sensitive or selective does not concur with the changes in expression seen for the other prominent members of the Cpx regulon previously outlined. Other methods of Cpx induction such as overexpression of *prpA* (Missiakas and Raina, 1997), alkaline pH (Danese and Silhavy, 1997), or P-pilus component overexpression (Jones et al., 1997, Nevesinjac and Raivio, 2005) are possible, but are substantially less specific than the methodology adopted here. In addition to the test strains analysed and discussed during this study, empty P_{BAD} vector controls in SL1344 WT and *cpxR* deletion strains were employed to remove any changes in expression as a result of NlpE changing growth conditions. Additional investigations discussing the general impact of NlpE overexpression through comparison of SL1344p*nlpE* and SL1344pBAD data sets would provide a more full characterisation of this inducing cue. As the means of Cpx activation by NlpE still remains illusive, these additional data could provide new information on the mechanisms of NlpE induction and any transient effects resulting from accumulation of this lipoprotein.

3.5.1.3 Cell division

Cell morphology of an *E. coli cpxA** strain has been analysed by electron microscopy (Pogliano et al., 1998). Abnormal cell cleavage and septum formation were identified in 38% of cells during cell division (Pogliano et al., 1998). Of the key cell division genes (*minCDE*, *ftsQAZ*, *ftsYEX* and *zipA; amiA* and *amiC*, encoding two N-acetylmuramoyl-L-alanine amidases aiding daughter cell separation), *minCDE* has a CpxR-P binding motif and is described as likely to be under direct repression by Cpx (De Wulf et al., 2002). None of these cell division genes including *minCDE* saw significant changes to expression levels in our CpxR mutant or SL1344 WT strains

following Cpx induction. The irregular septation and nucleoid inheritance observed in this CpxA* strain of *E. coli* are not present in *cpxR* deletion strains and are not due to the rate of *ftsZ* synthesis or stability (Pogliano et al., 1998). Normal septation and division was observed by Pogliano et al. (1997) in WT *E. coli* strains with NlpE-activated Cpx signal transduction and no obvious CpxR-P binding consensuses (5'-GTAAAN$_{5-7}$GTAAA-3') were located upstream of the main cell division genes (*ftsQAZ*, *ftsYEX* and *zipA*). The growth conditions and means of NlpE overexpression presented here are equivalent to those utilised by Pogliano et al. (1997). To the best of our knowledge the irregular septation and nucleoid inheritance observed in CpxA* *E. coli* strains has not been seen for the equivalent mutation in any *Salmonella* species. Under the conditions tested here, there appears to be no transcriptional effects of Cpx pathway induction on *minCDE* or any of the other cell division genes, and, in this instance said genes do not appear to be members of the Cpx regulon of *S.* Typhimurium.

3.5.1.4 Chemotaxis and cell components

The *motAB-cheAW* genes encode flagella motor proteins and chemotaxis regulators respectively. A recent review of flagella structure and regulation in *Salmonella* provides a detailed analysis of this tightly controlled system, which is highly conserved across Gram-negative bacteria (Chevance and Hughes, 2008). All six genes are under direct, negative regulation by Cpx in *E. coli* (De Wulf et al., 1999, De Wulf et al., 2002) and evidence supporting Cpx involvement in regulating FlhDC, the master flagella regulatory complex, was provided by Raivio et al. (2013). *flhC* saw significant down regulation in EPEC and MC4100 *E. coli* following NlpE overexpression, in conditions similar to those presented here (Raivio et al., 2013). Expression of *motAB-cheAW* and *flhDC*, located directly upstream of the *mot* operon, remained unchanged throughout our investigation. To date no experimental evidence has been provided to confirm Cpx regulation of these motility genes in *Salmonella*. However, the serine chemoreceptor encoded by *tsr* was Cpx activated post NlpE overexpression (Table 23). The role of Cpx on motility in *Salmonella* therefore remains enigmatic and further experiments are required. qRT-PCR of the main members of the flagella regulon in our

investigative strains would provide initial evidence to confirm the non-significant changes in transcription witnessed during our study. Unfortunately, these investigations, along with others to elucidate this role of Cpx in *Salmonella*, were outside the remit of this study. Completing these investigations in the future could provide crucial evidence highlighting a significant difference between the roles of Cpx in *E. coli* and *Salmonella*.

3.5.1.5 Genes of unknown function

As was the case for the other Cpx-regulon studies described throughout this chapter, one of the largest groups of genes positively regulated by NlpE overexpression in *S*. Typhimurium were those encoding hypothetical proteins and genes of 'unknown function' (Table H1). Many of the same putative proteins were present in our study and those by Raivio et al., (2009, 2013) (*yccA*, *ycjS*, *ynfD*, *yncJ*, *yebE*, *yqaE*, *yqjA*). These findings highlight the need for further and continued investigation of these proteins of unknown function. The Cpx response is intimately associated with a number of important phenotypes: antibiotic resistance, regulation of proteins at the IM, adhesion factors and many more. These associations are proving to be intricately complex and understanding the multiple levels of regulation involved within these molecular networks is increasingly challenging. Phenotypic analysis of uncharacterised members of the Cpx regulon could highlight previously unknown, essential members of these processes, providing important genetic and molecular targets with potential biotechnological and biomedical implications. A number of investigations into the function of certain unknown or hypothetical proteins, within our list of newly proposed members of the Cpx regulon (Table 25), are presented in Chapter 4.

3.5.2 Novel Cpx regulated genes

The functions of the 116 genes identified during this transcriptome analysis as novel Cpx regulon members varied widely (Table 24). To determine the functional classes of genes regulated by Cpx and the variability of Cpx function, all 116 genes were grouped according to the Kyoto Encyclopaedia of Genes and Genomes (KEGG) and current literature (Figure 11).

3.5.2.1 Cpx and pathogenicity

HilA is the central, positive regulator of *Salmonella* Pathogenicity Island-1, and is activated by CpxA in a pH dependent manner (pH 6.0) (Nakayama et al., 2003). Although HilA is an essential regulator of invasion gene expression, it does not appear to directly sense environmental cues (Johnston et al., 1996). The sensor kinase CpxA (but not CpxR) is required, presumably to act as this environmental sensor and induce *hilA* transcription; a *cpxA* mutant presents reduced invasiveness in INT 407 (HeLa derived) cells at pH 6.0 (Nakayama et al., 2003). Despite this, CpxAR mutants are slightly (but significantly) more invasive than WT *S*. Typhimurium for reasons unknown (Nakayama et al., 2003, Humphreys et al., 2004). When the Cpx system was induced, *hilA* expression increased 7.64-fold in Δ*cpxR* compared to SL1344 WT (Table 22), suggesting a repressive role for CpxR on *hilA*. If *hilA* regulation were independent of CpxR, as was observed by Nakayama et al. (2003), this differential regulation of *hilA* between SL1344 WT and Δ*cpxR* backgrounds would not have been observed. The mechanisms behind this apparent repressive role of CpxR, especially due to the complex nature of *hilA* regulation through multiple regulators, warrants further investigation. In addition to CpxR, the response regulator SirA is one of three other known regulators of HilA. The other two HilC and RtsA, are activated by HilD (Johnston et al., 1996). SilA regulation of *hilA* highlights a signal cascade of transcription factor synthesis that is important for invasion. Although both *hilC* and *hilD* are encoded within SPI-1, only *hilD* saw a significant change in expression (4.28-fold reduction), in our SL1344 WT strain compared to Δ*cpxR*. Expression of *hilC* was reduced ~2-fold by CpxR, but did not pass the statistical filtering employed. No significant change in *rtsA* expression was seen, encoded on a *Salmonella* specific insert (15 kb in length) located up/downstream of the gene for $tRNA^{PheU}$.

SlrP is a host specific virulence factor secreted by SPI-1 and SPI-2 TTSS. This protein mediates ubiquitination of ubiquitin and thioredoxin during host cell infection (Bernal-Bayard and Ramos-Morales, 2009). LeuO, Lon, and the two-component system PhoQ/PhoP are novel *slrP* regulators (Cordero-Alba and Ramos-Morales, 2014). It was proposed that under SPI-2 inducing

conditions PhoP interacts with the *slrP* promoter directly, activating transcription, whereas LeuO and Lon function through HilD under SPI-1-inducing conditions. *slrP* and SPI-1 expression are coordinated and *slrP* is subsequently induced by overexpression of HilC, HilD, and RtsA (Ellermeier and Slauch, 2004, Ellermeier and Slauch, 2003). As *slrP* was repressed 2.21-fold by Cpx during our study (Table 22), we wanted to confirm this reduction was not due to transient effects of NlpE overexpression on these SlrP regulators. Of the regulators outlined here, RtsA is stated as the best inducer of *slrP*. With transcription of *rtsA* unchanged between our SL1344 WT and *cpxR* deletion strains, repression of *slrP* from changes to RtsA levels are highly unlikely. Also, none of the three most recently characterised regulators of *slrP*: LeuO, Lon and the 2CST system PhoQ/PhoP (Cordero-Alba and Ramos-Morales, 2014), saw significant changes to their transcription levels in our data. As HilD is a positive regulator of *slrP*, any decrease in *hilD* expression may result in transient effects on *slrP* transcription. As levels of *slrP* transcription were repressed by CpxR (2.2-fold), and regulation of *hilD* also decreased under the same conditions (4.28-fold), these changes in SlrP expression may be due to down-regulation of HilD by CpxR and not from any direct Cpx regulation. However, the presence of a CpxR binding motif within the promoter region of *slrP* (Table 27; Chapter 4) makes direct down-regulation by CpxR a possibility and direct regulation of *slrP* by CpxR-P is investigated further in Chapter 4.

As well as influencing regulation of SPI-1 TTSS and its regulators, the Cpx response may also contribute towards survival strategies employed within host immune cells. Neutrophils are the first line of defense for host cells against invading microorganisms. Once phagocytosed, the oxidative and non-oxidative pathways are employed by the immune cells to kill the invader. One component of non-oxidative killing is the use of proteinases, sugar hydrolyzing, membrane permeabilising and proteolytic enzymes (Eggers et al., 2004). Neutrophil elastase (NE) is one such proteolytic enzyme secreted by host immune cells. NE targets the OM protein OmpA, where it cleaves causing permeability of the OM that persists even throughout renewed bacterial growth (Belaaouaj et al., 2000). An OmpA deletion in *E. coli*

perturbs the affect of NE, confirming OmpA as a specific target, and NE deficient mice are more susceptible to killing by Gram-negatives (Belaaouaj et al., 2000, Belaaouaj et al., 1998). One novel Cpx-regulon member described during this work was *eco*, encoding the dimeric periplasmic protein ecotin. This protein conserved across *E. coli* and related Gram-negatives inhibits many trypsin-fold serine proteases, the pancreatic digestive peptidases trypsin and chymotrypsin, and is important for *E. coli* survival post NE treatment (Rawlings et al., 2004, Eggers et al., 2004). The fact that NE targets the OM protein OmpA resulting in severe membrane leakage and envelope disruption would make this proteolytic enzyme an understandable target for the ESR systems, such as Cpx. The *eco* gene was induced ~5-fold by Cpx-induction in *S*. Typhimurium (Table 23) and a CpxR-P consensus motif is located ~250-bp upstream of the *eco* initiation codon (Table 27, Appendix K).

3.5.3 sRNAs

Several regulatory sRNAs were identified as Cpx regulon members during our investigations (Vogt et al., 2014). Transcription of *csrB* was repressed 2.58-fold by the Cpx system in *S*. Typhimurium (Table 22). This untranslated sRNA forms the *csrA*/*B* system with the protein CsrA (Liu et al., 1997). CsrB is believed to act as a positive regulator of CsrA, adjusting the free concentration of this protein through binding to ~18-20 CsrA molecules, antagonising its activity. The increase in *csrB* expression observed in our data is comparable to the 1.9-fold increase observed by Bury-Mone et al. (2009). However, CsrB was not identified as a Cpx-regulon member by Price and Raivio (2009) or Vogt et al. (2014). This latter study provided the first comprehensive evidence to show that Cpx regulates, and is regulated by, sRNAs. Both studies utilised NlpE overexpression as a means of Cpx induction and used comparable growth conditions to those presented here. Therefore the genetic backgrounds were the only substantial difference, adding further weight to *csrB* as a member of the Cpx regulon in *Salmonella*.

Transcription of both *omrA* and *omrB* increased ~3-fold (Table 23) when CpxR was present. These two sRNAs are directly involved in regulation of

“curli control cascade” downstream components and are regulated in response to high osmolarity by EnvZ/OmpR (Guillier and Gottesman, 2006). Both sRNAs therefore contribute to regulation of OM components during periods of environmental stress. Consequently, their regulation by CpxR proposed here would be fitting given the contribution of this ESR system to controlling continuity of the OM. OmrA and OmrB have been shown to differentially control *csgD*, a known Cpx regulon member in *E. coli*, through direct binding to *csgD* mRNA, resulting in a reduction of expression levels (Mika and Hengge, 2014). These results suggested another level of Cpx-mediated regulation, through the use of sRNA at the translational level. This negative regulation would provide one explanation as to why no alterations in *csgD* expression, or other members of the ‘curli phenotype’ operon *csgDEFG*, were observed during our investigations.

In conclusion, the continued expansion of the Cpx regulon may result from the large number of cellular regulators, regulatory sRNAs and sigma factors that are under CpxR regulation. Two new, uncharacterised regulators that appear to be under Cpx induction in *S*. Typhimurium are *SL3646* and *SL3361*. The growing number of unknown and hypothetical proteins under Cpx control could further enhance the wide-range of phenotypes and molecular mechanisms associated with this ESR system. The key differences presented in this study between RpoH regulation in *E. coli* and *S.* Typhimurium, and the possible differential regulation of flagellae in these two species, further highlight the importance of understanding the specific function of Cpx in different organisms. With regulation of numerous effector and invasion proteins, regulators of TTSS and protease inhibitors falling under Cpx control, Cpx is also becoming as established contributor to *Salmonella* pathogenicity. Investigations to confirm Cpx regulation of the genes presented during this chapter are continued in Chapter 4. Along with investigations to shed further light on the function of several unknown or hypothetical proteins described so far.

4 Phenotypic analysis of newly discovered and uncharacterised members of the Cpx regulon

4.1 Introduction

4.1.1 Analysis of new Cpx regulon members – An introduction

As presented in Chapter 3, microarray analysis of *S*. Typhimurium revealed 144 genes differentially regulated in SL1344 WT and Δ*cpxR* strains after induction of the Cpx ESR pathway. Investigations presented in Chapter 4 expand upon these initial transcriptomic analyses, focusing on confirming direct regulation of these genes by CpxR and how the proteins they encode contribute towards the Cpx ESR.

Following a review of current literature, 28 of the 144 differentially regulated genes had previously been identified as members of the Cpx-regulon in other Enterobacteriaceae, highlighted yellow in Table H1, leaving 116 genes regulated in a CpxR dependent manner that have not had their regulatory mechanisms associated with the Cpx ESR previously. We have compiled a shortlist of 27 genes, across 18 transcriptional units, to be selected for further analysis (Table 25). These genes were chosen because 1) their regulatory mechanisms remained unknown 2) they are hypothesised as CpxR regulated, but experimental confirmation is lacking and/or 3) they had been characterised as Cpx regulated in a different genetic background during prior studies, but the function of the gene product and function remains unknown. At least 10 of these 27 genes have unknown functions or functions which are yet to be determined in *Salmonella* species (Chapter 3).

After confirming direct or indirect regulation of these genes by CpxR, the role that they play in the *S.* Typhimurium response to envelope stress, specifically through copper tolerance, antibiotic and oxidative stress, polyamine homeostasis and biofilm formation (specifically adhesion to abiotic surfaces) was the focus of the research presented in this chapter. The contribution of Cpx to biofilm formation, antibiotic and AMP stress were summarised during the main introduction. The contribution of the Cpx ESR to copper tolerance is outlined below, along with an introduction to polyamine homeostasis.

4.1.2 *Salmonella* response to copper stress and the contribution of CpxAR to copper tolerance

4.1.2.1 An introduction to metal stress

Metal ions of copper, iron, manganese and zinc are critical components of metalloenzymes, making them essential for the survival of both prokaryotic and eukaryotic cells (Agranoff and Krishna, 1998). One estimate approximates that half of all proteins contain metal ions in their structure and up to a third of enzymes require metals to function correctly (Thomson and Gray, 1998, Waldron and Robinson, 2009). Despite their necessity in biology, metals are toxic if intracellular levels are not strictly controlled. Ironically, the toxic effects of many metals result from the properties that make them so important. For example the redox cycling of Cu^{+} [Cu(I)] and Cu^{2+} [Cu(II)] ions allows this metal to be a critical component of proteins involved in numerous cellular processes i.e. denitrification, oxidative respiration, electron transport (Fraústo da Silva and Williams, 2001, Arguello et al., 2013). However, cellular imbalance of Cu^{+} ions can aid hydroxyl radical formation through reactions with H_2O_2 (via Fenton chemistry). This results in nucleic acid, protein and membrane lipid damage, nitric oxide production through interactions with *S*-nitrosothiols and destabilisation of iron-sulphur cluster enzymes (Williams, 1999, Hiniker et al., 2005, Macomber and Imlay, 2009). In *E. coli* elevated intracellular copper does not cause significant DNA oxidative damage *in vivo*, suggesting copper toxicity occurs (in this instance) through a combination of the other processes described (Macomber et al., 2007). During metal deficiency, intracellular reserves are mobilised and transcription of metal carriers and influx systems are increased. The synthesis of storage proteins, an array of excretion systems, regulators and pumps (e.g. CopA, GesABC, ZntR, ZntAB, ZitB, YiiP, RcnA, Fur, Mur, MntR) help to neutralise the threats exhibited from elevated metal ion concentrations. For a review of metal sensing in *Salmonella* and the impact on pathogenicity see Osman and Cavet (2011).

4.1.2.2 Impact of copper on virulence of Salmonella

Elevated and depleted levels of metal ions in an intracellular environment can have a negative impact on virulence. Systems allowing iron, zinc, manganese, and copper uptake contribute significantly to virulence in pathogenic bacteria (Osman and Cavet, 2011, Guilhen et al., 2013, Crane et al., 2011, Eijkelkamp et al., 2015, Subashchandrabose and Mobley, 2015, Parrow et al., 2013). The importance of copper in bacterial pathogenicity and host immune systems is emphasised by the high infection rates experienced by patients suffering from the lethal Cu-deficiency disorder Menke's disease (Uno and Arya, 1987, Gunn et al., 1984, Kreuder et al., 1993, Agertt et al., 2007). Farm animals with Cu-deficient diets also experience a marked increase in microbial infection occurrence and susceptibility (Samanovic et al., 2012).

During infection, *Salmonella* must overcome an array of stressful and diverse environments present within the host. This includes host-induced reductions in metal availability and metal-mediated toxicity. Although the levels of bioavailable iron are low in humans, neutrophils and macrophages further reduce availability at sites of infection through: iron uptake (Diaz-Ochoa et al., 2014), synthesis of the hormone hepcidin (Nicolas et al., 2001, Nicolas et al., 2002, Park et al., 2001, Nemeth et al., 2003) and iron storage proteins, e.g. transferrin (Nemeth et al., 2003, Armitage et al., 2011) and lactoferrin (Masson et al., 1969, Steinbakk et al., 1990, Goetz et al., 2002). Neutrophils and epithelial cells also release lipocalin-2, an antimicrobial protein that sequesters siderophores, including enterobactin, to limit the bacterial response to reduced iron (Aujla et al., 2008, Bachman et al., 2009, Raffatellu et al., 2009). However salmochelin, a derivative of enterobactin synthesised by *Salmonella* sp., *Klebsiella* sp. and UPEC, cannot be bound by lipocalin-2, making *S*. Typhimurium lipochalin-2 resistant (Hantke et al., 2003, Raffatellu et al., 2009, Bachman et al., 2011). Zinc and manganese are sequestered by more general metal ion binding proteins, such a calprotectin, an antimicrobial protein that comprises 50% of neutrophil cytosolic content (Hessian et al., 1993). Macrophages also utilise the toxic effects of copper during bacterial killing. The cytokine IFN-γ stimulates copper uptake in macrophages by

increasing expression of CTR1, a high affinity copper importer (White et al., 2009). This may have the added benefit of further reducing extracellular copper that is bioavailable. In addition, copper is exported from the Golgi to the phagosomal compartment through the ATP7A copper transporter, enhancing bactericidal activity of macrophages (White et al., 2009). White and colleagues (2009) showed that the copper transporting ATPase, CopA, helps *E. coli* overcome this copper-mediated killing. A *copA* deletion renders the bacteria hypersensitive to killing by murine macrophages, in an ATP7A dependant manner. These descriptions of mammalian host manipulations of metals during immune response to infection is by no means exhaustive; see Diaz-Ochoa et al., (2014) for a comprehensive review. However, this summary provides an insight into the onslaught pathogens such as *Salmonella* must overcome when establishing an infection.

4.1.2.3 Salmonella response to copper

Salmonella has evolved multiple DNA-binding metal responsive transcription factors: CueR, Fur, Zur, MntR, NikR, GolS and RcnR, allowing optimisation of metal acquisition while affording protection from metal-mediated toxicity inflicted upon it within host immune cells (for full review see Osman and Cavet (2011). In addition to these metal-specific regulatory networks, *Salmonella* employs multiple global stress responses in response to excess copper and zinc (Pontel et al., 2014). As a result of Cu^{+} ion induced membrane damage, both CpxAR and SoxRS stress responses are activated by high copper concentrations (Kershaw et al., 2005, Yamamoto and Ishihama, 2006). Of these, the Cpx response appears to be critically important for copper stress in *E. coli*. Double *cpxAR* deletion strains exhibit higher sensitivity to copper than their WT equivalent, and transcriptomic analysis of the Cpx response revealed CpxA/R dependent regulation of 27 transcriptional units following copper exposure (Yamamoto and Ishihama, 2006, Yamamoto and Ishihama, 2005).

Unlike *E. coli*, which has the *cue*- and *cus*- copper homeostatic systems, *Salmonella* lack *cusCFBA*, encoding an RND-type copper-transporting efflux system. Despite this absence, *Salmonella* can support higher copper

concentrations than *E. coli* during anaerobic growth (Pontel and Soncini, 2009). *Salmonella*, and many other species that lack a functional *cus*-operon (i.e. *Yersina* and *Erwinia*) instead possess a novel copper binding protein, CueP (Pontel and Soncini, 2009). This periplasmic protein sequesters free intracellular copper ions to reduce toxicity and is required for *S*. Typhimurium copper tolerance under anaerobic conditions (Osman et al., 2010, Pontel and Soncini, 2009). The Cu^{+} inducible sensor/transcriptional regulator CueR regulates expression of the *cueP* gene (STM3650/SL3616) (Pontel and Soncini, 2009). However, transcriptome data presented in Chapter 3 of this thesis provided evidence to support further, positive regulation of *cueP* by CpxR. The Cpx system of *Salmonella* may therefore provide additional compensation for the absence of *cus*- through CueP activation, making this ESR system an even greater contributor to copper tolerance in *Salmonella* than *E. coli*.

S. Typhimurium also has a multi-copper oxidase, CueO (alias CuiD), which converts Cu^{+} ions to the less reactive Cu^{2+}. In the absence of CueO, *S*. Typhimurium is copper sensitive and exhibits significant attenuation in murine infection models (Achard et al., 2010). This attenuation is, however, confined to the liver and spleen, with no significant differences in Δ*cueO* or WT strains recovered from Peyer's patches or mesenteric lymph nodes. S. Typhimurium Δ*cueO* strains therefore show some similarity to the phenotype of SPI-2 mutants, growth of which is confined to the Peyer's patch (Cirillo et al., 1998).

4.1.3 Role of polyamines in Enteric bacteria

The YdgFE (MdtJI) multidrug efflux system of *E. coli* contributes towards polyamine homeostasis, preventing cell toxicity and inhibition of growth associated with spermidine overaccumulation within the cell (Higashi et al., 2008). Our transcriptomic data implied CpxR-medicated regulation of the *ydgFE* genes in *S*. Typhimurium (Chapter 3). The role of YdgFE in the *Salmonella* response to spermidine stress is yet to be investigated and is one area of investigation during this chapter. An introduction to the

importance of polyamines and polyamine homeostasis in *E. coli* and *Salmonella* is included here.

Polyamines are associated with a wide range of core physiological processes and their crucial role in *Salmonella* pathogenesis is becoming increasingly apparent (Schroll et al., 2014, Jelsbak et al., 2012). Spermidine [*N*-(3-aminopropyl)butane-1,4-diamine] is a ubiquitous, aliphatic, cationic polyamine. Polyamines, of which the most widely distributed cellular polyamines are putrescine, cadaverine, spermidine and spermine (Figure 13), are multifunctional and essential for life of both prokaryotes and eukaryotic cells (Cohen, 1997). These compounds are produced during the catabolism of proteins and function through the formation of complexes with nucleic acids, promoting stability and desirable structural changes in RNA and DNA which influence DNA binding proteins and protein synthesis (Tabor and Tabor, 1985, Cohen, 1997, Wortham et al., 2007, Potter and Paton, 2014).

4.1.3.1 Polyamine synthesis and homeostasis

In *S*. Typhimurium there are two pathways of putrescine synthesis, from *L*-ornithine by the ornithine decarboxylases SpeC or SpeF or from *L*-arginine by SpeA and SpeB (Figure 13). SpeE subsequently converts putrescine to spermidine. Inhibition of protein synthesis is the proposed cause of accumulated spermidine. The resulting toxicity arises through unregulated binding of spermidine at acidic sites of nucleic acids, proteins and membranes, as well as the displacement of cations, e.g. Mg^{2+}, at such sites (Morris, 1991, Fukuchi et al., 1995, Pegg, 2013). Polyamine catabolism also results in the production of toxic metabolites, including ammonia and reactive aldehydes, e.g. H_2O_2 and acrolein, causing further damage to proteins and DNA (Pegg, 2013). Combined, these lead to DNA precipitation, inhibition of growth and, if unregulated, cell death. Polyamines have, however, also been associated with protection from free radicals and acid stress. Polyamine-deficient *E. coli* cells are killed by H_2O_2 at concentrations that are sub-lethal for WT or polyamine treated mutants (Chattopadhyay et al., 2003) and the *cadBA* operon (encoding a lysine-carboxylase and lysine-cadaverine

antiporter respectively) has been linked, through the regulator CadC, to acid stress tolerance in *Salmonella* (Lee et al., 2007). Tight regulation of polyamine levels is therefore essential for healthy cell function and controlled amino acid metabolism.

PotE has putrescine-ornithine antiporter activity and CadB, a cadaverine-lysine antiporter, excreting putrescine and cadaverine respectively at acidic pH (Kashiwagi et al., 2002, Kashiwagi et al., 2000, Vassylyev et al., 1998, Soksawatmaekhin et al., 2004). Both aid uptake of their respective polyamines at a neutral pH (Kashiwagi et al., 2000, Soksawatmaekhin et al., 2004). Degradation, excretion and uptake systems are all believed to contribute towards polyamine homeostasis. However, investigations into the mechanisms of polyamine homeostasis are limited to few organisms and spermidine efflux pumps especially have only recently been characterised (Higashi et al., 2008, Chan and Chua, 2010).

Monoacetylation is one method of maintaining intracellular levels of spermidine in both eukaryotic and prokaryotic cells that has been investigated in more detail. Acetyl group addition at the N^1 or N^8 positions of spermidine occurs at approximately equal frequencies. Spermidine N^1-acetyltransferase, encoded by *speG* in *E. coli*, is constitutively expressed during all stages of growth and is required to maintain non-toxic spermidine levels at low temperatures (Carper et al., 1991, Limsuwun and Jones, 2000). The protein product of this *E. coli* gene (SpeG) and the spermidine N^1-acetyltransferase of *S*. Typhimurium, situated at locus *stm1502*, share 91% sequence homology at the amino acid level (data not shown).

Analysis of spermidine acetylation in *E. coli* showed diamine putrescine and spermidine as the two most prevalent polyamines during log phase of growth (Carper et al., 1991). However, monoacetylspermidine accumulates in response to several stresses, including extreme temperature fluctuations, alkaline shift (pH 6.5-8.5) and ethanol stress (Carper et al., 1991). Despite the obvious involvement of polyamines in cellular stresses, the only evidence to date linking ESRs and polyamine toxicity has been found in *Borkholderia*

pseudomallei. The *speG* gene is a novel member of the *B. pseudomallei* σ^E regulon, providing indirect regulon of spermidine levels through the σ^E response during times of oxidative stress (Jitprasutwit et al., 2014).

4.1.3.2 Polyamines and virulence

In addition to their essential functions within cells, the impact of polyamines on, and their involvement in, bacterial pathogenesis and host-pathogen interactions is a more recent research focus. A host of evidence has been presented highlighting the role of these compounds in response to oxidative and acid stresses, biofilm formation, bacteriocin production and escape from phagolysosomes (Shah and Swiatlo, 2008, Lee et al., 2007, Chattopadhyay et al., 2003, Di Martino et al., 2013). Regarding *Salmonella* pathogenicity, deletions of the *spe-* operon, required for spermidine biosynthesis, results in a significant reduction in invasion of epithelial cells as both putrescine and spermidine are required for full induction of SPI-1 genes *hilA*, *invF* and *sipB* (Jelsbak et al., 2012). This study also highlighted the importance of polyamines for intracellular survival and proliferation of *S*. Typhimurium in epithelial cells. Strains lacking *spe-* observed a 4-fold reduction in survival and a net replication of <1 compared to WT cells, due to reduced expression of several SPI-2 genes and some of its effectors (Jelsbak et al., 2012). Although polyamines affect biofilm formation in *Yersinia pestis* (Di Martino et al., 2013), spermidine mutants of *S*. Typhimurium exhibit no reduction in adhesion to Int-407 human epithelial cells (Jelsbak et al., 2012).

In the poultry restricted pathogen *S*. Gallinarum, polyamines are essential for virulence, despite evolutionary decay of the *spe-* genes in this host-specialist (Schroll et al., 2014). The *speC* genes of *S*. Typhi and *S*. Gallinarum are pseudogenes, occurring through independent evolutionary events and both serovars are therefore considered ornithine decarboxylase (ODC) negative (Thomson et al., 2008). *S*. Gallinarum is attenuated for intraperitoneal infection when putrescine import and synthesis are not disrupted and in the absence of both *speE* (encoding a spermidine synthase which catalyses the formation of spermidine from putrescine and S-adenosylmethioninamine) and the spermidine influx system PotCD (Schroll et al., 2014). Although

these results show the requirement of polyamines for infection of this specific serovar, they also indicate distinct roles for putrescine and spermidine during systemic infections. Polyamines are therefore an important avenue of investigation due to the diverse range of cellular functions they are involved in, many of which overlap with processes associated with the Cpx stress response. Combined, polyamines and virulence, spermidine toxicity and the regulation of *speG* and *ydgFE* by σ^E and Cpx respectively, all highlight potential involvement of the ESRs (and the Cpx system specifically) in polyamine stress adding to the diverse range of stresses Cpx helps to combat.

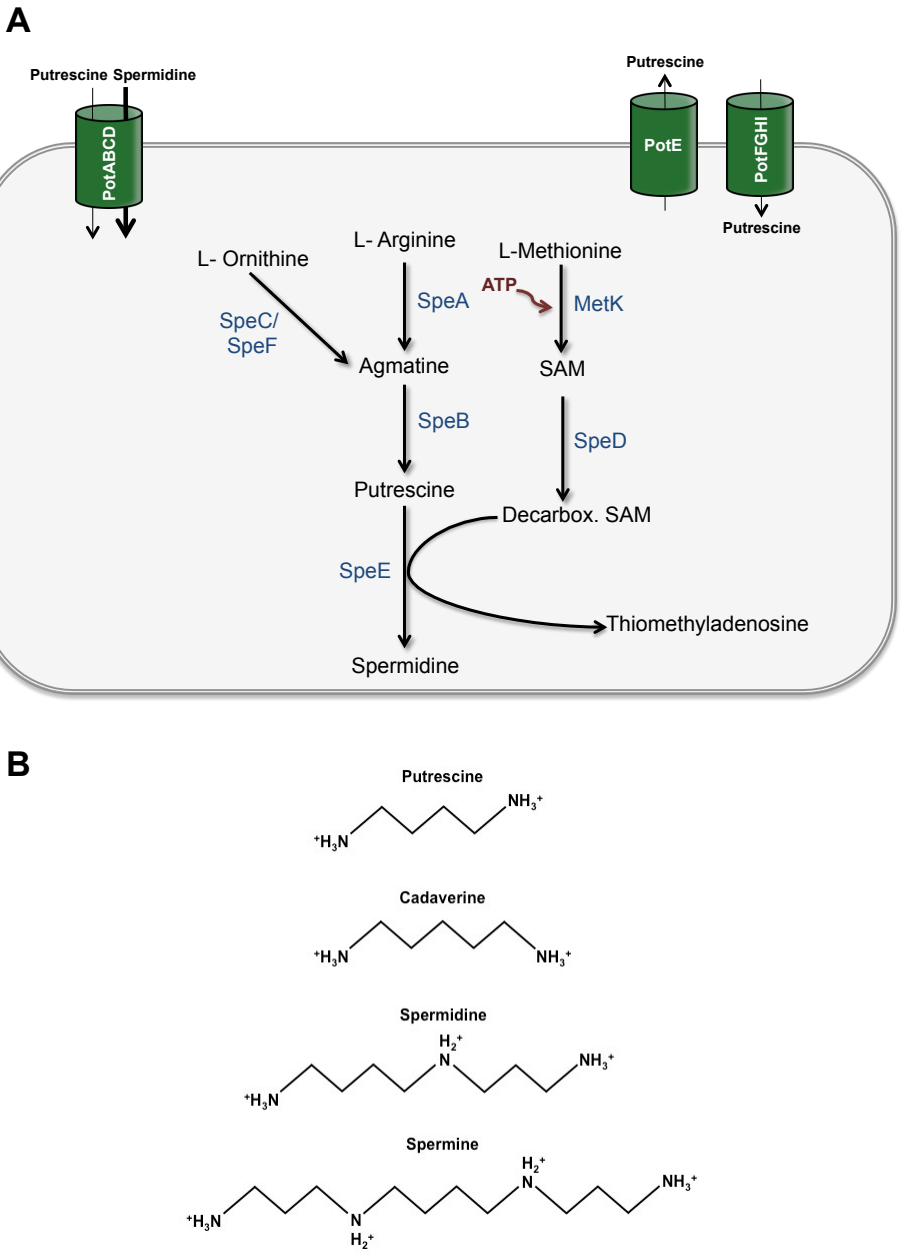

Figure 13: Polyamine synthesis and transport. A) Graphic representation of putrescine and spermidine transport and biosynthesis pathways in *E. coli*. **B**) Structure of the four most common polyamines in microbial cells. Adapted from Schroll et al., (2014) and Shah and Swiatlo (2008).

4.2 Aim

Following identification of new Cpx regulon members in Chapter 3, we aimed to 1) ascertain evidence of direct regulation of specified Cpx regulon members, 2) provide further information as to the function of the protein products of these genes in *S*. Typhimurium and 3) ascertain any involvement of cross regulation between these new members of the Cpx regulon and other ESRs.

4.3 Experimental design

All assays were conducted in biological and technical triplicate, as a minimum, to allow for statistical analysis unless otherwise stated.

4.3.1 Purification of His_{10}-CpxR protein

Two *cpxR* overexpression constructs were made. The ORF of SL1344 *cpxR* (*SL4009*) was cloned into pBAD *myc* His A, in frame with the pBAD L-arabinose inducible promoter and C-terminal 6xHis tag (pBAD*cpxR*). A pET16b construct with 10xHis*cpxR*, under the control of an IPTG inducible promoter, was synthesised by GenScript (10xHis*cpxR*). Both constructs were confirmed by sequencing and transduced into *E. coli* BL21 strains. Overexpression of *cpxR* was induced by the addition of 0.02% (w/v) arabinose or 0.1M IPTG in 1 L volumes of LB Amp and Tet. Cells were lysed by French Press and His tagged CpxR purified from the supernatant using a GE HisTrap column on a GE AKTA FPLC. Fraction samples were resolved by SDS-PAGE (15% v/v) to confirm >95% purity and further confirmed by immunoblotting. Fractions were concentrated, washed and buffer exchanged into CpxR storage buffer via centrifugation with 30KDa size exclusion centrifugation columns. This removed residual imidazole carryover from protein elution. A_{280} analysis on a NanoDrop 2000c UV-Vis spectrophotometer (Thermo Scientific), Bradford assay and Qubit™ Protein Assay Kits with a Qubit® 2.0 Fluorometer (Invitrogen) confirmed final protein concentrations. Only His_{10}-CpxR was purified to a sufficient concentration (5 mg mL^{-1}) and all experiments described subsequently used this N-terminal His-tagged protein.

4.3.2 Electrophoretic motility shift assays (EMSAs)

4.3.2.1 CpxR phosphorylation

Phosphorylation of His_{10}-CpxR was required for the protein to take its active form. CpxR-P was produced as described by (Hung et al., 2001) with minor alterations. Purified CpxR protein (100 pmol) was incubated in phosphorylation buffer: 100 mM Tris [pH 7.5], 10 mM $MgCl_2$, 125 mM KCl, 50 mM acetyl phosphate (lithium potassium salt; Sigma), in a final volume of 50 µL, at 30˚C, for one hour.

4.3.2.2 EMSA probe production

EMSA 6-FAM™-fluorescein labelled probes were generated by PCR amplification of positive control (*cpxP*), negative control (*wraB*) and target gene promoter regions. Controls were selected as *cpxP* is a known member of the Cpx regulon and a CpxR binding site (with CpxR binding previously confirmed) is situated within its promoter region. No such motif or regulation had been observed for *wraB* and expression of this negative control was invariant throughout our previous transcriptomic analysis of the CpxR regulon (Chapter 3). PCR products were purified and diluted 1:50 to minimise carry over of unlabelled DNA and used as templates for universal 6-FAM™-fluorescein labelled primers. This second PCR round generated 6-FAM™ labelled probes. Labelled probes were purified before use in EMSA reactions.

4.3.2.3 EMSA reaction and gel imaging

EMSAs were conducted as described by Shimada et al. (2013) with minor alterations. CpxR-P at 2.5, 5, 10 and 20 pmol concentrations were incubated (30˚C, one hour) with 6-FAM™ tagged probes (0.5 pmol) in EMSA buffer (10 mM Tris-HCl [pH 7.5], 10 mM NaCl, 1 mM $MgCl_2$, 1 mM EDTA [pH 8.0], 5 mM DTT, 5% glycerol and 30 mM acetyl phosphate) in the presence and absence of the non-specific competitor poly(dI•dC) (1 µg). DNA loading dye solution (40% glycerol, 0.025% bromophenol blue, 0.025% xylene cyanol) (1:5) was added and the reaction mix immediately subjected to 6% native PAGE in 1 x TBE buffer, 30 mA, at 4°C. Gels were visualised on a Typhoon

FLA 9500 laser scanner (GE Healthcare) with LBP/BPB1 emission filter, Exmax 495 nm Emmax 576 nm, at 50 µM resolution.

4.3.3 β-Galactosidase assays

β-Galactosidase assays for SL1344 WT or ESR deletion mutants (Δ*baeR*, Δ*baeR*Δ*cpxAR*, Δ*cpxR*, Δ*cpxAR*, Δ*rpoE*, Δ*zraSR*, Δ*cpxAR*Δ*baeR*Δ*zraSR*) were conducted as described in 2.4.12.

4.3.4 Sensitivity spot plates

Overnight cultures of SL1344 WT (control), Δ*cpxR*, *cpxA**, Δ*scsA*, Δ*STM3388*, Δ*SL3646*, Δ*ybiJ*, Δ*ydgFE*, Δ*yncJ*, Δ*yqaE* and strains harbouring pR*scsA* were serial diluted (10-fold) in 1 x PBS to 10^{-8} using aseptic technique. A 10 µL aliquot of dilutions (typically 10^{-2} to 10^{-8}) were spotted onto control (LB agar (1.5% w/v) and test media (LB agar 1.5% w/v) with either 4 mM $CuSO_4$ or spermidine (2 mM, 4 mM, 6 mM or 8 mM). Plates were dried at RT (~one hour) and incubated at 37˚C (12 hours minimum) or until distinct single colonies were visible (~48 hours for plates containing 4 mM $CuSO_4$ or spermidine). CFU mL^{-1} and survival percentages were calculated.

4.3.5 Disc diffusion assays

Overnight cultures of SL1344 WT (control), Δ*stm3388*, Δ*SL3646*, Δ*ybiJ*, Δ*ydgEF*, Δ*yncJ* and Δ*yqaE* were used in disc diffusion assays as described in 2.4.11.2.

4.3.6 Spermidine survival assays

LB (50 mL) flasks were inoculated with 1:100 (v/v) SL1344 WT (control) and Δ*ydgFE* overnight cultures. Spermidine (2 mM) added at *t*=0 or at *t*=3 hours growth. LB only control cultures were grown in tandem. Cultures were incubated for 48 hours at 37°C, 200 rpm. Samples (100 µL) were removed at regular intervals and spread at 10^{-4}, 10^{-5} and 10^{-6} dilutions onto LB agar (1.5% w/v). Plates were dried at RT, incubated at 37°C overnight and CFU mL^{-1} calculated.

4.3.7 Real-time quantitative PCR

All qRT-PCR experiments were performed as described by (Appia-Ayme et al., 2012) and 2.4.22, with three independent total RNA preparations of SL1344p*nlpE* and Δ*cpxR*p*nlpE*, cultured under NlpE inducing and non-inducing conditions Gene specific primers (~60°C Tm) were designed to amplify an average product of 100 bp. Real-time PCR quantifications were realised on a five-times dilution of the total cDNA obtained, using SensiMix™ SYBR No-ROX kit (Bioline) and Bio-Rad CFX96™ real-time PCR detection system. The calculated threshold cycle (Ct) for each gene was normalised to Ct of the *rpoD* gene, which expression is invariant across a large range of growth conditions.

4.4 Results

4.4.1 Shortlist of new Cpx regulon members for further analysis

Following analysis of our SL1344 WT and Δ*cpxR* transcriptomes (Table H1), and specifically the 116 not identified as Cpx-regulon members in previous studies (Table 24) a shortlist of 27 genes across 18 transcriptional units were chosen for further analysis as described previously (Table 27). In addition, *cpxP,* encoding the Cpx accessory protein, was included as a positive control during further analysis. The *tsr* gene has been used as a genetic and biochemical verification of CpxR-P targets during bioinformatic analysis (De Wulf et al., 2002). However, as our *tsr* expression data differ to that presented by De Wulf et al., (2002) (our results show *tsr* is Cpx activated in *S.* Typhimurium whereas De Wulf et al. (2002) presented negative regulation of *tsr* by Cpx in *E. coli*), this gene was included for investigative purposes only. RpoH was also included in our 27-gene shortlist despite binding to the *rpoH1* promoter by CpxR-P being observed in *E. coli* (Danese and Silhavy, 1997). We wished to directly confirm this regulation in *Salmonella* due to the differing roles of stress sigma factors in *S*. Typhimurium and *E. coli*.

The information currently available in the literature for these 27 genes has already been described (3.4.2). Prior to investigations into the function of these genes, and involvement of CpxR in their regulation, we used

bioinformatic analyses of the promoter regions of the 19 operons to identify the presence or absence of CpxR recognition sites (Appendix K, Figure K1). Our 27 genes of interest are summarised in Table 25.

Table 25: **Shortlist of 27 genes differentially regulated >2-fold (FDR <0.05) during our transcriptomic analyses selected for further investigation.** This condensed list contains genes that are not previously shown to be Cpx regulated, whose proposed regulation has not been proven experimentally or requires further investigation. Genes are ordered according to locus. A broken line separates each transcriptional unit.

Locus Tag	Gene Name	Description	Fold Change[†]
SL0776	*slrP*	Leucine-rich repeat-containing protein	2.31
SL0799	*ybiJ*	Hypothetical protein	0.08
SL1025	*yccA*	Hypothetical protein	0.02
SL1052	*scsA*	Suppression of copper sensitivity protein A	0.15
SL1053	*scsB*	Suppression of copper sensitivity protein B	0.31
SL1054	*scsC*	Suppression of copper sensitivity protein C	0.27
SL1055	*scsD*	Suppression of copper sensitivity protein D	0.31
SL1412	*ydgF*	Multidrug efflux system protein MdtJ	0.32
SL1413	*ydgE*	Multidrug efflux system protein MdtI	0.38
SL1699	*chaA*	Calcium/sodium: proton antiporter	0.14
SL2232	*eco*	Precursor of the serine protease Ecotin	0.21
SL2780	*yqaE*	Putative transport protein	0.04
SL3009	-	Hypothetical protein	0.05
SL3010	-	Ail/OmpX-like protein	0.11
SL3350	*yedY*	Putative sulfite oxidase subunit	0.17
SL3351	*yedZ*	Putative sulfite oxidase subunit	0.22
SL3361	-	Putative signal transduction protein	0.36
SL3533	*rpoH**	RNA polymerase factor sigma-32	0.32
SL3616	*cueP*	Hypothetical protein; proposed copper sensitivity protein	0.08
SL3646	-	Putative transcriptional regulator	0.31
SL3782	*ccmE;ccmD*	Cytochrome c-type biogenesis protein	2.88
SL3783	*ccmC*	Haem exporter protein	2.93
SL3784	*ccmB*	Haem exporter protein	2.75
SL3944	*yihE*	Serine/threonine protein kinase	0.31
SL4463	*yjiY*	Putative carbon starvation protein	2.38
SL4464	*tsr**	Methyl-accepting chemotaxis protein I	0.36
SL4495	*deoA*	Thymidine phosphorylase	0.41

[†]Denotes change in expression level in Δ*cpxR*p*nlpE* compared to SL1344p*nlpE* following NlpE overexpression. Values <0.5 = reduction in expression. Values >2 = increase in expression.

4.4.2. Regulation of proposed Cpx regulon members was confirmed by qRT-PCR

Further confirmation of the transcriptional changes observed for our proposed Cpx regulated genes was achieved by qRT-PCR analysis. Our shortlisted 27 genes are grouped into 18 transcriptional units (Table 25). Relative fold expression levels for the first 18 genes of these operons in our NlpE overexpression strains (SL1344p*nlpE* and Δ*cpxR*p*nlpE*) were calculated (Figure 14, A to R). The mean expression values obtained for each and the standard deviation (SD) across replicates are summarised in Table 26.

qRT-PCR data for all 18 selected genes concurred with the expression values observed during microarray analyses (Figure 14, A-R; Table 26); no genes exhibited divergent expression. Of these, 16 genes were Cpx activated and only two genes, *yjiY* and *slrP*, had expression levels decrease in the presence of CpxR (3.39-fold and 2.85-fold respectively) (Figure 14, D and E). For 10 genes (*slrP*, *ybiJ*, *yedY*, *rpoH*, *cueP*, *SL3646*, *yihE*, *yjiY*, *tsr* and *deoA*), expression values obtained by qRT-PCR and microarray analyses were very similar, falling within 1-1.46-fold of each other (Table 26). For the other eight selected genes (*cpxP*, *scsA*, *ydgF*, *eco*, *yqaE*, *SL3009*, *SL3010* and *stm3388*), changes in relative expression between SL1344 WT and Δ*cpxR* backgrounds were greater in data collected by qRT-PCR, relative to our array values, despite the same trends in transcription being seen (Table 26). Expression of *SL3009* and *SL3010* (Figure 14, O and I respectively) differed the greatest between the two methods of analysis. Although induction by CpxR was still seen, increases in expression of *SL3009* and *SL3010* were 3.9-fold and 5.6-fold lower respectively in our qRT-PCR analysis, compared to microarray expression values (Table 26). Expression of *scsA* (Figure 14, H) was 2.73-fold lower in our qRT-PCR data compared to microarray values, and *ydgF* (Figure 14, B) and *eco* (Figure 14, Q) also had expression reduce (~1.7-fold) post qRT-PCR analysis, compared to microarray fold-change. Although qRT-PCR and microarray analysis provided similar expression values for *yedY* (Figure 14, M) and *stm3388* (Figure 14, A) in our Δ*cpxR* background, the fold-changes observed

during microarray analysis were 1.27- and 1.62-fold greater than the values acquired from qRT-PCR (Table 26).

4.4.3 *in silico* analysis of CpxR binding motifs within the promoter regions of identified Cpx regulon members in SL1344

CpxR binding recognition sequences have been used in previous studies to identify reliable target promoters. The PRODORIC® database (Prokaryotic database of gene regulation) (Munch et al., 2003) was used during this study as a bioinformatic tool to analyse and visualise the presence of predicted CpxR-P consensus-binding motifs (CpxR binding boxes), within the promoter regions of our 27 shortlisted genes requiring further analysis. DNA regions of 500-1000 bp in length, immediately upstream of the 18 operons were analysed using Virtual Footprint (Version 3.0) promoter analysis software, against the CpxR (*E. coli* str. K-12) position weight matrix (PWM). Position weight matrices are built based on a set of aligned, known sequences, using the information theory approach by Schneider et al. (1986) (Munch et al., 2003, Schneider et al., 1986). The CpxR *E. coli* str. K-12 position weight matrix uses 17 independent binding sites, mean score 13.16 with a SD of 0.86 (Munch et al., 2003). The sequence logo for this binding site, produced using WebLogo (Version 2.8.2) (http://weblogo.berkeley.edu/) from 17 CpxR binding motifs present on the PRODORIC® database, is shown in Figure 15, A.

Of the 18 promoter regions analysed, 15 were found to contain a CpxR binding region, 16 bp in length. The CpxR-P binding consensus sequences identified for each and their location (bp upstream of gene initiation codon) are summarised in Table 27. Using these new binding motifs, a second sequence logo was made (Figure 15, B) to produce a CpxR binding motif more representative of that present within *S*. Typhimurium. The *E. coli* and *S*. Typhimurium CpxR binding motifs both contain the conserved GTAAA-n_x-GTAAA motif described by De Wulf et al. (2002), however there is slightly

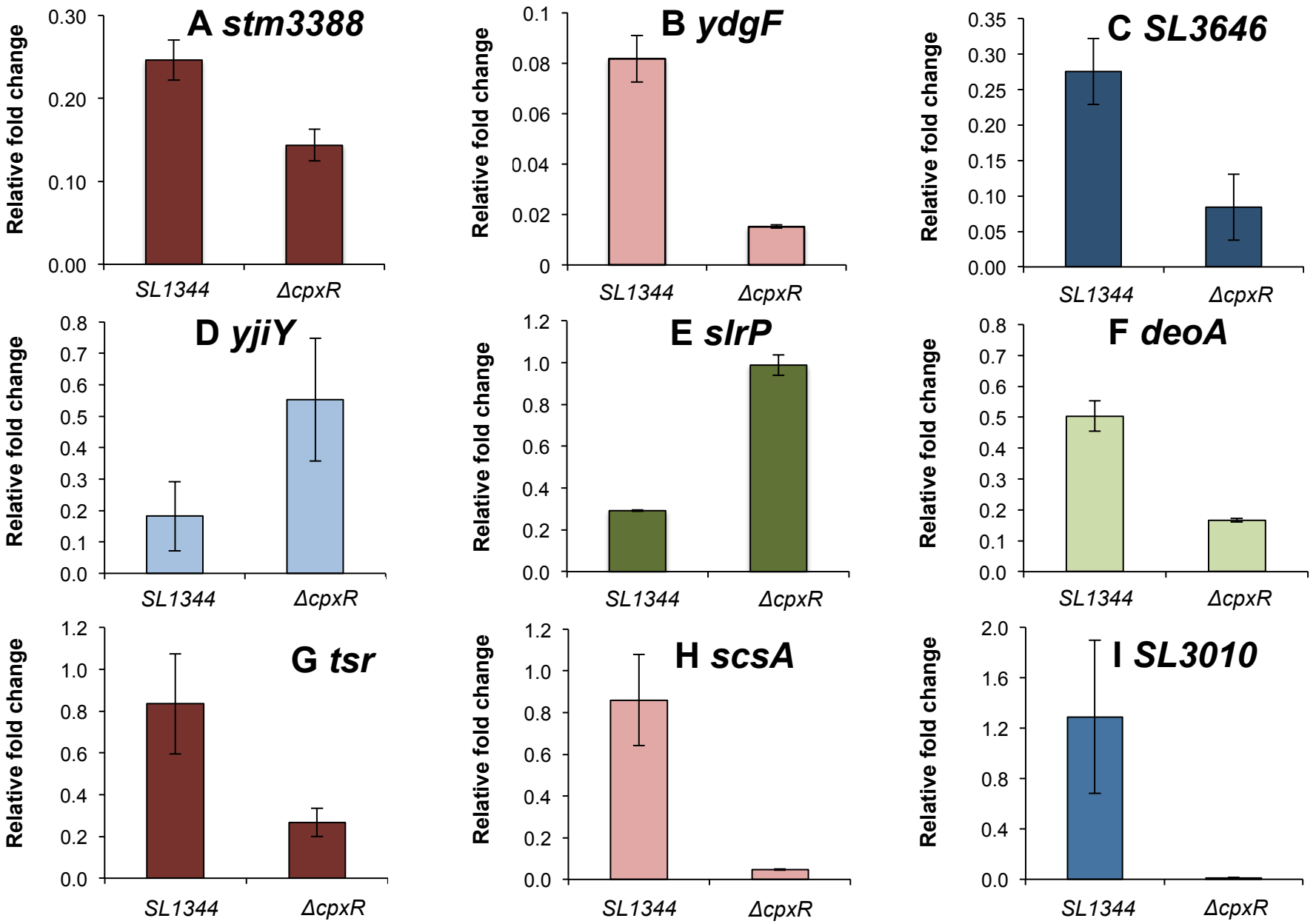
A stm3388
B ydgF
C SL3646
D yjiY
E slrP
F deoA
G tsr
H scsA
I SL3010
Relative fold change
SL1344
ΔcpxR

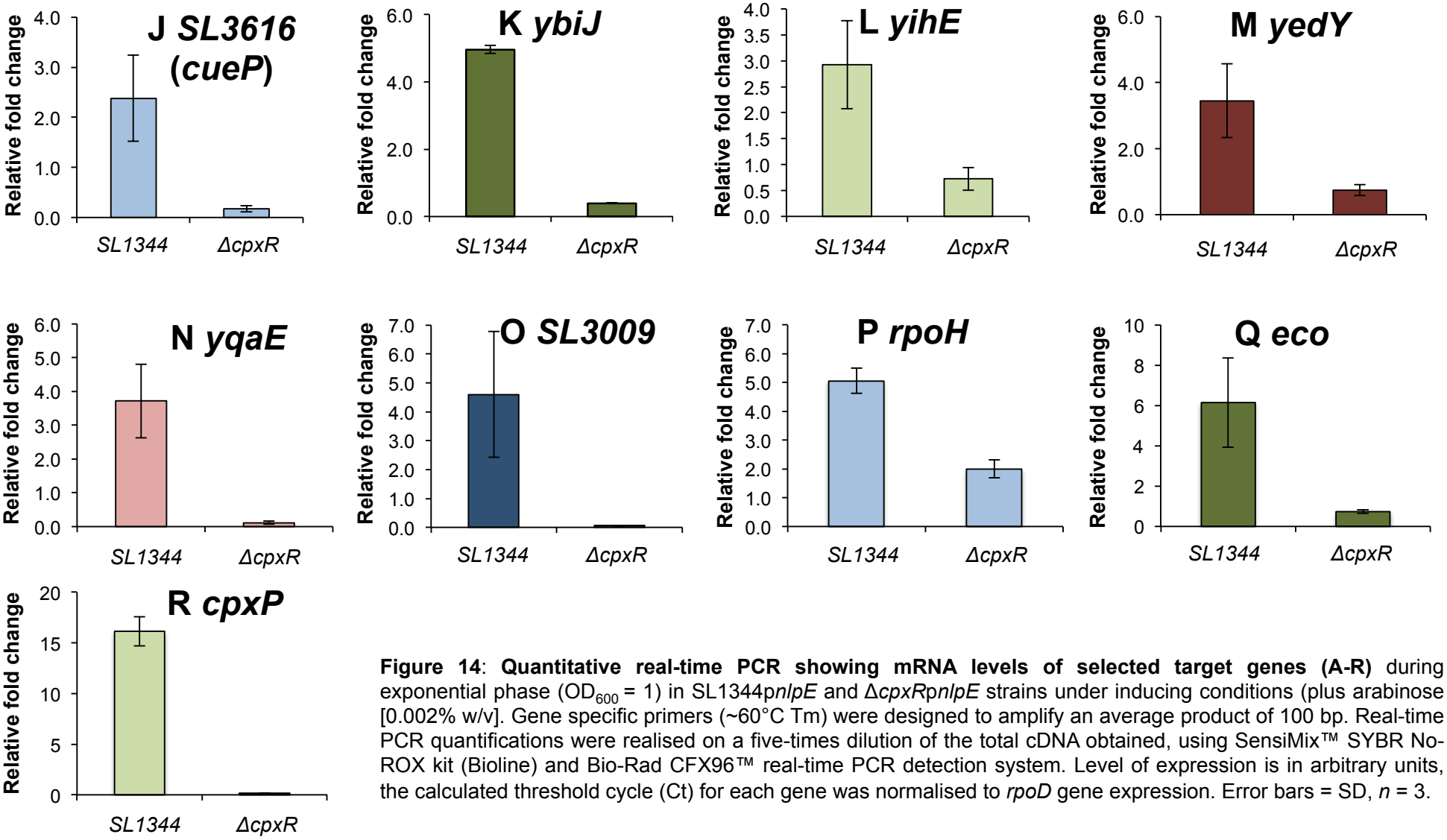

Figure 14: **Quantitative real-time PCR showing mRNA levels of selected target genes (A-R)** during exponential phase (OD_{600} = 1) in SL1344p*nlpE* and Δ*cpxR*p*nlpE* strains under inducing conditions (plus arabinose [0.002% w/v]. Gene specific primers (~60°C Tm) were designed to amplify an average product of 100 bp. Real-time PCR quantifications were realised on a five-times dilution of the total cDNA obtained, using SensiMix™ SYBR No-ROX kit (Bioline) and Bio-Rad CFX96™ real-time PCR detection system. Level of expression is in arbitrary units, the calculated threshold cycle (Ct) for each gene was normalised to *rpoD* gene expression. Error bars = SD, *n* = 3.

Table 26: Summary of qRT-PCR results confirming expression levels observed during microarray analysis. mRNA levels for target genes and operons in SL1344p*nlpE* and Δ*cpxR*p*nlpE* under inducing conditions (plus arabinoses [0.002% w/v]) when OD_{600} = 1. Levels of expression are in arbitrary units and have been normalised to *rpoD* control gene expression. Standard error (SE) was calculated from data for three biological replicates analysed in technical triplicate (as a minimum).

Locus Tag	Gene Name	Description	Fold Change†	Expression levels qRT-PCR (±SE)
SL4009	***cpxP***	Extracytoplasmic stress protein for protein-mediated toxicities	>-100	- 132.8 (±0.83)
SL0776	***slrP***	Leucine-rich repeat-containing protein	+2.31 up	+ 3.39 (±0.002)
SL0799	***ybiJ***	Hypothetical protein	- 12.5	- 12.45 (±0.07)
SL1052	***scsA***	Suppression of copper sensitivity protein A	- 6.74	- 18.4 (±0.13)
SL1412	***ydgF***	Multidrug efflux system protein MdtJ	- 3.13	- 5.36 (±0.005)
SL2232	***eco***	Ecotin precursor	- 4.76	- 8.38 (±1.29)
SL2780	***yqaE***	Putative transport protein	- 25	- 33.45 (±0.63)
SL3009	**-**	Hypothetical protein	- 20	- 79.18 (±1.26)
SL3010	**-**	Ail/OmpX-like protein	- 9.24	- 51.8 (±0.05)
SL3350	***yedY***	Putative sulfite oxidase subunit	- 5.88	- 4.63 (±0.65)
SL3361	**-**	Putative signal transduction protein	- 2.77	- 1.71 (±0.01)
SL3533	***rpoH****	RNA polymerase factor sigma-32	- 2.53	- 3.15 (±0.25)
SL3616	***cueP***	Hypothetical protein; proposed copper sensitivity protein	- 12.5	- 13.62 (±0.5)
SL3646	**-**	Putative transcriptional regulator	- 2.74	- 3.13 (±0.03)
SL3944	***yihE***	Serine/threonine protein kinase	- 3.23	- 4.03 (±0.49)
SL4463	***yjiY***	Putative carbon starvation protein	+ 2.38	+ 2.84 (±0.05)
SL4464	***tsr***	Methyl-accepting chemotaxis protein I	- 2.74	- 3.13 (±0.14)
SL4495	***deoA***	Thymidine phosphorylase	- 2.38	- 2.84 (±0.03)

†Denotes change in expression level in SL1344Δ*cpxR* compared to WT SL1344 following overexpression of *nlpE* obtained by microarray.

more variation within the nucleotides between these repeats in *S*. Typhimurium. Diagrammatic representation of the consensus sequences position and raw analyses of the 500-1000 bp fragments analyses are listed in Appendix K. An example for *yccA* is shown in Figure 15, C.

4.4.4 Confirmation of CpxR-mediated regulation of new Cpx regulon members and CpxR-P:DNA complex formation

4.4.4.1 Purification of S. Typhimurium CpxR (SL4009) for use in DNA binding assays

qRT-PCR analysis concurred with our microarray analysis, providing additional evidence in support of CpxR-mediated regulation of our 18 transcriptional units. In addition to the combined approach of microarray and qRT-PCR transcriptional studies, we wished to confirm the mechanism of CpxR regulation and whether this occurred in a direct or indirect manner. To test this, purified CpxR from *S*. Typhimurium was needed to carry out DNA binding assays.

His-tagged CpxR was purified following overexpression in *E. coli* BL21 (DE3). The amount of CpxR-His6 purified from a C-terminal 6xHis tagged *cpxR* construct (pBAD*cpxR*) was insufficient for the number of DNA binding assays we wished to complete (data not shown). Following successful overexpression of a synthesised construct (10xHis*cpxR*; Table 4) 10His-CpxR was purified as described in 2.4.15 (Figure 16, A). Bands corresponding to the molecular mass of 10His-CpxR (~30 kDa) were clearly visible and immunoblot analysis with HRP conjugated anti-His antibody (QIAGEN) confirmed the presence of His-tagged CpxR (Figure 16, B). Fractions were concentrated and buffer exchanged into CpxR storage buffer through 30KDa size exclusion centrifugation columns. This also removed any protein contaminants of <30KDa visible following SDS-PAGE analysis. The fractions visualised here (Figure 16, A) were used during all phosphorylation reactions and DNA binding assays described.

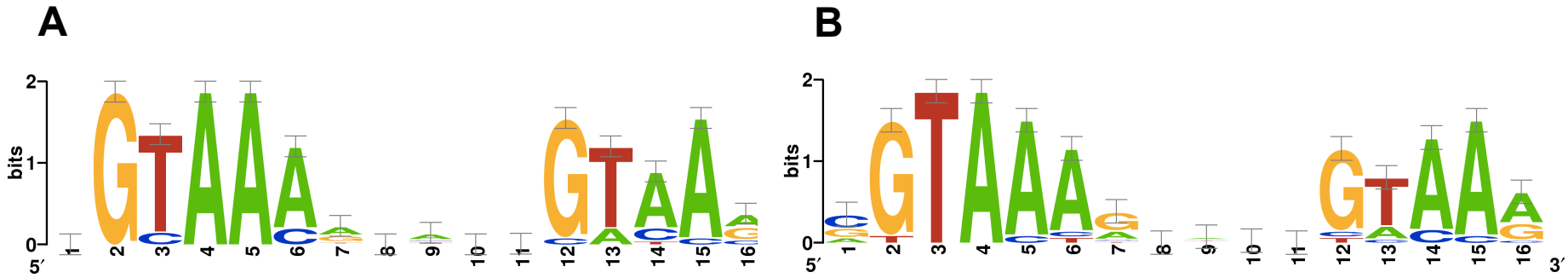

C ***yccA***

Promoter Sequence: *Salmonella* Typhimurium (strain ATCC 700720 / SGSC1412 / LT2)|complete chromosome (500bp upstream of *yccA*)					
1 GTAACCCCTT GTTTAATCTG GCGGAAGCGC AGAGATTCGA ACTCTGGAAC CCTTTCGGGT CGCCGGTTTT CAAGACCGGT 80 81 GCCTTCAACC GCTCGGCCAC ACTTCCGGAA TGAGGCGCAC TATAAACATC CCGGTGCGCC ATGTAAAGAC CGAATGTGTT 160 161 CGTTTGCGTG AAAAACAGGC AAAATTTCGT TAATTGCCTG AAATAGCGGC ACATTGACCA TTTCTTCAAC ACAAAACTGG 240 241 CTGAATACGT ATTGATCGCC TCCACTGTTT CACCGCTGTG ATTAGCGATT TTTTTATCGG TAACGCGTGG TTGGCGCTGC 320 321 CGCCTGTTTT ATGGCGTAGC GCCAGGCATG AGCAGACCGT TTTAACGACG GTAATCACCT GAAATCTCTT AAGGAAACTA 400 401 AACGTAAACG AATGCGTAAA GATGGGTAAA ACCACTGGGT GACAGTGACT GTTTTTATTA TTCTCCTTTA TTAATTACAT 480 480 CTGTCATAAG AGAGTGACTA ATG					
PWM (species)	**Start Position**	**End Position**	**Strand**	**Score**	**Sequence**
CpxR | Escherichia coli (strain K12)	415	430	+	13.62	CGTAAAGATGGGTAAA

Figure 15: Sequence logo for the CpxR-P recognition weight matrix in *E. coli* (A) and *Salmonella* (B), produced using WebLogo (Version 2.8.2) (http://weblogo.berkeley.edu/) from 17 CpxR binding motifs present on the PRODORIC® database (A) and PRODORIC® database analyses of CpxR regulon members of *S.* Typhimurium SL1344 (B), as shown in Table 4. Sequence motif A was utilised during promoter analyses of 27 genes of interest. Relative height of each base represents base conservation, measured in bits (Schneider and Stephens, 1990). Total sequence conservation is 13.16 ± 0.86 bits. An example promoter sequence for *yccA* is shown in C). Proposed CpxR binding motif is highlighted in grey. Additional promoter sequence figures for the remaining genes listed in Table 26 are found in Appendix K.

Table 27: **Presence and location of CpxR-P binding motifs** within the promoter regions of 27 proposed members of the Cpx regulon of *S*. Typhimurium. Genes under the control of the same promoter are grouped into their respective operons.

Gene/Operon	Description	Fold Change†	CpxR Binding Motif		
			Motif Presence	Sequence (5'-3')	Location (5' of ATG)
yccA	Hypothetical protein	0.02	✓	CGTAAAGATGGGTAAA	415-430 bp
yqaE	Putative transport protein	0.04	✓	CGTAAAGGAGGGTAAA	388-403 bp
SL3009-30 (STM3030-31)	Hypothetical protein; Ail/OmpX-like protein	0.05	✗		
cueP	Proposed copper sensitivity protein	0.08	✓	GGTAAAGTAATGCAAA	411-426 bp
ybiJ	Hypothetical protein	0.08	✓	GGTAAAGAAAAGTCAG	213-228 bp
chaA	Calcium/sodium: proton antiporter	0.14	✓	CGTAAAACTACGTAAA	400-415 bp
scsABCD	Suppression of copper sensitivity proteins	0.15; 0.31; 0.31; 0.27; 0.31	✗		
yedYZ	Putative sulfite oxidase subunits	0.17; 0.22	✗		
eco	Ecotin precursor	0.21	✓	GGTAAAGACCCGTAAA	249-264 bp
yihE	Serine/threonine protein kinase	0.31	✓	AGTAAAACCTTGTAAG	420-435 bp
SL3646/STM3681	Putative transcriptional regulator	0.31	✓	ATTACTTTCCTTTACG	426-441 bp
ydgFE	Multidrug efflux system proteins; MdtJI	0.32	✓	GGTAAAGAAGTGAAAA	164-179 bp
rpoH	RNA polymerase factor sigma-32	0.32	✓	AGTAAAGTGACGTAAA	731-746 bp
SL3362 (*STM3388*)	Putative signal transduction protein	0.36	✗		
tsr	Methyl-accepting chemotaxis protein I	0.36	✓	CGTAAAGTTAGGTAAA [see *yjiY*]	
deoA	Thymidine phosphorylase	0.41	✓	CGTAAAACTCTGAAAG	266-281 bp
slrP	Leucine-rich repeat-containing protein	2.31	✓	CGTAACCTAAAGTAAC	464-479 bp
yjiY	Putative carbon starvation protein	2.38	✓	CGTAAAGTTAGGTAAA	371-386 bp
ccmBCDE	Haem transporter proteins; cytochrome *c*-type biogenesis proteins	2.88	✓	GGTAAAAGATGCACAG	893-903 bp

†Denotes change in expression level in SL1344Δ*cpxR* compared to WT SL1344 following overexpression of *nlpE*.

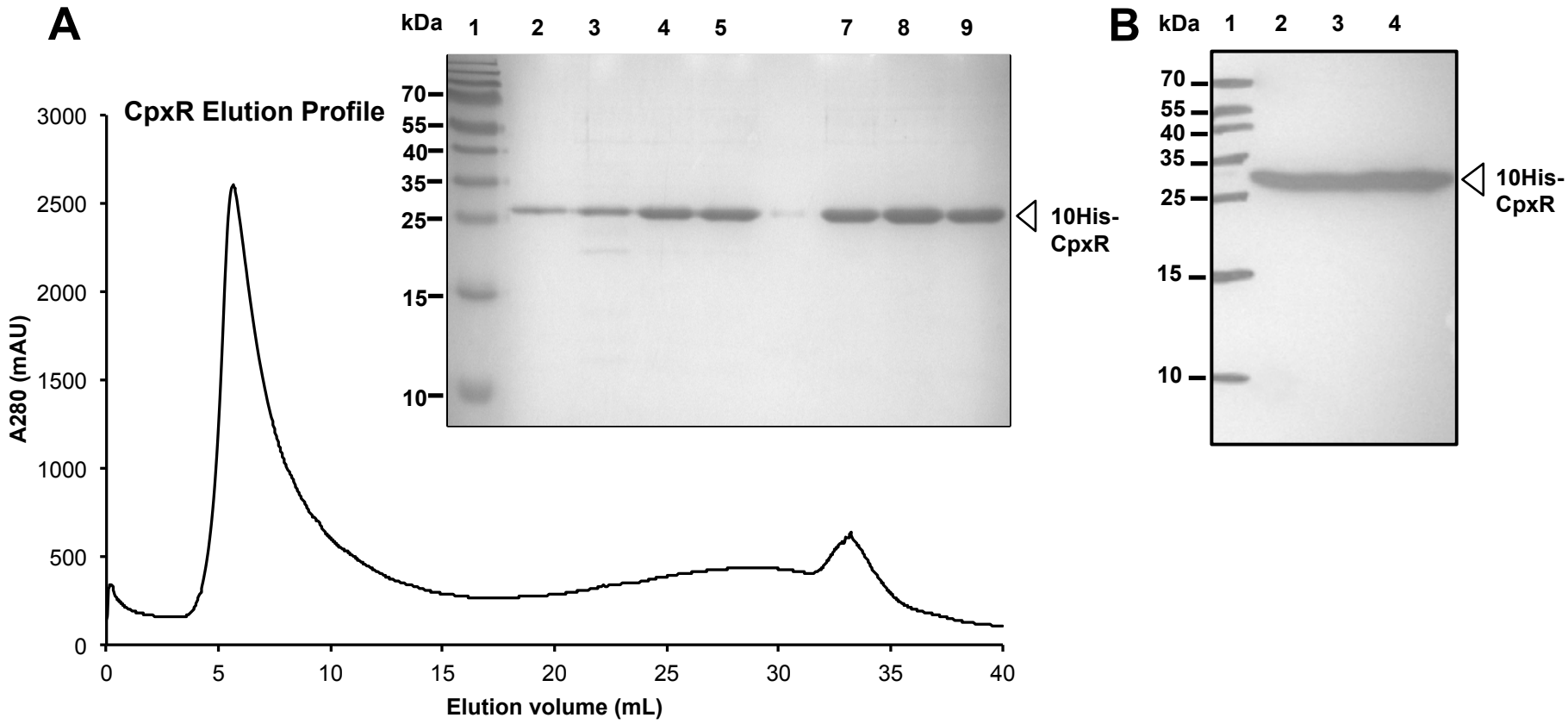

Figure 16: **Purification of N-terminal 10xHis tagged CpxR purification at >95% purity as judged by SDS-PAGE.** A) Elution profile and samples from seven fractions (*lanes 2-5*, *7-9*) collected during the elution stage of purification procedure were resolved by 15% SDS-PAGE. Proteins were stained with SimplyBlue™ SafeStain Coomassie® G-250 stain. *Lane 1*, PageRuler™ Prestained Protein Ladder. B) Immunoblot of three 10His-CpxR samples (*lanes 2,3 and 4*) after buffer exchange and fraction concentration. This 10His-CpxR was used in all phosphorylation and EMSA reactions.

4.4.4.2 Visualisation of DNA:CpxR-P Interactions – Direct regulation of cstA, yqaE, SL3646, yccA, ydgF, eco, slrP and ybiJ by CpxR-P confirmed through the formation of promoter-CpxR-P complexes

Our purified CpxR protein was phosphorylated to produce its active form (4.3.2.1). CpxR-P was used in electromobility shift assays (EMSAs) to ascertain direct binding of CpxR-P to the promoter regions of our 15 target operons, with potential CpxR-P binding motifs identified during *in silico* analysis.

Initial EMSAs using our positive and negative control probes confirmed no CpxR-P binding to our *wraB* probe [0.5 pmol] (negative control) and CpxR-P:DNA complex formation for our *cpxP* probe [0.5 pmol] (positive control) in the presence of CpxR-P [10 pmol] (Figure 17). Of the 15 operons identified as having potential CpxR-P consensus binding motifs, CpxR-P:DNA complex formation was confirmed for eight: *yccA*, *cstA*, *yqaE*, *SL3646*, *ydgF*, *slrP*, *ybiJ* and *eco* (Figure 17). DNA shifts were seen in the absence of poly(dI•dC) for *tsr*, *yihE* and *deoA* DNA probes [0.5pmol] when incubated with 10 pmol CpxR-P (Figure 18, A-C). Initial investigations could not reproduce such shifts when poly(dI•dC) (1 µg) was added to the reaction (data not shown). Surprisingly, no shift was observed for our *rpoH* probe in the presence of poly(dI•dC) (data not shown), or in its absence when incubated with 10 pmol CpxR-P (Figure 18, D). Only when CpxR-P was present in excess [20 pmol] was a possible shift in the absence of poly(dI•dC) observed (Figure 18, D).

4.4.5 Phenotypic analysis of uncharacterised, newly identified *S.* Typhimurium Cpx-regulon members

Transcriptomic analysis and EMSAs confirmed our selected genes as new members of the Cpx regulon in *S*. Typhimurium, either under direct or indirect regulation from CpxR. Our investigations now focused on ascertaining the function of the unknown and uncharacterised genes from our shortlist of 27 (Table 25) in *S*. Typhimurium. Deletion mutants of Δ*ydgFE*, Δ*stm3388*, Δ*ybiJ*, Δ*SL3646*, Δ*yncJ*, Δ*yqaE*, Δ*SL3009 and* Δ*SL3010/09* were made using the λ-red system and confirmed by PCR. The phenotypic

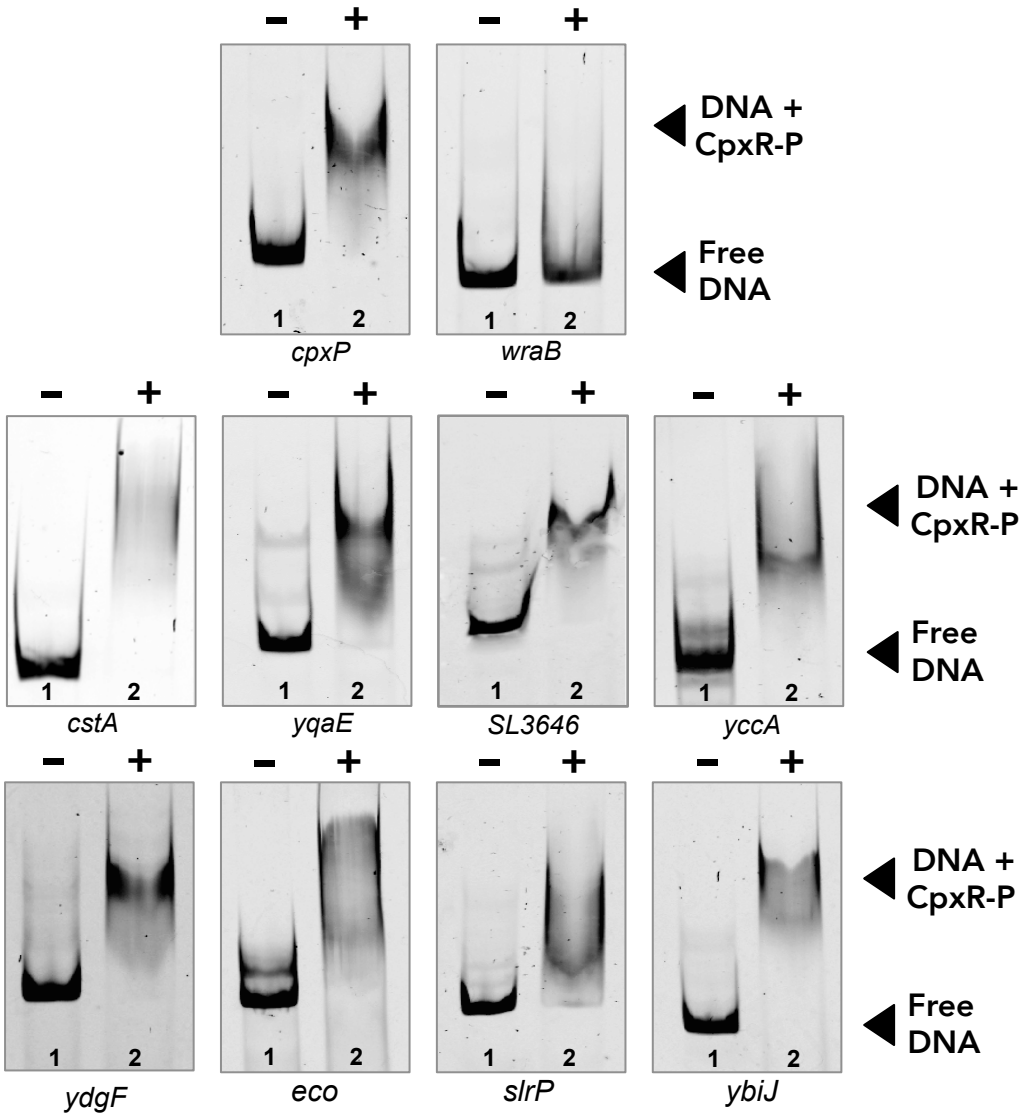

Figure 17: **Formation of CpxR-P-promoter complexes for *cstA*, *yqaE*, *SL3646*, *yccA, ydgF*, *eco*, *slrP* and *ybiJ* 6-FAM fluorescein labelled promoter regions.** 6-FAM fluorescein labelled DNA probes [0.5 pmol] for *wraB,* negative control, *cpxP*, positive control and test probes *cstA*, *yqaE*, *SL3646*, *yccA, ydgF*, *eco*, *slrP* and *ybiJ* were used in EMSAs as described in 4.3.2, with poly(dI•dC) [1 µg] and with (+) or without (-) CpxR-P [10 pmol]. Arrows highlight free DNA (6-FAM fluorescein labelled DNA probes unbound to CpxR-P) and CpxR-P-promoter complexes.

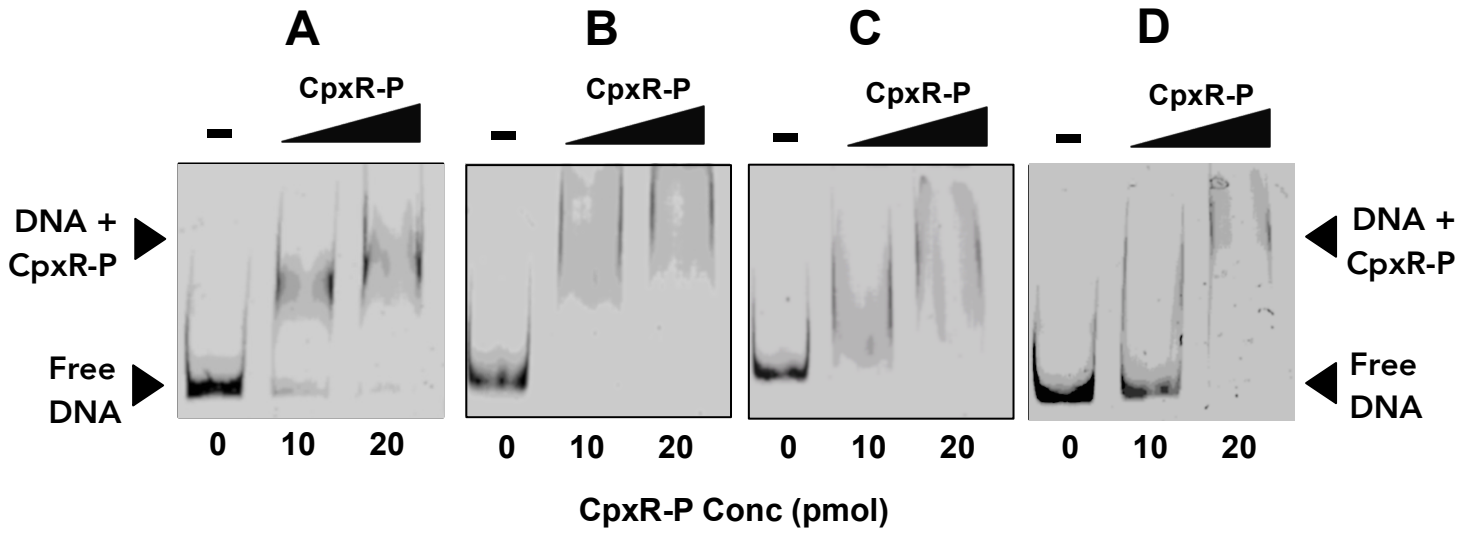

Figure 18: **Formation of CpxR-P-promoter complexes for *yihE*, *tsr*, *deoA* and *rpoH* 6-FAM fluorescein labelled promoter regions in the absence of poly(dI•dC).** 6-FAM fluorescein labelled DNA probes [0.5 pmol] for *yihE* (A), *tsr* (B), *deoA* (C) and *rpoH* (D) were incubated in EMSA buffer with (*lane* 1 to 3) 0, 10 and 20 pmol CpxR-P. Reactions were resolved on 6% NATIVE PAGE, 4°C, ~45 min and imaged using a Typhoon FLA 9500 laser system. Arrows highlight free DNA (6-FAM fluorescein labelled DNA probes unbound to CpxR-P) and CpxR-P-promoter complexes.

screens presented here took into account any hypothesised functions for these genes from other studies (as described in Chapter 3) in other organisms or putative functions assigned from *in silico* sequence or structural analysis.

4.4.5.1 Antibiotic and antimicrobial compound screens suggest yqaE involvement in response to ampicillin and oxidative stress

Six of our deletion mutants (Δ*ydgFE*, Δ*stm3388*, Δ*ybiJ*, Δ*SL3646*, Δ*yncJ*, Δ*yqaE*) were screened for their susceptibility to a selection of 22 compounds including antibiotics, antimicrobial compounds and oxidative stress (hydrogen peroxide and HU screens) (Table 28). Compounds were chosen due to their involvement in inducing the Cpx response, phenotypes observed by *Salmonella* WT, Cpx deletion strains or by deletion strains of Cpx regulated genes, their current use as a therapeutic treatment for *Salmonella* and/or their modes of action and the impact they have on the bacterial envelope. Unfortunately, due to time restrictions, not all deletions mutants could be tested against all compounds. See Table 28 for the combination of compounds tested.

Of the six mutant strains (Δ*stm3388*, Δ*SL3646*, Δ*yqaE*, Δ*ydgFE*, Δ*ybiJ* and Δ*yncJ*) and 22 compounds tested, only Δ*yqaE* exhibited a phenotype significantly different to that observed for our SL1344 WT strain (Table 28 and Figure 19). As determined by disc diffusion assays, *yqaE* deletion increases sensitivity of *S*. Typhimurium to the β-lactam antibiotic ampicillin [10 μg mL^{-1}] and H_2O_2 [30% and 15% v/v] (Figure 19). However, no increased sensitivity was observed for Δ*yqaE* to carbenicillin, the only other β-lactam antibiotic screened and a structural homologue of ampicillin. Hydrogen peroxide and HU induce oxidative stress and hydroxyl-radical mediated cell death. Although Δ*yqaE* strains were significantly (Student's *t* test $p<0.01$) more sensitive to H_2O_2 than SL1344 (Figure 19), they did not exhibit any significant sensitivity to HU at the concentrations tested [760 μg].

None of the six mutant strains screened showed an increase in resistance to any of the 22 compounds tested, compared to SL1344 WT.

Table 28: **Sensitivity screens of *S*. Typhimurium SL1344 WT and six deletion mutants.** Phenotypes of Δ*stm3388*, Δ*SL3646*, Δ*yqaE*, Δ*ydgFE*, Δ*ybiJ* and Δ*yncJ* when exposed to 22 compounds during disc diffusion assays. Zones of inhibition (mm^2) were calculated and compared to SL1344 WT after ~18 hours growth, 37°C. Data summarised as no significant difference (-) or increased sensitivity (+) compared to SL1344 WT values. Statistical analysis = Student's *t* test ($p<0.01$), n = 3. Absence of marker indicates no data collected.

Compound and concentration

Mutants	**Aminoglycosides** *Amikacin* (500 µg)	**Aminocoumarins** *Novobiocin* (30µg)	**Azolidines** *Nitrofurantoin* (200 µg)	*Nitrofurantoin*(100 µg)	**Benzenoids** *Chloramphenicol* (30 µg)	*Tetracyclin* (50 µg)	**β-lactams** *Ampicillin* (10 µg)	*Carbenicillin* (100 µg)	*Cloxacillin* (5 µg)	**Carboxylic Acids and Derivatives** *Colistin* (500 µg)	*Polymyxin B* (300 units)	**Cephalosporins** *Ceftriaxone* (30 µg)	*Ceftsulodin* (30 µg)	**Dihydrofolate Reductase Inhibitors (DHRIs)** *Trimethoprim* (1.25 µg)	**Fluoroquinolones** *Ciprofloxacin* (10 µg)	**Naphthyridines** *Nalidixic Acid* (300 µg)	**Organic Phosphonic Acids** *Phosphomycin* (650 µg)	**Peptidomimetics** *Bacitracin* (10 µg)	**Sulfonamide** *Sulfamethoxazole* (100 µg)	**Thiazines** *Cephalothin* (30 µg)	**Oxidative Stress Screens** *H_2O_2* (30 %)	*H_2O_2* (15 %)	*Hydroxyurea (HU)* (760 µg)
Δ*stm3388*	-	-	-	-	-	-	-	-	-	-	-	-	-	-	-	-	-	-	-	-	-	-	-
Δ*SL3646*	-	-	-	-	-	-	-	-	-	-	-	-	-	-	-	-	-	-	-	-	-	-	-
Δ*yqaE*	-	-	-	-	-	-	+	-		-	-	-	-	-	-	-	-			-	+	+	-
Δ*ydgFE*	-				-		-	-	-			-	-		-			-	-		-	-	
Δ*ybiJ*	-				-		-	-	-			-	-		-			-	-		-	-	
Δ*yncJ*																					-	-	-

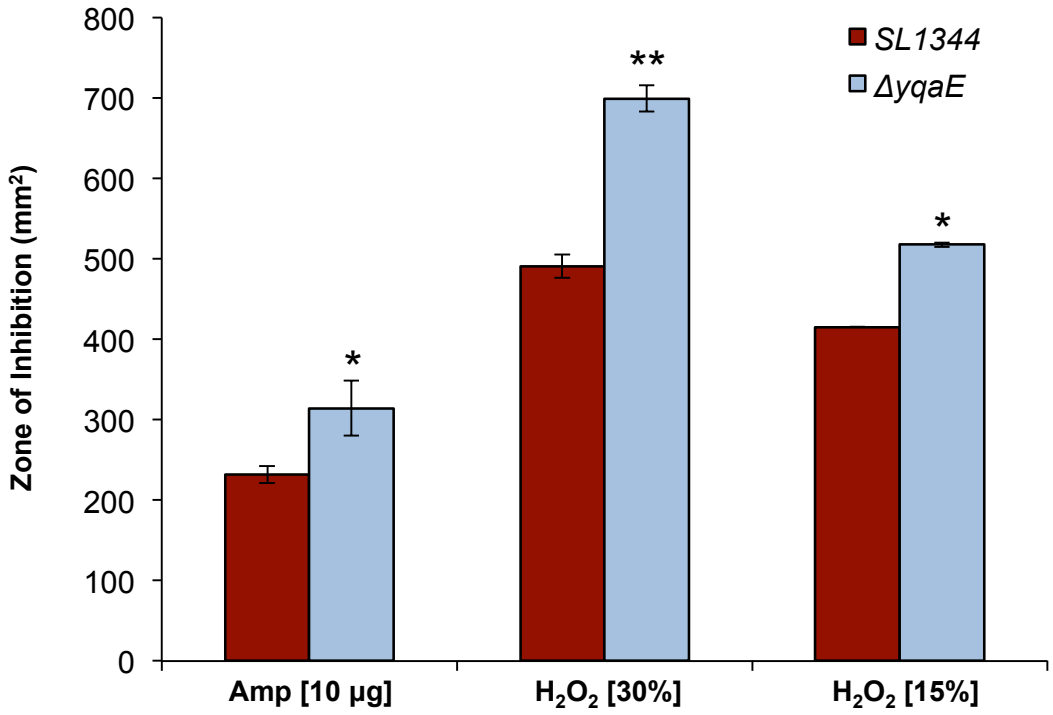

Figure 19: Deletion of *yqaE* renders *S.* Typhimurium more sensitive to ampicillin [10 µg] and hydrogen peroxide [30% and 15% v/v]. SL1344 WT and Δ*yqaE* were tested for ampicillin and H_2O_2 sensitivity by a disc diffusion assay. Significant differences to WT SL1344 shown by * ($p<0.05$) and ** ($p<0.01$). Error bars = SE, $n = 3$.

4.4.5.2 YdgFE contributes to S. Typhimurium survival during spermidine stress

Based on protein sequence analyses *SL1412* and *SL1413* (*ydgFE*) were predicted to encode a drug transporter system and later confirmed as novel drug resistance genes in *E. coli* (Nishino and Yamaguchi, 2001). Prior to the work presented in this thesis, no studies had investigated the regulation of this drug efflux system, or its function, in any *Salmonella* species. One study had highlighted a role for YdgFE (MdtJI) in maintaining non-toxic levels of polyamines within the cytoplasm of *E. coli*, with double *mdtJI* mutants of *E. coli* CAG2242 (*speG*$^-$) having defective growth in the presence of 2mM spermidine (Higashi et al., 2008).

Our SL1344 Δ*ydgFE* deletion strain, along with SL1344 WT, was subjected to 2 mM spermidine survival assays, as described by Higashi et al. (2008) (Figure 20, A and B). Spermidine was added to LB batch cultures at

inoculation (*t* = 0) (Figure 20, A) and post-lag phase (*t* = 3) (Figure 20, B) and viable cell counts (CFU mL^{-1}) recorded for SL1344 WT and Δ*ydgFE* after 6, 24 and 48-hours growth. In liquid culture, a Δ*ydgFE* double mutant grew as SL1344 WT in the presence of spermidine, regardless of when polyamine addition occurred (Figure 20, A and B). Both strains had a higher CFU mL^{-1} after 6 hours growth in the presence of 2 mM spermidine compared to LB control cultures. However, after this initial increase in cell number, spermidine negatively impacted growth of both SL1344 WT and Δ*ydgFE* over time. After 48-hours, the CFU mL^{-1} for all spermidine exposed SL1344 WT and Δ*ydgFE* cultures was, on average, 58% and 50% lower (respectively) than the CFU mL^{-1} for their equivalent LB control cultures (Figure 20, A and B). Despite the sensitivity exhibited by both strains to high spermidine concentrations, Δ*ydgFE* was not significantly more sensitive than WT SL1344 during these investigations in liquid culture. There was no significant difference ($p>0.05$, Student's *t* test) in the final CFU mL^{-1} of the two strains, after 48-hours growth in the presence of 2 mM spermidine (Figure 20).

When sensitivity to spermidine was examined during growth on solid media (LB agar 1.5% w/v) containing 2 mM spermidine, no difference in survival was again observed for WT SL1344 or Δ*ydgFE* (Figure 21). However, increasing spermidine concentrations to 4 mM, 6 mM and 8 mM produced an average 10% reduction in Δ*ydgFE* viable cells, compared to LB controls (Figure 22). In contrast, growth of SL1344 WT increased by ~8% on LB 4 mM spermidine agar (Figure 22). On media containing 6 mM spermidine, SL1344 WT also grew better, or at least equal to, the LB agar control plates (Figure 22). Only once spermidine concentrations increased to 8 mM did SL1344 WT survival rates drop below those witnessed on LB controls (Figure 22).

The increase in SL1344 WT survival on 4 mM and 6 mM concurs with the initial increase in CFU mL^{-1} seen for SL1344 WT, after 6-hours growth in liquid culture with 2 mM spermidine (Figure 21, A and B). This was not the case for Δ*ydgFE*. In liquid culture, the increase in survival observed for

Δ*ydgFE* (in the first 6-hours of exposure to 2 mM spermidine) (Figure 20, A and B) was not repeated when solid media supplemented with spermidine >4 mM (Figure 22).

In addition to these spermidine sensitivity assays, our *ΔydgFE* strain was screened for sensitivity against 10 antimicrobial compounds at a range of concentrations (Table 28). However, no adverse affect on growth or survival was observed for any compounds tested.

4.4.5.3 ScsA, as well as ScsBCD, contributes towards copper sulphate tolerance in S. Typhimurium

Work by Anwar et al. (2013) highlighted ScsABCD as a novel virulence cluster in *S.* Typhimurium. Although all four genes are situated on the same DNA strand, *scsA* and *scsBCD* are read in two separate transcriptional units. Anwar et al. (2013) showed ScsBCD, but not ScsA, is required for copper chloride tolerance. A single *scsA* deletion mutant was made in our SL1344 background using the λ-red system and confirmed by PCR. Deletion of *scsA* had no negative impact on SL1344 growth (data not shown) under standard growth conditions (LB media, aerated, 37°C). SL1344 WT, Δ*cpxR*, *cpxA** and Δ*scsA* were grown on LB agar supplemented with 4 mM $CuSO_4$ and LB agar only controls. All strains grew to a comparable level on LB agar control plates (data not shown), but growth on solid media containing $CuSO_4$ [4mM] was fatal to Δ*cpxR* and Δ*scsA* (Figure 23). Growth of SL1344 WT and *cpxA** was stunted on $CuSO_4$ [4mM] compared to controls, but *cpxA** presented an increase in copper tolerance compared to the isogenic parent strain in the presence of 4 mM $CuSO_4$ (Figure 23). SL1344 WT, Δ*cpxR*, *cpxA**, Δ*cpxP*, Δ*scsA*, Δ*cpxR*Δ*scsA,* were also subjected to copper sensitivity assays in liquid LB culture, supplemented with 3 mM or 4 mM $CuSO_4$. Sensitivity of Δ*scsA* (μ=0.44 hr^{-1}) and Δ*cpxR*Δ*scsA* (μ=0.54 hr^{-1}) strains was observed in the presence of 3 mM $CuSO_4$, reaching final ODs (24-hours) 18.7-fold and 16.7-fold lower than the WT strain (Figure 24, A). Δ*cpxR* was not sensitive to 3 mM $CuSO_4$, growing to a final OD slightly, but not significantly, higher than SL1344 WT (Figure 24, A). The growth rates of SL1344 WT and Δ*cpxR* were

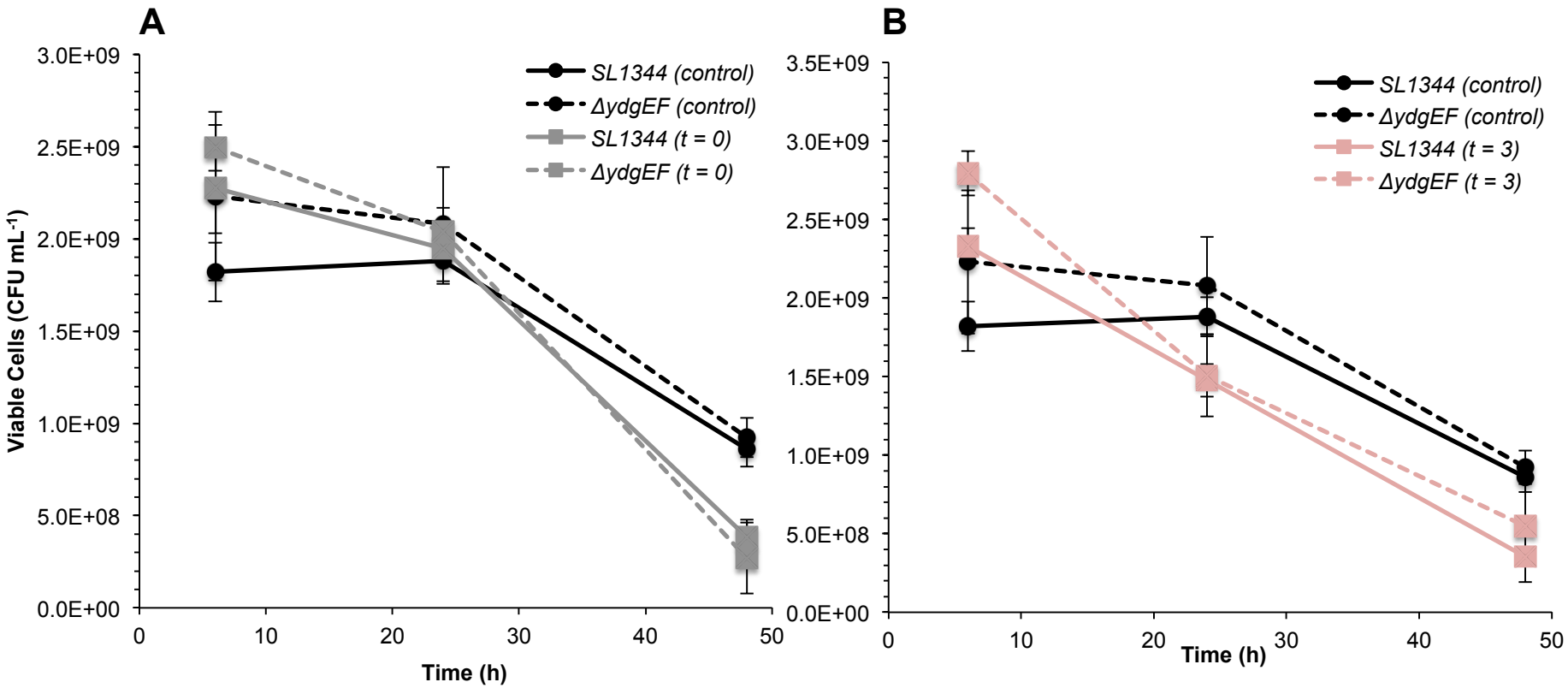

Figure 20: ***S*. Typhimurium SL1344 WT and Δ*ydgFE* double mutants do not differ in sensitivity to spermidine (2 mM) when grown in liquid culture.** Samples of WT SL1344 and Δ*ydgFE* were collected after 6, 24 and 48 hours growth in LB (batch culture) with (■) and without (●) 2 mM spermidine (added at *t* = 0; **A**, and *t* = 3; **B**), 37°C, 200 rpm. Serial dilutions (10^{-3}, 10^{-4} and 10^{-5}) in 1 x PBS were plated onto LB agar and viability counts (CFU mL^{-1}) were calculated after overnight incubation at 37°C. Error bars = SE, *n* = 3.

virtually identical, μ=0.64 hr^{-1} and μ=0.63 hr^{-1} respectively, in these 3 mM $CuSO_4$ cultures. Despite growing better than SL1344 WT on LB agar 4 mM $CuSO_4$, *cpxA** reached a final OD 1.7-fold lower than WT SL1344 in liquid culture at this lower (3 mM) $CuSO_4$ concentration (Figure 24, A). However, as determined for Δ*cpxR*, the final OD for *cpxA** was not significantly different ($p>0.05$ Student's *t* test) to SL1344 WT.

As expected, no growth was observed for Δ*scsA* and Δ*cpxR*Δ*scsA* in 4 mM $CuSO_4$ (Figure 25). Δ*cpxR* also experienced defective growth at this higher concentration compared to WT SL1344 (Figure 25), although this was not as extreme as the phenotype observed on solid media containing 4 mM $CuSO_4$ (Figure 23)

If the copper sulphate sensitivity displayed by our *scsA* mutant was due to deletion of the *scsA* gene, and not a result of polar effects of *scsA* deletion on *scsBCD* then growth should be restored through complementation. We therefore tested sensitivity of Δ*scsA* to 3 mM $CuSO_4$ when *scsA* was expressed *in trans*. SL1344 WT, Δ*cpxR* and Δ*scsA* were transformed with the *scsA* overexpression vector pBAD*scsA*, the *scsA* gene of *S*. Typhimurium (SL1052) cloned into pBAD myc/His A under the control of an arabinose inducible promoter. Complementation strains SL1344p*scsA*, Δ*cpxR*p*scsA*, Δ*scsA*p*scsA* and strains harbouring empty pBAD controls, were grown in LB batch cultures supplemented with 3 mM $CuSO_4$, Amp to maintain the plasmid and *L*-arabinose (0.02% w/v) to induce *scsA* transcription from the overexpression vector. Overexpression of an empty pBAD control vector had no adverse effects on growth of WT SL1344, Δ*cpxR* or Δ*scsA* (data not shown). All complementation strains reached an OD of 1.24-1.41 after 24-hours growth (Figure 24, B). Our Δ*scsA*pscsA strain reached a final OD ~8-fold higher than Δ*scsA* when ScsA was overexpressed *in trans* (Figure 24, B). However, growth of Δ*scsA*p*scsA* was not restored to that seen for the isogenic parent strain and SL1344p*scsA* and Δ*cpxR*p*scsA* grew ~2.3-fold and ~2.5-fold less than SL1344 WT respectively under the same conditions (Figure 24, A and B).

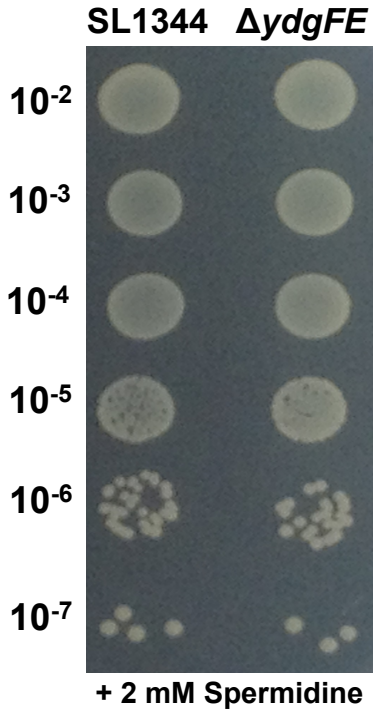

Figure 21: *S*. Typhimurium SL1344 and *ydgFE* double mutants do not differ in sensitivity to spermidine (2mM) when grown on solid media. SL1344 WT and Δ*ydgFE* cultures were serial diluted in to 1xPBS (10^{-2} to 10^{-6}) and spotted on to LB agar with and without spermidine (2 mM). Plates were imaged once single colonies were visible, ~18 hours for LB controls and ~48 hours for 2 mM spermidine plates.

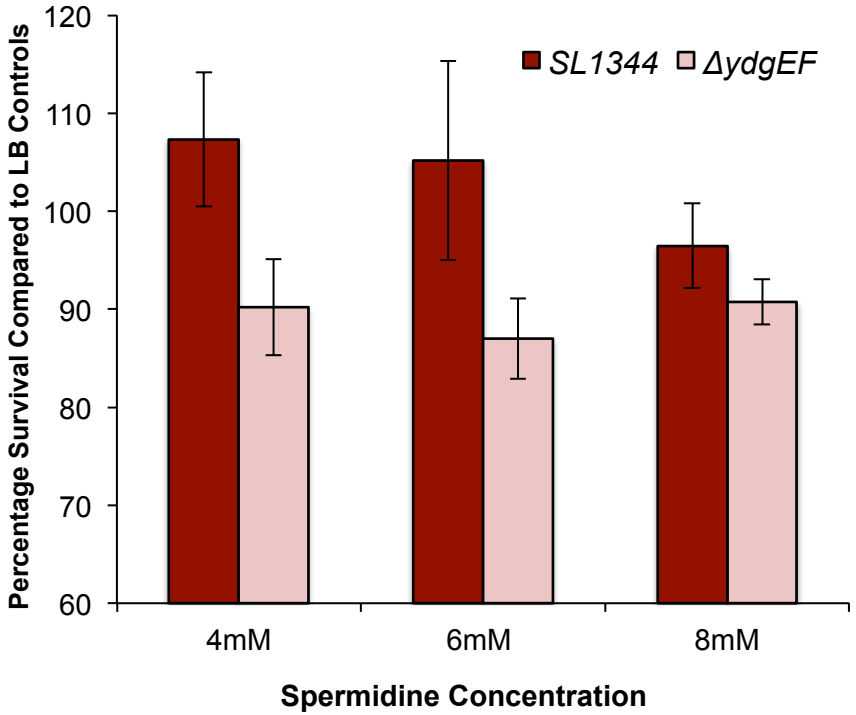

Figure 22: S. Typhimurium *ydgFE* double mutant exhibits sensitivity to spermidine at concentrations greater than 4 mM when grown on solid media. SL1344 WT and Δ*ydgFE* cultures were serial diluted into 1xPBS (10^{-2} to 10^{-6}) and spotted in on to LB agar with and without spermidine (4 mM, 6 mM and 8 mM). CFU mL^{-1} were calculated (at ~18 h for LB controls, ~48 h for spermidine plates. Error bars = SE, *n* =3.

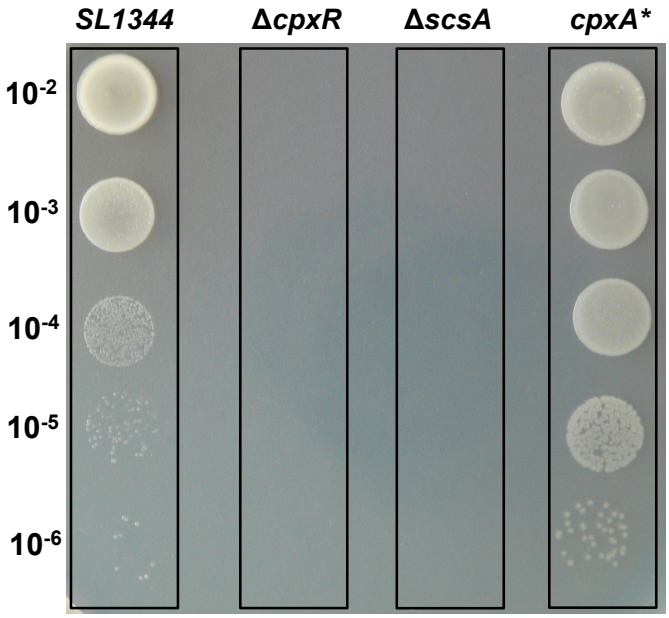

Figure 23: Growth of SL1344 WT, Δ*cpxR*, Δ*scsA* and *cpxA strains on LB agar containing 4 mM $CuSO_4$, under aerobic conditions, at 37°C for ~48 hours.** Exposure to 4mM $CuSO_4$ was fatal for Δ*cpxR* and Δ*scsA* strains. No differences in growth were observed for all strains under the same conditions on LB agar control plates (data not shown).

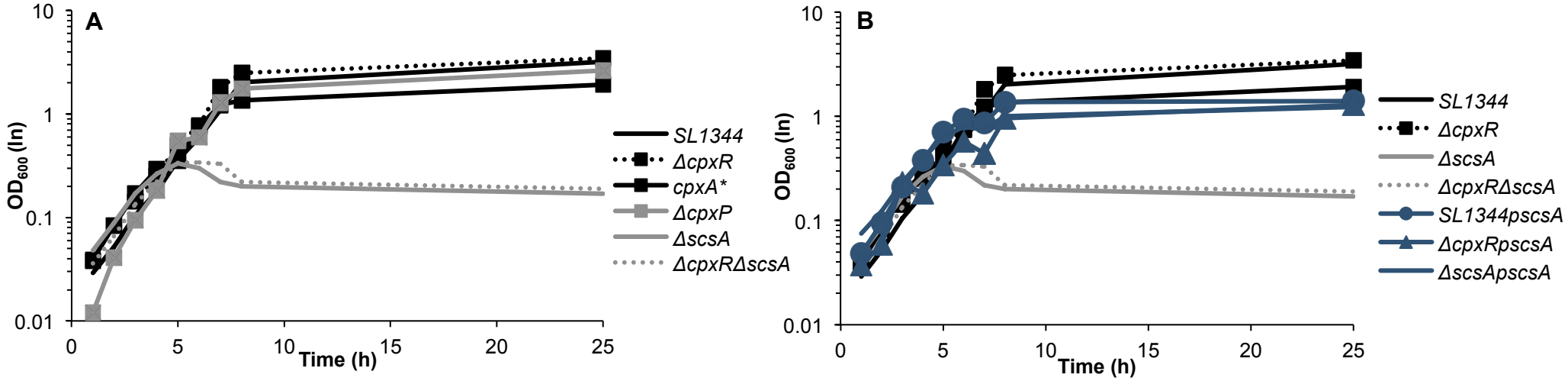

Figure 24 (above): Sensitivity of Δ*scsA* and Δ*cpxR*Δ*scsA* to 3 mM $CuSO_4$ (A) cannot be fully complemented when Δ*scsA* is expressed *in trans* (B). A. SL1344 WT, Δ*cpxR*, *cpxA**, Δ*cpxP*, Δ*scsA* and Δ*cpxR*Δ*scsA* were grown in LB 3mM $CuSO_4$ at 37°C, 200rpm, and OD_{600} recorded over 25 hours. B. Cultures were repeated for strains expressing the *scsA* complementation vector pBADscsA, SL1344p*scsA*, Δ*cpxR*p*scsA* and Δ*scsA*p*scsA*, with Amp and arabinose [0.02% w/v].

Figure 25 (below): Sensitivity of Δ*scsA* and Cpx mutants to 4 mM $CuSO_4$ when grown overnight in batch culture (LB). SL1344 WT, Δ*cpxP*, Δ*cpxR*, Δ*scsA* and Δ*cpxR*Δ*scsA* were grown in LB with 4 mM $CuSO_4$ at 37°C, 200rpm, overnight. OD_{600} was recorded after 15 hours growth.

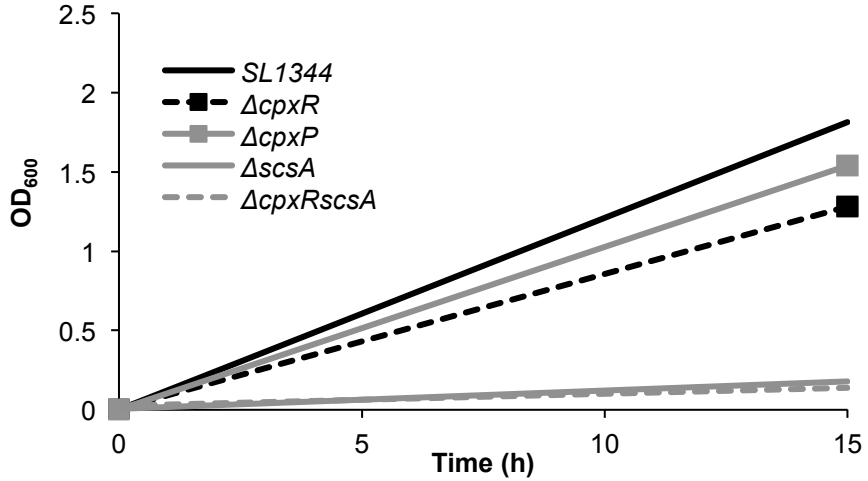

4.4.5.4 Characterisation of the SL3010/3009 operon: Expression levels across growth phases and regulation by other ESRs

Cross-talk between the ESRs means that certain Cpx regulon members are regulated by multiple ESRs, such as σ^E (i.e. *htrA*, *skp*, *rpoD*, *rpoE*, *rpoH*, *rseABC*) or the 2CST system BaeSR (i.e. *spy, acrD*, *mdtA*). We wanted to assess if this was true for any of our new Cpx regulon members, especially for those genes where no regulatory information had been identified. *lacZ*-promoter fusion constructs were used in β-galactosidase assays to assess promoter activity of these Cpx regulon members, in a variety of ESR deletion mutant backgrounds. This methodology also allowed us to evaluate the expression levels of our genes of interest across different phases of growth.

Unfortunately, only *lacZ*-promoter fusion constructs for the SL3010/SL3009 operon could be made and verified during this investigation. However, there have been limited investigations into the function of this uncharacterised operon and therefore any additional regulatory information would be essential to elucidating its function in *Salmonella*.

4.4.5.4.1 SL3010 and SL3009 are up-regulated upon entry into stationary phase and increasing cell density

The promoter-containing region of *SL3010* (~1000 bp 5' of the *SL3010* initiation codon) was cloned into the low-copy expression vector pMP220, producing the SL3010-*lacZ* transcriptional fusion plasmid (pR3009/10), confirmed by sequencing. This construct and empty pMP220 (control) were transduced into SL1344 WT and seven ESR mutants: Δ*cpxR*, Δ*cpxAR*, Δ*baeR*, Δ*rpoE* Δ*zraSR*, Δ*cpxAR*Δ*baeR*, Δ*cpxR*Δ*baeR*Δ*zraSR*. β-galactosidase assays were performed as described in 4.3.3 and relative expression of this operon during lag, early-log, mid-log, late-log and stationary phases of growth was determined (Miller units) (Figure 26). Values were normalised by subtracting any background expression recorded for the pMP220 control. In an SL1344 WT background, expression levels for SL3010/09 increased across all phases of growth with a ~5-fold increase in SL3010/09 promoter activity observed between lag and stationary phases (Figure 26).

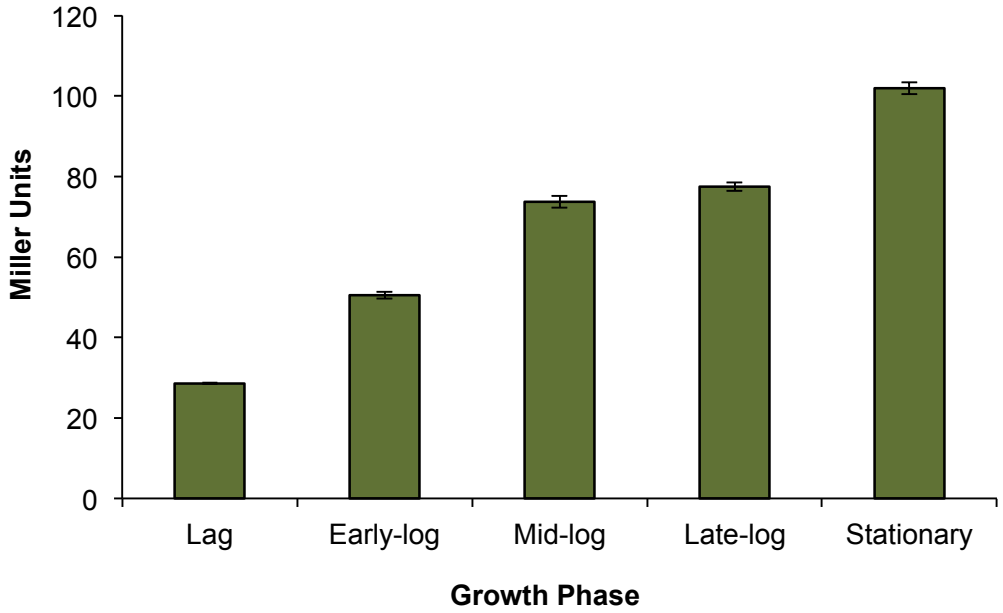

Figure 26: β-galactosidase assays of SL3010/3009 *lacZ*-promoter fusions show increased SL3010/3009 expression upon entry into stationary phase and with increased cell density. Relative expression of the SL3010/3009 operon increases across five growth phases from lag to stationary phase. Units have been normalised by subtracting background expression levels observed for empty pMP220 control vector. Error bars = SE. *n* = 3.

When relative expression levels of SL3010/09 in Δ*cpxR*, Δ*cpxAR*, Δ*baeR*, Δ*rpoE* Δ*zraSR*, Δ*cpxAR*Δ*baeR* and Δ*cpxR*Δ*baeR*Δ*zraSR* were determined, a reduction in SL3010/09 expression was observed in all mutants lacking CpxR, BaeR and ZraR response regulators (Figure 27). In SL1344 mutants where the histidine sensor kinases CpxA and ZraS had been deleted, a significant reduction ($p<0.01$ Student's *t* test) in SL3010/09 expression was seen upon entry into stationary phase (Figure 27). When comparing SL3010/3009 expression in SL1344 WT and Δ*rpoE* backgrounds, no differences in expression were observed during early log phase, followed by a significant increase in expression during mid-log phase of growth ($p<0.05$ Student's *t* test), before a further reduction in expression in late-log and stationary phases of growth ($p<0.01$ Student's *t* test) (Figure 27).

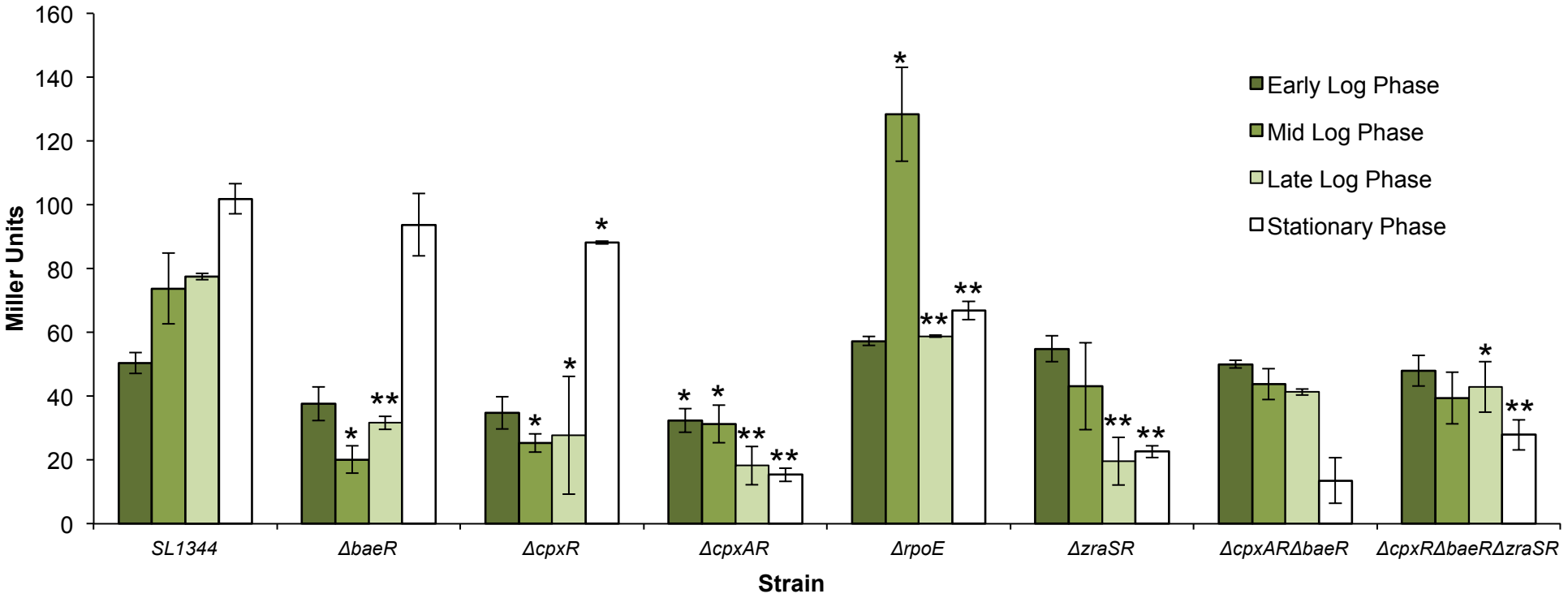

Figure 27: **β-galactosidase assays of SL3010/3009 *lacZ*-promoter fusions show cross-regulation of this uncharacterised operon by Cpx, Bae and Zra ESRs.** Relative expression of SL3010/09 (miller units) was determined across four growth phases: early log, mid-log, late-log and stationary phase. Units have been normalised by subtracting background expression levels obtained for empty pMP220 control vector. Significant differences to WT SL1344 shown by * ($p<0.05$) and ** ($p<0.01$). Error bars = SE, $n = 3$.

4.4.5.4.2 Involvement of SL3010/09 in adhesion of S. Typhimurium to abiotic surfaces

As summarised in 1.7.3, the Cpx pathway plays a key role in regulation of adhesion through induced gene expression, with mutations in the *cpxA* gene reducing biofilm formation through disruption of essential component of solid-surface adhesion (Dorel et al., 1999, Otto and Silhavy, 2002). Several members of the *E. coli* Cpx regulon encode critical components of the cell surface assembly, involved in biofilm formation and conjugation, such as *csgA* (curli), *pap* (pili P) and *tra* (pili F) (Prigent-Combaret et al., 2001, Hernday et al., 2004, Gubbins et al., 2002b). Activation of the Cpx pathway results in impairment of F pili, P pili and curli biogenesis. P pili and curli regulation changes occur at the transcriptional levels, whereas Cpx modifies F pili expression at the post-transcriptional level (Dorel et al., 2006).

Hancock et al. (2010) suggested that *ybiJ*, a gene of unknown function, could encode a small, low-molecular weight protein that contributes towards biofilm formation of UPEC *E. coli* (strain CFT073). We wanted to assess if *ybiJ*, or other genes described during this work as Cpx regulated, were involved in biofilm formation of *S*. Typhimurium. SL1344 WT and Δ*ybiJ*, Δ*stm3388*, Δ*SL3646*, Δ*yqaE*, Δ*ydgFE*, Δ*SL3009* and Δ*SL3010*Δ*SL3009* were subjected to biofilm assays (24 and 48 hours) in polycarbonate 96-well plates (2.4.25). After 48 hours, both Δ*SL3009* and Δ*SL3010*Δ*SL3009* exhibited significantly increased biofilm formation (30% and 54% respectively) compared to WT SL1344 (Figure 28). No significant difference in relative biofilm formation (OD_{595}) was observed for Δ*ybiJ* or Δ*ydgFE* compared to WT SL1344 at either time points tested (Figure 29). Unfortunately, data obtained for Δ*stm3388*, Δ*SL3646*, Δ*yqaE* was inconclusive (data not shown) and further investigations for these strains are needed.

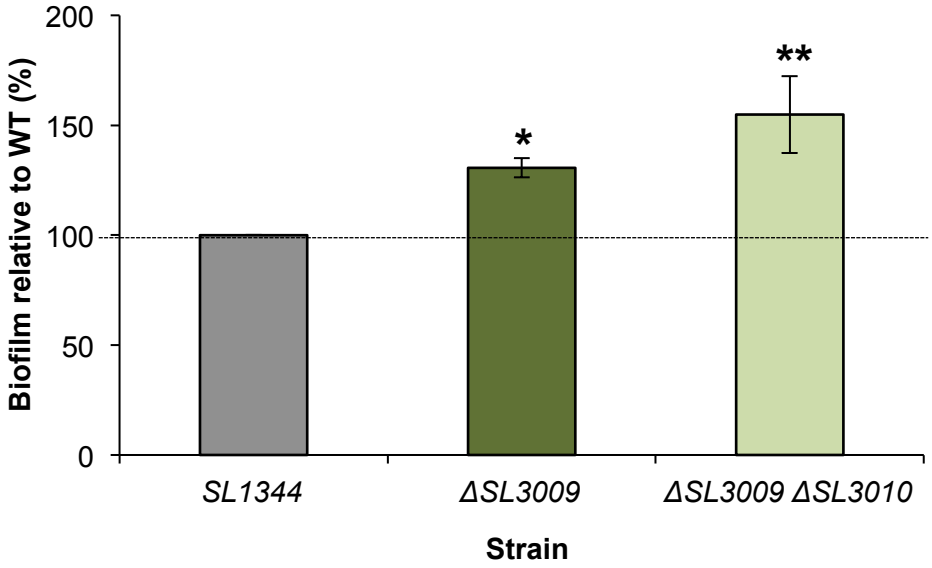

Figure 28: **Increased biofilm formation of Δ*SL3009* and Δ*SL3010*Δ*SL3009* mutants compared to SL1344 WT**. Relative biofilm formation (percentage of WT SL1344) for sample and control plates (CFA only) calculated after 48 hours growth at 28° C. Data were normalised by subtracting any background from media control. Significant differences to SL1344 WT shown by Student's *t* test $p<0.05$ (*) and $p<0.01$ (**). Error bars = SE, *n* = 2.

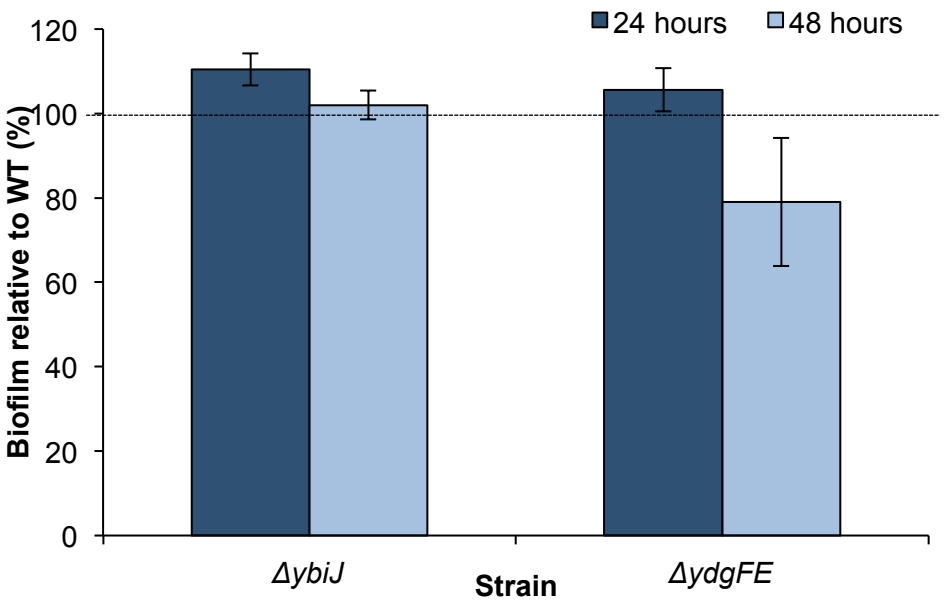

Figure 29: **Biofilm formation of Δ*ybiJ* and Δ*ydgFE* mutants does not significantly differ to WT SL1344 (100%) (Student's *t* test p>0.05).** Relative biofilm formation (percentage of WT SL1344) for sample and control plates (CFA only) calculated after 48 hours growth at 28°C. Data were normalised by subtracting any background from media control. Error bars = SE, *n* = 2.

4.5 Discussion and future work

CpxR falls into the OmpR subfamily of RRs, classified as a winged helix-turn-helix DNA binding protein (Kenney, 2002). As is the case for many RR of its type, CpxR has a higher affinity for its target-binding motif following phosphorylation compared to its unphosphorylated form (Hoch, 2000). Receiver (REC) domains, conserved across all RRs, act as a molecular switch in response to phosphorylation and primarily exist in their inactive conformation. However, continuous fluctuations between both active and inactive conformations occur, within a microsecond timescale, and phosphorylation is required to shift this pre-existing equilibrium resulting in stabilisation of the RR's conformational state (Gardino and Kern, 2007). Due to the winged helix-turn-helix homology of CpxR, once phosphorylated CpxR-P is believed to form direct contacts with the carboxy-terminal domain of the α-subunit of RNA polymerase, stimulating transcription (MacRitchie et al., 2008a).

The consensus of the CpxR binding site or its orientation have little impact on the strength of Cpx regulation, with the location of the CpxR binding box being the most important factor (Price and Raivio, 2009). Price and Raivio (2009) state that the presence of a CpxR binding site within the initial 100 bp upstream from the transcriptional start site is imperative for strong regulation by CpxR. Although none of the proposed CpxR-P binding motifs presented during our investigation appear within this section (Table 27), the fold changes as a result of Cpx induction for many of our newly proposed Cpx-regulon members are significant and often substantial (> 5-fold) which suggests strong induction of these genes by CpxR. EMSAs confirmed CpxR-P binding to the promoter regions of eight genes; *yccA*, *cstA*, *yqaE*, *SL3646*, *ydgF*, *slrP*, *ybiJ* and *eco*, in the presence of the non-specific competitor poly(dI•dC) (Figure 17). This binding of CpxR-P occurred in the absence of any other external factors, strongly suggesting direct regulation of these genes by CpxR through binding to the 17-bp CpxR-P motif, located in the centre of our fluorescein labelled promoter probes, that has sequence homology to a previously identified CpxR consensus motif in *E. coli* (GTAAAAGCTTGTAAG) (De Wulf et al., 2002). Preliminary investigations

also suggested direct binding of CpxR-P to the promoters of *yihE*, *tsr*, *deoA* and *rpoH* (Figure 18). However, DNA shifts for these three promoter probes were not reproducible in the presence of poly(dI•dC). These EMSAs need to be repeated with an increasing CpxR-P pmol gradient and the addition of poly dI•dC to confirm this CpxR-P:DNA complex is not forming due to non-specific binding. *tsr* has been defined as CpxR regulated in *E.coli* with confirmation of direct CpxR-P binding to a 212-bp *tsr* promoter fragment containing the CpxR-P recognition consensus box in the centre (De Wulf et al., 1999). De Wulf et al. (1999) conducted *tsr* EMSAs at a CpxR-P/DNA ratio of 20 (200 pmol/10 pmol) in the presence of 500-fold molar excess competitor DNA (in this case sheared herring sperm DNA). Although the CpxR-P/DNA ratio during our *tsr* EMSAs was 20 (10 pmol/0.5 pmol) and 40 (20 pmol/0.5 pmol) (Figure 18), the total concentration of CpxR-P protein was substantially lower. This may contribute to the lack of band shifts seen in the presence of poly(dI•dC). Increasing CpxR-P concentrations to 200 pmol was not possible within the reaction parameters of our EMSAs and the CpxR-P/DNA ratio used should have been sufficient, however further investigations and protocol modifications are required before direct binding of CpxR-P to the *tsr* promoter fragment of *S*. Typhimurium (and *yihE*, *deoA* and *rpoH*) can be ruled out.

Although binding of CpxR-P to our 6-FAM fluorescein labelled DNA probes was visualised through EMSAs, the exact position of CpxR-P binding and promoter-binding affinity were not possible within the time frame of our investigations. Repeating these EMSAs across an extended protein concentration gradient would allow more specific CpxR-P binding concentrations to be determined. Our promoter probes spanned a 17-bp section of DNA, identified through bioinformatic analysis, to share sequence similarity with a previous published CpxR binding motif. Confirmation of the specific bases involved and their contribution to these CpxR-P:DNA interactions could be confirmed through site-directed mutagenesis of these motifs or the synthesis of multiple oligonucleotide fragments containing point mutations within the CpxR-P motif. Chromatin Immunoprecipitation (ChIP) assays would further confirm the direct interactions presented here, providing

additional evidence to support CpxR regulation of all of our newly described Cpx regulon members *in vivo* and a more comprehensive overview of CpxR regulated genes in *Salmonella* as a whole. Our investigations allowed an updated CpxR binding motif in *S*. Typhimurium to be produced (Figure 15), contributing to our understanding of this system and hopefully providing a more accurate binding motif should these future experiments take place.

4.5.1 The multidrug efflux system YdgFE assists *S*. Typhimurium in overcoming spermidine toxicity

Despite the involvement of polyamines in cellular stresses, biofilm formation, bacteriocin production and escape from phagolysosomes (Shah and Swiatlo, 2008, Lee et al., 2007, Chattopadhyay et al., 2003, Di Martino et al., 2013), only the *speG* gene of *B. pseudomallei* is associated with the ESRs as it is under σ^E regulation in this species (Jitprasutwit et al., 2014).

One operon positively regulated by CpxR during our transcriptomic analysis was YdgFE, encoded by *SL1412* and *SL1413* respectively (Chapter 3). No regulatory information for this system had previously been presented in any organism. However, work by Higashi et al. (2008) highlighted a role for this system in response of *E. coli* to spermidine toxicity at a neutral pH. As YdgFE was identified as a multidrug efflux system during analysis of putative drug transporter genes (Nishino and Yamaguchi, 2001), evidence for YdgFE involvement in maintaining intracellular levels of spermidine through the excretion of this polyamine was unsurprising and provided a viable explanation to their function based on sequence analysis. Expression of *ydgFE in trans* increases cell viability of a *speG*$^-$ *E. coli* strain in the presence of 2 mM spermidine >1000-fold (Higashi et al., 2008). This recovery was also seen when spermidine concentrations were increased to 12 mM. However, no recovery was observed when either gene was expressed individually, and as *ydgFE* are co-expressed (Nishino and Yamaguchi, 2001), this indicates the requirement of both genes in maintaining viability during intracellular accumulation of spermidine (Higashi et al., 2008). Prior to Higashi et al. (2008), no spermidine efflux systems had been discovered in *E. coli* and, to the best of our knowledge, none have been characterised in *Salmonella*. We

therefore wished to determine what role, if any, YdgFE of *S*. Typhimurium had in the *Salmonella* response to spermidine stress. Deletion of *ydgFE* in our SL1344 WT did not result in sensitivity to 2 mM spermidine, both WT and Δ*ydgFE* strains grew equally well in liquid culture, and on solid media, containing 2 mM spermidine (Figure 20; Figure 21). However, when exposed to higher spermidine levels (4 mM, 6 mM and 8 mM), Δ*ydgFE* growth reduced by ~10% compared to minus spermidine controls, a difference of nearly 20% compared to SL1344 WT grown in the presence of 4 mM and 6 mM spermidine (Figure 22). Our Δ*ydgFE* strain was made in an SL1344 background, without deleting *speG*, encoding a spermidine *N*1-acetyltransferase. SpeG monoacetylates spermidine during periods of excess resulting in polyamine catabolism. Lack of Δ*ydgFE* sensitivity at lower spermidine concentrations (2 mM) could be due to spermidine monoacetylation by STM1502, a homologue of *E. coli* SpeG in *S*. Typhimurium (data not shown), relieving toxicity by compensating for increases in intracellular spermidine as a result of YdgFE deletion. The SpeG protein of *E. coli* and STM1502 of *S*. Typhimurium share 91% sequence homology at the amino acid level (data not shown). An SL1344 Δ*stm1502* (*speG*-) background was not available at the time of these experiments, but conducting spermidine sensitivity assays in a triple Δ*speG*Δ*ydgFE* mutant of SL1344, or expressing *ydgFE in trans* in an *stm1502* deletion mutant, would clarify involvement of YdgFE in the response of *S*. Typhimurium to spermidine toxicity. If STM1502 is able to compensate for the loss of *ydgFE* at lower concentrations, the sensitivity of Δ*ydgFE* to spermidine at >4 mM may be a result of excessive intracellular accumulation and levels that can no longer be sustained by monoacetylation alone.

It is not yet known if other spermidine efflux systems are functional in *Salmonella* under the conditions tested here. If present they may contribute to spermidine efflux, further counteracting any growth inhibitions from YdgFE deletion. Incubation with radiolabelled spermidine, [^{14}C]spermidine, followed by cell harvesting and counting radioactivity of the supernatant by a liquid scintillation counter would allow quantification of intracellular spermidine levels, measuring any increases hypothesised in Δ*ydgFE* or Δ*speG*Δ*ydgFE*

mutants. Variations in spermidine efflux between SL1344 WT and Δ*ydgFE* strains could also be measured in this manner. However, incubation with non-labelled spermidine and analysis by high-performance liquid chromatography would be required to measure excreted polyamines, as described by Higashi et al. (2008). Such investigations could be extended to other polyamines, e.g. putrescine, cadaverine and spermine (which with spermidine make up the four most common polyamines in microbial cells; Figure 13) to establish if YdgFE is a specific spermidine efflux system or if these proteins function to maintain intracellular concentrations of all polyamines.

Although the Cpx ESR has not previously been associated with regulating spermidine toxicity, the role of Cpx in antibiotic resistance phenotypes is well established (Mahoney and Silhavy, 2013, Raivio et al., 2013). Links between exogenous spermidine concentrations and the antibiotic susceptibility of bacteria has been observed for a variety of human pathogens, including *S*. Typhimurium (Kwon and Lu, 2007). Such links are unsurprising given the crossover observed between known polyamine transport systems in other species and antibiotic uptake and efflux. Aminoglycosides largely mimic polyamines and regularly utilise influx systems of polyamines to allow entry into prokaryotic and eukaryotic cells (Van Bambeke et al., 2000). One such example is the spermidine efflux system Blt, a MDR transporter in Gram-positive bacteria, which is also involved in fluoroquinolone (FQ) efflux (Woolridge et al., 1997, Poole, 2000).

Given the large number of processes polyamines are involved in, including virulence and infection strategies, it is surprising that so few investigations have focused on spermidine homeostasis in pathogens like *Salmonella*. One role of spermidine of particular interest is its ability to scavenge free radicals within the nucleus of eukaryotic cells, reducing DNA damage from oxidative stress (Ha et al., 1998). This protective role was demonstrated in prokaryotes shortly after (Tkachenko et al., 2001), with polyamine synthesis pathways (Figure 13) also up-regulated upon exposure to hydrogen peroxide in *E. coli* (Tkachenko and Nesterova, 2003). Because of this protective role,

polyamines would be an important component of the ESR of *Salmonella* during oxidative stress inflicted upon it within the host macrophages.

As *speG* of *B. pseudomallei* is the only gene involved in polyamine homeostasis known to be regulated by an ESR (Jitprasutwit et al., 2014), if YdgFE is confirmed as a spermidine efflux system in *Salmonella*, it will be the first of its kind associated with any ESR, not just the Cpx pathway. *ydgFE* analysis presented in this thesis confirms, through a combination of transcriptomic analyses (microarray and qRT-PCR) and EMSAs, direct regulation of YdgFE by CpxR. As described during Chapter 1 and Chapter 3, there is significant overlap between the regulons of σ^E and Cpx and their inducing cues. Cross-talk between these two ESR with regards to spermidine would allow fine tuning of polyamine homeostasis, intracellular concentrations to be adjusted during oxidative stress as wells as maintaining polyamine levels for the other essential cell functions polyamines are involved (4.1.5)

4.5.2 *yqaE* Involvement in *S*. Typhimurium response to ampicillin and oxidative stress

Very little is known about the function of YqaE, despite it being a predicted membrane protein that is highly conserved across species (De Lay and Gottesman, 2009). In the plant model *Arabidopsis thaliana*, expression of *yqaE* homologues increases during periods of stress, specifically low temperatures, osmotic shock and dehydration (Capel et al., 1997, Medina et al., 2001). Although no function has been assigned to YqaE in bacteria, previous investigations in *E. coli* confirmed negative regulation of *yqaE*, at the post-transcriptional level, by the small non-coding RNA CyaR (De Lay and Gottesman, 2009) and transcriptomic analysis (Chapter 3; Figure 14, N) and EMSAs (Figure 17) presented throughout this work add *yqaE* to the growing number of genes directly regulated by CpxR in *Salmonella*.

An *S*. Typhimurium *yqaE* (*SL2780*) deletion strain exhibits significantly increased sensitivity to the β-lactam antibiotic ampicillin [10 μg] and hydrogen peroxide [30% and 15%] compared to the isogenic parent strain

(Figure 19; Table 28). Hydrogen peroxide reacts with transition metal ions to produce hydroxyl radicals (Fenton, 1894). These damage DNA directly or indirectly through oxidisation of deoxynucleotides, prior to their incorporation into DNA (Imlay, 2008, Liu and Imlay, 2013). This hydrogen peroxide sensitivity suggests YqaE may function in protecting the cell from oxidative damage. However, as Δ*yqaE* is a not sensitive to HU, a direct role of YqaE in preventing oxidative damage is unlikely. YqaE is a predicted membrane protein and deletion could damage the integrity of the cell envelope. Such damage would be exacerbated by exposure to the high levels of H_2O_2 present during our disc diffusion assays (Figure 19) and assessing the affect of *yqaE* deletion on membrane integrity, for example through sensitivity to osmotic shock, extreme temperatures and vancomycin, would confirm if this is the case. The OM of healthy Gram-negative bacteria acts as a barrier to vancomycin, a bactericidal antibiotic predominately used to treat Gram-positive infections. If this OM is compromised, which could be the case for Δ*yqaE*, vancomycin would be able to permeate the cell envelope and kill the cell through inhibition of cell wall synthesis. Permeability assays, for example through the uptake of the fluorescent probe 1-N-phenylnaphthylamine (NPN) (Helander and Mattila-Sandholm, 2000) would allow quantification of the affect of *yqaE* deletion. These additional phenotypic screens could also be used during further analysis of the deletion strains produced during this work, especially those where genes of unknown function or proposed membrane components are removed.

Increased sensitivity of Δ*yqaE* to ampicillin [10 μg] (Figure 19) was unexpected as no differences in sensitivity were seen for SL1344 WT and Δ*yqaE* to carbenicillin [100 μg] (another β-lactam antibiotic and a structural isomer of ampicillin) (Table 28). Both antibiotics are semi-synthetic penicillins that block transpeptidation through association with penicillin-binding proteins (PBPs). This leads to the rupture of cell walls and the death of actively growing cells. The structure of carbenicillin differs from ampicillin in that the carboxyl group situated at the alpha position is substituted for an amino group. Ampicillin is also more susceptible to β-lactamase degradation than carbenicillin (Ouellette, 2014). The possibility of Δ*yqaE* sensitivity to β-

lactam antibiotics needs further investigation, a repeat of the disk diffusion analysis and MIC assays including a wider range and concentration of antibiotics.

4.5.3 Cross-regulation of SL3010/SL3009 by Cpx, Bae and Zra ESRs and the influence Cpx regulated genes on biofilm formation

Stationary phase is a known activating condition of the ESRs and β-galactosidase assays indicate up-regulation of SL3009 and SL3010 upon entry into stationary phase and with increasing cell density (Figure 26). When expression of SL3010/09 in a range of ESR mutants was determined, levels increased ~2-fold during mid-log phase in a Δ*rpoE* background when compared to the isogenic parent (Figure 26). This most likely results from increased CpxR levels due to a lack of negative regulation by σ^E. However, this spike is short lived and expression of the SL3010/09 operon reduces significantly ($p<0.01$ Student's *t* test) during late-log and stationary phases of growth in a Δ*rpoE* background (Figure 26). It is possible that increased CpxP subsequently suppresses CpxAR during these late growth phases and the subsequent reduction in SL3010/09 expression occurs.

SL3010/09 expression reduced in all mutants lacking Δ*cpxR*, Δ*baeR* and Δ*rpoE* (Figure 26), highlighting a clear role for all three of these ESRs in the induction of this operon. A reduction in STM3031 (SL3010) protein levels has been shown in Δ*baeR* and Δ*cpxAR* strains of *S*. Typhimurium (Hu et al., 2005). However, regulation of the SL3010/09 operon at the transcriptional level by either of the Bae or Cpx systems had not been determined prior to our study. A reduction in stationary phase expression of SL3010/09 in strains lacking *cpxA* or *zraS* (Figure 27) highlights the importance of these histidine SKs in SL3010/09 regulation and provides evidence for cross regulation of this operon between the ESRs. Cross regulation by ESRs has been observed for a variety of genes previously, e.g. *spy, acrD*, *mdtA, htrA*, *skp*, *rpoD*, *rpoE*, *rpoH* and *rseABC*. This coordinated regulation of SL3010/09 suggests the need for fine-tuning of this operon and possible induction in response to a variety of envelope stresses, due to the multiple inducing cues of the Cpx, Bae and σ^E ESRs. The lack of a CpxR binding motif within the

promoter region of SL3010 and the evidence presented here implying multiple regulatory components, suggests indirect regulation of SL3010/09 by the Cpx system.

The CpxAR system is known to have a role in biofilm formation (1.7.3) (Dorel et al., 1999, Yang et al., 2008, Steenackers et al., 2012) and any of the uncharacterised Cpx regulon members identified during this study could contribute towards this. Hancock et al. (2010) highlighted *ybiJ* involvement in biofilm formation and motility of both uropathogenic (CFT073) and probiotic (Nissle 1917) strains of *E. coli*, when grown in the presence of human urine. This reduction in biofilm formation was also reproduced in laboratory minimal media, albeit to a lesser extent (Hancock et al., 2010). Deleting *ybiJ* in *S*. Typhimurium SL1344 had no adverse impact on adhesion to an abiotic surface (Figure 29) when cultured in CFA media. This suggests a possible alternative function of *ybiJ* in *Salmonella*, or a less pronounced role for YbiJ in biofilm formation compared to *E. coli* strains. Screening our Δ*ybiJ* strain for biofilm formation and motility in a variety of media, especially those of physiological relevance (i.e. adhesion to gallstones; presence of bile salts) would categorically define this role of YbiJ in *Salmonella*. One significant phenotype associated with SL3009 and SL3010/09 deletion was an increase in biofilm formation, approximately 30% and 55% respectively (Figure 28). SL3009 could play a crucial role in inhibiting biofilm formation. SL3010 has sequence similarity to Omp X-like and Pag-C like OM virulence proteins. Omp X proteins promote bacterial adhesion and entry into mammalian cells and an SL3010 homolog in *Yersinia pestis* is associated with virulence and cell adhesion (Vogt and Schulz, 1999). SL3010 is therefore a possible adhesion factor with SL3009 contributing to this interaction. However, the exact involvement of SL3010 in *S*. Typhimurium biofilm formation can only be determined through analysis of a single Δ*SL3010* deletion strain, which was not possible during our study. Motility assays and macrophage infection studies involving *SL3009* and *SL3010* single and double mutants would provide a more detailed understanding of the function of this operon in bacterial-host cell interactions and *Salmonella* invasion and infection strategies. As expression of SL3009 and SL3010 increased during stationary

phase of growth and with increasing cell density (Figure 26), up-regulation of this operon may also correlate with *Salmonella* biofilm formation and the transition between planktonic and biofilm growth forms. By reducing biofilm formation, i.e. through the suppression of adhesion factors or the promotion of cell motility, SL3009 could allow release from biofilms and a return to planktonic growth. This would result in escape from the GIT/gallbladder into the environment, promoting spreading to the next host. The exact method through which SL3009 inhibits biofilm formation warrants further investigation. A combination of microscopy and transcriptomic analysis of SL3009 (and SL3010) during biofilm growth, motility and adhesion studies would establish how SL3009 impacts on *Salmonella* biofilms.

4.5.4 Confirmation of Scs operon involvement in copper tolerance of *S.* Typhimurium

The host, in direct response to infection, alters metal ion concentrations within macrophages. Zinc and copper concentrations decrease and increase respectively, due to the up-regulation and release of metal-binding antimicrobial proteins and NRAMP1 generated metal flux across phagosomal membranes (Collins, 2008, Wessling-Resnick, 2010, White et al., 2009, Kehl-Fie and Skaar, 2010, Jabado et al., 2000, Goswami et al., 2001, Osman and Cavet, 2011). Responding to fluctuations in metal availability and metal-mediated toxicity is critical for *S*. Typhimurium survival, especially as copper is redistributed within murine macrophages in response to *Salmonella* infection, with increased copper increasing bacterial killing (White et al., 2009, Achard et al., 2012). In the presence of the copper chelator BCS (bathocuproinedisulfonic acid), intracellular survival of *S*. Typhimurium increases, providing further evidence to link the importance of copper tolerance and successful colonisation (Achard et al., 2012).

Work by Yamamoto and Ishihama (2006) established the Cpx ESR as a regulator of copper homeostasis, defining the copper-inducible CpxR regulon in *E. coli*, including *cpxP*, *spy* and *yccA*. A *cpxAR* deletion strain of *E. coli* BW25113 is more sensitive to both copper chloride and copper sulphate than WT (Yamamoto and Ishihama, 2006). This sensitivity to $CuSO_4$ was

confirmed during our investigations (Figure 23; Figure 24), with our *cpxA** strain of SL1344 also exhibiting increased copper tolerance when exposed to $CuSO_4$, as was the case for BW25113 *cpxA** (Yamamoto and Ishihama, 2006). The *yccA* gene of *E. coli* was described by Yamamoto and Ishihama (2006) as CpxR regulated, in the presence of copper and independently. The work presented during this thesis confirms *yccA* as CpxR regulated in *S*. Typhimurium (Chapter 3) and through direct binding of CpxR-P to the promoter region of this gene (Figure 17), most likely to a 17bp motif sharing similarity to that presented by Yamamoto and Ishihama (2006) $GTAAA(N)_{4-8}GTAAA$.

The *scsABCD* operon of *Salmonella*, absent from *E. coli*, has also previously been linked to copper tolerance in *S*. Typhimurium (Anwar et al., 2013). Our microarray (Chapter 3) and qRT-PCR analysis (Figure 14, H) confirmed CpxR-mediated regulation of this operon. However as no CpxR binding motif was found during *in silico* analysis of the promoter regions of the two transcriptional units that encode the *scs* genes, the means of this regulation remains enigmatic. Anwar et al. (2013) dismissed ScsA involvement in copper tolerance of *Salmonella*. However, when our Δ*scsA* mutant was subjected to $CuSO_4$ sensitivity assays, growth on solid media containing $CuSO_4$ [4mM] was fatal to Δ*cpxR* and Δ*scsA* strains (Figure 23), however Δ*cpxR* did not exhibit sensitivity in batch culture containing 3 mM $CuSO_4$ (Figure 24, A). The lack of sensitivity exhibited by Δ*cpxR* strains in LB 3 mM $CuSO_4$ liquid culture was unexpected, given that Δ*scsA* grew half as well as SL1344 WT at this $CuSO_4$ concentration. A Δ*scsBCD* strain is sensitive to copper chloride, but Anwar et al. (2013) were unable to complement this copper sensitive phenotype. Expression of *scsA in trans* by the means of an arabinose inducible promoter on the pBAD plasmid saw SL1344 WT, Δ*cpxR* and Δ*scsA* strains reach ODs of no significant difference ($p>0.05$) after 24-hours growth in LB $CuSO_4$ [3mM] (Figure 14, A). Additions of Amp (100 µg) and *L*-arabinose (0.02% w/v) were required to maintain the pBAD*scsA* plasmid and induce *scsA* expression. SL1344 WT and Δ*cpxR* saw a reduction in final OD following *scsA* overexpression, compared to strains lacking the pBAD*scsA* plasmid (Figure 14, B) and overexpression of *scsA*

therefore negatively affected growth of SL1344 WT and Δ*cpxR*. Overexpression of empty pBAD *myc*/His A plasmid did not affect the growth rate or final OD of any of the strains tested (data not shown), therefore the addition of ampicillin, although it is known to from complexes with copper ions (Mukherjee and Ghosh, 1995), or *L*-arabinose do not affect growth. The levels of arabinose present needs to be reassessed to optimise *scsA* expression *in trans* if complementation is to be successful. The antibiotic cassette replacing *scsA* also needs to be removed and these experiments repeated to confirm that no transient effects from *scsA* deletion on *scsBCD* expression is occurring in our Δ*scsA* deletion strain.

4.5.5 Summary

The 18 operons, encoding 27 genes that were studied in more detail during this chapter were only a snapshot of the 144 genes differentially regulated between SL1344 WT and Δ*cpxR* following activation of the Cpx pathway, and a small selection of the 116 genes from this list not previously associated with regulation by Cpx. The additional transcriptomic analysis presented during this chapter confirmed the expression levels witnessed during our microarray analysis for these 18 transcriptional units, providing further evidence to support their inclusion within the Cpx-regulon of *Salmonella*. Our EMSAs added strong evidence to support direct regulation of nearly half of these operons by CpxR, and preliminary investigations into a number of new Cpx-regulated genes of hypothetical or unknown function links the Cpx a new cellular process, polyamine homeostasis. The transcriptomic data and phenotypic screens presented in Chapter 3 and Chapter 4, and the production of several knockout mutants, provide a wealth of data for further investigation of the Cpx-regulon in *S*. Typhimurium.

One ESR that has recently been proposed in *S*. Typhimurium is ZraSR, mentioned briefly during this chapter in relation to SL3010/09 regulation with the Cpx and Bae systems. The ZraSR 2CST system regulates a molecular chaperone of similar structure and function to the CpxAR accessory protein CpxP, called ZraP. The contribution of ZraPSR to the ESR of *Salmonella*

was the focus of investigations presented in the final two results chapters of this thesis.

5 Characterisation of the *S.* Typhimurium ZraPSR ESR

5.1 Introduction

In addition to expanding our knowledge of the Cpx regulon of *S*. Typhimurium, we wanted to broaden our analysis to a newly identified ESR in *Salmonella*, ZraPSR. As a proposed zinc-responsive system, which also contributes towards envelope homeostasis (Leonhartsberger et al., 2001, Appia-Ayme et al., 2012), this poorly characterised operon has the potential to be involved in numerous regulatory networks, given the huge array of processes zinc ions are associated with.

5.1.1 The Zra 2CST system

As outlined during Chapter 1, the ZraSR 2CST system exhibits sequence similarity to NtrBC and was originally associated with regulation of hydrogenase 3 formation in *E. coli* (Stoker et al., 1989). However, Leonhartsberger et al. (2001) revealed ZraR regulation of the *hyc* genes, encoding hydrogenase 3, was a result of non-specific cross-talk. Direct binding of phosphorylated ZraR to the intergenic region between *zraS* and *zraP* however was observed (Leonhartsberger et al., 2001) (Figure 30), and to date these two genes remain the only confirmed ZraR regulon members.

Lead, zinc and tungstate have been shown to activate expression of the ZraSR operon (Appia-Ayme et al., 2011, Leonhartsberger et al., 2001), concurring with the actions of ZraP as a zinc responsive molecular chaperone. Yamamoto et al. (2005) conducted *in vitro* functional characterisation of all 2CST systems in *E. coli.* Their results showed *in vitro* phosphorylation of ZraR by a second HK in addition to ZraS, called UhpB. The UhpB HK belongs to the UhpB-UhpC-UhpA phosphorelay system that controls production of the sugar phosphate transporter UhbT (Weston and Kadner, 1988, Island et al., 1992, Wright and Kadner, 2001). Cross-talk between ZraS and other 2CST systems was also observed, with ZraS phosphorylating two RRs, RssB (also referred to as SprE in *E. coli* and MviA in *S. enterica*) and YfhA *in vitro*, in addition to ZraR. YfhA is a predicted RR in a 2CST system with the HK YfhK with an as yet unknown function (Rudd, 2000, Riley et al., 2006). In *S. enterica*, the RR MviA is an adaptor protein, which in its phosphorylated form directly interacts with RpoS and the ClpXP

protease to facilitate RpoS degradation (Moreno et al., 2000, Schweder et al., 1996, Klauck et al., 2001). Degradation of RpoS by ClpXP is rapid (during exponential phase RpoS has a half-life of 3 minutes; Lange and Hengge-Aronis (1994), Schweder et al. (1996)) and is an important component of the complex network that regulates RpoS expression and activity. As the master regulator for the general stress response, accumulation of RpoS occurs in response to unfavourable growth conditions through suppression of RpoS degradation by ClpXP. These conditions include entry into stationary phase and increasing cell density, nutrient limitation, fluctuations in pH and osmolarity and DNA damage (Battesti et al., 2011, Landini et al., 2014).

Although these results were observed in a synthetic environment they provide evidence to suggest ZraSR may respond to multiple signals and regulate genes involved in a wider range of cellular processes than originally thought i.e. RpoS regulation, growth phase dependence and as a contributor to the global stress response; glucose-6-phosphate uptake and metabolism of sugars. With experimental evidence confirming ZraSR activation by so few environmental cues, the fact this 2CST system appears to only regulate itself and *zraP* is surprising, and the physiological relevance of the Zra system and the genes regulated by it warrant further investigation.

5.1.2 ZraR is a σ^{54} bacterial enhancer binding protein (bEBP)

In addition to its role as a RR, ZraR functions as a bacterial enhancer binding protein (bEBP), an activator of RpoN (σ^{N}/σ^{54}) dependent transcription. Unlike the σ^{70} family of sigma factors, transcription initiated by σ^{54} is completely dependent upon bEBPs. This means σ^{54} transcription is tightly regulated and occurs in a specific and rapid manner.

bEBPs contain three domains: a loosely conserved N-terminal regulatory domain, a highly conserved central AAA+ domain and a C-terminal DNA binding domain. Five classical groups (I-V) of bEBPs exist, grouped according to their domain organisation. As ZraR has an N-terminal response

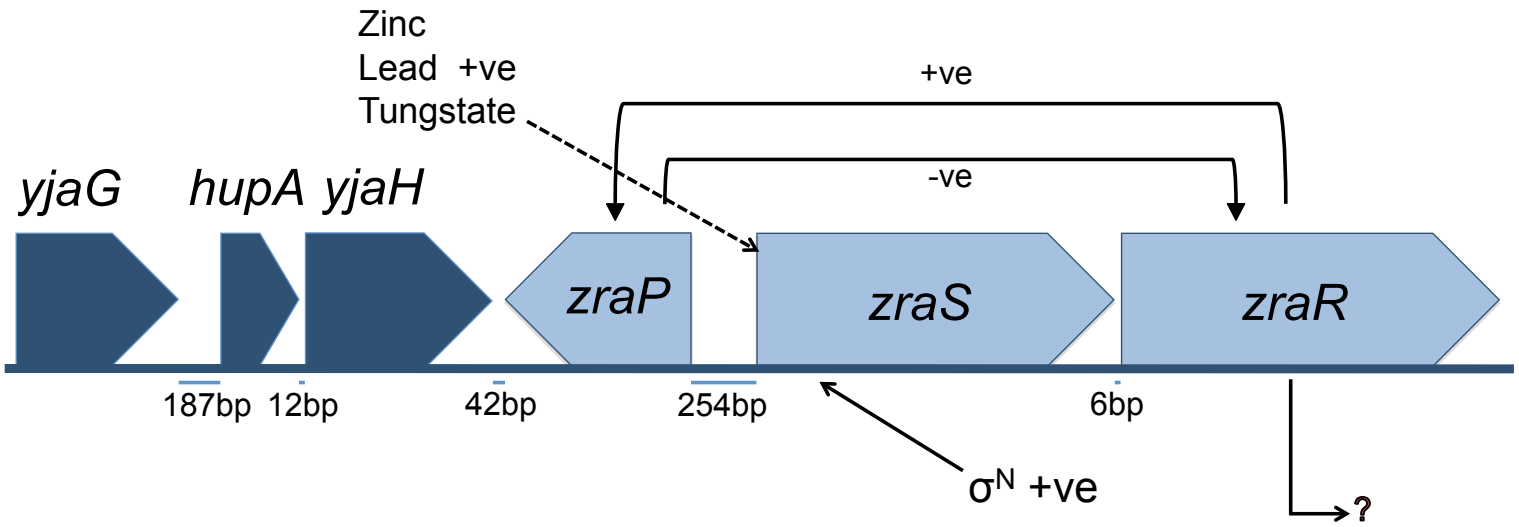

Gene Summary
hupA = transcriptional regulator
yjaH = inner membrane protein
zraP = zinc responsive periplasmic chaperone
zraS = sensor kinase
zraR = response regulator and enhancer binding protein

Figure 30: Diagram of *zraPSR* operon. The 2CST system ZraSR is induced by zinc, lead and tungstate in *E. coli* and are RpoN (σ^N/σ^{54}) regulated. ZraP and ZraR regulate each other in a feedback loop. The ZraR regulon remains unknown. See in text for references.

regulatory domain, it belongs to bEBP Group I with fellow RRs NtrC, NtrC1, NtrC4, DctA and FlgR (Bush and Dixon, 2012). For σ^{54} transcription initiation to take place, bEBPs bind ~80bp to 250 bp upstream of their target promoter at a region designated the enhancer site or upstream activator sequence (UAS). Of the three bEBP structural domains, it is the central AAA+ domain that is essential for σ^{54} dependant transcription, coupling the energy generated from ATP hydrolysis to the isomeration of the RNA polymerase-σ^{54} closed complex (Schumacher et al., 2004, Bush and Dixon, 2012). Activity of this AAA+ domain must be tightly regulated in response to an inducing cue to maintain bEBP specificity. Negative regulation of the catalytic domain by the regulatory domain is believed to be the dominant mechanism of control (Shingler, 1996). Regulation of the ZraR AAA+ domain remains unknown. However, due to structural similarities of ZraR and NtrC1/DctD it is proposed to be under negative regulation (Lee et al., 2003, Shingler, 1996).

Characterisation of the σ^{54} regulon by Samuels et al. (2013) confirmed σ^{54} mediated regulation of *zraP* and *zraSR* (Figure 30). This, coupled with the role ZraR plays as a bEBP, will be taken into consideration during analysis of the Zra regulated transcriptome, described within the results section of this chapter.

5.1.3 Zinc: How bacteria respond to fluctuations in zinc availability and maintenance of zinc homeostasis

Zinc ions are ubiquitous in the environment and imperative in biological chemistry, with zinc binding proteins composing 8.8% of the eukaryotic proteome and 5% and 6% of the bacteria and archaea proteomes respectively (Andreini et al., 2006). Zinc in its natural form, Zn(II) (Zn^{2+}), has no redox activity under physiological conditions (Nies, 1999). However it can function in a signalling, catalytic and structural capacity, facilitate the correct folding of protein domains and provide stability during protein-protein and protein-macromolecule interactions (Berg and Shi, 1996). Intracellular zinc, calcium and iron are all present at the same levels in *E. coli* (approximately 10^{-4} M) despite zinc being referred to as a trace element (Outten and O'Halloran, 2001). As is the case for all metals, intracellular Zn^{2+} levels are

tightly controlled as accumulation is toxic; zinc can interact with thiols and block essential reactions in the cell, and deficiency negatively impacts growth (Graham et al., 2009, Hantke, 2005, Porcheron et al., 2013).

In addition to the cytoplasm, Gram-negative bacteria need zinc within the periplasm to function correctly, with several periplasmic enzymes requiring zinc as a cofactor (e.g. SodC and FtsK amongst others) (Hantke, 2005). In *Neisseria meningitidis*, ZnuD (zinc uptake component D) has been identified as a TonB-dependent OM receptor involved in zinc and haem uptake across the OM (Stork et al., 2010, Hubert et al., 2013). ZnuD is produced under zinc limitation, binds free zinc and is regulated by either Zur or Fur, members of the Fur family of global metal responsive transcription factors (Stork et al., 2010). Despite the presence of ZnuD in all 223 strains of *N. meningitidis* and ZnuD homologues in other bacteria, many of which are respiratory pathogens (e.g. *Actinobacillus pleuropneumoniae*, *Bordetella pertussis*, *Haemophilus parasuis*) (Stork et al., 2010, Hubert et al., 2013), no ZnuD homologues have been found to date in any γ-proteobacteria. Zinc is unable to passively diffuse across the OM of Gram-negative bacteria and one theory suggests Zn^{2+} uptake occurs via diffusion through non-selective porins (Hood and Skaar, 2012, Minnock et al., 2000). The discovery of OM transporters in non γ-proteobacteria, such as ZnuD, puts this method of zinc uptake across the OM of Enterobacteria into question and the specific means of zinc uptake in the γ-proteobacteria remains unknown (Figure 30).

Several protein families are involved in Zn^{2+} trafficking across the IM of Gram-negatives, including ABC transporters, broad-spectrum metal ion import systems and low-affinity ZIP-type transporters [for review see (Blencowe and Morby, 2003, Osman and Cavet, 2011, Porcheron et al., 2013, Hantke, 2005)]. Zn^{2+} uptake predominantly occurs via ZnuACB, a Zn^{2+} inducible ATP dependent ABC transporter made up of the periplasmic, zinc-binding protein ZnuA, the IM spanning ZnuB and the ATPase subunit ZnuC (Figure 31) (Patzer and Hantke, 2000). Homologues of this system have been identified in numerous species, including *Listeria monocytogenes*, *Neisseria gonorrhoeae, Haemophilus* sp.*, Streptococcus* sp.*,* and

Treponema pallidum (Blencowe and Morby, 2003, Dalet et al., 1999, Chen and Morse, 2001, Lu et al., 1997, Lu et al., 1998, Lewis et al., 1999, Dintilhac et al., 1997, Janulczyk et al., 1999, Lee et al., 1999). During periods of Zn^{2+} excess, Zur represses *znuACB* transcription. Zn^{2+}-bound Zur dimers bind to the *znu* operon regulatory sequence, blocking RNA polymerase and inhibiting zinc uptake (Patzer and Hantke, 2000, Blencowe and Morby, 2003). Zur can sense sub-femtomolar concentrations of cytosolic zinc, only allowing activation of ZnuACB at exceptionally low Zn^{2+} levels. This suggests zinc starvation occurs at very low concentrations and Outten and O'Halloran (2001) found that the minimal zinc content required for *E. coli* growth is 2 x 10^5 atoms/cell, approximately 0.2 mM. When Zn^{2+} starvation occurs, ZnuA passes Zn^{2+} into the cytosol through a pore formed by ZnuB dimers in the IM, fuelled by the ATPase subunit ZnuC (Figure 31) (Patzer and Hantke, 1998). Both Gram-negative and Gram-positive bacteria possess a ZnuACB accessory protein, ZinT (formally known as YodA) (Panina et al., 2003). ZinT forms ZinT-ZnuA complexes in the presence of zinc and acts as a Zn^{2+} buffering protein to deliver Zn^{2+} to ZnuA, further aiding Zn^{2+} uptake (Petrarca et al., 2010, Cerasi et al., 2013, Ilari et al., 2014).

During periods of moderate zinc availability ZupT, is the primary system of zinc uptake (Figure 31) (Porcheron et al., 2013). This low-affinity transporter belongs to the ZIP family of iron and zinc transporters and was the first ZIP protein characterised in bacteria (Grass et al., 2002). Despite having a broad substrate spectrum in addition to zinc (transporting iron, cobalt, copper, cadmium and possibly manganese), ZupT preferentially binds zinc over other divalent metals and depends upon the proton motive force to energise Zn^{2+} trafficking (Grass et al., 2005a, Grass et al., 2002, Karlinsey et al., 2010, Taudte and Grass, 2010). Unlike ZnuACB, ZupT does not appear to be metal regulated in *E. coli* and is constitutively expressed at low levels (Grass et al., 2005a). However, in *Cupriavidus metallidurans, zupT* is up-regulated during zinc starvation and directly repressed by FurC during periods of zinc sufficiency (Schmidt et al., 2014).

Zinc export is achieved through ZntA, a P_{1B}-type ATPase, and two cation diffusion facilitators (CDF), ZitB and YiiP (Figure 31). ZitB and YiiP are Zn^{+2}/H^{+} antiporters (although YiiP also transports Cd^{2+}) and both maintain zinc homeostasis during periods of normal growth (Wang et al., 2012). ZntA however is critical for *E. coli* survival at times of high zinc concentrations (Wang et al., 2012, Rensing et al., 1997), efficiently pumping Zn^{2+} into the periplasmic space. As mentioned earlier the means of Zn^{2+} transportation across the OM in γ-proteobacteria (during acquisition or export) remains elusive. As a newly characterised zinc inducible 2CST system, ZraSRP may contribute towards zinc homeostasis and maintenance of envelope homeostasis during periods of zinc stress. Transcriptomic analyses and structure function analysis of ZraP, the periplasmic accessory protein to the ZraSR system, may answer these fundamental problems regarding periplasmic zinc regulation and trafficking, and are areas of investigation throughout this chapter and Chapter 5.

5.1.4 Importance of zinc in host-pathogen interactions and *Salmonella* virulence

Acquisition of zinc from the host environment is a critical hurdle pathogens must overcome when establishing an infection. Vertebrate hosts can manipulate the availability of metal ions to invading pathogens in a process termed 'nutritional immunity' (Weinberg, 2009). In infected tissues, the neutrophil antimicrobial protein calprotectin (a heterodimeric S100 protein comprising 40-50% of the neutrophil cytosol) is secreted at high levels and sequesters manganese and zinc to virtually undetectable concentrations (Corbin et al., 2008, Teigelkamp et al., 1991, Steinbakk et al., 1990). Acute cecal inflammation and neutrophil influx are key markers of *S*. Typhimurium infection and two calprotectin subunits (*S100a8* and *S100a9*) are highly up-regulated during *S*. Typhimurium colonisation (Godinez et al., 2008, Raffatellu et al., 2008). Liu et al. (2012) showed a 4-fold reduction of faecal zinc concentrations from *S*. Typhimurium infected mice, suggesting that the high-affinity uptake system ZnuABC could provide an advantage to *Salmonella* within the gut environment. Deletion of *znuA* does not negatively

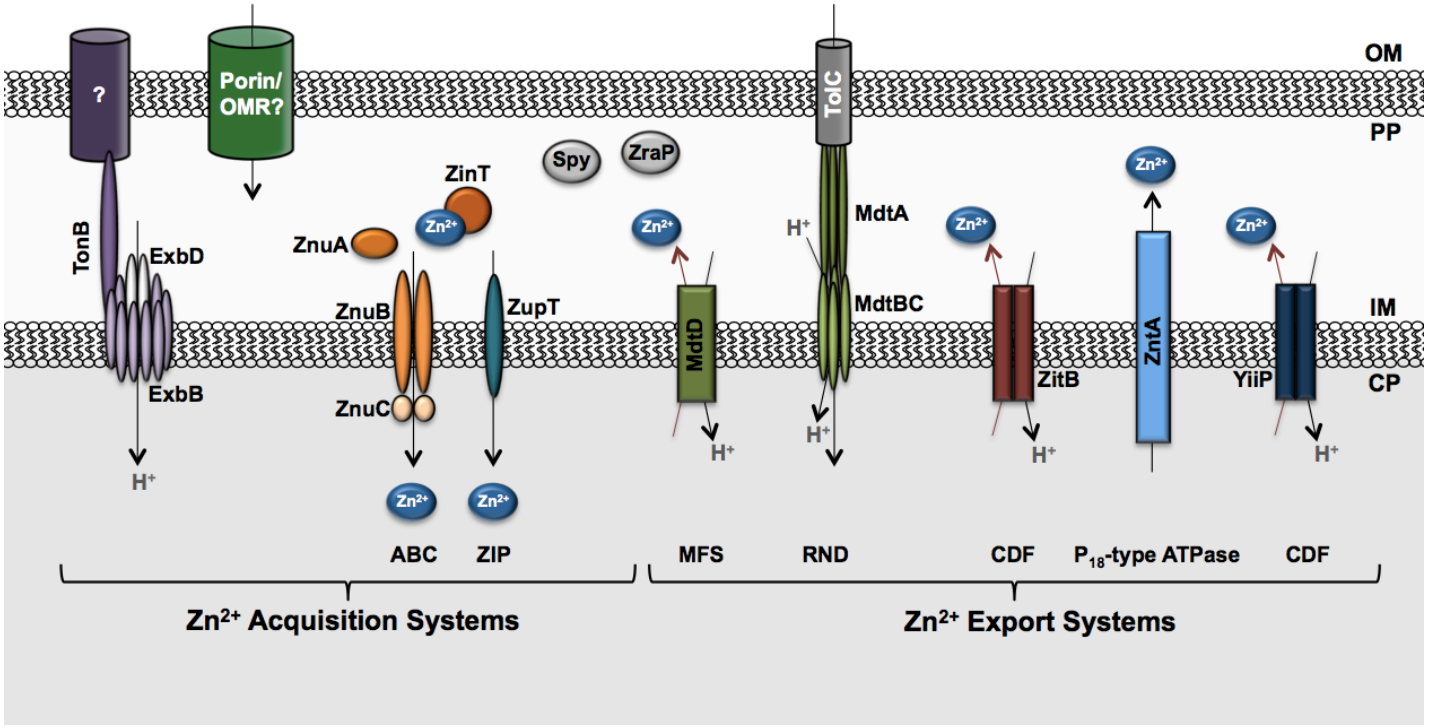

Figure 31: Zinc transporters in Enterobacteria. Cartoon representation of zinc uptake and export systems. As no ZnuD OMP homologue is present in Enterobacteria, the uptake and removal of zinc across the OM remains unknown. Adapted from Porcheron et al., (2013).

affect virulence of *S*. Typhimurium, but colonisation rates of a Δ*znuA* strain is 200-fold lower than those observed for an avirulent *S*. Typhimurium strain lacking SPI-1 and SPI-2 activity through deletion of *invA* and *spiB* (Liu et al., 2012). This was a result of reduced Δ*znuA* fitness compared to competing microbiota within the gut. ZnuABC therefore only offers a growth advantage to the bacteria during periods of inflammation, i.e. at times of high calprotectin presence and zinc sequestration, and is critical for *S*. Typhimurium to resist the antimicrobial actions of calprotectin, promote competition with commensal bacteria and promote *S*. Typhimurium colonisation in the inflamed gut (Liu et al., 2012). Macrophages can also limit intracellular metal ion availability through induction of the zinc transporters ZIP8 (SLC39A family) and ZnTs (SLC30A family), and NRAMP1, which pumps iron and zinc out of the phagosome following phagocytosis (Porcheron et al., 2013, Desrosiers et al., 2010, Jabado et al., 2000, Forbes and Gros, 2003). The presence of LPS is a key inducer of SLC30A transporter up-regulation (Kitamura et al., 2006), but intracellular zinc depletion also occurs in response to fungal infections (Winters et al., 2010), suggesting this is a universal defence mechanism employed by macrophages against an array of microbial pathogens. This depletion of zinc must be carefully balanced to ensure the necessary metal ions remain available to the host cell for crucial enzymatic redox activities, such as iNOS, NADPH oxidase and myeloperoxidase (Cellier et al., 2007). Very few functional studies have been published to date on macrophage mediated metal regulation in response to infection and there are conflicting reports that macrophages actively increase zinc within the phagosome as an antimicrobial response (Stafford et al., 2013). This intracellular accumulation of zinc occurs in human macrophages in response to *Mycobacterium tuberculosis* infection and TNFα and IFNγ promote zinc accumulation in the phagosome of *Mycobacterium avium* infected murine macrophages (Wagner et al., 2005).

The specific type of zinc response elicited by macrophages may be dependent on multiple factors, including time, infection stage or the type of pathogen. The increase and reduction of intracellular zinc by immune cells

are designed to inhibit microbial growth and proliferation. The underlying mechanism behind which response (metal limitation or excess) the host cell selects does require further investigation, but regardless of the zinc status inflicted upon pathogens by the host immune system, microbes must maintain their zinc levels at an optimum concentration to survive. As well as zinc acquisition systems during times of limitation, pathogens have evolved a range of metal stress responses to cope with excessive metal ion exposure (Nies, 1999, Osman and Cavet, 2011), and how these systems contribute to bacterial virulence are outlined below.

Compared to other metals, there are a relatively low number of zinc importers in most bacterial species (Cerasi et al., 2013) and many established members of the Enterobacteria zinc regulatory system have a critical role in virulence. These important factors make the regulation of zinc homeostasis an exciting avenue through which to uncover potentially novel drug targets.

Ammendola et al. (2007) state that *S.* Typhimurium and *S.* Enteritidis strains lacking *znuA* are attenuated in BALB/c mice. This study showed that a complete ZnuABC transport system was required for zinc uptake during macrophage colonisation and a *znuC* mutant of *S*. Typhimurium also exhibits reduced intracellular survival compared to the WT strain (Ammendola et al., 2007, Campoy et al., 2002). The reduced virulence of Δ*znuA* was not observed by Liu et al. (2012) in WT C57BL/6 or S100A9$^{-/-}$ mice as described earlier, as Δ*znuA* strains produced similar levels of inflammation and expression of calprotectin and cytokines to the isogenic parent strain. However, both studies agreed that a functioning ZnuABC system is required for intracellular survival of *S*. Typhimurium, with Liu et al. (2012) contributing the additional observations that ZnuABC offers a growth advantage to *Salmonella* when competing with the host microbiota.

The zinc uptake system ZupT is required for *S*. Typhimurium virulence in NRAMP$^{+/+}$ mice (Karlinsey et al., 2010), i.e. mice where NRAMP1 is present to pump zinc and iron out of the phagosome and a metal ion limited

intracellular environment is produced. However, as ZupT transports a range of divalent metal ions it is unclear if this phenotype is due to reduced acquisition of zinc by the bacteria or as a result of reduction in uptake of other metals. Cerasi et al. (2014) showed the importance of ZupT in promoting *S*. Typhimurium colonisation of host tissues and zinc homeostasis *in vivo*. Their finding that Δ*znuABC*Δ*zupT* mutants are less able to colonise the spleen of NRAMP$^{+/+}$ mice than Δ*znuABC* strains, suggests ZupT is active and involved in zinc acquisition during infection (Cerasi et al., 2014). ZupT and ZnuABC component mutants also have reduced or attenuated virulence in other Enterobacteria, including *E. coli* (UPEC), *Yersinia* sp., and *Proteus mirabilis* (Sabri et al., 2009, Patzer and Hantke, 1998, Campoy et al., 2002, Desrosiers et al., 2010, Gabbianelli et al., 2011, Gunasekera et al., 2009, Nielubowicz et al., 2010).

In addition to these established members of the Enterobacteria zinc regulatory systems, the zinc responsive RR at the focus of our investigations, ZraR, may also be associated with *S*. Typhimurium virulence as up-regulation of ZraR was witnessed during infection of pigs (Huang et al., 2007b). It remains unknown if this increase in expression results from exposure of *S*. Typhimurium to higher zinc concentrations in the pig GIT due to dietary zinc supplementation, or if *zraR* is up-regulated during infection, as observed in *E. coli* during within the human gut (John et al., 2005). The contribution of the ZraPSR system to *S*. Typhimurium virulence remains enigmatic and detailed studies involving a range of infection models is needed to answer these questions.

5.1.5 Contribution of the Bae ESR system to zinc tolerance

As outlined in 1.11, the BaeSR classical two-component system comprises the response regulator BaeR and the histidine kinase BaeS and was the third ESR to be identified (Raffa and Raivio, 2002). Although limited characterisation of the Bae-regulon has been conducted to date, all members are involved in multidrug efflux (*acrD*, *mdtABCD*) and protein folding (*spy*) (Leblanc et al., 2011) (Figure 32). Appia-Ayme et al. (2011) showed a regulatory link, either directly or indirectly, between the ZraSR and

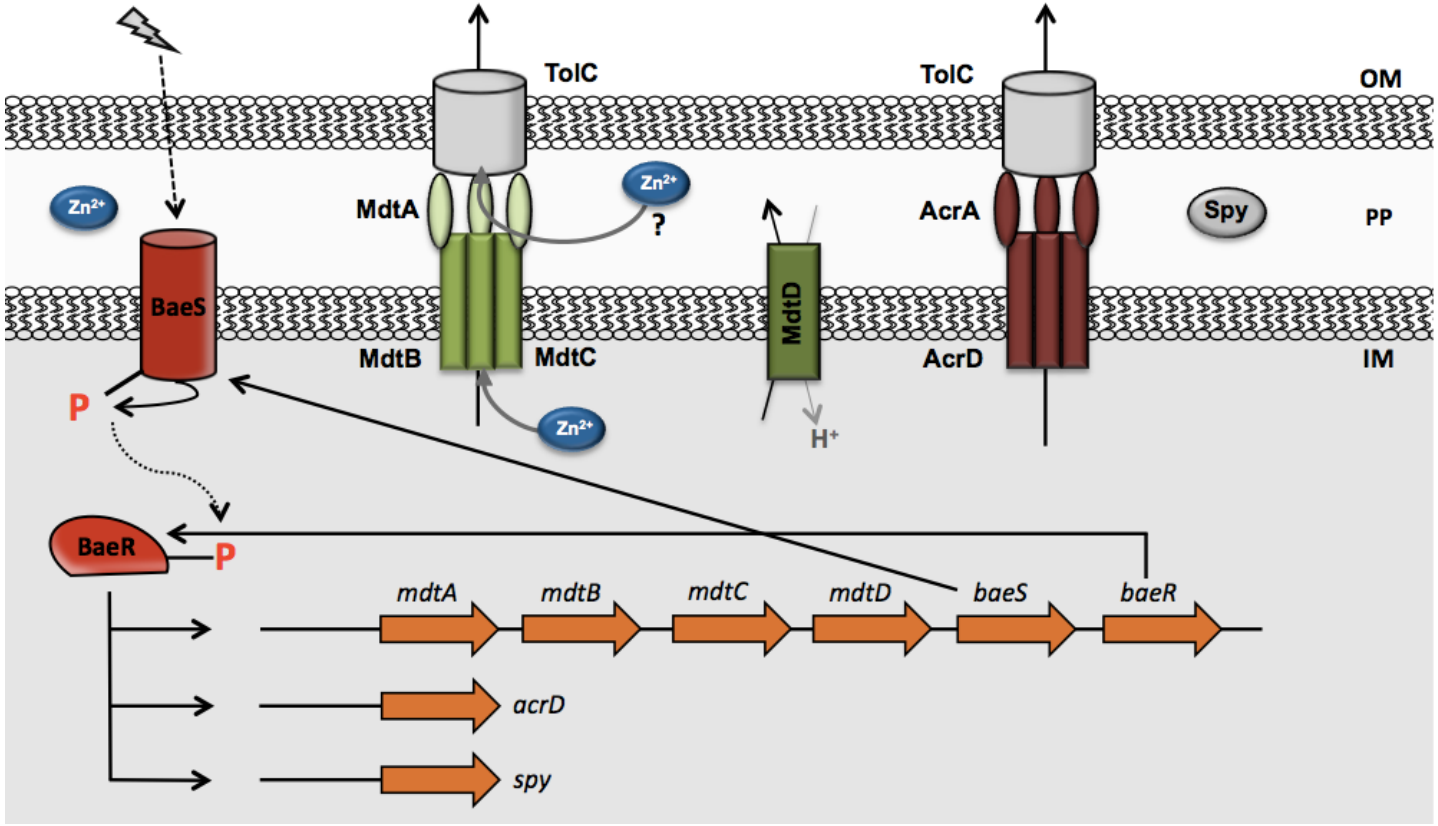

Figure 32: **Representation of Bae regulon and members involvement in zinc tolerance**. Adapted from Nishino et al. (2007) and Runkel et al. (2013).

Bae systems, with *zraSR* and *zraP* up-regulated in a *baeR* mutant background upon exposure to tungstate. This possible overlap between these two, 2CST systems is intriguing and requires further investigation, especially because Bae has also been associated with zinc tolerance in *S.* Typhimurium and *E. coli* strains. In *S*. Typhimurium, Nishino et al. (2007) demonstrated severe growth defects under high zinc conditions for Bae mutants and a similar phenotype was observed in MG1655 (Wang and Fierke, 2013). However these results were inconsistent to those observed for Bae mutants of *S*. Typhimurium SL1344 during our investigations (Appia-Ayme *unpublished observations*). These discrepancies made us question the reproducibility of these phenotypes associated with the Bae system in the serovar Typhimurium, and the establishment of Bae as a zinc responsive system in *E. coli* or *Salmonella*. The contribution of Bae as well as ZraSR to zinc tolerance in *S*. Typhimurium will be investigated during this chapter

5.2 Aims

The aim of this chapter was 1) to define the function of the ZraSR two-component system in *S*. Typhimurium through a combination of transcriptomic and phenotypic analysis, and 2) to assess the contribution of ZraPSR and BaeSR ESR system to zinc homeostasis and stress tolerance in *Salmonella* species.

5.3 Experimental Design

5.3.1 Growth assays

For measurement of aerobic growth, LB broth or MOPS minimal media were used for batch cultures (2.3.4). For analysis of anaerobic growth, strains were cultured in MGN^+ media (2.3.5).

5.3.2 ZraR overexpression and microarray analysis

SL1344pBAD and SL1344p*zraR* strains were grown in aerobic batch culture (2.3.4) until an OD_{600} of 1. *L*-arabinose (0.02% w/v) was added and cultures incubated for four hours to allow subsequent induction of *zraR* (2.3.4). Cells

were collected (2.4.2), total RNA extracted (2.4.20), cDNA synthesised (2.4.21.1) and subjected to microarray analysis (2.4.22).

5.3.3 Real-time quantitative PCR

All qRT-PCR experiments were performed as described in 2.4.21. The calculated threshold cycle (Ct) for each gene was normalised to Ct of the control genes *ampD* or *rpoD*.

5.3.4 LT-CSS and CSIXR assays

SL1344 WT and Δ*rpoE*, Δ*baeR*, Δ*cpxAR*, Δ*cpxR*, Δ*baeR*Δ*cpxAR*, Δ*zraSR* and Δ*baeR*Δ*cpxAR*Δ*zraSR* were subjected to LT-CSS and CSIXR assays as performed by Kenyon et al. (2002) (2.4.13 and 2.4.14).

5.4 Results

5.4.1 Zinc sensitivity of SL1344 following deletion of ZraSR and the Cpx family of molecular chaperones

As the *zraPSR* operon is induced upon exposure to high zinc concentrations in *E. coli*, and is believed to contribute to zinc tolerance (Leonhartsberger et al., 2001), we first assessed SL1344 cell growth in the presence of increasing zinc concentrations to define the MIC for our WT strain. Zinc toxicity in *E. coli* has been investigated previously by recording bacterial growth rate in rich media (LB only and LB zinc supplemented) and defined (MOPS) media (Wang and Fierke, 2013, Nishino et al., 2007). MOPS medium was specifically designed for Enterobacteria and allows growth of both *E. coli* spp. and *Salmonella* spp. at levels comparable to traditional media (i.e. LB broth) (Neidhardt et al., 1974). Phosphate can form strong complexes with heavy metals (Belkin and Gu, 2010), therefore MOPS is preferred to rich media as each macronutrient (i.e. phosphate, sulphate, nitrogen) is present at sufficiently low levels to prevent interference and allow reproducible nutritional studies (Neidhardt et al., 1974). Zinc chloride ($ZnCl_2$) and zinc sulphate ($ZnSO_4$) were both used to ensure any differences in growth associated with zinc bioavailability was taken into account.

The addition of 0.5 mM $ZnSO_4$ or $ZnCl_2$ to LB cultures had no impact on the growth rate of SL1344 WT (Figure 33). WT cells grew without compromise in $ZnCl_2$ up to 1 mM, presented a reduced growth rate and final cell density at 1.5 mM $ZnCl_2$ and failed to grow at $ZnCl_2$ concentrations >2 mM (Figure 33, A). WT cells exposed to $ZnSO_4$ presented a reduced growth rate and final cell density at all concentrations >0.5 mM, with no growth was observed at $ZnSO_4$ concentrations ≥1.5 mM (Figure 33, B). The number of moles of Zn^{2+} ions are equal within both solutions, meaning the lower MIC observed for $ZnSO_4$ compared to $ZnCl_2$ must be due to the formation of SO_4^- ions within the culture e.g. when dissolved $ZnSO_4$ forms Zn^{2+} and SO_4^- ions and $ZnCl_2$ forms Zn^{2+} and Cl^- ions. $ZnSO_4$ and $ZnCl_2$ dissociate in a 1:1 ratio to give 1 mole of Zn^{2+} and 1 mole of SO_4^- and 1 mole of Zn^{2+} and 1 mole of Cl^- respectively. The type of anion present is the only difference between our two growth conditions.

We next assessed the impact of deleting *zraSR* on *Salmonella* growth when exposed to high zinc. As the only proposed function of this 2CST system is in regulation of zinc tolerance, one expected to observe zinc dependent growth defects for this mutant strain. SL1344 WT and Δ*zraSR* were cultured in MOPS defined medium, with and without 1 mM $ZnCl_2$. This zinc concentration was chosen because it was the highest $ZnCl_2$ concentration tested which did not impede our WT strain in rich media (LB) (Figure 33). Growth inhibition is likely to be accentuated in MOPS due to the reduced levels of phosphate present and the associated increase in Zn^{2+} bioavailability. SL1344 WT and Δ*zraSR* grew in non-supplemented MOPS medium to a comparable final OD (Figure 33, C). The addition of 1 mM $ZnCl_2$ to MOPS cultures significantly reduced the growth rate and final cell densities of both SL1344 WT and Δ*zraSR*. But, as was the case when cultured in LB broth, no significant differences between the two strains were observed (Figure 33, C).

The only known member of the Zra regulon, other than *zraSR* itself, is the zinc dependent molecular chaperone ZraP (Appia-Ayme et al., 2012). ZraP and the abundant periplasmic chaperone Spy are also associated with zinc

tolerance (Wang and Fierke, 2013, Appia-Ayme et al., 2012), presumably through their role as molecular chaperones in responding to the increase in protein damage associated with metal stress. Growth assays of SL1344 WT, Δ*zraSR*, Δ*zraP,* Δ*spy* and a Δ*zraP*Δ*spy*Δ*cpxP* triple mutant, with all three CpxP chaperone family members absent, were performed as described by Wang and Fierke (2013) and Nishino et al. (2007). These methodologies have previously been adopted to characterise involvement of the ESR BaeSR in zinc tolerance (Wang and Fierke, 2013, Nishino et al., 2007). SL1344 WT and Δ*zraSR* presented no sensitivity to $ZnSO_4$ in LB at 600 μM (Figure 34, A) or in MOPS at 300 μM (Figure 34, B). An *E. coli* Δ*spy* strain is highly sensitive to $ZnSO_4$ in MOPS (Wang and Fierke, 2013). However, an SL1344 Δ*spy* strain, and strains lacking *zraP* or all three members of the Cpx family of chaperones, exhibited no growth defects compared to SL1344 WT in MOPS or LB media during both conditions tested (Figure 33). We conclude that deletion of *zraSR* or the molecular chaperone it regulates, *zraP*, does not appear to increase sensitivity of *S*. Typhimurium to zinc, during growth in aerated batch culture. Contrary to data collected in *E. coli* (Wang and Fierke, 2013), deletion of *spy*, the important molecular chaperone under regulation of both the Cpx and Bae ESRs, also has no negative impact on SL1344 zinc tolerance.

It is possible that any zinc stress response systems, influx/efflux pumps and transporters that may be under ZraSR control, have multiple regulators. Therefore deletion of this 2CST system alone may not negatively affect cell viability under the conditions presented here due to functional redundancy. Given our slightly unexpected results we wished to investigate which zinc stress responses and transport systems, if any, are under ZraSR control through analysis of the SL1344 transcriptome. Firstly, we wished to confirm specific conditions of ZraSR induction and how this system senses high periplasmic Zn^{2+}, as proposed by Leonhartsberger et al. (2001).

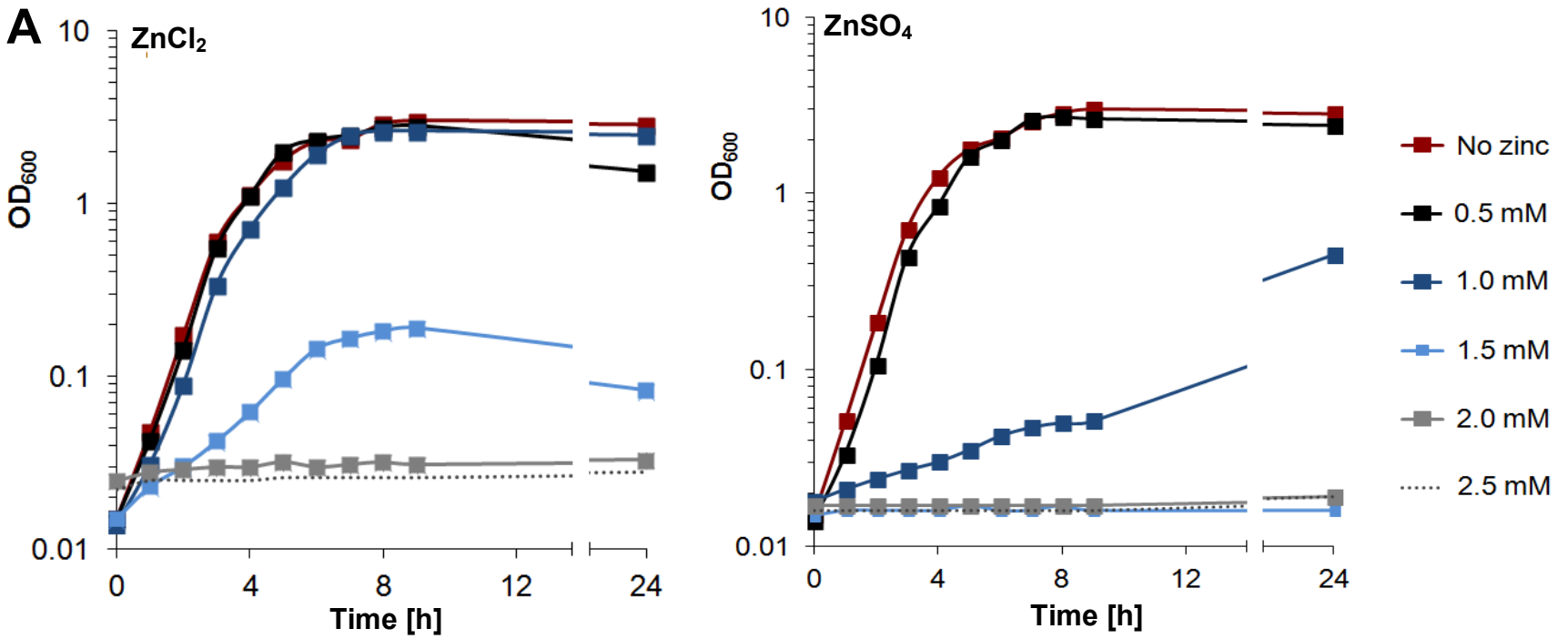

$ZnCl_2$ [mM]	0	0.5	1.0	1.5	2.0	2.5
SL1344 μ (hr^{-1})	1.87	2.04	2.08	0.72	0.03	0

$ZnSO_4$ [mM]	0	0.5	1.0	1.5	2.0	2.5
SL1344 μ (hr^{-1})	1.90	2.07	0.22	0	0	0

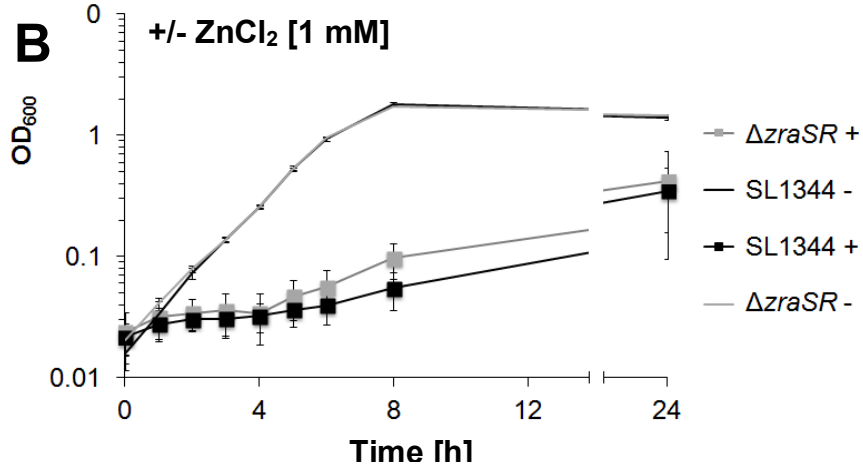

Strain and condition	SL1344-	Δ*zraSR*-	SL1344+	Δ*zraSR*+
SL1344 μ (hr^{-1})	1.26	1.19	0.06	0.08

Figure 33: Impacts of high $ZnCl_2$ and $ZnSO_4$ concentrations on the growth rate (μ) of SL1344 (A) and the effect of *zraSR* deletion on zinc tolerance (B). SL1344 WT was cultured in rich (LB) media supplemented with $ZnCl_2$ or $ZnSO_4$ at six concentrations (0 - 2.5 mM) (A). SL1344 WT and Δ*zraSR* strains were cultured in MOPS defined media supplemented with 1 mM $ZnCl_2$ (B). Deletion of the ZraSR 2CST system has no negative affect on *S.* Typhimurium tolerance to elevated zinc, when compared to SL1344 WT (B). μ was calculated during exponential growth using Equation 1 and presented for each strain and condition under the corresponding graph. All cultures were grown at 37°C, 200 rpm and the OD_{600} recorded at regular intervals over 24 hours. A, *n=1*. B *n=3*, Error bars = SD.

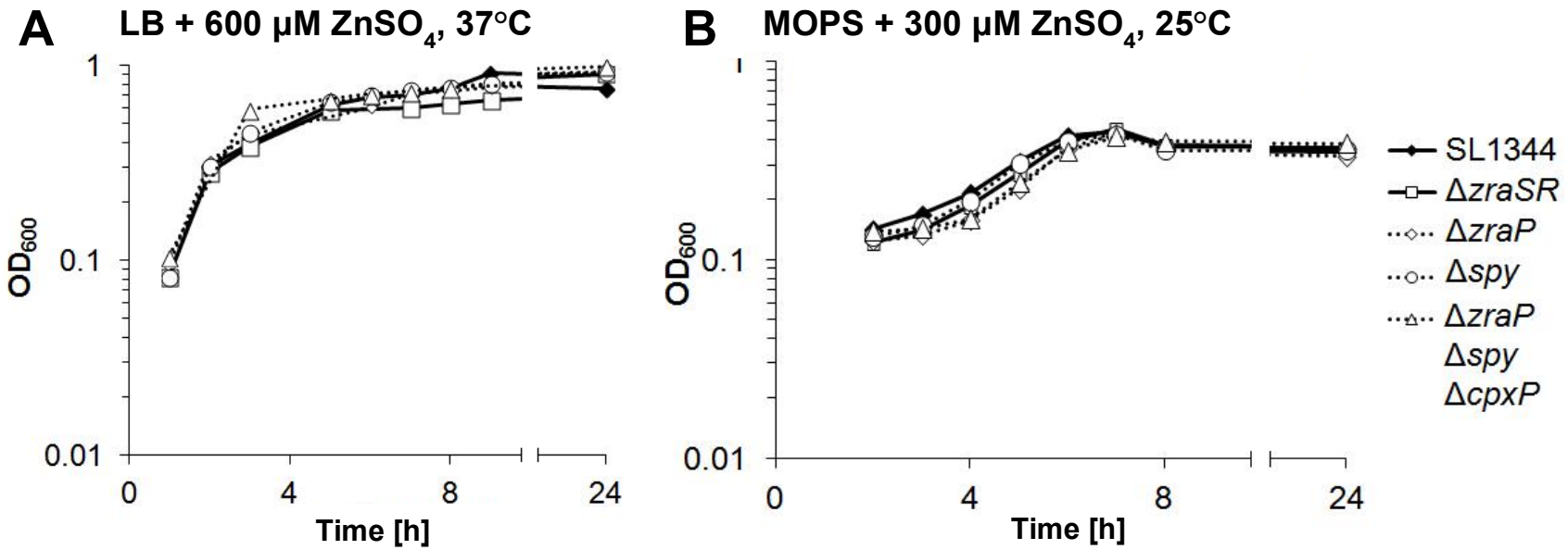

Figure 34: **Growth of SL1344 WT and strains lacking *zraSR*, *zraP* and the Cpx family of molecular chaperones are unaffected by exposure to $ZnSO_4$.** SL1344 WT, Δ*zraSR*, Δ*zraP*, Δ*spy*, and Δ*zraP*Δ*spy*Δ*cpxP* strains were cultured in rich (LB) media supplemented with 600 µM $ZnSO_4$ (A), and defined (MOPS) media supplemented with 300 µM $ZnSO_4$, at 37°C, 200rpm. The OD_{600} was recorded at regular intervals over 24 hours. Growth rates (µ) were calculated during exponential growth using Equation 1. *n=3*, Error bars = SD.

5.4.2 Transcription of *zraR* increases in response to elevated environmental zinc

When *E. coli* MC4100 cells are cultured in rich media supplemented with 1 mM $ZnCl_2$, cellular levels of ZraR are greatly increased (Leonhartsberger et al., 2001). We wished to confirm up-regulation of ZraR in response to 1 mM $ZnCl_2$ in our SL1344 background, especially as *zraSR* null strains grow as WT when exposed to elevated zinc (Figure 33; Figure 34). We used qRT-PCR to analyse relative expression levels of *zraR* when SL1344 cells were cultured in MOPS medium containing increasing $ZnCl_2$ concentrations (0-1 mM) (Figure 35) The decision to use MOPS instead of LB was taken to ensure that all zinc concentrations present were accurate, and no discrepancies in Zn^{2+} availability occurred due to media composition.

Expression of *zraR* increased significantly ($p<0.05$, $p<0.01$, Student's *t* test) when SL1344 was exposed to all four $ZnCl_2$ concentrations tested (Figure 35). Surprisingly, exposure to 250 µM, 500 µM and 1 mM $ZnCl_2$ produced similar results, an ~2-fold increase in *zraR* expression compared to growth in MOPS minus $ZnCl_2$ supplementation (Figure 35). The addition of 750 µM $ZnCl_2$ produced the greatest increase in *zraR* expression levels, an ~2.5-fold increase compared to all other $ZnCl_2$ concentrations, and an ~5-fold increase compared to *zraR* expression in MOPS only cultures (Figure 35). As a zinc sensing system, one would have expected *zraR* levels to increase proportionally with an increase in environmental zinc, or reach a desired threshold that was maintained in response to zinc exposure regardless of concentration. These results imply *zraR* expression increases following exposure to zinc. However this increase does not appear to increase proportionally with concentration. As growth of SL1344 is not negatively affected by 1 mM $ZnCl_2$ in LB (Figure 33, A), we cannot attribute this reduction in ZraR expression at 1 mM $ZnCl_2$ to increased cell death. It is possible that an optimal expression level for ZraR has been reached, after which ZraR is no longer required, or if another zinc responsive system or ESR are also activated at 1 mM $ZnCl_2$ to work in conjunction with ZraR, and therefore expression of this specific 2CST system is reduced when compared to growth conditions with slightly lower $ZnCl_2$ present.

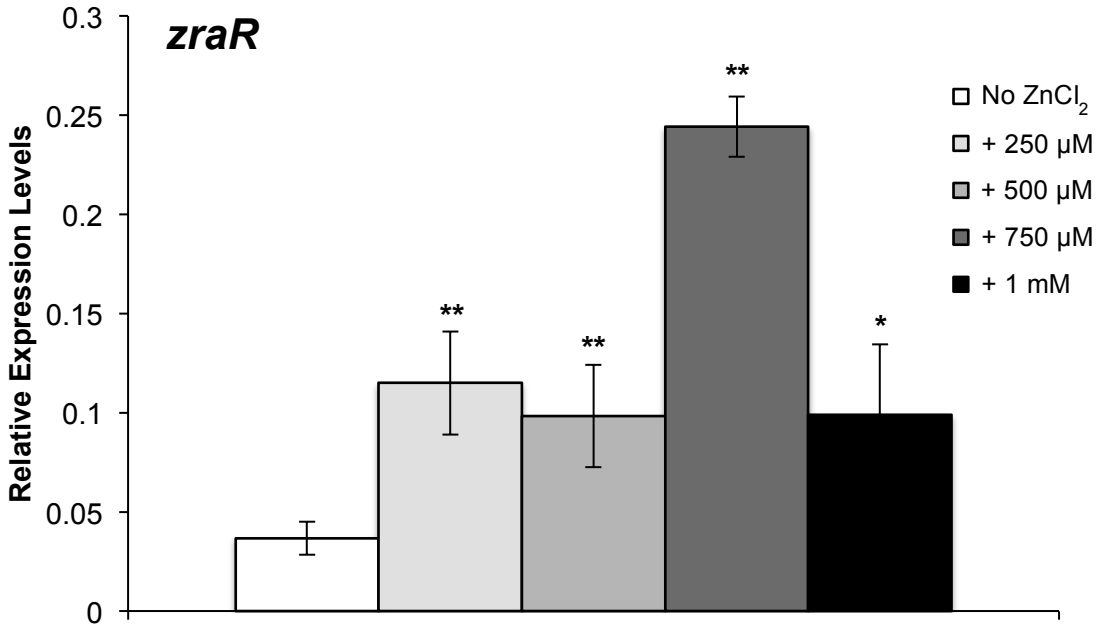

Figure 35: **Expression of *zraR* in a SL1344 WT background when cultured in MOPS with increasing $ZnCl_2$ concentrations (0-1 mM).** The addition of $ZnCl_2$ approximately doubles *zraR* expression levels at all concentrations tested bar 750 µM when *zraR* transcription levels increased ~5-fold. Significant difference indicated by * $p<0.05$ and ** $p<0.01$ (Student's *t* test) when compared to growth in MOPS minus $ZnCl_2$ supplementation (white bar). *n* = 6, Error bars = SD. Control gene was *ampD*.

Now that we have evidence in *S*. Typhimurium to confirm ZraR up-regulation in response to elevated external zinc concentrations, despite *zraSR* deletion having no detrimental impact on growth of our SL1344 strain, we focused our attention on identifying why this up-regulation happens and how ZraR helps *Salmonella* respond to zinc stress, if at all, through the genes ZraR regulates.

5.4.3 ZraR is negatively regulated by its cognate, periplasmic protein ZraP and expression of both genes correlates with this feedback inhibition across growth phases in SL1344

Appia-Ayme et al. (2012) reported negative regulation of ZraR by ZraP. This negative feedback loop was confirmed during our analysis, with relative expression of ZraR at 1.0 OD (~ 4 hours growth) ~halved when ZraP was overexpressed (Figure 36, B). The ESRs σ^E and Bae are induced during stationary phase of growth, a known stress inducing condition (Appia-Ayme

et al., 2011). To investigate if expression of ZraR and ZraP are growth phase linked, transcription of both genes was measured across a 24-hour period in aerated LB cultures. Transcription of *zraR* peaks at 3 hours growth, followed by a peak in *zraP* expression at 4 hours (Figure 36, A). ZraR levels then subsequently drop in concurrence with ZraP expression levels, confirming the negative feedback observed for ZraP on ZraR following ZraP up-regulation (Figure 36, A). These results suggest maximal ZraR expression occurs as SL1344 cells enter the exponential phase of growth and not stationary phase as is observed for the σ^E and Bae ESR systems.

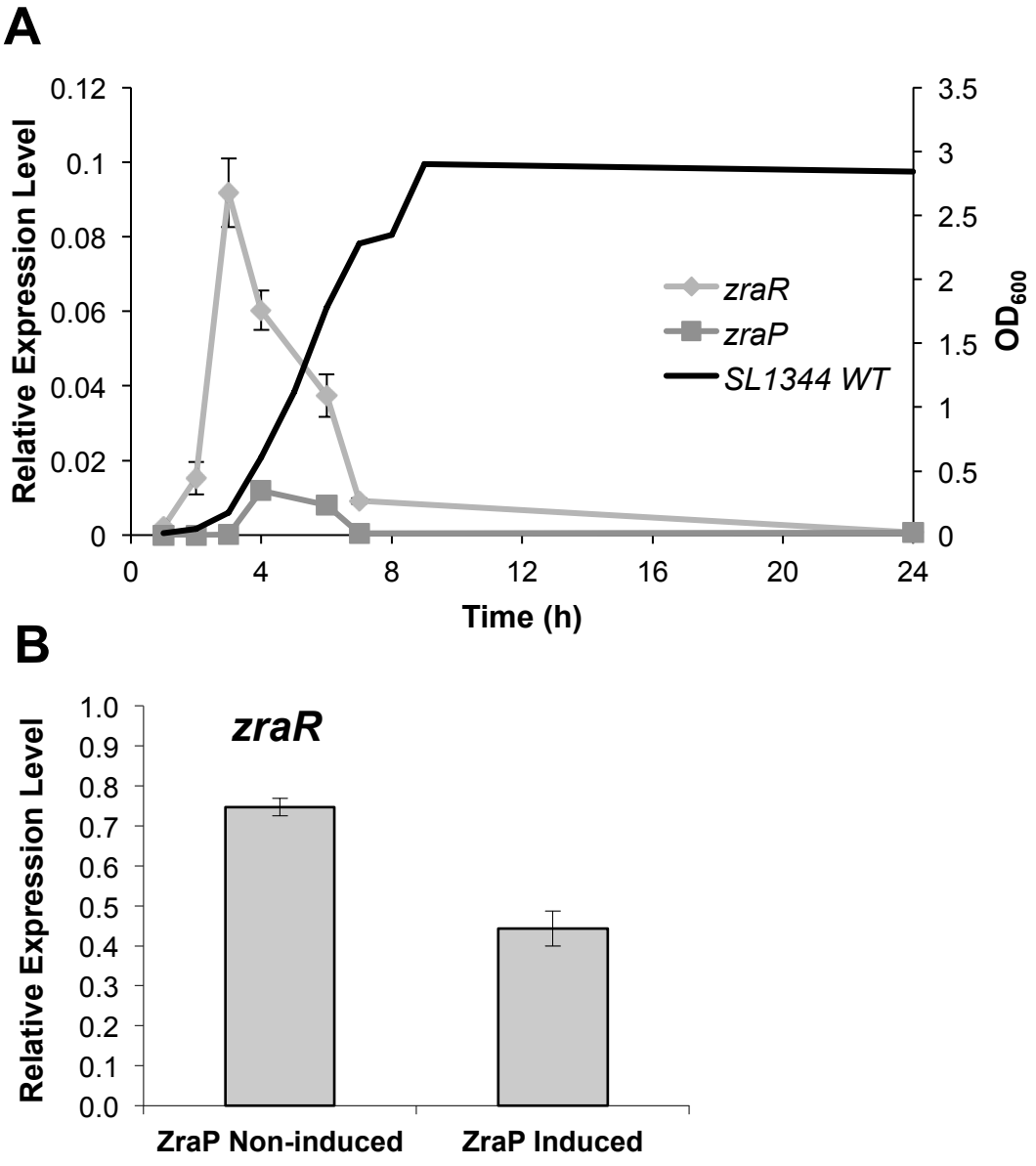

Figure 36: **Expression of *zraR* and *zraP* peak upon entry into exponential growth phase.** After 3 hours, ZraR expression reduces as a result of negative regulation by ZraP (A) confirmed by qRT-PCR analysis (B). Relative expression levels for *zraR* and *zraP* were compared to the control gene *ampD*. *n* = 3, Error bars = SD.

5.4.4 Contribution of ZraSR to carbon starvation induced cross-resistance (CSIXR) of *S*. Typhimurium

The starvation stress response (SSR) is induced during periods of nutrient limitation, predominantly a lack of carbon, phosphate and nitrogen sources, and functions to maintain long-term carbon starvation survival (LT-CSS) and generate cross-resistance to other environmental stress (termed carbon starvation induced cross-resistance; CSIXR) (Kenyon et al., 2002). Two ESRs are linked with LT-CSS and CSIXR in *Salmonella*. σ^E, which has a role in both LT-CSS and CSIXR in response to heat, acidic pH, and the cAMP polymyxin B (Spector et al., 1999, Spector and Kenyon, 2012), while constitutive expression of σ^E and Cpx ESRs increased resistance of both P- and N-starved cells to the aminoglycoside antibiotic gentamycin (Moreau, 2014).

The general stress sigma factor RpoS (σ^s) works with σ^E to regulate the SSR of *Salmonella*. Given the importance of the σ^E and Cpx ESRs in regulation of SSR and the fact that ZraS has been shown to phosphorylate the RpoS adaptor RR RssB from *E. coli in vitro* (Yamamoto and Ishihama, 2005), we wished to determine if ZraSR was involved in the SSR of *S*. Typhimurium through contributing to LT-CSS and CSIXR.

Our data confirmed σ^E contribution to LT-CSS in *S*. Typhimurium, concurring with the results of (Kenyon et al., 2002). However none of the other six ESR mutants (Δ*baeR*, Δ*cpxAR*, Δ*cpxR*, Δ*baeR*Δ*cpxAR*, Δ*zraSR* and Δ*baeR*Δ*cpxAR*Δ*zraSR*) presented any significant difference in LT-CSS when compared to SL1344 WT (data not shown). These data confirm σ^E as the only ESR involved in LT-CSS of *S*. Typhimurium, even when functional overlap is taken into account.

Because σ^E deletion mutants present severe sensitivity to heat and cAMPs when carbon starved (Kenyon et al., 2002), an SL1344 Δ*rpoE* strain was used as a comparative control to assess the contribution of ZraSR to CSIXR. ZraSR contributes to CSIXR in response to heat stress and cAMP stress, specifically polymyxin B, to a similar level for that observed for σ^E (Figure

37). When a Δ*zraSR* strain carbon starved for 24-hours was subjected to polymyxin B treatment, 50% fewer cells survived than SL1344 WT, only 10% more than the highly sensitive Δ*rpoE* strain (Figure 37, A). ZraSR deletion strains were even more sensitive to heat after carbon starvation with survival percentages reducing to ~17% of the isogenic parent strain, only 2% more than that observed for Δ*rpoE*. These severe phenotypes of carbon starved Δ*zraSR* strains provide strong evidence to support the contribution of this 2CST system to the SSR as well as maintenance of the bacterial envelope during carbon starvation.

5.4.5 Overexpression of ZraR and analysis of the ZraR regulated transcriptome in SL1344

If we are to fully elucidate the importance of the ZraSR system in *Salmonella*, investigations must focus on the gene members of the Zra regulon and regulation of the *zraPSR* operon itself, in addition to the physiological signals sensed by the Zra proteins and phenotypes associated with *zraSR* deletion.

In silico sequence and structural analysis of ZraR has shown this protein as an uncharacterised transcriptional regulator and bEBP (Chaudhuri et al., 2004, Sallai and Tucker, 2005). With the exception of *zraP* and itself, no other members of the ZraR regulon have been identified. Previous investigations have highlighted ZraR up-regulation in response to zinc, lead and tungstate (Leonhartsberger et al., 2001, Appia-Ayme et al., 2011) and work presented here has shown ZraR induction in SL1344 when grown in defined media supplemented with up to 1 mM $ZnCl_2$ (Figure 35), and upon entry into exponential (logarithmic) phase of growth (Figure 36). Acquiring SL1344 total RNA at a concentration suitable for microarray analysis under zinc inducing conditions was problematic (data not shown). As an alternative, a ZraR overexpression construct (p*zraR*, Table 4) was made, where the ORF of *S*. Typhimurium SL1344 *zraR* was cloned into the P_{BAD} Myc His A overexpression vector. DNA transcribing the original stop codon remained to ensure ZraR was expressed without the addition of the *myc* epitope or HIS tag present within P_{BAD} Myc His A. p*zraR* was made in the same way as

pBAD*nlpE*, utilised for analysis of the Cpx regulated transcriptome (Chapter 3).

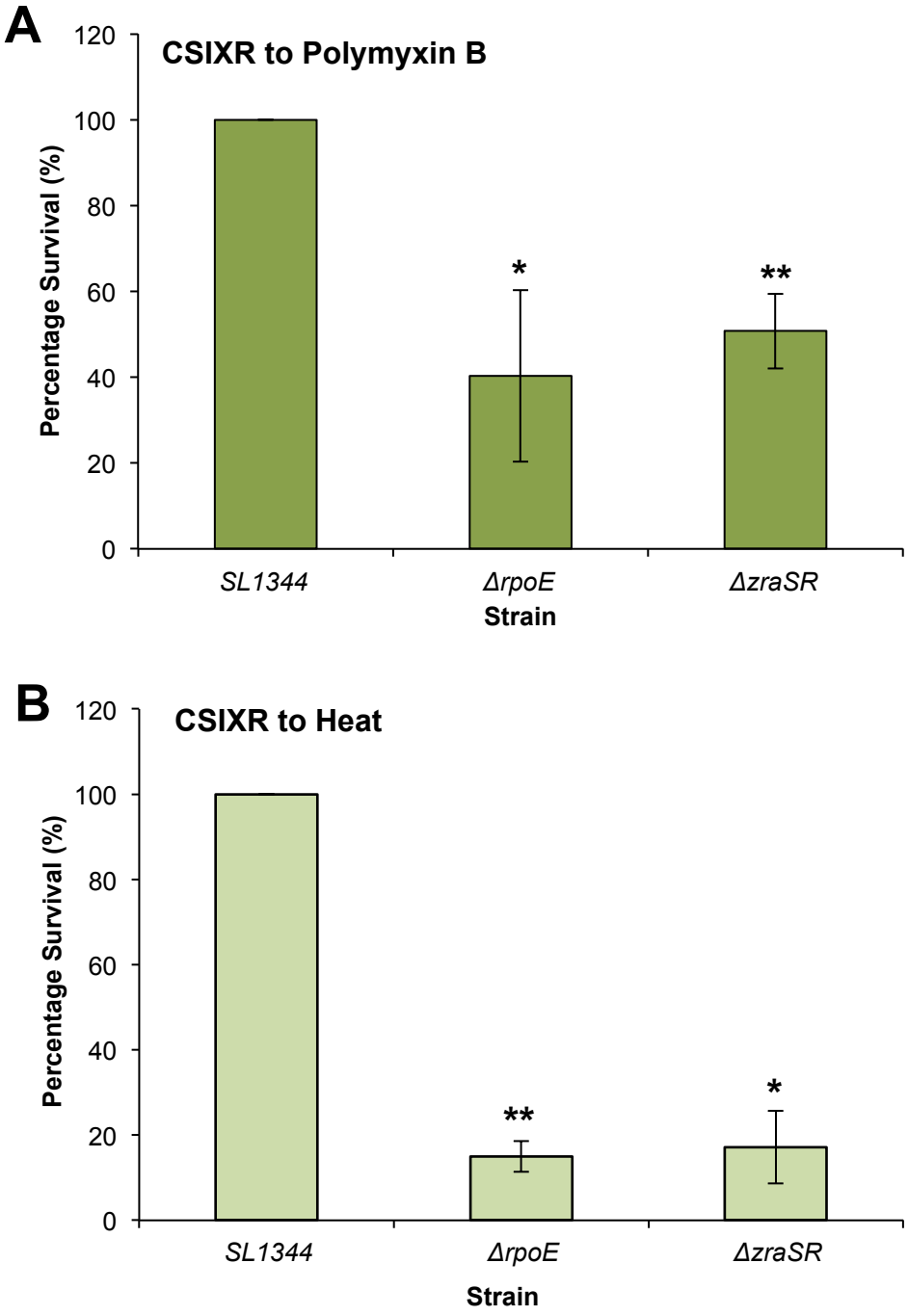

Figure 37: ZraSR contributes towards *S*. Typhimurium CSIXR to cAMP and heat. Survival of 24 hour carbon-starved cells following treatment with 0.1 mg ml^{-1} polymyxin B (A) or heat shock at 55°C (B). *n* = 2, Error bars = SE. Statistical analysis * = p<0.05), ** = p<0.01 (Student's *t* test) compared to SL1344 under comparable conditions.

When cultured in LB medium under *zraR* inducing conditions, no significant difference in μ was observed between SL1344p*zraR* and SL1344pBAD (μ = 1.17 and 1.21 respectively) (data not shown). Our SL1344p*zraR* and SL1344pBAD strains were subsequently used in microarray studies to analyse changes in the SL1344 transcriptome after ZraR overexpression. This provided the first broad-scale study of the Zra regulon in any species. Following statistical filtering (2-fold threshold, FDR<0.05), 186 genes were differentially regulated in SL1344p*zraR* and SL1344pBAD (Appendix L; Table L1). Of these 186 genes, 147 were induced by ZraR overexpression (Table L2), and 39 were repressed (Table L3; Figure 38). As a zinc inducible system, we hypothesised that a number of genes contributing towards zinc homeostasis and metal ion trafficking would be up regulated in our SL1344p*zraR* strain. Figure 38 summarises these changes in gene expression.

5.4.5.1 Comparison of transcriptomic data from ZraR overexpression in SL1344 to current literature

The 186 genes differentially regulated post ZraR overexpression were compared to the current literature to investigate their function and resolve the physiological processes associated with the Zra regulon in *Salmonella*. We initially compared these 186 genes to processes previously associated with the Zra system. Our data provided evidence to support Zra involvement in the regulation of chaperones, stress response proteins, hydrogenase 3 formation and numerous putative, unknown or hypothetical proteins previously uncharacterised in *Salmonella*. Surprisingly, our transcriptome analysis in SL1344 revealed no involvement of ZraR in regulating any zinc tolerance systems.

The known ZraSR regulon members, *zraP* and *zraS*, saw an ~123-fold and 4.7-fold increase respectively when ZraR was overexpressed (Appendix L, Table L1). These data further confirm the auto-regulation of the Zra operon

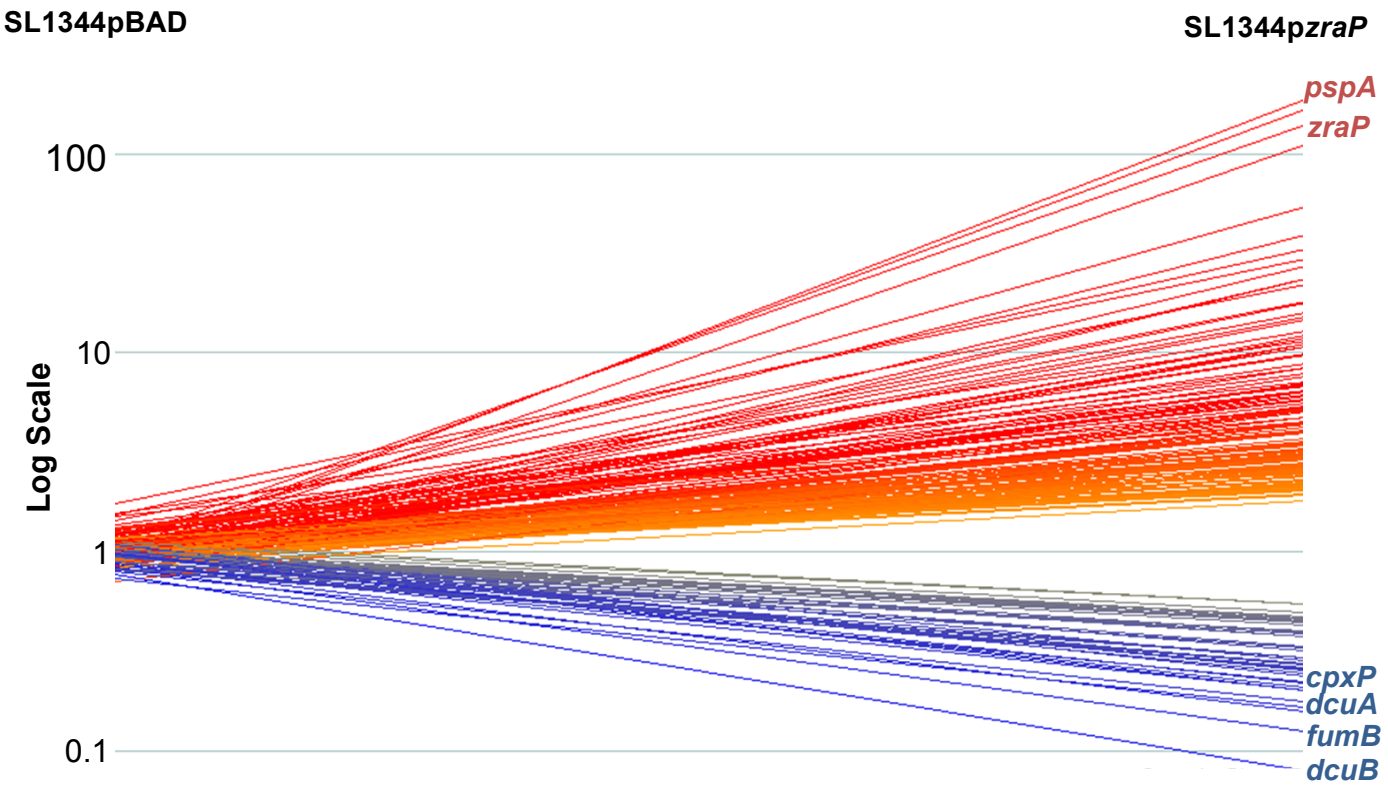

Figure 38: **Diagrammatic summary of transcription changes to 186 genes differentially regulated >2-fold following ZraR overexpression in *S.* Typhimurium SL1344**. The position of selected of genes described during Chapter 5 are shown in parenthesis.

by ZraR previously identified (Leonhartsberger et al., 2001, Appia-Ayme et al., 2011). Both of these studies linked the *zraPSR* operon to zinc tolerance. However, no genes involved in zinc homeostasis or zinc ion trafficking saw transcription levels change in our data set. Of all genes involved in metal homeostasis, only *mntH* (formerly *yfeP*), encoding an NRAMP1-like transporter, was induced by ZraR overexpression (~2.5-fold) (Table L1). The metal sensing RRs MntR and Fur both negatively regulate *mntH* in reaction to elevated manganese and iron concentrations (Ikeda et al., 2005). Transcription of Fur and MntR was unaffected by ZraR overexpression suggesting the significant increase in *mntH* expression seen is not a result of cross-talk with MntR or Fur. Further investigations would be needed to confirm the mechanisms of ZraR-mediated MntH regulation as this was outside the scope of our investigation. Although defined as a manganese transporter, MntH is a divalent metal transporter transporting cadmium, cobalt, zinc and to a lesser extent copper and nickel (Makui et al., 2000), which could contribute towards the zinc responsive phenotype associated with ZraSR, discussed in more detail during 5.5. The phage shock protein (PSP) ESR has been linked with *MntH* activity; Mn^{2+} uptake by MntH was reduced in a *pspA* deletion strain (Karlinsey et al., 2010). Although the PSP ESR was up-regulated >2-fold during our transcriptomic analysis of the ZraR regulon, this was concluded to be a result of increased σ^{54} activity following ZraR overexpression and not due to direct ZraR regulation. Reduced MntH activity in *pspA* deletion strains was likely due to disruption of the PMF, which drives MntH activity, and not because of PSP-mediated regulon of this transporter. We can therefore assume that the up-regulation of MntH expression observed during our study was not as a result of increased PSP levels.

5.4.5.1.1 ESR genes: Comparisons to Bae, Cpx, and σ^E regulons and genes involved in envelope homeostasis

The ZraSR 2CST system has been described in *Salmonella* as a new ESR due to its regulation of the periplasmic chaperone ZraP and the structural similarity of this periplasmic protein to the important chaperones CpxP and Spy. Regulation of these three CpxP family members involves the CpxAR,

BaeSR and ZraSR ESRs. We therefore wished to determine if any overlap existed between the Zra regulon and those of other ESRs in *Salmonella*.

Studies by Nishino et al. (2007) and Wang and Fierke (2013) highlight involvement of the Bae ESR in zinc tolerance, and Appia-Ayme et al. (2012) suggested a regulatory link, either directly or indirectly, between the ZraSR and BaeSR systems. Bae regulon members and their involvement in zinc tolerance in *E. coli*, as described by Nishino et al. (2007) are depicted in Figure 32. As no zinc tolerance systems were differentially regulated by ZraR overexpression, we compared the Bae regulon to our 186 Zra-regulated genes (Table L1) to ascertain if any zinc responsive phenotypes associated with Zra are due to functional overlap of these two, 2CST systems. Eight genes are defined as belonging to the Bae regulon: *mdtABCD*, *baeSR*, *acrD* and *spy*. Transcription levels of all eight were unaffected (<2-fold; FDR <0.05) by ZraR overexpression. Any influence of these two systems on zinc tolerance does not appear to result from cross talk between the Bae and Zra ESRs.

The Cpx ESR has also been linked to metal tolerance, with CpxAR regulating several copper resistance genes (i.e. *yccA*, *ybaJ*, *yihE*, *yobB*, *ycfS*, *ydeH*, *yebE*), as highlighted in this work and previous studies (Chapter 3) (Yamamoto and Ishihama, 2006, Yamamoto and Ishihama, 2005). Chapter 3 of this thesis analysed the Cpx regulated transcriptome of SL1344. During this analysis 144 genes were differentially regulated in SL1344 WT and Δ*cpxR* backgrounds, when cultured under Cpx inducing conditions (Table H1). When this gene list was compared to all >2-fold ZraR-regulated genes (Table L1), only two were present in both, *cpxP* and *dcuB*. CpxP, the CpxAR accessory protein and chaperone, was repressed ~4.5-fold following ZraR overexpression (Table L3). *dcuB*, encoding an anaerobic-C4-carboxylase transporter, saw transcription reduce ~9.8-fold by ZraR overexpression (Table L3) and 4.1-fold by Cpx induction (Table H1). *dcuA*, another anaerobic-C4-carboxylase transporter encoded at a different location of the SL1344 genome, was also down-regulated (~4-fold) but to a lesser extent than *dcuB*. To date CpxR is the only known direct regulator of *cpxP*.

Inclusion of *cpxP* on our gene list was therefore unexpected, especially as transcription of *cpxA* and *cpxR* remained unaltered during our analysis.

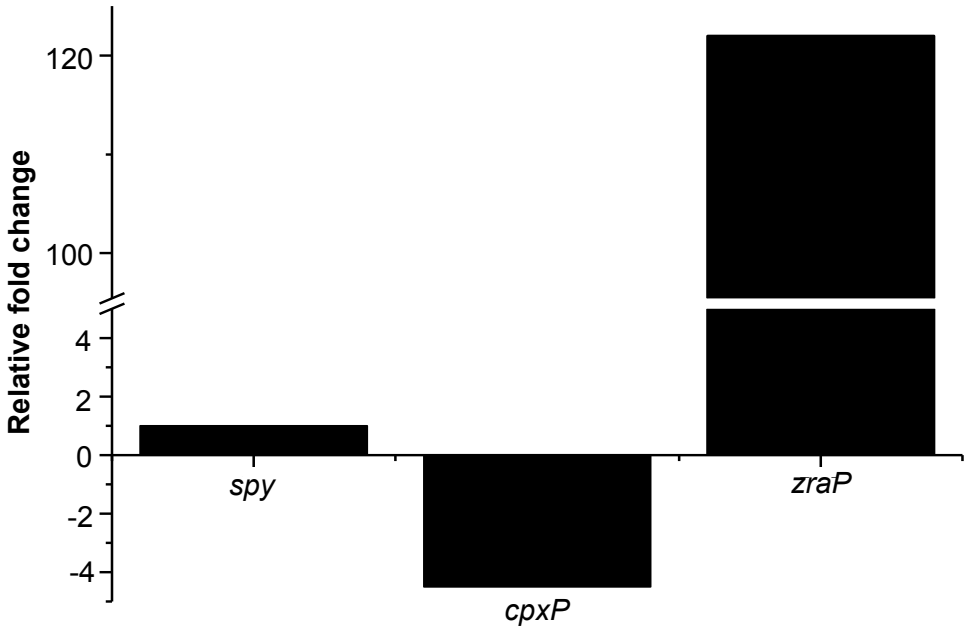

Figure 39: **Fold change of the CpxP family of molecular chaperones following transcriptomic analysis (microarray) in *S*. Typhimurium SL1344 following ZraR overexpression.**

Table 29: 97 genes up-regulated by ZraR overexpression in *S.* Typhimurium SL1344 that do not belong to the σ^{54} regulon. Adapted from Table L1 using σ^{54} regulon data published by Samuels et al., (2013).

Locus		Gene Name	Description	Fold Change[†]
SL Number	STM Number			
Putative or unknown function and hypothetical proteins				
SL3775	STM3808		Unknown	15.10
SL3776	STM3809		Unknown	13.62
SL1374	STM1442	*ydhJ*	putative multidrug resistance efflux pump	8.91
		rlgA	Unknown	8.68
SL2327	STM2358		putative cytoplasmic protein	8.30
C0664			Unknown	7.49
SL1062	STM1124		Unknown	6.84
SL4483	STM4552		putative inner membrane protein	6.52
SL0862	STM0886		putative sulfatase	6.20
	STM14_5288		hypothetical protein	4.93
SL1187	STM1251		putative molecular chaperone	4.75
SL3744	STM3778		putative DNA-binding protein	4.29
SLP1_0064			Unknown	3.98
SL2787	STM2716		putative regulatory protein	3.97
SLP1_0062			Unknown	3.91
SL3484	STM3517		putative DNA-damage-inducible protein	3.76
SL1615	STM1685	*ycjX*	putative ATPase	3.64
SL4110	STM4171	*yjaH*	putative inner membrane protein	3.46
SL3012	STM3034		putative cytoplasmic protein	3.22
SL0480	STM0487		Unknown	3.20
SL2157	STM2180		putative transcriptional regulator	3.18

Table 29 continued

Locus		Gene Name	Description	Fold Change[†]
SL Number	STM Number			
SLP2_0011			Unknown	3.14
STnc630	STM14_5162		Unknown	3.14
PSLT026			putative periplasmic protein	3.13
STM2724			hypothetical protein	3.09
SL2197	STM2220	*yejG*	hypothetical protein	3.08
SL1503	STM1572	*nmpC*	putative outer membrane porin precursor	3.00
SLP1_0081			Unknown	2.93
SLP1_0063			Unknown	2.89
SL0274	STM0279		putative cytoplasmic protein	2.88
SL1417	STM1487	*ynfL*	putative transcriptional regulator	2.87
SL0467	STM0474	*ybaJ*	hypothetical protein	2.82
	istR		Unknown	2.75
SLP1_0002		*traX*	Unknown	2.74
SLP1_0087			Unknown	2.63
SL0957	STM2621		hypothetical protein	2.57
	oxyS		Unknown	2.56
STnc310			Unknown	2.53
SL0497	STM0504	*ybbN*	putative thioredoxin protein	2.50
STM3797A	STM14_4583		Unknown	2.42
SL0275	STM0280		putative outer membrane lipoprotein	2.40
SL4264	STM4327	*fxsA*	Putative membrane protein	2.40
STM3796B	STM14_4584		Unknown	2.39
SLP1_0060			Unknown	2.37
SL0519	STM0526	*ylbA*	hypothetical protein	2.36
SL0624	STM0636	*ybeD*	hypothetical protein	2.35

Table 29 continued

Locus		Gene Name	Description	Fold Change[†]
SL Number	**STM Number**			
SLP1_0055		*parA*	Unknown	2.30
SLP1_0005		*trbH*	Unknown	2.30
SLP2_0003			Unknown	2.27
STM4287	STM14_5157		Unknown	2.26
SL3059	STM3083		putative mannitol dehydrogenase	2.20
SLP1_0080		*ccdA*	Unknown	2.20
SL3475	STM3508		putative cytoplasmic protein	2.19
STM0895			hypothetical protein	2.16
SL3977	STM4031		putative cytoplasmic protein	2.16
SL2978	STM3000	*ppdA*	hypothetical protein	2.15
SL1076	STM1139	*csgG*	putative curli operon transcriptional regulator	2.15
SL1453	STM1523	*yneJ*	putative transcriptional regulator	2.14
SL2154	STM2177		putative flutathione S-transferase	2.13
SL3743	STM3777		putative cytoplasmic protein	2.11
STM14_4997			hypothetical protein	2.10
SL4406			Unknown	2.09
STM4008	STM14_4821		Unknown	2.07
SL4269	STM4332	*yjeJ*	putative inner membrane protein	2.05
SL3297	STM3325	*yrbL*	hypothetical protein	2.04
SL0271	STM0276		putative cytoplasmic protein	2.04
SLP1_0074			putative inner membrane protein	2.03
SL3979	STM14_4847		Unknown	2.02
Metabolism				
SL2776	STM2792	*gabT*	4-aminobutyrate aminotransferase	7.31
SL3995	STM4046	*rhaA*	L-rhamnose isomerase	6.74

Table 29 continued

Locus		Gene Name	Description	Fold Change[†]
SL Number	STM Number			
SL2886	STM2907	*pphB*	serine/threonine-specific protein phosphatase 2	6.62
SL2323	STM2354	*hisJ*	histidine transport protein	5.85
SL3425	STM3458	*yheR*	glutathione-regulated potassium-efflux system ancillary protein KefG	4.86
SL3528	STM3562	*livM*	leucine/isoleucine/valine transporter permease subunit	3.69
SL2322	STM2353	*hisQ*	histidine/lysine/arginine/ornithine transport protein	3.18
SL4034	STM4085	*glpX*	fructose 1,6-bisphosphatase II	2.97
SL4118	STM4183	*aceB*	malate synthase	2.67
SL2166	STM2189	*mglA*	galactose/methyl galaxtoside transporter ATP-binding protein	2.24
SL2377	STM2409	*nupC*	nucleoside transport	2.21
SL3965	STM4019	*yihQ*	alpha-glucosidase	2.11
Chaperones				
SL0012	STM0012	*dnaK*	molecular chaperone DnaK	5.17
SL4266	STM4329	*groES*	co-chaperonin GroES	3.64
SL4267	STM4330	*groEL*	chaperonin GroEL	3.36
SL2620	STM2660	*clpB*	protein disaggregation chaperone	2.81
Virulence				
PSLT043			type II secretion system protein	3.74
SL0466	STM0473	*hha*	hemolysin expression-modulating protein	3.12
SL2613	STM2649	*trxC*	thioredoxin 2	2.27
Stress Responses				
SL3883	STM3924	*wecD*	TDP-fucosamine acetyltransferase, required for ECA formation	2.77
SL1621	STM1691	*pspF*	phage shock protein operon transcriptional activator	2.14
Hydrogenase-3 formation				
SL2839	STM2859	*fhlA*	formate hydrogen-lyase transcriptional activator	5.71
	STM14_3433		hydrogenase maturation protein	4.75

Table 29 continued

Locus		Gene Name	Description	Fold Change[†]
SL Number	**STM Number**			
Transporters				
SL2360	STM2391	*fadL*	long-chain fatty acid outer membrane transporter	6.43
SL3594	STM3628	*dppC*	dipeptide transporter	2.50
Respiration				
SL0437	STM0443	*cyoA*	cytochrome o ubiquinol oxidase subunit II	6.09
Metal Transport				
SL2376	STM2408	*mntH*	manganese transport protein MntH	2.49
Other				
SL3011	STM3033		plasmid maintenance protein	2.43

5.4.5.1.2 Functional groups with members differentially regulated by ZraR over expression

Two other genes that contribute towards the stress responses of *Salmonella*, *wecD* and *pspF*, were up-regulated 2.77-fold and 2.14-fold respectively by ZraR (Table 29). The former encodes a TDP-fucosamine acetyltransferase, required for the final formation step of the glycolipid Enterobacterial common antigen (ECA)(Kuhn et al., 1988). This protein is found on the OM of all *Enterobacteriaceae* and is involved in resistance of *S. enterica* to bile salts, Shiga-toxin-producing *E. coli* (STEC) to organic acids and indirectly contributes towards virulence (Nnalue and Stocker, 1987, Valtonen et al., 1976, Hung et al., 2006, Danese et al., 1998, Ramos-Morales et al., 2003). However, none of the other members of the *wec-wzx* operon saw their transcription significantly altered by ZraR overexpression. The PspF protein is a constitutively active bEBP and activator of the σ^{54}-dependant phage shock protein response operon *pspABCDE* (Dworkin et al., 1997). This ESR contributes towards maintaining membrane potential during stress (see Chapter 1, 1.8) and all other *psp* operon members were significantly up-regulated by ZraR overexpression (Table L2). Like other bEBPs expression of *pspF* must be tightly regulated to prevent transactivation of σ^{54}-regulated promoters. Up-regulation of PspF as a result of ZraR overexpression may have contributed to the large number of σ^{54} regulon members present within our differentially expressed genes (Table L1) and the up-regulation observed for the *psp* operon. Because of this, direct regulation of the PSP ESR by ZraSR is questionable and more investigations are needed.

Interestingly ZraR overexpression resulted in up-regulation of two genes involved in hydrogenase-3 formation, *fhlA* and STM14_3433 (Table 29). The Zra system was originally proposed to be a regulator of hydrogenase-3 formation (Stoker et al., 1989), but this was later dismissed by Leonhartsberger et al., (2001) as unspecific cross talk. *fhlA*, up-regulated 5.71-fold by ZraR overexpression (Table 29), encodes a formate hydrogen lyase transcriptional activator and controls the transcription of the operons involved in formate metabolism (i.e. *hypABCDE* and *hycA*). None of these genes directly regulated by FhlA saw >2-fold changes to transcription levels

during our microarray analysis. The only *hyp* gene to see a >2-fold change in our data was *hypO* (-2.5-fold), which is transcribed on a separate transcriptional unit with *hybABCDEFG*. Of this operon *hybABC* passed our statistical filtering and are included within our significantly down-regulated genes (~-3-fold) (Table L2). The *hypO-hyb* operon encodes subunits of hydrogenase 2, suggesting ZraSR involvement in anaerobic metabolism, in addition to or instead of hydrogenase 3 as originally suggested (Stoker et al., 1989). Whether ZraSR regulation of the hydrogenases differs between *S*. Typhimurium and *E. coli,* used by Stoker et al. (1989), remains inconclusive. The second protein encoded by STM14_3433 is a provisional hydrogenase maturation protein (Chaudhuri et al., 2004), however there is no further information on the function of this gene in the literature.

Genes of the *hyb* operon are not the only genes involved in anaerobic growth affected by ZraR overexpression. Of the 41 genes down regulated by ZraR overexpression, 12 (~30%) were associated with anaerobic respiration with 60% of these linked to fumarate metabolism (*dcuA*, *dcuB*, *fumB*, *frd*-operon) (Table L3). As previously mentioned the *dcuA* and *dcuB* anaerobic-C4-dicarboxylate transporters were two of the most significantly down-regulated genes in our data set (Table L2, Figure 38), and function at the IM to catalyse fumarate/succinate transport (Bauer et al., 2011). The *frd*- operon (*frdABCD*) encodes fumarate reductase, and *fumB* encodes the fumarate hydratase Fumarase B and is located directly downstream of the *dcuB* gene.

5.4.6 Analysis of *zraSR* and *zraP* during anaerobic growth

Leonhartsberger et al., (2007) presented evidence of *zraSR* induction during anoxic conditions when grown in buffered rich medium (TGYEP, pH 6.5) supplemented with sodium formate. When cultured in MGN minimal media supplemented with sodium nitrate and glycerol as the e^- acceptor and carbon source (MGN^+), Δ*zraSR* grew as WT SL1344 and presented no growth defects (Figure 40). The same result was obtained for strains lacking *baeR*, neither mutant stain presented significant differences in μ or final cell density compared to WT SL1344 cells (data not shown). This anaerobic growth methodology was used because of the materials and media available from

other projects within the laboratory at the time. Based on our transcriptomic data collected after ZraR overexpression, ZraR appears to regulate a number of proteins required for fumarate metabolism. Anaerobic growth assays of ZraSR deletion strains utilising fumarate as a carbon source would be a more appropriate indication of the contribution of the ZraSR 2CST system to the anaerobic respiration of *Salmonella*. Our anaerobic growth curves in MGN^{+} media were included here to show that ZraSR did not impact anaerobic growth in this instance and alternative e^{-} acceptors and carbon sources should be used during future investigations.

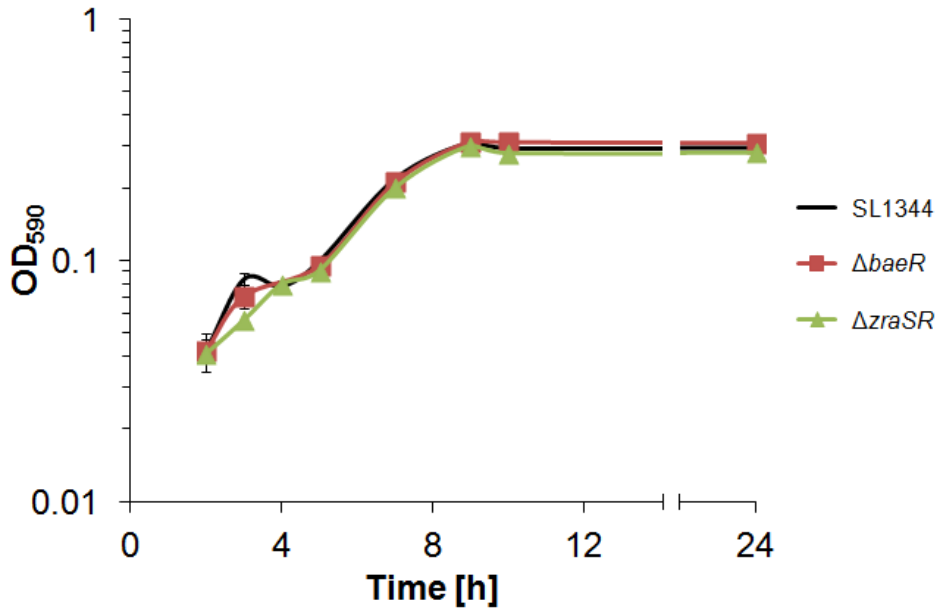

Figure 40: **Anaerobic growth of *S.* Typhimurium SL1344 is unaffected by deletion of *zraSR* or *baeR*.** SL1344 WT, Δ*baeR* and Δ*zraSR* cells were cultured in hungate tubes containing MGN+ media under anaerobic conditions. All cultures were grown at 37°C and the OD_{590} recorded at regular intervals over 24 hours. *n=3*, Error bars = SD.

5.4.7 The contribution of the Bae ESR to zinc tolerance in *S.* Typhimurium, *S.* Enteritidis and *E. coli* is not universal

Investigations by Wang and Fierke (2013) and Nishino et al. (2007) have established Bae as a key contributor to zinc tolerance. Deletions of Bae and Bae regulon members resulted in growth defects for both *E. coli* BW25113 and *S.* Typhimurium ATCC 14028s, when exposed to high zinc concentrations (Wang and Fierke, 2013, Nishino et al., 2007). These studies highlighted a previously unseen role for the AcrD and MdtABC multidrug efflux systems in metal resistance. Because these results did not concur with

phenotypes observed for Bae mutants of SL1344 in our hands (Appia-Ayme et al., *unpublished observations*), we wished to investigate this proposed function of the Bae ESR further. As zinc tolerance is becoming a widely accepted function of the Bae system, these inconsistencies needed to be addressed.

In the present study we assessed sensitivity of *S*. Typhimurium SL1344, *S*. Typhimurium NCTC 12023 (ATCC 14028), *S*. Enteritidis PT4 and *E. coli* MG1655, WT and Δ*baeR* mutants to $ZnSO_4$ under the same growth conditions presented by Wang and Fierke (2013) and Nishino et al. (2007). Average μ constants and mean generation/doubling time (Td) were also calculated for all strains in the presence and absence of excess $ZnSO_4$ (Figure 42).

The methodologies adopted by Wang and Fierke (2013) and Nishino et al. (2007) were reproduced to firstly confirm the phenotypes observed for Bae mutants of *E. coli* and *S*. Typhimurium respectively, and investigate the role of Bae on zinc tolerance in SL1344 strains. Nishino et al. (2007) assessed sensitivity of *S*. Typhimurium ATCC 14028s Δ*baeSR*, Δ*tolC* and Δ*acrD mdtABC* mutants to 600 μM $ZnSO_4$ by cell growth assays in rich (LB) media (37°C). Although all three mutants grew more poorly than the WT ATCC 14028s strain, the Δ*baeSR* mutant presented the most severe growth defect when exposed to $ZnSO_4$ (Nishino et al., 2007). All of our *S*. Typhimurium, *S*. Enteritidis and *E. coli* MG1655 WT and Δ*baeR* deletion strains grew to a comparable cell density in control cultures (LB medium, 37°C, 200rpm agitation) across a 24-hour period (Figure 41, A). When exposed to 600 μM $ZnSO_4$, Δ*baeR* mutants of all serovars and strains presented no significant growth defects when compared to their isogenic parent strain (Figure 41, B) ($p>0.05$, Student's *t* test). The *E. coli* MG1655 strains had a slightly reduced *Td* when exposed to high $ZnSO_4$ than the three *S. enterica* serovars tested, but cell growth of MG1655 WT and Δ*baeR* strains were virtually identical and the difference between the two species was not significant ($p>0.05$, Student's *t* test) (Figure 41, B).

Wang and Fierke (2013) investigated the growth rates of *E. coli* MG1655 *baeR* and *baeS* single deletion mutants, as well as a range of Bae regulon member mutants, in MOPS defined medium. When exposed to 300 μM $ZnSO_4$, Wang and Fierke (2013) presented slower growth rates than the isogenic parent strain for all Bae mutants tested, during early and late stages of growth (Wang and Fierke, 2013). Our MG1655 WT and *baeR* deletion strains were subjected to identical growth analyses as presented by Wang and Fierke (2013) (MOPS media with and without 300 μM $ZnSO_4$, 25°C) and we observed no significant difference in μ or *Td* between the two strains in the presence or absence of excess $ZnSO_4$ (Figure 41 C and D). This was also the case for all *S. enterica* strains tested (Figure 41, C and D). In direct contrast to data presented by Wang and Fierke (2013) all of our tested strains presented faster growth rates and reduced doubling times compared to MOPS only control growth assays (Figure 42). Our strains therefore appear to grow faster in MOPS containing 300 μM $ZnSO_4$ (although these differences were not significant $p>0.05$, Student's *t* test), despite reaching a reduced final cell density compared to MOPS only cultures.

Absence of the RR BaeR therefore does not result in a zinc sensitive phenotype in any of the strains we tested. These results differ to those observed for *S*. Typhimurium strain 14028s WT and a *baeSR* double mutant (Nishino et al., 2007), or *baeR* or *baeS* single mutants in *E. coli* BW25113 (Wang and Fierke, 2013). If the Bae 2CST system is involved in zinc tolerance, our data suggest this response occurs in a BaeS dependent manner, independently of the response regulator BaeR. Unfortunately *baeS* single or *baeSR* deletion strains were not available to us at the time these experiments were undertaken. It is also possible that this involvement of Bae in zinc tolerance may be subspecies or growth condition specific. However, our results are reproducible across the *S*. Typhimurium, *S*. Enteritidis and *E. coli* genetic backgrounds available. This casts doubt on the level of Bae involvement in zinc tolerance, providing evidence that this function of Bae is not universal in response to elevated environmental zinc concentrations and deletion of *baeR* does not produce as severe a phenotype as previously presented.

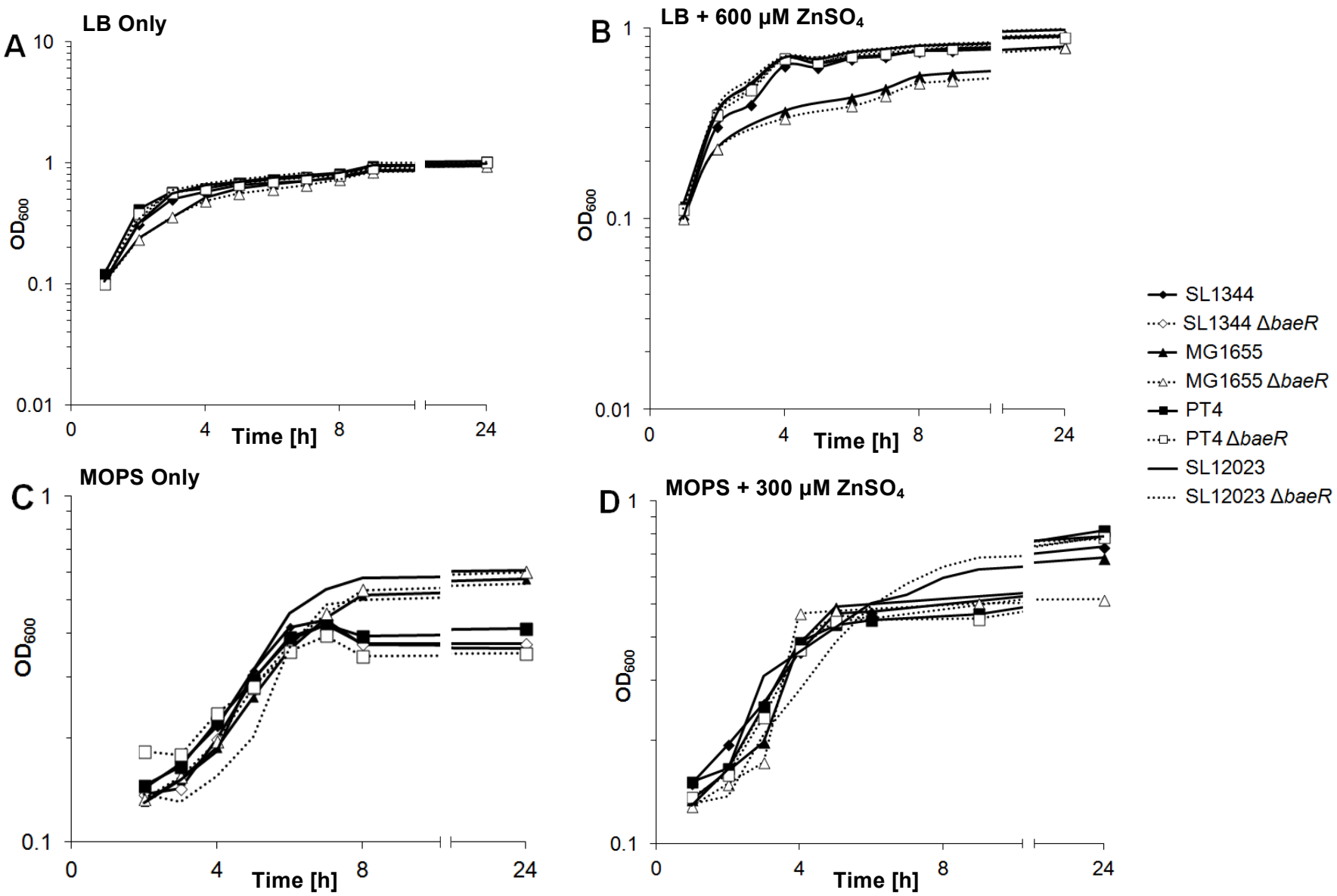

Figure 41: Deletion of *baeR* does not impact on zinc tolerance. When cultured in rich (A and B) or defined (C and D) medium supplemented with $ZnSO_4$ deletion of BaeR had no negative impact on cell survival and does not concur with zinc sensitivity phenotypes presented by Wang and Fierke (2013) and Nishino et al., (2007) for *bae* deletion strains in *S*. Typhimurium and *E. coli* genetic backgrounds. *n*=3, error bars = SD.

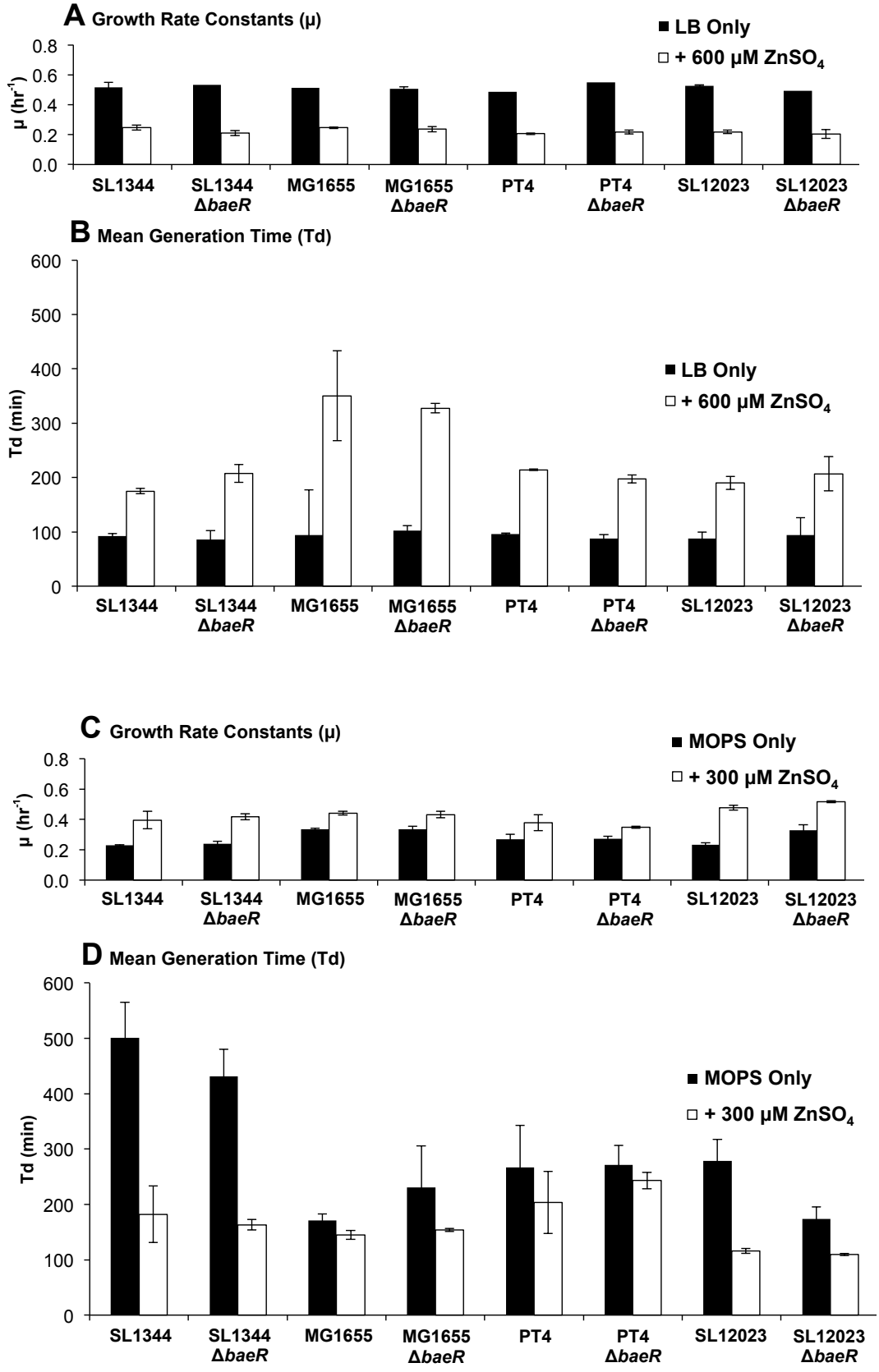

Figure 42: **Growth rate constants (μ) and mean generation times (*Td*) of *baeR* deletion mutants are unchanged compared to WT equivalents when exposed to $ZnSO_4$ in rich (A and B) and minimal (C and D) media**. Calculated using Equation1 from growth assays presented in Figure 40. *n* = 3, Error bars = SD

5.5 Discussion and future work

In this study a combined physiological and transcriptional approach was used to characterise the contribution of the ZraSR 2CST system to zinc tolerance in *S*. Typhimurium and provide the first broad-scale analysis of the ZraR regulon in any organism.

Our initial characterisation of SL1344 *zraSR* mutants revealed that deletion of this system did not affect *S*. Typhimurium's ability to respond to excess zinc, across a range of concentrations and growth conditions (Figure 34). As one of the only phenotypes experimentally linked to the ZraPSR system was differential regulation of this operon in response to fluctuations in zinc and lead concentrations (Leonhartsberger et al., 2001, Graham et al., 2009), we expected to see some level of zinc sensitivity for our *zraSR* double deletion strain. Despite this, qRT-PCR analysis confirmed up-regulation of *zraR* transcription in response to elevated environmental zinc concentrations (Figure 35), concurring with results published by Leonhartsberger et al., (2001) and confirming *zraSR* as a zinc responsive system in *S*. Typhimurium.

We hoped that through analysis of the *S*. Typhimurium SL1344 transcriptome after ZraR overexpression, we could identify the reason for ZraR up-regulation in response to elevated extracellular zinc and identify the physiological processes regulated by ZraSR. Our data revealed no known zinc uptake/efflux systems or metallochaperones as members of the ZraR regulon, and had no impact on the established regulators of these systems (Zur and Fur). With ZraSR having no direct influence on the regulation of these crucial components of zinc homeostasis, the lack of zinc sensitivity observed for a *zraSR* deletion strain is explained. Despite being zinc responsive, the ZraSR 2CST system does not function as a regulator of metal homeostasis.

Our transcriptomic analyses highlighted *mntH* as the only metal ion trafficking protein regulated by ZraR, up-regulated ~2.5-fold upon ZraR overexpression (Table 29). As an orthologue of the NRAMP1 divalent metal

transporter, MntH transports manganese and to a lesser extent, iron, into the cell at times of limitation. The primary regulator of MntH, MntR, is highly selective for manganese (and cadmium) and binds to the promoter region of *mntH* in its Mn^{2+} bound state to block transcription (Guedon and Helmann, 2003, Golynskiy et al., 2006). OxyR (a positive regulator of MntH during oxidative stress) and Fur induce *mntH* expression in metal depleted conditions (Botteldoorn et al., 2006). If ZraSR directly regulates *mntH* transcription, what links induction of ZraSR by high zinc and the 'switching on' of a manganese transporter?

MntH has been identified as a virulence factor for *Y. pestis* and *Salmonella*, especially during infection of *Salmonella* in NRAMP1$^{+/+}$ mice (Zaharik et al., 2004, Perry et al., 2012, Runyen-Janecky et al., 2006). These experiments highlight the importance of MntH within the host environment. The NRAMP transporters of the host are located at the phagosomal membrane and pump divalent metal ions out of the phagosome after phagocytosis to produce a metal limited environment (Kehres et al., 2000, Zaharik et al., 2004). There is evidence to suggest immune cells are able to substantially increase and decrease the concentrations of metal ions within their cytosol in response to infection (Stafford et al., 2013, Hood and Skaar, 2012), termed 'nutrient immunity' (Winters et al., 2010). A sudden increase in metal ions (predominantly copper and zinc) can damage proteins through non-specific binding to thiols and the production of hydroxyl radicals. Severe limitation prevents the bacteria from attaining the required levels of metal cofactors critical for central metabolic processes, DNA replication and maintaining protein stability. Although 'nutrient immunity' is yet to be fully understood, an increase in zinc concentrations within immune cells occurs as a direct response to infection and significantly reduces pathogen infection rates (Stafford et al., 2013, Hood and Skaar, 2012). Induction of ZraSR by high zinc concentrations within the phagosome could induce MntH activity to increase the concentrations of Mn^{2+} and Fe^{2+} within the bacteria before extreme nutritional limitation occurs as a result of host induction of zinc transporters ZIP8 (SLC39A family) and ZnTs (SLC30A family), and NRAMP1 (Porcheron et al., 2013, Desrosiers et al., 2010, Jabado et al., 2000, Forbes

and Gros, 2003). ZraSR may therefore not regulate genes involved in zinc homeostasis or the response to zinc deficiency directly (e.g. *znuABC*, *zinT*, *zupT*), but may provide an additional sensing mechanism for high zinc concentrations within the intracellular environment.

Evidence presented by Leonhartsberger et al. (2001) stating ZraR up-regulation during anoxic conditions. Up-regulation of Zra during *Salmonella* and *E. coli* infection of pigs and humans has also been observed (Huang et al., 2007b, John et al., 2005). Growth in anoxic conditions and up-regulation within the mammalian host provide evidence to support the theory of ZraSR as a zinc sensing system within the host environment. A clear induction of ZraR and ZraP at the transcriptional level was observed upon transition from lag phase into exponential (logarithmic) phase (Figure 36, A), followed by a decrease in expression consistent with feedback inhibition from ZraP (Figure 36, B). Botteldoorn et al. (2006) showed maximal *mntH* expression occurs at early exponential phase, correlating with an increase in ZraR expression during the transition from lag to exponential phase of growth (Figure 36). These data confirm ZraR and MntH are co-expressed during the same period of growth. If ZraR is a positive regulator of MntH, as suggested by our *S*. Typhimurium transcriptome data, this could be in preparation for entering a host environment, during fluctuating metal ion concentrations within the macrophage, in response to oxidative stress within phagocytes or a combination of the above. Unfortunately macrophage infection assays were one area of investigation outside the remit of our study. These assays, with our Zra deletion strains and Δ*zraSR*Δ*mntH* strains, would be required to determine the role *zraSR* plays, if any, within host immune cells. Our investigations into the affect of *zraSR* deletion on *S*. Typhimurium anaerobic growth were limited (Figure 40) and need to be extended to include a range of electron donors/acceptors to experimentally assess ZraSR growth within the GIT of hosts. *Salmonella* catabolises glucose within macrophages and glycolysis is required for infection of macrophages and mice (Bowden et al., 2009). *In vitro* studies by Yamamoto et al. (2005) showed ZraR phosphorylation by a non-cognate HK UhpB, involved in the regulation of carbohydrate transport into the bacteria. In addition, the fructose 1,6-

bisphosphatase II GlpX, which functions within the glycolysis pathway was up-regulated in *S*. Typhimurium ~3-fold by ZraR overexpression (Table 29). Given our data suggesting ZraSR involvement in stress sensing within host immune cells, this possible link between ZraSR and carbohydrate transport and glycolysis is an interesting observation and could provide more evidence to link ZraSR activity with *Salmonella* growth within immune cells.

Additional evidence to support involvement of *zraSR* in response to nutrient immunity of the host was the inclusion of several molecular chaperones: *zraP*, *groEL*, *groSL*, *dnaK* and *clpB*, within the list of genes up-regulated upon ZraR overexpression (Table 29). GroEL-GroES form a megadalton protein complex that resides in the cytoplasm, are conserved across all form of life and are members of the RpoH heat shock regulon to assist in refolding of thermally damaged proteins (Horwich et al., 1993, Rosen and Ron, 2002). Both GroEL and DnaK are induced in *S*. Typhi cells exposed to heat stress and deletion of GroEL-GroES in *E. coli* is lethal at all temperatures; they are therefore critical for the correct folding of at least one essential protein (Fayet et al., 1989, Tang et al., 1997). DnaK (Hsp70 member) along with DnaJ (Hsp40 member) and GrpE also form chaperone machinery involved in the response to thermally induced protein damage (Schroder et al., 1993), and the forth chaperone up-regulated by ZraR overexpression, *clpB*, functions in cooperation with DnaK, DnaJ and GrpE to aid cell recovery. In addition, these proteins contribute towards *Salmonella* pathogenicity as *clpB* deletion strains present attenuation in chicks and DnaK-DnaJ-GrpE is essential for invasion of epithelial cells (Turner et al., 1998, Takaya et al., 2004). As previously mentioned, the toxic conditions within macrophages are known to include metal stress. In eukaryotic cells, zinc is a well-known, potent inducer of HSPs, especially the Hsp70 protein family (Hatayama et al., 1993, Arslan et al., 2006). The HSPs described above are induced upon *S*. Typhimurium infection of macrophages (Buchmeier and Heffron, 1990, Perez-Perez et al., 1996, Wu et al., 1994), making possible up-regulation of these chaperones by a zinc responsive system more intriguing. The up-regulation of chaperones by ZraSR, possibly in response to zinc stress within macrophages, could help counteract the damaging environment of the

phagosome. The influence of ZraSR on the heat shock response specifically is yet to be investigated as all growth assays presented during this work were carried out at 37°C or 25°C and is one avenue of current investigation. It remains unclear if the transcriptional changes in HSP chaperones observed are a result of direct or indirect regulation by ZraR, or as a transient response to increased ZraR concentrations and knock-on effects from this. The ZraR-mediated regulation of HSPs observed in our array data requires confirmation through qRT-PCR, and as is the case for all potential ZraR regulated genes described during this chapter, ZraR-DNA binding assays (EMSAs) would provide evidence to support direct regulation by ZraR. Purification of ZraR from a σ^{54} deletion background would allow this protein to be used in EMSAs or Chip-Seq experiments to support our description of the ZraR regulon without influencing expression of the σ^{54} regulon, and include any other genes missed by the arbitrary 2-fold threshold applied to our data set. A DNA binding motif for ZraR is yet to be characterised. This future work could result in the formation of a conserved motif to be used during additional *in silico* analysis to investigate the Zra regulon further in *Salmonella* and related species.

It is important to note a possible link between the sensitivity of a Δ*zraSR* strain to heat following carbon starvation (Figure 37), and the apparent regulation of HSP chaperones by the ZraSR system (Table 29). Following carbon starvation, bacteria undergo radical metabolic remodelling resulting in distinct morphology compared to actively growing cells (Kenyon et al., 2002). These physiological changes have the added benefit of affording protection to environmental stresses, such as fluctuations in osmolarity, heat and pH. We conducted LT-CSS and CSIXR assays to determine if ZraSR is involved in the response of *S*. Typhimurium to carbon starvation and found that although *zraSR* deletion strains are no more sensitive than SL1344 WT to stresses during LT-CSS (data not shown), they are highly sensitive to heat and cAMPs after carbon starvation (Figure 37). These data strongly imply ZraSR as a contributor to *Salmonella* CSIXR. The CpxP family of molecular chaperones, including the ZraSR regulated ZraP, are critically required for resistance to polymyxin B (Appia-Ayme et al., 2012). The polymyxin B

sensitivity observed for *zraSR* during CSIXR is likely to result from lack of *zraP* expression. Both the σ^E and Cpx ESRs contribute towards CSIXR of *Salmonella* (Spector et al., 1999, Spector and Kenyon, 2012, Moreau, 2014) and the contribution of ZraSR helps to further establish this 2CST system as an ESR.

In vitro analysis by Yamamoto et al. (2005) showed phosphorylation of MviA by ZraS and five other HKs (RstB, DcuS, NtrB, NarQ). MviA purified from *E. coli* is also phosphorylated *in vitro* by acetyl phosphate (Bouche et al., 1998). When phosphorylated, MviA shuttles σ^S to the ClpXP protease complex for degradation, as described earlier, to suppress σ^S levels in the absence of stress. σ^S, in coordination with σ^E, contributes towards regulation of the SSR in *Salmonella* (Kenyon et al., 2002, O'Neal et al., 1994, Spector et al., 1999). However, a non-phosphorylated MviA protein (due to mutations within the phosphorylation site) still has some activity *in vivo* (Bougdour et al., 2006). It is possible that the sensitivity of *zraSR* mutants to cAMP and heat stress during carbon starvation are a result of deregulation of MviA activity in the absence of ZraSR. Battesti and Gottesman (2013) state during their investigations of MviA function that this protein is an orphan regulator (i.e. it has no HK associated with it) and the means of MviA phosphorylation *in vivo* are still unknown. One would expect that in the absence of ZraS, MviA phosphorylation would not occur, σ^S degradation by ClpXP would become deregulated and σ^S would accumulate, inducing the SSR. This does not concur with the sensitivity of our Δ*zraSR* strain during CSIXR analyses. However, the regulation of MviA and σ^S is a complex, multifaceted network involving multiple anti-adaptor proteins (i.e. IraP, IraD, IraM) (Bougdour et al., 2006, Battesti and Gottesman, 2013, Battesti et al., 2013). If *in vivo* phosphorylation of MviA by ZraS occurs then this SK could function as a crucial regulator of σ^S. However a more detailed analysis of any interaction between ZraS and MviA is required to understand the CSIXR sensitivity presented here. Both *in vitro* and *in vivo* analyses of the ZraSR contribution to *Salmonella* MviA phosphorylation are needed to link the results presented during this investigation and those presented by Yamamoto et al. (2005) in *E. coli*. Additional investigations into the sensitivity of *zraSR* deletion strains

during carbon stress are also needed to categorically confirm ZraSR involvement in the SSR of *S*. Typhimurium.

One interesting observation when looking at our proposed ZraR regulon as a whole (all 186 differentially regulated genes – Appendix L, Table L1), is the inclusion of a number of genes associated with *Salmonella* survival within the SCV, supporting the hypothesis of a role for ZraR in this microenvironment. *Salmonella* survive within these membrane bound vacuoles in macrophages (preferentially), epithelial, dendritic and fibroblast-like cells (García-del Portillo et al., 2008, Prost et al., 2007, Monack et al., 2004). In the latter cell type, *S. enterica* is able to establish a long-lasting infection with limited proliferation, completing very few rounds of replication during both acute and chronic infections (Cano et al., 2003). The SCV is a stressful environment for bacteria, with limited levels of Mn^{2+}, Fe^{2+}, PO_4^{3-} and Mg^{2+}; see Thompson et al. (2006) for review. The concentration of zinc within host immune cells may vary between cell types and the amount of labile zinc available for *Salmonella* growth is very low because it is stably bound by intracellular proteins. When ZraR is overexpressed, the Mn^{2+} (and Fe^{2+}) transporter *mntH* is up-regulated (as described above) allowing manganese uptake at times of limitation. The fatty acid transporter *fadL* was also up-regulated (~6.5-fold) by ZraR, and work by Fang et al. (2005) showed *S*. Typhimurium uses fatty acids and acetate as its main source of carbon during chronic infections. Proteins responding to stress, such as the PSP ESR, and numerous σ^{54} regulated genes (including many bEBPs) are also up-regulated by *Salmonella* within this intracellular environment (García-del Portillo et al., 2008). Of the 186 genes differentially regulated by ZraSR overexpression, 89 belonged to the σ^{54} regulon, including all of the PSP operon. We hypothesised that this increase was due to ZraR function as a bEBP, resulting in the illusion that these genes were directly ZraR regulated; overexpression of the AAA+ domain of bEBPs had previously been used as an inducing tool for σ^{54} activation (Samuels et al., 2013). However, this may be incorrect and ZraR could be more involved in regulating these σ^{54} regulon members than we expected. The Cyo and Cyd terminal reductases are strongly down regulated in the SCV of fibroblasts and anaerobic respiration

proteins up-regulated to compensate for the hypoxic conditions (García-del Portillo et al., 2008). *cyoA* and several genes involved in anaerobic metabolism were also differentially regulated in our WT and ZraR overexpression strains. Although we saw *cyoA* transcription increase ~6-fold, and expression of *frdABCD*, *dcuAB*, *hybABC*, *hypO* decrease (all >2-fold) after ZraR overexpression, these results do suggest ZraR involvement in the regulation of these operons. The SPI-2 transcriptional regulator SlyA saw transcription decrease in *S*. Typhimurium post ZraR overexpression. SlyA confers resistance to oxyradicals and acts through the direct regulation of the SsrAB 2CST system to regulate function of SPI-2 and expression of SPI-2 associated genes (Linehan et al., 2005, Okada et al., 2007). *S*. *enterica* serovars containing insertions in the *slyA* gene exhibit attenuation in mouse models (Kaneko et al., 2002) and sensitivity to oxidative stress and cAMPs in macrophages (Linehan et al., 2005, Libby et al., 1994, Daniels et al., 1996). Down regulation of *slyA* by ZraR suggests fine-tuning of SlyA activity and consequently SPI-2 expression by ZraSR. When coupled with our proposed ZraR-mediated regulation of *mntH*, *fadL*, and the ability of ZraR to activate the PSP ESR and σ^{54} regulon, analysis of the ZraR regulon under anaerobic and SCV mimicking conditions would be needed to assess to what level, if any, our hypothesis is correct.

As described by Appia-Ayme et al. (2012) ZraP is a negative regulator of the ZraSR 2CST system and our qRT-PCR results concur with this analysis (Figure 36, B). A similar method of regulation is observed for the CpxAR ESR where CpxP represses activity of CpxR (Raivio et al., 1999), through the formation of CpxP-CpxA complexes (Tschauner et al., 2014). ZraS-ZraP associations are yet to be demonstrated but this would be the most obvious means through which ZraP conducts this means of feedback inhibition. A membrane-Strep-tagged protein interaction (mSPINE) experiment as used by Tschauner et al. (2014) to demonstrate CpxA-CpxP interactions could be used in this instance to observe ZraR-ZraP interactions *in vivo* and would be the most refined methodology to confirm this protein:protein interaction.

As proposed by Yamamoto et al., (2005) the fact that ZraR is phosphorylated independently of its cognate sensor kinase ZraS supports the point that this RR is activated by numerous inducing conditions. Although we were unable to ascertain any additional inducing conditions for ZraSR during our investigation, with the exception of entry into exponential growth, the inclusion of numerous unknown and uncharacterised genes as potential Zra regulon members highlights the potential ZraSR has for involvement in a variety of cellular processes. We originally wished to conduct our microarray comparing SL1344 WT and Δ*zraSR* strains in MOPS defined medium with excess zinc as a Zra inducing cue. However, as collecting the required concentration of total RNA under these conditions proved problematic, ZraR overexpression was the logical alternative. Completing these arrays for SL1344 and Δ*zraSR* strains after exposure to high zinc would help filter out the large number of σ^{54} regulon members present within our data set. If the same selection of genes were present within this second array as our ZraR overexpression data, this would add further weight to their categorisation as Zra regulated genes.

Since initial studies by Nishino et al., (2007) and Wang and Fierke (2009) assigned contribution to zinc tolerance as a key function of the Bae ESR system, this involvement has become widely accepted and unquestioned. Reproducing the methodologies adopted by these two groups for a variety of *E. coli* and *S. enterica* strains lacking *baeR* produced results that did not concur with those published (Figure 41, Figure 42). At the transcriptional level there is growing evidence to support Bae regulation of multiple efflux systems and the chaperone *spy* following exposure to high zinc concentrations (Srivastava et al., 2014, Yamamoto et al., 2008, Pletzer and Weingart, 2014). However, our growth analysis of Δ*baeR* strains shows that the influence of BaeR deletion on zinc tolerance in *E. coli* and *Salmonella* strains is not as severe as previously stated. Growth rates and *Td* values for *baeR* deletion mutants cultured in high zinc media do not differ significantly ($p>0.05$) from WT values (Figure 42) and are not representative of those previously published by Wang and Fierke (2013). The contribution of Bae to the bacterial zinc stress response we believe has been overstated and if

BaeSR ESR does contribute towards zinc homeostasis in these enteric species, the level of contribution is not sufficient to impact on survival of either species when the RR for this system, BaeR, is deleted.

Combined this work suggests Zra may help *Salmonella* survive the stresses inflicted upon it within the host immune system, not through direct regulation of zinc efflux systems, but through the regulation of a host of chaperones, HSPs and RRs. Even if future intracellular survival and infection assays do not highlight a function for the ZraSR 2CST system for maintaining viability and growth within the SCV, this study has provided more evidence to support ZraSR as an ESR and regulator of protein homeostasis.

To conclude, these investigations have expanded upon primary investigations of the newly characterised ESR ZraPSR (Leonhartsberger et al., 2001, Graham et al., 2009, Appia-Ayme et al., 2012). We have confirmed the feedback inhibition controlling Zra regulation and the first preliminary results to characterise the Zra regulon in *S*. Typhimurium. The final results chapter of this thesis focuses on the periplasmic component of the ZraPSR system, ZraP, and how this protein's structure affects its function as a molecular chaperone.

6 Analysis of ZraP function and structure – How zinc influences ZraP chaperone activity and quaternary structure

6.1 Introduction

6.1.1 Biochemical analysis of ZraP

It is crucial for bacterial adaptation and survival that signals denoting changes in envelope homeostasis and the occurrence of damaging environmental stresses (such as metal stress) are transduced to the cytoplasm, where an appropriate transcriptomic response can be elicited. In Gram-negative bacteria, these signals must transverse the OM and periplasm, in addition to the cell wall and IM present in Gram-positives. As has been described in previous chapters, the ESRs increase the transcription of proteases, chaperones and isomerases to repair and replace damaged envelope components. These quality control proteins are present throughout the periplasm and cytoplasm to ensure the whole cell envelope is protected.

The CpxP family of molecular chaperones consists of CpxP, Spy and ZraP, regulated by CpxAR, BaeSR and ZraSR ESRs respectively (see 1.5 to 1.10). Spy belongs to the CpxR and BaeR regulons and transcriptomic analysis presented in Chapter 5 suggests ZraSR involvement in induction of CpxP, independently of CpxAR (Figure 39). The X-ray crystal structures of all three proteins have been solved and the coordinates deposited in the RCSB protein data bank (PDB): CpxP (PDB ID: 3QZC) (Zhou et al., 2011), Spy (PDB ID: 3O39) (Kwon et al., 2010) and ZraP (PDB ID: 3LAY) (Centre for Structural Genomics of Infectious Diseases) (Figure 43). Despite ZraP and Spy sharing only 13% sequence identity at the amino acid level, and ZraP and CpxP 12% identity, all three chaperones possess similar structures and functions based on recent characterisations (Appia-Ayme et al., 2012, Quan et al., 2011, Zhou et al., 2011). ZraP structure was resolved as a decamer, with each ZraP monomer comprising two α-helices with a disordered tail region (residues 123-151). Both Spy and CpxP have a third α-helix that is lacking from ZraP (Figure 43) (Kwon et al., 2010, Quan et al., 2011), which, if present would interfere with the multimeric structure of ZraP. Appia-Ayme et al. (2012) describe the key structural differences between ZraP, CpxP and Spy. One residue of Spy (Pro56) and two residues of CpxP (Pro71 and

Pro72) contribute towards complete structural disorder in the N-terminal α-helix of these proteins. This disordered region is lacking from ZraP, but the ZraP N-terminal α-helix is kinked due to a broken hydrogen bond between the carbonyl of Thr61 and the amide of Ser64, resulting in increased stability of this region in ZraP compared to CpxP or Spy (Appia-Ayme et al., 2012). All three proteins have a conserved LTXXQ motif located within the N-terminal region of the protein: CpxP, LTEHQ residues 51 to 55, Spy, LTDAQ residues 57 to 61 and ZraP, LTTEQ residues 44-48. Spy and CpxP have a second C-terminal LTXXQ motif forming hairpins at the end of a central helix that aids the formation of stable homodimers (Kwon et al., 2010, Quan et al., 2011). ZraP however only possesses the single N- terminal LTTEQ motif.

In relation to zinc homeostasis, none of the CpxP chaperone family members are up-regulated >1.25-fold during zinc deficiency (Graham et al., 2009). Despite ZraP being characterised as a zinc binding protein, no Zn^{2+} ions are present in the ZraP structure deposited in the PDB and no zinc binding sites were located within ZraP using the prediction software TEMSP (3D Template based Metal Site Prediction) (Zhao et al., 2011, Appia-Ayme et al., 2012). Noll et al. (1998) described two zinc-binding domains, HMGMGH and HGGHGM, in ZraP (YjaI) of *Proteus mirabilis*. These domains are not present within the ZraP of *S*. Typhimurium (STM4172), however a similar domain, HRGGGH (residues 130-135) is found. Zn^{2+} ions predominantly form tetra-coordinate complexes, in addition to penta- and hexahedral geometries, with amino acid side chains and occasionally non-protein ligands (Alberts et al., 1998). As reviewed by Daniel and Farrell (2014) the function and dynamics of a specific Zn^{2+} binding site is dependant upon the type of ligand bound. Zinc sites are classified according to the type of amino acid and their position within the sequence, i.e. the pattern of the coordinated amino acids (Daniel and Farrell, 2014). Histidine was regarded as the most common Zn^{2+} ligand, followed by glutamine (Glu, Q), aspartic acid (Asp, D) and cysteine (Cys, C) (Vallee and Auld, 1993). However, analysis of X-ray and NMR structures shows that Cys has a 50-75% propensity to be a zinc ligand in structural proteins, with His averaging ~35% (Patel et al., 2007). Cysteines bind zinc with high affinity and Zn^{2+}-Cys complexes contribute

towards protein catalysis and regulation as well as structure (Tainer et al., 1991, Giles et al., 2003). There is only one Cys located within the amino acid sequence of *S*. Typhimurium ZraP, Cys132, which is flanked by Gly (G) residues and a Tyr (Y) (see Appendix M for peptide sequences of CpxP superfamily members). There are four histidines in ZraP, residues His28 and His29 and two within the C-terminal HRGGGH motif at residues His44 and His49 (Appendix M). The glycines separating these His residues confer flexibility to this motif.

Zinc also has the propensity to influence quaternary protein structure. In this case zinc-binding ligands are found at the interface between two proteins and the zinc site that results has the coordination properties of a catalytic or structural Zn^{2+} binding site (Auld, 2001). As the proposed zinc-binding domains of *S*. Typhimurium ZraP (HRGGGH and the cysteine containing motif GGCGGY) are found in the disordered tail of the protein, it is possible that this flexible loop is involved in stabilising quaternary protein structure. Along with the N-terminal LTXXQ motif known to stabilise dimerization of CpxP and Spy, this zinc-binding domain could compensate for the lack of a C-terminal LTXXQ motif in ZraP, present in CpxP and Spy.

The involvement of the N-terminal LTTEQ motif of ZraP in the formation of ZraP multimeric structures will be investigated throughout this chapter. The possible involvement of ZraP residues 130-135 (HRGGGH) and 120-125 (GGCGGY) in zinc binding will also be looked at to establish the importance of zinc in ZraP chaperone function and if any zinc ions bound contribute towards the stability of ZraP higher-order oligomers.

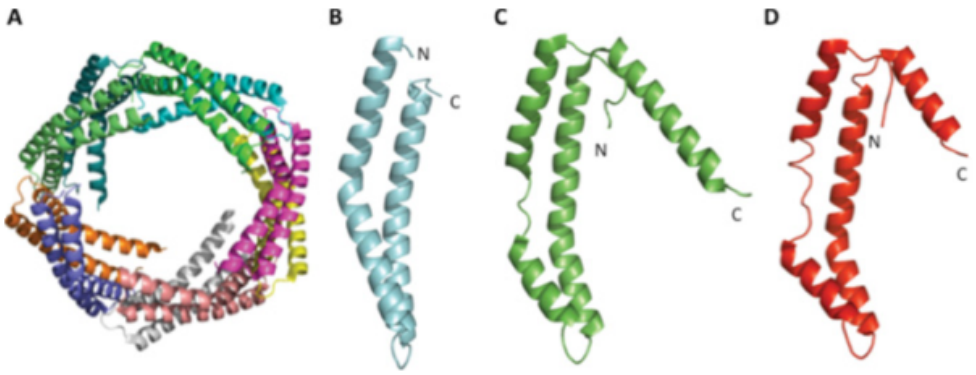

Figure 43: Diagrammatic representations of the known crystal structures of the Cpx family of molecular chaperones. A cartoon representation of the decameric ZraP protein (PDB ID: 3LAY) (**A**) is depicted alongside residues Leu44–Glu122 of the ZraP monomer (**B**). Residues His44–Lys151 of the CpxP monomer (**C**) (PDB ID: 3QZC) and residues Phe29–Thr124 of the Spy monomer (D) (PDB ID: 3O39). The third α-helix present in CpxP and Spy, but absent from ZraP is clearly visible. Taken from Appia-Ayme et al. (2012).

6.1.2 ZraP higher-order structure analysis

One methodology used during our analysis of ZraP structure is analytical ultracentrifugation (AUC, also referred to as sedimentation velocity [SV], SV-AUC or AU), described in 6.3.5. This technique is advantageous to size exclusion chromatography as solutes can be analysed in a range of solvents (e.g. changing pH and ionic strength conditions), across a broad range of solute concentrations, it is non-destructive (samples can be recovered post analysis) and samples can be analysed in their native state and under biologically relevant conditions (Cole et al., 2008). Appia-Ayme et al. (2012) used AUC to ascertain the role Zn^{2+} plays on ZraP conformation, confirming ZraP forms a zinc-dependant higher order structure. The presence of Zn^{2+} increases the overall size of ZraP oligomers from an average molecular weight (M_w^{av}) of 73 ±1 KDa (in the presence of the chelator EDTA) to 202 ±10 KDa, when 60 μM $ZnCl_2$ was included in the AUC buffer (Appia-Ayme et al., 2012). Our work presented during this chapter extends these studies, investigating how the LTXXQ (residues 44-48) motif and two proposed zinc-binding domains of ZraP, HRGGGH (residues 130-135) and GGCGGY (residues 120-125), contribute to the oligomeric structure of ZraP.

In summary, AUC experiments will help us to understand how the CpxP-like chaperone family function within the periplasm and the active forms they take. These investigations are needed if we are to understand the target of these chaperones, their mechanism of protection and their specificity.

6.2 Aims

This chapter compliments the transcriptomic analysis of ZraSR outlined in Chapter 5 through structure and functional analysis of ZraP, an accessory protein and negative regulator of the ZraSR 2CST system. Chapter 6 aims to confirm 1) the location of ZraP zinc-binding domains and 2) the contribution of the LTXXQ motif to ZraP higher-order oligomerisation. Together these aims help elucidate the role of zinc in ZraP function and structural stability.

6.3 Experimental Design

6.3.1 Site-directed mutagenesis (SDM)

All polymerase chain reactions (PCRs) were conducted as per 2.4.1 using ultra-stable *Taq* DNA Polymerase and *Phusion*™ high-fidelity DNA polymerase and their reagents (Table 5). Elongation time was calculated as one minute per one kilobase-pair (Kbp) of product (Table 7) using a DNA engine PTC 300 (BIORAD) PCR machine. All primers used during this work were synthesised by Integrated DNA Technologies (IDT) (Table 5).

SDM template DNA was pBAD*zraP* plasmid DNA (Table 4). Specific amino acids of ZraP (Table 11) were mutated at the codon level using a QuikChange® Lightning Site-Directed Mutagenesis Kit (Agilent Technologies) (2.4.9).

6.3.2 Purification of WT and recombinant ZraP protein

E. coli (Top10) harbouring ZraP WT (p*zraP*) or plasmids containing mutated cDNA (pLTXXA, pAAAAA, pHRGGAH or pSDMB) was grown in the presence of Amp and *L*-arabinose (0.02% w/v) (2.4.15.2). Cells were

harvested and protein purified (2.4.15) and fractions analysed by SDS-PAGE to assess purity (2.4.16). Sample concentrations were assessed by Bradford assay (2.4.19) and by measuring A_{280} on a Nanodrop 2000. Samples were aliquoted into appropriate volumes, snap frozen and stored at -80˚C.

6.3.3 Protein aggregation assays

MDH protein aggregation assays were as described in 2.4.24.

6.3.4 Malate dehydrogenase (MDH) activity assays

Residual activity of MDH after guanidine hydrochloride (GdnHCl) treatment was measured in the absence and presence of ZraP (2.4.25). Raw data were normalised to background levels of scattering and plotted against time (min).

6.3.5 Analytical ultracentrifugation (AUC)

AUC is a proven methodology for the characterisation and quantification of macromolecules in free solution (Lebowitz et al., 2002, Cole et al., 2008, Zhao et al., 2013, Howlett et al., 2006). By measuring the sedimentation rate, the rate at which molecules move in response to centrifugal force, AUC utilises the fundamental laws of gravitation and the principle properties of mass to define the size and shape of a macromolecule, as well as interactions between macromolecules.

Samples are loaded into small chambers (cells) and spun at high speeds in an analytical ultracentrifuge. The centrifugal force applied to the sample gradually moves the solute (our protein) away from the centre of the centrifuge over time. This movement slowly increases the solute concentration at the outer edge of the rotor, producing a concentration gradient across the cell. Centrifugation continues until sedimentation equilibrium is reached, i.e. until all of the protein is concentrated at the outside of the cell. This concentration distribution across the cell is measured at regular time points throughout the centrifugation process. These values can then be plotted against their position within the cell ($radius^2$) to calculate the rate of sedimentation, the sedimentation coefficient. The sedimentation coefficient depends on the molecular weight and size of the solute (the larger

the protein the faster sedimentation takes place). Sedimentation velocity experiments were performed using a Beckman Optima XL- I equipped with absorbance optics as described in 2.4.23.

6.3.6 Native PAGE and formaldehyde chemical cross-linking of protein oligomers

Our WT ZraP protein and four ZraP variants ZraP-LTTEA, ZraP-AAAAA, ZraP-HRGGAH and ZraP-SDMB were subjected to formaldehyde chemical cross-linking (2.4.17). Samples were visualised on native polyacrylamide gels (6% acrylamide w/v) (Table 16).

6.4 Results

6.4.1 ZraP protects MDH from denaturation by guanidine hydrochloride (GdnHCl)

By measuring the residual NADH oxidase activity of malate dehydrogenase (MDH), post denaturation in the presence of ZraP, one can determine to what extent ZraP protects protein function. MDH samples were incubated with and without ZraP and exposed to the chemical denaturant GdnHCl at a range of concentrations (0-2 M). Initial rates of NADH oxidation by MDH, using oxaloacetate as a substrate, were determined for each GdnHCl concentration tested. MDH oxidase activity reduced proportionally as GdnHCl concentration increased, confirming MDH denaturation and loss of function (Figure 44). When ZraP was added during chemical denaturation of MDH, MDH oxidase activity subsequently improved. Initial NADH oxidation rates were higher for all MDH samples in the presence of ZraP, when incubated with GdnHCl concentrations <1.6 M (Figure 44). No MDH function was observed following exposure to GdnHCl ≥1.6 M (Figure 44). This preliminary investigation provides us with an accurate and appropriate assay for measuring chaperone activity and could be expanded to investigate other denaturing conditions including heat, organic solvents and other chemical denaturants.

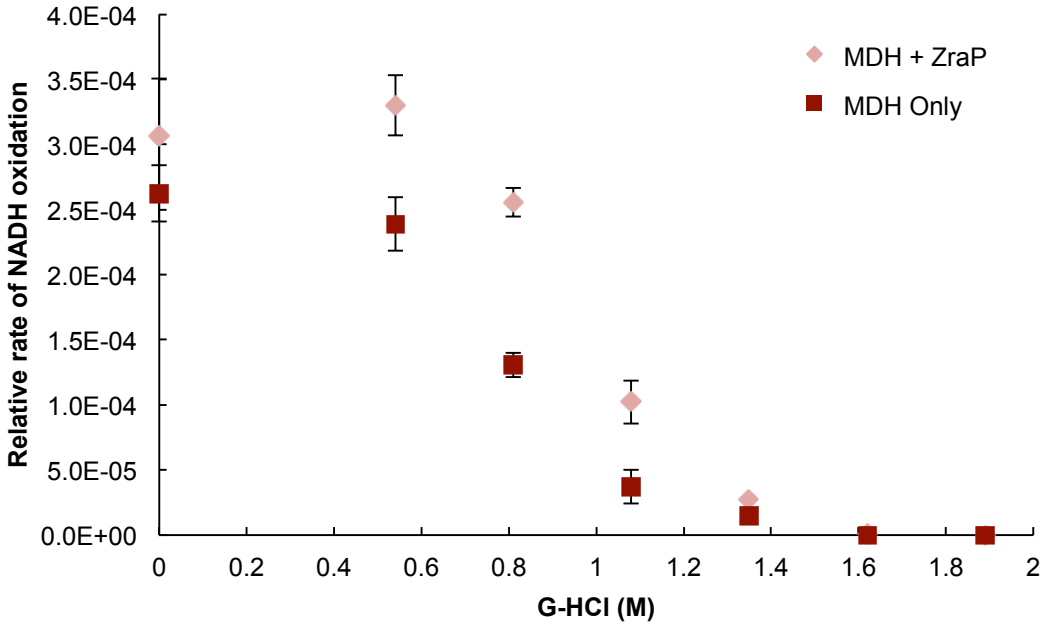

Figure 44: ZraP protects MDH function during chemical denaturation with GdnHCl. Residual NADH oxidase activity of 70 µM MDH in 50 mM HEPES/HCl, pH 7.4, 1 mM $ZnCl_2$, 0.1 mM NADH after incubation at RT with GdnHCl (0 - 1.89 M) in 50 mM HEPES, 1 mM $ZnCl_2$ (■). Assays were repeated with the addition of 70 µM ZraP WT (◆). *n* = 4, Error bars = SD.

6.4.2 Production and purification of ZraP site-directed mutants

Amino acid substitutions within three ZraP motifs of interest, LTTEQ, HRGGGH and GGCGGY were made by site-directed mutagenesis (SDM) (using a QuikChange® Lightning SDM Kit) or included when pSDMB was synthesised (GenScript). A summary of the amino acid substitutions resulting from site-specific point mutations incorporated into the cDNA of ZraP are summarised in Table 10.

The LTTEQ motif of ZraP was one focus of investigations because of the involvement of similar LTXXQ motifs in stabilising CpxP and Spy homodimers (Kwon et al., 2010, Quan et al., 2011). Due to the relatively low resolution of the X-ray crystal structure of ZraP (PDB ID: 3LAY), it is unknown whether this LTTEQ motif contributes towards stability of the decameric barrel structure formed by ZraP in its multimeric state (Figure 43). We aimed to produce six mutated versions of this LTXXQ motif to establish 1) what contribution, if any, LTTEQ makes in ZraP higher-order

oligomerisation and 2) which specific amino acids are involved. These six recombinant versions included single alanine substitutions at each residue of this motif (L44A, T45A, T46A, E47A, Q48A) and replacement of all five LTTEQ amino acids with alanines (LTTEQ to AAAAA). Unfortunately, only two of these six mutations were successfully made and confirmed by sequencing, a Q48A mutation (plasmid pLTTEA) and a full motif replacement of LTTEQ to alanines, AAAAA (plasmid pAAAAA) (Table 10).

The C-terminal HRGGGH motif of ZraP was suggested to be a zinc-binding domain by Appia-Ayme et al. (2012), due to similarity in sequence and position to the zinc binding domains of *Proteus mirabilis* ZraP (HMGMGH and HGGHGM) (Noll et al., 1998). Once again we aimed to produce six mutated versions of this HRGGGH motif to establish 1) what contribution, if any, HRGGGH makes to ZraP-Zn^{2+} binding, i.e. if these amino acids are zinc ligands forming a zinc binding pocket and 2) which specific amino acids are involved. However, only a single alanine amino acid substitution at Gly134 was successfully made (plasmid pHRGGAH) (Table 4). The GGCGGY motif (residues 120-125) was of interest as a possible second zinc-binding site as cysteines are the most common ligands for zinc when it functions to stabilise protein structure and Cys132 is the only Cys residue present in *S.* Typhimurium ZraP. This Cys132 residue along with four surrounding glycines (G130, G131, G133 and G134) and a tyrosine (Y135) were substituted for alanines (plasmid pSDMB). This recombinant *zraP* cDNA was synthesised by GenScript (pUC57*zraP*SDMB) and sub-cloned into pBAD Myc His A to produce the pSDMB plasmid (Table 4). This was a faster and cleaner method than constructing the site-directed mutant through PCR, as was the case for pLTTEA, pAAAAA and pHRGGAH.

The presence of cDNA mutations was confirmed by sequencing. All four C-terminal 10xHis-tagged recombinant constructs, pLTTEA, pAAAAA, pHRGGAH and pSDMB were successfully transformed into *E. coli* TOP10 cells and expression of recombinant ZraP proteins induced by the addition of 0.2% (w/v) *L*-arabinose (data not shown). Overexpression and purification was conducted as described in 2.4.15. Elution profiles of ZraP-LTTEQ, ZraP-

AAAAA, ZraP-HRGGAH and ZraP-SDMB are shown in Figure 45. Fractions spanning the elution phase of purification were resolved by 15% SDS-PAGE, confirming recombinant ZraP purification at >95% purity as judged by eye (Figure 45). WT ZraP has a molecular weight of 13.5 KDa and bands corresponding to the molecular weights of N-terminal polyhistidine (6xHis) tagged ZraP-LTTEA, ZraP-AAAAA, ZraP-HRGGAH and ZraP-SDMB are clearly visible at ~15KDa. By combining our purification fractions for each protein, samples were able to be further concentrated and buffer exchanging into 50 mM HEPES buffer through 10,000 Da size exclusion centrifugation columns removed any protein contaminants of <10KDa visible following SDS-PAGE analysis. The fractions visualised here (Figure 45) were used during all ZraP assays described.

6.4.3 Chaperone activity of ZraP is zinc dependent, requires residues G120-Y125 and occurs independently of an LTXXQ motif conserved within the CpxP-like superfamily of molecular chaperones

Chaperone activity of purified WT ZraP and recombinant site-directed mutants, (ZraP-AAAAA, ZraP-HRGGAH and ZraP-SDMB) were determined and compared, as described previously by Quan et al. (2011). This protein aggregation assay measures the rate of MDH thermal aggregation (43°C, 20 min), in 50 mM HEPES buffer with or without our proteins of interest, by means of light scattering. As thermal aggregation increases, so does light scattering, measured at $\lambda_{excitation}/\lambda_{emission}$ of 360 nm with a CARY Eclipse fluorimeter (2.4.24). WT ZraP has a protective role during this process, reducing the rate at which MDH aggregates under thermal stress (Appia-Ayme et al., 2012). This protective nature was enhanced in the presence of zinc, highlighting the importance of Zn^{2+} ions for ZraP to function correctly. By comparing light scattering levels when MDH is incubated with WT ZraP or our recombinant ZraP proteins during non-specific thermal aggregation, we are able to assess if our amino acid substitutions have altered key sites important for ZraP chaperone function. These experiments were repeated in

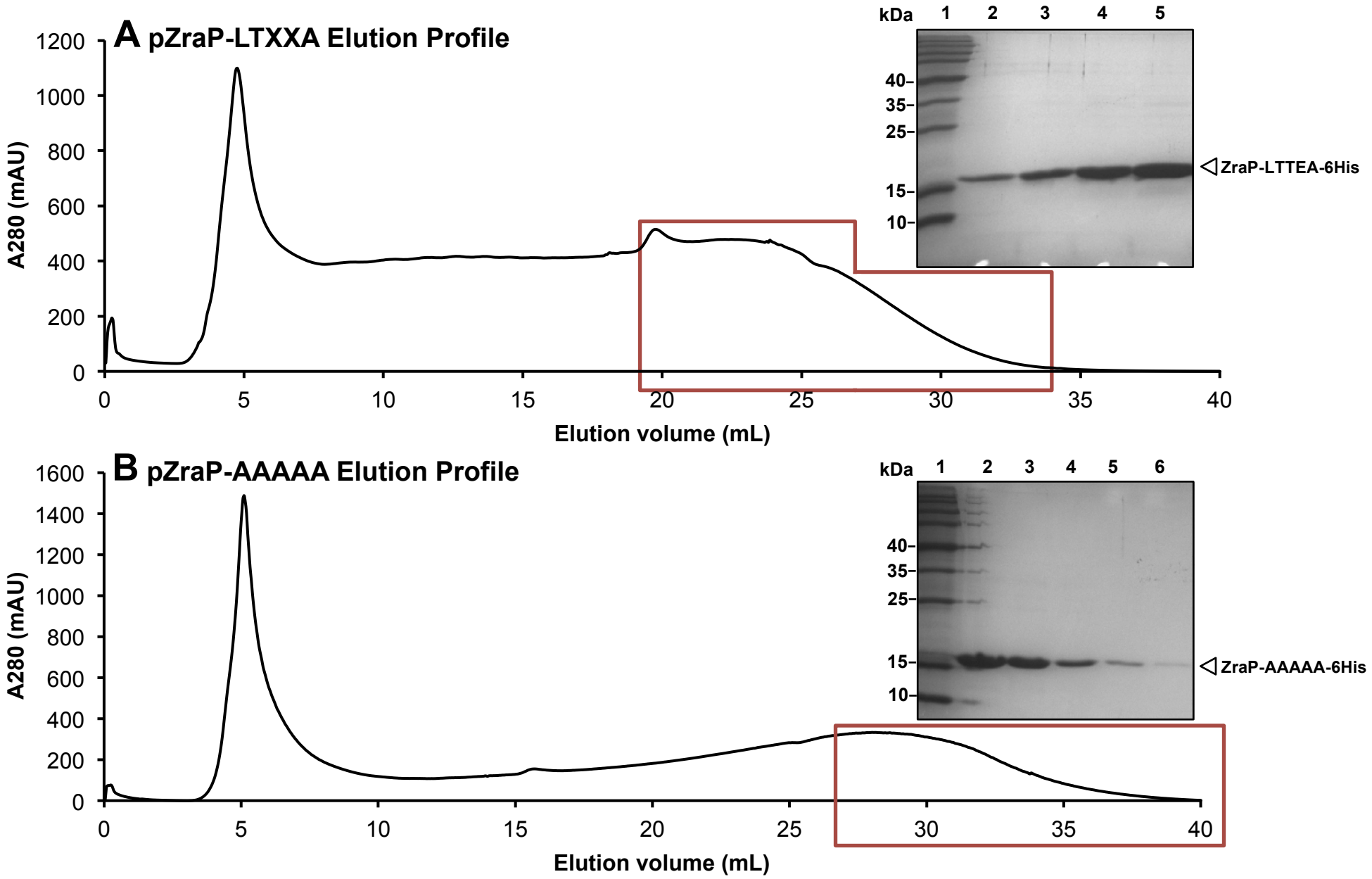
A pZraP-LTXXA Elution Profile
A280 (mAU)
Elution volume (mL)
kDa
1
2
3
4
5
40
35
25
15
10
ZraP-LTTEA-6His
B pZraP-AAAAA Elution Profile
A280 (mAU)
Elution volume (mL)
kDa
1
2
3
4
5
6
40
35
25
15
10
ZraP-AAAAA-6His

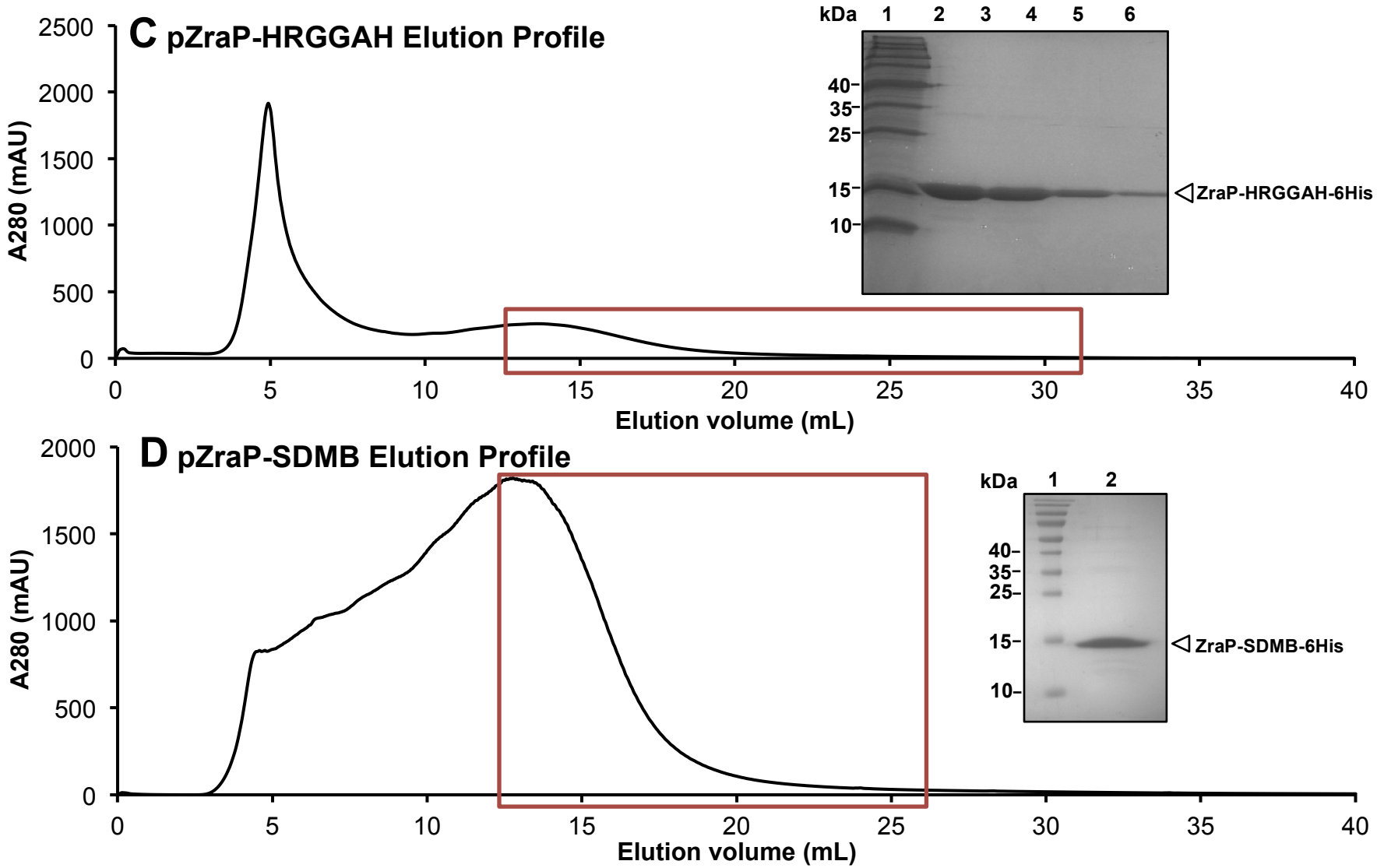

Figure 45: **Elution profiles and SDS-PAGE analysis of ZraP recombinant proteins.** Gel images show a sample of combined fractions from red box on elution profiles A) ZraP-LTTEA (*lanes 2-5*), B) ZraP-AAAAA (*lanes 2-6*), C) ZraP-HRGGAH (*lanes 2-5*) and D) ZraP-SDMB (*lane 2*). Proteins were stained with SimplyBlue™ SafeStain Coomassie® G-250 stain. PageRuler™ Prestained Protein Ladder was used as a molecular marker on all gels (*Lane 1*).

buffers containing differing concentrations of zinc to determine the impact these mutations have on zinc binding, affording a direct comparison between zinc binding and function. Our ZraP-LTTEA mutant was not included during these screens, as any negative impact of ZraP function by the Q48A substitution would be observed during analysis of ZraP-AAAAA. If this ZraP-AAAAA mutant showed differing chaperone function to ZraP WT than each residue in turn would be investigated.

Our experiments confirmed the results seen by Appia-Ayme et al., (2012) with ZraP WT suppressing the onset of light scattering, and therefore thermal aggregation of MDH, in a similar pattern to that observed for Spy (Quan et al., 2011) (Figure 46, A). Protection afforded by ZraP WT was again improved in the presence of zinc (Figure 46, A). The addition of $ZnCl_2$ alone had no affect on MDH aggregation (data not shown). ZraP WT, recombinant ZraP proteins and buffer only controls were run in parallel to confirm no influence on MDH aggregation and light scattering (Figure 46; Figure 47). Our recombinant ZraP proteins were subjected to the same assays, and for ZraP-AAAAA (Figure 46, B) and ZraP-HRGGAH (Figure 46, C) the results concurred with those observed for WT ZraP. Thermal aggregation of MDH reduced by 100-150 units from ~330 units with the addition of 198 nM ZraP WT, ZraP-AAAAA or ZraP-HRGGAH (Figure 46). The protective nature of ZraP-AAAAA and ZraP-HRGGAH was enhanced with $ZnCl_2$ (10 μM) addition, concurring with data obtained for ZraP WT under the same conditions (Figure 46, A; Appia-Ayme et al., 2012). The mutations introduced within LTTEQ and HRGGGH motifs therefore had no detrimental effect on the chaperone activity of ZraP *in vitro* and our recombinant proteins performed as WT during our MDH aggregation assay.

The most intriguing results were recorded for the ZraP variant ZraP-SDMB (ZraP site-directed mutant B), harbouring six alanine substitutions (G120A, G121A, C122A, G123A, G124A, Y125A) within a second possible zinc-binding site proposed during this study (6.1.1). MDH thermal aggregation reduced with the addition of 198 nM ZraP-SDMB in the absence of zinc by ~150 units (Figure 47, A), comparable to levels seen for ZraP WT, ZraP-

AAAAA and ZraP-HRGGAH under the same conditions. However, the addition of $ZnCl_2$ did not enhance ZraP-SDMB chaperone function, as was the case for ZraP-WT, ZraP-AAAAA and ZraP-HRGGAH. ZraP-SDMB in 50 mM HEPES supplemented with 10 μM $ZnCl_2$ returned final MDH aggregation levels only slightly lower than that observed for MDH in the absence of a chaperone, ~310 units (Figure 47, A). When these results were repeated with the addition of $ZnCl_2$ at 10-fold increments (0 μM, 0.1 μM, 1 μM and 10 μM), aggregation of MDH increased correspondingly (Figure 47, B). In the presence of ZraP-SDMB, addition of 10 μM $ZnCl_2$ increased the rate of MDH thermal aggregation the most (~150 units), compared to 0 μM $ZnCl_2$ (Figure 47, B). Although ZraP-SDMB with 1 μM $ZnCl_2$ present produced slightly higher levels of MDH thermal aggregation than 0.1 μM, the differences in MDH aggregation at these two $ZnCl_2$ concentrations was negligible. Yet both conditions reduce chaperone activity of ZraP-SDMB compared to no zinc, and offer better protection than 10 μM $ZnCl_2$ (Figure 47).

6.4.4 ZraP-SDMB is unable to form higher order multimers

6.4.4.1 ZraP-SDMB predominantly forms monomers as seen by chemical cross-linking

As described in 6.4.3, protein aggregation assays alluded to alterations in ZraP function as a result of site-specific amino acid substitutions present in our recombinant ZraP protein ZraP-SDMB. However, additional analysis of the structure of all four of our recombinant proteins must be ascertained if the impacts of these point mutations are to be fully understood.

One means of visualising ZraP multimers was through chemical cross-linking of our purified proteins. By comparing the protein-protein interactions within our WT and recombinant ZraP samples we can visualise any discrepancies in oligomer formation as a result of our amino acid substitutions.

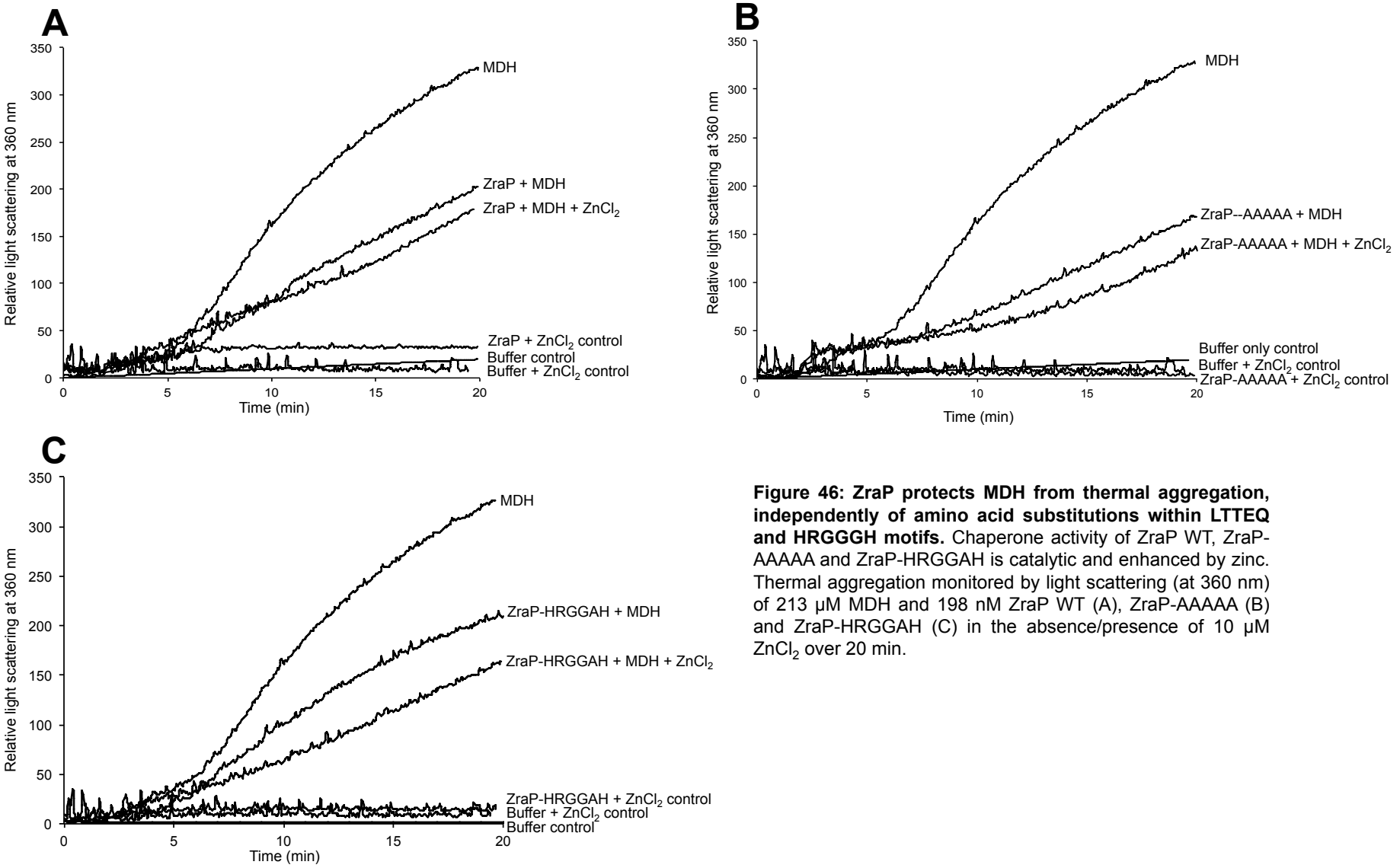

Figure 46: ZraP protects MDH from thermal aggregation, independently of amino acid substitutions within LTTEQ and HRGGGH motifs. Chaperone activity of ZraP WT, ZraP-AAAAA and ZraP-HRGGAH is catalytic and enhanced by zinc. Thermal aggregation monitored by light scattering (at 360 nm) of 213 µM MDH and 198 nM ZraP WT (A), ZraP-AAAAA (B) and ZraP-HRGGAH (C) in the absence/presence of 10 µM $ZnCl_2$ over 20 min.

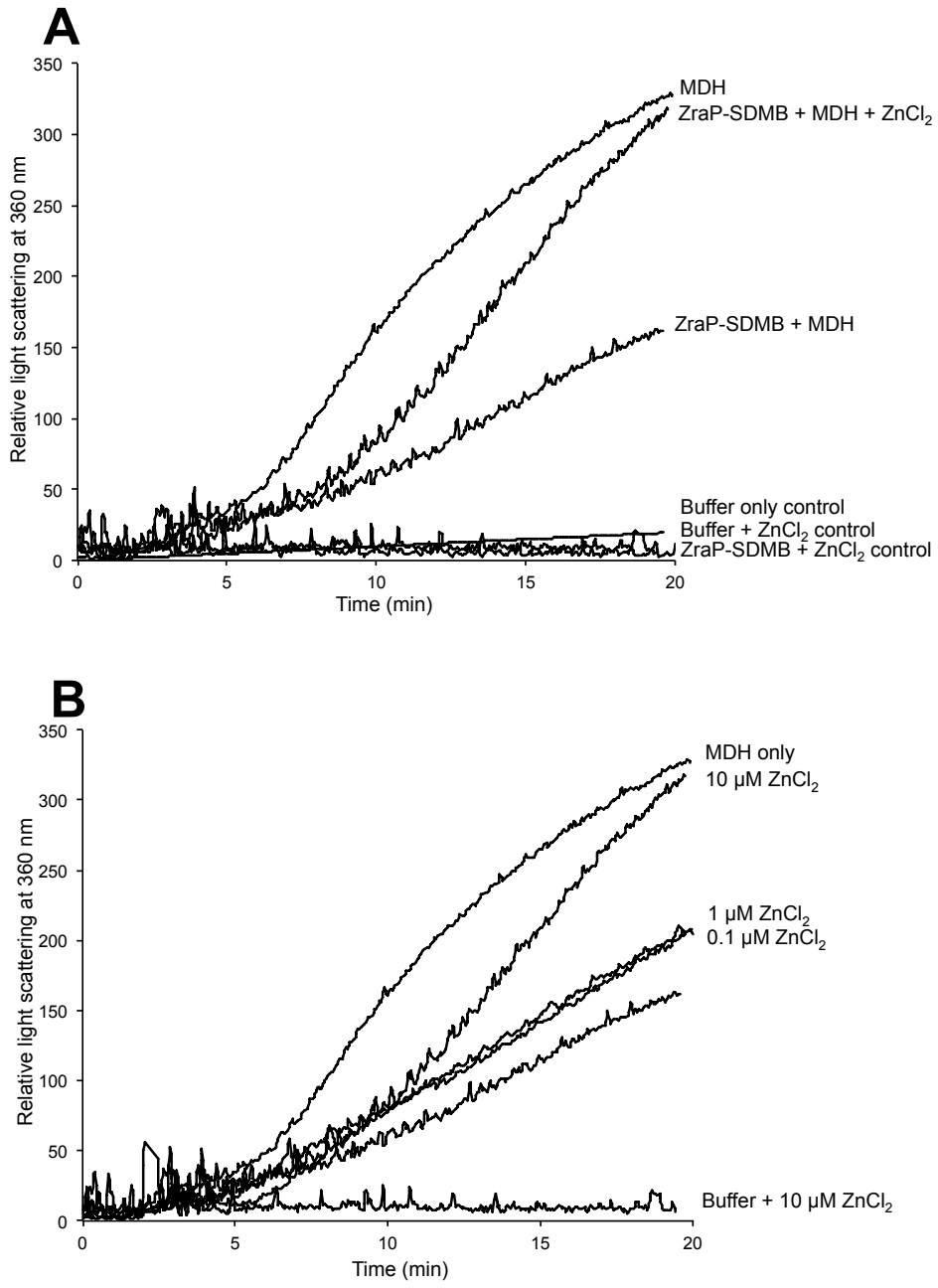

Figure 47: ZraP-SDMB protects MDH from thermal aggregation, activity that is lost upon the addition of zinc chloride. Thermal aggregation monitored by light scattering (at 360 nm) of 213 μM MDH and 198 nM ZraP-SDMB (A) in the absence/ presence of 10 μM $ZnCl_2$ over 20 min and (B) with increasing zinc concentrations (0 μM, 0.1 μM, 1 μM and 10 μM). Increasing $ZnCl_2$ concentrations negatively affects ZraP-SDMB chaperone activity.

Following formaldehyde cross-linking and resolving by native PAGE, we saw a marked reduction in the size of higher order oligomeric complexes formed by our ZraP variant ZraP-SDMB (Figure 48, lane 3) compared to ZraP WT (Figure 48, lane 2). Our remaining ZraP variants, ZraP-LTTEA, ZraP-AAAAA and ZraP-HRGGAH (Figure 48, lane 4, 5 and 6) presented little or no difference to the WT protein sample after chemical cross-linking. Although multimers are present at 35 kDa and 15 kDa in all five samples, the majority of the purified ZraP-SDMB is 15kDa in size, suggesting this ZraP variant predominantly resides in its monomeric state. ZraP monomers are present in the other four samples tested (lanes 2, 4, 5 and 6), but the most common multimer present in these ZraP-WT, ZraP-LTTEA, ZraP-AAAAA and ZraP-HRGGAH samples are ~35kDa in size, likely to be protein dimers. No ZraP-SDMB complexes larger than ~35kDa were observed in our ZraP-SDM sample, whereas high molecular weight complexes of >70 kDa were formed by ZraP-WT, ZraP-LTTEA, ZraP-AAAAA and ZraP-HRGGAH.

These results imply that mutating the proposed zinc-binding site GGCGGY in ZraP (G120A, G121A, C122A, G123A, G124A, Y125A) hinders the ability of ZraP to form larger, multimeric complexes, with dimers being the largest complex formed by the ZraP-SDMB variant. Formaldehyde cross-linking stabilises protein-protein interactions, including those of a transient nature (Klockenbusch and Kast, 2010). Although this methodology only provides a ‘snap shot’ of our ZraP samples at one moment of time, it gives our first suggestion that the GGCGGY motif is crucial for ZraP oligomerisation or that this specific region of the ZraP protein is involved at the interface between ZraP monomers, when higher order multimers are formed. Although this *in vitro* data does not conclusively show that ZraP-SDMB is completely unable to form higher order oligomers, it is suggestive of instability when larger multimers are formed and that the ZraP-SDMB variant, when compared to ZraP-LTTEQ, ZraP-AAAAA or ZraP-HRGGAH is the most likely to exhibit differential quaternary structure to the WT equivalent.

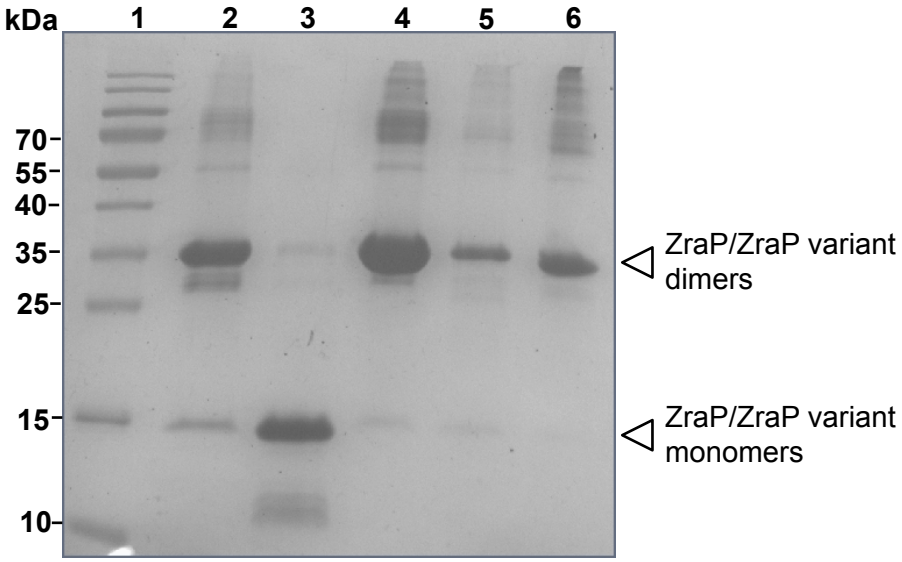

Figure 48: **Native PAGE of formaldehyde cross-linked ZraP WT and ZraP variants**. Protein samples (1 mg/mL) ZraP WT (2), ZraP-SDMB (3), ZraP-LTTEA (4), ZraP-AAAAA (5) and ZraP-HRGGAH (6) were treated with 1% (v/v) formaldehyde, pH 8, for 1 min. 2 M glycerol was added to halt the reaction before samples were resolved by native PAGE. Proteins were stained with SimplyBlue™ SafeStain Coomassie® G-250 stain. PageRuler™ Prestained Protein Ladder was used as a molecular marker (*Lane 1*).

6.4.4.2 Mutations within the ZraP-SDMB motif impacts on the formation of multimeric structures of ZraP

Sedimentation velocity experiments permitted the biophysical properties of recombinant ZraP proteins to be examined and an apparent weight average molecular mass for each to be calculated in the presence of zinc and the chelator EDTA. During preliminary experiments, a total of five scans per sample were recorded during centrifugation (6.3.5), once equilibrium had been reached. A single species model (Demelar, 2005) in Ultrascan II was used to fit the sample scans and the average molecular mass (M_w^{av}) taken to be the concentration at the middle point, using Equation 2. Fitted data for all four recombinant proteins are plotted in Figure 49 (lower panels) for both scan speeds (7,000 rpm and 10,000 rpm). Plotting ln absorbance versus radius^2-radius$_{(ref)}^2$ produces a linear line, where the gradient is proportional to the molecular mass of the single species. The residual absorbance, calculated by subtracting the experimental data from the simulated fit, shows the quality of fit between the experimental and the simulated best-fit data presented in Figure 49 upper panels.

Fitting each absorbance profile to a single species gave an M_w^{av} of ~238 kDa for ZraP-LTTEA, 330 kDa for ZraP-AAAAA, ~208 kDa for ZraP-HRGGAH and ~268 kDa for ZraP-SDMB, in the presence of 60 μM $ZnCl_2$. ZraP has a predicted molecular mass of 13.5 kDa in its monomeric state. Our results suggest ZraP-LTTEA forms an oligomer of ~18 monomers in the presence of $ZnCl_2$, compared to ~25 monomers for ZraP-AAAAA, ~15 monomers for ZraP-HRGGAH or ~20 monomers for ZraP-SDMB. Under the same conditions, ZraP WT has a molecular weight of ~202 kDa, comprising an oligomer of ~15 monomer (Appia-Ayme et al., 2012), a value almost identical to that observed for ZraP-HRGGAH. The remaining three recombinant proteins form oligomers larger than that obtained for ZraP WT, the largest of which for ZraP-AAAAA contains ~10 more monomers than the oligomeric form of ZraP WT.

The AUC data presented in Figure 49 for ZraP-LTTEA, ZraP-AAAAA and ZraP-HRGGAH concurs with the higher order oligomerisation observed during our native page analysis (Figure 48). However, the data in Figure 49 for ZraP-SDMB suggests that this ZraP variant is able to produce oligomers not observed during our native page analysis when 60 μM $ZnCl_2$ is present (Figure 48). From these preliminary experiments (Figure 49) we designed a second round of AUC to investigate the affect of EDTA addition on ZraP oligomerisation. All four recombinant ZraP samples were subjected to AUC using the same buffers as previously, but with the addition of 10 mM EDTA and no surplus $ZnCl_2$. Absorbance was again measured at 280 nm but samples were subjected to higher spin speeds of 23,000 rpm and 30,000 rpm to ensure equilibrium was reached should smaller protein species be present. The data no longer fitted a single species model suggesting a heterogeneous population of protein complexes. Fitting each absorbance profile to a two-component model gave an M_w^{av} of 20kDa and 68kDa (at ~1:3 ratio) for ZraP-LTTEA, 18kDa and 136 kDa (at an ~2:1 ratio) for ZraP-AAAAA, and our ZraP-HRGGAH samples contained 18kDa and 109kDa species (at ~2:1 ratio) (Table 30). The protein species present in all three samples (18-20 kDa) are indicative of the formation of monomers or a

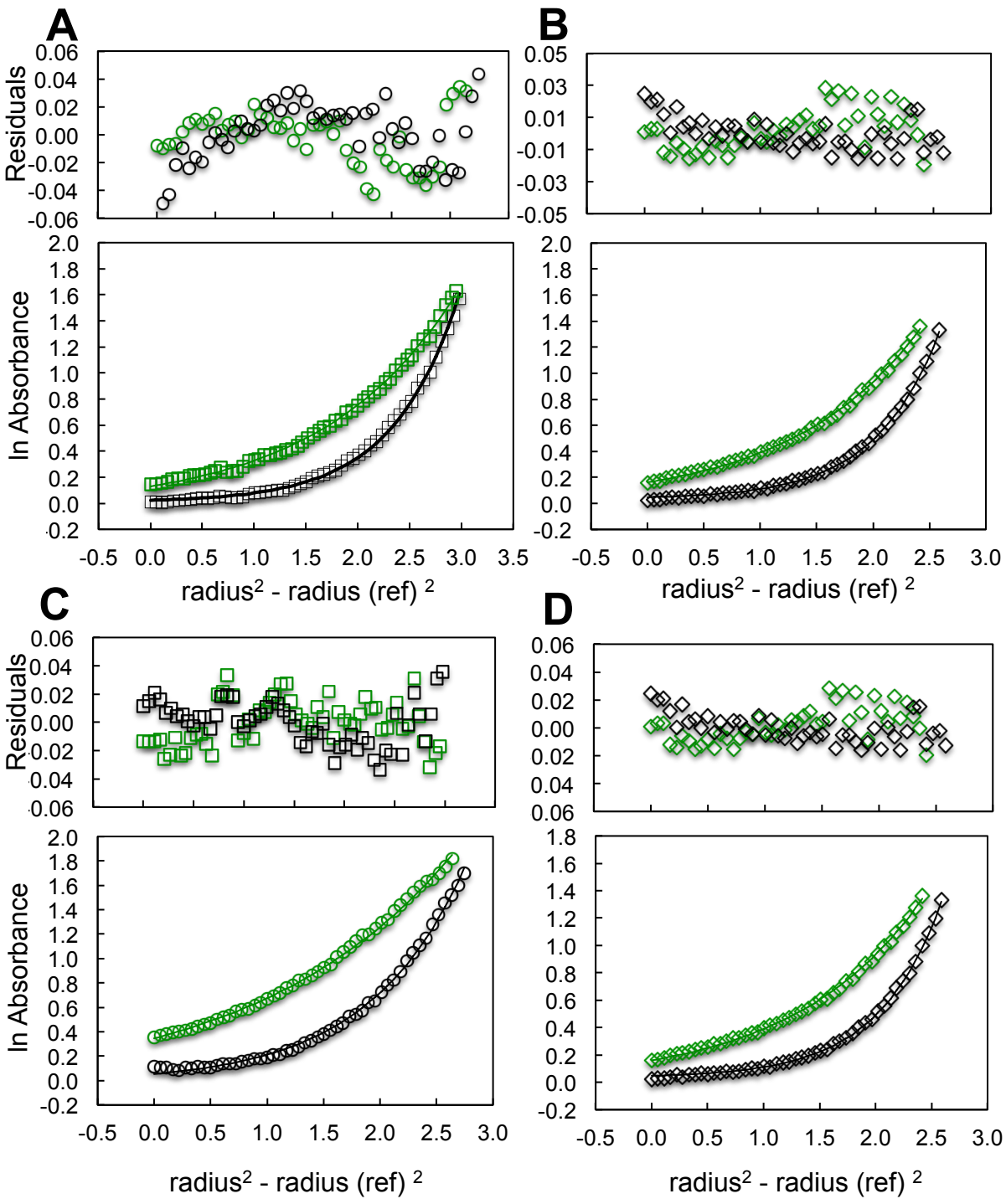

Figure 49: Preliminary sedimentation equilibrium analysis of recombinant ZraP oligomers at 7,000 rpm (GREEN) and 10,000 rpm (BLACK): *Lower panels.* Absorbance profile of 198 nM recombinant ZraP: **A**) ZraP-LTTEA, **B**) ZraP-AAAAA, **C**) ZraP-HRGGAH and **D**) ZraP-SDMB, measured at A_{280} in the presence of 60 μM $ZnCl_2$. Each profile was fitted to a single species, non-interacting model (**solid line**). Absorbance data in the non-linear range of 0 - 0.02 AU have been excluded from the plot. *Upper panels:* residual difference between the experimental data for each absorbance profile and fitted curves.

heterogeneous mixture containing ZraP oligomers 5 to 10 subunits (68-136kDa) during metal chelation (Figure 50). These second AUC results (Figure 50) again agree with the native page analysis of ZraP-LTTEA, ZraP-AAAAA and ZraP-HRGGAH where a population of different sized oligomers was seen (Figure 48). ZraP-WT presented a M_w^{av} of 73±1 kDa when incubated with 10 mM EDTA i.e. a complex containing approximately five ZraP monomers (Appia-Ayme et al., 2012). ZraP-LTTEA incubated with EDTA produces results virtually identical to those observed for the WT protein.

Initial AUC data for ZraP-SDMB with 10 mM EDTA only fits a single species model, and gave an average molecular mass of ~6 kDa (Figure 49). This result suggested loss of all oligomerisation and possible tertiary structure for this recombinant protein in the presence of EDTA. Data was only available for the higher spin speed of 30,000 rpm, as 23,000 rpm did not result in equilibrium being reached (data not shown). Our ZraP-SDMB protein was therefore subjected to a third round of AUC, with three conditions analysed, 60 µM $ZnCl_2$, 120 µM $ZnCl_2$ and 10 mM EDTA (Figure 51, A-C). In the presence of $ZnCl_2$, ZraP-SDMB produced multimeric complexes of the same size (20 monomers) with an M_w^{av} of 268 kDa and 270 kDa respectively. However, in the presence of 10 mM EDTA, ZraP-SDMB produced monomers (~17 kDa) and probable dimers at ~35 kDa (Figure 51, B). This third round of AUC produced results almost identical to our native page analysis of ZraP-SDM (Figure 49), where this ZraP variant was only present in its monomeric and dimeric forms when no excess zinc was present.

Table 30: Summary of AUC data for ZraP WT and ZraP variants

Sample	M_w^{av} for each condition (kDa)		
	60 µM $ZnCl_2^{\Psi}$	10 mM EDTA$^{\Phi}$	120 µM $ZnCl_2^{\Psi}$
ZraP- WT	202*	-	-
ZraP-LTTEA	238	20, 68	-
ZraP-AAAAA	330	18, 136	-
ZraP-HRGGAH	208	18, 109	-
ZraP-SDMB	268	17, 35	270

*Appia-Ayme et al. (2012) $^{\Psi}$one-component model, $^{\Phi}$two-component model, - no data collected.

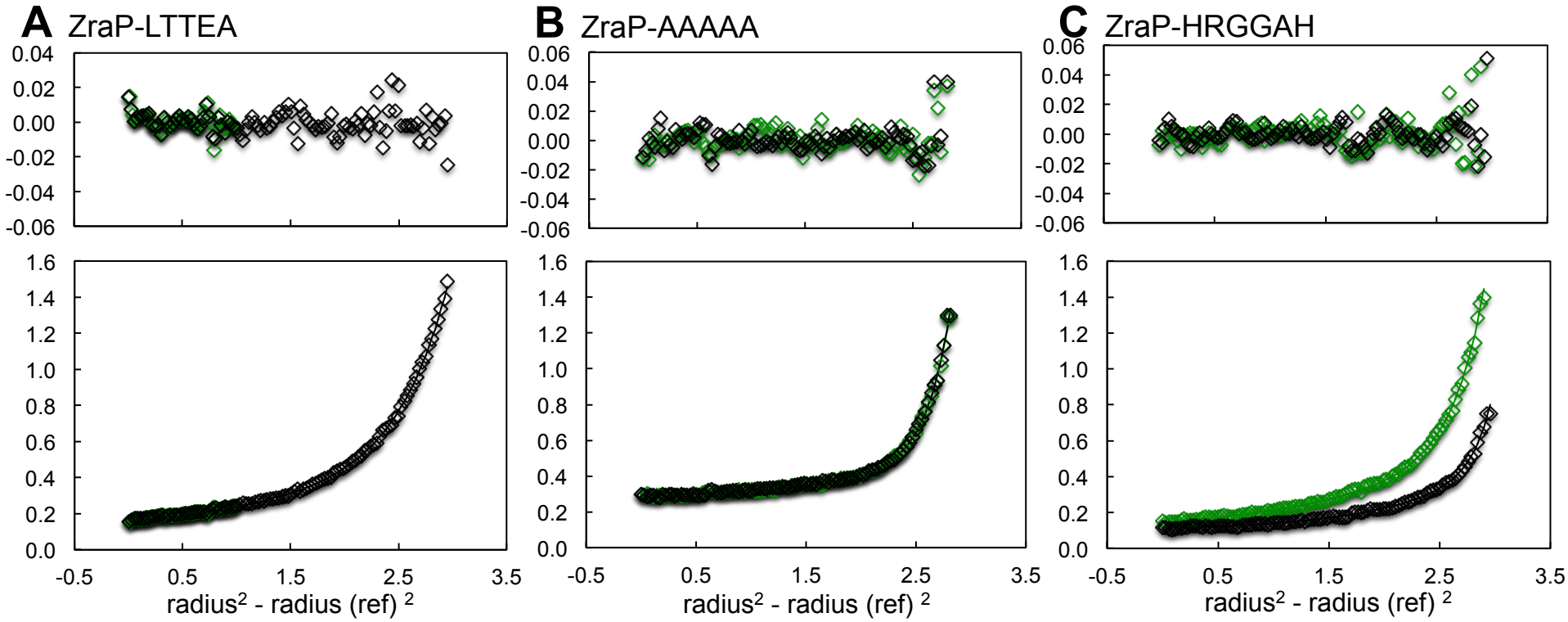

Figure 50: Sedimentation equilibrium analysis of recombinant ZraP oligomers at 23,000 rpm (GREEN) and 30,000 rpm (BLACK): *Lower panels.* Absorbance profile of 198 nM recombinant ZraP **A**) ZraP-LTTEA, **B**) ZraP-AAAAA and **C**) ZraP-HRGGAH measured at A_{280} in the presence of 10 mM EDTA for. Each profile was fitted to a two-component model (**solid line**). Absorbance data in the non-linear range of 0 - 0.02 AU have been excluded from the plot. *Upper panels:* residual difference between the experimental data for each absorbance profile and fitted curves.

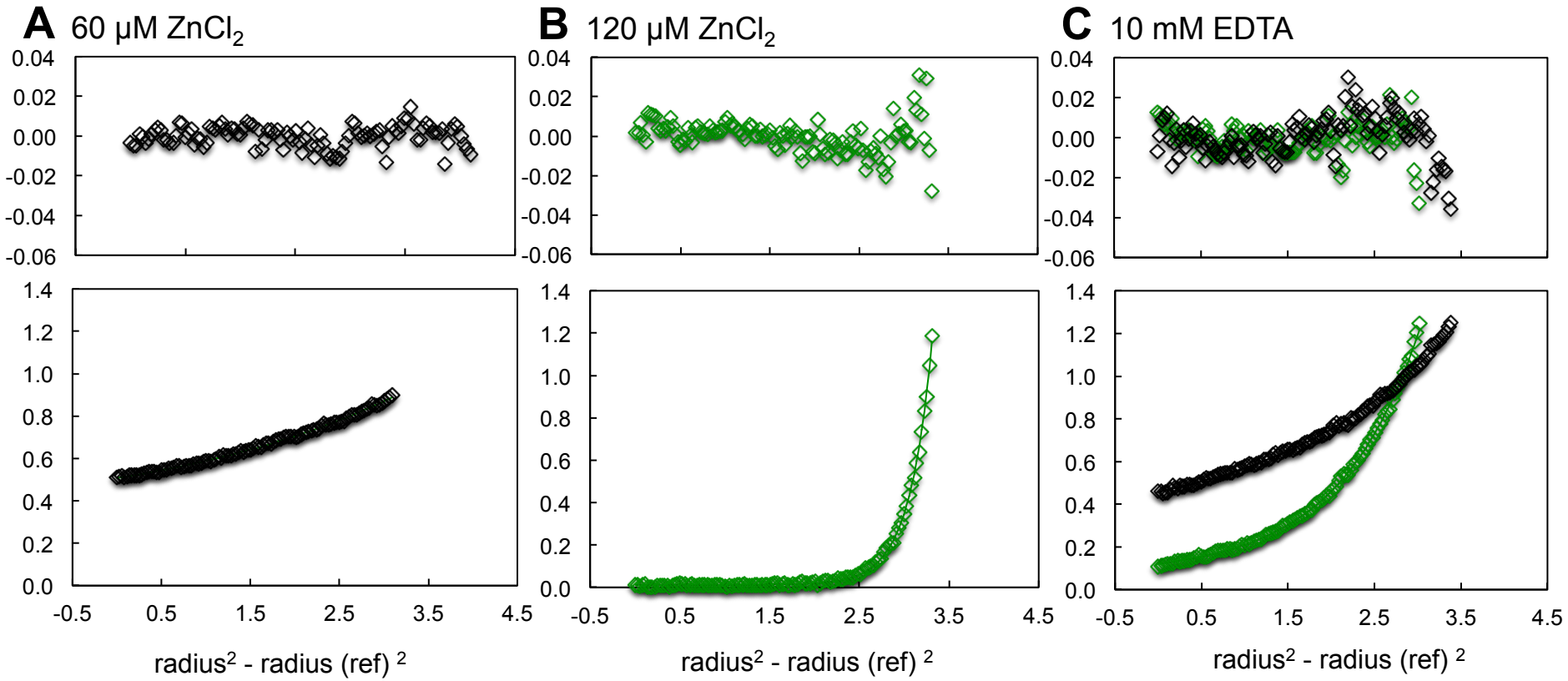

Figure 51: Sedimentation equilibrium analysis of recombinant ZraP-SDMB oligomers at 23,000 rpm (GREEN) and 30,000 rpm (BLACK): *Lower panels.* Absorbance profile of 198 nM recombinant ZraP-SDMB measured at 280 nm in the presence of 60 μM $ZnCl_2$ (**A**), 120 μM $ZnCl_2$ (**B**) and 10 mM EDTA (**C**). **C** was fitted to a two-component model and **A** and **B** are fitted to a single component model (**solid line**). Absorbance data in the non-linear range of 0 - 0.02 AU have been excluded from the plot. *Upper panels:* residual difference between the experimental data for each absorbance profile and fitted curves.

6.5 Discussion and future work

ZraP acts in a negative feedback loop to inhibit the ZraSR 2CST system, and functions as an ATP-independent chaperone (Appia-Ayme et al., 2012). This chaperone activity is enhanced in the presence of zinc. Despite a probable role for ZraP in zinc homeostasis: this protein preferentially binding zinc over other metals and is zinc inducible (Noll et al., 1998, Graham et al., 2012, Lee et al., 2005), no investigations prior to this study explored the importance of zinc binding for ZraP chaperone activity. As outlined in Chapter 4, deletion of *zraP* has no negative impact on *S*. Typhimurium zinc toxicity. We hypothesised that Zn^{2+} functions to stabilize the oligomeric form of ZraP, which is in turn required for chaperone activity, deduced from initial ZraP characterization studies performed by Appia-Ayme et al. (2012). Three residues of interest: LTXXQ, HRGGGH and GGCGGY, were identified due to structural and sequence comparison with the other two members of the CpxP-like family of molecular chaperones, CpxP and Spy, and similarity to other zinc binding domains (Quan et al., 2011, Kwon et al., 2010, Noll et al., 1998). Site-specific amino acid substitutions within these motifs were produced by site-directed mutagenesis and the recombinant proteins purified (ZraP-LTXXQ, ZraP-AAAAA, ZraP-HRGGAH and ZraP-SDMB). Biochemical techniques were employed to explore the importance of these regions in zinc association and complex formation. Any impact on ZraP decameric structure, as shown by X-ray crystallography (PDB ID: 3LAY, Filippova and colleagues unpublished) and AUC (Appia-Ayme et al., 2012), was also investigated.

6.5.1 ZraP chaperone activity and higher order oligomerisation is hindered by alanine substitution mutations at residues G120-Y125

Our MDH aggregation assays (light scatter assays) confirmed the results seen by Appia-Ayme et al. (2012). ZraP suppressed the onset of MDH thermal aggregation in a similar pattern to that observed for Spy (Quan et al., 2011) (Figure 46). This chaperone mechanism was catalytic, independent of ATP and required zinc for optimum activity. ZraP mutants containing alanine substitutions within the LTTEQ and HRGGGH motifs, ZraP-AAAAA (Figure 46, B) and ZraP-HRGGAH (Figure 46, C), exhibited the same catalytic chaperone activity of WT ZraP, with and without excess $ZnCl_2$ additions.

These initial findings suggested these two residues do not directly influence ZraP chaperone activity, or at least the mutations did not significantly alter ZraP structure to inhibit chaperone function, observations which concur with multimer formation seen during native page analysis (Figure 48). As neither ZraP-AAAAA nor ZraP-HRGGAH exhibited any disruption in ZraP function, they do not appear to influence ZraP chaperone activity under the conditions tested here, and further investigation into their role in ZraP oligomerisation and zinc binding is required. MDH activity assays (Figure 44), could only be conducted for WT ZraP during this study and are currently being extended to include all three recombinant ZraP proteins produced during this study. This further work will provide a quantifiable value to the levels of protection offered by ZraP-AAAAA, ZraP-HRGGAH and ZraP-SDMB to MDH during chemical denaturation.

ZraP-SDMB, a ZraP variant with six alanine substitutions at residues 120-125 presented activity that differed from ZraP WT, was the recombinant ZraP protein of the most interest. Not only did alanine substitutions within the GGCGGY motif inhibit chaperone function at high zinc concentrations (Figure 47), but in the presence of no excess zinc (Figure 48) and 10 mM EDTA (Figure 51; Table 30) ZraP-SDMB resides predominantly in its monomeric state. Because the other proposed zinc-binding domain ZraP-HRGGAH did not see any difference in quaternary structure to ZraP WT during either AUC (Figure 49 and Figure 50), native PAGE (Figure 48) analysis or chaperone function (Figure 46), one can conclude that if zinc does bind at the N-terminal HRGGGH motif of ZraP, this motif is of less importance to ZraP structure and function than GGCGGY. The next step in our analysis of this GGCGGY motif is to confirm the importance of Cys132 through the site-directed mutagenesis of this specific residue, without interfering with the surrounding residues.

Although ZraP-SDMB protected MDH from thermal aggregation at a similar rate to WT ZraP in the absence of zinc (Figure 47, A), this chaperone activity was removed almost entirely following $ZnCl_2$ (10 μM) addition and partially hindered when lower $ZnCl_2$ concentrations (0.1 μM and 1 μM) were present

(Figure 47, B). If GGCGGY conferred a zinc-binding site in ZraP, then our specific mutations within ZraP-SDMB (G120A, G121A, C122A, G123A, G124A, Y125A) should remove zinc ligands and perturb Zn^{2+} binding. ZraP-SDMB should therefore provide similar levels of protection to MDH in both zinc deplete and replete conditions. This was not the case. Excess $ZnCl_2$ negatively impacted on ZraP-SDMB chaperone activity, with MDH aggregating at a rate comparable to that seen when no chaperone was present (Figure 47). Exactly why the presence of excess $ZnCl_2$ would negatively effect ZraP-SDMB activity is unclear. Stability and rigidity of flexible polypeptide chains, such as that found within at the C-terminal tail of ZraP, is improved through binding around tetrahedrally coordinated Zn^{2+} complexes. If zinc is not bound directly at residues G120-Y125, it is possible that our alanine substitutions within the C-terminal flexible tail of ZraP resulted in significant movement of the zinc ion from its native position in the WT protein, diminishing chaperone activity. Zinc binding itself may not be impeded in ZraP-SDMB, but the new position of the Zn^{2+} complex as a result of these structural changes may negatively impact ZraP function. The zinc-binding domain proposed by Appia-Ayme et al. (2012), HRGGGH, is located five residues from the alanine substitutions in ZraP-SDMB. If our hypothesis is correct then Zn^{2+} could still be binding at this HRGGGH motif, but in an altered confirmation. Our ZraP-HRGGAH mutant exhibited no alteration in chaperon function compared to the WT protein under all conditions tested (Figure 46, C). This single G144A mutation may not be sufficient to hinder zinc binding at this site. Investigations involving a library of site-specific ZraP mutants would be required to categorically confirm this HRGGGH motif as a site of Zn^{2+} binding in ZraP, alongside MDH activity assays as mentioned previously.

Both GGCGGY and HRGGGH motifs may therefore be important for zinc coordination in ZraP. One additional explanation for the altered function of ZraP-SDMB when zinc is present is that conformational changes in ZraP-SDMB result in 1) binding of additional zinc ions or 2) these mutations changed the properties of an existing zinc binding site, altering structure and activity, both of which can also inhibit ZraP function. This has been seen for

recombinant thermolysin proteins where catalytic activity was hindered in the presence of excess zinc due to additional metal ion binding (Holland et al., 1995). When a ligand within an existing metal binding site, for example GGCGGY, is changed to a smaller, non-coordinating ligand (e.g. alanine or glycine) a cavity within the binding site can be produced. This is defined as 'cavity complementation' in the field of metal binding site engineering (Lu and Valentine, 1997). This could explain why ZraP-SDMB functions differently in the presence of zinc; ZraP may be binding zinc at GGCGGY but presenting a different functionality to ZraP WT. Determining zinc-binding affinity for ZraP WT and our ZraP mutants by metal ion affinity chromatography would be one useful direction of future investigations. High throughput techniques such as X-ray absorption spectroscopy would also allow detection and identification of bound zinc ions, a well as quantifying the number present (Lippi et al., 2012). However, both of these techniques were beyond the scope of this thesis.

The rate of intracellular protein degradation depends on the proteins involved and the presence or absence of molecular chaperones. According to the chaperone-folding model, chaperones interact with and stabilise (partially) unfolded protein subunits and protect them from degradation during translocation through the periplasm (Driessen and Nouwen, 2008). A proteolysis assay involving our purified WT ZraP and three ZraP variants would help determine what protection, if any, ZraP offers the proteins it interacts with within the periplasm from protease degradation. The precise mechanism of ZraP, CpxP and Spy protection, and their target protein specificities is unclear. CpxP-like family members may target specific periplasmic proteins for protection, a specific protein type or protection may occur in a more general manner. Specificity can be investigated by measuring the ability of ZraP to stabilise a host of periplasmic proteins, for example PapE, MalE and NapA, or well-known model proteins such as alcohol dehydrogenase or GFP, in a range of denaturants including thermal stress, guanidine hydrochloride or ethanol. Investigations could be extended to include CpxP and Spy, giving a more detailed overview of how this chaperone family operates.

The formation of higher order multimers is thought to be essential for ZraP chaperone function (Appia-Ayme et al., 2012). ZraP has a predicted molecular mass of 13.5 kDa and results by Appia-Ayme *et al.*, (2012) gave a M_w^{av} for ZraP WT, in the presence of 60 μM $ZnCl_2$, of ~202 kDa. This suggested ZraP forms an oligomer of ~15 monomers in the presence of $ZnCl_2$. ZraP formed oligomers of half the size, ~6-7 monomers, in the presence of $MgCl_2$ or EDTA (Appia-Ayme et al., 2012). ZraP monomers share significant structural similarity to CpxP and Spy (Figure 43), which form stable homodimers through interactions between conserved N- and C-terminal LTXXQ motifs forming hairpins at the end of a central helix (Kwon et al., 2010, Quan et al., 2011). This third α-helix is absent from ZraP, which only possesses one LTXXQ motif at the N-terminal end (Figure 43). The crystal structure of *E. coli* ZraP was resolved as a decameric barrel (Figure 43), a structure that would be impeded if this third α-helix were present. This raised the question of what functional form ZraP takes and if oligomerisation was critical to chaperone activity, how is this quaternary structure stabilised? AUC was employed to determine the higher order oligomer formation of our three recombinant ZraP proteins and what part these motifs play in stabilisation of these structures (Figure 49-51). Through sedimentation velocity analysis, M_w^{av} for all four recombinant ZraP proteins were calculated in the presence of 60 μM $ZnCl_2$ (Table 30). In comparison to data obtained by Appia-Ayme et al. (2012) the M_w^{av} obtained for ZraP-LTTEA (~238 kDa) and ZraP-AAAAA (~330 kDa) suggest these recombinant versions form larger oligomers than the WT protein and oligomerisation remained unaffected by the specific amino acid mutations. ZraP-HRGGAH and ZraP WT multimers contained the same number of ~15 monomers and ZraP-AAAAA differed the most from ZraP WT, containing ~10 more monomers than the oligomeric form of the WT protein. If the LTXXQ motif is involved at the interface between ZraP monomers, residue substitutions within this region could result in a reversible association, a weaker interface promoting dissociation and reforming of higher component species. As ZraP WT structure was resolved as a decamer (Figure 43) and ZraP-AAAAA multimers contain ~10 monomers more than the WT form, it is possible that

conformational changes at the N-terminal end of ZraP are allowing association between multiple ZraP decamers. If a single multimeric species is present, the alanine substitutions within the LTTEQ motif may alter the secondary structure of ZraP to produce a new interface allowing these higher order oligomers to form. Although this is possible, it is difficult to ascertain if the molecular weight calculated for ZraP-AAAAA is for a single species or a heterogeneous mix. The residual spread data for ZraP-AAAAA (Figure 50) suggests possible shifting between oligomeric forms, a population possibly consisting of ZraP-AAAAA in variety of dimeric, decameric, 20-mers or larger multimeric states. This heterogeneous population still implies an association change between ZraP-AAAAA monomers, an unstable association between ZraP-AAAAA monomers leading to reversible association.

Both hypotheses 1) the formation of higher order multimers or 2) a heterogeneous ZraP-AAAAA population, both imply possible involvement of LTXXQ in ZraP oligomerisation. However, our chaperone activity assays (Figure 46) indicate that if this is the case, mutations within LTTEQ do not affect ZraP chaperone function. Whether the larger oligomers for ZraP-AAAAA were caused by direct involvement at the interface between monomers or because of alterations to secondary structure, caused by alanine substitutions that physically hinder or block association, is yet to be determined. Repeating sedimentation velocity experiments for this recombinant mutant at a range of sedimentation speeds and sample concentrations would help specify the dominant species if a heterogeneous population is present.

As zinc can function in a signalling, catalytic and structural capacity (Berg and Shi, 1996) both zinc ion binding sites and the LTTEQ motif may be required to stabilise ZraP oligomerisation. Especially as ZraP lacks the C-terminal LTXXQ motif conserved in CpxP and Spy, which contributes towards stability of homodimers. Zinc ions, in a structural capacity, are usually tetrahedrally coordinated to ligands across two proteins, stabilising protein-protein interfaces. A zinc-binding site at the C-terminal tail of ZraP may compensate for the lack of the LTXXQ motif. However, any zinc ions

bound to ZraP may be more important to the catalytic activity of ZraP than stability of the higher order structure. For example, ZraP-AAAAA does not form the correct quaternary structure due to critical mutations within the LTXXQ motif, disrupting ZraP tertiary structure and the interface between ZraP-AAAAA monomers. ZraP-AAAAA is still able to bind zinc, but because of the alterations in tertiary structure, the coordinated Zn^{2+} ions (bound at either GGCGGY or HRGGGH) are unable to bind to ligands between the interacting monomers and stabilise higher order oligomers. Chaperone activity of ZraP-AAAAA was therefore not hindered under the conditions tested here, despite the increases in oligomerisation suggested by AUC, as zinc was still bound at the correct functional site within the protein. ZraP-AAAAA AUC analysis suggested this ZraP variant existed as a heterogeneous population of dimers to larger (>20-mer) species. ZraP-AAAAA may still possess chaperone activity in its dimeric form as long as zinc is coordinated correctly within the binding pocket of ZraP.

In addition to the data presented here, other members of the Rowley research group and collaborators are working to resolve the X-ray crystal structures of our recombinant ZraP proteins, and ZraP WT at an improved resolution to that deposited by Filippova and colleagues in the RCSB protein data bank (PDB 3LAY). WT ZraP crystals have been obtained at 0.2 M $MgCl_2$ and 0.1 M BIS-TRIS, pH 5.50, and ThermoFluor analysis is also being conducted on the WT protein to determine to optimum buffer conditions. This work, which is on going, would shed further light on any structural changes as well as the coordination of zinc ions present within the structure of ZraP. All four recombinant proteins are also in the process of being purified with a removable polyhistidine tag. A suitable vector allowing ZraP purification with a cleavable purification tag, either polyhistidine or a Strep-II fusion tag, was not available when our recombinant ZraP proteins were made. As ZraP is a relatively small protein of 13.5kDa, the C-terminal *Myc* epitope and 6xHis tag attached to our WT and recombinant ZraP proteins is comparatively large and could interfere with protein folding and quaternary structure. Although this does no appear to be the case from the protein aggregation data collected during this study, any future analysis and crystallisation trials will be

conducted with purified ZraP minus purification tag to minimise interference. As our mutated ZraP cDNA constructs were overexpressed in an *E. coli* host strain, TOP10, it is possible that *E. coli* WT ZraP at very low concentrations could have been co-purified with our recombinant proteins following overexpression in this host strain. It is therefore advisable that all recombinant proteins are purified from *E. coli zraP* deletion strains in future to prevent this minimal carry over. As *zraP* deletion does not negatively impact on cell grow (data not shown), this should not be problematic.

7 General discussion

As the results of each chapter have been discussed individually, this general discussion chapter will highlight the major outcomes of this study, the wider context and potential impact of this research.

7.1 Context

Salmonella spp. cause a range of diseases in humans and animals, from gastroenteritis (food poisoning) and bacteraemia to enteric fever. Despite improving sanitation, clinical practice and understanding of disease prevention, *Salmonella* remain some of the most deadly pathogens in low and middle-income countries (LMICs) (Mogasale et al., 2014). The increasing prevalence of MDR strains and iNTS, the continued difficulties presented by HIV/AIDS, malaria and malnutrition are making management of *Salmonella* infections ever more complex. These environmental factors, when coupled with a lack of life-long *S*. Typhi vaccines (and no licenced vaccine against paratyphoid or NTS serotypes available), make the need for new treatments and drug targets crucial. Research into *Salmonella* host-pathogen interactions and the ESRs of this Genus have led to the discovery of essential virulence factors and the development of potential vaccine candidates in humans and animal hosts (Humphreys et al., 2004, Humphreys et al., 1999, Tacket et al., 1997, Zhu et al., 2015, Si et al., 2015, Nandre et al., 2014). By improving our understanding of these ESRs further, we hope to identify novel ESR co-regulated genes which we hypothesise are critical for virulence of *Salmonella*, leading to the development of new treatments and infection prevention. This development of vaccines for both humans and animals is needed for the prevention and treatment of Typhoid fever, iNTS strains and the spread of gastroenteritis from *Salmonella* reservoirs within the food chain, such as pigs, chickens and their eggs.

Salmonella encounter stresses at every stage of its life cycle in non-host (water, soil, industrial processes etc.) and host environments. In order to successfully adapt to and move between changing environments, *Salmonella* must sense the stresses inflicted upon it and respond to prevent damage or repair any damage already sustained. The host's innate and adaptive immune responses are quickly activated following oral infection and

Salmonella have evolved a sophisticated set of defence mechanisms to thrive despite this attack. For example, upon entering a new host, *Salmonella* initiates an acid tolerance response (ATR) to survive stomach acid (low pH); up-regulates RpoS-mediated general stress responses upon exposure to detergent-like bile salts and switches to anaerobic metabolism to adapt to reducing oxygen availability within the host GIT. As infection becomes established, inflammation and the adaptive immune response to *Salmonella* (for review see Griffin and McSorley (2011)) must also be overcome.

7.1.1 Why study the ESRs of *Salmonella*?

The bacterial envelope is the interface between Gram-negative bacteria and the outside world and the point at which external stresses are first sensed. This makes the periplasm more susceptible to environmental changes than the cytoplasm, and protein-quality control within the periplasm, and our understanding of the processes involved, is crucial for our understanding of bacterial survival mechanisms. The sensing and repair of defective proteins within the bacterial cytoplasm is well defined, but this is not the case for the periplasm. During biogenesis, proteins are translocated across the IM, refolded or modified within the periplasmic space (Sec translocated proteins) and then inserted into the OM (if required). Disruption of protein formation and folding can occur at any stage of this process. Molecular chaperones function to promote correct folding and prevent aggregation during this process of normal biogenesis and during stresses (Zhou et al., 1988), such as heat shock, that increase protein denaturation and misfolding.

For Gram-negative bacteria, adapting to and surviving environmental stresses is dependent upon the detection and transduction of extracellular signals across this envelope, and the integration of these signals into transcriptional networks. The ESR systems are essential components of this mechanism because their influence on the regulation of protein quality control is critical to *Salmonella* survival and pathogenicity. If protein quality control measures are not in place, misfolded, damaged and degraded proteins form toxic aggregates within the periplasm, hindering the action of other protein components and disrupting membrane integrity. Maintaining

envelope integrity requires the combined efforts of molecular chaperones, proteases, isomerases and folding catalysts, expressed as a result of ESR activation. These stress response proteins assist in: the refolding and reassembly of damaged envelope proteins, LPS biogenesis and modification, the regulation of macromolecular surface structures, maintenance of the PMF and multidrug efflux, to name a few.

The majority of our knowledge surrounding ESR systems has come from investigations using *E. coli* model organisms and, more recently, pathogenic *E. coli* strains (e.g. EPEC and UPEC). Those investigations focusing on the ESRs of *Salmonella* have highlighted critical differences between the ESRs of these closely related, but distinct, species (1.6.2). Therefore our understanding of these survival mechanisms in *S.* Typhimurium, is ever more important. In order to provide a more comprehensive overview of the ESRs in *S.* Typhimurium, this thesis has examined the regulon of an established (CpxAR) and hypothesised (ZraSR) ESR system in SL1344 for the first time and investigated their contribution to *Salmonella* physiology, stress response and their regulation of potential (and known i.e. SPI-1) virulence factors. The research presented here offers various directions for future work including the importance of ESR systems in intracellular survival and expanding the regulatory networks regulated/co-regulated by the ESRs.

7.2 ZraSR – More than a zinc sensing system?

Appia-Ayme et al. (2011) reported co-regulation of ZraSR and BaeSR ESR pathways in *S*. Typhimurium. With *zraPSR* induction by an array of conditions that cause envelope stress (i.e. metal stress [lead and zinc], indole, high temperatures, osmotic stress and nitric oxide), this co-regulation with the Bae system made ZraPSR a prime candidate for further analysis as a potential, new ESR system (Leonhartsberger et al., 2001, Appia-Ayme et al., 2012, Appia-Ayme et al., 2011, Huang et al., 2007b). pH fluctuations, the presence of bile salts, growth phase, oxygen limitation and osmolarity are all ESR inducing conditions that are implicated in the control of virulence genes (Huang et al., 2007b). The CpxAR and σ^E ESR systems are associated with the virulence of *Salmonella* spp., *E. coli* spp., *Vibrio cholera*, *Haemophilus*

influenza, *Yersinia enterocolitica*, *Pseudomonas aeruginosa* and *Mycobacterium tuberculosis* during a range of infection studies (Redford and Welch, 2006, Humphreys et al., 2004, Humphreys et al., 1999, Debnath et al., 2013, Kovacikova and Skorupski, 2002, Acosta et al., 2015, Craig et al., 2002, Martin et al., 1994, Li et al., 1996, Yu et al., 1995, Collins et al., 1995). Two infection studies have highlighted a potential role for ZraSR in virulence. The first showed up-regulation of the ZraS during EHEC O157:H7 infection within the human gut (John et al., 2005), and the second showed ZraS expression during *S*. Typhimurium infection of pigs (Huang et al., 2007b). These results linking ZraSR to envelope homeostasis and pathogenicity were intriguing and warranted further investigation.

In vivo expression data from Huang et al. (2007b) was of particular interest to us with regards to the function of ZraSR as a zinc responsive system. ZraS is up-regulated in *S*. Typhimurium ATCC 14028 (transformed with a genomic library of *S*. Typhimurium strain 798) isolated from both the tonsils and intestine of infected pigs (Huang et al., 2007b). Pig feed is often supplemented with zinc to prevent deficiency of this essential nutrient; especially as the high levels of phytic acid (from soybeans) and calcium present in pig feed impede zinc absorption (Church and Pond, 1989). Pigs have a zinc dietary requirement of 50-100 ppm, higher than other livestock (Table 31) (Berger, 1987) and humans (age and gender dependant) (Sandstead, 1985), with a zinc deficiency in pigs presenting as a reduced growth rate and parakeratosis, a skin disease manifesting in raised red lesions. High zinc diets (e.g. 2000-3000 ppm), commonly supplemented with zinc sulphate, zinc oxide, zinc chloride, zinc carbonate and zinc chelates (Berger, 1987), are used to promote fast growth rates and development in young pigs (National Research Council, 2008). Organic zinc at 75mg/kg was recently determined to be the optimum concentration for the development of lean, fast growing animals (Hill et al., 2014). Zinc concentrations within the pig GIT are 12-43 fold higher (location dependent) in weaned animals fed ZnO supplemented food (2000 mg/kg) compared to non-weaned pigs of the same age (Davin et al., 2012). This shows a direct correlation between feed supplementation and the amount of bioavailable zinc within the GIT of this

host. As cases of post-weaning diarrhoea, predominantly caused by *E. coli* infections (Fairbrother et al., 2005), are reduced in pigs fed on high zinc diets, this suggests a link between zinc-rich food and a reduction in bacterial infection rates. It is hypothesised that this reduced infection results from improvement in the structure and/or immunological integrity of the intestinal mucosal barrier (Huang et al., 1999) (zinc is absorbed through the small intestine at 5-40% of dietary intake (Berger, 1987) and zinc stimulation of the host immune defences (King et al., 1995). However this is yet to be determined and the results extended to investigate other enteric pathogens, including *Salmonella* spp. *Salmonella* spp. are passed between pigs with subclinical *Salmonella* infections and naive pigs during transportation and lairage (resting places at market and slaughter houses) (Loynachan and Harris, 2005). Acute infection of pig alimentary and non-alimentary tract tissues with *S. enterica* serovars has been shown in market-weight pigs when exposed to an environment contaminated with lairage representative doses ($<10^6$ Salmonellae) (Loynachan and Harris, 2005), and within three hours of intranasal inoculation (Loynachan et al., 2004). Because of the elevated concentration of zinc within the diets and GIT of swine, it could be beneficial for *Salmonella* to employ zinc sensing and metal stress response systems, such as ZraSR, within this host environment, allowing adaptation to this zinc rich environment to promote growth and infection. This could give *Salmonella* an advantage not only for survival within the GIT, but also during colonisation if the presence of high zinc disrupts gut flora and competition were reduced. The affect of high zinc on pig gut flora requires more detailed analysis, but supplementation with ZnO alone does not appear to affect bacterial diversity within the microbiota (only when zinc and copper were supplemented in tandem was a reduction on microbiota diversity observed) (Perez et al., 2011).

Because of *Salmonella* exposure to high zinc within the GIT of pigs, one would expect to observe up-regulation of zinc responsive systems in this environment. We confirmed ZraR up-regulation in *S.* Typhimurium as a response to elevated zinc concentrations *in vitro* (Chapter 5, Figure 35),

concurring with results observed in *E. coli* (Leonhartsberger et al., 2001). If ZraSR were up-regulated is response to high zinc concentrations *in vivo*, as

Table 31: Zinc requirements and toxic levels[*]

Animal	Zinc Requirement in Diet (ppm)	Toxic Level in Total Diet (ppm)
Beef Cattle	30	500[ϕ]
Dairy Cattle	23-63	300-1000
Swine	50 (50-100)	2000-4000
Horse	40	Over 700
Sheep	20-33	750
Goats	45-75	750
Chickens	40-50	800-3000
Turkeys	40-75	4000

[*]Levels recommended by NRC committee unless otherwise stated. [ϕ]Maximal tolerance level in diet. Adapted from Berger (1987).

would be the case in the GIT of pigs fed with zinc supplements, one would expect to see a down-regulation of zinc acquisition systems and an induction of metal stress response proteins as a response. Expression of *mntH* correlates with an increase in ZraR expression upon entry into exponential growth (Figure 36) (Botteldoorn et al., 2006). *mntH* is also induced in response to oxidative stress (H_2O_2) and up-regulated in *Salmonella* once phagocytosed by NRAMP1 expressing macrophages (Kehres et al., 2000, Botteldoorn et al., 2006, Huang et al., 2007b, Runyen-Janecky et al., 2006). We show a strong link between ZraSR induction and exponential growth (Figure 36). If ZraR is a positive regulator of MntH, as suggested by our *S*. Typhimurium transcriptome data, this could be in preparation for entering a host environment, in response to reduced metal ions within the macrophage during times of nutritional-immunity, in response to oxidative stress within phagocytes or a combination of the above. During infection, macrophages decrease nutrients and metal ion availability, termed 'nutritional immunity' (Weinberg, 2009), through secretion of calprotectin (Corbin et al., 2008, Teigelkamp et al., 1991, Steinbakk et al., 1990), induction of the zinc

transporters ZIP8 and ZnTs (Porcheron et al., 2013, Desrosiers et al., 2010) and activation of NRAMP1 transporters at the plasma membrane (Jabado et al., 2000, Forbes and Gros, 2003, Hood and Skaar, 2012). MntH is a virulence determinant for a number of species because it is required to compete with calprotectin and host NRAMP1 transporters expressed in the phagosome, aiding maintenance of Mn^{2+} homeostasis (Perry et al., 2012, Champion et al., 2011, Anderson et al., 2009, Runyen-Janecky et al., 2006, Agranoff and Krishna, 1998, Zaharik et al., 2004, Kehl-Fie et al., 2013). Manganese is crucial for many physiological processes (i.e. as a biological cofactor), but it is also important for surviving oxidative stress within the phagosome. Mn^{2+} functions as a cofactor of Mn-SOD and forms non-proteinaceous manganese antioxidants that scavenge superoxide anion radicals (Aguirre and Culotta, 2012). ZraSR, OxyR, Fur and MntR could offer coordinated regulation of MntH to ensure Mn^{2+} and Fe^{2+} uptake within host immune cells during metal ion limitation and oxidative stress inflicted upon the bacteria from the host. If MntH activation and Mn^{2+} uptake is linked to high environmental zinc and lead concentrations (ZraSR inducers), because of the important function Mn^{2+} plays in the bacterial response to oxidative stress, increasing intracellular manganese through *mntH* induction could be an important pre-emptive response to prevent cellular damage from free radicals, which result from excess metal concentrations. As *mntH* is essential for *E. coli* survival during peroxide stress (Anjem et al., 2009), any link between ZraSR, MntH and peroxide stress would be the most logical area for further investigations. Sensitivity of *zraSR* deletion strains to peroxide stress was not determined during our investigations, but could be easily investigated through sensitivity and disc diffusion assays now an SL1344 Δ*zraSR* strain has been produced in this work.

Induction of ZraSR during anoxic growth (Leonhartsberger et al., 2001) could ensure MntH expression upon entry into the host GIT, priming the bacteria for nutrient limitation and competition for resources with the gut microbiome, as well as the reduction in bioavailable metals instigated by the host immune response outlined above. These other possibilities will need further analysis (i.e. macrophage infection studies) to fully elucidate the level of *mntH*

regulation by ZraSR and the impact this has on *Salmonella* physiology and pathogenicity.

Our hypothesis of ZraSR as a novel stress response system was supported by results presented in Chapter 5 and Chapter 6, where an array of chaperones were positively (ZraP, GroEL, GroES, DnaK and ClpB) and negatively (CpxP) regulated by ZraR overexpression. The GroEL-GroES chaperone machinery and DnaK-DnaJ-GrpE are HSPs, activated by the heat shock response sigma factor RpoH. Differential regulation of *rpoH* was not observed during our transcriptomic analysis of ZraR overexpression, suggesting any direct regulation of these heat shock chaperones may occur independently of RpoH. This notion is supported by the fact that ZraS is significantly up-regulated at higher growth temperatures (42°C) (Huang et al., 2007b) and could therefore be acting alongside *rpoH* to induce expression of these chaperones and prevent protein degradation and misfolding within the cytoplasm at high temperatures. While cattle have a similar body temperature to humans of 36.7-39.3°C (depending on breed), some *Salmonella* host species have a much higher body temperature: the normal rectal temperature of pigs is 38.7-39.8°C and chickens 40.6-43°C, (Robertshaw, 2004). As previously mentioned, Huang et al. (2007b) showed up-regulation of ZraS in pigs when infected with *S*. Typhimurium. Our proposed regulation of heat shock chaperones by ZraR coupled with ZraS expression data by Huang et al. (2007b) adds more weight to suggestion of ZraSR involvement in *Salmonella* infection of swine. However, it remains unclear if ZraS up-regulation in pigs is due to *S*. Typhimurium temperature stress, exposure to high zinc within the pig GIT or if ZraSR is up-regulated within all hosts. To the best of our knowledge, increased expression of either ZraS or ZraR is yet to be determined during *S*. Typhimurium infection of chickens, an *S*. Typhimurium host with the highest body temperature. However, as chickens also have their feed supplemented with zinc, this would also need to be taken into account during any infection studies in this species.

In addition to elevated environmental zinc, our data provides evidence of ZraSR involvement in regulation of anaerobic growth. Several components of anaerobic metabolism were down-regulated following ZraR overexpression (*frdABCD*, *dcuAB*, *hybABC*, *hypO*) (Chapter 5), including fumarase reductase, C4-dicarboxylate transporter and hydrogenase-2 activity. ZraS is induced during anoxic conditions (Leonhartsberger et al., 2001) but the *zraSR* deletion did not affect *S*. Typhimurium growth in either aerobic or anaerobic cultures (Figure 34; Figure 40). This transcriptomic analysis suggests involvement of ZraSR in oxygen sensing, which complements the proposed function of this 2CST system in response to oxidative stress. Total RNA for our microarray analysis was collected from aerobic batch cultures. A more targeted analysis of ZraR regulated genes during growth in the absence of oxygen would provide a more detailed analysis of ZraR regulation, analysis which could be extended to include a variety of physiologically relevant growth conditions linked with ZraSR as a result of our investigations i.e. intracellular environments, high zinc.

John et al. (2005) showed up-regulation of EHEC O157 *zraS* in the GIT of patients suffering from haemolytic-uremic syndrome (HUS). Obviously the dietary zinc levels of the four patients involved in this study are unknown and therefore the impact of zinc on ZraS induction in this instance remains unclear. As fever is usually mild or not present in HUS sufferers (as stated by the Mayo Clinic, USA: http://www.mayoclinic.org/diseases-conditions/hemolytic-uremic-syndrome/basics/symptoms/con-20029487), induction of ZraS as a result of temperature stress would be unusual on this occasion. As ZraSR is induced by several factors present during infection (i.e. anaerobic environment of the host GIT, high zinc, high temperature, general envelope stress, cross-talk with other ESRs) it remains unknown if all, some, or a combination of these *zraSR*-inducing cues contributes to expression of this system during infection in humans. The results presented by John et al. (2005) in an EHEC genetic background do imply ZraS/ZraR involvement during infection of hosts other than swine, possibly suggesting that in human hosts the links between *zraSR* expression and anaerobic growth, growth phase and stresses associated with nutritional immunity may

be the more important contributing factors. Up-regulation of ZraS in pigs may occur for the same reasons as up-regulation in a human host, with elevated zinc concentrations within the pig GIT an unfortunate red herring and distraction, unrelated to the natural inducing conditions for ZraS.

7.3 The CpxP-like family of periplasmic chaperones

As previously mentioned, several chaperones (cytoplasmic and periplasmic) were induced by ZraR overexpression. Of these, the structure and function of the periplasmic chaperone ZraP was investigated in more detail during Chapter 6. Enteric bacteria possess the CpxP family of molecular chaperones: CpxP, Spy and ZraP. Despite sharing only 12% and 13% homology at the amino acid level respectively, CpxP and ZraP and Spy and ZraP have very similar tertiary structures and all function as chaperones within the periplasm, as described during the introduction to this thesis (1.7.6). A triple CpxP family chaperone mutant in *S*. Typhimurium SL1344 is highly sensitive to the AMP polymyxin B (Appia-Ayme et al., 2012) showing functional redundancy between these chaperones and their combined importance as possible novel therapeutic targets. ZraP is the most recently described member of this chaperone family, with ATP-independent chaperone activity and regulation by ZraSR confirmed by Appia-Ayme et al. (2012). Our results presented in Chapter 6 further confirmed this positive regulation by ZraSR, and the negative inhibition on this system by ZraP as a result of this up-regulation (Figure 36). The importance of zinc for ZraP chaperone activity was described by Appia-Ayme et al. (2012), but the affect of oligomerisation on ZraP function was the main focus of our research. We concluded through biochemical and biophysical analysis of ZraP that five residues (G120, G121, C122, G123, G124, Y125) are critical to the stability of ZraP multimers, most likely due to zinc binding at this site and the formation of zinc-binding interfaces between ZraP monomers (7.4.2). Conserved residues in ZraP that have structural and sequence homology with both CpxP and Spy (LTXXQ), and a second proposed zinc-binding motif HRGGGH, did not appear to influence ZraP oligomerisation during our investigations (Chapter 6). Determining a specific binding affinity for the GGCGGY site, and our ZraP-SDMB site-directed mutant, was outside the

remit of this work but would be required to confirm this observation, as would confirmation of the X-ray crystal structure of our recombinant ZraP proteins. This work is on going by our research group, including crystallisation trials of the ZraP variants produced during this study. The MDH activity assays presented in Chapter 5 showed that ZraP protects MDH during chemical denaturation with GdnHCl. These MDH activity assays are currently being repeated for our recombinant ZraP proteins to confirm the involvement of the GCCGGY motif in ZraP chaperone activity, and the ensure no loss of ZraP function occurs as a result of mutations at the LTTEQ or HRGGAH motifs. Our MDH activity assays are more sensitive compared to our protein aggregation assays and provide a quantifiable analysis of ZraP chaperone activity (2.4.24), and are therefore the preferred choice for future analysis and investigations into chaperone function of CpxP-like family members. Although our work provided an insight into the formation of ZraP multimeric complexes and the importance of higher order oligomerisation for chaperone activity *in vitro*, how this structural conformation is important for ZraP protection within the *Salmonella* periplasm *in vivo* would be the next avenue of investigation. The mechanisms of protection adopted by the CpxP family of molecular chaperones remain unknown, as are their protein targets; is protection provided at a general level or in a protein specific manner? MDH was used as a model protein during our chaperone activity assays because of the readiness of established techniques within our laboratory to measure this enzymes residual activity, its low cost and availability. However these assays should be expanded to investigate a host of periplasmic proteins, for example PapE, MalE and NapA, or well-known model proteins such as alcohol dehydrogenase or GFP.

This biophysical and biochemical analysis of ZraP was one area of our investigations because of its association with the ZraSR stress response and its structural similarity to the Cpx auxiliary protein CpxP. There are still unanswered questions surrounding the similarity of these chaperones, their function within the periplasm and their signal sensing ability. Signal sensing by CpxP is poorly understood and is not currently associated with detection of any known Cpx inducing conditions (Vogt and Raivio, 2012, Raivio et al.,

1999, DiGiuseppe and Silhavy, 2003). CpxP may be involved in the prevention of unnecessary CpxA induction and fine-tuning of this response, or it may have as yet unidentified signal sensing capabilities (Raivio et al., 1999, Vogt and Raivio, 2012). The same could be said for ZraP. The zinc binding property of ZraP and the involvement of Zn^{2+} in stabilising ZraP higher order multimers could have a secondary function in zinc ion sensing. Although no zinc ions were present within the crystal structure of ZraP (PDB: 3LAY) and the ZraP regulator ZraR does not regulate any zinc ion trafficking systems, zinc ions were found in the CpxP crystal structure and crystallisation of CpxP occurred in the presence of high zinc concentrations (Thede et al., 2011). Both ZraP and CpxP also share structural homologies with CnrX (PDB ID: 3EPV), a metal sensing protein that binds nickel, cobalt and (possibly) copper (Liesegang et al., 1993, Grass et al., 2000, Grass et al., 2005b, Maillard et al., 2015, Monchy et al., 2007). The similarities in CpxP, ZraP and CnrX structure, and the role of CpxAR as a regulator of *Salmonella* copper tolerance, makes the metal sensing role of CpxP a logical area of future research. Levels of *cpxP* mRNA (with *zraP* and *spy*) increased in response to zinc (Lee et al., 2005), CpxP transcription is reduced by ZraR overexpression (Figure 10; Table L3) and experimental evidence supports metal binding of ZraP and CrnX. Together, these results would suggest CpxP involvement in metal sensing through direct CpxP-metal ion binding and not just as a transcriptional response to protein misfolding from high metal ion concentrations in the periplasm.

Any contribution of the CpxP-like family to *Salmonella* virulence is also yet to be assessed. Our research group has a library of CpxP-like family deletion strains available for infection studies in human, porcine and murine macrophages. The use of non-phagocytic cell lines (e.g. human epithelial cells, Hela and porcine monocytes 3D4/31) will ensure assessment of defects in adhesion, invasiveness and intracellular survival can take place. If these studies provided evidence of CpxP-like chaperones in *S*. Typhimurium virulence, infection studies in non-vertebrate model organisms (*C. elegans* and *Galleria mellonella*) are also available and could be conducted.

The application of the ZraP chaperone research presented here would extend beyond our organism of choice due to conservation of the CpxP family of molecular chaperones across a range of socially and economically important pathogens, including *E. coli* sp., *Yersinia* sp., *Shigella* sp. and *Vibrio* sp. With more recent publications establishing Cpx as a significant virulence regulator in these pathogens (Table 1, see 1.7.3 for more details), these studies emphasise the importance of the Cpx ESR for infection across bacterial species and the application of Cpx research to clinical microbiology as a whole. Regarding periplasmic chaperones in general, their mechanisms of protection and how environmental signals are integrated into transcriptional networks represent two major areas of interest within this research field. Research into the CpxP chaperone family could provide useful answers to these questions and knowledge applicable to other periplasmic chaperones, improving our understanding of periplasmic protein quality control and their function in the absence of ATP.

7.4 The Cpx ESR and *Salmonella* virulence

The most recent research on the Cpx ESR has focused on understanding the signalling proteins that regulate this system, the diverse phenotypes associated with the Cpx response and interplay between Cpx and other ESRs (for review see Raivio (2013)). Our transcriptomic approach has added new information to this body of work as well as confirming Cpx regulation of specific genes, and involvement of Cpx in cellular processes previously described in species related and unrelated to *Salmonella*. In addition, our results highlight a number of proteins with unknown or putative functions in *Salmonella* that are regulated in response to Cpx induction, providing a *Salmonella* specific analysis of this stress response and avenues for further investigation. Microarray analysis of the *E. coli* Cpx regulon conducted at the same time as our transcriptomic study (Raivio et al., 2013) shows that the Cpx regulon of this organism may contain several hundred genes. This concurred with the broader cellular role for Cpx implicated by our analysis in *S*. Typhimurium and the huge range of characterised and uncharacterised genes induced in response to Cpx induction.

Principal investigations established the Cpx system as a mechanism for recognising and maintaining envelope homeostasis, predominantly through the regulation of protein folding and degradation factors. As Cpx investigations continued, it quickly became apparent that Cpx has a broader cellular role, including the positive and negative regulation of virulence factors (i.e. pili, curli fimbriae, type III and IV secretion systems, virulence regulators) in several bacterial species, directly or as a result of downstream effects from other Cpx-regulated proteins. In *S.* Typhimurium specifically, Humphreys et al. (2004) showed a reduction in host cell adhesion as a result of constitutive *cpxA* expression, although the exact mechanisms behind this phenotype were unknown. It has been suggested that down-regulation of non-essential proteins by Cpx, especially cell surface structures, may allow for energy conservation at times of stress and/or reduce the workload on the periplasmic protein folding machinery when protein aggregates are present (MacRitchie et al., 2008a, De Wulf et al., 1999). Our study supports these hypotheses and further confirms involvement of Cpx in *Salmonella* virulence as we observed down-regulation of OM proteins (SL1190), fimbrin (*fimA*) and SPI-1 (Figure 12) post Cpx induction (Table 22). The type-III secretion system encoded by SPI-1 is a major cell surface complex that promotes the invasion of intestinal epithelial cells, localised inflammatory response following invasion and the survival and persistence of *Salmonella* following compartmentalisation within host cells (Coombes et al., 2005, Hapfelmeier et al., 2004, Brawn et al., 2007, Lawley et al., 2006, Steele-Mortimer et al., 2002)(see Que et al. (2013) and Srikanth et al. (2011) for most recent SPI-1 reviews). Although Cpx-mediated activation of the SPI-1 regulator HilA has been identified in a pH dependant manner (at pH 6) previously (Nakayama et al., 2003), this regulation occurred in a CpxA dependant manner, independently of CpxR. Nakayama et al. (2003) hypothesised that CpxA may interact with regulator(s) other than CpxR at a low pH to activate SPI-1 expression through HilA. Our results show that Cpx-mediated repression of *Salmonella* invasion genes can occur when the Cpx ESR is induced by an endogenous signal (NlpE overexpression) and that in this instance CpxR is the regulator involved. Our results and those of Nakayama et al. (2003) therefore show Cpx regulation of invasion genes under two differing

conditions, activation at a low pH by CpxA through an alternative RR to CpxR, and repression of SPI-1 by CpxR during periods of envelope stress (Table 22; Figure 12).

Two SPI-1 genes down regulated in *S*. Typhimurium post Cpx induction, were *sipB* and *sipC* (Table 22). Both are required for adhesion to epithelial cells (Lara-Tejero and Galán, 2009) providing one possible explanation for the reduced invasiveness of HEp2 and Caco-2 epithelial cells by *S*. Typhimurium *cpxA** seen by Humphreys et al. (2004). The Humphreys et al. (2004) study assessed the virulence of multiple *cpx*- mutants and showed that levels of *S*. Typhimurium virulence correlated inversely with the amount of CpxR-P present within the cell (Humphreys et al., 2004), concurring with the negative regulation of SPI-1 genes observed during our investigations.

Although the Cpx-mediated regulation of SPI-1 presented during our study requires further investigation to confirm the specific means by which this regulation occurs, it is an exciting discovery given the importance of this major virulence determinant in *Salmonella*. There are numerous studies reporting the involvement of SPI-1 encoded proteins during intestinal colonisation of *S*. Typhimurium, in many animal models (bovine, porcine, poultry and murine) (Boyen et al., 2006, Coombes et al., 2005, Hapfelmeier et al., 2004, Turner et al., 1998). Despite SPI-1 of *S*. Enteritidis being involved in, but not essential for the systemic spread of infection in chickens (Desin et al., 2009), and human gastroenteritis from *S*. Senftenberg occurring in the absence of this pathogenicity island (Hu et al., 2008), SPI-1 is still an important contributor to *Salmonella enterica* virulence and contains possible targets for future treatment and vaccines.

Cpx involvement in virulence is not limited to those processes outlined above. The SPI-1 and SPI-2 secreted protein SlrP is directly repressed by CpxR through the proposed binding of CpxR-P to a 17bp CpxR binding motif within the *slrP* promoter (Figure 17; Appendix J). Encoding an E3 ubiquitin ligase, expression of SlrP in HeLa cells results in a significant reduction in thioredoxin activity and induces apoptosis of host cells (Bernal-Bayard and

Ramos-Morales, 2009). Interestingly, the SPI-1 effector protein SipB, also down regulated by CpxR during our transcriptomic analysis, is involved in rapid pyroptosis and delayed apoptosis of *Salmonella* infected macrophages through an unknown association with Caspase-1 (Fink and Cookson, 2007, Knodler and Finlay, 2001). *Salmonella*-induced apoptosis is one weapon *Salmonella* uses to manipulate host cell functions for its advantage, and there is much evidence supporting *Salmonella*-induced macrophage and neutrophil cell death (Richter-Dahlfors et al., 1997, Lindgren et al., 1996, Chen et al., 1996). Although it appears that both the bacteria and host immune cell are responsible for this programmed death (activated macrophages are more cytotoxic than unactivated cells after *Salmonella* infection), the process is SPI-1 dependent because invasive but non-replicating *S*. Typhimurium strains are still able to induce apoptosis of murine macrophages *in vitro* (Monack et al., 1996, Chen et al., 1996). The theory behind this pathogen-induced cell death is that through apoptosis and pyroptosis *Salmonella* can, at the appropriate time 1) escape the host cell and increase infection and 2) remove host immune response cells to weaken the localised host immune response (Knodler and Finlay, 2001). To the best of our knowledge, Cpx has not been implicated in this process before. Down-regulation of apoptosis inducers by Cpx could help fine-tune this process to ensure host cell death does not occur too early. Rapid killing of the macrophages would be detrimental to the bacteria as *Salmonella* would be unable to establish itself within the SCV, replicate and escape to invade new host cells. Although we provide evidence to support direct repression of *slrP* by CpxR-P in *S*. Typhimurium, western blot analysis of chromosomally epitope tagged SlrP protein in our SL1344 WT and *cpxR* deletion strains would allow quantification of post-translational SlrP levels and comparison to the changes in transcription observed for SlrP during our microarray (Table 22) and qRT-PCR (Figure 14, E) analyses.

7.5 Concluding remarks

The work presented during this thesis expanded our understanding of ESRs in *S*. Typhimurium. In particular, the results discussed here for the Cpx and ZraSR stress responses give more weight to involvement of these systems in

Salmonella pathogenicity, specifically establishing an infection within host immune cells and surviving within that microenvironment. The large number of uncharacterised and unknown genes highlighted as Cpx or ZraSR regulated during this study further enhances our need to understand the function of these stress response systems and the untapped potential they offer when it comes to understanding *Salmonella* physiology.

There are many avenues of future work as a result of this research. Specific experiments are described during the 'Discussion and future work' sections of each results chapter and cover theses main areas: 1) Host-pathogen interactions: Identifying involvement of ZraPSR during *Salmonella* infection, specifically survival within phagocytic immune cells and the SCV, 2) characterisation of previously unidentified and unknown members of the Cpx and Zra regulons, broadening our understanding of these envelope stress responses and their influence on *Salmonella* physiology and 3) the methods utilised by periplasmic chaperones (specifically the CpxP family) to control periplasmic protein quality and integration of this signals into transcriptional networks. This knowledge could provide targets for new treatment strategies of *Salmonella* infections and expanding this research beyond our model strain to clinical isolates could provide additional insights into the infection strategies of *Salmonella* serovars associated with the ESRs. Given the increasing prevalence of antibiotic resistance and the evolution of iNTS strains, alternative means of treatment are desperately needed to perturb the global social and economic impact of *Salmonella* spp. Although this research has added to the wealth of ESR knowledge in general, and provided the first major investigation into Cpx and ZraSR regulated genes in any *Salmonella* species, there is still more to be discovered and understood if we are to fully understand the molecular and physiological functions associated with the envelope stress responses of this important pathogen.

8 References

ABBOTT, S. L., NI, F. C. Y. & JANDA, J. M. 2012. Increase in Extraintestinal Infections Caused by *Salmonella* enterica Subspecies II–IV. *Emerg Infect Dis,* 18**,** 637-9.

ABRIATA, L. A., PONTEL, L. B., VILA, A. J., DAL PERARO, M. & SONCINI, F. C. 2014. A dimerization interface mediated by functionally critical residues creates interfacial disulfide bonds and copper sites in CueP. *J Inorg Biochem,* 140**,** 199-201.

ACHARD, M. E., STAFFORD, S. L., BOKIL, N. J., CHARTRES, J., BERNHARDT, P. V., SCHEMBRI, M. A., SWEET, M. J. & MCEWAN, A. G. 2012. Copper redistribution in murine macrophages in response to *Salmonella* infection. *Biochem J,* 444**,** 51-7.

ACHARD, M. E., TREE, J. J., HOLDEN, J. A., SIMPFENDORFER, K. R., WIJBURG, O. L., STRUGNELL, R. A., SCHEMBRI, M. A., SWEET, M. J., JENNINGS, M. P. & MCEWAN, A. G. 2010. The multi-copper-ion oxidase CueO of *Salmonella* enterica serovar Typhimurium is required for systemic virulence. *Infect Immun,* 78**,** 2312-9.

ACHTMAN, M., WAIN, J., WEILL, F. X., NAIR, S., ZHOU, Z., SANGAL, V., KRAULAND, M. G., HALE, J. L., HARBOTTLE, H., UESBECK, A., DOUGAN, G., HARRISON, L. H. & BRISSE, S. 2012. Multilocus sequence typing as a replacement for serotyping in *Salmonella* enterica. *PLoS Pathog,* 8**,** e1002776.

ACOSTA, N., PUKATZKI, S. & RAIVIO, T. L. 2015. The Cpx system regulates virulence gene expression in *Vibrio cholerae*. *Infect Immun,* 83**,** 2396-408.

AGERTT, F., CRIPPA, A. C., LORENZONI, P. J., SCOLA, R. H., BRUCK, I., PAOLA, L., SILVADO, C. E. & WERNECK, L. C. 2007. Menkes' disease: case report. *Arq Neuropsiquiatr,* 65**,** 157-60.

AGRANOFF, D. D. & KRISHNA, S. 1998. Metal ion homeostasis and intracellular parasitism. *Mol Microbiol,* 28**,** 403-12.

AGUIRRE, J. D. & CULOTTA, V. C. 2012. Battles with iron: manganese in oxidative stress protection. *J Biol Chem,* 287**,** 13541-8.

ALBA, B. M. & GROSS, C. A. 2004. Regulation of the *Escherichia coli* sigma-dependent envelope stress response. *Mol Microbiol,* 52**,** 613-9.

ALBERTS, I. L., NADASSY, K. & WODAK, S. J. 1998. Analysis of zinc binding sites in protein crystal structures. *Protein Sci,* 7**,** 1700-16.

ALPUCHE ARANDA, C. M., SWANSON, J. A., LOOMIS, W. P. & MILLER, S. I. 1992. *Salmonella* typhimurium activates virulence gene transcription within acidified macrophage phagosomes. *Proc Natl Acad Sci U S A,* 89**,** 10079-83.

ALSTON, M. J., SEERS, J., HINTON, J. C. & LUCCHINI, S. 2010. BABAR: an R package to simplify the normalisation of common reference design microarray-based transcriptomic datasets. *BMC Bioinformatics,* 11**,** 73.

ALTIER, C. 2005. Genetic and environmental control of *Salmonella* invasion. *J Microbiol,* 43 Spec No**,** 85-92.

ALTMAN, E. & SEGAL, G. 2008. The response regulator CpxR directly regulates expression of several *Legionella pneumophila* icm/dot components as well as new translocated substrates. *J Bacteriol,* 190**,** 1985-96.

ALTSCHUL, S. F., GISH, W., MILLER, W., MYERS, E. W. & LIPMAN, D. J. 1990. Basic local alignment search tool. *J Mol Biol,* 215**,** 403-10.

AMMENDOLA, S., PASQUALI, P., PISTOIA, C., PETRUCCI, P., PETRARCA, P., ROTILIO, G. & BATTISTONI, A. 2007. High-affinity Zn2+ uptake system ZnuABC is required for bacterial zinc homeostasis in intracellular environments and contributes to the virulence of *Salmonella enterica*. *Infect Immun,* 75**,** 5867-76.

ANDERSON, E. S., PAULLEY, J. T., GAINES, J. M., VALDERAS, M. W., MARTIN, D. W., MENSCHER, E., BROWN, T. D., BURNS, C. S. & ROOP, R. M., 2ND 2009. The manganese transporter MntH is a critical virulence determinant for *Brucella abortus* 2308 in experimentally infected mice. *Infect Immun,* 77**,** 3466-74.

ANDREINI, C., BANCI, L., BERTINI, I. & ROSATO, A. 2006. Zinc through the three domains of life. *J Proteome Res,* 5**,** 3173-8.

ANJEM, A., VARGHESE, S. & IMLAY, J. A. 2009. Manganese import is a key element of the OxyR response to hydrogen peroxide in *Escherichia coli*. *Mol Microbiol,* 72**,** 844-58.

ANWAR, N., SEM, X. H. & RHEN, M. 2013. Oxidoreductases that act as conditional virulence suppressors in *Salmonella enterica* serovar Typhimurium. *PLoS One,* 8**,** e64948.

APPIA-AYME, C., HALL, A., PATRICK, E., RAJADURAI, S., CLARKE, T. A. & ROWLEY, G. 2012. ZraP is a periplasmic molecular chaperone and a repressor of the zinc-responsive two-component regulator ZraSR. *Biochem J,* 442**,** 85-93.

APPIA-AYME, C., PATRICK, E., SULLIVAN, M. J., ALSTON, M. J., FIELD, S. J., ABUOUN, M., ANJUM, M. F. & ROWLEY, G. 2011. Novel inducers of the envelope stress response BaeSR in *Salmonella* Typhimurium: BaeR is critically required for tungstate waste disposal. *PLoS One,* 6**,** e23713.

ARGUELLO, J. M., RAIMUNDA, D. & PADILLA-BENAVIDES, T. 2013. Mechanisms of copper homeostasis in bacteria. *Front Cell Infect Microbiol,* 3**,** 73.

ARMITAGE, A. E., EDDOWES, L. A., GILEADI, U., COLE, S., SPOTTISWOODE, N., SELVAKUMAR, T. A., HO, L. P., TOWNSEND, A. R. & DRAKESMITH, H. 2011. Hepcidin regulation by innate immune and infectious stimuli. *Blood,* 118**,** 4129-39.

ARSLAN, M. A., CSERMELY, P. & SOTI, C. 2006. Protein homeostasis and molecular chaperones in aging. *Biogerontology,* 7**,** 383-9.

AUDRAIN, B., FERRIÈRES, L., ZAIRI, A., SOUBIGOU, G., DOBSON, C., COPPÉE, J.-Y., BELOIN, C. & GHIGO, J.-M. 2013. Induction of the Cpx Envelope Stress Pathway Contributes to *Escherichia coli* Tolerance to Antimicrobial Peptides. *Applied and Environmental Microbiology,* 79**,** 7770-7779.

AUJLA, S. J., CHAN, Y. R., ZHENG, M., FEI, M., ASKEW, D. J., POCIASK, D. A., REINHART, T. A., MCALLISTER, F., EDEAL, J., GAUS, K., HUSAIN, S., KREINDLER, J. L., DUBIN, P. J., PILEWSKI, J. M., MYERBURG, M. M., MASON, C. A., IWAKURA, Y. & KOLLS, J. K. 2008. IL-22 mediates mucosal host defense against Gram-negative bacterial pneumonia. *Nat Med,* 14**,** 275-81.

AULD, D. S. 2001. Zinc coordination sphere in biochemical zinc sites. *Biometals,* 14**,** 271-313.

BACHMAN, M. A., MILLER, V. L. & WEISER, J. N. 2009. Mucosal lipocalin 2 has pro-inflammatory and iron-sequestering effects in response to bacterial enterobactin. *PLoS Pathog,* 5**,** e1000622.

BACHMAN, M. A., OYLER, J. E., BURNS, S. H., CAZA, M., LEPINE, F., DOZOIS, C. M. & WEISER, J. N. 2011. *Klebsiella pneumoniae* yersiniabactin promotes respiratory tract infection through evasion of lipocalin 2. *Infect Immun,* 79**,** 3309-16.

BADER, M. W., NAVARRE, W. W., SHIAU, W., NIKAIDO, H., FRYE, J. G., MCCLELLAND, M., FANG, F. C. & MILLER, S. I. 2003. Regulation of *Salmonella* Typhimurium virulence gene expression by cationic antimicrobial peptides. *Mol Microbiol,* 50**,** 219-30.

BALAJI, B., O'CONNOR, K., LUCAS, J. R., ANDERSON, J. M. & CSONKA, L. N. 2005. Timing of induction of osmotically controlled genes in *Salmonella enterica* Serovar Typhimurium, determined with quantitative real-time reverse transcription-PCR. *Appl Environ Microbiol,* 71**,** 8273-83.

BANG, I. S., AUDIA, J. P., PARK, Y. K. & FOSTER, J. W. 2002. Autoinduction of the ompR response regulator by acid shock and control of the *Salmonella enterica* acid tolerance response. *Mol Microbiol,* 44**,** 1235-50.

BANG, I. S., FRYE, J. G., MCCLELLAND, M., VELAYUDHAN, J. & FANG, F. C. 2005. Alternative sigma factor interactions in *Salmonella*: sigma and sigma promote antioxidant defences by enhancing sigma levels. *Mol Microbiol,* 56**,** 811-23.

BARQUIST, L., LANGRIDGE, G. C., TURNER, D. J., PHAN, M. D., TURNER, A. K., BATEMAN, A., PARKHILL, J., WAIN, J. & GARDNER, P. P. 2013. A comparison of dense transposon insertion libraries in the *Salmonella* serovars Typhi and Typhimurium. *Nucleic Acids Res,* 41**,** 4549-64.

BARROW, P. A. 1991. Experimental infection of chickens with *Salmonella* enteritidis. *Avian Pathol,* 20**,** 145-53.

BATCHELOR, E., WALTHERS, D., KENNEY, L. J. & GOULIAN, M. 2005. The *Escherichia coli* CpxA-CpxR envelope stress response system regulates expression of the porins OmpF and OmpC. *J Bacteriol,* 187**,** 5723-31.

BATTESTI, A. & GOTTESMAN, S. 2013. Roles of adaptor proteins in regulation of bacterial proteolysis. *Curr Opin Microbiol,* 16**,** 140-7.

BATTESTI, A., HOSKINS, J. R., TONG, S., MILANESIO, P., MANN, J. M., KRAVATS, A., TSEGAYE, Y. M., BOUGDOUR, A., WICKNER, S. & GOTTESMAN, S. 2013. Anti-adaptors provide multiple modes for regulation of the RssB adaptor protein. *Genes Dev,* 27**,** 2722-35.

BATTESTI, A., MAJDALANI, N. & GOTTESMAN, S. 2011. The RpoS-mediated general stress response in *Escherichia coli*. *Annu Rev Microbiol,* 65**,** 189-213.

BAUER, J., FRITSCH, M. J., PALMER, T. & UNDEN, G. 2011. Topology and accessibility of the transmembrane helices and the sensory site in the bifunctional transporter DcuB of *Escherichia coli*. *Biochemistry,* 50**,** 5925-38.

BAUMLER, A. J., KUSTERS, J. G., STOJILJKOVIC, I. & HEFFRON, F. 1994. *Salmonella* Typhimurium loci involved in survival within macrophages. *Infect Immun,* 62**,** 1623-30.

BAUMLER, A. J., TSOLIS, R. M., FICHT, T. A. & ADAMS, L. G. 1998. Evolution of host adaptation in *Salmonella enterica*. *Infect Immun,* 66**,** 4579-87.

BEARSON, B. L., WILSON, L. & FOSTER, J. W. 1998. A low pH-inducible, PhoPQ-dependent acid tolerance response protects *Salmonella* Typhimurium against inorganic acid stress. *J Bacteriol,* 180**,** 2409-17.

BECKER, L. A., BANG, I. S., CROUCH, M. L. & FANG, F. C. 2005. Compensatory role of PspA, a member of the phage shock protein operon, in *rpoE* mutant *Salmonella enterica* serovar Typhimurium. *Mol Microbiol,* 56**,** 1004-16.

BELAAOUAJ, A., MCCARTHY, R., BAUMANN, M., GAO, Z., LEY, T. J., ABRAHAM, S. N. & SHAPIRO, S. D. 1998. Mice lacking neutrophil elastase reveal impaired host defense against gram negative bacterial sepsis. *Nat Med,* 4**,** 615-8.

BELAAOUAJ, A. A., KIM, K. S. & SHAPIRO, S. D. 2000. Degradation of Outer Membrane Protein A in *Escherichia coli* Killing by Neutrophil Elastase. *Science,* 289**,** 1185-1187.

BELKIN, S. & GU, M. B. 2010. *Whole Cell Sensing Systems II - Applications*, Springer-Verlag Berlin Heidelberg GmbH & Co. KG.

BELOIN, C., VALLE, J., LATOUR-LAMBERT, P., FAURE, P., KZREMINSKI, M., BALESTRINO, D., HAAGENSEN, J. A., MOLIN, S., PRENSIER, G., ARBEILLE, B. & GHIGO, J. M. 2004. Global impact of mature biofilm lifestyle on *Escherichia coli* K-12 gene expression. *Mol Microbiol,* 51**,** 659-74.

BERG, J. M. & SHI, Y. 1996. The galvanization of biology: a growing appreciation for the roles of zinc. *Science,* 271**,** 1081-5.

BERGER, L. L. 1987. *Salt and trace minerals for livestock, poultry and other animals,* Alexandria, VA., Salt Institute.

BERNAL-BAYARD, J. & RAMOS-MORALES, F. 2009. *Salmonella* type III secretion effector SlrP is an E3 ubiquitin ligase for mammalian thioredoxin. *J Biol Chem,* 284**,** 27587-95.

BERTANI, G. 1951. Studies on lysogenesis. I. The mode of phage liberation by lysogenic Escherichia coli. *J Bacteriol,* 62**,** 293-300.

BEUZON, C. R., MERESSE, S., UNSWORTH, K. E., RUIZ-ALBERT, J., GARVIS, S., WATERMAN, S. R., RYDER, T. A., BOUCROT, E. & HOLDEN, D. W. 2000. *Salmonella* maintains the integrity of its intracellular vacuole through the action of SifA. *Embo j,* 19**,** 3235-49.

BEUZON, C. R., SALCEDO, S. P. & HOLDEN, D. W. 2002. Growth and killing of a *Salmonella* enterica serovar Typhimurium *sifA* mutant strain in the cytosol of different host cell lines. *Microbiology,* 148**,** 2705-15.

BHAN, M. K., BAHL, R. & BHATNAGAR, S. 2005. Typhoid and paratyphoid fever. *Lancet,* 366**,** 749-62.

BHUTTA, Z. A. 2006. Current concepts in the diagnosis and treatment of typhoid fever. *Bmj,* 333**,** 78-82.

BHUTTA, Z. A., PUNJWANI, N. & LINDBLAD, B. S. 1996. Concomitant bacteraemia as a risk factor for diarrhoeal disease mortality in

Karachi: a case-control study of hospitalized children. *Acta Paediatr,* 85**,** 809-13.
BITTO, E. & MCKAY, D. B. 2003. The periplasmic molecular chaperone protein SurA binds a peptide motif that is characteristic of integral outer membrane proteins. *J Biol Chem,* 278**,** 49316-22.
BLANC-POTARD, A. B., SOLOMON, F., KAYSER, J. & GROISMAN, E. A. 1999. The SPI-3 pathogenicity island of *Salmonella enterica*. *J Bacteriol,* 181**,** 998-1004.
BLENCOWE, D. K. & MORBY, A. P. 2003. Zn(II) metabolism in prokaryotes. *FEMS Microbiol Rev,* 27**,** 291-311.
BLONDEL, C. J., JIMENEZ, J. C., CONTRERAS, I. & SANTIVIAGO, C. A. 2009. Comparative genomic analysis uncovers 3 novel loci encoding type six secretion systems differentially distributed in *Salmonella* serotypes. *BMC Genomics,* 10**,** 354.
BOCHNER, B. R. 1984. Curing bacterial cells of lysogenic viruses by using UCB indicator plates. *Biotechniques,* 2**,** 234-240.
BOOR, K. J. 2006. Bacterial stress responses: what doesn't kill them can make then stronger. *PLoS Biol,* 4**,** e23.
BORATYN, G. M., CAMACHO, C., COOPER, P. S., COULOURIS, G., FONG, A., MA, N., MADDEN, T. L., MATTEN, W. T., MCGINNIS, S. D., MEREZHUK, Y., RAYTSELIS, Y., SAYERS, E. W., TAO, T., YE, J. & ZARETSKAYA, I. 2013. BLAST: a more efficient report with usability improvements. *Nucleic Acids Research,* 41**,** W29-W33.
BORUKHOV, S. & NUDLER, E. 2003. RNA polymerase holoenzyme: structure, function and biological implications. *Curr Opin Microbiol,* 6**,** 93-100.
BOTSFORD, J. L. & DEMOSS, R. D. 1972. *Escherichia coli* tryptophanase in the enteric environment. *J Bacteriol,* 109**,** 74-80.
BOTTELDOORN, N., VAN COILLIE, E., GRIJSPEERDT, K., WERBROUCK, H., HAESEBROUCK, F., DONNE, E., D'HAESE, E., HEYNDRICKX, M., PASMANS, F. & HERMAN, L. 2006. Real-time reverse transcription PCR for the quantification of the mntH expression of *Salmonella enterica* as a function of growth phase and phagosome-like conditions. *J Microbiol Methods,* 66**,** 125-35.
BOUCHE, S., KLAUCK, E., FISCHER, D., LUCASSEN, M., JUNG, K. & HENGGE-ARONIS, R. 1998. Regulation of RssB-dependent proteolysis in *Escherichia coli*: a role for acetyl phosphate in a response regulator-controlled process. *Mol Microbiol,* 27**,** 787-95.
BOUGDOUR, A., WICKNER, S. & GOTTESMAN, S. 2006. Modulating RssB activity: IraP, a novel regulator of σ(S) stability in *Escherichia coli*. *Genes Dev,* 20**,** 884-97.
BOWDEN, S. D., ROWLEY, G., HINTON, J. C. D. & THOMPSON, A. 2009. Glucose and Glycolysis Are Required for the Successful Infection of Macrophages and Mice by *Salmonella* enterica Serovar Typhimurium. *Infect Immun,* 77**,** 3117-26.
BOYEN, F., PASMANS, F., VAN IMMERSEEL, F., MORGAN, E., ADRIAENSEN, C., HERNALSTEENS, J. P., DECOSTERE, A., DUCATELLE, R. & HAESEBROUCK, F. 2006. *Salmonella* Typhimurium SPI-1 genes promote intestinal but not tonsillar colonization in pigs. *Microbes Infect,* 8**,** 2899-907.

BOYLE, E. C., BISHOP, J. L., GRASSL, G. A. & FINLAY, B. B. 2007. *Salmonella*: from Pathogenesis to Therapeutics. *J Bacteriol,* 189**,** 1489-95.

BRADFORD, M. M. 1976. A rapid and sensitive method for the quantitation of microgram quantities of protein utilizing the principle of protein-dye binding. *Anal Biochem,* 72**,** 248-54.

BRASS, J. M., HIGGINS, C. F., FOLEY, M., RUGMAN, P. A., BIRMINGHAM, J. & GARLAND, P. B. 1986. Lateral diffusion of proteins in the periplasm of *Escherichia coli*. *J Bacteriol,* 165**,** 787-95.

BRAWN, L. C., HAYWARD, R. D. & KORONAKIS, V. 2007. *Salmonella* SPI1 effector SipA persists after entry and cooperates with a SPI2 effector to regulate phagosome maturation and intracellular replication. *Cell Host Microbe,* 1**,** 63-75.

BRISSETTE, J. L., RUSSEL, M., WEINER, L. & MODEL, P. 1990. Phage shock protein, a stress protein of *Escherichia coli. Proc Natl Acad Sci U S A,* 87**,** 862-6.

BROKX, S. J., ROTHERY, R. A., ZHANG, G., NG, D. P. & WEINER, J. H. 2005. Characterization of an *Escherichia coli* sulfite oxidase homologue reveals the role of a conserved active site cysteine in assembly and function. *Biochemistry,* 44**,** 10339-48.

BROWN, R. N. & GULIG, P. A. 2009. Roles of RseB, sigmaE, and DegP in virulence and phase variation of colony morphotype of *Vibrio vulnificus*. *Infect Immun,* 77**,** 3768-81.

BRUMELL, J. H., ROSENBERGER, C. M., GOTTO, G. T., MARCUS, S. L. & FINLAY, B. B. 2001. SifA permits survival and replication of *Salmonella* Typhimurium in murine macrophages. *Cell Microbiol,* 3**,** 75-84.

BRUSCH, J. L., GARVEY, T., CORALES, R. & SCHMITT, S. K. 2015. *Typhoid Fever Medication* [Online]. http://emedicine.medscape.com/article/231135: Medscape. [Accessed 25-02 2015].

BUCHMEIER, N. A. & HEFFRON, F. 1990. Induction of *Salmonella* stress proteins upon infection of macrophages. *Science,* 248**,** 730-2.

BUCKLE, G. C., WALKER, C. L. & BLACK, R. E. 2012. Typhoid fever and paratyphoid fever: Systematic review to estimate global morbidity and mortality for 2010. *J Glob Health,* 2**,** 010401.

BUELOW, D. R. & RAIVIO, T. L. 2005. Cpx signal transduction is influenced by a conserved N-terminal domain in the novel inhibitor CpxP and the periplasmic protease DegP. *J Bacteriol,* 187**,** 6622-30.

BUELOW, D. R. & RAIVIO, T. L. 2010. Three (and more) component regulatory systems - auxiliary regulators of bacterial histidine kinases. *Mol Microbiol,* 75**,** 547-66.

BURY-MONE, S., NOMANE, Y., REYMOND, N., BARBET, R., JACQUET, E., IMBEAUD, S., JACQ, A. & BOULOC, P. 2009. Global analysis of extracytoplasmic stress signaling in *Escherichia coli*. *PLoS Genet,* 5**,** e1000651.

BUSH, M. & DIXON, R. 2012. The Role of Bacterial Enhancer Binding Proteins as Specialized Activators of σ(54)-Dependent Transcription. *Microbiol Mol Biol Rev,* 76**,** 497-529.

CAMPOY, S., JARA, M., BUSQUETS, N., PEREZ DE ROZAS, A. M., BADIOLA, I. & BARBE, J. 2002. Role of the high-affinity zinc uptake *znuABC* system in *Salmonella* enterica serovar Typhimurium virulence. *Infect Immun,* 70**,** 4721-5.

CANO, D. A., PUCCIARELLI, M. G., MARTINEZ-MOYA, M., CASADESUS, J. & GARCIA-DEL PORTILLO, F. 2003. Selection of small-colony variants of *Salmonella* enterica serovar Typhimurium in nonphagocytic eucaryotic cells. *Infect Immun,* 71**,** 3690-8.

CAO, J., WOODHALL, M. R., ALVAREZ, J., CARTRON, M. L. & ANDREWS, S. C. 2007. EfeUOB (YcdNOB) is a tripartite, acid-induced and CpxAR-regulated, low-pH Fe^{2+} transporter that is cryptic in *Escherichia coli* K-12 but functional in *E. coli* O157:H7. *Mol Microbiol,* 65**,** 857-75.

CAPEL, J., JARILLO, J. A., SALINAS, J. & MARTINEZ-ZAPATER, J. M. 1997. Two homologous low-temperature-inducible genes from *Arabidopsis* encode highly hydrophobic proteins. *Plant Physiol,* 115**,** 569-76.

CAPOOR, M. R. & NAIR, D. 2010. Quinolone and Cephalosporin Resistance in Enteric Fever. *J Glob Infect Dis,* 2**,** 258-62.

CAPRA, E. J. & LAUB, M. T. 2012. Evolution of two-component signal transduction systems. *Annu Rev Microbiol,* 66**,** 325-47.

CARLSSON, K. E., LIU, J., EDQVIST, P. J. & FRANCIS, M. S. 2007a. Extracytoplasmic-stress-responsive pathways modulate type III secretion in *Yersinia pseudotuberculosis*. *Infect Immun,* 75**,** 3913-24.

CARLSSON, K. E., LIU, J., EDQVIST, P. J. & FRANCIS, M. S. 2007b. Influence of the Cpx extracytoplasmic-stress-responsive pathway on *Yersinia* sp.-eukaryotic cell contact. *Infect Immun,* 75**,** 4386-99.

CARPER, S. W., WILLIS, D. G., MANNING, K. A. & GERNER, E. W. 1991. Spermidine acetylation in response to a variety of stresses in *Escherichia coli*. *J Biol Chem,* 266**,** 12439-41.

CELLIER, M. F., COURVILLE, P. & CAMPION, C. 2007. NRAMP1 phagocyte intracellular metal withdrawal defense. *Microbes Infect,* 9**,** 1662-70.

CENTERS FOR DISEASE CONTROL AND PREVENTION (CDC) 2014. National *Salmonella* Surveillance Annual Report (2012). Atlanta, Georgia: US Department of Health and Human Services, CDC.

CERASI, M., AMMENDOLA, S. & BATTISTONI, A. 2013. Competition for zinc binding in the host-pathogen interaction. *Front Cell Infect Microbiol,* 3**,** 108.

CERASI, M., LIU, J. Z., AMMENDOLA, S., POE, A. J., PETRARCA, P., PESCIAROLI, M., PASQUALI, P., RAFFATELLU, M. & BATTISTONI, A. 2014. The ZupT transporter plays an important role in zinc homeostasis and contributes to *Salmonella enterica* virulence. *Metallomics,* 6**,** 845-53.

CHAMPION, O. L., KARLYSHEV, A., COOPER, I. A., FORD, D. C., WREN, B. W., DUFFIELD, M., OYSTON, P. C. & TITBALL, R. W. 2011. *Yersinia pseudotuberculosis mntH* functions in intracellular manganese accumulation, which is essential for virulence and survival in cells expressing functional NRAMP1. *Microbiology,* 157**,** 1115-22.

CHAN, Y. Y. & CHUA, K. L. 2010. Growth-related changes in intracellular spermidine and its effect on efflux pump expression and quorum sensing in *Burkholderia pseudomallei*. *Microbiology,* 156**,** 1144-54.

CHASSAING, B. & DARFEUILLE-MICHAUD, A. 2013. The sigmaE pathway is involved in biofilm formation by Crohn's disease-associated adherent-invasive *Escherichia coli*. *J Bacteriol,* 195**,** 76-84.

CHASSAING, B., GARÉNAUX, E., CARRIERE, J., ROLHION, N., GUÉRARDEL, Y., BARNICH, N., BONNET, R. & DARFEUILLE-MICHAUD, A. 2015. Analysis of σ^E regulon in Crohn disease-associated *E. coli* revealed *waaWVL* operon involved in biofilm formation. *Journal of Bacteriology*.

CHATFIELD, S. N., STRAHAN, K., PICKARD, D., CHARLES, I. G., HORMAECHE, C. E. & DOUGAN, G. 1992. Evaluation of *Salmonella* Typhimurium strains harbouring defined mutations in *htrA* and *aroA* in the murine salmonellosis model. *Microb Pathog,* 12**,** 145-51.

CHATTOPADHYAY, M. K., TABOR, C. W. & TABOR, H. 2003. Polyamines protect *Escherichia coli* cells from the toxic effect of oxygen. *Proceedings of the National Academy of Sciences,* 100**,** 2261-2265.

CHAU, T. T., CAMPBELL, J. I., GALINDO, C. M., VAN MINH HOANG, N., DIEP, T. S., NGA, T. T., VAN VINH CHAU, N., TUAN, P. Q., PAGE, A. L., OCHIAI, R. L., SCHULTSZ, C., WAIN, J., BHUTTA, Z. A., PARRY, C. M., BHATTACHARYA, S. K., DUTTA, S., AGTINI, M., DONG, B., HONGHUI, Y., ANH, D. D., CANH DO, G., NAHEED, A., ALBERT, M. J., PHETSOUVANH, R., NEWTON, P. N., BASNYAT, B., ARJYAL, A., LA, T. T., RANG, N. N., PHUONG LE, T., VAN BE BAY, P., VON SEIDLEIN, L., DOUGAN, G., CLEMENS, J. D., VINH, H., HIEN, T. T., CHINH, N. T., ACOSTA, C. J., FARRAR, J. & DOLECEK, C. 2007. Antimicrobial drug resistance of *Salmonella enterica* serovar Typhi in asia and molecular mechanism of reduced susceptibility to the fluoroquinolones. *Antimicrob Agents Chemother,* 51**,** 4315-23.

CHAUDHURI, R. R., KHAN, A. M. & PALLEN, M. J. 2004. coliBASE: an online database for *Escherichia coli*, *Shigella* and *Salmonella* comparative genomics. *Nucleic Acids Res,* 32**,** D296-9.

CHEN, C. Y. & MORSE, S. A. 2001. Identification and characterization of a high-affinity zinc uptake system in *Neisseria gonorrhoeae*. *FEMS Microbiol Lett,* 202**,** 67-71.

CHEN, L. M., KANIGA, K. & GALAN, J. E. 1996. *Salmonella* spp. are cytotoxic for cultured macrophages. *Mol Microbiol,* 21**,** 1101-15.

CHEN, R. & HENNING, U. 1996. A periplasmic protein (Skp) of *Escherichia coli* selectively binds a class of outer membrane proteins. *Mol Microbiol,* 19**,** 1287-94.

CHEREPANOV, P. P. & WACKERNAGEL, W. 1995. Gene disruption in *Escherichia coli*: TcR and KmR cassettes with the option of Flp-catalyzed excision of the antibiotic-resistance determinant. *Gene,* 158**,** 9-14.

CHEVANCE, F. F. & HUGHES, K. T. 2008. Coordinating assembly of a bacterial macromolecular machine. *Nat Rev Microbiol,* 6**,** 455-65.

CHURCH, D. C. & POND, W. G. 1989. *Basic Animal Nutrition and Feeding,* New York, John Wiley and Sons.

CIRILLO, D. M., VALDIVIA, R. H., MONACK, D. M. & FALKOW, S. 1998. Macrophage-dependent induction of the *Salmonella* pathogenicity island 2 type III secretion system and its role in intracellular survival. *Mol Microbiol,* 30**,** 175-88.

CLARK, M. A., JEPSON, M. A., SIMMONS, N. L. & HIRST, B. H. 1994. Preferential interaction of *Salmonella* Typhimurium with mouse Peyer's patch M cells. *Res Microbiol,* 145**,** 543-52.

CLARKE, D. J. 2012. The Rcs Phosphorelay: Biofilm Formation and Virulence. *In:* GROSS, R. & BEIER, D. (eds.) *Two-component Systems in Bacteria.* Norfolk, UK: Caister Academic Press.

COBURN, B., GRASSL, G. A. & FINLAY, B. B. 2007. *Salmonella*, the host and disease: a brief review. *Immunol Cell Biol,* 85**,** 112-8.

COHEN, S. S. 1997. *A Guide to the Polyamines,* New York, NY, Oxford University Press.

COLE, J. L., LARY, J. W., MOODY, T. & LAUE, T. M. 2008. Analytical Ultracentrifugation: Sedimentation Velocity and Sedimentation Equilibrium. *Methods Cell Biol,* 84**,** 143-79.

COLLINS, D. M., KAWAKAMI, R. P., DE LISLE, G. W., PASCOPELLA, L., BLOOM, B. R. & JACOBS, W. R., JR. 1995. Mutation of the principal sigma factor causes loss of virulence in a strain of the *Mycobacterium tuberculosis* complex. *Proc Natl Acad Sci U S A,* 92**,** 8036-40.

COLLINS, H. L. 2008. Withholding iron as a cellular defence mechanism--friend or foe? *Eur J Immunol,* 38**,** 1803-6.

CONNOLLY, L., DE LAS PENAS, A., ALBA, B. M. & GROSS, C. A. 1997. The response to extracytoplasmic stress in *Escherichia coli* is controlled by partially overlapping pathways. *Genes Dev,* 11**,** 2012-21.

COOMBES, B. K., COBURN, B. A., POTTER, A. A., GOMIS, S., MIRAKHUR, K., LI, Y. & FINLAY, B. B. 2005. Analysis of the contribution of *Salmonella* pathogenicity islands 1 and 2 to enteric disease progression using a novel bovine ileal loop model and a murine model of infectious enterocolitis. *Infect Immun,* 73**,** 7161-9.

CORBIN, B. D., SEELEY, E. H., RAAB, A., FELDMANN, J., MILLER, M. R., TORRES, V. J., ANDERSON, K. L., DATTILO, B. M., DUNMAN, P. M., GERADS, R., CAPRIOLI, R. M., NACKEN, W., CHAZIN, W. J. & SKAAR, E. P. 2008. Metal chelation and inhibition of bacterial growth in tissue abscesses. *Science,* 319**,** 962-5.

CORDERO-ALBA, M. & RAMOS-MORALES, F. 2014. Patterns of Expression and Translocation of the Ubiquitin Ligase SlrP in *Salmonella enterica* Serovar Typhimurium. *J Bacteriol,* 196**,** 3912-22.

COSMA, C. L., DANESE, P. N., CARLSON, J. H., SILHAVY, T. J. & SNYDER, W. B. 1995. Mutational activation of the Cpx signal transduction pathway of *Escherichia coli* suppresses the toxicity conferred by certain envelope-associated stresses. *Mol Microbiol,* 18**,** 491-505.

COSTERTON, J. W., STEWART, P. S. & GREENBERG, E. P. 1999. Bacterial biofilms: a common cause of persistent infections. *Science,* 284**,** 1318-22.

COYNAULT, C., ROBBE-SAULE, V. & NOREL, F. 1996. Virulence and vaccine potential of *Salmonella* Typhimurium mutants deficient in the expression of the RpoS (sigma S) regulon. *Mol Microbiol,* 22**,** 149-60.

CRAIG, J. E., NOBBS, A. & HIGH, N. J. 2002. The extracytoplasmic sigma factor, final sigma(E), is required for intracellular survival of nontypeable *Haemophilus influenzae* in J774 macrophages. *Infect Immun,* 70**,** 708-15.

CRANE, J. K., BYRD, I. W. & BOEDEKER, E. C. 2011. Virulence inhibition by zinc in shiga-toxigenic *Escherichia coli*. *Infect Immun,* 79**,** 1696-705.

CRAWFORD, R. W., ROSALES-REYES, R., RAMÍREZ-AGUILAR, M. D. L. L., CHAPA-AZUELA, O., ALPUCHE-ARANDA, C. & GUNN, J. S. 2010. Gallstones play a significant role in *Salmonella* spp. gallbladder colonization and carriage. *Proceedings of the National Academy of Sciences,* 107**,** 4353-4358.

CROUCH, M. L., BECKER, L. A., BANG, I. S., TANABE, H., OUELLETTE, A. J. & FANG, F. C. 2005. The alternative sigma factor sigma is required for resistance of *Salmonella* enterica serovar Typhimurium to anti-microbial peptides. *Mol Microbiol,* 56**,** 789-99.

CRUMP, J. A., LUBY, S. P. & MINTZ, E. D. 2004. The global burden of typhoid fever. *Bull World Health Organ,* 82**,** 346-53.

CRUMP, J. A. & MINTZ, E. D. 2010. Global trends in typhoid and paratyphoid Fever. *Clin Infect Dis,* 50**,** 241-6.

D'AMELIO, R., TAGLIABUE, A., NENCIONI, L., DI ADDARIO, A., VILLA, L., MANGANARO, M., BORASCHI, D., LE MOLI, S., NISINI, R. & MATRICARDI, P. M. 1988. Comparative analysis of immunological responses to oral (Ty21a) and parenteral (TAB) typhoid vaccines. *Infect Immun,* 56**,** 2731-5.

DALET, K., GOUIN, E., CENATIEMPO, Y., COSSART, P. & HECHARD, Y. 1999. Characterisation of a new operon encoding a Zur-like protein and an associated ABC zinc permease in *Listeria monocytogenes*. *FEMS Microbiol Lett,* 174**,** 111-6.

DALEY, D. O., RAPP, M., GRANSETH, E., MELEN, K., DREW, D. & VON HEIJNE, G. 2005. Global topology analysis of the *Escherichia coli* inner membrane proteome. *Science,* 308**,** 1321-3.

DANESE, P. N., OLIVER, G. R., BARR, K., BOWMAN, G. D., RICK, P. D. & SILHAVY, T. J. 1998. Accumulation of the enterobacterial common antigen lipid II biosynthetic intermediate stimulates *degP* transcription in *Escherichia coli*. *J Bacteriol,* 180**,** 5875-84.

DANESE, P. N. & SILHAVY, T. J. 1997. The sigma(E) and the Cpx signal transduction systems control the synthesis of periplasmic protein-folding enzymes in *Escherichia coli*. *Genes Dev,* 11**,** 1183-93.

DANESE, P. N. & SILHAVY, T. J. 1998. CpxP, a stress-combative member of the Cpx regulon. *J Bacteriol,* 180**,** 831-9.

DANESE, P. N., SNYDER, W. B., COSMA, C. L., DAVIS, L. J. & SILHAVY, T. J. 1995. The Cpx two-component signal transduction pathway of *Escherichia coli* regulates transcription of the gene specifying the stress-inducible periplasmic protease, DegP. *Genes Dev,* 9**,** 387-98.

DANIEL, A. G. & FARRELL, N. P. 2014. The dynamics of zinc sites in proteins: electronic basis for coordination sphere expansion at structural sites. *Metallomics,* 6**,** 2230-41.

DANIELS, J. J., AUTENRIETH, I. B., LUDWIG, A. & GOEBEL, W. 1996. The gene *slyA* of *Salmonella* Typhimurium is required for destruction of M

cells and intracellular survival but not for invasion or colonization of the murine small intestine. *Infect Immun,* 64**,** 5075-84.
DARTIGALONGUE, C., MISSIAKAS, D. & RAINA, S. 2001. Characterization of the *Escherichia coli* sigma E regulon. *J Biol Chem,* 276**,** 20866-75.
DARTIGALONGUE, C. & RAINA, S. 1998. A new heat-shock gene, *ppiD*, encodes a peptidyl-prolyl isomerase required for folding of outer membrane proteins in *Escherichia coli*. *Embo j,* 17**,** 3968-80.
DARWIN, A. J. 2005. The phage-shock-protein response. *Mol Microbiol,* 57**,** 621-8.
DATSENKO, K. A. & WANNER, B. L. 2000. One-step inactivation of chromosomal genes in *Escherichia coli* K-12 using PCR products. *Proc Natl Acad Sci U S A,* 97**,** 6640-5.
DAVIES, B. W., KOHANSKI, M. A., SIMMONS, L. A., WINKLER, J. A., COLLINS, J. J. & WALKER, G. C. 2009. Hydroxyurea induces hydroxyl radical-mediated cell death in *Escherichia coli*. *Mol Cell,* 36**,** 845-60.
DAVIN, R., MANZANILLA, E. G., KLASING, K. C. & PEREZ, J. F. 2012. Evolution of zinc, iron, and copper concentrations along the gastrointestinal tract of piglets weaned with or without in-feed high doses of zinc oxide compared to unweaned littermates. *J Anim Sci,* 90 Suppl 4**,** 248-50.
DAVIS, B. D. 1987. Mechanism of bactericidal action of aminoglycosides. *Microbiol Rev,* 51**,** 341-50.
DE JONG, H. K., PARRY, C. M., VAN DER POLL, T. & WIERSINGA, W. J. 2012. Host-pathogen interaction in invasive Salmonellosis. *PLoS Pathog,* 8**,** e1002933.
DE LAS PENAS, A., CONNOLLY, L. & GROSS, C. A. 1997. SigmaE is an essential sigma factor in *Escherichia coli*. *J Bacteriol,* 179**,** 6862-4.
DE LAY, N. & GOTTESMAN, S. 2009. The Crp-activated small noncoding regulatory RNA CyaR (RyeE) links nutritional status to group behavior. *J Bacteriol,* 191**,** 461-76.
DE WULF, P., KWON, O. & LIN, E. C. 1999. The CpxRA signal transduction system of *Escherichia coli*: growth-related autoactivation and control of unanticipated target operons. *J Bacteriol,* 181**,** 6772-8.
DE WULF, P., MCGUIRE, A. M., LIU, X. & LIN, E. C. 2002. Genome-wide profiling of promoter recognition by the two-component response regulator CpxR-P in *Escherichia coli*. *J Biol Chem,* 277**,** 26652-61.
DEBNATH, I., NORTON, J. P., BARBER, A. E., OTT, E. M., DHAKAL, B. K., KULESUS, R. R. & MULVEY, M. A. 2013. The Cpx Stress Response System Potentiates the Fitness and Virulence of Uropathogenic *Escherichia coli*. *Infect Immun,* 81**,** 1450-9.
DEEN, J., VON SEIDLEIN, L., ANDERSEN, F., ELLE, N., WHITE, N. J. & LUBELL, Y. 2012. Community-acquired bacterial bloodstream infections in developing countries in south and southeast Asia: a systematic review. *Lancet Infect Dis,* 12**,** 480-7.
DEMELAR, B. 2005. UltraScan - A Comprehensive Data Analysis Software Package for Analytical Ultracentrifugation Experiments. *In:* SCOTT, D. J., HARDING, S. E. & ROWE, A. J. (eds.) *Analytical Ultracentrifugation: Techniques and Methods.* The Royal Society of Chemistry.

DESIN, T. S., LAM, P. K. S., KOCH, B., MICKAEL, C., BERBEROV, E., WISNER, A. L. S., TOWNSEND, H. G. G., POTTER, A. A. & KÖSTER, W. 2009. *Salmonella* enterica Serovar Enteritidis Pathogenicity Island 1 Is Not Essential for but Facilitates Rapid Systemic Spread in Chickens. *Infect Immun,* 77**,** 2866-75.

DESROSIERS, D. C., BEARDEN, S. W., MIER, I., ABNEY, J., PAULLEY, J. T., FETHERSTON, J. D., SALAZAR, J. C., RADOLF, J. D. & PERRY, R. D. 2010. Znu Is the Predominant Zinc Importer in *Yersinia pestis* during In Vitro Growth but Is Not Essential for Virulence. *Infection and Immunity,* 78**,** 5163-5177.

DI MARTINO, M. L., CAMPILONGO, R., CASALINO, M., MICHELI, G., COLONNA, B. & PROSSEDA, G. 2013. Polyamines: emerging players in bacteria-host interactions. *Int J Med Microbiol,* 303**,** 484-91.

DIAZ-OCHOA, V. E., JELLBAUER, S., KLAUS, S. & RAFFATELLU, M. 2014. Transition metal ions at the crossroads of mucosal immunity and microbial pathogenesis. *Front Cell Infect Microbiol,* 4.

DIGIUSEPPE, P. A. & SILHAVY, T. J. 2003. Signal detection and target gene induction by the CpxRA two-component system. *J Bacteriol,* 185**,** 2432-40.

DINTILHAC, A., ALLOING, G., GRANADEL, C. & CLAVERYS, J. P. 1997. Competence and virulence of *Streptococcus pneumoniae*: Adc and PsaA mutants exhibit a requirement for Zn and Mn resulting from inactivation of putative ABC metal permeases. *Mol Microbiol,* 25**,** 727-39.

DOERRLER, W. T. & RAETZ, C. R. 2005. Loss of outer membrane proteins without inhibition of lipid export in an *Escherichia coli* YaeT mutant. *J Biol Chem,* 280**,** 27679-87.

DONG, J., IUCHI, S., KWAN, H. S., LU, Z. & LIN, E. C. 1993. The deduced amino-acid sequence of the cloned *cpxR* gene suggests the protein is the cognate regulator for the membrane sensor, CpxA, in a two-component signal transduction system of *Escherichia coli*. *Gene,* 136**,** 227-30.

DONLAN, R. M. & COSTERTON, J. W. 2002. Biofilms: survival mechanisms of clinically relevant microorganisms. *Clin Microbiol Rev,* 15**,** 167-93.

DOOLITTLE, R. F., FENG, D. F., TSANG, S., CHO, G. & LITTLE, E. 1996. Determining divergence times of the major kingdoms of living organisms with a protein clock. *Science,* 271**,** 470-7.

DOREL, C., LEJEUNE, P. & RODRIGUE, A. 2006. The Cpx system of *Escherichia coli*, a strategic signaling pathway for confronting adverse conditions and for settling biofilm communities? *Research in Microbiology,* 157**,** 306-314.

DOREL, C., VIDAL, O., PRIGENT-COMBARET, C., VALLET, I. & LEJEUNE, P. 1999. *Involvement of the Cpx signal transduction pathway of E. coli in biofilm formation*.

DORSEY-ORESTO, A., LU, T., MOSEL, M., WANG, X., SALZ, T., DRLICA, K. & ZHAO, X. 2013. YihE Kinase Is a Central Regulator of Programmed Cell Death in Bacteria. *Cell Reports,* 3**,** 528-537.

DOUCHIN, V., BOHN, C. & BOULOC, P. 2006. Down-regulation of porins by a small RNA bypasses the essentiality of the regulated

intramembrane proteolysis protease RseP in *Escherichia coli*. *J Biol Chem,* 281**,** 12253-9.
DRIESSEN, A. J. & NOUWEN, N. 2008. Protein translocation across the bacterial cytoplasmic membrane. *Annu Rev Biochem,* 77**,** 643-67.
DU, H., SHENG, X., ZHANG, H., ZOU, X., NI, B., XU, S., ZHU, X., XU, H. & HUANG, X. 2011a. RpoE may promote flagellar gene expression in *Salmonella* enterica serovar Typhi under hyperosmotic stress. *Curr Microbiol,* 62**,** 492-500.
DU, H., WANG, M., LUO, Z., NI, B., WANG, F., MENG, Y., XU, S. & HUANG, X. 2011b. Coregulation of gene expression by sigma factors RpoE and RpoS in *Salmonella enterica* serovar Typhi during hyperosmotic stress. *Curr Microbiol,* 62**,** 1483-9.
DWORKIN, J., JOVANOVIC, G. & MODEL, P. 1997. Role of upstream activation sequences and integration host factor in transcriptional activation by the constitutively active prokaryotic enhancer-binding protein PspF. *J Mol Biol,* 273**,** 377-88.
DWYER, D. J., KOHANSKI, M. A., HAYETE, B. & COLLINS, J. J. 2007. *Gyrase inhibitors induce an oxidative damage cellular death pathway in Escherichia coli*.
EGGERS, C. T., MURRAY, I. A., DELMAR, V. A., DAY, A. G. & CRAIK, C. S. 2004. The periplasmic serine protease inhibitor ecotin protects bacteria against neutrophil elastase. *Biochem J,* 379**,** 107-18.
EIJKELKAMP, B. A., MCDEVITT, C. A. & KITTEN, T. 2015. Manganese uptake and streptococcal virulence. *Biometals*.
ELDERKIN, S., BORDES, P., JONES, S., RAPPAS, M. & BUCK, M. 2005. Molecular determinants for PspA-mediated repression of the AAA transcriptional activator PspF. *J Bacteriol,* 187**,** 3238-48.
ELDERKIN, S., JONES, S., SCHUMACHER, J., STUDHOLME, D. & BUCK, M. 2002. Mechanism of action of the *Escherichia coli* phage shock protein PspA in repression of the AAA family transcription factor PspF. *J Mol Biol,* 320**,** 23-37.
ELLERMEIER, C. D. & SLAUCH, J. M. 2003. RtsA and RtsB coordinately regulate expression of the invasion and flagellar genes in *Salmonella* enterica serovar Typhimurium. *J Bacteriol,* 185**,** 5096-108.
ELLERMEIER, C. D. & SLAUCH, J. M. 2004. RtsA coordinately regulates DsbA and the *Salmonella* pathogenicity island 1 type III secretion system. *J Bacteriol,* 186**,** 68-79.
ERICKSON, J. W. & GROSS, C. A. 1989. Identification of the sigma E subunit of *Escherichia coli* RNA polymerase: a second alternate sigma factor involved in high-temperature gene expression. *Genes Dev,* 3**,** 1462-71.
ERICKSON, K. D. & DETWEILER, C. S. 2006. The Rcs phosphorelay system is specific to enteric pathogens/commensals and activates ydeI, a gene important for persistent *Salmonella* infection of mice. *Mol Microbiol,* 62**,** 883-94.
ERIKSSON, S., LUCCHINI, S., THOMPSON, A., RHEN, M. & HINTON, J. C. 2003. Unravelling the biology of macrophage infection by gene expression profiling of intracellular *Salmonella* enterica. *Mol Microbiol,* 47**,** 103-18.

EVANS, D. G., EVANS, D. J., JR. & TJOA, W. 1977. Hemagglutination of human group A erythrocytes by enterotoxigenic *Escherichia coli* isolated from adults with diarrhea: correlation with colonization factor. *Infect Immun,* 18**,** 330-7.

EVANS, M. L., SCHMIDT, J. C., ILBERT, M., DOYLE, S. M., QUAN, S., BARDWELL, J. C., JAKOB, U., WICKNER, S. & CHAPMAN, M. R. 2011. *E. coli* chaperones DnaK, Hsp33 and Spy inhibit bacterial functional amyloid assembly. *Prion,* 5**,** 323-34.

FAIRBROTHER, J. M., NADEAU, E. & GYLES, C. L. 2005. *Escherichia coli* in postweaning diarrhea in pigs: an update on bacterial types, pathogenesis, and prevention strategies. *Anim Health Res Rev,* 6**,** 17-39.

FANG, F. C., LIBBY, S. J., CASTOR, M. E. & FUNG, A. M. 2005. Isocitrate lyase (AceA) is required for *Salmonella* persistence but not for acute lethal infection in mice. *Infect Immun,* 73**,** 2547-9.

FARRIS, C., SANOWAR, S., BADER, M. W., PFUETZNER, R. & MILLER, S. I. 2010. Antimicrobial peptides activate the Rcs regulon through the outer membrane lipoprotein RcsF. *J Bacteriol,* 192**,** 4894-903.

FASS, E. & GROISMAN, E. A. 2009. Control of *Salmonella* pathogenicity island-2 gene expression. *Curr Opin Microbiol,* 12**,** 199-204.

FATICA, M. K. & SCHNEIDER, K. R. 2011. *Salmonella* and produce: survival in the plant environment and implications in food safety. *Virulence,* 2**,** 573-9.

FAYET, O., ZIEGELHOFFER, T. & GEORGOPOULOS, C. 1989. The *groES* and *groEL* heat shock gene products of *Escherichia coli* are essential for bacterial growth at all temperatures. *J Bacteriol,* 171**,** 1379-85.

FEASEY, N. A., DOUGAN, G., KINGSLEY, R. A., HEYDERMAN, R. S. & GORDON, M. A. 2012. Invasive non-typhoidal *Salmonella* disease: an emerging and neglected tropical disease in Africa. *Lancet,* 379**,** 2489-99.

FEI, Y. Y., GAI, J. Y. & ZHAO, T. J. 2013. Identification of regulated genes conferring resistance to high concentrations of glyphosate in a new strain of *Enterobacter*. *FEMS Microbiol Lett,* 349**,** 135-43.

FENG, Y., LIU, W.-Q., SANDERSON, K. E. & LIU, S.-L. 2011. Comparison of *Salmonella* Genomes*,* Norfolk, UK, Caister Academic Press.

FENTON, H. J. H. 1894. Oxidation of tartaric acid in presence of iron. *Journal of the Chemical Society, Transactions,* 65**,** 899-910.

FIELDS, P. I., SWANSON, R. V., HAIDARIS, C. G. & HEFFRON, F. 1986. Mutants of *Salmonella* Typhimurium that cannot survive within the macrophage are avirulent. *Proc Natl Acad Sci U S A,* 83**,** 5189-93.

FIGUEIRA, R. & HOLDEN, D. W. 2012. Functions of the *Salmonella* pathogenicity island 2 (SPI-2) type III secretion system effectors. *Microbiology,* 158**,** 1147-61.

FINK, S. L. & COOKSON, B. T. 2007. Pyroptosis and host cell death responses during *Salmonella* infection. *Cell Microbiol,* 9**,** 2562-70.

FOOKES, M., SCHROEDER, G. N., LANGRIDGE, G. C., BLONDEL, C. J., MAMMINA, C., CONNOR, T. R., SETH-SMITH, H., VERNIKOS, G. S., ROBINSON, K. S., SANDERS, M., PETTY, N. K., KINGSLEY, R. A., BAUMLER, A. J., NUCCIO, S. P., CONTRERAS, I., SANTIVIAGO, C. A., MASKELL, D., BARROW, P., HUMPHREY, T., NASTASI, A.,

ROBERTS, M., FRANKEL, G., PARKHILL, J., DOUGAN, G. & THOMSON, N. R. 2011. *Salmonella bongori* provides insights into the evolution of the Salmonellae. *PLoS Pathog,* 7**,** e1002191.
FORBES, J. R. & GROS, P. 2003. Iron, manganese, and cobalt transport by NRAMP1 (Slc11a1) and NRAMP2 (Slc11a2) expressed at the plasma membrane. *Blood,* 102**,** 1884-92.
FOREST, C. G., FERRARO, E., SABBAGH, S. C. & DAIGLE, F. 2010. Intracellular survival of *Salmonella* enterica serovar Typhi in human macrophages is independent of *Salmonella* pathogenicity island (SPI)-2. *Microbiology,* 156**,** 3689-98.
FOSTER, J. W. 1991. *Salmonella* acid shock proteins are required for the adaptive acid tolerance response. *J Bacteriol,* 173**,** 6896-902.
FRANKE, S., GRASS, G. & NIES, D. H. 2001. The product of the *ybdE* gene of the *Escherichia coli* chromosome is involved in detoxification of silver ions. *Microbiology,* 147**,** 965-72.
FRASER, A., PAUL, M., GOLDBERG, E., ACOSTA, C. J. & LEIBOVICI, L. 2007. Typhoid fever vaccines: systematic review and meta-analysis of randomised controlled trials. *Vaccine,* 25**,** 7848-57.
FRAÚSTO DA SILVA, J. J. R. & WILLIAMS, R. J. P. 2001. *The Biological Chemistry of the Elements: The Inorganic Chemistry of Life* Oxford, Oxford University Press.
FREEMAN, J. A., OHL, M. E. & MILLER, S. I. 2003. The *Salmonella* enterica serovar Typhimurium translocated effectors SseJ and SifB are targeted to the *Salmonella*-containing vacuole. *Infect Immun,* 71**,** 418-27.
FU, Y. & GALAN, J. E. 1999. A *Salmonella* protein antagonizes Rac-1 and Cdc42 to mediate host-cell recovery after bacterial invasion. *Nature,* 401**,** 293-7.
FUKUCHI, J., KASHIWAGI, K., YAMAGISHI, M., ISHIHAMA, A. & IGARASHI, K. 1995. Decrease in cell viability due to the accumulation of spermidine in spermidine acetyltransferase-deficient mutant of *Escherichia coli*. *J Biol Chem,* 270**,** 18831-5.
GABBIANELLI, R., SCOTTI, R., AMMENDOLA, S., PETRARCA, P., NICOLINI, L. & BATTISTONI, A. 2011. Role of ZnuABC and ZinT in *Escherichia coli* O157:H7 zinc acquisition and interaction with epithelial cells. *BMC Microbiol,* 11**,** 36.
GAL-MOR, O. & SEGAL, G. 2003. Identification of CpxR as a positive regulator of *icm* and *dot* virulence genes of *Legionella pneumophila*. *J Bacteriol,* 185**,** 4908-19.
GALAN, J. E. 2008. Energizing type III secretion machines: what is the fuel? *Nat Struct Mol Biol,* 15**,** 127-8.
GALAN, J. E. & ZHOU, D. 2000. Striking a balance: modulation of the actin cytoskeleton by *Salmonella*. *Proc Natl Acad Sci U S A,* 97**,** 8754-61.
GAMAZO, C. & IRACHE, J. M. 2007. *Salmonella Vaccines*, Formatex.
GANGAIAH, D., ZHANG, X., FORTNEY, K. R., BAKER, B., LIU, Y., MUNSON, R. S., JR. & SPINOLA, S. M. 2013. Activation of CpxRA in *Haemophilus ducreyi* primarily inhibits the expression of its targets, including major virulence determinants. *J Bacteriol,* 195**,** 3486-502.
GAO, R. & STOCK, A. M. 2009. Biological insights from structures of two-component proteins. *Annu Rev Microbiol,* 63**,** 133-54.

GARCIA-DEL PORTILLO, F., FOSTER, J. W. & FINLAY, B. B. 1993a. Role of acid tolerance response genes in *Salmonella* Typhimurium virulence. *Infect Immun,* 61**,** 4489-92.
GARCÍA-DEL PORTILLO, F., NÚÑEZ-HERNÁNDEZ, C., EISMAN, B. & RAMOS-VIVAS, J. 2008. Growth control in the *Salmonella*-containing vacuole. *Current Opinion in Microbiology,* 11**,** 46-52.
GARCIA-DEL PORTILLO, F., ZWICK, M. B., LEUNG, K. Y. & FINLAY, B. B. 1993b. *Salmonella* induces the formation of filamentous structures containing lysosomal membrane glycoproteins in epithelial cells. *Proc Natl Acad Sci U S A,* 90**,** 10544-8.
GARDINO, A. K. & KERN, D. 2007. Functional dynamics of response regulators using NMR relaxation techniques. *Methods Enzymol,* 423**,** 149-65.
GARMENDIA, J., BEUZON, C. R., RUIZ-ALBERT, J. & HOLDEN, D. W. 2003. The roles of SsrA-SsrB and OmpR-EnvZ in the regulation of genes encoding the *Salmonella* Typhimurium SPI-2 type III secretion system. *Microbiology,* 149**,** 2385-96.
GERKEN, H. & MISRA, R. 2010. MzrA-EnvZ interactions in the periplasm influence the EnvZ/OmpR two-component regulon. *Journal of bacteriology,* 192**,** 6271-6278.
GERLACH, R. G., CLAUDIO, N., ROHDE, M., JACKEL, D., WAGNER, C. & HENSEL, M. 2008. Cooperation of *Salmonella* pathogenicity islands 1 and 4 is required to breach epithelial barriers. *Cell Microbiol,* 10**,** 2364-76.
GILES, N. M., WATTS, A. B., GILES, G. I., FRY, F. H., LITTLECHILD, J. A. & JACOB, C. 2003. Metal and redox modulation of cysteine protein function. *Chem Biol,* 10**,** 677-93.
GODINEZ, I., HANEDA, T., RAFFATELLU, M., GEORGE, M. D., PAIXAO, T. A., ROLAN, H. G., SANTOS, R. L., DANDEKAR, S., TSOLIS, R. M. & BAUMLER, A. J. 2008. T cells help to amplify inflammatory responses induced by *Salmonella* enterica serotype Typhimurium in the intestinal mucosa. *Infect Immun,* 76**,** 2008-17.
GOETZ, D. H., HOLMES, M. A., BORREGAARD, N., BLUHM, M. E., RAYMOND, K. N. & STRONG, R. K. 2002. The neutrophil lipocalin NGAL is a bacteriostatic agent that interferes with siderophore-mediated iron acquisition. *Mol Cell,* 10**,** 1033-43.
GOLYNSKIY, M. V., GUNDERSON, W. A., HENDRICH, M. P. & COHEN, S. M. 2006. Metal binding studies and EPR spectroscopy of the manganese transport regulator MntR. *Biochemistry,* 45**,** 15359-72.
GONZALEZ-ESCOBEDO, G., MARSHALL, J. M. & GUNN, J. S. 2011. Chronic and acute infection of the gall bladder by *Salmonella* Typhi: understanding the carrier state. *Nat Rev Microbiol,* 9**,** 9-14.
GOSWAMI, T., BHATTACHARJEE, A., BABAL, P., SEARLE, S., MOORE, E., LI, M. & BLACKWELL, J. M. 2001. Natural-resistance-associated macrophage protein 1 is an H+/bivalent cation antiporter. *Biochem J,* 354**,** 511-9.
GOTTESMAN, S. 2004. The small RNA regulators of *Escherichia coli*: roles and mechanisms*. *Annu Rev Microbiol,* 58**,** 303-28.
GRAHAM, A. I., HUNT, S., STOKES, S. L., BRAMALL, N., BUNCH, J., COX, A. G., MCLEOD, C. W. & POOLE, R. K. 2009. Severe zinc depletion

of *Escherichia coli*: roles for high affinity zinc binding by ZinT, zinc transport and zinc-independent proteins. *J Biol Chem,* 284**,** 18377-89.
GRAHAM, A. I., SANGUINETTI, G., BRAMALL, N., MCLEOD, C. W. & POOLE, R. K. 2012. Dynamics of a starvation-to-surfeit shift: a transcriptomic and modelling analysis of the bacterial response to zinc reveals transient behaviour of the Fur and SoxS regulators. *Microbiology,* 158**,** 284-92.
GRASS, G., FRANKE, S., TAUDTE, N., NIES, D. H., KUCHARSKI, L. M., MAGUIRE, M. E. & RENSING, C. 2005a. The metal permease ZupT from *Escherichia coli* is a transporter with a broad substrate spectrum. *J Bacteriol,* 187**,** 1604-11.
GRASS, G., FRICKE, B. & NIES, D. H. 2005b. Control of expression of a periplasmic nickel efflux pump by periplasmic nickel concentrations. *Biometals,* 18**,** 437-48.
GRASS, G., GROSSE, C. & NIES, D. H. 2000. Regulation of the *cnr* cobalt and nickel resistance determinant from *Ralstonia* sp. strain CH34. *J Bacteriol,* 182**,** 1390-8.
GRASS, G., WONG, M. D., ROSEN, B. P., SMITH, R. L. & RENSING, C. 2002. ZupT is a Zn(II) uptake system in *Escherichia coli*. *J Bacteriol,* 184**,** 864-6.
GRIFFIN, A. J. & MCSORLEY, S. J. 2011. Development of protective immunity to *Salmonella*, a mucosal pathogen with a systemic agenda. *Mucosal Immunol,* 4**,** 371-382.
GUBBINS, M. J., LAU, I., WILL, W. R., MANCHAK, J. M., RAIVIO, T. L. & FROST, L. S. 2002. The positive regulator, TraJ, of the *Escherichia coli* F plasmid is unstable in a *cpxA** background. *J Bacteriol,* 184**,** 5781-8.
GUEDON, E. & HELMANN, J. D. 2003. Origins of metal ion selectivity in the DtxR/MntR family of metalloregulators. *Mol Microbiol,* 48**,** 495-506.
GUILHEN, C., TAHA, M. K. & VEYRIER, F. J. 2013. Role of transition metal exporters in virulence: the example of *Neisseria meningitidis*. *Front Cell Infect Microbiol,* 3**,** 102.
GUILLIER, M. & GOTTESMAN, S. 2006. Remodelling of the *Escherichia coli* outer membrane by two small regulatory RNAs. *Mol Microbiol,* 59**,** 231-47.
GUNASEKERA, T. S., HERRE, A. H. & CROWDER, M. W. 2009. Absence of ZnuABC-mediated zinc uptake affects virulence-associated phenotypes of uropathogenic *Escherichia coli* CFT073 under Zn(II)-depleted conditions. *FEMS Microbiol Lett,* 300**,** 36-41.
GUNN, T. R., MACFARLANE, S. & PHILLIPS, L. I. 1984. Difficulties in the neonatal diagnosis of Menkes' kinky hair syndrome--trichopoliodystrophy. *Clin Pediatr (Phila),* 23**,** 514-6.
GUO, M. S., UPDEGROVE, T. B., GOGOL, E. B., SHABALINA, S. A., GROSS, C. A. & STORZ, G. 2014. MicL, a new sigmaE-dependent sRNA, combats envelope stress by repressing synthesis of Lpp, the major outer membrane lipoprotein. *Genes Dev,* 28**,** 1620-34.
GUPTA, S. D., WU, H. C. & RICK, P. D. 1997. A *Salmonella* Typhimurium genetic locus which confers copper tolerance on copper-sensitive mutants of *Escherichia coli*. *J Bacteriol,* 179**,** 4977-84.

GUYER, M. S., REED, R. R., STEITZ, J. A. & LOW, K. B. 1981. Identification of a sex-factor-affinity site in *E. coli* as gamma delta. *Cold Spring Harb Symp Quant Biol,* 45 Pt 1**,** 135-40.

HA, H. C., SIRISOMA, N. S., KUPPUSAMY, P., ZWEIER, J. L., WOSTER, P. M. & CASERO, R. A., JR. 1998. The natural polyamine spermine functions directly as a free radical scavenger. *Proc Natl Acad Sci U S A,* 95**,** 11140-5.

HAGENMAIER, S., STIERHOF, Y. D. & HENNING, U. 1997. A new periplasmic protein of *Escherichia coli* which is synthesized in spheroplasts but not in intact cells. *J Bacteriol,* 179**,** 2073-6.

HALL-STOODLEY, L. & STOODLEY, P. 2009. Evolving concepts in biofilm infections. *Cell Microbiol,* 11**,** 1034-43.

HAMILTON, S., BONGAERTS, R. J., MULHOLLAND, F., COCHRANE, B., PORTER, J., LUCCHINI, S., LAPPIN-SCOTT, H. M. & HINTON, J. C. 2009. The transcriptional programme of *Salmonella* enterica serovar Typhimurium reveals a key role for tryptophan metabolism in biofilms. *BMC Genomics,* 10**,** 599.

HAN, T. H., LEE, J. H., CHO, M. H., WOOD, T. K. & LEE, J. 2011. Environmental factors affecting indole production in *Escherichia coli*. *Res Microbiol,* 162**,** 108-16.

HANCOCK, V., VEJBORG, R. M. & KLEMM, P. 2010. Functional genomics of probiotic *Escherichia coli* Nissle 1917 and 83972, and UPEC strain CFT073: comparison of transcriptomes, growth and biofilm formation. *Mol Genet Genomics,* 284**,** 437-54.

HANEDA, T., ISHII, Y., DANBARA, H. & OKADA, N. 2009. Genome-wide identification of novel genomic islands that contribute to *Salmonella* virulence in mouse systemic infection. *FEMS Microbiol Lett,* 297**,** 241-9.

HANNING, I. B., NUTT, J. D. & RICKE, S. C. 2009. Salmonellosis outbreaks in the United States due to fresh produce: sources and potential intervention measures. *Foodborne Pathog Dis,* 6**,** 635-48.

HANTKE, K. 2005. Bacterial zinc uptake and regulators. *Curr Opin Microbiol,* 8**,** 196-202.

HANTKE, K., NICHOLSON, G., RABSCH, W. & WINKELMANN, G. 2003. Salmochelins, siderophores of *Salmonella* enterica and uropathogenic *Escherichia coli* strains, are recognized by the outer membrane receptor IroN. *Proc Natl Acad Sci U S A,* 100**,** 3677-82.

HAPFELMEIER, S., EHRBAR, K., STECHER, B., BARTHEL, M., KREMER, M. & HARDT, W. D. 2004. Role of the *Salmonella* pathogenicity island 1 effector proteins SipA, SopB, SopE, and SopE2 in *Salmonella* enterica subspecies 1 serovar Typhimurium colitis in streptomycin-pretreated mice. *Infect Immun,* 72**,** 795-809.

HARAGA, A., OHLSON, M. B. & MILLER, S. I. 2008. *Salmonella*e interplay with host cells. *Nat Rev Microbiol,* 6**,** 53-66.

HARDT, W. D., CHEN, L. M., SCHUEBEL, K. E., BUSTELO, X. R. & GALAN, J. E. 1998. *S*. Typhimurium encodes an activator of Rho GTPases that induces membrane ruffling and nuclear responses in host cells. *Cell,* 93**,** 815-26.

HATAYAMA, T., ASAI, Y., WAKATSUKI, T., KITAMURA, T. & IMAHARA, H. 1993. Regulation of hsp70 synthesis induced by cupric sulfate and zinc sulfate in thermotolerant HeLa cells. *J Biochem,* 114**,** 592-7.

HAUTEFORT, I., THOMPSON, A., ERIKSSON-YGBERG, S., PARKER, M. L., LUCCHINI, S., DANINO, V., BONGAERTS, R. J., AHMAD, N., RHEN, M. & HINTON, J. C. 2008. During infection of epithelial cells *Salmonella* enterica serovar Typhimurium undergoes a time-dependent transcriptional adaptation that results in simultaneous expression of three type 3 secretion systems. *Cell Microbiol,* 10**,** 958-84.

HELANDER, I. M. & MATTILA-SANDHOLM, T. 2000. Fluorometric assessment of gram-negative bacterial permeabilization. *J Appl Microbiol,* 88**,** 213-9.

HELMANN, J. D. 2002. The extracytoplasmic function (ECF) sigma factors. *Adv Microb Physiol,* 46**,** 47-110.

HENGGE-ARONIS, R. 1996. Back to log phase: sigma S as a global regulator in the osmotic control of gene expression in *Escherichia coli*. *Mol Microbiol,* 21**,** 887-93.

HENNECKE, G., NOLTE, J., VOLKMER-ENGERT, R., SCHNEIDER-MERGENER, J. & BEHRENS, S. 2005. The periplasmic chaperone SurA exploits two features characteristic of integral outer membrane proteins for selective substrate recognition. *J Biol Chem,* 280**,** 23540-8.

HERBERT, E. E., COWLES, K. N. & GOODRICH-BLAIR, H. 2007. CpxRA regulates mutualism and pathogenesis in *Xenorhabdus nematophila*. *Appl Environ Microbiol,* 73**,** 7826-36.

HERBERT TRAN, E. E. & GOODRICH-BLAIR, H. 2009. CpxRA contributes to *Xenorhabdus nematophila* virulence through regulation of *lrhA* and modulation of insect immunity. *Appl Environ Microbiol,* 75**,** 3998-4006.

HERNDAY, A. D., BRAATEN, B. A., BROITMAN-MADURO, G., ENGELBERTS, P. & LOW, D. A. 2004. Regulation of the Pap Epigenetic Switch by CpxAR: Phosphorylated CpxR Inhibits Transition to the Phase ON State by Competition with Lrp. *Molecular Cell,* 16**,** 537-547.

HESSIAN, P. A., EDGEWORTH, J. & HOGG, N. 1993. MRP-8 and MRP-14, two abundant Ca($^{2+}$)-binding proteins of neutrophils and monocytes. *J Leukoc Biol,* 53**,** 197-204.

HEUSIPP, G., SCHMIDT, M. A. & MILLER, V. L. 2003. Identification of *rpoE* and *nadB* as host responsive elements of *Yersinia enterocolitica*. *FEMS Microbiol Lett,* 226**,** 291-8.

HIGASHI, K., ISHIGURE, H., DEMIZU, R., UEMURA, T., NISHINO, K., YAMAGUCHI, A., KASHIWAGI, K. & IGARASHI, K. 2008. Identification of a spermidine excretion protein complex (MdtJI) in *Escherichia coli*. *J Bacteriol,* 190**,** 872-8.

HILL, G. M., MAHAN, D. C. & JOLLIFF, J. S. 2014. Comparison of organic and inorganic zinc sources to maximize growth and meet the zinc needs of the nursery pig. *J Anim Sci,* 92**,** 1582-94.

HINCHLIFFE, S. J., HOWARD, S. L., HUANG, Y. H., CLARKE, D. J. & WREN, B. W. 2008. The importance of the Rcs phosphorelay in the

survival and pathogenesis of the enteropathogenic yersiniae. *Microbiology,* 154**,** 1117-31.

HINDLE, Z., CHATFIELD, S. N., PHILLIMORE, J., BENTLEY, M., JOHNSON, J., COSGROVE, C. A., GHAEM-MAGHAMI, M., SEXTON, A., KHAN, M., BRENNAN, F. R., EVEREST, P., WU, T., PICKARD, D., HOLDEN, D. W., DOUGAN, G., GRIFFIN, G. E., HOUSE, D., SANTANGELO, J. D., KHAN, S. A., SHEA, J. E., FELDMAN, R. G. & LEWIS, D. J. 2002. Characterization of *Salmonella* enterica derivatives harboring defined *aroC* and *Salmonella* pathogenicity island 2 type III secretion system (ssaV) mutations by immunization of healthy volunteers. *Infect Immun,* 70**,** 3457-67.

HINIKER, A., COLLET, J. F. & BARDWELL, J. C. 2005. Copper stress causes an i*n vivo* requirement for the *Escherichia coli* disulfide isomerase DsbC. *J Biol Chem,* 280**,** 33785-91.

HIRAKAWA, H., INAZUMI, Y., MASAKI, T., HIRATA, T. & YAMAGUCHI, A. 2005. Indole induces the expression of multidrug exporter genes in *Escherichia coli*. *Mol Microbiol,* 55**,** 1113-26.

HIRAKAWA, H., NISHINO, K., HIRATA, T. & YAMAGUCHI, A. 2003. Comprehensive studies of drug resistance mediated by overexpression of response regulators of two-component signal transduction systems in *Escherichia coli*. *J Bacteriol,* 185**,** 1851-6.

HIRANO, Y., HOSSAIN, M. M., TAKEDA, K., TOKUDA, H. & MIKI, K. 2007. Structural studies of the Cpx pathway activator NlpE on the outer membrane of *Escherichia coli*. *Structure,* 15**,** 963-76.

HOCH, J. A. 2000. Two-component and phosphorelay signal transduction. *Curr Opin Microbiol,* 3**,** 165-70.

HOISETH, S. K. & STOCKER, B. A. 1981. Aromatic-dependent *Salmonella* Typhimurium are non-virulent and effective as live vaccines. *Nature,* 291**,** 238-9.

HOLLAND, D. R., HAUSRATH, A. C., JUERS, D. & MATTHEWS, B. W. 1995. Structural analysis of zinc substitutions in the active site of thermolysin. *Protein Sci,* 4**,** 1955-65.

HOLTJE, J. V. 1998. Growth of the stress-bearing and shape-maintaining murein sacculus of *Escherichia coli*. *Microbiol Mol Biol Rev,* 62**,** 181-203.

HOOD, M. I. & SKAAR, E. P. 2012. Nutritional immunity: transition metals at the pathogen–host interface. *Nat Rev Micro,* 10**,** 525-537.

HORWICH, A. L., LOW, K. B., FENTON, W. A., HIRSHFIELD, I. N. & FURTAK, K. 1993. Folding *in vivo* of bacterial cytoplasmic proteins: role of GroEL. *Cell,* 74**,** 909-17.

HOWLETT, G. J., MINTON, A. P. & RIVAS, G. 2006. Analytical ultracentrifugation for the study of protein association and assembly. *Curr Opin Chem Biol,* 10**,** 430-6.

HU, Q., COBURN, B., DENG, W., LI, Y., SHI, X., LAN, Q., WANG, B., COOMBES, B. K. & FINLAY, B. B. 2008. *Salmonella* enterica Serovar Senftenberg Human Clinical Isolates Lacking SPI-1. *J Clin Microbiol,* 46**,** 1330-6.

HU, W. S., LI, P. C. & CHENG, C. Y. 2005. Correlation between ceftriaxone resistance of *Salmonella* enterica serovar Typhimurium and

expression of outer membrane proteins OmpW and Ail/OmpX-like protein, which are regulated by BaeR of a two-component system. *Antimicrob Agents Chemother,* 49**,** 3955-8.

HU, W. S., LIN, J. F., LIN, Y. H. & CHANG, H. Y. 2009. Outer membrane protein STM3031 (Ail/OmpX-like protein) plays a key role in the ceftriaxone resistance of *Salmonella* enterica serovar Typhimurium. *Antimicrob Agents Chemother,* 53**,** 3248-55.

HUANG, S. X., MCFALL, M., CEGIELSKI, A. C. & KIRKWOOD, R. N. 1999. Effect of dietary zinc supplementation on *Escherichia coli* septicemia in weaned pigs. *J Swine Health Prod,* 7**,** 109-111.

HUANG, X., XU, H., SUN, X., OHKUSU, K., KAWAMURA, Y. & EZAKI, T. 2007a. Genome-Wide Scan of the Gene Expression Kinetics of *Salmonella* enterica Serovar Typhi during Hyperosmotic Stress. *International Journal of Molecular Sciences,* 8**,** 116-135.

HUANG, Y., LEMING, C. L., SUYEMOTO, M. & ALTIER, C. 2007b. Genome-wide screen of *Salmonella* genes expressed during infection in pigs, using in vivo expression technology. *Appl Environ Microbiol,* 73**,** 7522-30.

HUBERT, K., DEVOS, N., MORDHORST, I., TANS, C., BAUDOUX, G., FERON, C., GORAJ, K., TOMMASSEN, J., VOGEL, U., POOLMAN, J. T. & WEYNANTS, V. 2013. ZnuD, a Potential Candidate for a Simple and Universal *Neisseria meningitidis* Vaccine. *Infection and Immunity,* 81**,** 1915-1927.

HUMPHREYS, S., ROWLEY, G., STEVENSON, A., ANJUM, M. F., WOODWARD, M. J., GILBERT, S., KORMANEC, J. & ROBERTS, M. 2004. Role of the two-component regulator CpxAR in the virulence of *Salmonella* enterica serotype Typhimurium. *Infect Immun,* 72**,** 4654-61.

HUMPHREYS, S., STEVENSON, A., BACON, A., WEINHARDT, A. B. & ROBERTS, M. 1999. The alternative sigma factor, sigmaE, is critically important for the virulence of *Salmonella* Typhimurium. *Infect Immun,* 67**,** 1560-8.

HUNG, D. L., RAIVIO, T. L., JONES, C. H., SILHAVY, T. J. & HULTGREN, S. J. 2001. Cpx signaling pathway monitors biogenesis and affects assembly and expression of P pili. *Embo j,* 20**,** 1508-18.

HUNG, M. N., RANGARAJAN, E., MUNGER, C., NADEAU, G., SULEA, T. & MATTE, A. 2006. Crystal structure of TDP-fucosamine acetyltransferase (WecD) from *Escherichia coli*, an enzyme required for enterobacterial common antigen synthesis. *J Bacteriol,* 188**,** 5606-17.

HUNKE, S., KELLER, R. & MULLER, V. S. 2012. Signal integration by the Cpx-envelope stress system. *FEMS Microbiol Lett,* 326**,** 12-22.

HUVET, M., TONI, T., SHENG, X., THORNE, T., JOVANOVIC, G., ENGL, C., BUCK, M., PINNEY, J. W. & STUMPF, M. P. 2011. The evolution of the phage shock protein response system: interplay between protein function, genomic organization, and system function. *Mol Biol Evol,* 28**,** 1141-55.

IKEDA, J. S., JANAKIRAMAN, A., KEHRES, D. G., MAGUIRE, M. E. & SLAUCH, J. M. 2005. Transcriptional regulation of sitABCD of

Salmonella enterica serovar Typhimurium by MntR and Fur. *J Bacteriol,* 187**,** 912-22.

ILARI, A., ALALEONA, F., TRIA, G., PETRARCA, P., BATTISTONI, A., ZAMPARELLI, C., VERZILI, D., FALCONI, M. & CHIANCONE, E. 2014. The *Salmonella* enterica ZinT structure, zinc affinity and interaction with the high-affinity uptake protein ZnuA provide insight into the management of periplasmic zinc. *Biochim Biophys Acta,* 1840**,** 535-44.

IMLAY, J. A. 2008. Cellular defenses against superoxide and hydrogen peroxide. *Annu Rev Biochem,* 77**,** 755-76.

ISAAC, D. D., PINKNER, J. S., HULTGREN, S. J. & SILHAVY, T. J. 2005. The extracytoplasmic adaptor protein CpxP is degraded with substrate by DegP. *Proc Natl Acad Sci U S A,* 102**,** 17775-9.

ISLAND, M. D., WEI, B. Y. & KADNER, R. J. 1992. Structure and function of the *uhp* genes for the sugar phosphate transport system in *Escherichia coli* and *Salmonella* Typhimurium. *J Bacteriol,* 174**,** 2754-62.

ISSENHUTH-JEANJEAN, S., ROGGENTIN, P., MIKOLEIT, M., GUIBOURDENCHE, M., DE PINNA, E., NAIR, S., FIELDS, P. I. & WEILL, F.-X. 2014. Supplement 2008–2010 (no. 48) to the White–Kauffmann–Le Minor scheme. *Research in Microbiology,* 165**,** 526-530.

IVANOFF, B., LEVINE, M. M. & LAMBERT, P. H. 1994. Vaccination against typhoid fever: present status. *Bull World Health Organ,* 72**,** 957-71.

JABADO, N., JANKOWSKI, A., DOUGAPARSAD, S., PICARD, V., GRINSTEIN, S. & GROS, P. 2000. Natural resistance to intracellular infections: natural resistance-associated macrophage protein 1 (NRAMP1) functions as a pH-dependent manganese transporter at the phagosomal membrane. *J Exp Med,* 192**,** 1237-48.

JANULCZYK, R., PALLON, J. & BJORCK, L. 1999. Identification and characterization of a *Streptococcus pyogenes* ABC transporter with multiple specificity for metal cations. *Mol Microbiol,* 34**,** 596-606.

JELSBAK, L., THOMSEN, L. E., WALLRODT, I., JENSEN, P. R. & OLSEN, J. E. 2012. Polyamines are required for virulence in *Salmonella* enterica serovar Typhimurium. *PLoS One,* 7**,** e36149.

JIANG, X., ROSSANESE, O. W., BROWN, N. F., KUJAT-CHOY, S., GALAN, J. E., FINLAY, B. B. & BRUMELL, J. H. 2004. The related effector proteins SopD and SopD2 from *Salmonella* enterica serovar Typhimurium contribute to virulence during systemic infection of mice. *Mol Microbiol,* 54**,** 1186-98.

JIN, H. H. & LEE, S. Y. 2007. Combined effect of aqueous chlorine dioxide and modified atmosphere packaging on inhibiting *Salmonella* Typhimurium and *Listeria monocytogenes* in mungbean sprouts. *J Food Sci,* 72**,** M441-5.

JIN, Y. 2008. Enteric fever in south China: Guangxi province. *J Infect Dev Ctries,* 2**,** 283-8.

JITPRASUTWIT, S., ONG, C., JUNTAWIENG, N., OOI, W. F., HEMSLEY, C. M., VATTANAVIBOON, P., TITBALL, R. W., TAN, P. & KORBSRISATE, S. 2014. Transcriptional profiles of *Burkholderia*

pseudomallei reveal the direct and indirect roles of Sigma E under oxidative stress conditions. *BMC Genomics,* 15**,** 787.

JOHANSEN, J., RASMUSSEN, A. A., OVERGAARD, M. & VALENTIN-HANSEN, P. 2006. Conserved small non-coding RNAs that belong to the sigmaE regulon: role in down-regulation of outer membrane proteins. *J Mol Biol,* 364**,** 1-8.

JOHN, M., KUDVA, I. T., GRIFFIN, R. W., DODSON, A. W., MCMANUS, B., KRASTINS, B., SARRACINO, D., PROGULSKE-FOX, A., HILLMAN, J. D., HANDFIELD, M., TARR, P. I. & CALDERWOOD, S. B. 2005. Use of *in vivo*-induced antigen technology for identification of *Escherichia coli* O157:H7 proteins expressed during human infection. *Infect Immun,* 73**,** 2665-79.

JOHNSON, K., CHARLES, I., DOUGAN, G., PICKARD, D., O'GAORA, P., COSTA, G., ALI, T., MILLER, I. & HORMAECHE, C. 1991. The role of a stress-response protein in *Salmonella* Typhimurium virulence. *Mol Microbiol,* 5**,** 401-7.

JOHNSTON, C., PEGUES, D. A., HUECK, C. J., LEE, A. & MILLER, S. I. 1996. Transcriptional activation of *Salmonella* Typhimurium invasion genes by a member of the phosphorylated response-regulator superfamily. *Mol Microbiol,* 22**,** 715-27.

JOHNSTON, V., STOCKLEY, J. M., DOCKRELL, D., WARRELL, D., BAILEY, R., PASVOL, G., KLEIN, J., USTIANOWSKI, A., JONES, M., BEECHING, N. J., BROWN, M., CHAPMAN, A. L., SANDERSON, F. & WHITTY, C. J. 2009. Fever in returned travellers presenting in the United Kingdom: recommendations for investigation and initial management. *J Infect,* 59**,** 1-18.

JOLY, N., BURROWS, P. C., ENGL, C., JOVANOVIC, G. & BUCK, M. 2009. A lower-order oligomer form of phage shock protein A (PspA) stably associates with the hexameric AAA(+) transcription activator protein PspF for negative regulation. *J Mol Biol,* 394**,** 764-75.

JOLY, N., ENGL, C., JOVANOVIC, G., HUVET, M., TONI, T., SHENG, X., STUMPF, M. P. & BUCK, M. 2010. Managing membrane stress: the phage shock protein (Psp) response, from molecular mechanisms to physiology. *FEMS Microbiol Rev,* 34**,** 797-827.

JONES, A. L., NEEDHAM, R. H. & RUBENS, C. E. 2003. The Delta subunit of RNA polymerase is required for virulence of *Streptococcus agalactiae*. *Infect Immun,* 71**,** 4011-7.

JONES, B. D., GHORI, N. & FALKOW, S. 1994. *Salmonella* Typhimurium initiates murine infection by penetrating and destroying the specialized epithelial M cells of the Peyer's patches. *J Exp Med,* 180**,** 15-23.

JONES, C. H., DANESE, P. N., PINKNER, J. S., SILHAVY, T. J. & HULTGREN, S. J. 1997. The chaperone-assisted membrane release and folding pathway is sensed by two signal transduction systems. *Embo j,* 16**,** 6394-406.

JONES, T. F., INGRAM, L. A., CIESLAK, P. R., VUGIA, D. J., TOBIN-D'ANGELO, M., HURD, S., MEDUS, C., CRONQUIST, A. & ANGULO, F. J. 2008. Salmonellosis outcomes differ substantially by serotype. *J Infect Dis,* 198**,** 109-14.

JUDICIAL COMMISSION OF THE INTERNATIONAL COMMITTEE ON THE SYSTEMATICS OF PROKARYOTES 2005. The type species of the

genus *Salmonella* Lignieres 1900 is *Salmonella* enterica (ex Kauffmann and Edwards 1952) Le Minor and Popoff 1987, with the type strain LT2T, and conservation of the epithet enterica in *Salmonella* enterica over all earlier epithets that may be applied to this species. Opinion 80. *Int J Syst Evol Microbiol,* 55**,** 519-20.

KABIR, M. S., YAMASHITA, D., KOYAMA, S., OSHIMA, T., KUROKAWA, K., MAEDA, M., TSUNEDOMI, R., MURATA, M., WADA, C., MORI, H. & YAMADA, M. 2005. Cell lysis directed by sigmaE in early stationary phase and effect of induction of the *rpoE* gene on global gene expression in *Escherichia coli*. *Microbiology,* 151**,** 2721-35.

KADER, A., SIMM, R., GERSTEL, U., MORR, M. & ROMLING, U. 2006. Hierarchical involvement of various GGDEF domain proteins in rdar morphotype development of *Salmonella* enterica serovar Typhimurium. *Mol Microbiol,* 60**,** 602-16.

KANEKO, A., MITA, M., SEKIYA, K., MATSUI, H., KAWAHARA, K. & DANBARA, H. 2002. Association of a regulatory gene, *slyA* with a mouse virulence of *Salmonella* serovar Choleraesuis. *Microbiol Immunol,* 46**,** 109-13.

KAPPLER, U. 2011. Bacterial sulfite-oxidizing enzymes. *Biochimica et Biophysica Acta (BBA) - Bioenergetics,* 1807**,** 1-10.

KARASOVA, D., SEBKOVA, A., HAVLICKOVA, H., SISAK, F., VOLF, J., FALDYNA, M., ONDRACKOVA, P., KUMMER, V. & RYCHLIK, I. 2010. Influence of 5 major *Salmonella* pathogenicity islands on NK cell depletion in mice infected with *Salmonella* enterica serovar Enteritidis. *BMC Microbiol,* 10**,** 75.

KARLINSEY, J. E., MAGUIRE, M. E., BECKER, L. A., CROUCH, M. L. & FANG, F. C. 2010. The phage shock protein PspA facilitates divalent metal transport and is required for virulence of *Salmonella enterica* sv. Typhimurium. *Mol Microbiol,* 78**,** 669-85.

KASHIWAGI, K., INNAMI, A., ZENDA, R., TOMITORI, H. & IGARASHI, K. 2002. The ATPase activity and the functional domain of PotA, a component of the sermidine-preferential uptake system in *Escherichia coli*. *J Biol Chem,* 277**,** 24212-9.

KASHIWAGI, K., KURAISHI, A., TOMITORI, H., IGARASHI, A., NISHIMURA, K., SHIRAHATA, A. & IGARASHI, K. 2000. Identification of the putrescine recognition site on polyamine transport protein PotE. *J Biol Chem,* 275**,** 36007-12.

KEHL-FIE, T. E. & SKAAR, E. P. 2010. Nutritional immunity beyond iron: a role for manganese and zinc. *Curr Opin Chem Biol,* 14**,** 218-24.

KEHL-FIE, T. E., ZHANG, Y., MOORE, J. L., FARRAND, A. J., HOOD, M. I., RATHI, S., CHAZIN, W. J., CAPRIOLI, R. M. & SKAAR, E. P. 2013. MntABC and MntH contribute to systemic *Staphylococcus aureus* infection by competing with calprotectin for nutrient manganese. *Infect Immun,* 81**,** 3395-405.

KEHRES, D. G., ZAHARIK, M. L., FINLAY, B. B. & MAGUIRE, M. E. 2000. The NRAMP proteins of *Salmonella* Typhimurium and *Escherichia coli* are selective manganese transporters involved in the response to reactive oxygen. *Mol Microbiol,* 36**,** 1085-100.

KELLY, B. G., VESPERMANN, A. & BOLTON, D. J. 2009. The role of horizontal gene transfer in the evolution of selected foodborne bacterial pathogens. *Food Chem Toxicol,* 47**,** 951-68.

KENNEY, L. J. 2002. Structure/function relationships in OmpR and other winged-helix transcription factors. *Curr Opin Microbiol,* 5**,** 135-41.

KENYON, W. J., SAYERS, D. G., HUMPHREYS, S., ROBERTS, M. & SPECTOR, M. P. 2002. The starvation-stress response of *Salmonella enterica* serovar Typhimurium requires sigma(E)-, but not CpxR-regulated extracytoplasmic functions. *Microbiology,* 148**,** 113-22.

KEREN, I., WU, Y., INOCENCIO, J., MULCAHY, L. R. & LEWIS, K. 2013. Killing by bactericidal antibiotics does not depend on reactive oxygen species. *Science,* 339**,** 1213-6.

KERSHAW, C. J., BROWN, N. L., CONSTANTINIDOU, C., PATEL, M. D. & HOBMAN, J. L. 2005. The expression profile of *Escherichia coli* K-12 in response to minimal, optimal and excess copper concentrations. *Microbiology,* 151**,** 1187-1198.

KHAN, S. A., STRATFORD, R., WU, T., MCKELVIE, N., BELLABY, T., HINDLE, Z., SINHA, K. A., ELTZE, S., MASTROENI, P., PICKARD, D., DOUGAN, G., CHATFIELD, S. N. & BRENNAN, F. R. 2003. *Salmonella* Typhi and *S*. Typhimurium derivatives harbouring deletions in aromatic biosynthesis and *Salmonella* Pathogenicity Island-2 (SPI-2) genes as vaccines and vectors. *Vaccine,* 21**,** 538-48.

KIM, S., GRANT, R. A. & SAUER, R. T. 2011. Covalent linkage of distinct substrate degrons controls assembly and disassembly of DegP proteolytic cages. *Cell,* 145**,** 67-78.

KING, L. E., OSATI-ASHTIANI, F. & FRAKER, P. J. 1995. Depletion of cells of the B lineage in the bone marrow of zinc-deficient mice. . *Immunology,* 85**,** 69-73.

KINGSLEY, R. A., MSEFULA, C. L., THOMSON, N. R., KARIUKI, S., HOLT, K. E., GORDON, M. A., HARRIS, D., CLARKE, L., WHITEHEAD, S., SANGAL, V., MARSH, K., ACHTMAN, M., MOLYNEUX, M. E., CORMICAN, M., PARKHILL, J., MACLENNAN, C. A., HEYDERMAN, R. S. & DOUGAN, G. 2009. Epidemic multiple drug resistant *Salmonella* Typhimurium causing invasive disease in sub-Saharan Africa have a distinct genotype. *Genome Res,* 19**,** 2279-87.

KIRKPATRICK, B. D., MCKENZIE, R., O'NEILL, J. P., LARSSON, C. J., BOURGEOIS, A. L., SHIMKO, J., BENTLEY, M., MAKIN, J., CHATFIELD, S., HINDLE, Z., FIDLER, C., ROBINSON, B. E., VENTRONE, C. H., BANSAL, N., CARPENTER, C. M., KUTZKO, D., HAMLET, S., LAPOINTE, C. & TAYLOR, D. N. 2006. Evaluation of *Salmonella* enterica serovar Typhi (Ty2 *aroC-ssaV*-) M01ZH09, with a defined mutation in the *Salmonella* pathogenicity island 2, as a live, oral typhoid vaccine in human volunteers. *Vaccine,* 24**,** 116-123.

KIRKPATRICK, B. D., TENNEY, K. M., LARSSON, C. J., O'NEILL, J. P., VENTRONE, C., BENTLEY, M., UPTON, A., HINDLE, Z., FIDLER, C., KUTZKO, D., HOLDRIDGE, R., LAPOINTE, C., HAMLET, S. & CHATFIELD, S. N. 2005. The novel oral typhoid vaccine M01ZH09 is well tolerated and highly immunogenic in 2 vaccine presentations. *J Infect Dis,* 192**,** 360-6.

KITAMURA, H., MORIKAWA, H., KAMON, H., IGUCHI, M., HOJYO, S., FUKADA, T., YAMASHITA, S., KAISHO, T., AKIRA, S., MURAKAMI, M. & HIRANO, T. 2006. Toll-like receptor-mediated regulation of zinc homeostasis influences dendritic cell function. *Nat Immunol,* 7**,** 971-7.

KLAUCK, E., LINGNAU, M. & HENGGE-ARONIS, R. 2001. Role of the response regulator RssB in sigma recognition and initiation of sigma proteolysis in *Escherichia coli*. *Mol Microbiol,* 40**,** 1381-90.

KLEEREBEZEM, M., CRIELAARD, W. & TOMMASSEN, J. 1996. Involvement of stress protein PspA (phage shock protein A) of *Escherichia coli* in maintenance of the protonmotive force under stress conditions. *Embo j,* 15**,** 162-71.

KLOCKENBUSCH, C. & KAST, J. 2010. Optimization of formaldehyde cross-linking for protein interaction analysis of non-tagged integrin beta1. *J Biomed Biotechnol,* 2010**,** 927585.

KNODLER, L. A. & FINLAY, B. B. 2001. *Salmonella* and apoptosis: to live or let die? *Microbes Infect,* 3**,** 1321-6.

KNODLER, L. A. & STEELE-MORTIMER, O. 2005. The *Salmonella* effector PipB2 affects late endosome/lysosome distribution to mediate Sif extension. *Mol Biol Cell,* 16**,** 4108-23.

KNODLER, L. A., VALLANCE, B. A., HENSEL, M., JACKEL, D., FINLAY, B. B. & STEELE-MORTIMER, O. 2003. *Salmonella* type III effectors PipB and PipB2 are targeted to detergent-resistant microdomains on internal host cell membranes. *Mol Microbiol,* 49**,** 685-704.

KNOWLES, T. J., SCOTT-TUCKER, A., OVERDUIN, M. & HENDERSON, I. R. 2009. Membrane protein architects: the role of the BAM complex in outer membrane protein assembly. *Nat Rev Microbiol,* 7**,** 206-14.

KOBAYASHI, R., SUZUKI, T. & YOSHIDA, M. 2007. *Escherichia coli* phage-shock protein A (PspA) binds to membrane phospholipids and repairs proton leakage of the damaged membranes. *Mol Microbiol,* 66**,** 100-9.

KOHANSKI, M. A., DWYER, D. J. & COLLINS, J. J. 2010. How antibiotics kill bacteria: from targets to networks. *Nat Rev Microbiol,* 8**,** 423-35.

KOHANSKI, M. A., DWYER, D. J., HAYETE, B., LAWRENCE, C. A. & COLLINS, J. J. 2007. A common mechanism of cellular death induced by bactericidal antibiotics. *Cell,* 130**,** 797-810.

KOHANSKI, M. A., DWYER, D. J., WIERZBOWSKI, J., COTTAREL, G. & COLLINS, J. J. 2008. Mistranslation of Membrane Proteins and Two-Component System Activation Trigger Antibiotic-Mediated Cell Death. *Cell,* 135**,** 679-690.

KOHBATA, S., YOKOYAMA, H. & YABUUCHI, E. 1986. Cytopathogenic effect of *Salmonella* Typhi GIFU 10007 on M cells of murine ileal Peyer's patches in ligated ileal loops: an ultrastructural study. *Microbiol Immunol,* 30**,** 1225-37.

KOVACIKOVA, G. & SKORUPSKI, K. 2002. The alternative sigma factor sigma(E) plays an important role in intestinal survival and virulence in *Vibrio cholerae*. *Infect Immun,* 70**,** 5355-62.

KREUDER, J., OTTEN, A., FUDER, H., TUMER, Z., TONNESEN, T., HORN, N. & DRALLE, D. 1993. Clinical and biochemical consequences of copper-histidine therapy in Menkes disease. *Eur J Pediatr,* 152**,** 828-32.

KROGER, C., COLGAN, A., SRIKUMAR, S., HANDLER, K., SIVASANKARAN, S. K., HAMMARLOF, D. L., CANALS, R., GRISSOM, J. E., CONWAY, T., HOKAMP, K. & HINTON, J. C. 2013. An infection-relevant transcriptomic compendium for *Salmonella* enterica Serovar Typhimurium. *Cell Host Microbe,* 14**,** 683-95.

KROGER, C., DILLON, S. C., CAMERON, A. D., PAPENFORT, K., SIVASANKARAN, S. K., HOKAMP, K., CHAO, Y., SITTKA, A., HEBRARD, M., HANDLER, K., COLGAN, A., LEEKITCHAROENPHON, P., LANGRIDGE, G. C., LOHAN, A. J., LOFTUS, B., LUCCHINI, S., USSERY, D. W., DORMAN, C. J., THOMSON, N. R., VOGEL, J. & HINTON, J. C. 2012. The transcriptional landscape and small RNAs of *Salmonella* enterica serovar Typhimurium. *Proc Natl Acad Sci U S A,* 109**,** E1277-86.

KUBORI, T., MATSUSHIMA, Y., NAKAMURA, D., URALIL, J., LARA-TEJERO, M., SUKHAN, A., GALAN, J. E. & AIZAWA, S. I. 1998. Supramolecular structure of the *Salmonella* Typhimurium type III protein secretion system. *Science,* 280**,** 602-5.

KUBORI, T., SUKHAN, A., AIZAWA, S. I. & GALAN, J. E. 2000. Molecular characterization and assembly of the needle complex of the *Salmonella* Typhimurium type III protein secretion system. *Proc Natl Acad Sci U S A,* 97**,** 10225-30.

KUEHN, M. J. & KESTY, N. C. 2005. Bacterial outer membrane vesicles and the host-pathogen interaction. *Genes Dev,* 19**,** 2645-55.

KUHN, H. M., MEIER-DIETER, U. & MAYER, H. 1988. ECA, the enterobacterial common antigen. *FEMS Microbiol Rev,* 4**,** 195-222.

KWON, D. H. & LU, C. D. 2007. Polyamine effects on antibiotic susceptibility in bacteria. *Antimicrob Agents Chemother,* 51**,** 2070-7.

KWON, E., KIM, D. Y., GROSS, C. A., GROSS, J. D. & KIM, K. K. 2010. The crystal structure *Escherichia coli* Spy. *Protein Sci,* 19**,** 2252-9.

LABANDEIRA-REY, M., BRAUTIGAM, C. A. & HANSEN, E. J. 2010. Characterization of the CpxRA Regulon in *Haemophilus ducreyi*. *Infection and Immunity,* 78**,** 4779-4791.

LABANDEIRA-REY, M., MOCK, J. R. & HANSEN, E. J. 2009. Regulation of expression of the *Haemophilus ducreyi* LspB and LspA2 proteins by CpxR. *Infect Immun,* 77**,** 3402-11.

LACEY, M. M., PARTRIDGE, J. D. & GREEN, J. 2010. *Escherichia coli* K-12 YfgF is an anaerobic cyclic di-GMP phosphodiesterase with roles in cell surface remodelling and the oxidative stress response. *Microbiology,* 156**,** 2873-86.

LANDINI, P., EGLI, T., WOLF, J. & LACOUR, S. 2014. sigmaS, a major player in the response to environmental stresses in *Escherichia coli*: role, regulation and mechanisms of promoter recognition. *Environ Microbiol Rep,* 6**,** 1-13.

LANGE, R. & HENGGE-ARONIS, R. 1994. The cellular concentration of the sigma S subunit of RNA polymerase in *Escherichia coli* is controlled at the levels of transcription, translation, and protein stability. *Genes Dev,* 8**,** 1600-12.

LANGRIDGE, G. C., PHAN, M. D., TURNER, D. J., PERKINS, T. T., PARTS, L., HAASE, J., CHARLES, I., MASKELL, D. J., PETERS, S. E., DOUGAN, G., WAIN, J., PARKHILL, J. & TURNER, A. K. 2009.

Simultaneous assay of every *Salmonella* Typhi gene using one million transposon mutants. *Genome Res,* 19**,** 2308-16.
LARA-TEJERO, M. & GALÁN, J. E. 2009. *Salmonella* enterica Serovar Typhimurium Pathogenicity Island 1-Encoded Type III Secretion System Translocases Mediate Intimate Attachment to Nonphagocytic Cells. *Infect Immun,* 77**,** 2635-42.
LAUBACHER, M. E. & ADES, S. E. 2008. The Rcs phosphorelay is a cell envelope stress response activated by peptidoglycan stress and contributes to intrinsic antibiotic resistance. *J Bacteriol,* 190**,** 2065-74.
LAUPLAND, K. B., SCHONHEYDER, H. C., KENNEDY, K. J., LYYTIKAINEN, O., VALIQUETTE, L., GALBRAITH, J. & COLLIGNON, P. 2010. *Salmonella enterica* bacteraemia: a multi-national population-based cohort study. *BMC Infect Dis,* 10**,** 95.
LAWLEY, T. D., CHAN, K., THOMPSON, L. J., KIM, C. C., GOVONI, G. R. & MONACK, D. M. 2006. Genome-wide screen for *Salmonella* genes required for long-term systemic infection of the mouse. *PLoS Pathog,* 2**,** e11.
LEBLANC, S. K., OATES, C. W. & RAIVIO, T. L. 2011. Characterization of the induction and cellular role of the BaeSR two-component envelope stress response of *Escherichia coli. J Bacteriol,* 193**,** 3367-75.
LEBOWITZ, J., LEWIS, M. S. & SCHUCK, P. 2002. Modern analytical ultracentrifugation in protein science: A tutorial review. *Protein Sci,* 11**,** 2067-79.
LECLERC, G. J., TARTERA, C. & METCALF, E. S. 1998. Environmental regulation of *Salmonella* Typhi invasion-defective mutants. *Infect Immun,* 66**,** 682-91.
LEE, L. J., BARRETT, J. A. & POOLE, R. K. 2005. Genome-Wide Transcriptional Response of Chemostat-Cultured *Escherichia coli* to Zinc. *Journal of Bacteriology,* 187**,** 1124-1134.
LEE, S. Y., DE LA TORRE, A., YAN, D., KUSTU, S., NIXON, B. T. & WEMMER, D. E. 2003. Regulation of the transcriptional activator NtrC1: structural studies of the regulatory and AAA+ ATPase domains. *Genes Dev,* 17**,** 2552-63.
LEE, Y. H., DEKA, R. K., NORGARD, M. V., RADOLF, J. D. & HASEMANN, C. A. 1999. *Treponema pallidum* TroA is a periplasmic zinc-binding protein with a helical backbone. *Nat Struct Biol,* 6**,** 628-33.
LEE, Y. H., KIM, B. H., KIM, J. H., YOON, W. S., BANG, S. H. & PARK, Y. K. 2007. CadC Has a Global Translational Effect during Acid Adaptation in *Salmonella* enterica Serovar Typhimurium. *Journal of Bacteriology,* 189**,** 2417-2425.
LEONHARTSBERGER, S., HUBER, A., LOTTSPEICH, F. & BOCK, A. 2001. The *hydH/G* Genes from *Escherichia coli* code for a zinc and lead responsive two-component regulatory system. *J Mol Biol,* 307**,** 93-105.
LEVINE, M. M., BLACK, R. E. & LANATA, C. 1982. Precise estimation of the numbers of chronic carriers of *Salmonella* Typhi in Santiago, Chile, an endemic area. *J Infect Dis,* 146**,** 724-6.
LEWIS, C., SKOVIEROVA, H., ROWLEY, G., REZUCHOVA, B., HOMEROVA, D., STEVENSON, A., SHERRY, A., KORMANEC, J. & ROBERTS, M. 2008. Small outer-membrane lipoprotein, SmpA, is

regulated by sigmaE and has a role in cell envelope integrity and virulence of *Salmonella* enterica serovar Typhimurium. *Microbiology,* 154**,** 979-88.

LEWIS, C., SKOVIEROVA, H., ROWLEY, G., REZUCHOVA, B., HOMEROVA, D., STEVENSON, A., SPENCER, J., FARN, J., KORMANEC, J. & ROBERTS, M. 2009. *Salmonella enterica* Serovar Typhimurium HtrA: regulation of expression and role of the chaperone and protease activities during infection. *Microbiology,* 155**,** 873-81.

LEWIS, D. A., KLESNEY-TAIT, J., LUMBLEY, S. R., WARD, C. K., LATIMER, J. L., ISON, C. A. & HANSEN, E. J. 1999. Identification of the znuA-encoded periplasmic zinc transport protein of *Haemophilus ducreyi*. *Infect Immun,* 67**,** 5060-8.

LI, J., NAKAYASU, E. S., OVERALL, C. C., JOHNSON, R. C., KIDWAI, A. S., MCDERMOTT, J. E., ANSONG, C., HEFFRON, F., CAMBRONNE, E. D. & ADKINS, J. N. 2015a. Global analysis of *Salmonella* alternative sigma factor E on protein translation. *J Proteome Res*.

LI, J., OVERALL, C., NAKAYASU, E. S., KIDWAI, A., JONES, M., JOHNSON, R., NGUYEN, N., MCDERMOTT, J., ANSONG, C., HEFFRON, F., CAMBRONNE, E. D. & ADKINS, J. N. 2015b. Analysis of the *Salmonella* regulatory network suggests involvement of SsrB and H-NS in σ^E-regulated SPI-2 gene expression. *Frontiers in Microbiology,* 6.

LI, S. R., DORRELL, N., EVEREST, P. H., DOUGAN, G. & WREN, B. W. 1996. Construction and characterization of a *Yersinia enterocolitica* O:8 high-temperature requirement (*htrA*) isogenic mutant. *Infect Immun,* 64**,** 2088-94.

LIBBY, S. J., GOEBEL, W., LUDWIG, A., BUCHMEIER, N., BOWE, F., FANG, F. C., GUINEY, D. G., SONGER, J. G. & HEFFRON, F. 1994. A cytolysin encoded by *Salmonella* is required for survival within macrophages. *Proc Natl Acad Sci U S A,* 91**,** 489-93.

LIESEGANG, H., LEMKE, K., SIDDIQUI, R. A. & SCHLEGEL, H. G. 1993. Characterization of the inducible nickel and cobalt resistance determinant cnr from pMOL28 of *Alcaligenes eutrophus* CH34. *J Bacteriol,* 175**,** 767-78.

LIMSUWUN, K. & JONES, P. G. 2000. Spermidine acetyltransferase is required to prevent spermidine toxicity at low temperatures in *Escherichia coli. J Bacteriol,* 182**,** 5373-80.

LINDGREN, S. W., STOJILJKOVIC, I. & HEFFRON, F. 1996. Macrophage killing is an essential virulence mechanism of *Salmonella* Typhimurium. *Proc Natl Acad Sci U S A,* 93**,** 4197-201.

LINEHAN, S. A., RYTKONEN, A., YU, X. J., LIU, M. & HOLDEN, D. W. 2005. SlyA regulates function of *Salmonella* pathogenicity island 2 (SPI-2) and expression of SPI-2-associated genes. *Infect Immun,* 73**,** 4354-62.

LIPINSKA, B., FAYET, O., BAIRD, L. & GEORGOPOULOS, C. 1989. Identification, characterization, and mapping of the *Escherichia coli htrA* gene, whose product is essential for bacterial growth only at elevated temperatures. *J Bacteriol,* 171**,** 1574-84.

LIPPI, M., PASSERINI, A., PUNTA, M. & FRASCONI, P. 2012. Metal Binding in Proteins: Machine Learning Complements X-Ray Absorption Spectroscopy. *In:* FLACH, P., DE BIE, T. & CRISTIANINI, N. (eds.) *Machine Learning and Knowledge Discovery in Databases.* Springer Berlin Heidelberg.

LIU, J. Z., JELLBAUER, S., POE, A. J., TON, V., PESCIAROLI, M., KEHL-FIE, T. E., RESTREPO, N. A., HOSKING, M. P., EDWARDS, R. A., BATTISTONI, A., PASQUALI, P., LANE, T. E., CHAZIN, W. J., VOGL, T., ROTH, J., SKAAR, E. P. & RAFFATELLU, M. 2012. Zinc sequestration by the neutrophil protein calprotectin enhances *Salmonella* growth in the inflamed gut. *Cell Host Microbe,* 11**,** 227-39.

LIU, M. C., KUO, K. T., CHIEN, H. F., TSAI, Y. L. & LIAW, S. J. 2015. New Aspects of RpoE in Uropathogenic *Proteus mirabilis*. *Infect Immun,* 83**,** 966-77.

LIU, M. Y., GUI, G., WEI, B., PRESTON, J. F., 3RD, OAKFORD, L., YUKSEL, U., GIEDROC, D. P. & ROMEO, T. 1997. The RNA molecule CsrB binds to the global regulatory protein CsrA and antagonizes its activity in *Escherichia coli*. *J Biol Chem,* 272**,** 17502-10.

LIU, S. L., EZAKI, T., MIURA, H., MATSUI, K. & YABUUCHI, E. 1988. Intact motility as a *Salmonella* Typhi invasion-related factor. *Infect Immun,* 56**,** 1967-73.

LIU, Y. & IMLAY, J. A. 2013. Cell death from antibiotics without the involvement of reactive oxygen species. *Science,* 339**,** 1210-3.

LONETTO, M. A., BROWN, K. L., RUDD, K. E. & BUTTNER, M. J. 1994. Analysis of the *Streptomyces coelicolor* sigE gene reveals the existence of a subfamily of eubacterial RNA polymerase sigma factors involved in the regulation of extracytoplasmic functions. *Proc Natl Acad Sci U S A,* 91**,** 7573-7.

LOSCHI, L., BROKX, S. J., HILLS, T. L., ZHANG, G., BERTERO, M. G., LOVERING, A. L., WEINER, J. H. & STRYNADKA, N. C. 2004. Structural and biochemical identification of a novel bacterial oxidoreductase. *J Biol Chem,* 279**,** 50391-400.

LOYNACHAN, A. T. & HARRIS, D. L. 2005. Dose Determination for Acute *Salmonella* Infection in Pigs. *Appl Environ Microbiol,* 71**,** 2753-5.

LOYNACHAN, A. T., NUGENT, J. M., ERDMAN, M. M. & HARRIS, D. L. 2004. Acute infection of swine by various *Salmonella* serovars. *J Food Prot,* 67**,** 1484-8.

LU, D., BOYD, B. & LINGWOOD, C. A. 1997. Identification of the key protein for zinc uptake in *Hemophilus influenzae*. *J Biol Chem,* 272**,** 29033-8.

LU, D., BOYD, B. & LINGWOOD, C. A. 1998. The expression and characterization of a putative adhesin B from *H. influenzae*. *FEMS Microbiol Lett,* 165**,** 129-37.

LU, Y. & VALENTINE, J. S. 1997. Engineering metal-binding sites in proteins. *Curr Opin Struct Biol,* 7**,** 495-500.

LYON, C. E., SADIGH, K. S., CARMOLLI, M. P., HARRO, C., SHELDON, E., LINDOW, J. C., LARSSON, C. J., MARTINEZ, T., FELLER, A., VENTRONE, C. H., SACK, D. A., DENEARING, B., FINGAR, A., PIERCE, K., DILL, E. A., SCHWARTZ, H. I., BEARDSWORTH, E. E., KILONZO, B., MAY, J. P., LAM, W., UPTON, A., BUDHRAM, R. &

KIRKPATRICK, B. D. 2010. In a randomized, double-blinded, placebo-controlled trial, the single oral dose typhoid vaccine, M01ZH09, is safe and immunogenic at doses up to 1.7 × 1010 colony-forming units. *Vaccine,* 28**,** 3602-3608.
MACE, C., SEYER, D., CHEMANI, C., COSETTE, P., DI-MARTINO, P., GUERY, B., FILLOUX, A., FONTAINE, M., MOLLE, V., JUNTER, G. A. & JOUENNE, T. 2008. Identification of biofilm-associated cluster (bac) in *Pseudomonas aeruginosa* involved in biofilm formation and virulence. *PLoS One,* 3**,** e3897.
MACLENNAN, C. A., MARTIN, L. B. & MICOLI, F. 2014. Vaccines against invasive *Salmonella* disease: current status and future directions. *Hum Vaccin Immunother,* 10**,** 1478-93.
MACOMBER, L. & IMLAY, J. A. 2009. The iron-sulfur clusters of dehydratases are primary intracellular targets of copper toxicity. *Proc Natl Acad Sci U S A,* 106**,** 8344-9.
MACOMBER, L., RENSING, C. & IMLAY, J. A. 2007. Intracellular Copper Does Not Catalyze the Formation of Oxidative DNA Damage in *Escherichia coli. Journal of Bacteriology,* 189**,** 1616-1626.
MACRITCHIE, D. M., BUELOW, D. R., PRICE, N. L. & RAIVIO, T. L. 2008a. Two-component signaling and gram negative envelope stress response systems. *Adv Exp Med Biol,* 631**,** 80-110.
MACRITCHIE, D. M., WARD, J. D., NEVESINJAC, A. Z. & RAIVIO, T. L. 2008b. Activation of the Cpx Envelope Stress Response Down-Regulates Expression of Several Locus of Enterocyte Effacement-Encoded Genes in Enteropathogenic *Escherichia coli*. *Infection and Immunity,* 76**,** 1465-1475.
MAHONEY, T. F. & SILHAVY, T. J. 2013. The Cpx stress response confers resistance to some, but not all, bactericidal antibiotics. *J Bacteriol,* 195**,** 1869-74.
MAILLARD, A. P., KUNNEMANN, S., GROSSE, C., VOLBEDA, A., SCHLEUDER, G., PETIT-HARTLEIN, I., DE ROSNY, E., NIES, D. H. & COVES, J. 2015. Response of CnrX from *Cupriavidus metallidurans* CH34 to nickel binding. *Metallomics,* 7**,** 622-31.
MAJDALANI, N., HECK, M., STOUT, V. & GOTTESMAN, S. 2005. Role of RcsF in signaling to the Rcs phosphorelay pathway in *Escherichia coli*. *J Bacteriol,* 187**,** 6770-8.
MAKUI, H., ROIG, E., COLE, S. T., HELMANN, J. D., GROS, P. & CELLIER, M. F. 2000. Identification of the *Escherichia coli* K-12 NRAMP orthologue (MntH) as a selective divalent metal ion transporter. *Mol Microbiol,* 35**,** 1065-78.
MALINVERNI, J. C., WERNER, J., KIM, S., SKLAR, J. G., KAHNE, D., MISRA, R. & SILHAVY, T. J. 2006. YfiO stabilizes the YaeT complex and is essential for outer membrane protein assembly in *Escherichia coli*. *Mol Microbiol,* 61**,** 151-64.
MANFREDI, R., DONZELLI, C., TALO, S., GUZMAN, S. M. & CHIODO, F. 1998. Typhoid fever and HIV infection: a rare disease association in industrialized countries. *Int J Infect Dis,* 3**,** 105-8.
MANIATIS, T. 1982. Molecular Cloning: A Laboratory Manual. 68.

MARCUS, S. L., BRUMELL, J. H., PFEIFER, C. G. & FINLAY, B. B. 2000. *Salmonella* pathogenicity islands: big virulence in small packages. *Microbes Infect,* 2**,** 145-56.

MARTIN, D. W., SCHURR, M. J., YU, H. & DERETIC, V. 1994. Analysis of promoters controlled by the putative sigma factor AlgU regulating conversion to mucoidy in *Pseudomonas aeruginosa*: relationship to sigma E and stress response. *J Bacteriol,* 176**,** 6688-96.

MASSON, P. L., HEREMANS, J. F. & SCHONNE, E. 1969. Lactoferrin, an iron-binding protein in neutrophilic leukocytes. *J Exp Med,* 130**,** 643-58.

MATAMOUROS, S. & MILLER, S. I. 2015. *S*. Typhimurium strategies to resist killing by cationic antimicrobial peptides. *Biochim Biophys Acta*.

MATHUR, R., OH, H., ZHANG, D., PARK, S. G., SEO, J., KOBLANSKY, A., HAYDEN, M. S. & GHOSH, S. 2012. A mouse model of *Salmonella* Typhi infection. *Cell,* 151**,** 590-602.

MATSUYAMA, S., TAJIMA, T. & TOKUDA, H. 1995. A novel periplasmic carrier protein involved in the sorting and transport of *Escherichia coli* lipoproteins destined for the outer membrane. *Embo j,* 14**,** 3365-72.

MATSUYAMA, S., YOKOTA, N. & TOKUDA, H. 1997. A novel outer membrane lipoprotein, LolB (HemM), involved in the LolA (p20)-dependent localization of lipoproteins to the outer membrane of *Escherichia coli*. *Embo j,* 16**,** 6947-55.

MAYRAND, D. & GRENIER, D. 1989. Biological activities of outer membrane vesicles. *Can J Microbiol,* 35**,** 607-13.

MAZURKIEWICZ, P., THOMAS, J., THOMPSON, J. A., LIU, M., ARBIBE, L., SANSONETTI, P. & HOLDEN, D. W. 2008. SpvC is a *Salmonella* effector with phosphothreonine lyase activity on host mitogen-activated protein kinases. *Mol Microbiol,* 67**,** 1371-83.

MCBROOM, A. J. & KUEHN, M. J. 2005. *Outer membrane vesicles. In EcoSal – Escherichia coli and Salmonella,* Washington, DC, American Society for Microbiology Press.

MCBROOM, A. J. & KUEHN, M. J. 2007. Release of outer membrane vesicles by Gram-negative bacteria is a novel envelope stress response. *Mol Microbiol,* 63**,** 545-58.

MCCLELLAND, M., SANDERSON, K. E., SPIETH, J., CLIFTON, S. W., LATREILLE, P., COURTNEY, L., PORWOLLIK, S., ALI, J., DANTE, M., DU, F., HOU, S., LAYMAN, D., LEONARD, S., NGUYEN, C., SCOTT, K., HOLMES, A., GREWAL, N., MULVANEY, E., RYAN, E., SUN, H., FLOREA, L., MILLER, W., STONEKING, T., NHAN, M., WATERSTON, R. & WILSON, R. K. 2001. Complete genome sequence of *Salmonella* enterica serovar Typhimurium LT2. *Nature,* 413**,** 852-856.

MCCORMICK, B. A., MILLER, S. I., CARNES, D. & MADARA, J. L. 1995. Transepithelial signaling to neutrophils by Salmonellae: a novel virulence mechanism for gastroenteritis. *Infect Immun,* 63**,** 2302-9.

MCEWEN, J., SAMBUCETTI, L. & SILVERMAN, P. M. 1983. Synthesis of outer membrane proteins in *cpxA cpxB* mutants of *Escherichia coli* K-12. *J Bacteriol,* 154**,** 375-82.

MCEWEN, J. & SILVERMAN, P. 1980. Chromosomal mutations of *Escherichia coli* that alter expression of conjugative plasmid functions. *Proc. Natl. Acad. Sci. USA,* 77**,** 513-517.
MCEWEN, J. & SILVERMAN, P. M. 1982. Mutations in genes *cpxA* and *cpxB* alter the protein composition of *Escherichia coli* inner and outer membranes. *J Bacteriol,* 151**,** 1553-9.
MCGHIE, E. J., HAYWARD, R. D. & KORONAKIS, V. 2001. Cooperation between actin-binding proteins of invasive *Salmonella*: SipA potentiates SipC nucleation and bundling of actin. *Embo j,* 20**,** 2131-9.
MCMAHON, M. A., XU, J., MOORE, J. E., BLAIR, I. S. & MCDOWELL, D. A. 2007. Environmental stress and antibiotic resistance in food-related pathogens. *Appl Environ Microbiol,* 73**,** 211-7.
MEDINA, J., CATALA, R. & SALINAS, J. 2001. Developmental and stress regulation of RCI2A and RCI2B, two cold-inducible genes of arabidopsis encoding highly conserved hydrophobic proteins. *Plant Physiol,* 125**,** 1655-66.
MERDANOVIC, M., CLAUSEN, T., KAISER, M., HUBER, R. & EHRMANN, M. 2011. Protein quality control in the bacterial periplasm. *Annu Rev Microbiol,* 65**,** 149-68.
MERMIN, J. H., VILLAR, R., CARPENTER, J., ROBERTS, L., SAMARIDDEN, A., GASANOVA, L., LOMAKINA, S., BOPP, C., HUTWAGNER, L., MEAD, P., ROSS, B. & MINTZ, E. D. 1999. A massive epidemic of multidrug-resistant typhoid fever in Tajikistan associated with consumption of municipal water. *J Infect Dis,* 179**,** 1416-22.
MERSELIS, J. G., JR., KAYE, D., CONNOLLY, C. S. & HOOK, E. W. 1964. QUANTITATIVE BACTERIOLOGY OF THE TYPHOID CARRIER STATE. *Am J Trop Med Hyg,* 13**,** 425-9.
MESTECKY, J., NGUYEN, H., CZERKINSKY, C. & KIYONO, H. 2008. Oral immunization: an update. *Curr Opin Gastroenterol,* 24**,** 713-9.
MIKA, F. & HENGGE, R. 2014. Small RNAs in the control of RpoS, CsgD, and biofilm architecture of *Escherichia coli*. *RNA Biol,* 11**,** 494-507.
MINAMINO, T. & NAMBA, K. 2008. Distinct roles of the FliI ATPase and proton motive force in bacterial flagellar protein export. *Nature,* 451**,** 485-8.
MINNOCK, A., VERNON, D. I., SCHOFIELD, J., GRIFFITHS, J., PARISH, J. H. & BROWN, S. B. 2000. Mechanism of Uptake of a Cationic Water-Soluble Pyridinium Zinc Phthalocyanine across the Outer Membrane of *Escherichia coli*. *Antimicrob Agents Chemother,* 44**,** 522-7.
MIOT, M. & BETTON, J. M. 2004. Protein quality control in the bacterial periplasm. *Microb Cell Fact,* 3**,** 4.
MIRZA, S. H., BEECHING, N. J. & HART, C. A. 1996. Multi-drug resistant typhoid: a global problem. *J Med Microbiol,* 44**,** 317-9.
MISSIAKAS, D., BETTON, J. M. & RAINA, S. 1996. New components of protein folding in extracytoplasmic compartments of *Escherichia coli* SurA, FkpA and Skp/OmpH. *Mol Microbiol,* 21**,** 871-84.
MISSIAKAS, D. & RAINA, S. 1997. Signal transduction pathways in response to protein misfolding in the extracytoplasmic compartments of *E. coli:* role of two new phosphoprotein phosphatases PrpA and PrpB. *Embo j,* 16**,** 1670-85.

MISSIAKAS, D. & RAINA, S. 1998. The extracytoplasmic function sigma factors: role and regulation. *Mol Microbiol,* 28**,** 1059-66.

MITICKA, H., ROWLEY, G., REZUCHOVA, B., HOMEROVA, D., HUMPHREYS, S., FARN, J., ROBERTS, M. & KORMANEC, J. 2003. Transcriptional analysis of the *rpoE* gene encoding extracytoplasmic stress response sigma factor sigmaE in *Salmonella* enterica serovar Typhimurium. *FEMS Microbiol Lett,* 226**,** 307-14.

MITOBE, J., ARAKAWA, E. & WATANABE, H. 2005. A sensor of the two-component system CpxA affects expression of the type III secretion system through posttranscriptional processing of InvE. *J Bacteriol,* 187**,** 107-13.

MIYADAI, H., TANAKA-MASUDA, K., MATSUYAMA, S. & TOKUDA, H. 2004. Effects of lipoprotein overproduction on the induction of DegP (HtrA) involved in quality control in the *Escherichia coli* periplasm. *J Biol Chem,* 279**,** 39807-13.

MODEL, P., JOVANOVIC, G. & DWORKIN, J. 1997. The *Escherichia coli* phage-shock-protein (*psp*) operon. *Mol Microbiol,* 24**,** 255-61.

MOGASALE, V., MASKERY, B., OCHIAI, R. L., LEE, J. S., MOGASALE, V. V., RAMANI, E., KIM, Y. E., PARK, J. K. & WIERZBA, T. F. 2014. Burden of typhoid fever in low-income and middle-income countries: a systematic, literature-based update with risk-factor adjustment. *The Lancet Global Health,* 2**,** e570-e580.

MONACK, D. M., BOULEY, D. M. & FALKOW, S. 2004. *Salmonella* Typhimurium persists within macrophages in the mesenteric lymph nodes of chronically infected NRAMP1+/+ mice and can be reactivated by IFNgamma neutralization. *J Exp Med,* 199**,** 231-41.

MONACK, D. M., RAUPACH, B., HROMOCKYJ, A. E. & FALKOW, S. 1996. *Salmonella* Typhimurium invasion induces apoptosis in infected macrophages. *Proc Natl Acad Sci U S A,* 93**,** 9833-8.

MONCHY, S., BENOTMANE, M. A., JANSSEN, P., VALLAEYS, T., TAGHAVI, S., VAN DER LELIE, D. & MERGEAY, M. 2007. Plasmids pMOL28 and pMOL30 of *Cupriavidus metallidurans* are specialized in the maximal viable response to heavy metals. *J Bacteriol,* 189**,** 7417-25.

MOREAU, P. L. 2014. Protective role of the RpoE (sigmaE) and Cpx envelope stress responses against gentamicin killing of nongrowing *Escherichia coli* incubated under aerobic, phosphate starvation conditions. *FEMS Microbiol Lett,* 357**,** 151-6.

MORENO, M., AUDIA, J. P., BEARSON, S. M., WEBB, C. & FOSTER, J. W. 2000. Regulation of sigma S degradation in *Salmonella enterica* var Typhimurium: in vivo interactions between sigma S, the response regulator MviA (RssB) and ClpX. *J Mol Microbiol Biotechnol,* 2**,** 245-54.

MORGAN, E., CAMPBELL, J. D., ROWE, S. C., BISPHAM, J., STEVENS, M. P., BOWEN, A. J., BARROW, P. A., MASKELL, D. J. & WALLIS, T. S. 2004. Identification of host-specific colonization factors of *Salmonella enterica* serovar Typhimurium. *Mol Microbiol,* 54**,** 994-1010.

MORGAN, J. K., VENDURA, K. W., STEVENS, S. M., JR. & RIORDAN, J. T. 2013. RcsB determines the locus of enterocyte effacement (LEE)

expression and adherence phenotype of *Escherichia coli* O157 : H7 spinach outbreak strain TW14359 and coordinates bicarbonate-dependent LEE activation with repression of motility. *Microbiology,* 159**,** 2342-53.

MORRIS, D. R. 1991. A new perspective on ornithine decarboxylase regulation: prevention of polyamine toxicity is the overriding theme. *J Cell Biochem,* 46**,** 102-5.

MORRIS, J. F. & NEWMAN, E. B. 1980. Map location of the *ssd* mutation in *Escherichia coli* K-12. *J Bacteriol,* 143**,** 1504-5.

MUKHERJEE, G. & GHOSH, T. 1995. Metal ion interaction with penicillins--Part VII: Mixed-ligand complex formation of cobalt(II), nickel(II), copper(II), and Zinc(II) with ampicillin and nucleic bases. *J Inorg Biochem,* 59**,** 827-33.

MULLER, C., BANG, I. S., VELAYUDHAN, J., KARLINSEY, J., PAPENFORT, K., VOGEL, J. & FANG, F. C. 2009. Acid stress activation of the sigma(E) stress response in *Salmonella* enterica serovar Typhimurium. *Mol Microbiol,* 71**,** 1228-38.

MUNCH, R., HILLER, K., BARG, H., HELDT, D., LINZ, S., WINGENDER, E. & JAHN, D. 2003. PRODORIC: prokaryotic database of gene regulation. *Nucleic Acids Res,* 31**,** 266-9.

NAKAYAMA, S., KUSHIRO, A., ASAHARA, T., TANAKA, R., HU, L., KOPECKO, D. J. & WATANABE, H. 2003. Activation of *hilA* expression at low pH requires the signal sensor CpxA, but not the cognate response regulator CpxR, in *Salmonella* enterica serovar Typhimurium. *Microbiology,* 149**,** 2809-17.

NAKAYAMA, S. & WATANABE, H. 1995. Involvement of *cpxA*, a sensor of a two-component regulatory system, in the pH-dependent regulation of expression of *Shigella sonnei virF* gene. *J Bacteriol,* 177**,** 5062-9.

NAKAYAMA, S. & WATANABE, H. 1998. Identification of *cpxR* as a positive regulator essential for expression of the *Shigella sonnei virF* gene. *J Bacteriol,* 180**,** 3522-8.

NANDRE, R., MATSUDA, K. & LEE, J. H. 2014. Efficacy for a new live attenuated *Salmonella* Enteritidis vaccine candidate to reduce internal egg contamination. *Zoonoses Public Health,* 61**,** 55-63.

NATIONAL RESEARCH COUNCIL 1988. *Minerals,* Washington, DC, National Academy Press.

NEIDHARDT, F. C., BLOCH, P. L. & SMITH, D. F. 1974. Culture medium for enterobacteria. *J Bacteriol,* 119**,** 736-47.

NEMETH, E., VALORE, E. V., TERRITO, M., SCHILLER, G., LICHTENSTEIN, A. & GANZ, T. 2003. Hepcidin, a putative mediator of anemia of inflammation, is a type II acute-phase protein. *Blood,* 101**,** 2461-3.

NEVESINJAC, A. Z. & RAIVIO, T. L. 2005. The Cpx envelope stress response affects expression of the type IV bundle-forming pili of enteropathogenic *Escherichia coli*. *J Bacteriol,* 187**,** 672-86.

NEWMAN, E. B., MALIK, N. & WALKER, C. 1982. L-serine degradation in *Escherichia coli* K-12: directly isolated ssd mutants and their intragenic revertants. *J Bacteriol,* 150**,** 710-5.

NICKERSON, C. A. & CURTISS, R., 3RD 1997. Role of sigma factor RpoS in initial stages of *Salmonella* Typhimurium infection. *Infect Immun,* 65**,** 1814-23.

NICOLAS, G., BENNOUN, M., DEVAUX, I., BEAUMONT, C., GRANDCHAMP, B., KAHN, A. & VAULONT, S. 2001. Lack of hepcidin gene expression and severe tissue iron overload in upstream stimulatory factor 2 (USF2) knockout mice. *Proc Natl Acad Sci U S A,* 98**,** 8780-5.

NICOLAS, G., BENNOUN, M., PORTEU, A., MATIVET, S., BEAUMONT, C., GRANDCHAMP, B., SIRITO, M., SAWADOGO, M., KAHN, A. & VAULONT, S. 2002. Severe iron deficiency anemia in transgenic mice expressing liver hepcidin. *Proc Natl Acad Sci U S A,* 99**,** 4596-601.

NICOLAY, T., VANDERLEYDEN, J. & SPAEPEN, S. 2015. Autotransporter-based cell surface display in Gram-negative bacteria. *Crit Rev Microbiol,* 41**,** 109-23.

NIELUBOWICZ, G. R., SMITH, S. N. & MOBLEY, H. L. 2010. Zinc uptake contributes to motility and provides a competitive advantage to Proteus mirabilis during experimental urinary tract infection. *Infect Immun,* 78**,** 2823-33.

NIES, D. H. 1999. Microbial heavy-metal resistance. *Appl Microbiol Biotechnol,* 51**,** 730-50.

NISHINO, K., NIKAIDO, E. & YAMAGUCHI, A. 2007. Regulation of multidrug efflux systems involved in multidrug and metal resistance of *Salmonella enterica* serovar Typhimurium. *J Bacteriol,* 189**,** 9066-75.

NISHINO, K. & YAMAGUCHI, A. 2001. Analysis of a complete library of putative drug transporter genes in *Escherichia coli*. *J Bacteriol,* 183**,** 5803-12.

NISINI, R., BISELLI, R., MATRICARDI, P. M., FATTOROSSI, A. & D'AMELIO, R. 1993. Clinical and immunological response to typhoid vaccination with parenteral or oral vaccines in two groups of 30 recruits. *Vaccine,* 11**,** 582-6.

NIXON, B. T., RONSON, C. W. & AUSUBEL, F. M. 1986. Two-component regulatory systems responsive to environmental stimuli share strongly conserved domains with the nitrogen assimilation regulatory genes *ntrB* and *ntrC*. *Proc Natl Acad Sci U S A,* 83**,** 7850-4.

NNALUE, N. A. & STOCKER, B. A. 1987. The effects of O-antigen character and enterobacterial common antigen content on the *in vivo* persistence of aromatic-dependent *Salmonella* sp. live-vaccine strains. *Microb Pathog,* 3**,** 31-44.

NOLL, M., PETRUKHIN, K. & LUTSENKO, S. 1998. Identification of a novel transcription regulator from *Proteus mirabilis*, PMTR, revealed a possible role of YJAI protein in balancing zinc in *Escherichia coli*. *J Biol Chem,* 273**,** 21393-401.

NUNEZ-HERNANDEZ, C., TIERREZ, A., ORTEGA, A. D., PUCCIARELLI, M. G., GODOY, M., EISMAN, B., CASADESUS, J. & GARCIA-DEL PORTILLO, F. 2013. Genome expression analysis of nonproliferating intracellular *Salmonella enterica* serovar Typhimurium unravels an acid pH-dependent PhoP-PhoQ response essential for dormancy. *Infect Immun,* 81**,** 154-65.

NUSS, A. M., GLAESER, J. & KLUG, G. 2009. RpoHII Activates Oxidative-Stress Defense Systems and Is Controlled by RpoE in the Singlet Oxygen-Dependent Response in *Rhodobacter sphaeroides*. *Journal of Bacteriology,* 191**,** 220-230.

O'NEAL, C. R., GABRIEL, W. M., TURK, A. K., LIBBY, S. J., FANG, F. C. & SPECTOR, M. P. 1994. RpoS is necessary for both the positive and negative regulation of starvation survival genes during phosphate, carbon, and nitrogen starvation in *Salmonella* Typhimurium. *J Bacteriol,* 176**,** 4610-6.

OCHMAN, H. & GROISMAN, E. A. 1996. Distribution of pathogenicity islands in *Salmonella* spp. *Infect Immun,* 64**,** 5410-2.

OCHMAN, H., SONCINI, F. C., SOLOMON, F. & GROISMAN, E. A. 1996. Identification of a pathogenicity island required for *Salmonella* survival in host cells. *Proc Natl Acad Sci U S A,* 93**,** 7800-4.

OGASAWARA, H., ISHIDA, Y., YAMADA, K., YAMAMOTO, K. & ISHIHAMA, A. 2007. PdhR (pyruvate dehydrogenase complex regulator) controls the respiratory electron transport system in *Escherichia coli*. *J Bacteriol,* 189**,** 5534-41.

OGASAWARA, H., TERAMOTO, J., HIRAO, K., YAMAMOTO, K., ISHIHAMA, A. & UTSUMI, R. 2004. Negative regulation of DNA repair gene (*ung*) expression by the CpxR/CpxA two-component system in *Escherichia coli* K-12 and induction of mutations by increased expression of CpxR. *J Bacteriol,* 186**,** 8317-25.

OHL, M. E. & MILLER, S. I. 2001. *Salmonella*: a model for bacterial pathogenesis. *Annu Rev Med,* 52**,** 259-74.

OKADA, N., OI, Y., TAKEDA-SHITAKA, M., KANOU, K., UMEYAMA, H., HANEDA, T., MIKI, T., HOSOYA, S. & DANBARA, H. 2007. Identification of amino acid residues of *Salmonella* SlyA that are critical for transcriptional regulation. *Microbiology,* 153**,** 548-60.

OSBORNE, S. E. & COOMBES, B. K. 2009. RpoE fine tunes expression of a subset of SsrB-regulated virulence factors in *Salmonella enterica* serovar Typhimurium. *BMC Microbiol,* 9**,** 45.

OSHIMA, T., AIBA, H., MASUDA, Y., KANAYA, S., SUGIURA, M., WANNER, B. L., MORI, H. & MIZUNO, T. 2002. Transcriptome analysis of all two-component regulatory system mutants of *Escherichia coli* K-12. *Mol Microbiol,* 46**,** 281-91.

OSMAN, D. & CAVET, J. S. 2011. Metal sensing in *Salmonella*: implications for pathogenesis. *Adv Microb Physiol,* 58**,** 175-232.

OSMAN, D., WALDRON, K. J., DENTON, H., TAYLOR, C. M., GRANT, A. J., MASTROENI, P., ROBINSON, N. J. & CAVET, J. S. 2010. Copper homeostasis in *Salmonella* is atypical and copper-CueP is a major periplasmic metal complex. *J Biol Chem,* 285**,** 25259-68.

OTTO, K. & SILHAVY, T. J. 2002. Surface sensing and adhesion of *Escherichia coli* controlled by the Cpx-signaling pathway. *Proc Natl Acad Sci U S A,* 99**,** 2287-92.

OUELLETTE, R. G. 2014. *e-Study Guide for Pharmacology For Nurse Anesthesiology,* online Amazon Media EU, Cram101.

OUTTEN, C. E. & O'HALLORAN, T. V. 2001. Femtomolar sensitivity of metalloregulatory proteins controlling zinc homeostasis. *Science,* 292**,** 2488-92.

OUTTEN, C. E., OUTTEN, F. W. & O'HALLORAN, T. V. 1999. DNA distortion mechanism for transcriptional activation by ZntR, a Zn(II)-responsive MerR homologue in *Escherichia coli*. *J Biol Chem,* 274**,** 37517-24.

PAKKANEN, S. H., KANTELE, J. M. & KANTELE, A. 2012. Cross-reactive gut-directed immune response against *Salmonella* enterica serovar Paratyphi A and B in typhoid fever and after oral Ty21a typhoid vaccination. *Vaccine,* 30**,** 6047-53.

PAKKANEN, S. H., KANTELE, J. M. & KANTELE, A. 2014. Cross-reactive immune response induced by the Vi capsular polysaccharide typhoid vaccine against *Salmonella* Paratyphi strains. *Scand J Immunol,* 79**,** 222-9.

PAKKANEN, S. H., KANTELE, J. M., SAVOLAINEN, L. E., ROMBO, L. & KANTELE, A. 2015. Specific and cross-reactive immune response to oral *Salmonella* Typhi Ty21a and parenteral Vi capsular polysaccharide typhoid vaccines administered concomitantly. *Vaccine,* 33**,** 451-8.

PANG, T., BHUTTA, Z. A., FINLAY, B. B. & ALTWEGG, M. 1995. Typhoid fever and other salmonellosis: a continuing challenge. *Trends Microbiol,* 3**,** 253-5.

PANINA, E. M., MIRONOV, A. A. & GELFAND, M. S. 2003. Comparative genomics of bacterial zinc regulons: enhanced ion transport, pathogenesis, and rearrangement of ribosomal proteins. *Proc Natl Acad Sci U S A,* 100**,** 9912-7.

PARK, C. H., VALORE, E. V., WARING, A. J. & GANZ, T. 2001. Hepcidin, a urinary antimicrobial peptide synthesized in the liver. *J Biol Chem,* 276**,** 7806-10.

PARROW, N. L., FLEMING, R. E. & MINNICK, M. F. 2013. Sequestration and scavenging of iron in infection. *Infect Immun,* 81**,** 3503-14.

PARRY, C. M., HIEN, T. T., DOUGAN, G., WHITE, N. J. & FARRAR, J. J. 2002. Typhoid fever. *N Engl J Med,* 347**,** 1770-82.

PASETTI, M. F., SIMON, J. K., SZTEIN, M. B. & LEVINE, M. M. 2011. Immunology of gut mucosal vaccines. *Immunol Rev,* 239**,** 125-48.

PASHA, I., SAEED, F., SULTAN, M. T., KHAN, M. R. & ROHI, M. 2014. Recent developments in minimal processing: a tool to retain nutritional quality of food. *Crit Rev Food Sci Nutr,* 54**,** 340-51.

PATEL, G. J., BEHRENS-KNEIP, S., HOLST, O. & KLEINSCHMIDT, J. H. 2009. The periplasmic chaperone Skp facilitates targeting, insertion, and folding of OmpA into lipid membranes with a negative membrane surface potential. *Biochemistry,* 48**,** 10235-45.

PATEL, K., KUMAR, A. & DURANI, S. 2007. Analysis of the structural consensus of the zinc coordination centers of metalloprotein structures. *Biochim Biophys Acta,* 1774**,** 1247-53.

PATERSON, G. K. & MASKELL, D. J. 2010. Recent advances in the field of *Salmonella* Typhi vaccines. *Hum Vaccin,* 6**,** 379-84.

PATZER, S. I. & HANTKE, K. 1998. The ZnuABC high-affinity zinc uptake system and its regulator Zur in *Escherichia coli*. *Mol Microbiol,* 28**,** 1199-210.

PATZER, S. I. & HANTKE, K. 2000. The zinc-responsive regulator Zur and its control of the *znu* gene cluster encoding the ZnuABC zinc uptake system in *Escherichia coli*. *J Biol Chem,* 275**,** 24321-32.
PEGG, A. E. 2013. Toxicity of polyamines and their metabolic products. *Chem Res Toxicol,* 26**,** 1782-800.
PEREZ, V. G., WAGUESPACK, A. M., BIDNER, T. D., SOUTHERN, L. L., FAKLER, T. M., WARD, T. L., STEIDINGER, M. & PETTIGREW, J. E. 2011. Additivity of effects from dietary copper and zinc on growth performance and fecal microbiota of pigs after weaning. *J Anim Sci,* 89**,** 414-25.
PEREZ-PEREZ, G. I., THIBERGE, J. M., LABIGNE, A. & BLASER, M. J. 1996. Relationship of immune response to heat-shock protein A and characteristics of *Helicobacter pylori*-infected patients. *J Infect Dis,* 174**,** 1046-50.
PERRY, R. D., CRAIG, S. K., ABNEY, J., BOBROV, A. G., KIRILLINA, O., MIER, I., JR., TRUSZCZYNSKA, H. & FETHERSTON, J. D. 2012. Manganese transporters Yfe and MntH are Fur-regulated and important for the virulence of *Yersinia pestis*. *Microbiology,* 158**,** 804-15.
PESCARETTI MDE, L., LOPEZ, F. E., MORERO, R. D. & DELGADO, M. A. 2010. Transcriptional autoregulation of the RcsCDB phosphorelay system in *Salmonella enterica* serovar Typhimurium. *Microbiology,* 156**,** 3513-21.
PETRARCA, P., AMMENDOLA, S., PASQUALI, P. & BATTISTONI, A. 2010. The Zur-Regulated ZinT Protein Is an Auxiliary Component of the High-Affinity ZnuABC Zinc Transporter That Facilitates Metal Recruitment during Severe Zinc Shortage. *Journal of Bacteriology,* 192**,** 1553-1564.
PFEIFER, C. G., MARCUS, S. L., STEELE-MORTIMER, O., KNODLER, L. A. & FINLAY, B. B. 1999. *Salmonella* Typhimurium virulence genes are induced upon bacterial invasion into phagocytic and nonphagocytic cells. *Infect Immun,* 67**,** 5690-8.
PLATE, C. A. 1976. Mutant of *Escherichia coli* defective in response to colicin
K and in active transport. *J. Bacteriol.,* 125**,** 467-474.
PLATE, C. A. & SUIT, J. L. 1981. The *eup* genetic locus of *Escherichia coli* and its role in H^+/solute symport. *J Biol Chem,* 256**,** 12974-80.
PLETZER, D. & WEINGART, H. 2014. Characterization of AcrD, a resistance-nodulation-cell division-type multidrug efflux pump from the fire blight pathogen *Erwinia amylovora*. *BMC Microbiol,* 14**,** 13.
POGLIANO, J., DONG, J. M., DE WULF, P., FURLONG, D., BOYD, D., LOSICK, R., POGLIANO, K. & LIN, E. C. 1998. Aberrant cell division and random FtsZ ring positioning in *Escherichia coli cpxA** mutants. *J Bacteriol,* 180**,** 3486-90.
POGLIANO, J., LYNCH, A. S., BELIN, D., LIN, E. C. & BECKWITH, J. 1997. Regulation of *Escherichia coli* cell envelope proteins involved in protein folding and degradation by the Cpx two-component system. *Genes Dev,* 11**,** 1169-82.

PONTEL, L. B., PEZZA, A. & SONCINI, F. C. 2010. Copper stress targets the *rcs* system to induce multiaggregative behavior in a copper-sensitive *Salmonella* strain. *J Bacteriol,* 192**,** 6287-90.
PONTEL, L. B., SCAMPOLI, N. L., PORWOLLIK, S., CHECA, S. K., MCCLELLAND, M. & SONCINI, F. C. 2014. Identification of a *Salmonella* ancillary copper detoxification mechanism by a comparative analysis of the genome-wide transcriptional response to copper and zinc excess. *Microbiology,* 160**,** 1659-69.
PONTEL, L. B. & SONCINI, F. C. 2009. Alternative periplasmic copper-resistance mechanisms in Gram negative bacteria. *Mol Microbiol,* 73**,** 212-25.
POOLE, K. 2000. Efflux-mediated resistance to fluoroquinolones in gram-positive bacteria and the mycobacteria. *Antimicrob Agents Chemother,* 44**,** 2595-9.
POPE, N. R. & COLE, J. A. 1982. Generation of a membrane potential by one of two independent pathways for nitrite reduction by *Escherichia coli*. *J Gen Microbiol,* 128**,** 219-22.
PORCHERON, G., GARENAUX, A., PROULX, J., SABRI, M. & DOZOIS, C. M. 2013. Iron, copper, zinc, and manganese transport and regulation in pathogenic Enterobacteria: correlations between strains, site of infection and the relative importance of the different metal transport systems for virulence. *Front Cell Infect Microbiol,* 3**,** 90.
PORWOLLIK, S., WONG, R. M. & MCCLELLAND, M. 2002. Evolutionary genomics of *Salmonella*: gene acquisitions revealed by microarray analysis. *Proc Natl Acad Sci U S A,* 99**,** 8956-61.
POTTER, A. J. & PATON, J. C. 2014. Spermidine biosynthesis and transport modulate pneumococcal autolysis. *J Bacteriol,* 196**,** 3556-61.
POWERS, E. T. & BALCH, W. E. 2011. Protein folding: Protection from the outside. *Nature,* 471**,** 42-3.
PREHNA, G., ZHANG, G., GONG, X., DUSZYK, M., OKON, M., MCINTOSH, L. P., WEINER, J. H. & STRYNADKA, N. C. 2012. A protein export pathway involving *Escherichia coli* porins. *Structure,* 20**,** 1154-66.
PRICE, N. L. & RAIVIO, T. L. 2009. Characterization of the Cpx regulon in *Escherichia coli* strain MC4100. *J Bacteriol,* 191**,** 1798-815.
PRIGENT-COMBARET, C., BROMBACHER, E., VIDAL, O., AMBERT, A., LEJEUNE, P., LANDINI, P. & DOREL, C. 2001. Complex regulatory network controls initial adhesion and biofilm formation in *Escherichia coli* via regulation of the *csgD* gene. *J Bacteriol,* 183**,** 7213-23.
PROKARIUM. 2015. *Typhella* [Online]. Available: http://prokarium.com/pipeline/typhella/ [Accessed 21-8-2015].
PROST, L. R., SANOWAR, S. & MILLER, S. I. 2007. *Salmonella* sensing of anti-microbial mechanisms to promote survival within macrophages. *Immunol Rev,* 219**,** 55-65.
PULLINGER, G. D., VAN DIEMEN, P. M., DZIVA, F. & STEVENS, M. P. 2010. Role of two-component sensory systems of *Salmonella enterica* serovar Dublin in the pathogenesis of systemic salmonellosis in cattle*.* Reading, England, Microbiology
QU, J., BEHRENS-KNEIP, S., HOLST, O. & KLEINSCHMIDT, J. H. 2009. Binding regions of outer membrane protein A in complexes with the

periplasmic chaperone Skp. A site-directed fluorescence study. *Biochemistry,* 48**,** 4926-36.
QUAN, S., KOLDEWEY, P., TAPLEY, T., KIRSCH, N., RUANE, K. M., PFIZENMAIER, J., SHI, R., HOFMANN, S., FOIT, L., REN, G., JAKOB, U., XU, Z., CYGLER, M. & BARDWELL, J. C. 2011. Genetic selection designed to stabilize proteins uncovers a chaperone called Spy. *Nat Struct Mol Biol,* 18**,** 262-9.
QUE, F., WU, S. & HUANG, R. 2013. *Salmonella* pathogenicity island 1(SPI-1) at work. *Curr Microbiol,* 66**,** 582-7.
RAFFA, R. G. & RAIVIO, T. L. 2002. A third envelope stress signal transduction pathway in *Escherichia coli*. *Mol Microbiol,* 45**,** 1599-611.
RAFFATELLU, M., GEORGE, M. D., AKIYAMA, Y., HORNSBY, M. J., NUCCIO, S. P., PAIXAO, T. A., BUTLER, B. P., CHU, H., SANTOS, R. L., BERGER, T., MAK, T. W., TSOLIS RÉ, M., BEVINS, C. L., SOLNICK, J. V., DANDEKAR, S. & BÄUMLER, A. J. 2009. Lipocalin-2 resistance of *Salmonella enterica* serotype Typhimurium confers an advantage during life in the inflamed intestine. *Cell Host Microbe,* 5**,** 476-86.
RAFFATELLU, M., SANTOS, R. L., VERHOEVEN, D. E., GEORGE, M. D., WILSON, R. P., WINTER, S. E., GODINEZ, I., SANKARAN, S., PAIXAO, T. A., GORDON, M. A., KOLLS, J. K., DANDEKAR, S. & BAUMLER, A. J. 2008. Simian immunodeficiency virus-induced mucosal interleukin-17 deficiency promotes *Salmonella* dissemination from the gut. *Nat Med,* 14**,** 421-8.
RAINWATER, S. & SILVERMAN, P. M. 1990. The Cpx proteins of *Escherichia coli* K-12: evidence that *cpxA*, *ecfB*, *ssd*, and *eup* mutations all identify the same gene. *J Bacteriol,* 172**,** 2456-61.
RAIVIO, T. L. 2013. Everything old is new again: An update on current research on the Cpx envelope stress response. *Biochim Biophys Acta*.
RAIVIO, T. L., LAIRD, M. W., JOLY, J. C. & SILHAVY, T. J. 2000. Tethering of CpxP to the inner membrane prevents spheroplast induction of the Cpx envelope stress response. *Mol Microbiol,* 37**,** 1186-97.
RAIVIO, T. L., LEBLANC, S. K. & PRICE, N. L. 2013. The *Escherichia coli* Cpx envelope stress response regulates genes of diverse function that impact antibiotic resistance and membrane integrity. *J Bacteriol,* 195**,** 2755-67.
RAIVIO, T. L., POPKIN, D. L. & SILHAVY, T. J. 1999. The Cpx envelope stress response is controlled by amplification and feedback inhibition. *J Bacteriol,* 181**,** 5263-72.
RAIVIO, T. L. & SILHAVY, T. J. 1997. Transduction of envelope stress in *Escherichia coli* by the Cpx two-component system. *J Bacteriol,* 179**,** 7724-33.
RAIVIO, T. L. & SILHAVY, T. J. 1999. The sigmaE and Cpx regulatory pathways: overlapping but distinct envelope stress responses. *Curr Opin Microbiol,* 2**,** 159-65.
RAIVIO, T. L. & SILHAVY, T. J. 2001. Periplasmic stress and ECF sigma factors. *Annu Rev Microbiol,* 55**,** 591-624.
RAMACHANDRAN, G., PERKINS, D. J., SCHMIDLEIN, P. J., TULAPURKAR, M. E. & TENNANT, S. M. 2015. Invasive *Salmonella*

Typhimurium ST313 with Naturally Attenuated Flagellin Elicits Reduced Inflammation and Replicates within Macrophages. *PLoS Negl Trop Dis,* 9**,** e3394.

RAMOS-MORALES, F., PRIETO, A. I., BEUZON, C. R., HOLDEN, D. W. & CASADESUS, J. 2003. Role for *Salmonella* enterica enterobacterial common antigen in bile resistance and virulence. *J Bacteriol,* 185**,** 5328-32.

RATHMAN, M., SJAASTAD, M. D. & FALKOW, S. 1996. Acidification of phagosomes containing *Salmonella* Typhimurium in murine macrophages. *Infect Immun,* 64**,** 2765-73.

RAVIKUMAR, S., YOO, I. K., LEE, S. Y. & HONG, S. H. 2011. A study on the dynamics of the *zraP* gene expression profile and its application to the construction of zinc adsorption bacteria. *Bioprocess Biosyst Eng,* 34**,** 1119-26.

RAWLINGS, N. D., TOLLE, D. P. & BARRETT, A. J. 2004. Evolutionary families of peptidase inhibitors. *Biochem J,* 378**,** 705-16.

REDFORD, P. & WELCH, R. A. 2006. Role of Sigma E-Regulated Genes in *Escherichia coli* Uropathogenesis. *Infect Immun,* 74**,** 4030-8.

RENSING, C., MITRA, B. & ROSEN, B. P. 1997. The *zntA* gene of *Escherichia coli* encodes a Zn(II)-translocating P-type ATPase. *Proc Natl Acad Sci U S A,* 94**,** 14326-31.

REZUCHOVA, B., MITICKA, H., HOMEROVA, D., ROBERTS, M. & KORMANEC, J. 2003. New members of the *Escherichia coli* sigmaE regulon identified by a two-plasmid system. *FEMS Microbiol Lett,* 225**,** 1-7.

RHODIUS, V. A., SUH, W. C., NONAKA, G., WEST, J. & GROSS, C. A. 2006. Conserved and variable functions of the sigmaE stress response in related genomes. *PLoS Biol,* 4**,** e2.

RICHTER-DAHLFORS, A., BUCHAN, A. M. & FINLAY, B. B. 1997. Murine salmonellosis studied by confocal microscopy: *Salmonella* Typhimurium resides intracellularly inside macrophages and exerts a cytotoxic effect on phagocytes *in vivo*. *J Exp Med,* 186**,** 569-80.

RILEY, M., ABE, T., ARNAUD, M. B., BERLYN, M. K. B., BLATTNER, F. R., CHAUDHURI, R. R., GLASNER, J. D., HORIUCHI, T., KESELER, I. M., KOSUGE, T., MORI, H., PERNA, N. T., PLUNKETT, G., RUDD, K. E., SERRES, M. H., THOMAS, G. H., THOMSON, N. R., WISHART, D. & WANNER, B. L. 2006. *Escherichia coli* K-12: a cooperatively developed annotation snapshot—2005. *Nucleic Acids Res,* 34**,** 1-9.

RIZZITELLO, A. E., HARPER, J. R. & SILHAVY, T. J. 2001. Genetic evidence for parallel pathways of chaperone activity in the periplasm of *Escherichia coli*. *J Bacteriol,* 183**,** 6794-800.

ROACH, J. C., GLUSMAN, G., ROWEN, L., KAUR, A., PURCELL, M. K., SMITH, K. D., HOOD, L. E. & ADEREM, A. 2005. The evolution of vertebrate Toll-like receptors. *Proc Natl Acad Sci U S A,* 102**,** 9577-82.

ROBERTSHAW, D. 2004. *Temperature regulation and the thermal environment,* Ichatha and London, Cornell University Press.

ROSEN, R. & RON, E. Z. 2002. Proteome analysis in the study of the bacterial heat-shock response. *Mass Spectrom Rev,* 21**,** 244-65.

ROUVIERE, P. E., DE LAS PENAS, A., MECSAS, J., LU, C. Z., RUDD, K. E. & GROSS, C. A. 1995. *rpoE*, the gene encoding the second heat-shock sigma factor, sigma E, in *Escherichia coli*. *Embo j,* 14**,** 1032-42.

ROWLEY, G., SKOVIEROVA, H., STEVENSON, A., REZUCHOVA, B., HOMEROVA, D., LEWIS, C., SHERRY, A., KORMANEC, J. & ROBERTS, M. 2011. The periplasmic chaperone Skp is required for successful *Salmonella* Typhimurium infection in a murine typhoid model. *Microbiology,* 157**,** 848-58.

ROWLEY, G., SPECTOR, M., KORMANEC, J. & ROBERTS, M. 2006. Pushing the envelope: extracytoplasmic stress responses in bacterial pathogens. *Nat Rev Micro,* 4**,** 383-394.

ROWLEY, G., STEVENSON, A., KORMANEC, J. & ROBERTS, M. 2005. Effect of inactivation of *degS* on *Salmonella enterica* serovar Typhimurium *in vitro* and *in vivo*. *Infect Immun,* 73**,** 459-63.

RUDD, K. E. 2000. EcoGene: a genome sequence database for *Escherichia coli* K-12. *Nucleic Acids Res,* 28**,** 60-4.

RUIZ, N., KAHNE, D. & SILHAVY, T. J. 2009. Transport of lipopolysaccharide across the cell envelope: the long road of discovery. *Nat Rev Microbiol,* 7**,** 677-83.

RUIZ-ALBERT, J., YU, X. J., BEUZON, C. R., BLAKEY, A. N., GALYOV, E. E. & HOLDEN, D. W. 2002. Complementary activities of SseJ and SifA regulate dynamics of the *Salmonella* Typhimurium vacuolar membrane. *Mol Microbiol,* 44**,** 645-61.

RUNKEL, S., WELLS, H. C. & ROWLEY, G. 2013. Living with Stress: A Lesson from the Enteric Pathogen *Salmonella enterica*. *Adv Appl Microbiol,* 83**,** 87-144.

RUNYEN-JANECKY, L., DAZENSKI, E., HAWKINS, S. & WARNER, L. 2006. Role and regulation of the *Shigella flexneri* Sit and MntH systems. *Infect Immun,* 74**,** 4666-72.

RUSSEL, M. 1994. Phage assembly: a paradigm for bacterial virulence factor export? *Science,* 265**,** 612-4.

SABBAGH, S. C., FOREST, C. G., LEPAGE, C., LECLERC, J.-M. & DAIGLE, F. 2010. So similar, yet so different: uncovering distinctive features in the genomes of *Salmonella enterica* serovars Typhimurium and Typhi.

SABRI, M., HOULE, S. & DOZOIS, C. M. 2009. Roles of the extraintestinal pathogenic *Escherichia coli* ZnuACB and ZupT zinc transporters during urinary tract infection. *Infect Immun,* 77**,** 1155-64.

SAIBIL, H. R. 2008. Chaperone machines in action. *Curr Opin Struct Biol,* 18**,** 35-42.

SALLAI, L. & TUCKER, P. A. 2005. Crystal structure of the central and C-terminal domain of the sigma(54)-activator ZraR. *J Struct Biol,* 151**,** 160-70.

SAMANOVIC, M. I., DING, C., THIELE, D. J. & DARWIN, K. H. 2012. Copper in microbial pathogenesis: meddling with the metal. *Cell Host Microbe,* 11**,** 106-15.

SAMUELS, D. J., FRYE, J. G., PORWOLLIK, S., MCCLELLAND, M., MRAZEK, J., HOOVER, T. R. & KARLS, A. C. 2013. Use of a promiscuous, constitutively-active bacterial enhancer-binding protein

to define the sigma(5)(4) (RpoN) regulon of *Salmonella* Typhimurium LT2. *BMC Genomics,* 14**,** 602.
SANDSTEAD, H. H. 1985. Requirement of zinc in human subjects. *J Am Coll Nutr,* 4**,** 73-82.
SCHAFER, U., BECK, K. & MULLER, M. 1999. Skp, a molecular chaperone of gram-negative bacteria, is required for the formation of soluble periplasmic intermediates of outer membrane proteins. *J Biol Chem,* 274**,** 24567-74.
SCHMIDT, C., SCHWARZENBERGER, C., GROSS, C. & NIES, D. H. 2014. FurC Regulates Expression of *zupT* for the Central Zinc Importer ZupT of *Cupriavidus metallidurans*. *J Bacteriol,* 196**,** 3461-71.
SCHMIDT, H. & HENSEL, M. 2004. Pathogenicity islands in bacterial pathogenesis. *Clin Microbiol Rev,* 17**,** 14-56.
SCHNEIDER, T. D., STORMO, G. D., GOLD, L. & EHRENFEUCHT, A. 1986. Information content of binding sites on nucleotide sequences. *J Mol Biol,* 188**,** 415-31.
SCHRODER, H., LANGER, T., HARTL, F. U. & BUKAU, B. 1993. DnaK, DnaJ and GrpE form a cellular chaperone machinery capable of repairing heat-induced protein damage. *EMBO J,* 12**,** 4137-44.
SCHROEDER, N., HENRY, T., DE CHASTELLIER, C., ZHAO, W., GUILHON, A. A., GORVEL, J. P. & MERESSE, S. 2010. The virulence protein SopD2 regulates membrane dynamics of *Salmonella*-containing vacuoles. *PLoS Pathog,* 6**,** e1001002.
SCHROLL, C., CHRISTENSEN, J. P., CHRISTENSEN, H., PORS, S. E., THORNDAHL, L., JENSEN, P. R., OLSEN, J. E. & JELSBAK, L. 2014. Polyamines are essential for virulence in *Salmonella enterica* serovar Gallinarum despite evolutionary decay of polyamine biosynthesis genes. *Vet Microbiol,* 170**,** 144-50.
SCHUMACHER, J., ZHANG, X., JONES, S., BORDES, P. & BUCK, M. 2004. ATP-dependent transcriptional activation by bacterial PspF AAA+protein. *J Mol Biol,* 338**,** 863-75.
SCHWEDER, T., LEE, K. H., LOMOVSKAYA, O. & MATIN, A. 1996. Regulation of *Escherichia coli* starvation sigma factor (sigma s) by ClpXP protease. *J Bacteriol,* 178**,** 470-6.
SETH-SMITH, H. M. 2008. SPI-7: *Salmonella*'s Vi-encoding Pathogenicity Island. *J Infect Dev Ctries,* 2**,** 267-71.
SHAH, D. H., LEE, M. J., PARK, J. H., LEE, J. H., EO, S. K., KWON, J. T. & CHAE, J. S. 2005. Identification of *Salmonella* Gallinarum virulence genes in a chicken infection model using PCR-based signature-tagged mutagenesis. *Microbiology,* 151**,** 3957-68.
SHAH, P. & SWIATLO, E. 2008. A multifaceted role for polyamines in bacterial pathogens. *Mol Microbiol,* 68**,** 4-16.
SHEA, J. E., HENSEL, M., GLEESON, C. & HOLDEN, D. W. 1996. Identification of a virulence locus encoding a second type III secretion system in *Salmonella* Typhimurium. *Proc Natl Acad Sci U S A,* 93**,** 2593-7.
SHI, L., ADKINS, J. N., COLEMAN, J. R., SCHEPMOES, A. A., DOHNKOVA, A., MOTTAZ, H. M., NORBECK, A. D., PURVINE, S. O., MANES, N. P., SMALLWOOD, H. S., WANG, H., FORBES, J., GROS, P., UZZAU, S., RODLAND, K. D., HEFFRON, F., SMITH, R.

D. & SQUIER, T. C. 2006. Proteomic analysis of *Salmonella* enterica serovar Typhimurium isolated from RAW 264.7 macrophages: identification of a novel protein that contributes to the replication of serovar Typhimurium inside macrophages. *J Biol Chem,* 281**,** 29131-40.

SHIMADA, K., OGASAWARA, H., YAMADA, K., SHIMURA, M., KORI, A., SHIMADA, T., YAMANAKA, Y., YAMAMOTO, K. & ISHIHAMA, A. 2013. Screening of promoter-specific transcription factors: multiple regulators for the *sdiA* gene involved in cell division control and quorum sensing. *Microbiology,* 159**,** 2501-12.

SHIMOHATA, N., CHIBA, S., SAIKAWA, N., ITO, K. & AKIYAMA, Y. 2002. The Cpx stress response system of *Escherichia coli* senses plasma membrane proteins and controls HtpX, a membrane protease with a cytosolic active site. *Genes Cells,* 7**,** 653-62.

SHINGLER, V. 1996. Signal sensing by sigma 54-dependent regulators: derepression as a control mechanism. *Mol Microbiol,* 19**,** 409-16.

SHPARGEL, J. S., BERARDI, R. S. & LENZ, D. 1985. *Salmonella* Typhi carrier state 52 years after illness with typhoid fever: a case study. *Am J Infect Control,* 13**,** 122-3.

SI, W., WANG, X., LIU, H., YU, S., LI, Z., CHEN, L., ZHANG, W. & LIU, S. 2015. Physiology, pathogenicity and immunogenicity of live, attenuated *Salmonella* enterica serovar Enteritidis mutants in chicks. *Microb Pathog,* 83-84**,** 6-11.

SINHA, A., SAZAWAL, S., KUMAR, R., SOOD, S., REDDAIAH, V. P., SINGH, B., RAO, M., NAFICY, A., CLEMENS, J. D. & BHAN, M. K. 1999. Typhoid fever in children aged less than 5 years. *Lancet,* 354**,** 734-7.

SINNOTT, C. R. & TEALL, A. J. 1987. Persistent gallbladder carriage of *Salmonella* typhi. *Lancet,* 1**,** 976.

SKOVIEROVA, H., ROWLEY, G., REZUCHOVA, B., HOMEROVA, D., LEWIS, C., ROBERTS, M. & KORMANEC, J. 2006. Identification of the sigmaE regulon of *Salmonella enterica* serovar Typhimurium. *Microbiology,* 152**,** 1347-59.

SNYDER, W. B., DAVIS, L. J., DANESE, P. N., COSMA, C. L. & SILHAVY, T. J. 1995. Overproduction of NlpE, a new outer membrane lipoprotein, suppresses the toxicity of periplasmic LacZ by activation of the Cpx signal transduction pathway. *J Bacteriol,* 177**,** 4216-23.

SOKSAWATMAEKHIN, W., KURAISHI, A., SAKATA, K., KASHIWAGI, K. & IGARASHI, K. 2004. Excretion and uptake of cadaverine by CadB and its physiological functions in *Escherichia coli*. *Mol Microbiol,* 51**,** 1401-12.

SPAINK, H. P., OKKER, R. J., WIJFFELMAN, C. A., PEES, E. & LUGTENBERG, B. J. 1987. Promoters in the nodulation region of the *Rhizobium leguminosarum* Sym plasmid pRL1JI. *Plant Mol Biol,* 9**,** 27-39.

SPECTOR, M. P., GARCIA DEL PORTILLO, F., BEARSON, S. M., MAHMUD, A., MAGUT, M., FINLAY, B. B., DOUGAN, G., FOSTER, J. W. & PALLEN, M. J. 1999. The *rpoS*-dependent starvation-stress response locus *stiA* encodes a nitrate reductase (*narZYWV*) required

for carbon-starvation-inducible thermotolerance and acid tolerance in *Salmonella* Typhimurium. *Microbiology,* 145 (Pt 11)**,** 3035-45.

SPECTOR, M. P. & KENYON, W. J. 2012. Resistance and survival strategies of *Salmonella enterica* to environmental stresses. *Food Res. Int.* **,** 455-481.

SPINOLA, S. M., FORTNEY, K. R., BAKER, B., JANOWICZ, D. M., ZWICKL, B., KATZ, B. P., BLICK, R. J. & MUNSON, R. S., JR. 2010. Activation of the CpxRA system by deletion of *cpxA* impairs the ability of *Haemophilus ducreyi* to infect humans. *Infect Immun,* 78**,** 3898-904.

SRIKANTH, C. V., MERCADO-LUBO, R., HALLSTROM, K. & MCCORMICK, B. A. 2011. *Salmonella* effector proteins and host-cell responses. *Cell Mol Life Sci,* 68**,** 3687-97.

SRIVASTAVA, S. K., LAMBADI, P. R., GHOSH, T., PATHANIA, R. & NAVANI, N. K. 2014. Genetic regulation of spy gene expression in *Escherichia coli* in the presence of protein unfolding agent ethanol. *Gene,* 548**,** 142-148.

STAFFORD, S. L., BOKIL, N. J., ACHARD, M. E. S., KAPETANOVIC, R., SCHEMBRI, M. A., MCEWAN, A. G. & SWEET, M. J. 2013. Metal ions in macrophage antimicrobial pathways: emerging roles for zinc and copper. *Biosci Rep,* 33.

STEADMAN, D., LO, A., WAKSMAN, G. & REMAUT, H. 2014. Bacterial surface appendages as targets for novel antibacterial therapeutics. *Future Microbiol,* 9**,** 887-900.

STEBBINS, C. E. & GALAN, J. E. 2003. Priming virulence factors for delivery into the host. *Nat Rev Mol Cell Biol,* 4**,** 738-43.

STEELE-MORTIMER, O., BRUMELL, J. H., KNODLER, L. A., MERESSE, S., LOPEZ, A. & FINLAY, B. B. 2002. The invasion-associated type III secretion system of *Salmonella enterica* serovar Typhimurium is necessary for intracellular proliferation and vacuole biogenesis in epithelial cells. *Cell Microbiol,* 4**,** 43-54.

STEENACKERS, H., HERMANS, K., VANDERLEYDEN, J. & DE KEERSMAECKER, S. C. J. 2012. *Salmonella* biofilms: An overview on occurrence, structure, regulation and eradication. *Food Research International,* 45**,** 502-531.

STEIN, M. A., LEUNG, K. Y., ZWICK, M., GARCIA-DEL PORTILLO, F. & FINLAY, B. B. 1996. Identification of a *Salmonella* virulence gene required for formation of filamentous structures containing lysosomal membrane glycoproteins within epithelial cells. *Mol Microbiol,* 20**,** 151-64.

STEINBAKK, M., NAESS-ANDRESEN, C. F., LINGAAS, E., DALE, I., BRANDTZAEG, P. & FAGERHOL, M. K. 1990. Antimicrobial actions of calcium binding leucocyte L1 protein, calprotectin. *Lancet,* 336**,** 763-5.

STENDER, S., FRIEBEL, A., LINDER, S., ROHDE, M., MIROLD, S. & HARDT, W. D. 2000. Identification of SopE2 from *Salmonella* Typhimurium, a conserved guanine nucleotide exchange factor for Cdc42 of the host cell. *Mol Microbiol,* 36**,** 1206-21.

STOCK, A. M., ROBINSON, V. L. & GOUDREAU, P. N. 2000. Two-component signal transduction. *Annu Rev Biochem,* 69**,** 183-215.

STOKER, K., REIJNDERS, W. N., OLTMANN, L. F. & STOUTHAMER, A. H. 1989. Initial cloning and sequencing of *hydHG*, an operon homologous to *ntrBC* and regulating the labile hydrogenase activity in *Escherichia coli* K-12. *J Bacteriol,* 171**,** 4448-56.

STORK, M., BOS, M. P., JONGERIUS, I., DE KOK, N., SCHILDERS, I., WEYNANTS, V. E., POOLMAN, J. T. & TOMMASSEN, J. 2010. An outer membrane receptor of *Neisseria meningitidis* involved in zinc acquisition with vaccine potential. *PLoS Pathog,* 6**,** e1000969.

STRAUCH, K. L. & BECKWITH, J. 1988. An *Escherichia coli* mutation preventing degradation of abnormal periplasmic proteins. *Proc Natl Acad Sci U S A,* 85**,** 1576-80.

STRELKAUSKAS, A. S., J.; MOSZYK-STRELKAUSKAS, D. 2010. Microbiology: A Clinical Approach. *Garland Science, Taylor and Francis Group, LLC.*

STROZEN, T. G., LANGEN, G. R. & HOWARD, S. P. 2005. Adenylate cyclase mutations rescue the *degP* temperature-sensitive phenotype and induce the sigma E and Cpx extracytoplasmic stress regulons in *Escherichia coli*. *J Bacteriol,* 187**,** 6309-16.

SU, H. S., LANG, B. F. & NEWMAN, E. B. 1989. L-serine degradation in *Escherichia coli* K-12: cloning and sequencing of the *sdaA* gene. *J Bacteriol,* 171**,** 5095-102.

SUAR, M. & RYAN, D. 2015. Small RNA in the acid tolerance response of *Salmonella* and their role in virulence. *Virulence,* 6**,** 105-6.

SUBASHCHANDRABOSE, S. & MOBLEY, H. L. 2015. Back to the metal age: battle for metals at the host-pathogen interface during urinary tract infection. *Metallomics*.

SUGAWARA, E. & NIKAIDO, H. 1992. Pore-forming activity of OmpA protein of *Escherichia coli*. *J Biol Chem,* 267**,** 2507-11.

SUGAWARA, E. & NIKAIDO, H. 1994. OmpA protein of *Escherichia coli* outer membrane occurs in open and closed channel forms. *J Biol Chem,* 269**,** 17981-7.

TABOR, C. W. & TABOR, H. 1985. Polyamines in microorganisms. *Microbiol Rev,* 49**,** 81-99.

TACKET, C. O., SZTEIN, M. B., LOSONSKY, G. A., WASSERMAN, S. S., NATARO, J. P., EDELMAN, R., PICKARD, D., DOUGAN, G., CHATFIELD, S. N. & LEVINE, M. M. 1997. Safety of live oral *Salmonella* Typhi vaccine strains with deletions in *htrA* and *aroC aroD* and immune response in humans. *Infect Immun,* 65**,** 452-6.

TAGLIABUE, A., VILLA, L., DE MAGISTRIS, M. T., ROMANO, M., SILVESTRI, S., BORASCHI, D. & NENCIONI, L. 1986. IgA-driven T cell-mediated anti-bacterial immunity in man after live oral Ty 21a vaccine. *J Immunol,* 137**,** 1504-10.

TAINER, J. A., ROBERTS, V. A. & GETZOFF, E. D. 1991. Metal-binding sites in proteins. *Curr Opin Biotechnol,* 2**,** 582-91.

TAKAYA, A., TOMOYASU, T., MATSUI, H. & YAMAMOTO, T. 2004. The DnaK/DnaJ Chaperone Machinery of *Salmonella enterica* Serovar Typhimurium Is Essential for Invasion of Epithelial Cells and Survival within Macrophages, Leading to Systemic Infection. *Infection and Immunity,* 72**,** 1364-1373.

TAM, F. C., WANG, M., DONG, B., LEUNG, D. T., MA, C. H. & LIM, P. L. 2008. New rapid test for paratyphoid a fever: usefulness, cross-detection, and solution. *Diagn Microbiol Infect Dis,* 62**,** 142-50.

TANG, S. W., ABUBAKAR, S., DEVI, S., PUTHUCHEARY, S. & PANG, T. 1997. Induction and characterization of heat shock proteins of *Salmonella* Typhi and their reactivity with sera from patients with typhoid fever. *Infect Immun,* 65**,** 2983-6.

TAUDTE, N. & GRASS, G. 2010. Point mutations change specificity and kinetics of metal uptake by ZupT from *Escherichia coli*. *Biometals,* 23**,** 643-56.

TEIGELKAMP, S., BHARDWAJ, R. S., ROTH, J., MEINARDUS-HAGER, G., KARAS, M. & SORG, C. 1991. Calcium-dependent complex assembly of the myeloic differentiation proteins MRP-8 and MRP-14. *J Biol Chem,* 266**,** 13462-7.

TENNANT, S. M. & LEVINE, M. M. 2015. Live attenuated vaccines for invasive *Salmonella* infections. *Vaccine,* 33, Supplement 3**,** C36-C41.

TENNANT, S. M., WANG, J. Y., GALEN, J. E., SIMON, R., PASETTI, M. F., GAT, O. & LEVINE, M. M. 2011. Engineering and preclinical evaluation of attenuated nontyphoidal *Salmonella* strains serving as live oral vaccines and as reagent strains. *Infect Immun,* 79**,** 4175-85.

TESTERMAN, T. L., VAZQUEZ-TORRES, A., XU, Y., JONES-CARSON, J., LIBBY, S. J. & FANG, F. C. 2002. The alternative sigma factor sigmaE controls antioxidant defences required for *Salmonella* virulence and stationary-phase survival. *Mol Microbiol,* 43**,** 771-82.

THANASSI, D. G., BLISKA, J. B. & CHRISTIE, P. J. 2012. Surface organelles assembled by secretion systems of Gram-negative bacteria: diversity in structure and function. *FEMS Microbiol Rev,* 36**,** 1046-82.

THEDE, G. L., ARTHUR, D. C., EDWARDS, R. A., BUELOW, D. R., WONG, J. L., RAIVIO, T. L. & GLOVER, J. N. 2011. Structure of the periplasmic stress response protein CpxP. *J Bacteriol,* 193**,** 2149-57.

THOMASSIN, J.-L., GIANNAKOPOULOU, N., ZHU, L., GROSS, J., SALMON, K., LECLERC, J.-M., DAIGLE, F., LE MOUAL, H. & GRUENHEID, S. 2015. The CpxRA two-component system is essential for *Citrobacter rodentium* virulence. *Infection and Immunity*.

THOME, B. M. & MULLER, M. 1991. Skp is a periplasmic *Escherichia coli* protein requiring SecA and SecY for export. *Mol Microbiol,* 5**,** 2815-21.

THOMPSON, A., ROWLEY, G., ALSTON, M., DANINO, V. & HINTON, J. C. 2006. *Salmonella* transcriptomics: relating regulons, stimulons and regulatory networks to the process of infection. *Curr Opin Microbiol,* 9**,** 109-16.

THOMSON, A. J. & GRAY, H. B. 1998. Bio-inorganic chemistry. *Current Opinion in Chemical Biology,* 2**,** 155-158.

THOMSON, N. R., CLAYTON, D. J., WINDHORST, D., VERNIKOS, G., DAVIDSON, S., CHURCHER, C., QUAIL, M. A., STEVENS, M., JONES, M. A., WATSON, M., BARRON, A., LAYTON, A., PICKARD, D., KINGSLEY, R. A., BIGNELL, A., CLARK, L., HARRIS, B., ORMOND, D., ABDELLAH, Z., BROOKS, K., CHEREVACH, I., CHILLINGWORTH, T., WOODWARD, J., NORBERCZAK, H., LORD, A., ARROWSMITH, C., JAGELS, K., MOULE, S., MUNGALL, K.,

SANDERS, M., WHITEHEAD, S., CHABALGOITY, J. A., MASKELL, D., HUMPHREY, T., ROBERTS, M., BARROW, P. A., DOUGAN, G. & PARKHILL, J. 2008. Comparative genome analysis of *Salmonella* Enteritidis PT4 and *Salmonella* Gallinarum 287/91 provides insights into evolutionary and host adaptation pathways. *Genome Res,* 18**,** 1624-37.

THONY-MEYER, L., FISCHER, F., KUNZLER, P., RITZ, D. & HENNECKE, H. 1995. *Escherichia coli* genes required for cytochrome c maturation. *J Bacteriol,* 177**,** 4321-6.

THORBJARNARDOTTIR, S. H., MAGNUSDOTTIR, R. A. & EGGERTSSON, G. 1978. Mutations determining generalized resistance to aminoglycoside antibiotics in *Escherichia coli*. *Mol. Gen. Genet. ,* 161**,** 89–98.

THRELFALL, E. J. & ROWE, B. W. L. 1991. Occurrence and treatment of multi-resistant *Salmonella* Typhi in the UK. *PHLS Microbiology Digest,* 8**,** 56-59.

TINDALL, B. J., GRIMONT, P. A., GARRITY, G. M. & EUZEBY, J. P. 2005. Nomenclature and taxonomy of the genus *Salmonella*. *Int J Syst Evol Microbiol,* 55**,** 521-4.

TKACHENKO, A., NESTEROVA, L. & PSHENICHNOV, M. 2001. The role of the natural polyamine putrescine in defense against oxidative stress in *Escherichia coli*. *Arch Microbiol,* 176**,** 155-7.

TKACHENKO, A. G. & NESTEROVA, L. Y. 2003. Polyamines as modulators of gene expression under oxidative stress in *Escherichia coli*. *Biochemistry (Mosc),* 68**,** 850-6.

TOBE, T., ANDO, H., ISHIKAWA, H., ABE, H., TASHIRO, K., HAYASHI, T., KUHARA, S. & SUGIMOTO, N. 2005. Dual regulatory pathways integrating the RcsC-RcsD-RcsB signalling system control enterohaemorrhagic *Escherichia coli* pathogenicity. *Mol Microbiol,* 58**,** 320-33.

TOBE, T., YOSHIKAWA, M., MIZUNO, T. & SASAKAWA, C. 1993. Transcriptional control of the invasion regulatory gene *virB* of *Shigella flexneri*: activation by *virF* and repression by H-NS. *J Bacteriol,* 175**,** 6142-9.

TRAN, T. H., NGUYEN, T. D., NGUYEN, T. T., NINH, T. T., TRAN, N. B., NGUYEN, V. M., TRAN, T. T., CAO, T. T., PHAM, V. M., NGUYEN, T. C., TRAN, T. D., PHAM, V. T., TO, S. D., CAMPBELL, J. I., STOCKWELL, E., SCHULTSZ, C., SIMMONS, C. P., GLOVER, C., LAM, W., MARQUES, F., MAY, J. P., UPTON, A., BUDHRAM, R., DOUGAN, G., FARRAR, J., NGUYEN, V. V. & DOLECEK, C. 2010. A randomised trial evaluating the safety and immunogenicity of the novel single oral dose typhoid vaccine M01ZH09 in healthy Vietnamese children. *PLoS One,* 5**,** e11778.

TSCHAUNER, K., HORNSCHEMEYER, P., MULLER, V. S. & HUNKE, S. 2014. Dynamic interaction between the CpxA sensor kinase and the periplasmic accessory protein CpxP mediates signal recognition in *E. coli*. *PLoS One,* 9**,** e107383.

TSOLIS, R. M., ADAMS, L. G., FICHT, T. A. & BAUMLER, A. J. 1999a. Contribution of *Salmonella* Typhimurium virulence factors to diarrheal disease in calves. *Infect Immun,* 67**,** 4879-85.

TSOLIS, R. M., KINGSLEY, R. A., TOWNSEND, S. M., FICHT, T. A., ADAMS, L. G. & BAUMLER, A. J. 1999b. Of mice, calves, and men. Comparison of the mouse typhoid model with other *Salmonella* infections. *Adv Exp Med Biol,* 473**,** 261-74.

TURNER, A. K., LOVELL, M. A., HULME, S. D., ZHANG-BARBER, L. & BARROW, P. A. 1998. Identification of *Salmonella* Typhimurium genes required for colonization of the chicken alimentary tract and for virulence in newly hatched chicks. *Infect Immun,* 66**,** 2099-106.

UNO, H. & ARYA, S. 1987. Neuronal and vascular disorders of the brain and spinal cord in Menkes kinky hair disease. *Am J Med Genet Suppl,* 3**,** 367-77.

VALDEZ, Y., FERREIRA, R. B. & FINLAY, B. B. 2009. Molecular mechanisms of *Salmonella* virulence and host resistance. *Curr Top Microbiol Immunol,* 337**,** 93-127.

VALENTIN-HANSEN, P., HAMMER-JESPERSEN, K., BOETIUS, F. & SVENDSEN, I. 1984. Structure and function of the intercistronic regulatory *deoC-deoA* element of *Escherichia coli* K-12. *Embo j,* 3**,** 179-83.

VALLEE, B. L. & AULD, D. S. 1993. New perspective on zinc biochemistry: cocatalytic sites in multi-zinc enzymes. *Biochemistry,* 32**,** 6493-500.

VALTONEN, M. V., LARINKARI, U. M., PLOSILA, M., VALTONEN, V. V. & MAKELA, P. H. 1976. Effect of enterobacterial common antigen on mouse virulence of *Salmonella* Typhimurium. *Infect Immun,* 13**,** 1601-5.

VAN ASTEN, A. J. & VAN DIJK, J. E. 2005. Distribution of "classic" virulence factors among *Salmonella* spp. *FEMS Immunol Med Microbiol,* 44**,** 251-9.

VAN BAMBEKE, F., BALZI, E. & TULKENS, P. M. 2000. Antibiotic efflux pumps. *Biochemical Pharmacology,* 60**,** 457-470.

VASSYLYEV, D. G., TOMITORI, H., KASHIWAGI, K., MORIKAWA, K. & IGARASHI, K. 1998. Crystal structure and mutational analysis of the *Escherichia coli* putrescine receptor. Structural basis for substrate specificity. *J Biol Chem,* 273**,** 17604-9.

VENECIA, K. & YOUNG, G. M. 2005. Environmental regulation and virulence attributes of the Ysa type III secretion system of *Yersinia enterocolitica* biovar 1B. *Infect Immun,* 73**,** 5961-77.

VINCENT, C. D., BUSCHER, B. A., FRIEDMAN, J. R., WILLIAMS, L. A., BARDILL, P. & VOGEL, J. P. 2006. Identification of non-dot/icm suppressors of the *Legionella pneumophila* DeltadotL lethality phenotype. *J Bacteriol,* 188**,** 8231-43.

VOGT, J. & SCHULZ, G. E. 1999. The structure of the outer membrane protein OmpX from *Escherichia coli* reveals possible mechanisms of virulence. *Structure,* 7**,** 1301-9.

VOGT, S. L., EVANS, A. D., GUEST, R. L. & RAIVIO, T. L. 2014. The Cpx envelope stress response regulates and is regulated by small noncoding RNAs. *J Bacteriol,* 196**,** 4229-38.

VOGT, S. L., NEVESINJAC, A. Z., HUMPHRIES, R. M., DONNENBERG, M. S., ARMSTRONG, G. D. & RAIVIO, T. L. 2010. The Cpx envelope stress response both facilitates and inhibits elaboration of the

enteropathogenic *Escherichia coli* bundle-forming pilus. *Mol Microbiol,* 76**,** 1095-110.

VOGT, S. L. & RAIVIO, T. L. 2012. Just scratching the surface: an expanding view of the Cpx envelope stress response. *FEMS Microbiol Lett,* 326**,** 2-11.

VUGIA, D. J., KIEHLBAUCH, J. A., YEBOUE, K., N'GBICHI, J. M., LACINA, D., MARAN, M., GONDO, M., KOUADIO, K., KADIO, A., LUCAS, S. B. & ET AL. 1993. Pathogens and predictors of fatal septicemia associated with human immunodeficiency virus infection in Ivory Coast, west Africa. *J Infect Dis,* 168**,** 564-70.

WAGNER, D., MASER, J., LAI, B., CAI, Z., BARRY, C. E., 3RD, HONER ZU BENTRUP, K., RUSSELL, D. G. & BERMUDEZ, L. E. 2005. Elemental analysis of *Mycobacterium avium*-, *Mycobacterium tuberculosis*-, and *Mycobacterium smegmatis*-containing phagosomes indicates pathogen-induced microenvironments within the host cell's endosomal system. *J Immunol,* 174**,** 1491-500.

WAHID, R., SIMON, R., ZAFAR, S. J., LEVINE, M. M. & SZTEIN, M. B. 2012. Live oral typhoid vaccine Ty21a induces cross-reactive humoral immune responses against *Salmonella* enterica serovar Paratyphi A and S. Paratyphi B in humans. *Clin Vaccine Immunol,* 19**,** 825-34.

WAHID, R., ZAFAR, S. J., MCARTHUR, M. A., PASETTI, M. F., LEVINE, M. M. & SZTEIN, M. B. 2014. Live Oral *Salmonella enterica* Serovar Typhi Vaccines Ty21a and CVD 909 Induce Opsonophagocytic Functional Antibodies in Humans That Cross-React with *S*. Paratyphi A and *S*. Paratyphi B. *Clinical and Vaccine Immunology,* 21**,** 427-434.

WAIN, J., HENDRIKSEN, R. S., MIKOLEIT, M. L., KEDDY, K. H. & OCHIAI, R. L. 2014. Typhoid fever. *Lancet*.

WALDRON, K. J. & ROBINSON, N. J. 2009. How do bacterial cells ensure that metalloproteins get the correct metal? *Nat Rev Microbiol,* 7**,** 25-35.

WALLRODT, I., JELSBAK, L., THOMSEN, L. E., BRIX, L., LEMIRE, S., GAUTIER, L., NIELSEN, D. S., JOVANOVIC, G., BUCK, M. & OLSEN, J. E. 2014. Removal of the phage-shock protein PspB causes reduction of virulence in *Salmonella enterica* serovar Typhimurium independently of NRAMP1. *J Med Microbiol,* 63**,** 788-95.

WALLRODT, I., JELSBAK, L., THORNDAHL, L., THOMSEN, L. E., LEMIRE, S. & OLSEN, J. E. 2013. The putative thiosulfate sulfurtransferases PspE and GlpE contribute to virulence of *Salmonella* Typhimurium in the mouse model of systemic disease. *PLoS One,* 8**,** e70829.

WANG, D. & FIERKE, C. A. 2013. The BaeSR regulon is involved in defense against zinc toxicity in *E. coli*. *Metallomics,* 5**,** 372-83.

WANG, D., HOSTEEN, O. & FIERKE, C. A. 2012. ZntR-mediated transcription of zntA responds to nanomolar intracellular free zinc. *J Inorg Biochem,* 111**,** 173-81.

WATTIAU, P., BOLAND, C. & BERTRAND, S. 2011. Methodologies for *Salmonella enterica* subsp. enterica Subtyping: Gold Standards and Alternatives. *Appl Environ Microbiol,* 77**,** 7877-85.

WEBER, R. F. & SILVERMAN, P. M. 1988. The Cpx proteins of *Escherichia coli* K12. Structure of the *cpxA* polypeptide as an inner membrane component. *J Mol Biol,* 203**,** 467-78.

WEINBERG, E. D. 2009. Iron availability and infection. *Biochim Biophys Acta,* 1790**,** 600-5.
WEISBLUM, B. & DAVIES, J. 1968. Antibiotic inhibitors of the bacterial ribosome. *Bacteriol Rev,* 32**,** 493-528.
WEISS, A., IBARRA, J. A., PAOLETTI, J., CARROLL, R. K. & SHAW, L. N. 2014. The delta subunit of RNA polymerase guides promoter selectivity and virulence in *Staphylococcus aureus*. *Infect Immun,* 82**,** 1424-35.
WERNER, J. & MISRA, R. 2005. YaeT (Omp85) affects the assembly of lipid-dependent and lipid-independent outer membrane proteins of *Escherichia coli*. *Mol Microbiol,* 57**,** 1450-9.
WESSLING-RESNICK, M. 2010. Iron homeostasis and the inflammatory response. *Annu Rev Nutr,* 30**,** 105-22.
WESTON, L. A. & KADNER, R. J. 1988. Role of *uhp* genes in expression of the *Escherichia coli* sugar-phosphate transport system. *J Bacteriol,* 170**,** 3375-83.
WHITE, C., LEE, J., KAMBE, T., FRITSCHE, K. & PETRIS, M. J. 2009. A role for the ATP7A copper-transporting ATPase in macrophage bactericidal activity. *J Biol Chem,* 284**,** 33949-56.
WILLIAMS, D. L. H. 1999. The chemistry of S-nitrosothiols. *Acc. Chem. Res.,* 32**,** 869–876.
WINTERS, M. S., CHAN, Q., CARUSO, J. A. & DEEPE, G. S. 2010. Metallomic Analysis of Macrophages Infected with Histoplasma capsulatum Reveals a Fundamental Role for Zinc in Host Defenses. *Journal of Infectious Diseases,* 202**,** 1136-1145.
WISNER, A. L. S., DESIN, T. S., WHITE, A., POTTER, A. A. & KOSTER, W. 2012. The *Salmonella* Pathogenicity Island-1 and -2 Encoded Type III Secretion Systems. *In:* KUMAR, Y. (ed.) *Salmonella - A Diversified Superbug.* Rijeka, Croatia: Intech.
WOOD, M. W., JONES, M. A., WATSON, P. R., HEDGES, S., WALLIS, T. S. & GALYOV, E. E. 1998. Identification of a pathogenicity island required for *Salmonella* enteropathogenicity. *Mol Microbiol,* 29**,** 883-91.
WOOD, W. B. 1966. Host specificity of DNA produced by *Escherichia coli*: bacterial mutations affecting the restriction and modification of DNA. *J Mol Biol,* 16**,** 118-33.
WOOLRIDGE, D. P., VAZQUEZ-LASLOP, N., MARKHAM, P. N., CHEVALIER, M. S., GERNER, E. W. & NEYFAKH, A. A. 1997. Efflux of the natural polyamine spermidine facilitated by the *Bacillus subtilis* multidrug transporter Blt. *J Biol Chem,* 272**,** 8864-6.
WORLD HEALTH ORGANISATION (WHO). 2015. *Typhoid* [Online]. [Accessed 21 August 2015].
WORTHAM, B. W., PATEL, C. N. & OLIVEIRA, M. A. 2007. Polyamines in bacteria: pleiotropic effects yet specific mechanisms. *Adv Exp Med Biol,* 603**,** 106-15.
WRIGHT, A. E. & LEISHMAN, W. B. 1900. Remarks on the Results which have been Obtained by the Antityphoid Inoculations and on the Methods which have been Employed in the Preparation of the Vaccine. *Br Med J,* 1**,** 122-9.

WRIGHT, J. S. & KADNER, R. J. 2001. The Phosphoryl Transfer Domain of UhpB Interacts with the Response Regulator UhpA. *Journal of Bacteriology,* 183**,** 3149-3159.
WU, T., MALINVERNI, J., RUIZ, N., KIM, S., SILHAVY, T. J. & KAHNE, D. 2005. Identification of a multicomponent complex required for outer membrane biogenesis in *Escherichia coli*. *Cell,* 121**,** 235-45.
WU, Y. L., LEE, L. H., ROLLINS, D. M. & CHING, W. M. 1994. Heat shock- and alkaline pH-induced proteins of *Campylobacter jejun*i: characterization and immunological properties. *Infect Immun,* 62**,** 4256-60.
YAKUSHI, T., MASUDA, K., NARITA, S., MATSUYAMA, S. & TOKUDA, H. 2000. A new ABC transporter mediating the detachment of lipid-modified proteins from membranes. *Nat Cell Biol,* 2**,** 212-8.
YAMAMOTO, K., HIRAO, K., OSHIMA, T., AIBA, H., UTSUMI, R. & ISHIHAMA, A. 2005. Functional characterization *in vitro* of all two-component signal transduction systems from *Escherichia coli*. *J Biol Chem,* 280**,** 1448-56.
YAMAMOTO, K. & ISHIHAMA, A. 2005. Transcriptional response of *Escherichia coli* to external copper. *Mol Microbiol,* 56**,** 215-27.
YAMAMOTO, K. & ISHIHAMA, A. 2006. Characterization of copper-inducible promoters regulated by CpxA/CpxR in *Escherichia coli*. *Biosci Biotechnol Biochem,* 70**,** 1688-95.
YAMAMOTO, K., OGASAWARA, H. & ISHIHAMA, A. 2008. Involvement of multiple transcription factors for metal-induced spy gene expression in Escherichia coli. *J Biotechnol,* 133**,** 196-200.
YANG, X., MA, Q. & WOOD, T. K. 2008. The R1 conjugative plasmid increases *Escherichia coli* biofilm formation through an envelope stress response. *Appl Environ Microbiol,* 74**,** 2690-9.
YOO, A. Y., YU, J. E., YOO, H., LEE, T. H., LEE, W. H., OH, J. I. & KANG, H. Y. 2013. Role of sigma factor E in regulation of *Salmonella* Agf expression. *Biochem Biophys Res Commun,* 430**,** 131-6.
YOON, B. Y., KIM, J. S., UM, S. H., JO, I., YOO, J. W., LEE, K., KIM, Y. H. & HA, N. C. 2014a. Periplasmic disulfide isomerase DsbC is involved in the reduction of copper binding protein CueP from *Salmonella enterica* serovar Typhimurium. *Biochem Biophys Res Commun,* 446**,** 971-6.
YOON, B. Y., YEOM, J. H., KIM, J. S., UM, S. H., JO, I., LEE, K., KIM, Y. H. & HA, N. C. 2014b. Direct ROS scavenging activity of CueP from *Salmonella enterica* serovar Typhimurium. *Mol Cells,* 37**,** 100-8.
YOON, H., MCDERMOTT, J. E., PORWOLLIK, S., MCCLELLAND, M. & HEFFRON, F. 2009. Coordinated regulation of virulence during systemic infection of *Salmonella enterica* serovar Typhimurium. *PLoS Pathog,* 5**,** e1000306.
YU, H., SCHURR, M. J. & DERETIC, V. 1995. Functional equivalence of *Escherichia coli* sigma E and *Pseudomonas aeruginosa* AlgU: *E. coli rpoE* restores mucoidy and reduces sensitivity to reactive oxygen intermediates in *algU* mutants of *P. aeruginosa*. *J Bacteriol,* 177**,** 3259-68.
ZAAT, S. A., WIJFFELMAN, C. A., SPAINK, H. P., VAN BRUSSEL, A. A., OKKER, R. J. & LUGTENBERG, B. J. 1987. Induction of the *nodA*

promoter of *Rhizobium leguminosarum* Sym plasmid pRL1JI by plant flavanones and flavones. *J Bacteriol,* 169**,** 198-204.

ZAHARIK, M. L., CULLEN, V. L., FUNG, A. M., LIBBY, S. J., KUJAT CHOY, S. L., COBURN, B., KEHRES, D. G., MAGUIRE, M. E., FANG, F. C. & FINLAY, B. B. 2004. The *Salmonella enterica* serovar typhimurium divalent cation transport systems MntH and SitABCD are essential for virulence in an NRAMP1G169 murine typhoid model. *Infect Immun,* 72**,** 5522-5.

ZASLOFF, M. 2002. Antimicrobial peptides of multicellular organisms. *Nature,* 415**,** 389-95.

ZHANG, X. & BREMER, H. 1995. Control of the *Escherichia coli rrnB* P1 promoter strength by ppGpp. *J Biol Chem,* 270**,** 11181-9.

ZHAO, H., BRAUTIGAM, C. A., GHIRLANDO, R. & SCHUCK, P. 2013. Overview of current methods in sedimentation velocity and sedimentation equilibrium analytical ultracentrifugation. *Curr Protoc Protein Sci,* Chapter 20**,** Unit20 12.

ZHAO, W., XU, M., LIANG, Z., DING, B., NIU, L., LIU, H. & TENG, M. 2011. Structure-based de novo prediction of zinc-binding sites in proteins of unknown function. *Bioinformatics,* 27**,** 1262-8.

ZHOU, D., MOOSEKER, M. S. & GALAN, J. E. 1999. Role of the *S*. Typhimurium actin-binding protein SipA in bacterial internalization. *Science,* 283**,** 2092-5.

ZHOU, X., KELLER, R., VOLKMER, R., KRAUSS, N., SCHEERER, P. & HUNKE, S. 2011. Structural basis for two-component system inhibition and pilus sensing by the auxiliary CpxP protein. *J Biol Chem,* 286**,** 9805-14.

ZHOU, Y. N., KUSUKAWA, N., ERICKSON, J. W., GROSS, C. A. & YURA, T. 1988. Isolation and characterization of *Escherichia coli* mutants that lack the heat shock sigma factor sigma 32. *J Bacteriol,* 170**,** 3640-9.

ZHU, C., XIONG, K., CHEN, Z., HU, X., LI, J., WANG, Y., RAO, X. & CONG, Y. 2015. Construction of an attenuated *Salmonella enterica* serovar Paratyphi A vaccine strain harboring defined mutations in *htrA* and *yncD*. *Microbiol Immunol,* 59**,** 443-51.

9 Appendices

Appendix A

Table A1: *Salmonella* pathogenicity islands (SPIs). Adapted from Wisner et al. (2012).

SPI	Size (kb)	Function	Reference
SPI-1	40.2	TTSS - Invasion of the intestinal epithelium	(Marcus et al., 2000) (Thomson et al., 2008) (van Asten and van Dijk, 2005)
SPI-2	39.8	TTSS - Systemic infection of mice, survival in intestinal epithelial cells and macrophages	(Marcus et al., 2000) (Thomson et al., 2008) (van Asten and van Dijk, 2005)
SPI-3	16.6	MgtC and B Mg^{2+} transporter, MisL T5SS Implicated in intramacrophage survival Certain components are important for *S*. Typhimurium infection of mice, calves and/or chicks	(Schmidt and Hensel, 2004) (Morgan et al., 2004) (Blanc-Potard et al., 1999) (Thomson et al., 2008) (van Asten and van Dijk, 2005)
SPI-4	25	Important for membrane ruffling and entry of polarised epithelial cells in conjunction with SPI-1 TTSS	(Morgan et al., 2004) (Gerlach et al., 2008) (Thomson et al., 2008) (Sabbagh et al., 2010)
SPI-5	6.6	SPI-1 TTSS effector SopB and its chaperone PipC SPI-2 TTSS effectors PipA and PipB; PipD Important for *S*. Dublin induced enteritis in cattle Important for *S*. Typhimurium systemic infection in chicks	(Marcus et al., 2000) (Morgan et al., 2004) (Tsolis et al., 1999a) (Wood et al., 1998) (Thomson et al., 2008) (van Asten and van Dijk, 2005)
SPI-6	17.6	A T6SS and *tcf* fimbrial operon that are absent in *S*. Enteritidis	(Blondel et al., 2009) (Sabbagh et al., 2010) (Thomson et al., 2008) (van Asten and van Dijk, 2005)

Table A1 continued

SPI	Size (kb)	Function	Reference
SPI-7	up to 134	Only present in *S*. Typhi, *S*. Paratyphi and some *S*. Dublin Largest PI identified so far, size varies between serovars	(Sabbagh et al., 2010) (Seth-Smith, 2008) (Thomson et al., 2008) (van Asten and van Dijk, 2005)
SPI-8	6-8	Resistance to bacteriocins Absent in *S*. Enteritidis and *S*. Typhimurium	(Sabbagh et al., 2010, Thomson et al., 2008) (van Asten and van Dijk, 2005)
SPI-9	16.3	The RTX protein is complete in *S*. Enteritidis but not *S*. Typhimurium	(Thomson et al., 2008) (van Asten and van Dijk, 2005)
SPI-10	10	*sef* fimbrial operon in *S*. Enteritidis Larger in other serovars (up to 34 kb)	(Sabbagh et al., 2010) (Thomson et al., 2008) (van Asten and van Dijk, 2005)
SPI-11	6.7	PagC, PagD and MsgA important for survival of *S*. Typhimurium in macrophages	(Sabbagh et al., 2010, Thomson et al., 2008)
SPI-12	5.8	SPI-2 TTSS effector *sspH2* Important for virulence of *S*. Typhimurium in mice	(Haneda et al., 2009, Sabbagh et al., 2010, Thomson et al., 2008)
SPI-13	25.3	Important for systemic infections in mice by *S*. Typhimurium	(Haneda et al., 2009, Shi et al., 2006, Thomson et al., 2008)
SPI-14	6.8	Electron transfer and putative regulatory genes	(Sabbagh et al., 2010) (Thomson et al., 2008)
SPI-15	Unstated	Five hypothetical proteins Not present in either *S*. Enteritidis or *S*. Typhimurium	(Sabbagh et al., 2010) (Thomson et al., 2008)
SPI-16	3.3	LPS modification High homology to SPI-17	(Sabbagh et al., 2010) (Thomson et al., 2008)

Table A1 continued

SPI	Size (kb)	Function	Reference
SPI-17	3.6	LPS modification High homology to SPI-16 Present in *S*. Enteritidis and *S*. Typhi but not *S*. Typhimurium	(Sabbagh et al., 2010) (Thomson et al., 2008)
SPI-18	Unstated	In *S*. Typhi encodes two genes for the cytolysin HlyE and the invasion TaiE	(Sabbagh et al., 2010) (Thomson et al., 2008)
SPI-19	14.1	T6SS likely non-functional in *S*. Enteritidis as most of the island has been deleted. Up to 45 kb in other serovars.	(Blondel et al., 2009) (Thomson et al., 2008)
SPI-20	34	Only identified in *S*. *enterica* subsp. *arizonae*	(Blondel et al., 2009, Thomson et al., 2008)
SPI-21	55	Only identified in *S. enterica* subsp. *arizonae*	(Blondel et al., 2009, Thomson et al., 2008)

Appendix B

Table B1: **Members of the RpoE regulons of *Salmonella* and *E. coli*.** Genes have a σ^E binding site identified or regulation by σ^E experimentally shown. CP, cytoplasmic protein; PP, periplasmic protein; IMP, inner membrane protein; HP, hypothetical protein; PPIase; peptidyl-prolyl-isomerase, ECF, extracytoplasmic function; LPS, lipopolysaccharide.

Gene	Gene Function	Reference
σ^E/σ^E regulation and other sigma factors		
rpoD	Housekeeping sigma factor D (σ^D or σ^{70})	(Dartigalongue et al., 2001)
rpoE	ECF sigma factor F	(Rouviere et al., 1995)
rpoH	Heat-shock sigma factor H (σ^H or σ^{32}); cytoplasmic branch of the heat shock response	(Skovierova et al., 2006)
rpoN	Nitrogen metabolism and sigma factor D (σ^{54})	(Rhodius et al., 2006)
rseA	Anti-sigma factor that binds and sequesters σ^E (IMP)	(Rouviere et al., 1995)
rseB	Binds to RseA; minor negative regulator of σ^E activity (PP)	(Rouviere et al., 1995)
rseC	Minor positive regulator of σ^E activity (IMP)	(Rouviere et al., 1995)
rseP (yaeL/ecfE)	Metalloprotease/carboxypeptidase that cleaves RseA at cytoplasmic site (IMP)	(Dartigalongue et al., 2001)
Primary metabolism, sensory-regulatory functions		
cca	tRNA nucleotidyl transferase	(Dartigalongue et al., 2001)
clpXlon	ATP-dependant specificity component of ClpP protease	(Rhodius et al., 2006)
cutC	Involved in copper tolerance and sensing (CP)	(Dartigalongue et al., 2001)
dnaE	α-subunit of DNA polymerase III	(Dartigalongue et al., 2001)
eno	Enolase (glycolysis)	(Skovierova et al., 2006)
fabZ	Fatty acid biosynthesis	(Dartigalongue et al., 2001)
fusA	Elongation factor G	(Skovierova et al., 2006)
greA	Transcription elongation factor	(Rhodius et al., 2006)
lhr	ATP-dependant helicase	(Rhodius et al., 2006)
malQ	4-α-glucanotransferase	(Rhodius et al., 2006)

Table B1 continued

Gene	Gene Function	Reference
mdoGH	Osmoregulated periplasmic glucan synthesis	(Dartigalongue et al., 2001)
(narY)narWV	Nitrate/Nitrite respiration	(Rhodius et al., 2006)
pioA	Putative general secretion pathway protein A	(Rhodius et al., 2006)
prfB	Peptide chain release factor RF-2	(Dartigalongue et al., 2001)
recD	Subunit of exonuclease V	(Skovierova et al., 2006)
recJ	Exonuclease; DNA repair	(Dartigalongue et al., 2001)
recR	DNA recombination and repair	(Rhodius et al., 2006)
rnhB	Ribonuclease HII	(Dartigalongue et al., 2001)
tufA	Translation unstable factor	
ybjWV	Nitrate/Nitrite respiration	(Rhodius et al., 2006)
ycdS	Transcription	(Rhodius et al., 2006)
PPs - Proteases/chaperones/folding enzymes		
asnB	Periplasmic *L*-asparaginase	(Rowley et al., 2006)
dsbC	Thiol:disulfide oxido-reductase/preint disulphide isomerase II	(Dartigalongue et al., 2001)
fkpA	FKBP-family PPIase	(Skovierova et al., 2006)
htrA (degP)	Periplasmic serine protease	(Erickson and Gross, 1989) (Lipinska et al., 1989)
yaeT	Serine protease and chaperone	(Dartigalongue et al., 2001)
skp	Chaperone involved in OMP assembly and folding; in operon with *lpxDA* (*skp lpxDA fabZ*)	(Dartigalongue et al., 2001)
surA	Parvulin-family PPIase and chaperone	(Dartigalongue et al., 2001)
ptr	Periplasmic protease III, exonuclease V β and α subunits	(Skovierova et al., 2006)
Phospholipid and LPS biogenesis/modification/OMP		
ahpF	Alkyl hydroperoxide reductase; lipid detoxification	(Rhodius et al., 2006)
fadD	acyl-coenzyme A synthase	(Rezuchova et al., 2003)
lpxA	UDP-3-O-(3-hydroxymyristoyl)-glucosamine N-acyltransferase involved in lipid A biosynthesis; in operon with lpxD (lpxDA fabZ)	(Dartigalongue et al., 2001)

Table B1 continued

Gene	Gene Function	Reference
lpxD	Cold-shock-induced palmitoleoyl transferase; adds palmitoleate to nascent lipid A of LPS	(Dartigalongue et al., 2001)
lpxB		(Dartigalongue et al., 2001)
lpxP (*ddg*)	Cold-shock-induced palmitoleoyl transferase; adds palmitoleate to nascent lipid A of LPS	(Skovierova et al., 2006)
ompX	OM protein	(Rhodius et al., 2006)
plsB	Glycerol-3-phosphate acyltransferase	(Rhodius et al., 2006)
psd	Phosphatidylserine decarboxylase; converts phosphatidylserine to phophatidylethanolamine	(Skovierova et al., 2006)
rfaD (*htrM*)	ADP-l-glycerol-d-mannoheptose-6-epimerase; first gene of *rfaDFCL* operon involved in LPS biosynthesis	(Rowley et al., 2006)
sixA	Phophohistidine phosphatase	(Rhodius et al., 2006)
smpA (*bamE*)	Small OM protein, component of BAM complex	(Rezuchova et al., 2003)
waaW	Predicted LPS biosynthesis	(Chassaing et al., 2015)
(wza)wzbwzc	OM translocon for capsular polysaccharides	(Rhodius et al., 2006) (Dong et al., 2006)
yfiO	Lipoprotein involved in YaeT mediated OMP folding	(Dartigalongue et al., 2001)
oppA	Periplasmic oligopeptide transport proteins of ABC family; putative voltage-gated potassium channel	(Skovierova et al., 2006)
tolR	Tol-Pal membrane system, cell envelope integrity, transport through the periplasm	(Skovierova et al., 2006)
IMPs - transport, unknown function		
bacA	Undecaprenyl pyrophosphate phosphatase; involved in bacitracin A resistance	(Rezuchova et al., 2003) (Rhodius et al., 2006)
gspApioO	Transport protein	(Rhodius et al., 2006)
ptsN	Phosphotransferase system enzyme IIA	(Rezuchova et al., 2003) (Skovierova et al., 2006)
sbmA	Putative transporter protein possibly involved in microcin B17 and J25 uptake; homologues in *Sinorhizobium meliloti* and *Brucella abortus* involved in intracellular survival; in operon with *yaiW*.	(Rezuchova et al., 2003)

Table B1 continued

Gene	Gene Function	Reference
***Salmonella* Pathogenicity Islands (SPIs)/Virulence Factors**		(Li et al., 2015b)
ssrB	Regulator of SPI-2	(Li et al., 2015b)
hns	DNA binding protein	(Osborne and Coombes,
sseB	Secreted effector protein	(Osborne and Coombes, 2009)
ssaG	Secreted effector protein	(Osborne and Coombes, 2009)
sseL	Secreted effector protein	(Osborne and Coombes, 2009)
sifA	Secreted effector protein	(Osborne and Coombes, 2009)
srfN	Secreted effector protein	
Miscellaneous		(Rhodius et al., 2006)
ybaB	Unknown function	(Rezuchova et al., 2003) (Rhodius et al., 2006)
ydhLJK	Predicted envelope proteins	(Rhodius et al., 2006)
yeaY	Unknown function	(Rezuchova et al., 2003) (Rhodius et al., 2006)
yecI	Ferritin-like protein	(Rhodius et al., 2006)
ybfG	Possible invovelment in biofilm	(Herzberg et al., 2006) (Rezuchova et al., 2003)
yiiS	Unknown function	(Rezuchova et al., 2003)
yiiT	Unknown function	(Rezuchova et al., 2003)
yfeY	Putative OM lipoprotein	(Rezuchova et al., 2003)
yaiW	Unknown function	(Skovierova et al., 2006)
yfeKyfeSyfeL	Putative periplasmic protein; penicillin-binding protein, putative membrane carboxypeptidase	(Rhodius et al., 2006)

Table B1 continued

Gene	Gene Function	Reference
ydcG	Putative periplasmic glucan biosynthese protein	(Skovierova et al., 2006)
stm1250	HP; putative molecular chaperone	(Skovierova et al., 2006)
yggT	Putative integral membrane resistance protein; HP; xanthosine triphosphate pyrophosphatase;	(Skovierova et al., 2006)
yggN	Putative periplasmic protein	(Dartigalongue et al., 2001)
dedD	Putative membrane protein	(Skovierova et al., 2006)
yabI	Putative DedA family membrane protein	(Skovierova et al., 2006)
ygiM	Putative IM protein, putative SH3 domain protein,	(Dartigalongue et al., 2001)
ycbK	Putative OM protein; putative metallo-b-lactamase	(Rhodius et al., 2006)
yraP	Putative OM lipoprotein	(Dartigalongue et al., 2001)
yeaY	Putative OM lipoprotein	(Skovierova et al., 2006)
yiaDE	Putative OM lipoprotein	(Skovierova et al., 2006), (Rhodius et al., 2006)
yifO	Putative OM lipoprotein; putative IM protein	(Skovierova et al., 2006)
yiiD	Putative acetyltransferase	(Skovierova et al., 2006)

Table B2: Summary of the functional categories regulated by σ^E in *S.* Typhimurium from Li et al. (2015b). The σ^E regulon was defined in rich media (LB) and acid minimal media (LPM) to mimic the early (4 hours) and late (20 hours) stages of infection. These data summarise the diverse range of cellular functions regulated by σ^E in *Salmonella*.

Functional Categories	Total from genome	Total measured by microarray	Up-regulated by σ^E			Down-regulated by σ^E		
			LB log	LPM (4h)	LPM (20h)	LB log	LPM (4h)	LPM (20h)
Amino acid biosynthesis	130	125	17	13	11	16	20	19
Biosynthesis of cofactors, prosthetic groups, and carriers	167	163	24	5	8	16	38	21
Cell envelope	479	437	45	77	44	90	54	34
Cellular processes	289	263	43	55	35	54	33	18
Central intermediary metabolism	170	160	14	16	11	19	30	18
DNA metabolism	166	150	18	17	13	21	22	19
Energy metabolism	610	563	111	53	34	55	76	59
Fatty acid and phospholipid metabolism	80	77	6	8	6	9	17	7
Hypothetical proteins	78	65	11	11	9	12	7	3
Mobile and extrachromosomal element functions	250	155	8	33	18	36	10	8
Protein fate	191	181	26	38	29	27	24	16
Protein synthesis	375	313	81	37	28	44	54	54
Purines, pyrimidines, nucleosides, and nucleotides	81	80	8	3	2	10	20	7
Regulatory functions	305	268	22	46	29	44	42	22
Signal transduction	26	20	3	3	4	6	4	2
Transcription	57	54	10	4	3	4	7	6
Transport and binding proteins	628	579	51	48	53	100	81	49
Unclassified	332	267	39	56	37	36	37	23
Unknown function	670	614	69	66	73	105	95	58

Appendix C

Table C1: Media composition

Media	Description
Luria-Bertani (LB) Broth **(g L^{-1})**	**(Bertani, 1951)**
10 Sodium chloride 10 Tryptone 5 Yeast Extract	Dissolve in ~800 mL dH_2O. Make up to 1 L with dH_2O and sterilise by autoclaving.
Luria-Bertani (LB) Agar **(g L^{-1})**	
10 Sodium chloride 10 Tryptone 5 Yeast Extract 1.5% (w/v) Agar	Prepare LB broth as described. Take 200 mL of LB and add 3 g of agar. Sterilise by autoclaving. *NB. For top agar plates reduce agar to 0.75%; 1.5g per 200 mL.*
Lennox Broth (LB Half Salt) **(g L^{-1})**	**Modified from (Bertani, 1951)**
5 Sodium chloride 10 Tryptone 5 Yeast Extract	Dissolve in ~800 mL dH_2O. Make up to 1 L with dH_2O and sterilise by autoclaving.
LBO Broth (LB broth minus salt) **(g L^{-1})**	**Modified from (Bertani, 1951)**
10 Tryptone 5 Yeast Extract	Made up to 1 L with dH_2O and sterilised by autoclaving.
LBO Agar (LB agar minus salt) **(g L^{-1})**	
10 Tryptone 5 Yeast Extract 1.5% (w/v) Agar	Prepare LBO broth as described and split in to five lots of 200 mL. Add 3 g of agar to each and sterilise by autoclaving.
M9 Minimal Medium **(g L^{-1})**	**Modified from (Maniatis, 1982)**
M9 Salts:	
64 Sodium phosphate dibasic heptahydrate 15 Monopotassium phosphate 2.5 Sodium chloride 5 Ammonium chloride	Dissolve in ~800 mL dH_2O, adjust to 1 L and sterilise by autoclaving.
1X M9 Minimal Media: 700 mL dH_2O* 200 mL M9 Salts* 2 mL 1 M Magnesium sulphate* 20 mL Glucose 20% (w/v) 0.1 mL 1 M Calcium chloride	Adjust 1X M9 minimal media to 1 L aseptically with sterile dH_2O
MGN Minimal Media **(per L)**	**Modified from (Pope and Cole, 1982)**
33 mM Dipotassium phosphate	Make up to 1 L with dH_2O and add

30 mM Potassium dihydrogen phosphate 8 mM Ammonium sulphate 2 mM Trisodium citrate 0.2 mM Magnesium sulphate heptahydrate 0.160 mM Iron (II) chloride tetrahydrate *Additions prior to autoclaving:* 1 µM Ammonium heptamolybdate* 1 µM Sodium selonate* 0.4 mM Magnesium chloride* 50 µM Magnesium chloride tetrahydrate* 9 µM Calcium chloride dehydrate* *Supplements:* *Nitrate Sufficient* 22 mM Sodium nitrate* 5 mM Glycerol* 0.1 mg Casamino acids¥ *Nitrate Limited* 5 mM Sodium nitrate* 20 mM Glycerol* 0.1 mg Casamino acids¥ *Autoclaved before use ¥ Filter sterilised before use	additions. Add appropriate supplements for sufficient or limited media.
MOPS Defined Medium	**(Neidhardt et al., 1974)**
10X MOPS: 83.72 MOPS 7.17 Tricine 0.01 M $FeSO_4$ Additional nutrients: 50 mL 1.9 M NH_4Cl 10 mL 0.276 M K_2SO_4 0.25 mL 0.02 M $CaCl_2.2H_2O$ 2.1 mL 2.5 M $MgCl_2$ 100 mL 5 M NaCl 0.2 mL Micronutrient stock Micronutrient stock: 9 mg Ammonium molybdate 62 mg Boric acid 18 mg Cobalt chloride 6 mg Cupric sulphate 40 mg Manganese chloride 7 mg Zinc sulphate 1X MOPS: 50 mL 10X MOPS 2.5 mL 0.132M K_2HPO_4	 Dissolve in ~300 mL dH_2O. Adjusted to pH 7.4, bring to 440 mL. Add 10 mL of freshly prepared $FeSO_4$ solution. Add additional nutrients in the order listed to avoid precipitation. Make up to 1 L with dH_2O and filter sterilise. Aliquot and store at -20˚C. Dissolve micronutrient stock components in 40 mL of dH_2O. Make up to 50 mL and store at RT. Make 1X MOPS up to 500 mL with dH_2O and filter sterilise.

25 µL 1 mg/mL Thiamine 250 µL 40 mg/mL Histidine Appropriate amount of glucose: HiC 4% LoC 0.03% NoC 0%.	
Colony Forming Antigen (CFA) Medium	**Modified CYE medium from (Evans et al., 1977)**
1.5 g Yeast extract 50 µg Magnesium sulphate 5 µg Manganese chloride	Dissolve in 900 µL and sterilise by autoclaving.
10 g Casamino acids	Dissolve casamino acids in 100 mL dH2O and filter sterilise before adding to 900 µL of media previously autoclaved.
UCB Indicator Plates (Green Plates) (g L^{-1})	**Modified from (Bochner, 1984)**
8 Tryptone 1 Yeast extract 5 Sodium chloride 1.5% Agar	Made up to 950 mL in dH_2O. Add 3 g of agar to separate 190 mL volumes and sterilise by autoclaving.
Additions (per 190 mL): 4 mL Glucose* 40% (w/v) 5 mL Alizarin yellow* 2.5% (w/v) 0.65 mL Aniline blue¥ 2% (w/v) *Autoclaved before use ¥ Filter sterilised before use	Add additions when cooled to ~ 55˚C. *NB. Alizarin yellow solution should be added when at ~ 60˚C to avoid precipitation.*
Congo Red Plates	**Modified from (Yoo et al., 2013)**
40 µg/mL Congo Red	Add to 200 mL of LBO agar (see Appendix CA) melted to ~ 60˚C, mix well by gentle agitation and pour into petri dishes immediately. *NB. Make and use congo red plates on same day.*

Table C2: Antibiotics. All antibiotics were aliquoted in 1 mL fractions and stored at -20˚C.

Antibiotic	Stock Concentration ($mg\ mL^{-1}$)	Final Concentration ($\mu g\ mL^{-1}$)
Ampicillin	100	100
Chloramphenicol*	10	10
Kanamycin	50	50
Tetracycline*¥	5	5
Vancomycin	65	65

*Made in 50:50 dH_2O: Ethanol
¥Light sensitive; stored in the dark

Appendix D

Buffers, Solutions and Assay Reagents

Table D1: General laboratory buffers and solutions

Solution	Description
CpxR Storage Buffer	**(Lima et al., 2012)**
10 mM Tris-HCl, pH 7.8 100 mM Potassium chloride 10 mM Magnesium chloride 0.1 mM EDTA, pH 8.0 1 mM Dithiothreitol (DTT) 50 % Glycerol	
Crystal Violet Solution (1%)	**Modified from (Hamilton et al., 2009)**
Solution A: 1 g Crystal Violet Powder (>99%) 20 mL Ethanol (>99%) *Solution B:* 0.8 g Ammonium oxalate 80 mL dH_2O	Combine solution A and B to produce a working crystal violet solution of 1% (f/c).
Microarray Wash Solutions	
Wash Solution 1 (1 L): 300 ml 20x SSPE 250 µL 20% N-Lauroylsarcosine 700 mL dH_2O	
Wash Solution 2 (1 L): 3 mL 20x SSPE 1.8 mL PEG200 995 mL dH2O	
20 x SSPE buffer: *175.3 g Sodium chloride* *27.6 g Sodium dihydrogen phosphate* *7.4 g Na_2EDTA*	*Dissolve SSPE components in ~ 800 mL dH_2O and adjust pH to 7.4 with 10 M NaOH (~27 mL/L).*
SDS Loading Buffer	
50 mM Tris-Cl (pH 6.8)	SDS gel-loading buffer, lacking β-

10% Glycerol 2% SDS 0.1% Bromophenol blue 5% β-mercaptoethanol	mercaptoethanol, can be stored at RT. When required add β-mercaptoethanol (1:19) to SDS loading buffer.
10 x Tris/Borate/EDTA (TBE) buffer 108 g Tris base 55 g Boric acid 20 mL 0.5M EDTA (pH 8.0)	Dissolve components in 1 L of dH_2O; solution pH should be ~ 8.3. When required dilute 1:10 in dH_2O to produced 1 x working concentration.
1 x Transfer Buffer Add methanol to 1 x TGS at f/c of 20%	Prepare TGS as outlined.
10 x Tris-buffered saline (TBS) 60.5 g Tris 87.6 g Sodium chloride	Dissolve components in ~800 mL of dH_2O. Adjust to pH 7.5 with concentrated HCl and bring to final volume of 1 L with dH_2O. When required dilute 1:10 in dH_2O to produced 1 x working concentration. Store at 4˚C.
10 x Tris-buffered saline TWEEN-20 (TBST) Add 1 mL TWEEN-20 per 1 L of 1 x TBS	Prepare TBS as outlined above.
10 x Tris-Glycine SDS-PAGE (TGS) 30.2 g Tris-base 144 g Glycine 20 g SDS	Dissolve components in ~800 mL of dH_2O and bring to final volume of 1 L. When required dilute 1:10 in dH_2O to produced 1 x working concentration.

Table D2: Assay reagents

ß- Galactosidase

Solution	Description
Z-buffer 0.06 M Na_2HPO_4 x 7 H_2O 0.04 M $Na_2H_2PO_4$ x H_2O 0.01 M KCl 0.001 M $MgSO_4$ 0.05 M β-mercaptoethanol	Z-buffer should be made fresh prior to each use. β-mercaptoethanol should be added directly before use. Adjust pH to 7.0
o-nitrophenyl-β-D-galactopyranoside (ONPG): 4 mg/mL	Dissolve in 0.1 M phosphate buffer
0.1 M phosphate buffer 0.06 M Na_2HPO_4 x 7 H_2O 0.04 M $Na_2H_2PO_4$ x H_2O	Dissolve in dH_2O

Appendix E

Site-Directed Mutagenesis (SDM)

Mutagenic Primer Design Guidelines

The mutagenic oligonucleotide primers for use in SDM were designed individually according to the desired mutation. Both mutagenic primers within the pair contained the desired mutation and annealed to the same sequence, on opposite strands of the template DNA. Primers were 39-45 bp in length, with melting temperatures (T_m) of 75-77.3°C. Primers were synthesised by Integrated DNA Technologies (IDT) and purified by desalting.

Formula I was used for estimating the T_m of primers; where N is the primer length in bases; values for %GC and % mismatch are whole numbers.

Formula I:

$$T_m = 81.5 + 0.41(\%GC)\ (675/N)\ \%\ \text{mismatch T}$$

The desired mutation was in the middle of the primer where possible with ~10–15 bases of original, un-mutated sequence on either side. A minimum GC content of 40% was adhered to and all primers terminated with one or more G/C bases.

Primers were used in SDM PCR reactions at excess concentrations of 125 ng (Table 9), calculated using Formula 2 to convert nanograms of oligonucleotide to picomoles.

Formula 2:

$$X \text{ pmoles of oligo} = \frac{\text{ng of oligo}}{330 \times \text{number of bases in oligo}} \times 1000$$

Appendix F

Table F1: **Restriction enzymes used and sequences** of their corresponding palindromic cut site. Position where phosphate backbone is broken is highlight with |.

Restriction Enzyme	Sequence of Cut Site
*Bam*HI	5'…G|GATCC…3' 3'…CCTAG|G…5'
*Eco*RI	5'…G|AATTC…3' 3'…CTTAA|G…5'
*Nco*I	5'…C|CATGG…3' 3'…GGTCA|A…5'
*Nde*I	5'…CA|TATG…3' 3'…GTAT|AC…5'
*Pst*I	5'…G|ACGTC…3' 3'…CTGCA|G…5'
*Xba*I	5'…T|CTAGA…3' 3'…AGATC|T…5'

Appendix G

Table G1: Known or putative members of the Cpx regulon in Enterobacteria.

Genes/ putative operon[Ψ]	Organism(s) where Cpx regulation identified	Gene product(s) description/function	Proposed Cpx regulation and fold change(s)* (if available)	CpxR-P binding site; binding conformation	Reference
acrD	*MC4100*	Component of efflux pump	Positive	N	(Hirakawa et al., 2005)
adhE	*ECL3502*	Iron dependent aldehyde-alcohol dehydrogenase, pyruvate-formate lyase-deactivase	Negative -2.0	Y; N	(De Wulf et al., 2002)
-aer	*ECL3502*	Aerotaxis receptor	Negative	N	(De Wulf et al., 1999) (De Wulf et al., 2002)
agp	*MG1655*	Periplasmic glucose-1-phosphatase	Negative -1.9	N	(Bury-Mone et al., 2009)
argA	*ECL3502*	*N*-acetylglutamate synthase	ND	Y; N	(De Wulf et al., 2002)
aroG	*BW21553*	Shikimate kinase I	Positive	N	(Yamamoto and Ishihama, 2006)
aroK	*ECL3502*	Ferritin-like protein	Positive	Y; N	(De Wulf et al., 2002)
bfp cluster	*E2348/59*	Type IV bundle-forming pili of EPEC	Positive	N	(Nevesinjac and Raivio, 2005)
C1109	*MC4100, E2348/59*	Unknown	Positive	N	(Raivio et al., 2013)
C2142	*MC4100, E2348/59*	Unknown	Positive	N	(Raivio et al., 2013)
C2257	*MC4100, E2348/59*	Unknown	Positive	N	(Raivio et al., 2013)
cpxP	*ECL3502 BW21553*	Regulator of the Cpx response and chaperone involved in extracytoplasmic stress	Positive 1.5 (3.3)	Y; Y	(Danese and Silhavy, 1998)
cpxRA	*MC4100*	Response regulator and sensor kinase of the Cpx ESR	Positive	Y;N	(De Wulf et al., 1999) (Raivio et al., 1999)
csgBAC	*MC4100*	Curlin fimbriae components	Negative	Y; N	(Dorel et al., 1999) (De Wulf et al., 2002)
csgDEFG	*MC4100*	Curlin regulatory components	Negative	Y; N	(Jubelin et al., 2005) (De Wulf et al., 2002)

Table G1 continued

Genes/ putative operon[Ψ]	Organism(s) where Cpx regulation identified	Gene product(s) description/function	Proposed Cpx regulation and fold change(s)* (if available)	CpxR-P binding site; binding conformation	Reference
cspD	*MG1655*	DNA replication inhibitor, induced by stress and glucose starvation, similarity to cold shock protein	Negative -2.5 (-2.5)	N	(Bury-Mone et al., 2009)
csrB	*MG1655*	Regulatory RNA/Carbon storage regulation	Positive 1.9	N	(Bury-Mone et al., 2009)
dacC	*MC4100, E2348/59*	D-Alanyl-D-alanine carboxypeptidase, PBP6	Positive 2.2 to 5.9	N	(Raivio et al., 2013)
dctA	*MC4100, E2348/59*	C4 carboxylate transporter	Negative	N	(Raivio et al., 2013)
efeU	*BW21553*	Elemental ferrous iron uptake permease	Negative	Y; Y	(Cao et al., 2007) (Yamamoto and Ishihama, 2006)
fadL	*MC4100, E2348/59*	Long chain fatty acid uptake	Negative -1.1 to -3.7	N	(Raivio et al., 2013)
flhC	*MC4100, E2348/59*	Transcriptional regulator of flagella	Negative -1.43 to -4.54	N	(Raivio et al., 2013)
ftnB	*BW21553*	Heat shock protease	Positive	N	(Yamamoto and Ishihama, 2006)
gatDCBAZY	*MG1655*	Galactitol specific enzyme IIC and IIB component of PTS	Negative -1.6; -2.6; -2.5; -1.6; -1.9; -1.4	N	(Bury-Mone et al., 2009)
gcvP ***gcvH gcvT***	*MG1655 ECL3502*	GcvH: lipoylprotein aminomethyltransferase; GcvT: tetrahydrofolate dependent subunit/glycine cleavage complex	Negative - ; -2.2; -1.8	Y; N	(Bury-Mone et al., 2009) (De Wulf et al., 2002)
glpA glpB glpC	*BW21553*	Glycerol-3-phosphate dehydrogenase subunits/glycerol degradation	Negative -2.3; -1.9; -3.0 (-8.8)	N	(Bury-Mone et al., 2009)
gspE	*MG1655*	General secretory pathway component, cryptic	Positive - ; - ; 2.7; - ; - ; - ; - ; - ; - ; - ; -	N	(Bury-Mone et al., 2009)
hns	*MG1655*	Global DNA-binding transcriptional dual regulator H-NS	Positive 2.3	N	(Bury-Mone et al., 2009)
htpX	*MC4100*	Proposed virulence factor	Positive ~4	N	(Shimohata et al., 2002)
***htrA* (*degP*)**	*MC4100*	Periplasmic serine endoprotease	Positive	N	(Danese et al., 1995) (Pogliano et al., 1997)
invE (virB)	*Shigella* spp.	Regulator of *mxi-spa* and *ipa* TTSS in *Shigella*		N	(Tobe et al., 1993) (Mitobe et al., 2005)
lamB	*MG1655*	OM porin, phage lambda receptor protein, maltose high-affinity receptor	Negative -2.5 (-9.8)	N	(Bury-Mone et al., 2009)

Table G1 continued

Genes/ putative operon[Ψ]	Organism(s) where Cpx regulation identified	Gene product(s) description/function	Proposed Cpx regulation and fold change(s)* (if available)	CpxR-P binding site; binding conformation	Reference
lgt thyA	*MG1655*	Lgt: prolipoprotein diacylglyceryl transferase, IM; ThyA: thymidylate synthetase	Positive 1.9; 1.5	N	(Bury-Mone et al., 2009)
mdtABDC	*MC4100*	Multidrug transporter unit	Positive	N	(Hirakawa et al., 2005)
mglB	*MC4100, E2348/59*	Galactose periplasmic binding protein	Negative	N	(Raivio et al., 2013)
minCDE	*MC4100 ECL3502*	Cell division inhibition; control of FtsZ ring formation	ND	N	(De Wulf et al., 2002) (Pogliano et al., 1998)
motAB-cheAW	*ECL3502*	Flagella motor and chemotaxis regulators	Negative	Y; Y	(De Wulf et al., 1999) (De Wulf et al., 2002)
mviM	*ECL3502*	Uracil-DNA glycosylase; proposed virulence factor	Positive	Y; N	(De Wulf et al., 2002)
mzrA	*MC4100*	IM protein, interacts with EnvZ as modulator of EnvZ/OmpR	Positive	Y; Y	(Gerken and Misra, 2010)
nanC	*MG1655*	NAN (*N*-acetylneuraminic acid) channel	Positive	ND	(Condemine et al., 2005)
nhaB	*MC4100, E2348/59*	Sodium/proton antiporter	Negative -1 to -3.57	N	(Raivio et al., 2013)
ompC	*ECL3502 MG1655 MC4100*	OM protein C	Positive	Y; N	(Price and Raivio, 2009) (De Wulf et al., 2002) (Batchelor et al., 2005)
ompF	*MC4100*	OM protein F	ND	Y	(De Wulf et al., 2002)
pap	*MC4100*	Uropathogenic *E. coli* P pilus subunits	Positive	Y;Y	(Hernday et al., 2004) (Hung et al., 2001)
pepT	*BW21553*	Peptidase T	Negative -2.3	N	(Oshima et al., 2002)
ppiA	*MC4100*	Periplasmic peptidyl iomerase A	Positive	Y; Y	(Pogliano et al., 1997)
ppiD	*MC4100*	Periplasmic peptidyl iomerase D	Positive	Y; N	(Raivio et al., 2013)
psd	*ECL3502*	Phosphatidyl serine decarboxylase	Positive	Y; Y	(De Wulf et al., 2002)
putP	*MC4100, E2348/59*	Sodium/proline symporter	Negative -2 to -2.63	N	(Raivio et al., 2013)
pykA	*MG1655*	Pyruvate kinase II/Anaerobic respiration, glycolysis	Negative -1.9	N	(Bury-Mone et al., 2009)
raiA	*MC4100, E2348/59*	Ribosome associated inhibitor	Positive 2.4 to 5.3	N	(Raivio et al., 2013)

Table G1 continued

Genes/ putative operon[Ψ]	Organism(s) where Cpx regulation identified	Gene product(s) description/function	Proposed Cpx regulation and fold change(s)* (if available)	CpxR-P binding site; binding conformation	Reference
rdoA (yihE)-dsbA	*MC4100*	Disulfide oxidoreductase	Positive	Y; Y	(Danese and Silhavy, 1997) (Pogliano et al., 1997)
rfaY	*MG1655*	Lipopolysaccharide core biosynthesis protein	Positive -;-;-;-;-;-;-; 2.0; -; -;	N	(Raivio et al., 2013)
rffA	*MG1655*	dTDP-4-oxo-6-deoxy-D-glucose transaminase/Lipopolysaccharide biosynthesis	Positive 1.9	N	(Bury-Mone et al., 2009)
rmf	*MC4100, E2348/59*	Ribosome associated inhibitor	Positive 2.1 to 4.1	N	(Raivio et al., 2013)
rpoE-rseABC	*ECL3502*	σ^E and regulators	Positive	Y; Y	(De Wulf et al., 2002)
rpoH	*ECL3502 MC4100*	Heat-shock sigma factor H (σ^H or σ^{32}); cytoplasmic branch of heat shock response	Negative	Y; Y	(De Wulf et al., 2002) (Danese and Silhavy, 1997) (Pogliano et al., 1997) (Nakayama et al., 2003)
sbmA	*MC4100, E2348/59*	Putative peptide importer	Positive 4.2 to 10.5	Y; N	(Raivio et al., 2013)
secA	*ECL3502*	Secretion subunit A	ND	N	(De Wulf et al., 2002)
skp (hlpA)	*ECL3502*	Chaperone involved in OMP assembly and folding, in operon with lpxDA (sky lpxDA fabZ); *Salmonella* virulence factor	ND	N	(De Wulf et al., 2002)
slt	*ECL3502*	Iron regulated shiga-like toxin	ND	Y; N	(De Wulf et al., 2002)
spy	*BW21553*	Periplasmic protein related to spheroplast formation	Positive 1.75 (39.3)	Y; Y	(Raffa and Raivio, 2002) (Raivio et al., 2000) (Yamamoto and Ishihama, 2005) (Nishino et al., 2005) (Yamamoto et al., 2008)
tnaL tnaA tnaB	*BW21553*	Tryptophan transport and utilisation	Negative -2.1; -2.9 (-58.5); -2.8	N	(Oshima et al., 2002)
tppB	*MC4100, E2348/59*	Proton dependent peptide transporter	Negative -2.86 to -5	N	(Raivio et al., 2013)
tsr	*ECL3502*	Serine chemotaxis	Negative	Y; Y	(De Wulf et al., 1999) (De Wulf et al., 2002)
ulaR	*MG1655*	DNA binding transcriptional dual regulator/represses transport and utilisation of L-ascorbate	Positive 2.0	N	(Bury-Mone et al., 2009)

Table G1 continued

Genes/ putative operon[Ψ]	Organism(s) where Cpx regulation identified	Gene product(s) description/function	Proposed Cpx regulation and fold change(s)* (if available)	CpxR-P binding site; binding conformation	Reference
ung	*ECL3502 BW21553 MC4100*	DNA metabolism, Uracil-DNA glycosylase	Positive	Y; N	(Ogasawara et al., 2004) (De Wulf et al., 1999) (De Wulf et al., 2002)
uspA	*MG1655*	Universal stress global response regulator	Negative -1.9	N	(Bury-Mone et al., 2009)
virF	*Shigella* spp.	Positive regulator of virulence plasmid *ipaBCD*	ND	N	(Nakayama and Watanabe, 1995)
vsr	*MG1655*	DNA mismatch endonuclease of very short patch repair	Positive 2.0	N	(Bury-Mone et al., 2009)
yafK	*MG1655*	Conserved periplasmic protein	Positive 3.0	N	(Nakayama and Watanabe, 1995) (Tobe et al., 1993)
yaiW	*MC4100, E2348/59*	Unknown	Positive 2.8 to 3.9	Y; N	(Raivio et al., 2013)
ybaJ	*BW21553*	Unknown	ND	N	(Yamamoto and Ishihama, 2005)
ybgC tolQ *tolR* ***tolA tolB*** *pal* ***ybgF***	*MG1655*	YbgC: predicted acyl- coA thioesterase; TolQRAB-YbgF: components of the Tol-Pal cell envelope complex	Positive 1.8; 2.4; - ;1.6 (2.5); 1.7; - ; 1.5	N	(Bury-Mone et al., 2009)
ybjS	*MG1655*	Predicted oxidoreductase with NAD(P)-binding domain	Positive 2.3	N	(Bury-Mone et al., 2009)
ycbB	*MC4100, E2348/59*	L-D-Transpeptidase	Positive 2.4 to 5.5	N	(Raivio et al., 2013)
yccA	*BW21553, MC4100, E2348/59*	IM protein, regulator of FtsH proteolysis, copper tolerance protein	Positive 2 to 7.5	Y; Y	(Price and Raivio, 2009) (Yamamoto and Ishihama, 2005)
yceJ yceI	*MG1655*	YceJ: predicted cytochrome b561; YceI: periplasmic protein induced at high pH and by osmotic shock	Positive 1.4; 2.1	N	(Bury-Mone et al., 2009)
ycfF	*BW21553*	Purine nucleoside phosphoramidase	ND	N	(Yamamoto and Ishihama, 2005)
ycfS	*BW21553*	Periplasmic protein with unknown function	ND	N	(Yamamoto and Ishihama, 2005)
yciX (C1744)	*MC4100, E2348/59*	Unknown	Negative -2.5 to -3.45	N	(Raivio et al., 2013)

Table G1 continued

Genes/ putative operon[Ψ]	Organism(s) where Cpx regulation identified	Gene product(s) description/function	Proposed Cpx regulation and fold change(s)* (if available)	CpxR-P binding site; binding conformation	Reference
ydeH	*BW21553*	Diguanylate cyclase	Positive	N	(Price and Raivio, 2009) (Yamamoto and Ishihama, 2005)
ydeK	*MG1655*	Predicted lipoprotein	Positive 2.2	N	(Bury-Mone et al., 2009)
ydeN	*MG1655*	Uncharacterised sulfatase	Negative -2.0 (-2.4)	N	(Bury-Mone et al., 2009)
ydiY	*MC4100, E2348/59*	Unknown	Negative -1.67 to -5.88	N	(Raivio et al., 2013)
yebE	*MG1655*	Conserved IM protein	Positive 9.8	Y; Y	(Bury-Mone et al., 2009)
ygaU	*MC4100, E2348/59*	LysM cell degradation motif	Positive 2.4 to 3.3	Y; N	(Raivio et al., 2013)
ygaW	*MG1655*	Predicted IM protein	Negative -2.0	N	(Bury-Mone et al., 2009)
ygjT	*ECL3502*	Putative transport protein	Positive	Y; Y	(De Wulf et al., 2002)
yhaH yhaI yhaJ	*MG1655*	Predicted IM protein; putative IM protein; predicted DNA binding transcriptional regulator	Positive 1.9; 3.2 (40.3); 2.0	N	(Bury-Mone et al., 2009)
yiaF	*MG1655*	Putative IM lipoprotein	Positive 5.9 (7.71)	N	(De Wulf et al., 2002)
yidZ	*MG1655*	HTH-type transcriptional regulator	Positive 1.9	N	(Bury-Mone et al., 2009)
yijP	*MC4100, E2348/59*	Unknown	Negative	N	(Raivio et al., 2013)
yjfN	*ECL3502*	Unknown	ND	Y; N	(De Wulf et al., 2002)
yjiY	*ECL3502*	Putative carbon starvation protein	ND	Y; N	(De Wulf et al., 2002)
yncJ	*MC4100, E2348/59*	Unknown	Positive 5.9 to 50.14	N	(Raivio et al., 2013)
ynfD	*MC4100, E2348/59*	Unknown	Positive 2.2 to 3.9	N	(Raivio et al., 2013)
yobB	*BW21553*	Proposed copper tolerance protein	ND	N	(Yamamoto and Ishihama, 2006)
yqaE	*MC4100, E2348/59*	Unknown	Positive 3 to 6.3	Y; N	(Raivio et al., 2013)

Table G1 continued

Genes/ putative operon[Ψ]	Organism(s) where Cpx regulation identified	Gene product(s) description/function	Proposed Cpx regulation and fold change(s)* (if available)	CpxR-P binding site; binding conformation	Reference
yqjA	*BW21553*	DedA-like predicated IM protein	ND	N	(Yamamoto and Ishihama, 2006)
ytfK	*MC4100, E2348/59*	Unknown	Positive 4.9 to 9.3	N	(Raivio et al., 2013)

[Ψ]*Genes are listed in alphabetical order and grouped by putative or known operon (ordered in direction of transcription). Genes whose expression were found to be significantly modulated are shown in* ***bold*** *(see appropriate reference for methodologies). Genes whose expression were determined by Q-PCR are* ***underlined****, and the fold change determined in indicated in parentheses after microarray fold-change values.*

** Fold changes indicate ratios of gene signal intensities of the relative ΔcpxR strain to reference signals (see appropriate reference for methodologies). Values correspond to, and follow, the gene order as presented in the first column. ND = Not determined. The ratio values of genes not significantly modulated are shown as "-". Numbers in italics indicate a p-value <0.01 in the case of microarray data or <0.05 in case of Q-PCR. Y=yes; N=no. Adapted from tables shown in (Bury-Mone et al., 2009, De Wulf et al., 2002, Price and Raivio, 2009, Rowley et al., 2006, Raivio et al., 2013).*

Appendix H

Table H1: All 144 genes whose expression levels changed significantly (>2-fold; FDR <0.05) in an SL1344Δ*cpxR* strain compared to SL1344 WT SL1344, when Cpx was induced by NlpE overexpression. Genes are listed in order of SL number loci; common gene names are stated if available. Genes highlighted have had Cpx regulation demonstrated previously in other species of Enterobacteriacae (see Appendix G).

Locus Tag		Gene Name	Description	Fold Change[†]
SL Number	STM Number			
SL0088	STM0087	*folA*	Dihydrofolate reductase	0.13
SL0210	STM0209	*htrA*	Serine endoprotease; also known as *degP*.	0.11
SL0226	STM0225	*hlpA*	Periplasmic chaperone	3.14
SL0407	STM0413	*tsx*	Nucleoside channel	2.35
SL0500	STM0507	*ybbA*	Putative ABC transporter ATP-binding protein	0.19
SL0536	STM0543	*fimA*	Fimbrin	3.15
SL0731	STM0749	*pal*	Peptidoglycan- associated outer membrane lipoprotein	0.44
SL0776	STM0800	*slrP*	Leucine-rich repeat-containing protein	2.31
SL0799	STM0823	*ybiJ*	Hypothetical protein	0.08
SL0808	STM0833	*ompX*	Outer membrane protein X	0.33
SL0839	STM0863	*dacC*	D-alanyl-D-alanine carboxypeptidase fraction C	0.47
SL1025	STM1085	*yccA*	Hypothetical protein	0.02
SL1030	STM1091	*sopB*	SigD; Salmonella outer protein B; Effector protein secreted by SPI-I, type-III secretion system	2.86
SL1052	STM1113	*scsA*	Suppression of copper sensitivity protein A	0.15
SL1053	STM1114	*scsB*	Suppression of copper sensitivity protein B	0.31
SL1054	STM1115	*scsC*	Suppression of copper sensitivity protein C	0.27
SL1055	STM1116	*scsD*	Suppression of copper sensitivity protein D	0.31
SL1152	STM1215	*ycfS*	Putative periplasmic protein	0.13
SL1177	STM1239		Putative cytoplasmic protein	2.14
SL1181	STM1242	*envE*	Putative envelope protein; Probable EnvE precursor	2.10
SL1184	STM1246	*pagC*	Virulence membrane protein PAGC precursor	2.43

Table H1 continued

Locus Tag		Gene Name	Description	Fold Change[†]
SL Number	STM Number			
SL1186	STM1250		Putative cytoplasmic protein	3.26
SL1189	STM1253		Putative inner membrane protein	3.30
SL1190	STM1254		Putative outer membrane lipoprotein	12.97
SL1243	STM1308	*spy*	Periplasmic protein; Induced by Cpx and BaeSR stress response systems	0.02
SL1260	STM1325	*ydiZ*	Putative cytoplasmic protein	0.35
SL1261	STM1326	*pfkB*	6-phosphofructokinase 2	0.32
SL1263	STM1328		Putative outer membrane protein	4.27
SL1265	STM1330		Putative DNA/RNA non-specific endonuclease	2.02
SL1278	STM1344	*ydiV*	Hypothetical protein; possible putative diguanylate cyclase/phosphodiesterase domain 1	2.23
SL1404	STM1473	*ompN*	Outer membrane protein N precursor	0.25
SL1412	STM1482	*ydgF*	Multidrug efflux system protein MdtJ	0.32
SL1413	STM1483	*ydgE*	Multidrug efflux system protein MdtI	0.38
SL1430	STM1500	*ynfD*	Putative outer membrane protein	0.21
SL1533	STM1603	*yncJ*	Putative periplasmic protein	0.02
SL1699	STM1771	*chaA*	Calcium/sodium: proton antiporter	0.14
SL1773	STM1844	*htpX*	Heat shock protein X; possible putative metalloprotease	0.07
SL1799	STM1867	*pagK*	PhoPQ-activated gene	2.14
SL1811	STM1877		Putative amidohydrolase	0.30
SL1814	STM1880	*yebE*	Putative inner membrane protein	0.02
SL1872	STM1939		Putative glucose-6-phosphate dehydrogenase	2.65
SL1996	STM2020	*cbiO*	Cobalt transporter ATP-binding subunit	2.28
SL1999	STM2023	*cbiM*	Cobalt transport protein	3.37
SL2000	STM2024	*cbiL*	Cobalt-precorrin-2 C (20)-methyltransferase	2.46
SL2001	STM2025	*cbiK*	Vitamin B12 biosynthetic protein	2.54

Table H1 continued

Locus Tag		Gene Name	Description	Fold Change[†]
SL Number	STM Number			
SL2003	STM2027	*cbiH*	Precorrin-3B C (17)-methyltransferase	2.91
SL2011	STM2035	*cbiA*	Cobyrinic acid a, c-diamide synthase	2.41
SL2020	STM2044	*pduH*	Propanediol dehydratase reactivation protein	2.25
SL2043	STM2066	*sopA*	Effector protein secreted by SPI-I, type-III secretion system	6.55
SL2056	STM2079	*wzzB*	Lipopolysaccharide O-antigen chain length regulator	2.57
SL2163	STM2186		Putative oxidoreductase	2.76
SL2225	STM2255	*napC*	Cytochrome C-type protein	3.31
SL2232	STM2262	*eco*	Ecotin precursor	0.21
SL2378	STM2410	*yfeA*	Hypothetical protein	2.66
SL2490	STM2528		Putative dimethylsulfoxide reductase	2.14
SL2521	STM2559	*cadA*	Lysine decarboxylase 1	2.65
SL2603	STM2639	*rseA*	Sigma-E factor regulatory protein	2.77
SL2604	STM2640	*rpoE*	RNA polymerase sigma-E factor (sigma-24)	2.48
SL2674	STM2703		Hypothetical protein	2.92
SL2780	STM2796	*yqaE*	Putative transport protein	0.04
SL2796	STM2811	*proX*	Glycine betaine-binding periplasmic protein precursor	2.90
SL2848	STM2868	*orgC*	Putative cytoplasmic protein	4.66
SL2850	STM2870	*orgA*	Needle complex assembly protein	6.40
SL2851	STM2871	*prgK*	Needle complex inner membrane lipoprotein	5.04
SL2852	STM2872	*prgJ*	Needle complex minor subunit	5.27
SL2853	STM2873	*prgI*	Needle complex major subunit	5.06
SL2854	STM2874	*prgH*	Needle complex inner membrane protein	6.76
SL2855	STM2875	*hilD*	Invasion protein regulatory protein	4.28
SL2856	STM2876	*hilA*	Invasion protein regulator	7.64
SL2857	STM2877	*iagB*	Invasion protein precursor	4.26

Table H1 continued

Locus Tag		Gene Name	Description	Fold Change[†]
SL Number	STM Number			
SL2858	STM2878	*sptP*	Protein tyrosine phosphatase/GTPase activating protein	2.82
SL2859	STM2879	*sicP*	Secretion chaperone	3.46
SL2860	STM2881	*iacP*	Acyl carrier protein	4.46
SL2861	STM2882	*sipA*	Secreted effector protein	3.61
SL2862	STM2883	*sipD*	Translocation machinery component	3.30
SL2863	STM2884	*sipC*	Translocation machinery component	3.20
SL2864	STM2885	*sipB*	Translocation machinery component	3.20
SL2865	STM2886	*sicA*	Secretion chaperone	3.58
SL2867	STM2888	*spaR*	Needle complex export protein	3.04
SL2868	STM2889	*spaQ*	Needle complex export protein	3.34
SL2869	STM2890	*spaP*	Surface presentation of antigens protein	6.37
SL2870	STM2891	*spaO*	Surface presentation of antigens protein	3.65
SL2871	STM2892	*invJ*	Needle length control protein	4.41
SL2873	STM2894	*invC*	Needle complex assembly protein	4.64
SL2874	STM2895	*invB*	Secretion chaperone	5.22
SL2875	STM2896	*invA*	Needle complex export protein	6.32
SL2876	STM2897	*invE*	Invasion protein	4.46
SL2877	STM2898	*invG*	Outer membrane secretin precursor	3.50
SL2878	STM2899	*invF*	Invasion regulatory protein	4.36
SL2879	STM2900	*invH*	Needle complex outer membrane lipoprotein precursor	6.10
SL3009	STM3030		Hypothetical protein	0.05
SL3010	STM3031		Ail/OmpX-like protein	0.11
SL3105	STM3131		Putative cytoplasmic protein	2.05
SL3112	STM3138		Putative methyl-accepting chemotaxis protein	5.92
SL3161	STM3187	*ygiB*	Hypothetical protein	0.19

Table H1 continued

Locus Tag		Gene Name	Description	Fold Change[†]
SL Number	STM Number			
SL3162	STM3188	*ygiC*	Putative glutathionyl spermidine synthase	0.25
SL3199	STM3226	*yqjA*	Hypothetical protein	0.20
SL3200	STM3227	*yqjB*	Hypothetical protein	0.26
SL3201	STM3228	*yqjC*	Putative periplasmic protein	0.33
SL3202	STM3230	*yqjE*	Putative inner membrane protein	0.43
SL3203	STM3231	*yqjK*	Putative inner membrane protein	0.40
SL3229	STM3256		Phosphotransferase system mannitol/fructose-specific IIA component	0.48
SL3350	STM3377	*yedY*	Putative sulfite oxidase subunit	0.17
SL3351	STM3378	*yedZ*	Putative sulfite oxidase subunit	0.22
SL3352	STM3379	*accB*	Acetyl-CoA carboxylase biotin carboxyl carrier protein subunit	0.35
SL3353	STM3380	*accC*	Acetyl-CoA carboxylase biotin carboxyl carrier protein subunit	0.37
SL3361	STM3388		Putative signal transduction protein	0.36
SL3365	STM3392	*yhdV*	Putative outer membrane lipoprotein	0.40
SL3437	STM3470	*fic*	Cell filamentation protein	0.34
SL3438	STM3471	*yhfG*	Hypothetical protein	0.29
SL3439	STM3472	*ppiA*	Peptidyl-prolyl cis-trans isomerase A (rotamase)	0.10
SL3533	STM3568	*rpoH*	RNA polymerase factor sigma-32	0.32
SL3616	STM3650	*cueP*	Hypothetical protein; proposed copper sensitivity protein	0.08
SL3646	STM3681		Putative transcriptional regulator	0.31
SL3782	STM3815	*ccmE;ccmD*	Cytochrome c-type biogenesis protein	2.88
SL3783	STM3817	*ccmC*	Haem exporter protein	2.93
SL3784	STM3818	*ccmB*	Haem exporter protein	2.75
SL3928	STM3974	*tatB*	Sec independent translocase protein	0.47
SL3944	STM3996	*yihE*	Serine/threonine protein kinase	0.31
SL3945	STM3997	*dsbA*	Periplasmic protein disulphide isomerase I	0.42

Table H1 continued

Locus Tag		Gene Name	Description	Fold Change†
SL Number	STM Number			
SL4007	STM4058	*cpxA*	Two-component sensor protein	0.05
SL4008	STM4059	*cpxR*	DNA-binding transcriptional regulator	0.12
SL4009	STM4060	*cpxP*	Periplasmic repressor protein	0.01
SL4124	STM4189	*yjbB*	Periplasmic transport protein	0.19
SL4238	STM4301	*dcuB*	Anaerobic C4-dicarboxylate transporter	4.10
SL4239	STM4302		Putative cytoplasmic protein	3.18
SL4248	STM4312		Hypothetical protein	7.36
SL4250	STM4314		Putative regulatory protein	3.55
SL4251	STM4315		Putative DNA-binding protein	10.73
SL4285	STM4348	*psd*	Phosphatidylserine decarboxylase	0.27
SL4294	STM4360	*miaA*	tRNA delta(2)-isopentenylpyrophosphate transferase	0.26
SL4298	STM4364	*hflC*	FtsH protease regulator	0.47
SL4450	STM4519		Putative NAD-dependent aldehyde dehydrogenase	0.37
SL4463	STM4532	*yjiY*	Putative carbon starvation protein	2.38
SL4464	STM4533	*tsr*	Methyl-accepting chemotaxis protein I	0.36
SL4495	STM4568	*deoA*	Thymidine phosphorylase	0.41
SL4509	STM4582	*slt*	Lytic murein transglycosylase	0.21
SL4510	STM4583	*trpR*	Probable Trp operon repressor	0.41
	STM2966	*csrB*	Possible regulatory RNA	2.58
		invR	Small non-coding regulatory RNA	3.14
		omrA	Small RNA	0.34
		omrB	Small RNA	0.33
	STM14_1500		Hypothetical protein; located directly upstream of PagC (outer membrane invasion protein [STM1246])	2.20
	STM3229	*yqjD*	Putative inner membrane protein	0.34

†Denotes change in expression level in SL1344Δ*cpxR* compared to SL1344 following overexpression of *nlpE*. Values <0.5 represent level of expression reduction: values <2 represent levels of expression increase.

Appendix I

Table I1: **Supplement to Table 2. Distribution of genes presenting differential regulation in SL1344 WT and SL1344Δ*cpxR* following NlpE overexpression**. All 38 categories structured according to the Kyoto Encyclopaedia of Genes and Genomes (KEGG), in combination with current literature. n=number of genes in category. Cut-off threshold 2-fold, FDR >0.05.

Functional Category	Number of Genes in Each Category	
	Up-regulated	Down-regulated
Amino Acid transport and metabolism (n=326)	3	1
Anaerobic Metabolism (n=59)	4	0
Biofilms from Array Data (n=200)	3	11
Biofilms from *E. coli* Mutants (n=97)	1	1
Carbohydrate Transport and Metabolism (n=343)	0	2
Cell Envelope Biogenesis and OM (n=223)	5	6
Cell Motility and Secretion (n=100)	3	1
Chemotaxis (n=22)	1	1
Chemotaxis and Flagella (n=62)	1	1
Coenzyme Metabolism (n=134)	3	1
Cold (n=6)	0	0
Drug Analogue and Resistance (n=23)	0	0
Energy Production and Conservation (n=244)	2	1
Global Regulatory Function (n=50)	2	2
Inorganic Ion Transport and Metabolism (n=157)	2	5
Islands (n=827)	46	6
Lipid Metabolism (n=67)	1	3
Membrane Stress (n=20)	2	4
Nucleotide Metabolism (n=73)	1	1
Oxidative Phosphorylation (n=34)	0	0
Oxidative Stress (n=20)	0	1
Protein Transport (n=14)	0	0
Putative Function (n=1397)	12	17
Regulators (n=107)	1	4
Signal Transduction (n=114)	4	3
SPI-1 (n=36)	24	0
SPI-2 (n=32)	0	0
SPI-3 (n=28)	0	0
SPI-4 (n=6)	0	0
SPI-5 (n=8)	0	0
SPI-1 to 5 (n=128)	28	0
Structural Genes (n=73)	0	0
Surface Structure (n=101)	1	0
Transcription (n=275)	4	3
Translation (n=172)	0	1
Transport (n=120)	1	1
Unknown Function List 1 (n=830)	12	17
Unknown Function List 2 (n=912)	13	19

Appendix J

Figure J1: **Bioinformatic analysis of proposed, new members of the *Salmonella* Cpx regulon** in the form of protein BLAST (blastp) analyses (http://blast.ncbi.nlm.nih.gov). * indicates identical sequences for '*Subject*' at the nucleotide level. (Boratyn et al., 2013, Altschul et al., 1990).

Alignment of *yccA S*. Typhimurium SL1344 (Query) and *E. coli* K-12 (Subject)

Sequence ID: lcl|37153 Length: 219 Number of Matches: 1

Range 1: 28 to 219 Graphics ▼ Next Match ▲ Previous Match

Score	Expect	Method	Identities	Positives	Gaps
358 bits(918)	1e-130	Compositional matrix adjust.	184/192(96%)	188/192(97%)	0/192(0%)

```
Query  1    MSLTLALSAITATASTVLMLPSPGLILTLVGMYGLMFLTYKTANKPVGILSAFAFTGFLG  60
            +SLTLA SAITATASTVLMLPSPGLILTLVGMYGLMFLTYKTANKP GI+SAFAFTGFLG
Sbjct  28   LSLTLAFSAITATASTVLMLPSPGLILTLVGMYGLMFLTYKTANKPTGIISAFAFTGFLG  87

Query  61   YILGPILNAYLSAGMGDVIGLALGGTALVFFCCSAYVLTTRKDMSFLGGMLMAGIVVVLI  120
            YILGPILN YLSAGMGDVI +ALGGTALVFFCCSAYVLTTRKDMSFLGGMLMAGIVVVLI
Sbjct  88   YILGPILNTYLSAGMGDVIAMALGGTALVFFCCSAYVLTTRKDMSFLGGMLMAGIVVVLI  147

Query  121  GMVANIFLQLPALHLAISAVFILISSGAILYETSNIIHGGETNYIRATVSLYVSLYNIFV  180
            GMVANIFLQLPALHLAISAVFILISSGAIL+ETSNIIHGGETNYIRATVSLYVSLYNIFV
Sbjct  148  GMVANIFLQLPALHLAISAVFILISSGAILFETSNIIHGGETNYIRATVSLYVSLYNIFV  207

Query  181  SLLSILGFASRD  192
            SLLSILGFASRD
Sbjct  208  SLLSILGFASRD  219
```

Alignment of *ybiJ S*. Typhimurium SL1344 (Query) and UPEC *E. coli* str. CFT073 (Subject)

Sequence ID: lcl|55415 Length: 121 Number of Matches: 1

Range 1: 4 to 121 Graphics ▼ Next Match ▲ Previous Match

Score	Expect	Method	Identities	Positives	Gaps
188 bits(477)	7e-67	Compositional matrix adjust.	99/118(84%)	103/118(87%)	0/118(0%)

```
Query  3    YWILLALAIATEITGTLSMKWASVGNGNAGFILMLVMITLSYIFLSFAVKKIALGVAYAL  62
            YWILL LAIATEITGTLSMKWASV  GN GFILMLVMI+LSYIFLSFAVKKIALGVAYAL
Sbjct  4    YWILLGLAIATEITGTLSMKWASVSEGNGGFILMLVMISLSYIFLSFAVKKIALGVAYAL  63

Query  63   WEGIGILFITIFSVLLFDEALSTMKIAGLLTLVAGIVLIKSGTRKPGKPVKEATRATI  120
            WEGIGILFIT+FSVLLFDE+LS MKIAGL TLVAGIVLIKSGTRK  KP  E     +
Sbjct  64   WEGIGILFITLFSVLLFDESLSLMKIAGLTTLVAGIVLIKSGTRKARKPELEVNHGAV  121
```

Alignment of *ydgE S*. Typhimurium SL1344 (Query) and *E. coli* K-12 str. MG1655/*E. coli* W3110* (Subject)

Sequence ID: lcl|39735 Length: 86 Number of Matches: 1

Range 1: 1 to 86 Graphics ▼ Next Match ▲ Previous Match

Score	Expect	Method	Identities	Positives	Gaps
110 bits(276)	1e-37	Compositional matrix adjust.	69/86(80%)	77/86(89%)	0/86(0%)

```
Query  1   MKTIKYAVAAIALSTLSFGAFAAEPVSASQTQNLHKIGVVSADGATTLDGLEAKLAEKAA  60
           MKTI   VAA+ALSTLSFG FAAEPV+ASQ QN++KIGVVSADGA+TLD LEAKLAEKAA
Sbjct  1   MKTINTVVAAMALSTLSFGVFAAEPVTASQAQNMNKIGVVSADGASTLDALEAKLAEKAA  60

Query  61  AAGASAYNITSAVGNDKMSGTAVIYK  86
           AAGAS Y+ITSA  N+K+SGTAVIYK
Sbjct  61  AAGASGYSITSATNNNKLSGTAVIYK  86
```

Alignment of *ydgF S.* Typhimurium SL1344 (Query) and *E. coli* K-12 str. MG1655/*E. coli* W3110* (Subject)

Sequence ID: lcl|55415 Length: 121 Number of Matches: 1

Range 1: 4 to 121 Graphics ▼ Next Match ▲ Previous Match

Score	Expect	Method	Identities	Positives	Gaps
188 bits(477)	7e-67	Compositional matrix adjust.	99/118(84%)	103/118(87%)	0/118(0%)

```
Query  3    YWILLALAIATEITGTLSMKWASVGNGNAGFILMLVMITLSYIFLSFAVKKIALGVAYAL  62
            YWILL LAIATEITGTLSMKWASV  GN GFILMLVMI+LSYIFLSFAVKKIALGVAYAL
Sbjct  4    YWILLGLAIATEITGTLSMKWASVSEGNGGFILMLVMISLSYIFLSFAVKKIALGVAYAL  63

Query  63   WEGIGILFITIFSVLLFDEALSTMKIAGLLTLVAGIVLIKSGTRKPGKPVKEATRATI  120
            WEGIGILFIT+FSVLLFDE+LS MKIAGL TLVAGIVLIKSGTRK  KP  E     +
Sbjct  64   WEGIGILFITLFSVLLFDESLSLMKIAGLTTLVAGIVLIKSGTRKARKPELEVNHGAV  121
```

Appendix K

Figure K1: **Supplement to Table 26 and Figure 15: PRODORIC® promoter sequence analyses.** Genes are listed in order of fold change A) Down regulated; greatest to least, B) Up regulated; least to greatest, as ordered in Table 26. Positions of CpxR binding motifs are highlighted in grey.

A ***yqaE***

Promoter Sequence: *Salmonella* Typhimurium (strain ATCC 700720 / SGSC1412 / LT2)|complete chromosome (500bp upstream of *yqaE*)

```
  1 AATGGACATC GTGCCTCCTT ATGGACAATA GAGATTCTTT AACGTGGCGA TAATCGTATT AACCGCCTCA TTTTTAATGA   80
 81 AATAGTGAAT GCGCTGGGCA TCGCGTTGAC TATCAATCAG CCCTTCTTCC CGCATCCGCG CCAGATGTTG CGACGTCGCG  160
161 GAGGGGCTTA GCCCGGTAAT GCGCGCCAGT TCGCCTGCGC TGGTTTTTGG CGAACCGCAA AGCATACATA AAATCAGTAA  240
241 TCTTTTTGGG TGGCTCATCG CTTTGAGCAG GGCCGCCGCC TGTTCTGCGC TGGCCTGAAG TTGTTCAAGC TCTGTCATAG  320
321 TTATTTAAGT ATTTTCTAAA TTTAGTTAAT TCTAAAATAA ACATCAACCT AATGCCAGCG TAAAGAGCGT AAAGGAGGGT  400
401 AAAAGCGCGG CGCGCGACTG GCAGGCTCAG GTAAACTGAC TATGCTTAGA GATAAAATCT CTTTTTAAAC AATGACTAAT  480
480 TTTGCTTGTA TGGAGTGTAT ATG
```

PWM (species)	Start Position	End Position	Strand	Score	Sequence
CpxR | Escherichia coli (strain K12)	388	403	+	13.57	CGTAAAGGAGGGTAAA

STM3650 (SL3616 – *cueP*)

Promoter Sequence: *Salmonella* Typhimurium (strain ATCC 700720 / SGSC1412 / LT2)|complete chromosome (500bp upstream of STM3650)

```
  1 CAAGAGTTAT CCATTAGATA CCCCTCGTAG TGCGCATTTC CTTAACGCTT AAAAAATCTG TAAAGCACGC CATAACGCCG   80
 81 AAAGGCACAC TTATTTTTTA AAAGGTAATA CACTATGTCC GGTAAAATGA CTGGTATCGT AAAATGGTTC AACGCTGATA  160
161 AAGGCTTCGG CTTTATTACT CCTGATGACG GTTCTAAAGA CGTGTTCGTA CACTTCTCCG CTATTCAGAA CGATGGTTAC  240
241 AAATCTCTGG ACGAAGGTCA GAAAGTTTCC TTCACCATCG AAAGCGGCGC TAAGGGCCCG GCAGCTGGCA ACGTAACCAG  320
321 CCTGTAAGCT TAAAAAGCTC AGCATTTTGA ATCCCTGCCT GATGGCGGGG ATTTTTTTTA TTCCAATTCC CCCCTCTCCC  400
401 CCAGCATAAC TTTGCATTAC TTTACCCTGC GTCCCTTTGA CCTTTCCCTT AGGGGAACCC CTATAGTAGG CAGGGAGATT  480
481 GTTCACAAGG AATTGAAGTT ATG
```

PWM (species)	Start Position	End Position	Strand	Score	Sequence
CpxR | Escherichia coli (strain K12)	411	426	-	12.77	GGTAAAGTAATGCAAA

ybiJ

Promoter Sequence: *Salmonella* Typhimurium (strain ATCC 700720 / SGSC1412 / LT2)|complete chromosome (500bp upstream of *ybiJ*)

```
  1  ACCATTGAAG ATGCCGTTGC CCGCGCTCGC GGCGAACTTC CCCACGGCGA AAGTCGCGAT GAATGCGAAT CTTGCGGCGA   80
 81  TCCTATCCCT GAAGCGCGGC GTAAAGCCGT GCCGGGCGTT CGGTTATGCA TAGCCTGCCA ACAGGAGAAA GATTTACATA  160
161  ACGCAACATT TTCAGGATAT AATCGTAGAG GTTCAAAAGA CAGCCAGTTA CGCTGACTTT TCTTTACCGA AACCGCCAGT  240
241  ATTATCCATT CCTTTACGCT CATGCTTTTT AGCGTTCTGC GTCGCAGAAT GTGCCGTTAA CCTCGACTCT GTAAAGCCAG  320
321  ATGACAAGAA AGGTAAATTC AACCGTTGAA TTAATTAATA ATCAATAGGT TATTTGTCAT TCAAAAATTT TGAGCAAGGC  400
401  AGTCAATTCT ATTCGATTTT ATCTTTCGCA AAAAACCGTG ATACTCATCA CATCGACGGA ACATCGTCCC ATAAACAGAA  480
481  TAACCTGCGA GAGATTAATC ATG
```

PWM (species)	Start Position	End Position	Strand	Score	Sequence
CpxR | Escherichia coli (strain K12)	213	228	-	13.26	GGTAAAGAAAAGTCAG

chaA

Promoter Sequence: *Salmonella* Typhimurium (strain ATCC 700720 / SGSC1412 / LT2)|complete chromosome (500bp upstream of *chaA*)

```
  1  CGTTTATTTT TTCTTATGCC ATTTATCATC CTCGCCTTTT TCATAATCGT TTTTAACCGC CGCCCAGGCG ACTTTGTGTG   80
 81  CGGTTTCCTC GCGGCTGGCG TCATCACGAC GATCGGCTTT ATCTTTATAT TGCTCCCAGG CGCTATTAAA CGCTTCTTTG  160
161  TAAATGTCCT GGGCATGGGC TGGAAGAACA TTCCGCACAT TATCGGGTAA ATCACTTTTG GCTTTATACG GCATCAGCGC  240
241  CTCCGTCTTC AGGGAAAACA TTAAGTGTGG TAAACAATGC GTTATTACGC CAGTCGAGGA GGATTTTTGC TTTTTACGGA  320
321  AATTAACTTT TTGTTATTTA AACACTGTTA AAACAAGATG CTTGTTTTAC TGACCTTGAA AGAAAAAAAT CGTCTACGCC  400
401  GTAAAACTAC GTAAAAAACC ACTAAAAAAA TACAAATTTC TGCTATTTTT ACCTTCTTTA CTCTTTCCAA AATATTAACA  480
481  CCTGCACAAG GGAGACCCTC ATG
```

PWM (species)	Start Position	End Position	Strand	Score	Sequence
CpxR | Escherichia coli (strain K12)	400	415	+	13.55	CGTAAAACTACGTAAA

eco

Promoter Sequence: *Salmonella* Typhimurium (strain ATCC 700720 / SGSC1412 / LT2)|complete chromosome (500bp upstream of *eco*)

```
  1  CGTTTCTCTG GCCCACGGCG GAAGAATCCC ATTGCTGGCG TTGCGCCAAC TGCCGGTCAA CATGCTTCGA CGGGATAAAT   80
 81  CAACCATGAT ATCGCCCTTC CATAACGACA CGCTTCCATA GGGAGTGAAT ACCAATAAAA ACCGTACAAT TTATGAGTAG  160
161  TTGTTTTTGT AAATAAGATA TTTCAGGATG TGTAAGAGAT GCATACCCCG ATAGAGGTAA ATGCTGTTGC CGGATCAAAA  240
241  GAGTGCCGGG TAAAGACCCG TAAACGTGCT TTTTCTCACA TTTCAATGAG TTATATAGAT ATTTATATAA CGAAAACCAC  320
321  TAATAGCTGA TAATTTCATT TACATTATCA ATATCAGAAT ATTCCACTAT ATAAAAAGAC GCTATTTTAT TAATAATCTT  400
401  GAAAATATGA GTAAATACAG ATTAATAGAT AATATGAATG TGTTAATCTG TTGTCAGTGA ATACCGAAAA CAGCAGAAAG  480
481  GAAATACTGT GAACAATCAA ATG
```

PWM (species)	Start Position	End Position	Strand	Score	Sequence
CpxR | Escherichia coli (strain K12)	249	264	+	12.96	GGTAAAGACCCGTAAA

yihE

Promoter Sequence: *Salmonella* Typhimurium (strain ATCC 700720 / SGSC1412 / LT2)|complete chromosome (500bp upstream of *yihE*)

```
  1  CAAGCAGACC TTTATCCGCA CCTCCCATCC GCCTGGCTTT ACCGCCTGCC AGCACCACGC CGGTTATTAC TTCATCCAGA   80
 81  TTCACCGATA TCGCCTCTTT TATTGTGGGA TTGACCCTGC TACCGTGTCT GTATCAAGAA TAAGGAGCAC AGCTATGAAA  160
161  TGTAAACGCC TGAATGAAGT CATTGAACTC CTCCAGCCAG CCTGGCAGAA AGAGCCTGAT CTTAATCTGA CGCAATTTTT  240
241  GCAGAAACTG GCGAAAGAGT CAGGTTTTGA CGGCAAACTG GAAGATTTAA CTGATGATAT CCTGATCTAC CATCTGAAAA  320
321  TGCGCGATTC CGCCAAAGAC GCCGCCATTC CAGGGATTCA AAAAGACTAT GAAGAGGACT TTAAAACGGC GCTTTTACGC  400
401  GCCCGCGGCG TTATTAAAGA GTAAAACCTT GTAAGCGGCG CCACCGAAAT CGCCACGAAA TGATATCCTG AATCATTCGT  480
481  AGTATTTTCC GGATGATGGG ATG
```

PWM (species)	Start Position	End Position	Strand	Score	Sequence
CpxR | Escherichia coli (strain K12)	420	435	+	13.93	AGTAAAACCTTGTAAG

STM3681 (SL3646)

Promoter Sequence: *Salmonella* Typhimurium (strain ATCC 700720 / SGSC1412 / LT2)|complete chromosome (500bp upstream of STM3681)

```
  1  TCCCAGGTTT CCGCTGTCGC CAACAGTTCG AGGTTTTGTT CCATCCGATC GGCGATCTTA AACAAGATAG CGGCACGGTC   80
 81  TTGTACTGAC GTATGCGCCC ACTTATCTTT CGCCTTATGC GCGGCGTCGA GCGCTAAATC GATATCTTTT TTACCGGAGG  160
161  AAGCGACTTC ACATAGCGGC TGGCCGGTCA CTGGCGTCAG GTTTTGATAA TATTCGCCGT CGGCGGGCGC AACCCAGTCA  240
241  CCACCAATAA AATTGTCATA GCGGGCTTTT AACTTCAGTG GGTACCCGTA TTCACCTGGC TGAATACGTG TTGAAGGGGG  320
321  ATTGTTCGTC ATGACCAACT CCTTATTGTA AAGGTACTCC ACAAGGGTAG ACGGTGCTGG TGAATTTTTC GCCAATGATT  400
401  TCCCGCTTTA CGACAGCAAT CACGAATTAC TTTCCTTTAC GTTTCTCCGT CTGGTTTTAG CCATACTAAA CAGGTGCCTG  480
481  TTTAACGTAC GGAGAACACT ATG
```

PWM (species)	Start Position	End Position	Strand	Score	Sequence
CpxR | *Escherichia coli* (strain K12)	426	441	-	13.87	CGTAAAGGAAAGTAAT

ydgF

Promoter Sequence: *Salmonella* Typhimurium (strain ATCC 700720 / SGSC1412 / LT2)|complete chromosome (500bp upstream of *ydgF*)

```
  1  CGGATACCGC TCAGAATAAC TACCAGCATT CCCAGCATAA TGACGATTTT TAGACCATTG AGCGTGATGA TCGGTTTTGC   80
 81  CATATCAGTC CCTGTTTTCT GATGCCGACA CGAATAATAA TGTGATGTCG GTCGACCTGT TCTGGTTAAA ATCAAACACT  160
161  TCAGGTAAAG AAGTGAAAAT ATTTTGAGTT AATTCCTGGC TTATGATACA AATCAGGCGT GTTCAACTAC CGAGGACAAT  240
241  TATCATCCGC GATGACGAGA AGCAACACTG CGGATAATTG TAATATTATG GACAATATGT TCAGCGCTTT TTTCTCCACG  320
321  CAAACGCATC TTCACTCTAC CTCCTTTTTC CTGCTTATCG GCGAGCAGCA CTGGCGTAAC GCACTTTAGT CTCTCACTTC  400
401  TGCCTGAGCT GGCGCAATGC GCTGTGCTAA CTGATTTTAT TTTTTAGTTT GCTGCGTGCA GCAGACTCGA AAGAGTATAT  480
481  TCTCATGCAG GAGAAGTGTC ATG
```

PWM (species)	Start Position	End Position	Strand	Score	Sequence
CpxR | Escherichia coli (strain K12)	164	179	+	12.86	GGTAAAGAAGTGAAAA

rpoH

Promoter Sequence: *Salmonella* Typhimurium (strain ATCC 700720 / SGSC1412 / LT2)|complete chromosome (1000bp upstream of *rpoH*)

```
  81 GGGCAGCTTC AGGCCGAGCA GGGCGTTGAG AAGGTCAACT ACCTGTCCCG TGAGGACGCG CTGGGAGAAT TCCGCAACTG  160
 161 GTCGGGTTTT GGCGGCGCGC TGGATATGCT GGAAGAGAAC CCGCTACCGG CGGTGGCGGT GGTGATCCCC AAGCTGGACT  240
 241 TTCAAAGTAC CGCCTCGCTT AATACGCTGC GCGACCGTAT CTCGCAGATT AACGGCATTG ACGAAGTCCG CATGGATGAT  320
 321 AGCTGGTTTG CGCGCCTGGC GGCGCTCACC GGGCTGGTGG GCCGCGTATC GGCGATGATC GGCGTGCTGA TGGTCGCGGC  400
 401 GGTCTTCCTC GTTATCGGCA ACAGCGTGCG CCTGAGCATT TTTGCCCGTC GCGACACCAT TAACGTGCAA AAGCTGATTG  480
 480 GCGCGACCGA TGGCTTTATC CTGCGTCCGT TCCTCTATGG CGGCGCGTTG CTCGGTTTTT CCGGCGCGTT TCTGTCACTG  560
 561 ATATTGTCTG AAATTTTGGT GATGCGTTTA TCATCGGCGG TGACTGAAGT GGCGCAGGTC TTCGGCACGA AGTTTGATCT  640
 641 CAATGGCTTA TCGTTCGATG AGTGCCTGTT GCTGCTGCTG GTCTGTTCCA TGATTGGCTG GATCGCCGCC TGGCTGGCCA  720
 721 CGGTGCAACA TTTACGTCAC TTTACTCCCG ATTGATAAAA TCGTGGTATA ATCTTTCCCT GCAATGGGCT TCCGTTCGCA  800
 801 GGGAAAGAGT CCCTGTTGTC TCTTCCCCGC GCGTCATCTT TATGTCACAA GATTTGTGCA AATTATGCAC AGTGTTACAT  880
 881 TGAACTTGTG GATAAAATCA CTGTCTGATA AAAGAGTGGG TGATATTCTC GTTGCTCATC GGCTTTGGCA CGGTTGTTGC  960
 961 TCGCTGACGG TGCCAGGCAA TACTGATTGA GAGGATTTGA ATG
```

PWM (species)	Start Position	End Position	Strand	Score	Sequence
CpxR | Escherichia coli (strain K12)	731	746	-	14.20	AGTAAAGTGACGTAAA

slrP

Promoter Sequence: *Salmonella* Typhimurium (strain ATCC 700720 / SGSC1412 / LT2)|complete chromosome (500bp upstream of *slrP*)

```
   1  CGGCGTCCTG ACAATGTGTC GATCGCCAGC GAGTCATCGT TACCATGGCT CGCTTTTGAG AATTTCAGTG CAATAGTAAG   80
  81  GGCTAAGTCA GTCAGGAATG AAAAACAGTG ACAGGCTTTG ACTAACGGGA TTGTCGAAAA ACTCAAAACA TCAATGGGGT  160
 161  AGCTAGTTTA ATCACAACTG AAGAAAATTA GCGTTGAGGC TGAACCCAAC GCTAATTTTC CCTCTCTCCT CGGCTATGAA  240
 241  AAAAAACGCC CCGTATTATC GGTATAGCTA TCCTTATGAT CGTCATTTTA ATCTTATATG AGTTCGTTGA AAGCGTGTCA  320
 321  TGGCAACAGA TTACATCATT CTACTTAAAA AAGAGGTGAT GGAAGCGCGA GCATCTATAA GTCAAGCGCT GCAAATACTG  400
 401  AATGATTTGT CCGAAATAAT GACGACTGTG ACCTCTTATT TAAAGTTGAG AATATCCTTA TCTGTTACTT TAGGTTACGT  480
 481  TCAGATCAGG TAGGGAAAAT ATG
```

PWM (species)	Start Position	End Position	Strand	Score	Sequence
CpxR | Escherichia coli (strain K12)	464	479	-	12.38	CGTAACCTAAAGTAAC

B

yjiY

Promoter Sequence: *Salmonella* Typhimurium (strain ATCC 700720 / SGSC1412 / LT2)|complete chromosome (500bp upstream of *yjiY*)

```
  1  GTTTGCAATA CGGTGAAGTT TTCTTTGTCA TTCTTCAGCG AGTTGAAGAA CAGCCCGCCG GATGTCAGTT GTAAAAGGCC   80
 81  AAATAGCGCC AATACCAGCA GTAAGCTGGT AACAATTTTA ATTCGCTTTA ACATGTTTTC TCTTTCCGCT AGACAGATAC  160
161  AGAATTTTCG GCCTGGAAAG GGAAAACTTT ATGGGATGCG CGCCATTAAT ATCACGATTA GCTCAGTGAA GTCGTTATGA  240
241  CGCCCCGCGC AACAAGGATC GTCCCATTTT ATATCGTGAT CTCAATCACA TAAAATAGCC CACGCCCTCC TCCGCGAAAC  320
321  CGCTTACCGG TACGTCCGAC CGCTTAAACC GCCATACAAC CACTCACTGA TTTACCTAAC TTTACGCGCG CGATGATCTG  400
401  GCAAGATCCT CTCAGCATAG CAGTCAATCT ACCTCCTCAA ACACGAACTC AATGTCCACC CAGCTTCGGC TGATAATTAA  480
481  ACTTACAACC AGGTTTTACT ATG
```

PWM (species)	Start Position	End Position	Strand	Score	Sequence
CpxR | Escherichia coli (strain K12)	371	386	-	13.99	CGTAAAGTTAGGTAAA

deoA

Promoter Sequence: *Salmonella* Typhimurium (strain ATCC 700720 / SGSC1412 / LT2)|complete chromosome (1000bp upstream of *deoA*)

```
  81 TGCCGTTGGA GAATGTCATG ACTGATTTAA AAGCAAGCAG CCTGCGTGCG CTCAAACTGA TGGATCTGAC CACTCTGAAC  160
 161 GATGACGACA CCAATGAAAA AGTGATCGCG TTGTGTCATC AGGCAAAAAC TCCGGTCGGG AATACGGCGG CGATTTGTAT  240
 241 TTACCCGCGT TTTATCCCGA TTGCGCGTAA AACTCTGAAA GAACAAGGTA CGCCGGACAT CCGCATTGCA ACGGTGACTA  320
 321 ACTTCCCGCA TGGCAATGAT GACATCGATA TTGCGCTGGC GGAAACCCGT GCGGCGATCG CCTACGGCGC TGACGAAGTG  401
 401 GACGTGGTAT TCCCGTACCG CGCGTTGATC GCCGGTAACG AGCAGGTGGG TTTTGACCTG GTAAAAGCCT GTAAAGACGC  480
 481 TTGTGCCGCA GCGAACGTAT TGCTGAAAGT GATTATCGAA ACCGGCGAGC TGAAAGAAGA GGCGCTGATT CGTAAAGCCT  561
 561 CTGAAATCTC CATTAAAGCC GGTGCGGATT TCATCAAAAC CTCTACCGGT AAAGTGCCGG TAAACGCTAC GCCGGAAAGC  640
 641 GCGCGCATCA TGATGGAAGT GATCCGCGAC ATGGGCGTTT CCAAAACCGT TGGCTTCAAA CCGGCGGGCG GCGTACGTAC  720
 721 GGCGGAAGAC GCGCAGAAAT TCCTCGCGAT TGCAGACGAA CTGTTTGGCG CTGACTGGGC AGATTCTCGT CACTACCGCT  800
 801 TTGGCGCATC CAGCCTGCTG GCAAGCCTGC TGAAAGCGCT GGGTCACGGC GACGGTAAGA GCGCCAGCAG CTACTAAGCT  880
 881 CTGATTTGCC GGATGGCGCT GCGCTTATCC GGCCTACAAA TCCAGGCCTG TAGGCCGGAT AAGGCGTTAG CCGCCATCCG  960
 961 GCGATGTAAG CCTTCTACTC TTTTCCCTCA GGAGGGTACC GTG
```

PWM (species)	Start Position	End Position	Strand	Score	Sequence
CpxR | Escherichia coli (strain K12)	460	475	+	14.02	GGTAAAAGCCTGTAAA
CpxR | Escherichia coli (strain K12)	266	281	+	13.06	CGTAAAACTCTGAAAG

ccmA

Promoter Sequence: *Salmonella* Typhimurium (strain ATCC 700720 / SGSC1412 / LT2)|complete chromosome (1000bp upstream of *ccmA*)

```
  81 CGTATGCCGC TAAATTACGT CAACCAGCCG CCGATGATCC CGCACAGCGT CGAGGGCTAC CAGGTGACGA CCAATACCAA   160
 161 CCGCTGTCTG CAATGCCACG GCGTGGAAAG TTATCGTACG ACGGGCGCGC CGCGTATCAG TCCGACGCAC TTTATGGACA   240
 241 GCGACGGTAA AGTGTCGGGC AACGTCGCGC CGCGTCGTTA TTTCTGCCTG CAGTGCCACG TACCGCAGTC TGATACCGCG   320
 321 CCGATTATCG ACAATACCTT TACCCCCTCG CAAGGTTACG GGAAATAAGA GGTCATTATG GAAAATTCTA ACCGTAAACC   401
 401 CGGCTGGATA AAGCGCGTCT GGCGATGGTG GCGCAGCCCC AGCCGCCTGG CGTTGGGGAC GCTGCTGTTA ATCGGTTTTA   480
 481 TCGGCGGCAT CATCTTCTGG GGCGGCTTCA ATACCGGAAT GGAAAAGGCT AACACCGAAG AGTTTTGTAT TAGCTGCCAT   561
 561 GAAATGCGCA ACACGGTGTA TGAGGAGTAT ATGGAAACCG TCCACTACAA CAACCGTAGC GGCGTTCGTG CCACCTGTCC   640
 641 TGACTGCCAT GTGCCGCATG AGTGGGGGCC GAAGATGATC CGTAAGATCA AAGCCAGTAA AGAGCTGTAT GCGAAGGTAT   720
 721 TTGGGCTGAT AGATACACCG CAGAAATTTG AAGCTCATCG CCTGACAATG GCACAAAATG AGTGGCGGCG CATGAAAGAC   800
 801 AACAACTCGC AGGAATGCCG TAACTGCCAC AATTTCGACT TTATGGATCT GACCGCGCAA AAAGGCGTCG CGGCGAAAAT   880
 881 GCACGATCAG GCGGTAAAAG ATGGACAGAC CTGTATCGAT TGCCACAAAG GGATCGCGCA TAAACTGCCG GATATGCGTG   960
 961 ATGTTAAACC AGGTTTCTGA CAGGACGTTG ATGAGTGGGA ATG
```

PWM (species)	Start Position	End Position	Strand	Score	Sequence
CpxR | Escherichia coli (strain K12)	893	908	+	12.43	GGTAAAAGATGGACAG

Appendix L

Table L1: All genes differentially expressed by ZraR overexpression in *Salmonella* Typhimurium SL1344. All genes were induced (green) or repressed (red) greater than 2-fold (FDR <0.05) in SL1344p*zraR* following ZraR overexpression, compared to SL1344pBAD empty vector. Genes are listed and sorted by operon. Fold change is shown to two decimal places. Genes highlighted yellow are also regulated by RpoN, as presented by Samuels et al. (2013).

Locus Tag		Gene Name	Description	Fold Change[†]
SL Number	STM Number			
		istR	Unknown	2.75
		oxyS	Unknown	2.56
PSLT026			Putative periplasmic protein	3.13
PSLT043			type II secretion system protein	3.74
		rlgA	Unknown	8.68
SL0012	STM0012	*dnaK*	Molecular chaperone DnaK	5.16
SL0122	STM0122	*ftsI*	Division specific transpeptidase	-2.99
SL0271	STM0276		Putative cytoplasmic protein	2.04
SL0274	STM0279		Putative cytoplasmic protein	2.88
SL0275	STM0280		Putative outer membrane lipoprotein	2.40
SL0312	STM0316	*pepD*	Aminoacyl-histidine dipeptidase	-2.05
SL0363	STM0368	*prpB*	2-methylisocitrate lyase	3.10
SL0364	STM0369	*prpC*	Methylcitrate synthase	5.76
SL0365	STM0369	*prpD*	2-methylcitrate dehydratase	16.44
SL0437	STM0443	*cyoA*	Cytochrome o ubiquinol oxidase subunit II	6.09
SL0456	STM0462	*glnK*	Nitrogen regulatory protein P-II 2	14.64
SL0457	STM0463	*amtB*	Ammonium transporter	27.42
SL0466	STM0473	*hha*	Hemolysin expression-modulating protein	3.12
SL0467	STM0474	*ybaJ*	Hypothetical protein	2.82
SL0480	STM0487		Unknown	3.20
SL0497	STM0504	*ybbN*	Putative thioredoxin protein	2.50

Table L1 continued

Locus Tag		Gene Name	Description	Fold Change[†]
SL Number	STM Number			
SL0519	STM0526	*ylbA*	Hypothetical protein; cupin 2 superfamily	2.36
SL0561	STM0573		Putative inner membrane protein	5.17
SL0562	STM0574		Putative PTS system mannose-specific enzyme IID	2.96
SL0563	STM0575		Putative inner membrane protein	2.86
SL0564	STM0576		Putative PTS system mannose-specific enzyme IIAB	14.23
SL0565	STM0577		Putative PTS system mannose-specific enzyme IIAB	10.20
SL0612	STM0624	*citC*	Citrate lyase synthetase	0.48
SL0614	STM0626	*dpiA*	Two-component response regulator DpiA	0.45
SL0624	STM0636	*ybeD*	Hypothetical protein; proposed lipoate regulatory protein	2.35
SL0637	STM0649		Unknown	46.33
SL0638	STM0650		Putative hydrolas	5.02
SL0639	STM0651		2-keto-3-deoxygluconate permease	2.45
SL0652	STM0663	*gltK*	Glutamate/aspartate transporter	5.50
SL0654	STM0665	*gltI*	Glutamate and aspartate transporter subunit	21.72
SL0803	STM0828	*glnQ*	Glutamine ABC transporter ATP-binding protein	2.49
SL0804	STM0829	*glnP*	Glutamine ABC transporter permease protein	2.58
SL0805	STM0830	*glnH*	Glutamine ABC transporter periplasmic protein	6.43
SL0862	STM0886		Putative sulfatase	6.20
SL0957	STM2621		Hypothetical protein	2.57
SL1006	STM1066	*rmf*	Ribosome modulation factor	-3.97
SL1010	STM1070	*ompA*	Outer membrane protein A	-2.20
SL1062	STM1124		Unknown	6.84
SL1076	STM1139	*csgG*	Putative curli operon transcriptional regulator	2.15
SL1187	STM1251		Putative molecular chaperone	4.75
SL1219	STM1284	*yeaH*	Hypothetical protein	3.53

Table L1 continued

Locus Tag		Gene Name	Description	Fold Change[†]
SL Number	STM Number			
SL1220	STM1285	*yeaG*	Putative serine protein kinase	6.65
SL1238	STM1303	*argD*	Bifunctional succinylornithine transaminase/acetylornithine Transaminase	15.48
SL1239	STM1304	*astA*	Arginine succinyltransferase	16.97
SL1374	STM1442	*ydhJ*	Putative multidrug resistance efflux pump	8.91
SL1376	STM1444	*slyA*	Transcriptional regulator SlyA	-2.22
SL1416	STM1486	*ynfM*	Putative transport protein	-2.76
SL1417	STM1487	*ynfL*	Putative transcriptional regulator	2.87
SL1427	STM1497		Putative dimethyl sulphoxide reductase	-4.64
SL1428	STM1498		Putative dimethyl sulphoxide reductase	-3.37
SL1453	STM1523	*yneJ*	Putative transcriptional regulator	2.14
SL1495	STM1565	*rpsV*	30S ribosomal subunit S22	-2.29
SL1503	STM1572	*nmpC*	Putative outer membrane porin precursor	3.00
SL1615	STM1685	*ycjX*	Putative ATPase	3.64
SL1617	STM1687	*pspD*	Peripheral inner membrane phage-shock protein	14.77
SL1618	STM0463	*pspC*	DNA-binding transcriptional activator PspC	24.80
SL1619	STM1689	*pspB*	Phage shock protein B	119.17
SL1620	STM1690	*pspA*	Phage shock protein PspA	164.56
SL1621	STM1691	*pspF*	Phage shock protein operon transcriptional activator	2.14
SL1854	STM1919	*cheM*	Methyl accepting chemotaxis protein II	-3.84
SL1972	STM14_1420		Unknown	-2.70
SL2154	STM2177		Putative flutathione S-transferase	2.13
SL2157	STM2180		Putative transcriptional regulator	3.18
SL2166	STM2189	*mglA*	Galactose/methyl galaxtoside transporter ATP-binding protein	2.24
SL2197	STM2220	*yejG*	Hypothetical protein	3.08
SL2269	STM2300		Putative cytoplasmic protein	-2.04

Table L1 continued

Locus Tag		Gene Name	Description	Fold Change[†]
SL Number	STM Number			
SL2322	STM2353	*hisQ*	Histidine/lysine/arginine/ornithine transport protein	3.18
SL2323	STM2354	*hisJ*	Histidine transport protein	5.85
SL2324	STM2355	*argT*	Lysine/arginine/ornithine transport protein	11.71
SL2327	STM2358		Putative cytoplasmic protein	8.30
SL2328	STM2359		Putative amino acid transporter	4.68
SL2330	STM2361		Putative regulatory protein; Conserved domains AAA superfamily/ PspF protein/PAS superfamily	2.99
SL2360	STM2391	*fadL*	Long-chain fatty acid outer membrane transporter	6.43
SL2376	STM2408	*mntH*	Manganese transport protein MntH	2.49
SL2377	STM2409	*nupC*	Nucleoside transport	2.21
SL2613	STM2649	*trxC*	Thioredoxin 2	2.27
SL2620	STM2660	*clpB*	Protein disaggregation chaperone	2.81
SL2658	STM2686	*yfjF*	Hypothetical protein	-2.11
SL2776	STM2792	*gabT*	4-aminobutyrate aminotransferase	7.31
SL2787	STM2716		Putative regulatory protein	3.97
SL2820	STM2840		Anaerobic nitric oxide reductase flavorubredoxin	7.93
SL2839	STM2859	*fhlA*	Formate hydrogen-lyase transcriptional activator	5.71
SL2886	STM2907	*pphB*	Serine/threonine-specific protein phosphatase 2	6.62
SL2918	STM2939	*ygcH*	Putative cytoplasmic protein	3.60
SL2978	STM3000	*ppdA*	Hypothetical protein; similar to *Escherichia coli* prepilin peptidase dependent protein A (AAC75865.1); putative component involved in type IV pilin biogenesis	2.15
SL3011	STM3033		Plasmid maintenance protein	2.43
SL3012	STM3034		Putative cytoplasmic protein	3.22
SL3052	STM3034	*tktA*	Transketolase	-2.26
SL3059	STM3083		Putative mannitol dehydrogenase	2.20

Table L1 continued

Locus Tag		Gene Name	Description	Fold Change[†]
SL Number	STM Number			
SL3121	STM3147	*hybC*	Hydrogenase 2 large subunit	-2.80
SL3122	STM3148	*hybB*	Putative hydrogenase 2 b cytochrome subunit	-3.22
SL3123	STM3149	*hybA*	Hydrogenase 2 protein HybA	-3.83
SL3124	STM3150	*hypO*	Hydrogenase 2 small subunit	-2.52
SL3255	STM3282	*pnp*	Polynucleotide phosphorylase/polyadenylase	-2.01
SL3297	STM3325	*yrbL*	Hypothetical protein; Protein Kinases, catalytic domain	2.04
SL3425	STM3458	*yheR*	Glutathione-regulated potassium-efflux system ancillary protein KefG	4.86
SL3475	STM3508		Putative cytoplasmic protein	2.19
SL3484	STM3517		Putative DNA-damage-inducibile protein	3.76
SL3485	STM3518	*rtcA*	RNA 3'-terminal-phosphate cyclase	11.24
SL3486	STM3519	*rtcB*	Putative cytoplasmic protein	10.54
SL3487	STM3521		Putative ribonucleoprotein related-protein	32.65
SL3528	STM3562	*livM*	Leucine/isoleucine/valine transporter permease subunit	3.69
SL3542	STM3577	*tcp*	Methyl-accepting transmembrane citrate/phenol chemoreceptor	-3.51
SL3594	STM3628	*dppC*	Dipeptide transporter	2.50
SL3732	STM3767		Putative cytoplasmic protein	11.28
SL3733	STM3768		Putative selenocysteine synthase	4.65
SL3735	STM3770		Putative phosphotransferase system enzyme IIC	13.89
SL3736	STM3771		Putative phosphotransferase system enzyme IIB	28.14
SL3737	STM3772		Putative phosphotransferase system enzyme IIA	5.97
SL3743	STM3777		Putative cytoplasmic protein	2.11
SL3744	STM3778		Putative DNA-binding protein	4.27
SL3775	STM3808		Unknown; in LT2 ibpB - heat shock chaperone IbpB	15.10
SL3776	STM3809		Unknown; in LT2 ibpA - heat shock protein IbpA	13.62
SL3883	STM3924	*wecD*	TDP-fucosamine acetyltransferase	2.77

Table L1 continued

Locus Tag		Gene Name	Description	Fold Change†
SL Number	STM Number			
SL3952	STM4005	*glnG*	Nitrogen regulation protein NR(I)	3.11
SL3953	STM4006	*glnL*	Nitrogen regulation protein NR(II)	2.19
SL3954	STM4007	*glnA*	Glutamine synthetase	6.77
SL3965	STM4019	*yihQ*	Alpha-glucosidase	2.11
SL3977	STM4031		Putative cytoplasmic protein	2.16
SL3979	STM14_4847		Unknown	2.02
SL3995	STM4046	*rhaA*	L-rhamnose isomerase	6.74
SL4009	STM4060	*cpxP*	Periplasmic repressor CpxP	-4.46
SL4034	STM4085	*glpX*	Fructose 1,6-bisphosphatase II	2.97
SL4110	STM4171	*yjaH*	Putative inner membrane protein	3.46
SL4111	STM4172	*zraP*	Zinc resistance protein	122.89
SL4112	STM4173	*hydH*	Sensor protein ZraS	4.71
SL4118	STM4183	*aceB*	Malate synthase	2.67
SL4180	STM4244	*pspG*	Phage shock protein G	5.63
SL4236	STM4299	*melB*	Melibiose:sodium symporter	-2.43
SL4237	STM4300	*fumB*	Fumarase B	-6.62
SL4238	STM4301	*dcuB*	Anaerobic C4-dicarboxylate transporter	-9.76
SL4262	STM4325	*dcuA*	Anaerobic C4-dicarboxylate transporter	-3.97
SL4264	STM4327	*fxsA*	FxsA	2.40
SL4266	STM4329	*groES*	Co-chaperonin GroES	3.64
SL4267	STM4330	*groEL*	Chaperonin GroEL	3.36
SL4269	STM4332	*yjeJ*	Putative inner membrane protein	2.05
SL4277	STM4340	*frdD*	Fumarate reductase subunit D	-4.48
SL4278	STM4341	*frdC*	Fumarate reductase subunit C	-4.03
SL4279	STM4342	*frdB*	Fumarate reductase iron-sulfur subunit	-4.92

Table L1 continued

Locus Tag		Gene Name	Description	Fold Change[†]
SL Number	STM Number			
SL4280	STM4343	*frdA*	Fumarate reductase flavoprotein subunit	-4.54
SL4406			Unknown; probable DNA polymerase III subunit	2.09
SL4444	STM4513	*yjiG*	Hypothetical protein; BLASTp nucleoside recognition domain-containing inner membrane protein	-3.13
SL4466	STM4535		Putative PTS permease	4.98
SL4467	STM4536		Putative PTS permease	4.15
SL4483	STM4552		Putative inner membrane protein	6.52
SL4492	STM4565	*yjjW*	Pyruvate formate lyase-activating enzyme	-2.07
SLP1_0002		*traX*	Unknown	2.74
SLP1_0005		*trbH*	Unknown	2.30
SLP1_0055		*parA*	Unknown	2.30
SLP1_0060			Unknown	2.37
SLP1_0062			Unknown	3.91
SLP1_0063			Unknown	2.89
SLP1_0064			Unknown	3.98
SLP1_0074		*PSLT033*	Putative inner membrane protein	2.03
SLP1_0080		*ccdA*	Unknown	2.20
SLP1_0081			Unknown	2.93
SLP1_0087			Unknown	2.63
SLP2_0003			Unknown	2.27
SLP2_0011			Unknown	3.14
SLP2_0086			Unknown	-2.19
SLP2_0088			Unknown	-2.17
SLP2_0091			Unknown	-2.73
STM0467			Unknown; miscRNA	-4.48
STM0895			Hypothetical protein; ATPase *Citrobacter*/*Salmonella* (97%,56%)	2.16

Table L1 continued

Locus Tag		Gene Name	Description	Fold Change[†]
SL Number	STM Number			
STM14_1810			Putative dimethyl sulphoxide reductase subunit A	-3.07
STM14_3433			Hydrogenase maturation protein	4.75
STM14_3965			Hypothetical protein	-2.82
STM14_4997			Hypothetical protein	2.10
STM14_5288			Hypothetical protein	4.93
STM2268	STM14_2799		Unknown	-5.50
STM3796B	STM14_4584		Unknown	2.39
STM3797A	STM14_4583		Unknown	2.42
STM4008	STM14_4821		Unknown	2.07
STM4287	STM14_5157		Unknown	2.26
STnc310			Unknown	2.53
STnc520			Unknown	-4.34
STnc630	STM14_5162		Unknown	3.14
sTnc800	STM4006	*glnL*	Unknown; nitrogen regulation protein NR(II)	13.24

[†]Denotes change in expression level in SL1344p*zraR* compared to SL1344pBAD.

Table L2: 147 genes up-regulated by ZraR overexpression in *Salmonella* Typhimurium SL1344. All genes were induced greater than 2-fold (FDR <0.05) in SL1344p*zraR* following ZraR overexpression, compared to SL1344pBAD. Genes are listed according to fold change (greatest to smallest) to two decimal places. The locus tags for both *Salmonella* Typhimurium LT2 (STM) and *Salmonella* Typhimurium SL1344 (SL) are shown. Genes highlighted yellow are also regulated by RpoN, as presented by Samuels et al. (2013).

Locus		Gene Name	Description	Fold Change[†]
SL Number	STM Number			
SL1620	STM1690	*pspA*	phage shock protein PspA	164.56
SL4111	STM4172	*zraP*	zinc resistance protein	122.89
SL1619	STM1689	*pspB*	phage shock protein B	119.17
SL0637	STM0649		Unknown	46.34
SL3487	STM3521		putative ribonucleoprotein related-protein	32.65
SL3736	STM3771		putative phosphotransferase system enzyme IIB	28.14
SL0457	STM0463	*amtB*	ammonium transporter	27.42
SL1618	STM0463	*pspC*	DNA-binding transcriptional activator PspC	24.80
SL0654	STM0665	*gltI*	glutamate and aspartate transporter subunit	21.72
SL1239	STM1304	*astA*	arginine succinyltransferase	16.97
SL0365	STM0369	*prpD*	2-methylcitrate dehydratase	16.44
SL1238	STM1303	*argD*	bifunctional succinylornithine transaminase/acetylornithine transaminase	15.48
SL3775	STM3808		Unknown	15.10
SL1617	STM1687	*pspD*	peripheral inner membrane phage-shock protein	14.77
SL0456	STM0462	*glnK*	nitrogen regulatory protein P-II 2	14.64
SL0564	STM0576		putative PTS system mannose-specific enzyme IIAB	14.23
SL3735	STM3770		putative phosphotransferase system enzyme IIC	13.89
SL3776	STM3809		Unknown	13.62
sTnc800	STM4006	*glnL*	Unknown; possible nitrogen regulation protein NR(II)	13.24
SL2324	STM2355	*argT*	lysine/arginine/ornithine transport protein	11.71
SL3732	STM3767		putative cytoplasmic protein	11.28
SL3485	STM3518	*rtcA*	RNA 3'-terminal-phosphate cyclase	11.24

Table L2 continued

Locus		Gene Name	Description	Fold Change[†]
SL Number	STM Number			
SL3486	STM3519	*rtcB*	putative cytoplasmic protein	10.54
SL0565	STM0577		putative PTS system mannose-specific enzyme IIAB	10.20
SL1374	STM1442	*ydhJ*	putative multidrug resistance efflux pump	8.91
		rlgA	Unknown	8.68
SL2327	STM2358		putative cytoplasmic protein	8.30
SL2820	STM2840		anaerobic nitric oxide reductase flavorubredoxin	7.93
C0664			Unknown	7.49
SL2776	STM2792	*gabT*	4-aminobutyrate aminotransferase	7.31
SL1062	STM1124		Unknown	6.84
SL3954	STM4007	*glnA*	glutamine synthetase	6.77
SL3995	STM4046	*rhaA*	L-rhamnose isomerase	6.74
SL1220	STM1285	*yeaG*	putative serine protein kinase	6.65
SL2886	STM2907	*pphB*	serine/threonine-specific protein phosphatase 2	6.62
SL4483	STM4552		putative inner membrane protein	6.52
SL2360	STM2391	*fadL*	long-chain fatty acid outer membrane transporter	6.43
SL0805	STM0830	*glnH*	glutamine ABC transporter periplasmic protein	6.43
SL0862	STM0886		putative sulfatase	6.20
SL0437	STM0443	*cyoA*	cytochrome o ubiquinol oxidase subunit II	6.09
SL3737	STM3772		putative phosphotransferase system enzyme IIA	5.97
SL2323	STM2354	*hisJ*	histidine transport protein	5.85
SL0364	STM0369	*prpC*	methylcitrate synthase	5.76
SL2839	STM2859	*fhlA*	formate hydrogen-lyase transcriptional activator	5.71
SL4180	STM4244	*pspG*	phage shock protein G	5.63
SL0652	STM0663	*gltK*	glutamate/aspartate transporter	5.50
SL0561	STM0573		putative inner membrane protein	5.17

Table L2 continued

Locus		Gene Name	Description	Fold Change[†]
SL Number	STM Number			
SL0012	STM0012	*dnaK*	molecular chaperone DnaK	5.17
SL0638	STM0650		putative hydrolas	5.02
SL4466	STM4535		putative PTS permease	4.98
	STM14_5288		hypothetical protein	4.93
SL3425	STM3458	*yheR*	glutathione-regulated potassium-efflux system ancillary protein KefG	4.86
SL1187	STM1251		putative molecular chaperone	4.75
	STM14_3433		hydrogenase maturation protein	4.75
SL4112	STM4173	*hydH(zraS)*	sensor kinase in 2CST system with ZraR	4.71
SL2328	STM2359		putative amino acid transporter	4.68
SL3733	STM3768		putative selenocysteine synthase	4.65
SL3744	STM3778		putative DNA-binding protein	4.29
SL4467	STM4536		putative PTS permease	4.15
SLP1_0064			Unknown	3.98
SL2787	STM2716		putative regulatory protein	3.97
SLP1_0062			Unknown	3.91
SL3484	STM3517		putative DNA-damage-inducibile protein	3.76
PSLT043			type II secretion system protein	3.74
SL3528	STM3562	*livM*	leucine/isoleucine/valine transporter permease subunit	3.69
SL1615	STM1685	*ycjX*	putative ATPase	3.64
SL4266	STM4329	*groES*	co-chaperonin GroES	3.64
SL2918	STM2939	*ygcH*	putative cytoplasmic protein	3.60
SL1219	STM1284	*yeaH*	hypothetical protein	3.53
SL4110	STM4171	*yjaH*	putative inner membrane protein	3.46
SL4267	STM4330	*groEL*	chaperonin GroEL	3.36
SL3012	STM3034		putative cytoplasmic protein	3.22

Table L2 continued

Locus		Gene Name	Description	Fold Change[†]
SL Number	STM Number			
SL0480	STM0487		Unknown	3.20
SL2322	STM2353	*hisQ*	histidine/lysine/arginine/ornithine transport protein	3.18
SL2157	STM2180		putative transcriptional regulator	3.18
SLP2_0011			Unknown	3.14
STnc630	STM14_5162		Unknown	3.14
PSLT026			putative periplasmic protein	3.13
SL0466	STM0473	*hha*	hemolysin expression-modulating protein	3.12
SL3952	STM4005	*glnG*	nitrogen regulation protein NR(I)	3.11
SL0363	STM0368	*prpB*	2-methylisocitrate lyase	3.10
STM2724			hypothetical protein	3.09
SL2197	STM2220	*yejG*	hypothetical protein	3.08
SL1503	STM1572	*nmpC*	putative outer membrane porin precursor	3.00
SL2330	STM2361		putative regulatory protein	2.99
SL4034	STM4085	*glpX*	fructose 1,6-bisphosphatase II	2.97
SL0562	STM0574		putative PTS system mannose-specific enzyme IID	2.96
SLP1_0081			Unknown	2.93
SLP1_0063			Unknown	2.89
SL0274	STM0279		putative cytoplasmic protein	2.88
SL1417	STM1487	*ynfL*	putative transcriptional regulator	2.87
SL0563	STM0575		putative inner membrane protein	2.86
SL0467	STM0474	*ybaJ*	hypothetical protein	2.82
SL2620	STM2660	*clpB*	protein disaggregation chaperone	2.81
SL3883	STM3924	*wecD*	TDP-fucosamine acetyltransferase	2.77
	istR		Unknown	2.75
SLP1_0002		*traX*	Unknown	2.74

Table L2 continued

Locus		Gene Name	Description	Fold Change[†]
SL Number	STM Number			
SL4118	STM4183	*aceB*	malate synthase	2.67
SLP1_0087			Unknown	2.63
SL0804	STM0829	*glnP*	glutamine ABC transporter permease protein	2.58
SL0957	STM2621		hypothetical protein	2.57
	oxyS		Unknown	2.56
STnc310			Unknown	2.53
SL3594	STM3628	*dppC*	dipeptide transporter	2.50
SL0497	STM0504	*ybbN*	putative thioredoxin protein	2.50
SL2376	STM2408	*mntH*	manganese transport protein MntH	2.49
SL0803	STM0828	*glnQ*	glutamine ABC transporter ATP-binding protein	2.49
SL0639	STM0651		2-keto-3-deoxygluconate permease	2.45
SL3011	STM3033		plasmid maintenance protein	2.43
STM3797A	STM14_4583		Unknown	2.42
SL4264	STM4327	*fxsA*	FxsA	2.40
SL0275	STM0280		putative outer membrane lipoprotein	2.40
STM3796B	STM14_4584		Unknown	2.39
SLP1_0060			Unknown	2.37
SL0519	STM0526	*ylbA*	hypothetical protein	2.36
SL0624	STM0636	*ybeD*	hypothetical protein	2.35
SLP1_0005		*trbH*	Unknown	2.30
SLP1_0055		*parA*	Unknown	2.30
SLP2_0003			Unknown	2.27
SL2613	STM2649	*trxC*	thioredoxin 2	2.27
STM4287	STM14_5157		Unknown	2.26
SL2166	STM2189	*mglA*	galactose/methyl galaxtoside transporter ATP-binding protein	2.24

Table L2 continued

Locus		Gene Name	Description	Fold Change[†]
SL Number	STM Number			
SL2377	STM2409	*nupC*	nucleoside transport	2.21
SL3059	STM3083		putative mannitol dehydrogenase	2.20
SLP1_0080		*ccdA*	Unknown	2.20
SL3953	STM4006	*glnL*	nitrogen regulation protein NR(II)	2.19
SL3475	STM3508		putative cytoplasmic protein	2.19
SL3977	STM4031		putative cytoplasmic protein	2.16
STM0895			hypothetical protein	2.16
SL2978	STM3000	*ppdA*	hypothetical protein	2.15
SL1076	STM1139	*csgG*	putative curli operon transcriptional regulator	2.15
SL1621	STM1691	*pspF*	phage shock protein operon transcriptional activator	2.14
SL1453	STM1523	*yneJ*	putative transcriptional regulator	2.14
SL2154	STM2177		putative flutathione S-transferase	2.13
SL3743	STM3777		putative cytoplasmic protein	2.11
SL3965	STM4019	*yihQ*	alpha-glucosidase	2.11
STM14_4997			hypothetical protein	2.10
SL4406			Unknown	2.09
STM4008	STM14_4821		Unknown	2.07
SL4269	STM4332	*yjeJ*	putative inner membrane protein	2.05
SL3297	STM3325	*yrbL*	hypothetical protein	2.04
SL0271	STM0276		putative cytoplasmic protein	2.04
SLP1_0074			putative inner membrane protein	2.03
SL3979	STM14_4847		Unknown	2.02

[†]Denotes change in expression level in SL1344p*zraR* compared to SL1344pBAD.

Table L3: **41 genes down regulated by ZraR overexpression in Salmonella Typhimurium SL1344**. All genes were repressed greater than 2-fold (FDR <0.05) in SL1344p*zraR* following ZraR overexpression, compared to SL1344pBAD. Genes are listed according to fold change (greatest to smallest) to two decimal places. The locus tags for both *Salmonella* Typhimurium LT2 (STM) and *Salmonella* Typhimurium SL1344 (SL) are shown.

Locus		Gene Name	Description	Fold Change[†]
SL Number	STM Number			
SL4238	STM4301	*dcuB*	anaerobic C4-dicarboxylate transporter	-9.76
SL4237	STM4300	*fumB*	fumarase B	-6.62
STM2268	STM14_2799		Unknown	-5.50
SL4279	STM4342	*frdB*	fumarate reductase iron-sulfur subunit	-4.92
SL1427	STM1497		putative dimethyl sulphoxide reductase	-4.64
SL4280	STM4343	*frdA*	fumarate reductase flavoprotein subunit	-4.54
SL4277	STM4340	*frdD*	fumarate reductase subunit D	-4.48
SL4009	STM4060	*cpxP*	periplasmic repressor CpxP	-4.46
STnc520			Unknown	-4.34
SL4278	STM4341	*frdC*	fumarate reductase subunit C	-4.03
SL4262	STM4325	*dcuA*	anaerobic C4-dicarboxylate transporter	-3.97
SL1006	STM1066	*rmf*	ribosome modulation factor	-3.97
SL1854	STM1919	*cheM*	methyl accepting chemotaxis protein II	-3.84
SL3123	STM3149	*hybA*	hydrogenase 2 protein HybA	-3.83
SL3542	STM3577	*tcp*	methyl-accepting transmembrane citrate/phenol chemoreceptor	-3.51
SL1428	STM1498		putative dimethyl sulphoxide reductase	-3.37
SL3122	STM3148	*hybB*	putative hydrogenase 2 b cytochrome subunit	-3.22
SL4444	STM4513	*yjiG*	hypothetical protein	-3.13
	STM14_1810		putative dimethyl sulphoxide reductase subunit A	-3.07
SL0122	STM0122	*ftsI*	division specific transpeptidase	-3.00
	STM14_3965		hypothetical protein	-2.82
SL3121	STM3147	*hybC*	hydrogenase 2 large subunit	-2.80

Table L3 continued

Locus		Gene Name	Description	Fold Change[†]
SL Number	STM Number			
SL4444	STM4513	*yjiG*	hypothetical protein	-3.13
SL1416	STM1486	*ynfM*	putative transport protein	-2.76
SLP2_0091			Unknown	-2.73
SL1972	STM14_1420		Unknown	-2.70
SL31 24	STM3150	*hypO*	Hydrogenase 2 small subunit	-2.52
SL4236	STM4299	*melB*	melibiose:sodium symporter	-2.43
SL1495	STM1565	*rpsV*	30S ribosomal subunit S22	-2.29
SL3052	STM3034	*tktA*	transketolase	-2.26
SL1376	STM1444	*slyA*	transcriptional regulator SlyA	-2.22
SL1010	STM1070	*ompA*	outer membrane protein A	-2.20
SLP2_0086			Unknown	-2.19
SLP2_0088			Unknown	-2.17
SL2658	STM2686	*yfjF*	hypothetical protein	-2.11
SL4492	STM4565	*yjjW*	pyruvate formate lyase-activating enzyme	-2.07
SL0312	STM0316	*pepD*	aminoacyl-histidine dipeptidase	-2.05
SL2269	STM2300		putative cytoplasmic protein	-2.04
SL3255	STM3282	*pnp*	polynucleotide phosphorylase/polyadenylase	-2.01

[†]Denotes change in expression level in SL1344p*zraR* compared to SL1344pBAD.

Appendix M

Amino acid sequences of CpxP family of chaperones. Motifs of interest are highlighted. Conserved LTXXQ motifs are shown in **RED** and possible zinc binding motifs in ZraP are shown in **BLUE**.

CpxP

```
         10         20         30         40         50
MRKVTAAVMA STLAFSFLSH AAEVVTSDNW HPGDGATQRS AQNHMFDGIS
         60         70         80         90        100
LTEHQRQQMR DLMQQARHEQ PPVNVSEMET MHRLVTAEKF DESAVRAQAE
        110        120        130        140        150
KMAQEQVARQ VEMARVRNQM YRLLTPEQQA VLNEKHQQRM EQLRDVAQWQ
        160
KSSSLKLLSS SNSRSQ
```

Spy

```
         10         20         30         40         50
MRKLTALFVA STLAMGAANL AHAAETTTAA PADAKPMMQH KGKFGPHHDM
         60         70         80         90        100
MFKNLNLTDA QKQQIRDIMK AQREQMKRPL LEERRAMHDI IASDTFDKAK
        110        120        130        140        150
AEAQITKMEA QRKANMLAHM ETQNKIYNVL TPEQKKQYNA NFEKRLTERP
        160
AQEGKMPAAA E
```

ZraP

```
         10         20         30         40         50
MKRNNKSAIA LIALSLLALS SGAAFAGHHW GNNDGMWQQG GSPLTTEQQA
         60         70         80         90        100
TAQKIYDDYY TQTSALRQQL ISKRYEYNAL LTASSPDTAK INAVAKEMES
        110        120        130        140        150
LGQKLDEQRV KRDVAMAQAG IPRGAGMGYG GCGGYGGGYH RGGGHMGMGN W
```